

UNIVERSITA' DEGLI STUDI DI MILANO

Doctorate School in Pharmaceutical Sciences

XXXV cycle



Development of small molecules as inhibitors of FtsZ and
RnpA acting as potential antimicrobial agents

Supervisor: Prof. Ermanno Valoti

PhD Coordinator: Prof. Giancarlo Aldini

Lorenzo Suigo

R12500

Summary

ABSTRACT	1
CHAPTER 1 – ANTIBIOTICS AND ANTIMICROBIAL RESISTANCE:	
INTRODUCTION	3
Pre-antibiotic era.....	3
Modern antibiotic era	4
The antimicrobial resistance phenomenon	5
Potential solutions to fight Antimicrobial Resistance: the WHO’s “Global Action Plan”	8
Antimicrobial research: the importance of new targets.....	9
CHAPTER 2 – BACTERIAL CELL DIVISION PROCESS: FtsZ	11
The bacterial cell division cycle	11
“Filamenting temperature sensitive Z” or FtsZ.....	11
FtsZ structural and functional characteristics.....	13
FtsZ inhibitors	14
GTP binding site.....	14
Interdomain cleft.....	15
2,6-difluorobenzamides FtsZ inhibitors	17
CHAPTER 3 – BACTERIAL RNA PROCESSING AND DEGRADATION: RnpA	30
Staphylococcus Aureus post-transcriptional regulation	30
Mechanisms of regulation.....	30
<i>S. aureus</i> RNA decay, processing and maturation machinery: RnpA	32
Discovery of <i>S. aureus</i> decay machinery.....	32
RnpA; the component of RNase P.....	33
RnpA inhibitors	34
RNPA1000.....	34
RNPA2000.....	35
The last discovered classes: Phenylcarbamoyl cyclic thiophenes and Piperidine carboxamides	38
Structure-activity evaluation of the novel classes of RnpA inhibitors	39
CHAPTER 4 – AIM OF THE WORK	42
Inhibitors of FtsZ	43
First set: modifications of the 1,2,4-oxadiazole ring.....	45
Second set: modifications of the linker between the two main moieties.....	45

Third set: modifications of the oxygen of the benzodioxane scaffold.....	46
Fourth set: cross-modifications of the substituent in 7-position, the linker between the two main moieties and the heteroatoms.....	47
<i>In-vitro</i> evaluation of the binding to <i>E. coli</i> FtsZ	49
Fifth set: hydroxylated and methylated derivatives	49
Inhibitors of RnpA	52
First set: modifications of JC1/JC2	53
Second set: modifications of the 2-furanyl moiety of RNPA2000	54
Third set: modifications of the <i>i</i> -propyl moiety of RNPA2000.....	55
Fourth set: modifications of the thiosemicarbazide moiety of RNPA2000	55
CHAPTER 5 – RESULTS AND DISCUSSION	57
Inhibitors of FtsZ	57
Structure-activity relationship exploration	57
In-vitro evaluation of the binding to <i>E. Coli</i> FtsZ.....	64
Structure-activity relationship exploration: fifth set of compounds	71
Inhibitors of RnpA	73
Structure-activity relationship exploration	73
<i>In-vitro</i> evaluation of the binding and inhibition of RnpA	75
Cellular evaluation of RnpA inhibition	78
CHAPTER 6 – CONCLUSIONS AND FUTURE WORK	80
Inhibitors of FtsZ	80
Inhibitors of RnpA	81
Overall conclusions	81
CHAPTER 7 – MATERIAL AND METHODS.....	82
Chemistry.....	82
FtsZ inhibitors: computation	82
Ligand preparation	82
Protein preparation.....	82
Docking studies	82
FtsZ inhibitors: <i>in vivo</i> evaluation	83
Antimicrobial activity evaluation on MSSA, MRSA and wt- <i>E. coli</i>	83
Antimicrobial activity evaluation on MDRSA, <i>E. coli</i> N43 and <i>E. coli</i> D22	83
Antimicrobial activity evaluation on <i>B. subtilis</i>	84
Thiazolyl Blue Tetrazolium Bromide (MTT) Cytotoxicity Assay.....	84

Transmission electron microscopy (TEM)	85
FtsZ inhibitors: <i>in vitro</i> evaluation	85
<i>E. coli</i> FtsZ protein purification	85
Fluorescent labelling of FtsZ	86
Fluorescent anisotropy binding experiments	86
Turbidity measurements	86
FtsZ inhibitors: confocal microscopy imaging	87
Preparation of bulk samples	87
Confocal microscopy measurements and data analysis	87
RnpA inhibitors: computation	87
Hotspot maps	87
Computational studies	87
RnpA inhibitors: biological study	88
Bacterial growth conditions	88
Antimicrobial susceptibility testing ATCC 29213 and ATCC 43300	88
RnpA protein purification.....	88
In-Vitro transcription of RNA	89
In vitro ptRNA processing assays	90
In vitro mRNA degradation assays	90
Cellular tRNA ^{Tyr} population measures.....	91
Cellular mRNA turnover assays	91
Bacterial RNA Isolation and Quantitative Reverse Transcription Polymerase Chain Reaction (qRT-PCR)	91
CHAPTER 8 – CHEMISTRY	93
Inhibitors of FtsZ	93
Synthesis of 5,6,7,8-Tetrahydronaphthalen-2,3-diol	93
Synthesis of first set compounds: derivatives I and II.....	94
Synthesis of second set compounds: derivatives III to VIII	95
Synthesis of third set compounds: derivatives IX to XIII	99
Synthesis of fourth set compounds: derivatives XIV to XX	100
Synthesis of fifth set compounds: derivatives XXI to XXIII.....	103
Inhibitors of RnpA	107
Synthesis of first set compounds: derivatives XXIV and XXVIII	107
Synthesis of second set compounds: derivatives XXIX and XXXII	107

Synthesis of third set compounds: derivatives XXXIII and XXXIV.....	108
Synthesis of fourth set compounds: derivatives XXXV to XL	108
CHAPTER 9 – EXPERIMENTAL	111
(1,4-naphthodioxan-2-yl)methanol	112
(1,4-naphthodioxan-2yl)methanesulfonate	113
(I) 3-(1,4-Naphthodioxan-2-yl)methoxy)-2,6-difluorobenzamide	114
5,6,7,8-Tetrahydronaphthalen-2-yl acetate	117
3-Acetyl-5,6,7,8-tetrahydro-2-naphthol	118
2-Acetyl-3-benzyloxy-5,6,7,8-tetrahydronaphthalene	119
2-Acetoxy-3-benzyloxy-5,6,7,8-tetrahydronaphthalene	120
2-Benzyloxy-5,6,7,8-tetrahydro-2-naphthol.....	121
5,6,7,8-Tetrahydronaphthalene-2,3-diol	122
(5,6,7,8-tetrahydro-1,4-naphthodioxan-2-yl)methanol	123
(5,6,7,8-tetrahydro-1,4-naphthodioxan-2-yl)methanesulfonate	124
(II) 3-(5,6,7,8-Tetrahydro-1,4-naphthodioxan-2-yl)methoxy)-2,6-difluorobenzamide .	125
3,4-Dibromobutanoic acid	128
Methyl 3,4-dibromobutanoate	129
Methyl 2-(1,4-benzodioxan-2-yl)-acetate.....	130
2-(1,4-Benzodioxane-2-yl)-ethanol.....	131
2-(1,4-Benzodioxane-2-yl)-ethyl methanesulfonate	132
(III) 3-(1,4-Benzodioxane-2-yl)ethoxy)-2,6-difluorobenzamide.....	133
Pent-4-en-1-yl methanesulfonate	136
2,6-Difluoro-3-(pent-4-en-1-yloxy)benzamide	137
2,6-Difluoro-3-(3-(oxiran-2-yl)propoxy)benzamide	138
2,6-Difluoro-3-((4-hydroxy-5-(2-hydroxyphenoxy)pentyl)oxy)benzamide	139
(IV) 3-(1,4-Benzodioxane-2-yl)propoxy)-2,6-difluorobenzamide	140
(1,4-Benzodioxan-2-yl)-carboxylic acid.....	143
(1,4-Benzodioxan-2-yl) carbonyl chloride.....	144
<i>N</i> -Methoxy- <i>N</i> -methyl-(1,4-benzodioxan-2-yl)carboxamide	145
1-(1,4-Benzodioxan-2-yl)-ethanone.....	146
1-(1,4-Benzodioxan-2-yl)-ethanol.....	147
1-(1,4-Benzodioxan-2-yl)-ethyl methanesulfonate	148
(V) 3-(1-(1,4-Benzodioxan-2-yl)-ethoxy)-2,6-difluorobenzamide.....	149
2-(1,4-Benzodioxan-2-yl)-propene	156

2-(1,4-Benzodioxan-2-yl)-1-propanol	157
2-(1,4-Benzodioxan-2-yl)-1-propyl methanesulfonate.....	158
(VI) 3-[2-(1,4-Benzodioxan-2-yl)-1-propyloxy]-2,6-difluorobenzamide	159
2-(1,4-Benzodioxan-2-yl)-acetic acid	166
2-(1,4-Benzodioxan-2-yl)-acetyl chloride	167
2-(1,4-Benzodioxan-2-yl)- <i>N</i> -methoxy- <i>N</i> -methyl-acetamide.....	168
1-(1,4-Benzodioxan-2-yl)-propan-2-one	169
1-(1,4-Benzodioxan-2-yl)-propan-2-ol	170
1-(1,4-Benzodioxan-2-yl)-propan-2-yl methanesulfonate.....	171
(VII) 3-[2-(1,4-Benzodioxan-2-yl)propan-2-yl]oxy)-2,6-difluorobenzamide	172
Methyl 3-(1,4-benzodioxan-2-yl)-buten-2-onate	173
Methyl 3-(1,4-benzodioxan-2-yl)-butanonate.....	174
3-(1,4-Benzodioxan-2-yl)-butan-1-ol	175
3-(1,4-Benzodioxan-2-yl)-butan-1-yl methanesulfonate.....	176
(VIII) 3-[2-(1,4-Benzodioxan-2-yl)butan-1-yl]oxy)-2,6-difluorobenzamide	177
Ethyl 1,4-benzoxathian-2-carboxylate and Ethyl 1,4-benzoxathian-3-carboxylate	184
2-(1,4-Benzoxathiane-2-yl)-ethanol and 2-(1,4-Benzoxathiane-3-yl)-ethanol.....	185
2-(1,4-Benzoxathiane-2-yl)-ethyl methanesulfonate and 2-(1,4-Benzoxathiane-3-yl)- ethyl methanesulfonate.....	186
(IX) and (X) 3-(1,4-Benzoxathiane-2-yl)methoxy)-2,6-difluorobenzamide and 2-(1,4- Benzoxathiane-3-yl)methoxy)-2,6-difluorobenzamide	187
Ethyl 1,4-benzodithian-2-carboxylate	194
2-(1,4-Benzodithian-2-yl)-ethanol	195
2-(1,4-Benzodithian-2-yl)-ethyl methanesulfonate.....	196
(XI) 3-(1,4-Benzodithian-2-yl)methoxy)-2,6-difluorobenzamide.....	197
(XII) 3-(1,4-Benzoxathiane-4,4-dioxide-2-yl)methoxy)-2,6-difluorobenzamide.....	200
(XIII) 3-(1,4-Benzoxathiane-4,4-dioxide-3-yl)methoxy)-2,6-difluorobenzamide.....	203
Methyl-(1,4-naphthodioxan-2-yl) acetate	206
2-Hydroxyethyl-1,4-naphthodioxane	207
2-Mesyloxyethyl-1,4-naphthodioxane.....	208
(XIV) 3-(1,4-Naphthodioxan-2-yl)ethoxy)-2,6-difluorobenzamide	209
Methyl-(5,6,7,8-tetrahydro-1,4-naphthodioxan-2-yl) acetate	212
2-(2-Hydroxyethyl)-5,6,7,8-tetrahydro-1,4-naphthodioxane.....	213
2-(2-Mesyloxyethyl)-5,6,7,8-tetrahydro-1,4-naphthodioxane.....	214
(XV) 3-(5,6,7,8-Tetrahydro-1,4-naphthodioxan-2-yl)ethoxy)-2,6-difluorobenzamide..	215

Methyl (7-cyano-1,4-benzodioxan-2-yl)-acetate.....	218
2-(2-Hydroxyethyl)-7-cyano-1,4-benzodioxane.....	219
2-(2-Mesyloxyethyl)-7-cyano-1,4-benzodioxane.....	220
3-[2-(7-Cyano-1,4-benzodioxan-2-yl)ethyloxy]-2,6-difluorobenzamide	221
3-[2-(7- <i>N'</i> -Hydroxycarbamimidoyl-1,4-benzodioxan-2-yl)ethyloxy]-2,6-difluorobenzamide.....	222
3-[2-(7-(5-Mercapto-1,2,4-oxadiazol-3-yl)-1,4-benzodioxan-2-yl)ethyloxy]-2,6-difluorobenzamide.....	223
(XVI) 3-[2-(7-(5-Methylthio-1,2,4-oxadiazol-3-yl)-1,4-benzodioxan-2-yl)ethyloxy]-2,6-difluorobenzamide.....	224
(XVII) 3-[2-(7-(5-Ethyl-1,2,4-oxadiazol-3-yl)-1,4-benzodioxan-2-yl)ethyloxy]-2,6-difluorobenzamide (VII)	227
(XVIII) 3-[2-(7-(5-Methyl-1,2,4-oxadiazol-3-yl)-1,4-benzodioxan-2-yl)ethyloxy]-2,6-difluorobenzamide.....	230
Methyl (1,4-benzoxathian-2-yl)-acetate.....	233
2-(1,4- Benzoxathian-2-yl)-ethanol.....	234
2-(1,4- Benzoxathian-2-yl)-ethyl methanesulfonate	235
(XIX) 3-(1,4-Benzoxathian-2-yl)ethoxy)-2,6-difluorobenzamide	236
3-(Naphthalen-2-yloxy)-1-propanol	239
3-(Naphthalen-2-yloxy)propyl methansulfonate.....	240
(XX) 3-(3-(Naphthalen-2-yloxy)propoxy)-2,6-difluorobenzamide	241
Ethyl (5,6,7,8-tetrahydro-1,4-naphthodioxane-2-yl)-carboxylate.....	244
(5,6,7,8-Tetrahydro-1,4-naphthodioxane-2-yl)-carboxylic acid	245
<i>N</i> -Methoxy- <i>N</i> -methyl-(5,6,7,8-tetrahydro-1,4-naphthodioxane-2-yl)-carboxamide..	246
1-(5,6,7,8-Tetrahydro-1,4-naphthodioxane-2-yl)-ethanone	247
2-Bromo-1-(5,6,7,8-tetrahydro-1,4-naphthodioxane-2-yl)-ethanone	248
<i>Erythro</i> and <i>Threo</i> -2-(5,6,7,8-tetrahydro-1,4-naphthodioxane-2-yl)-oxirane.....	249
<i>Erythro</i> (XXI) 3-(5,6,7,8-tetrahydro-1,4-naphthodioxane-2-yl)2-hydroxyethoxy)-2,6-difluorobenzamide.....	250
<i>Threo</i> (XXI) 3-(5,6,7,8-tetrahydro-1,4-naphthodioxane-2-yl)2-hydroxyethoxy)-2,6-difluorobenzamide.....	253
2-Bromo-1-(1,4-benzodioxan-2-yl)-ethanone	256
<i>Erythro</i> and <i>Threo</i> -2-(1,4-Benzodioxan-2-yl)-oxirane.....	257
<i>Erythro</i> (XXII) 3-(1,4-Benzodioxane-2-yl)2-hydroxyethoxy)-2,6-difluorobenzamide	258
<i>Threo</i> (XXII) 3-(1,4-Benzodioxane-2-yl)2-hydroxyethoxy)-2,6-difluorobenzamide	261
2-Methyl-3-butenic acid	264

3,4-Dibromo-2-methylbutanoic acid	265
Methyl 3,4-dibromo-2-methylbutanoate	266
<i>Erythro</i> and <i>Threo</i> Methyl 2-(5,6,7,8-tetrahydro-1,4-naphthodioxan-2-yl)-2-methylacetate	267
<i>Erythro</i> 2-(5,6,7,8-tetrahydro-1,4-naphthodioxan-2-yl)propan-1-ol.....	268
<i>Erythro</i> 2-(5,6,7,8-Tetrahydro-1,4-naphthodioxan-2-yl)prop-1-yl methanesulfonate .	269
(XXIII) <i>Erythro</i> 3-(2-(5,6,7,8-Tetrahydro-1,4-naphthodioxan-2-yl)prop-1-yloxy)-2,6-difluorobenzamide.....	270
<i>Threo</i> 2-(5,6,7,8-tetrahydro-1,4-naphthodioxan-2-yl)propan-1-ol	273
<i>Threo</i> 2-(5,6,7,8-Tetrahydro-1,4-naphthodioxan-2-yl)prop-1-yl methanesulfonate	274
(XXIII) <i>Threo</i> 3-(2-(5,6,7,8-Tetrahydro-1,4-naphthodioxan-2-yl)prop-1-yloxy)-2,6-difluorobenzamide.....	275
(XXIV) 1-(2-Biphenyl)-3-(2-methylpiperdin-1-yl)urea	278
(XXV) 1-(3-Biphenyl)-3-(2-methylpiperdin-1-yl)urea	281
(XXVI) 1-(4-Biphenyl)-3-(2-methylpiperdin-1-yl)urea	284
(XXVII) 1-(3,5-Dichlorophenyl)-3-(1,2,3,4-tetrahydroquinolin-1-yl)urea	287
(XXVIII) 1-(3,5-Dichlorophenyl)-3-(1,2,3,4-tetrahydroisoquinolin-1-yl)urea.....	290
Methyl 4- <i>i</i> -propylphenoxyacetate	293
4- <i>i</i> -Propylphenoxyacetohydrazide	294
(XXIX) 1-(4- <i>i</i> -Propylphenoxyacetyl)-4-(3,5-dichlorobenzoyl)thiosemicarbazide	295
(XXX) 1-(4- <i>i</i> -Propylphenoxyacetyl)-4-(3-chlorobenzoyl)thiosemicarbazide	298
(XXXI) 1-(4- <i>i</i> -Propylphenoxyacetyl)-4-(3-bromobenzoyl)thiosemicarbazide	301
(XXXII) 1-(4- <i>i</i> -Propylphenoxyacetyl)-4-(3,5-dibromobenzoyl)thiosemicarbazide	304
Methyl 4-biphenyloxyacetate	307
4-Biphenyloxyacetohydrazide	308
(XXXIII) 1-(4-Biphenyloxyacetyl)-4-(3,5-dichlorobenzoyl)thiosemicarbazide.....	309
Methyl 2-naphthoxyacetate	312
2-Naphthoxyacetohydrazide	313
(XXXIV) 1-(2-naphthoxyacetyl)-4-(3,5-dichlorobenzoyl)thiosemicarbazide	314
4- <i>i</i> -Propylphenoxyacetic acid.....	317
4- <i>i</i> -Propylphenoxyacetyl chloride	318
<i>N</i> -(<i>t</i> -Butoxycarbonylaminomethyl)-4- <i>i</i> -propylphenoxyacetamide.....	319
<i>N</i> -(Aminomethyl)-4- <i>i</i> -propylphenoxyacetamide	320
(XXXV) 3,5-Dichloro- <i>N</i> -((2-(4- <i>i</i> -propylphenoxy)acetamido)methyl)benzamide	321
<i>N</i> -(<i>t</i> -Butoxycarbonylaminoethyl)-3,5-dichlorobenzamide	324

<i>N</i> -(Aminoethyl)-3,5-dichlorobenzamide.....	325
(XXXVI) 3,5-Dichloro- <i>N</i> -((2-(4- <i>i</i> -propylphenoxy)acetamido)ethyl)benzamide	326
4- <i>t</i> -Butoxycarbonyl-1-(4- <i>i</i> -propylphenoxyacetyl)piperazine	329
1-(4- <i>i</i> -propylphenoxyacetyl)piperazine	330
(XXXVII) 4-(3,5-Dichlorobenzoyl)-1-(4- <i>i</i> -propylphenoxyacetyl)piperazine	331
4- <i>t</i> -Butoxycarbonylamino-1-(4- <i>i</i> -propylphenoxyacetyl)piperidine	334
4-amino-1-(4- <i>i</i> -propylphenoxyacetyl)piperidine	335
(XXXVIII) 4-(3,5-Dichlorobenzoylamino)-1-(4- <i>i</i> -propylphenoxyacetyl)piperidine	336
<i>N</i> -Boc-(3-(3,5-dichlorobenzamido)piperidine	339
3-(3,5-dichlorobenzamido)piperidine.....	340
(XXXIX) 3,5-dichloro- <i>N</i> -(1-(2-(4-isopropylphenoxy)acetyl)piperidin-3-yl)benzamide ...	341
<i>N</i> -Boc-(3-(4-isopropylphenoxy)acetamido)piperidine	342
3-(4-isopropylphenoxy)acetamido)piperidine.....	343
(XL) <i>N</i> -(1-(3,5-dichlorobenzoyl)piperidin-3-yl)-2-(4-isopropylphenoxy)acetamide	344
CHAPTER 10 – REFERENCES.....	345

ABSTRACT

The antimicrobial resistance (AMR) is nowadays one of the most worrying threats of modern medicine. Recently, AMR has been also called “the silent pandemic” because is as worrying as the COVID-19 outbreak, but without receiving the same public attention. The most important organizations such as World Health Organization (WHO) and Centres for Disease Control and Prevention (CDC) pointed out how the academic work on the development of new chemical entities as antimicrobials able to interact with new molecular targets remains one of the key actions to fight antimicrobial resistance (World Health Organization, 2015).

Within the present work, two innovative bacterial targets have been considered to develop new potential inhibitors: FtsZ and RnpA.

FtsZ is a 40 kDa protein with 40 -50% of conservation among all bacteria and archaea. This protein represents the main actor of the bacterial cell division cycle, the essential process that allows the parent cell to divide through binary fission into two daughter cells. At the beginning of the cycle, FtsZ polymerizes at the centre of the cell, constituting the “Z-ring”. This step serves as guide for the continuation of the process, therefore the inhibition of FtsZ leads to cell filamentation and death. For these reasons, FtsZ arose as a potential target for the development of new antimicrobials. In the first part of this work, starting from the insights gained in the last years, new families of benzodioxane-benzamides have been designed, synthesized, purified and evaluated as potential antimicrobials on *S. aureus*, *B. subtilis* and *E. coli*. Moreover, FtsZ was validated as the target of these compounds. In particular, *S. aureus* and *B. subtilis* FtsZs were validated as targets through specific cellular assays, while the capability of these compounds to interact with *E. coli* FtsZ was demonstrated through an *in vitro* study on the isolated protein. Moreover, the cytotoxicity of all the derivatives was evaluated, and most of the derivatives are characterized by low to non-detectable cytotoxicity on human cells.

RnpA is a small protein of *S. aureus* essential for two cellular processes: mRNA degradation and precursor tRNA (ptRNA) maturation. Indeed, RnpA alone can catalyse the degradation of bulk mRNA thus promoting mRNA turnover among different growth phases (exponential and stationary). Furthermore, RnpA is able to associate with a ribozyme to form RNase P, a riboprotein complex that promotes the removal of the 5' leader sequence from precursor

tRNA, inducing tRNA maturation. Shortly after the discovery of the essentiality of RnpA, the investigation of RnpA inhibitors as potential anti-staphylococcal compounds started. Within the second main body of this work, the structure-activity relationship (SAR) of two classes of known RnpA inhibitors was evaluated. Modifications of the structures of the two main RnpA inhibitors, JC2 and RNPA2000, have been designed and applied. The resulting compounds were tested as antimicrobials on *S. aureus*, both methicillin-sensitive and methicillin-resistant. Also in this case, the *in vitro* profile of inhibition of RnpA as well as the cytotoxicity of the obtained derivatives were assessed.

With the results obtained in the present work, the understanding of both FtsZ and RnpA inhibitors was significantly increased, speeding up the development of these important tools to fight antimicrobial resistance.

CHAPTER 1 – ANTIBIOTICS AND ANTIMICROBIAL RESISTANCE: INTRODUCTION

Pre-antibiotic era

Throughout history, mankind has always been menaced by viral and bacterial infectious diseases. Several historical evidence suggest us that the human being has been treating with infections since the beginnings. For instance, traces of tetracyclines have been found in numerous histological samples from skeletons dating 350 – 500 CE, which could derive only from the diet. Other examples came from the traditional Chinese medicine, in which *Artemisia* plant extracts were used for the treatment of several sicknesses (Aminov, 2010), and from traditional Indian ayurvedic medicine.

Nevertheless, despite these initial uses of antimicrobials, in the pre-antibiotic era the average life expectancy was 47 years, due to several reasons including infectious diseases such as cholera, diphtheria, smallpox, plaque etc (Adedeji W.A., 2021). Before the discovery of bacteria and of their role in the development of infections, the rational design of antimicrobials was, inevitably, impossible.

To the connection between microorganisms and diseases contributed Robert Koch in the 19th century. He discovered that it is always possible to isolate specific bacteria, not present in healthy individuals, from secretions of people suffering from a specific bacterial disease. Moreover, those same bacteria could replicate themselves in certain mediums and, if inoculated in healthy people, could induce the specific symptoms of the same disease. These discoveries gave birth to the idea of the cause-effect relation between microorganism and diseases.

Another great contribution came from Louis Pasteur, which in 1877 discovered that, in presence of what he called “common bacteria”, the anthrax bacteria produced a less deadly version of the disease, introducing the concept of antibiosis (Foye, 2005).

Although these initial findings were surely important and stimulating, only 50 years later the antibiotic research started to slowly evolve.

Modern antibiotic era

The beginning of the “Modern antibiotic era” is universally recognized to be related with the findings of Paul Ehrlich and Sir Alexander Fleming. Ehrlich was the first who ideate the idea of “*Compounds able to exert their full action exclusively on the parasite harboured within the organism*”, which gave birth to the concept of chemotherapy (Bosch and Rosich, 2008) (Paul Erlich Wikipedia, 2022). In parallel, in 1928, Fleming made his observations of the antimicrobial activity of *Penicillium*, which led to the isolation of Penicillin G in 1940 and to the mass production and distribution in 1945. Moreover, in the same period, in 1935, Josef Klarer and Fritz Mietzsch synthesized Prontosil, which was successively demonstrated to be a precursor of sulphanilamide, initiating the sulphonamides antimicrobial class.

Besides setting the base for the modern drug discovery process, these events gathered the attention of several researchers, resulting in the so-called “Golden era of antibiotic discoveries”, in which most of the antimicrobial classes still used nowadays were discovered.

Indeed, another important event in the history of antibiotics was the discovery in 1943 of streptomycin from *Actinomyces griseus*, the first aminoglycoside antibiotic. In addition to the activity towards Gram-positive strains, this compound showed high potencies against Gram-negative bacteria and mycobacteria such as *Mycobacterium tuberculosis*. Since penicillin was not active towards mycobacteria, this molecule represented the beginning of the treatment of mycobacteria-based diseases, like tuberculosis (Nicolaou and Rigol, 2018).

Shortly after, in 1945, chlortetracycline, the first member of the important class of the tetracyclines, was discovered. This compound was approved as broad-spectrum agent against both Gram-positive and Gram-negative bacteria in 1948. Thereafter, several other tetracyclines were discovered. Both streptomycin and tetracyclines are able to interact with the bacterial ribosome at the 30S subunit, exerting their antimicrobial activity.

All the antibiotics discovered between 1940s and 1960s are still used in clinical therapies, but their effectiveness has been strongly lowered by the development of antimicrobial resistance, a natural phenomenon speeded up by several factors.

The antimicrobial resistance phenomenon

The great success of antimicrobials in the late 50s, which culminated with the possibility to treat infectious diseases as never before, led General Surgeon William H. Stewart to make his famous statement: *“It is time to close the book on infectious diseases and declare the war against pestilence won”* (Sengupta, Chattopadhyay and Grossart, 2013). Also, one of the first studies about the possibility of penicillin to induce the development of antibiotic-resistance concluded that: *“Syphilis has now been treated with arsenicals for about 40 years without any indications of an increased incidence of arsenic--resistant infections, and this work gives grounds for hoping that the widespread use of penicillin will equally not result in an increasing incidence of infections resistant to penicillin”* (Rollo and Williamson, 1952).

Conversely to these predictions, after the large use of penicillin to control bacterial infections during Second World War, the emergence of penicillin-resistant strains started to be a major and severe threat. A short time later, the discoveries in 1961 in the UK and in 1968 in the US of methicillin-resistant *Staphylococcus aureus* officially raised the problem at the attention of the world (Lee Ventola, 2015).

As defined, Antimicrobial resistance (AMR) is a phenomenon that happens when microbials, such as bacteria or fungi, develop the ability to resist to a specific drug designed to kill them. This resistance occurs naturally; indeed, antibiotic resistance genes appeared in bacterial genome long ago in response to natural substances with antibiotic properties. Moreover, spontaneous mutations can also generate resistant species (Read and Woods, 2014). Nevertheless, resistant-mutants diffusion is accelerated by antibiotic-mediated selection, which occurs every time an antimicrobial fails to block their reproduction while eliminating the antimicrobial-sensitive competitors. As a conclusion, it is easy to understand how overuse of antibiotics represented and still represents an important cause of the antibiotic resistance worldwide diffusion.

In addition to this, several other human-related factors are responsible of the problem:

- Mistaken or inappropriate antibiotic prescription.
- Extensive use in agriculture.
- Regulatory limitations.
- Limited number of new antibiotics being developed.

As a result, nowadays AMR represents one of the major problems worldwide.

According to CDC antibiotic resistance report of 2019, 18 resistant germs are listed as “Concerning threats”, “Serious threats” or “Urgent threats” based on the gravity of the consequences of their existence nowadays (Figure 1). Some deserve a special mention: Carbapenem-resistant *Enterobacteriaceae*, which leads to severe infections in patients in healthcare facilities, or Multi-drug resistant *Neisseria gonorrhoeae*, which causes drug-resistant gonorrhoea, or again Methicillin-resistant *Staphylococcus aureus*, which is responsible for serious nosocomial infections (Centre for Disease Control and Prevention, 2019).

Urgent Threats

- Carbapenem-resistant *Acinetobacter*
- *Candida auris* (*C. auris*)
- *Clostridioides difficile* (*C. difficile*)
- Carbapenem-resistant Enterobacteriaceae (CRE)
- Drug-resistant *Neisseria gonorrhoeae* (*N. gonorrhoeae*)

Serious Threats

- Drug-resistant *Campylobacter*
- Drug-resistant *Candida*
- Extended-spectrum beta-lactamase (ESBL)-producing Enterobacteriaceae
- Vancomycin-resistant *Enterococci* (VRE)
- Multidrug-resistant *Pseudomonas aeruginosa* (*P. aeruginosa*)
- Drug-resistant nontyphoidal *Salmonella*
- Drug-resistant *Salmonella* serotype Typhi
- Drug-resistant *Shigella*
- Methicillin-resistant *Staphylococcus aureus* (MRSA)
- Drug-resistant *Streptococcus pneumoniae* (*S. pneumoniae*)
- Drug-resistant Tuberculosis (TB)

Concerning Threats

- Erythromycin-resistant group A *Streptococcus*
- Clindamycin-resistant group B *Streptococcus*

Figure 1: Germs listed as “Urgent”, “Serious” or “Concerning Threats” by CDC.

Beside this classification made by American CDC, in 2017 the World Health Organization (WHO) divided the antibiotic-resistant priority pathogens into three categories: “Priority 1:

Critical”, “Priority 2: High” and “Priority 3: Medium”, basing on multi-criteria analyses (Figure 2).

Priority 1: CRITICAL

- *Acinetobacter baumannii*, carbapenem-resistant
- *Pseudomonas aeruginosa*, carbapenem-resistant
- *Enterobacteriaceae*, carbapenem-resistant, ESBL-producing

Priority 2: HIGH

- *Enterococcus faecium*, vancomycin-resistant
- *Staphylococcus aureus*, methicillin-resistant, vancomycin-intermediate and resistant
- *Helicobacter pylori*, clarithromycin-resistant
- *Campylobacter spp.*, fluoroquinolone-resistant
- *Salmonellae*, fluoroquinolone-resistant
- *Neisseria gonorrhoeae*, cephalosporin-resistant, fluoroquinolone-resistant

Priority 3: MEDIUM

- *Streptococcus pneumoniae*, penicillin-non-susceptible
- *Haemophilus influenzae*, ampicillin-resistant
- *Shigella spp.*, fluoroquinolone-resistant

Figure 2: Pathogens classified into three different priority classes.

In the priority 1 class, in which germs are listed as “Critical”, we find the Gram-negative bacteria of the ESKAPE classification, while the Gram-positive ones are classified as “High” priority.

The ESKAPE bugs are a small group composed by *Enterococcus faecium*, *Staphylococcus aureus*, *Klebsiella pneumoniae*, *Acinetobacter baumannii*, *Pseudomonas aeruginosa* and *Enterobacter* species whose initials make the ESKAPE acronym. These bacteria are extremely important primarily because of their presence in the hospitals, which makes them responsible for several nosocomial infections, but also because of their increasing resistance to several antimicrobials (Rice, 2008).

As a result of the overwhelming severity of AMR today, in 2019 1.2 million people died as a direct result of antibiotic-resistant bacterial infections, making AMR a leading death cause worldwide, greater than malaria and HIV (University of Oxford, 2022). When the consequences are not lethal, infections with antibiotic resistant bugs can still result in longer illnesses, loss of protection for patients that underwent surgery or transplant, and prolonged stays in hospital. Moreover, the last also translates in higher costs for medical treatment and less productivity (of both animals and humans), which make AMR impacting on the world economy as well.

Taken together, all these data underline the importance to begin a deep work on AMR and to find solutions to overcome it.

Potential solutions to fight Antimicrobial Resistance: the WHO's "Global Action Plan"

In May 2015, the WHO compiled a "Global Action Plan on Antimicrobial Resistance" with the scope of maintain or improve the effectiveness of treatment and prevention of infectious diseases as long as possible. To achieve this final goal, the WHO set up 5 "strategic objectives", both social and scientific (World Health Organization, 2015):

- 1- Improve awareness and understanding of AMR.
- 2- Strengthen the knowledge and evidence base.
- 3- Reduce the incidence of infection.
- 4- Optimize the use of antimicrobial medicines in human and animal health.
- 5- Develop the economic case for sustainable investment and increase investment in new medicines, diagnostic tools, vaccines, and other intervention.

These objectives clearly underline how several social activities represent a priority and how behavioural changes are very important to significantly fight this problem. At the same time, also scientific actions must be taken to enhance prevention, diagnosis and, more importantly, treatment of multi-drug resistant bacterial infections.

It is clear that the antimicrobials research is less pursued by the pharmaceutical firms since the economic earnings are minor if compared to chronic diseases drugs. As a result, in 2021, the number of antimicrobial agents in clinical development is very far from the overall request to overcome or limit the problem (World Health Organization, 2021).

Antimicrobial research: the importance of new targets

As stated before, the antimicrobial research is deficient from a quantitative point of view, due to limited investments from industrials. At the same time, many of the new molecules being developed show small structural modifications of the existing drugs. Since most of the drugs used in therapy act on four crucial bacterial processes (protein synthesis, cell-wall synthesis, nucleic acid synthesis or folate synthesis) (Figure 3) (Lock and Harry, 2008), molecules deriving from them bind the same targets, allowing bacteria to rapidly develop resistance to the new molecules as well.

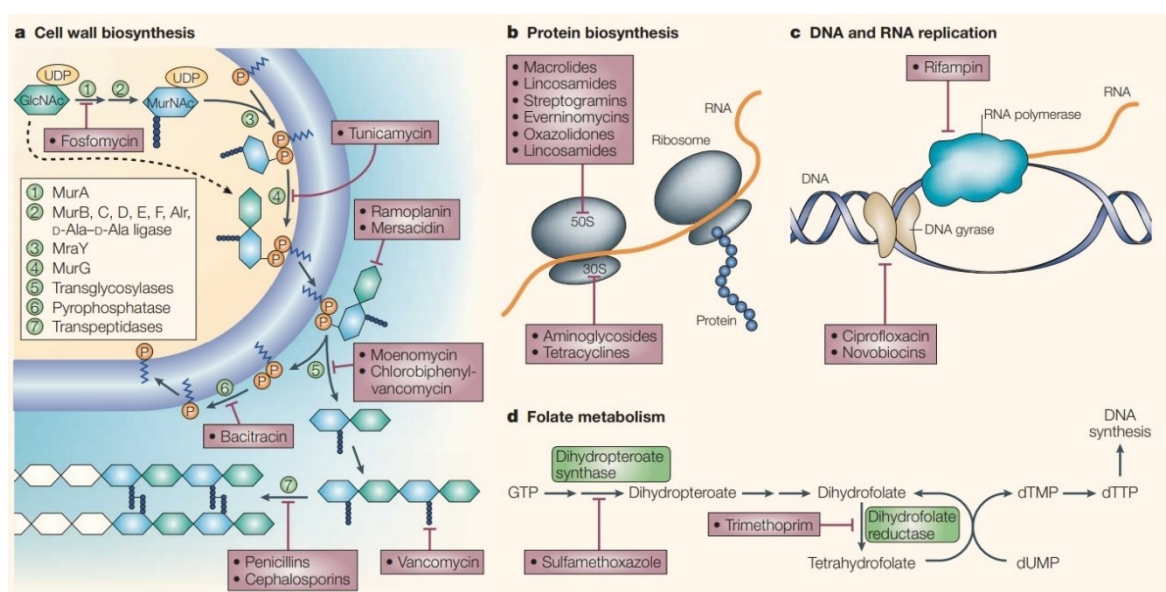


Figure 3: Targets of the antibiotics currently used in the market: Cell-wall biosynthesis (a), Protein biosynthesis (b), DNA and RNA replication (c) and Folate metabolism (d). Adapted from Mahmoud Sayed Doctoral Thesis, 2014.

These data highlight how gaining knowledge on crucial bacterial processes is essential to design new drugs able to overcome to current mechanisms of resistance and to delay as much as possible the insurgence of new resistance systems.

In this context, two processes have been recently recognized as exploitable for antimicrobial drug-discovery: the bacterial cell division cycle and the bacterial RNA processing and degradation. The former, which allows the parent cell to be divided into two daughter cells through binary fission, is based on FtsZ, a well-conserved protein among different species making it very interesting for target-driven antimicrobial drug discovery (Haeusser and Margolin, 2016). Even if the importance of this process is well-known from

several years has not be so exploited and, nowadays, only a few antibiotics acting on this target are in clinical development and no derivatives are currently marketed.

The latter, bacterial RNA processing and degradation, is another exploitable target. Conversely to the cell-division cycle, RNA processing and degradation is not promoted by a central conserved protein but by different protein elements that work in concert in different bacterial strains. Nonetheless, *S. aureus* RNA processing machinery has been recently described and the main actor, the protein RnpA, represents a promising target for developing anti-staphylococcal compounds, which are a huge clinically relevant medical need (Patrick D Olson *et al.*, 2011).

As a result, the present PhD thesis will start from these two important and crucial bacterial processes and will illustrate the development of new molecules acting on them. Each argument will be deeply described in the following chapters.

CHAPTER 2 – BACTERIAL CELL DIVISION PROCESS: FtsZ

The bacterial cell division cycle

Bacteria must divide in order to increase their number and take possession of the infection site. This, for the majority of bacteria, happens through binary fission that consists in the splitting of the mother cell into two daughter cells of approximately the same size (Haeusser and Margolin, 2016). The importance of this process is evident; any kind of inhibition will result in the impossibility of the bacterium to further colonize the host and, potentially, to develop the associated illness. This process is orchestrated by an elaborate protein complex named divisome, which formation starts with the polymerization of FtsZ, the key protein of the whole process.

“Filamenting temperature sensitive Z” or FtsZ

The history of the discoveries that led to the understanding of the importance of FtsZ in the cell division process begins in the 1960s. Several research groups screened for mutations on *E. coli* that impeded cell division at 42°C (*FtsZ Wikipedia page, 2022*) and this continued growth without achieving a correct division resulted in long filamentous cells. The genome of these mutants was later mapped, and the mutations identified on a gene adjacent to *FtsA*, which was named *FtsZ* (Lutkenhaus, Wolf-Watz and Donachie, 1980). FtsZ is a ~40 kDa protein highly conserved among bacteria and archaea that represents the homologue of the human tubulin (Figure 4).

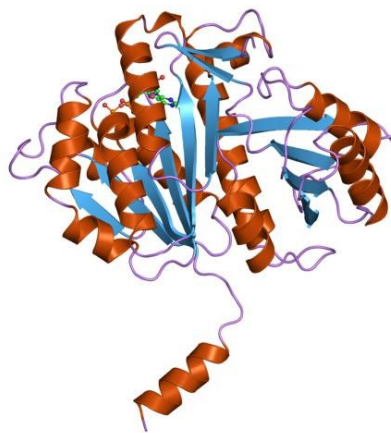


Figure 4: *E. coli* FtsZ (adapted from Wikipedia).

In more than 60 years of research, several discoveries have been made on FtsZ and its role on the cell division process, allowing the scientific community to construct a model of

bacterial division. At the beginning of the process, FtsZ localizes at the site of partition and, upon GTP binding, polymerizes forming the so-called Z-ring. Several regulatory systems intervene to correctly localize the Z-ring in the centre of the cell, and they divide into negative systems (that keep FtsZ polymers away from the poles and the nucleoid) and positive systems (that stimulate the polymerization at the right position). The proteins involved in these regulations differ among bacterial species (Monahan et al., 2014). Since FtsZ is a cytoplasmatic protein that is unable to interact with the membrane, other proteins mediate the link of the preformed Z-ring to the inner membrane. In *E. coli* this task is achieved by FtsA and ZipA (Rico, Krupka and Vicente, 2013), which are both essential for cytokinesis. Indeed, FtsA represents the second most conserved protein of the divisome (Haeusser and Margolin, 2016). In Gram-positive bacteria such as *B. subtilis*, SepF carries out the same function (Duman *et al.*, 2013).

The polymerization and the tethering of the Z-ring, also named proto-ring, represents only the first step of the formation of the divisome. Several second stage proteins intervene, such as FtsI which is responsible in *E. coli* for the synthesis of the peptidoglycan in the septum, or FtsB, FtsL and FtsQ, which functions have not been completely elucidated yet. Nevertheless, the coordinated action of the mature divisome in all its components allows the achieving of the daughter cells (Figure 5).

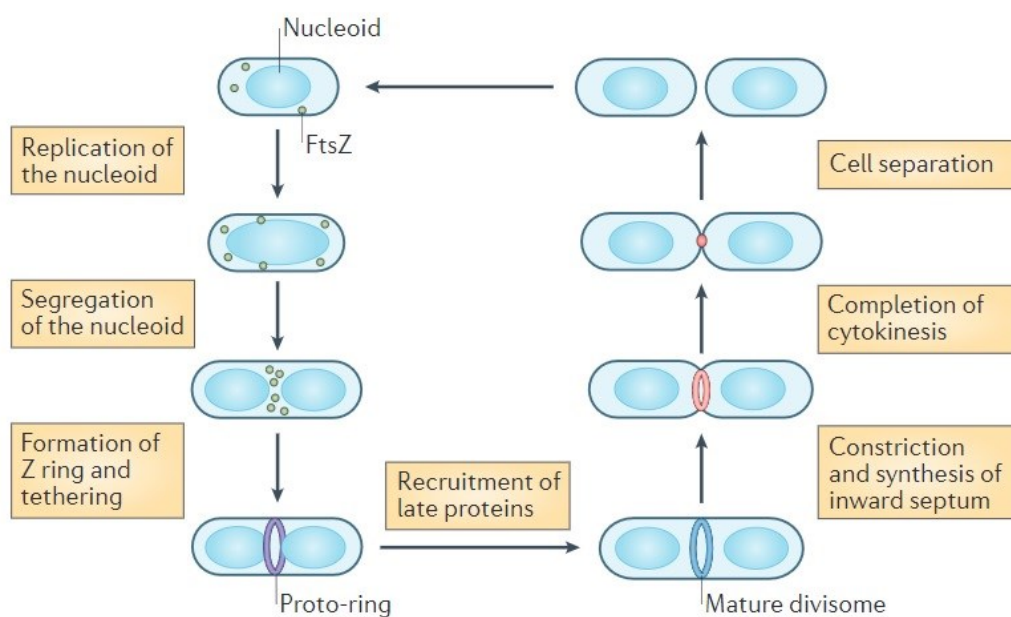


Figure 5: Bacterial cell division cycle: scheme adapted from Haeusser and Margolin, 2016.

When the process is complete, the GTPase activity possessed by FtsZ polymers promotes GTP hydrolysis, which is followed by FtsZ depolymerization. Thus, FtsZ is again freely present in the cytoplasm, able to repeat the cycle whenever necessary.

In addition to the centrality of the role of FtsZ in the bacterial binary fission, several other characteristics make this protein an interesting target for the antimicrobial therapy. Firstly, even if FtsZ represents the homologue of the human tubulin, their aminoacidic sequences significantly differ, with only a 20% of similarity (Nogales, Wolf and Downing, 1998). Moreover, FtsZ is highly conserved among bacteria and mycobacteria and possesses several essential protein partners. Given this, FtsZ inhibitors should represent potential broad-spectrum and low-cytotoxic antibiotics.

FtsZ structural and functional characteristics

Even if FtsZ is highly conserved among bacteria and mycobacteria, some structural differences can be identified. Nevertheless, all FtsZs can conceptually be divided into five regions, described starting from the N-terminal position of the protein (Casiraghi *et al.*, 2020; Levin and Janakiraman, 2021):

- **The N-terminal subunit**, characterized by variable length and poor structuration. The role of this subunit has not been completely elucidated yet.
- **The globular core**, which contains the GTP binding site and is generally highly conserved.
- **The C-terminal linker** that is usually scarcely conserved but its composition influences the polymers morphology and function *in vivo*.
- **The C-terminal peptide (also known as C-terminal tail)**, which is very important for several interactions that FtsZ achieve with other divisome proteins.
- **The C-terminal variable region (CTV)** able to influence lateral interactions between FtsZ protofilaments.

As anticipated before, in the globular core is contained the GTP binding site of FtsZ. Through GTP binding, FtsZ oligomers polymerize, bind FtsA, and progress in the division process. GTP hydrolysis is associated with polymers disassembling, allowing the cycle to be repeated (Erickson, 1997). This explains why the globular core of FtsZ is the most conserved site of the entire protein.

FtsZ inhibitors

Even if more and more insights are still being discovered about the bacterial cell division cycle physiology, the centrality of FtsZ has been widely demonstrated since the very first understandings of the process. This motivated the scientific community to investigate on FtsZ inhibitors and, in this ~25 years, several compounds have been discovered and studied. Today, FtsZ inhibitors can be classified basing on the nature (natural compounds vs synthetic), on the type (small molecules or peptides) or on the two binding sites. Indeed, almost all the known FtsZ inhibitors that are able to interfere with the protein bind in only two sites: the GTP binding site and the interdomain cleft (IDC) (Figure 6) (Casiraghi *et al.*, 2020).

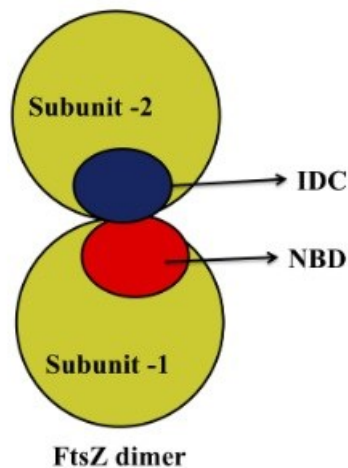


Figure 6: Localization of NBD (Nucleotide binding site) and IDC (Interdomain site) on FtsZ dimer – from Pradhan, Margolin and Beuria, 2021.

GTP binding site

The essentiality of the GTP binding site – also known as Nucleotide binding domain (NBD) (Pradhan, Margolin and Beuria, 2021) - coupled with the high conservation among several bacterial species moved the researchers to design inhibitors of FtsZ able to interfere with this important site within the protein. As anticipated before, the GTP binding site is held within the N-terminal domain and includes helices H1-H6 (plus the terminal part of H7), sheets S1-S6 and loops T1-T6. Each of these interact with different moieties of GTP (Löwe, 1998). Considering the similarities between the GTP binding sites of FtsZ and human tubulin, it is very likely that compounds able to bind and impede GTP binding in this position may exert cytotoxic action toward eukaryotic cells as well.

Nowadays, several FtsZ inhibitors able to interact with the NBD are known and they belong to different classes. For example, Pyrimidines (Figure 7) have been deeply investigated, achieving strong derivatives versus mainly Gram-positive bacteria, related with the inhibition of FtsZ. Indeed, these compounds proved to be bactericidal, by disrupting FtsZ and inhibiting the GTPase activity, inducing cell elongation (Fang, Li, *et al.*, 2019; Fang, Zheng, *et al.*, 2019).

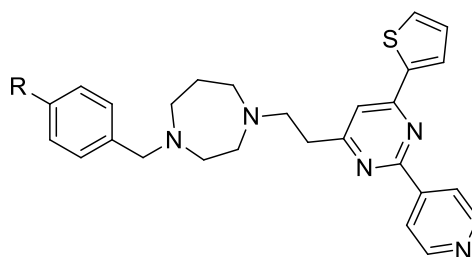


Figure 7: Structures of FtsZ pyrimidines inhibitors.

Other important compounds able to interfere with FtsZ function through the interaction with the GTP binding site are, logically, GTP analogues. BrGTP and MeOGTP (Figure 8) are the strongest derivatives, with a IC_{50} of 37 μ M and 10 μ M, respectively, versus FtsZ polymerization. Later, it was demonstrated that these compounds act by inducing polymerization while inhibiting GTPase activity, therefore impeding the normal functions of FtsZ (Casiraghi *et al.*, 2020).

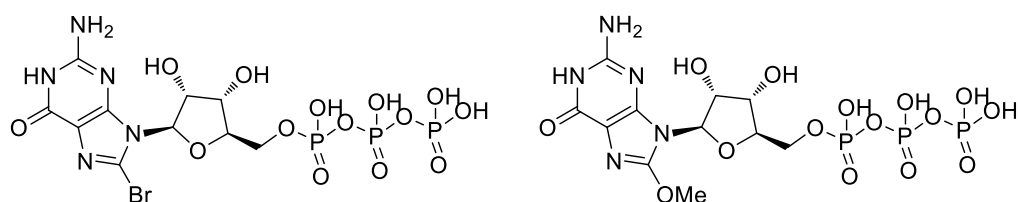


Figure 8: Structures of GTP analogues: BrGTP (left) and MeOGTP (right).

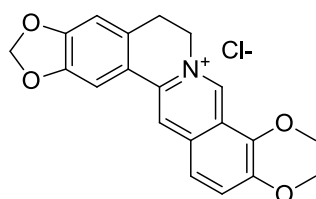
Pyrimidines and GTP analogues are two of the most studied classes of FtsZ inhibitors able to interact with the GTP binding site. Nevertheless, the worrying similarity between the GTP binding site of FtsZ and the one of human tubulin lowers the druggability of this site, making the second main inhibitor binding site of FtsZ, named Interdomain cleft (IDC), more taken in consideration during the development of potential drugs.

Interdomain cleft

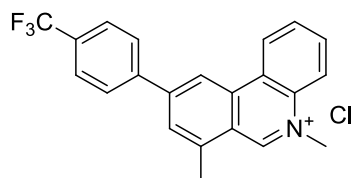
The C-terminal interdomain cleft, often simply referred as Interdomain site or Interdomain cleft, represents a better alternative for the development of antimicrobials acting on FtsZ.

Residues from the C-terminal β -sheet, T7 loop and H7 helix constitute this site (Sun *et al.*, 2014). Conversely to the NBD, the size and the aminoacidic sequence varies between different bacterial species, with a less degree of conservation in Gram-negative bacteria than Gram-positive bacteria. Overall, the IDC displays a less sequence conservation than the NBD.

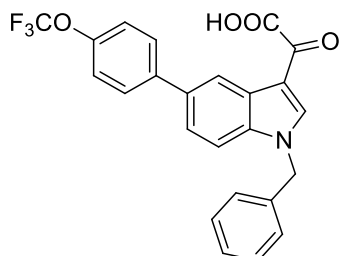
As introduced before, considering the similarity between FtsZ and α - β - tubulin, potential side effects on these systems must be always considered when designing FtsZ inhibitors. In analogy to FtsZ, tubulin polymers (known as microtubules) also possess allosteric inhibitor sites, where drugs like colchicine, vinblastine and taxane can bind and exert their activity (Lu *et al.*, 2012). Therefore, FtsZ inhibitors acting of the IDC could, hypothetically, exert off-target cytotoxic effects on mammalian cells. Nevertheless, since the IDC is quite different from chemotherapeutic drug sites on tubulin, only weak effects of FtsZ inhibitors on tubulins have been detected, with high differences in magnitude between the desired and the undesired activity (Pradhan, Margolin and Beuria, 2021). Thus, generally speaking, FtsZ inhibitors acting on the interdomain cleft rather than the NBD site are predicted to have a better toxicity profile with lower side effects on eukaryotic cells. This explains why the IDC site has been deeply studied and, nowadays, several inhibitors belonging to multiple structural classes are known. Among the high number of IDC-site related FtsZ inhibitors, the most studied are Berberine analogues, Phenanthridium derivatives, Indoles and 2,6-difluorobenzamides (Figure 9).



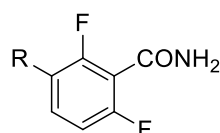
Berberine and derivatives



Phenanthridium derivatives



Indoles



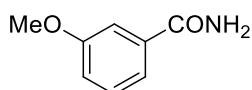
2,6-difluorobenzamides

Figure 9: Most known IDC-related FtsZ inhibitors.

Berberine analogues and Phenanthridium derivatives proved to be able to stabilize FtsZ polymers interfering with GTP hydrolysis (Sun *et al.*, 2014, 2017). Indoles strongly inhibit FtsZ, with effects that have been highly investigated through electron microscopy, polymerization assays and GTPase activity evaluation. The 2,6-difluorobenzamide class of FtsZ inhibitors deserve a special mention, and it will be deeply analysed in the following paragraph.

2,6-difluorobenzamides FtsZ inhibitors

2,6-difluorobenzamides represents the most studied class of compounds as FtsZ inhibitors. The interest of the scientific community on this chemical class was born with the discovery of the weak activity possessed by the 3-methoxybenzamide (3-MBA, Figure 10) on *Bacillus subtilis*, easily suppressed by the *brgA1* mutation on the *FtsZ* gene.



3-methoxybenzamide

Figure 10: Structure of 3-methoxybenzamide, the very first derivative of this class of inhibitors.

Incubation of *B. subtilis* with 10 mM 3-MBA resulted in filamentous cells, typical of a failed division (Ohashi *et al.*, 1999). The activity of 3-MBA coupled with the attractiveness of this scaffold (low molecular weight, high modifiability, good membrane permeability) made this compound an ideal starting point for rational antimicrobials design.

Stokes and collaborators, with the objective of increasing the activity while keeping the on-target effect on FtsZ pointed out the importance of fluorine atoms on positions 2 and 6, which led to an 8-fold increase of the activity. This noticeable improvement strongly underlined the importance of the fluorine atoms, which were therefore kept in all the subsequent derivatives.

In the same study, the homologation of the methoxy- up to 11 carbon atoms showed a further strong improvement of the activity, peaking at 0.125 $\mu\text{g}/\text{mL}$ vs *B. subtilis* and 0.5 $\mu\text{g}/\text{mL}$ vs *S. aureus* with the 2,6-difluoro-3-nonyloxybenzamide (DFNB, Figure 11) (Czaplewski *et al.*, 2009).

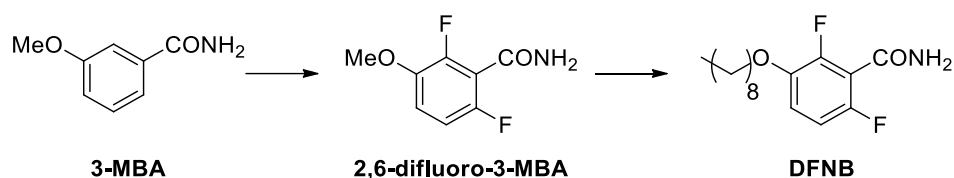


Figure 11: Structural improvements on the initial scaffold 3-MBA.

Shortly after, since 2,6-difluoro-3-nonyloxybenzamide possess several sub-optimal properties, a screening was performed to identify better benzamide derivatives. From more than 500 compounds, PC190723 arose as an even stronger anti-staphylococcal compound, with MICs that range from 0.5 to 1 $\mu\text{g}/\text{mL}$ versus both Methicillin-sensible and Methicillin-resistant *Staphylococcus aureus*, as well as clinically isolated multi-drug resistant *S. aureus*. Structurally, PC190723 is a thiazolopyridine linked to the benzamide by a methoxy linker (Figure 12) (Haydon *et al.*, 2008). The mechanism of action was deeply studied; PC190723 binds exclusively in the interdomain site of a specific conformation of FtsZ and stabilizes protofilaments, impeding the normal behaviour of FtsZ (Elsen *et al.*, 2012). PC190723 represented over the years the reference compound for FtsZ inhibitors, used as comparison for every derivative successively developed. Later, to improve the pharmacokinetic and biotechnological profiles of the molecule, both prodrugs and derivatives of PC190723 were designed and synthesized (Figure 12). Specifically, a trifluoromethyl moiety was introduced to block metabolization and the benzamide group was modified with a labile moiety to improve the poor solubility of the parent compound. TXY541 is indeed 143-times more soluble than PC190723 (Kaul *et al.*, 2013).

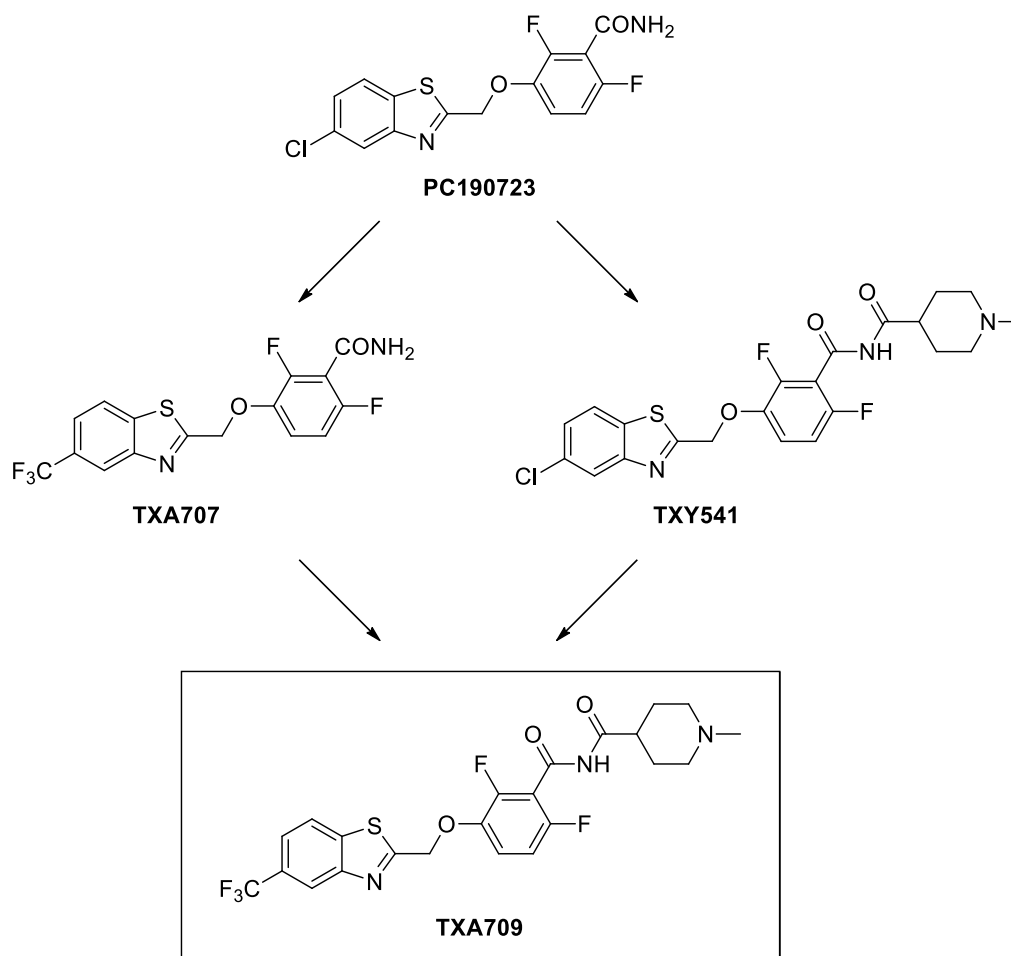


Figure 12: Chemical modifications to obtain PC190723 derivatives and prodrugs.

Over the years, PC190723 and its derivatives and prodrugs had demonstrated the ability to treat Staphylococcal infections *in vivo* throughout the inhibition of FtsZ and, currently, TXA709 and TXA707 are evaluated in clinical trials, alone or in association with other antimicrobials (TAXIS pharmaceuticals, inc., 2022) (Figure 12).

In the following years, several research groups focused on the development of novel 2,6-difluorobenzamides, mainly substituting the thiazolopyridine moiety of PC190723 with different substituted heterocycles. The very same group of Haydon, Stokes and collaborators developed a new class of FtsZ inhibitors, in which the PC190723 moiety was replaced by a substituted phenyl-bromo-oxazole, without modifying the pharmacophoric benzamide (Stokes *et al.*, 2013). Moreover, contextually, the methylene linker was substituted with a hydroxymethyl group (Figure 13).

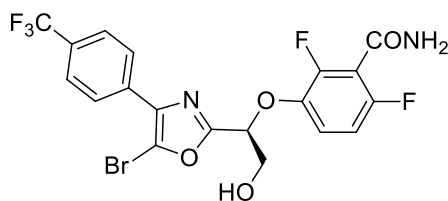


Figure 13: Lead compound of the phenyl-bromo-oxazole FtsZ inhibitors.

This compound displayed 4 to 32 times fold stronger activity than PC190723 towards *S. aureus* strains and, similarly to PC190723, complete inactivity vs Gram-negative bacteria. Also in this case, the activity exerted was linked to the inhibition of FtsZ, as demonstrated by microscopy assays, and the *in vivo* efficacy was demonstrated (Stokes *et al.*, 2013). In analogy to PC190723, a prodrug was designed to increase the solubility and enable *in vivo* assays at elevated concentrations.

In addition to this new chemical class, over the years, several benzamides were designed and developed: the isoxazole benzamides (Bi *et al.*, 2018), the 1,3,4-oxadiazol-2-one benzamides (Bi *et al.*, 2019), 3-aminobenzamides (Lui *et al.*, 2019) and much more.

The research group in which the present work was carried out started the evaluation and development of a novel class of FtsZ benzamide inhibitors: the benzodioxane-benzamides. Starting from the structure of PC190723, the thiazolopyridine moiety was replaced by a 1,4-benzodioxane ring, substituted in 2- position on the dioxane portion with the methoxy-2,6-difluorobenzamide.

The 1,4-benzodioxane scaffold was particularly appealing for bearing the pharmacophoric moiety since is widely known and applied in medicinal chemistry. The synthesis is well established, as well as the possible resolution of the stereocentre (which results from the substitution of this scaffold in position 2- or 3- of the dioxane moiety) and the toxicity profile is known. Indeed, the 1,4-benzodioxane moiety is encountered in many marketed drugs (Bolchi *et al.*, 2020).

The above-mentioned substitution led to Compound 1 (Figure 14), which represented the first compound for this chemical class of FtsZ inhibitors.

the same time, all the benzodioxane-benzamides evaluated in this phase showed no to little effects on human MRC-5 cells (Chiodini *et al.*, 2015). Starting from these initial findings, they started an in-depth study of the SAR of this class of compounds, mainly focused on three directions.

The structure of **1** was modified evaluating (Figure 16):

- The influence of a variety of substituents in positions 6- and 7- of the benzodioxane ring, preferring 7- position as suggested by the data obtained from compounds **2** and **3** (Series A).
- The effects on the replacement of the oxygens with nitrogen or carbon atoms (Series B).
- The effect on the activity when the position of the dioxane portion was changed or the benzodioxane ring opened (Series C).

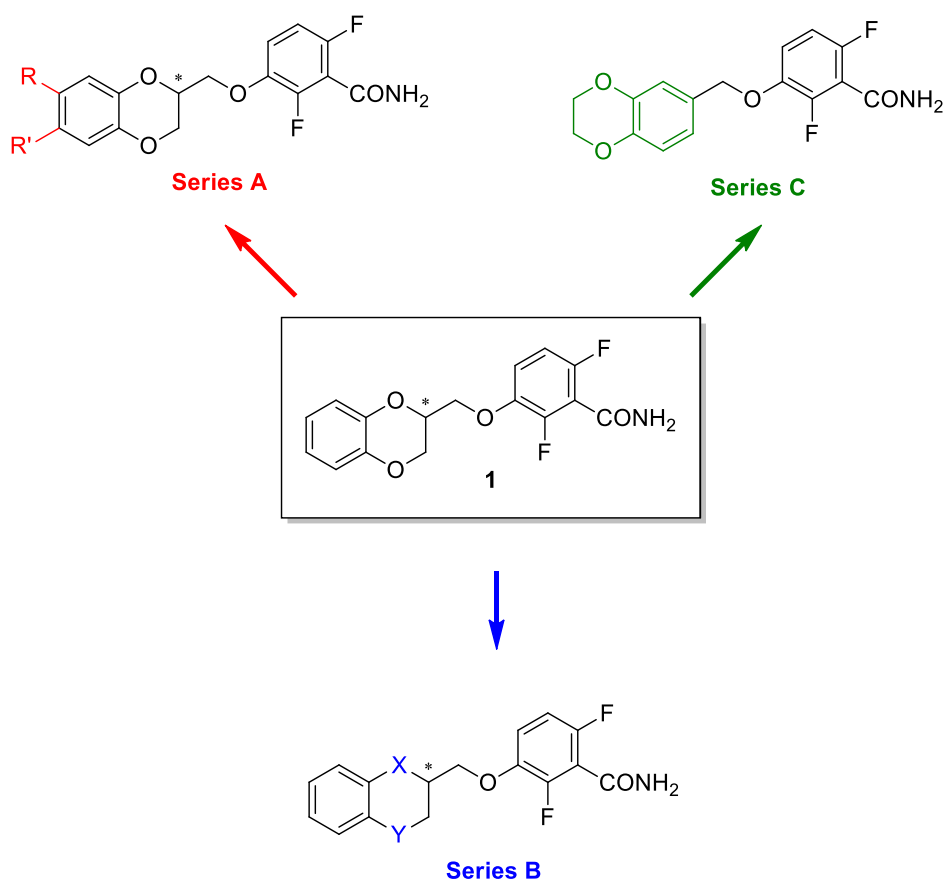
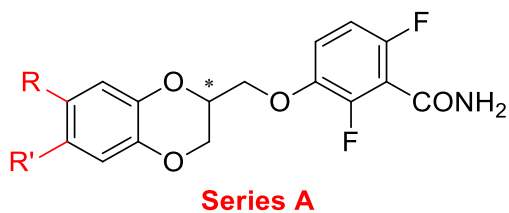


Figure 16: First in-depth evaluation of the SAR of the benzodioxane-benzamides.

Within this study, 26 derivatives of the series A, 7 derivatives of the series B and 2 derivatives of the series C were designed, synthesized, purified, and biologically evaluated

on both Methicillin-sensitive *S. aureus* (MSSA) and Methicillin-resistant *S. aureus* (MRSA), as well as on ESBL-*E. coli* (Straniero *et al.*, 2016, 2017).



Compound	R	R'	MIC vs <i>S. Aureus</i> ($\mu\text{g/mL}$)	TD ₉₀ vs MRC-5
4	Cl	Cl	2.5	<i>n.d.</i>
5	Br	H	0.625	>800
6	I	H	0.313	>800
7	F	H	2.5	<i>n.d.</i>
8	-C \equiv CH	H	0.313	400
9	-CH=CH ₂	H	0.625	>800
10	NO ₂	H	1.25	<i>n.d.</i>
11	NH ₂	H	100	<i>n.d.</i>
12	CF ₃	H	2.5	<i>n.d.</i>
13	NHSO ₂ CH ₃	H	>100	<i>n.d.</i>
14	CN	H	1.25	<i>n.d.</i>
15	COOCH ₃	H	0.625	>1280
16	CONH ₂	H	>100	<i>n.d.</i>
17	CONH- <i>n</i> -Bu	H	>100	<i>n.d.</i>
18	COOEt	H	0.6	>800
19	H	COOEt	5	>800
20	COO <i>i</i> Pr	H	5	>800
21	COOPh	H	5	>800
22	CH ₂ OCH ₃	H	5	400
23	COCH ₂ CH ₃	H	2.5	>800
24	CHO	H	5	400
25		H	100	<i>n.d.</i>

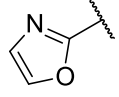
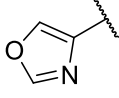
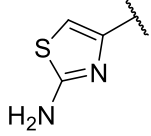
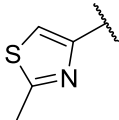
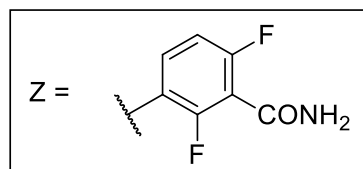
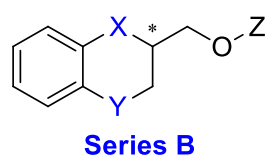
26		H	>100	<i>n.d.</i>
27		H	10	<i>n.d.</i>
28		H	>100	<i>n.d.</i>
29		H	10	<i>n.d.</i>

Table 1: Activity of benzodioxane-benzamides derivative **4-29**.

Inside the Series **A** (Table 1), all the stronger antimicrobial derivatives resulted to show substitution in 7- position, confirming the initial hypothesis of compound **2** and compound **3**. Regarding the nature of the substituents, 7- Br (**5**), 7-I (**6**), 7-C≡CH (**8**), 7-CH=CH₂ (**9**), and 7-COOMe (**15**) resulted to be active vs both MRSA and MSSA with activities below 1 µg/mL while retaining the activity on FtsZ, as showed by the evaluation of the morphological changes following incubation with the putative inhibitors (Straniero *et al.*, 2016, 2017). Surprisingly, conversely to PC190723 and derivatives, the metabolically stable CF₃ group insertion resulted in a slight loss of activity. As demonstrated from the biological data of this first series of compounds, polar or ionizable groups in position 7- of the 1,4-benzodioxane moiety seem to lead to the complete loss of activity, as for compounds **11**, **13**, **16**, **17** and **28**. Conversely, halogens and ester groups promote an increase of the activity. In particular, several kinds of esters, such as Ethyl, *i*-propyl and Phenyl, seem to be equally tolerated by the binding cleft.

None of these compounds resulted to be particularly toxic for human cells, although 7-C≡CH (**8**) displayed a higher toxicity compared to the others.

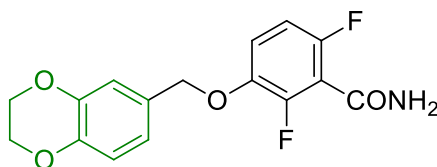
Conversely to these positive results, all the derivatives from series **B** (Table 2), in which the 1,4-benzodioxane moiety was modified, showed a worsening in the activity. In particular, the oxygen in position 1 resulted to be important for the retaining of the activity, whereas not so essential seemed to be oxygen in 4- position. Indeed, only compound **30** possess a weak antimicrobial activity.



Compound	X	Y	MIC vs <i>S. Aureus</i> ($\mu\text{g/mL}$)
30	O	CH ₂	5
31	CH ₂	O	100
32	CH ₂	CH ₂	>100
33	O	NMe	100
34	NMe	O	100
35	NMe	NMe	>100
36	N	N	100

Table 2: Activity of benzodioxane-benzamides compounds **30-36**.

Lastly, the derivatives from series **C** (Table 3), in which drastic modifications on the 1,4-benzodioxane scaffold were applied, show again a complete loss of activity. This strongly underlines the importance of the benzodioxane moiety, appropriately positioned, for the antimicrobial activity.



Series C

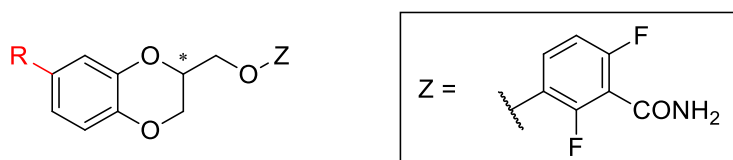
Compound	Structure	MIC vs <i>S. Aureus</i> ($\mu\text{g/mL}$)
37		100
38		>100

Table 3: Activity of compounds **37-38**.

At the end of this initial evaluation, all the tested compounds demonstrated a common range of activities on both MSSA and MRSA, confirming the viability of FtsZ as a new target for antimicrobial therapy to overcome the current mechanisms of resistance. Similarly to PC190723 and derivatives, also the benzodioxane-benzamides FtsZ inhibitors display no activity on *E. coli* strains (Chiodini *et al.*, 2015; Straniero *et al.*, 2016, 2017).

As anticipated before, the strong activity improvement achieved with lipophilic residues on position 7- of the 1,4-benzodioxane ring suggests how this lipophilic nature should be maintained to obtain a strong antimicrobial activity. Nevertheless, all the strongest abovementioned compounds (7-Br, 7-I, 7-CH=CH₂, 7-COOMe, etc.) are characterized by a low stability *in vivo* due to the nature of the substituent, making their development as potential antimicrobial drugs impossible.

For this reason, the research group focused on the development of a second series of compounds, in which the ester moiety of compound **15** was replaced by several ester bioisosters such as tetrazole, 1,2,4-oxadiazole, 5-methylthio-1,2,4-oxadiazole etc. (Straniero, Sebastián-Pérez, *et al.*, 2020) (Table 4). In the same study, the corresponding carboxylic acid bioisoster was included, to confirm the hypothesis of the negative contribution of polar groups in position 7. Thus, also the unsubstituted tetrazole and oxadiazoles were synthesized and evaluated.



Compound	Structure
39	
40	
41	

42	
43	
44	
45	
46	
47	
48	
49	

Table 4: Structures of compounds **39-49**.

Compounds **39-49** were tested on both MSSA and MRSA, as well as versus wt-*E. coli* to evaluate the influence of these modifications on the antimicrobial activity. Moreover, the toxicity of these derivatives was evaluated on human MRC-5 cells. Using the ratio between the toxicity and the antimicrobial activity, the therapeutic index was also calculated. The results are listed in Table 5, compared to the reference compound **15**, the 7-ester derivative.

Cpd	MSSA ATCC 29213			MRSA ATCC 43300			MRC-5
	MIC (µg/mL)	MBC (µg/mL)	MIC/MBC	MIC (µg/mL)	MBC (µg/mL)	MIC/MBC	MIC (µg/mL)
15	0.625	0.625	1	<i>n.d.</i>	<i>n.d.</i>	/	>800
39	>100	>100	/	>100	>100	/	/
40	>100	>100	/	>100	>100	/	/
41	80	100	/	80	100	/	/
42	2.5	2.5	36	2.5	2.5	36	90
43	>100	>100	/	>100	>100	/	/
44	>100	>100	/	>100	>100	/	/
45	>100	>100	/	>100	>100	/	/
46	>100	>100	/	>100	>100	/	/
47	0.6	0.6	1184	0.6	0.6	1184	740
48	2.5	2.5	>320	2.5	2.5	>320	>800
49	2.5	2.5	>320	2.5	2.5	>320	>800

Table 5: Antimicrobial activities and human cell toxicities of derivatives **39-49**.

The inactivity of compounds **39**, **41**, **44** and **46** confirms how the substitution in 7-position with polar groups is completely detrimental for the antimicrobial activity. At the same time, the higher activity of **42**, **47**, **48** and **49** when compared to the activities of **43** and **45** seems to underline how the linear structures of the 3-methyltetrazole or 5-methylthio-1,2,4-oxadiazole are significantly preferred over branched substitutions such as the 2-methyltetrazole or the *N*-methyl-1,2,4-oxadiazol-3-one ring.

At the end of this second evaluation, compound **47** demonstrated to be as strong as **15** versus both MSSA and MRSA, while possessing low toxicity on human cells. At the same time, the 5-methylthio-1,2,4-oxadiazole ring is characterized by a significantly higher stability in physiological hydrophilic environment if compared to the ester moiety of compound **15**, easily hydrolysable *in vivo* (Straniero, Sebastián-Pérez, *et al.*, 2020). For all the active compounds, FtsZ was validated as the target responsible of the antimicrobial

activity (Straniero, Sebastián-Pérez, *et al.*, 2020). Also in this case, all compounds **39-49** present complete inactivity versus wild type-*E. coli*.

All the work performed by Straniero and co-workers deeply improved the understanding behind the activity of benzodioxane-benzamides as FtsZ inhibitors, investigating the SAR of this important class of promising tools to fight back the antimicrobial resistance phenomenon.

CHAPTER 3 – BACTERIAL RNA PROCESSING AND DEGRADATION: RnpA

Staphylococcus Aureus post-transcriptional regulation

Staphylococcus Aureus, which belongs to the ESKAPE classification, is one of the most important germs from a clinical point of view. *S. aureus* colonizes the nasopharynx of 20-30% of human beings without consequences. Nevertheless, in specific conditions such as weakness of the immune system of the host, this bacterium can lead to severe pathologies (le Scornet and Redder, 2019). Especially due to the capability of *S. aureus* to exploit weaknesses of the host, this bacterium easily spreads in healthcare facilities, with ~330000 estimated cases of Methicillin-resistant *S. aureus* infections in hospitalized patients in 2017 only, which led to ~10000 estimated deaths (Centre for Disease Control and Prevention, 2019).

Unlike other bacterial species, *S. aureus* does not rely on several sigma factors to regulate expression, it rather exploits post-transcriptional expression tuning through a variety of pathways (le Scornet and Redder, 2019). Indeed, physiologically, the ability of causing infections of *S. aureus* strongly depends on the different expression of virulence factors in stationary or in exponential growth phase.

In the last decade, Olson and collaborators, demonstrated the importance of the RNase P protein component, named RnpA which is responsible of both mRNA degradation and tRNA processing (Patrick D Olson *et al.*, 2011).

After this assessment, the importance and the essentiality of RnpA in governing the expression of bacterial virulence factors, thus allowing the change from a less aggressive phenotype to a pathogenic one and vice versa, made this protein a valuable target for the development of anti-staphylococcal compounds.

Mechanisms of regulation

As anticipated before, *S. aureus* strongly relies on post-transcriptional regulation to modify gene expression, especially of virulence factors that are proteins able to promote growth and viability of the bacterium within the host. Generally, post-transcriptional regulation

involves RNA decay, processing and maturation and the mechanisms of virulence factors post-transcriptional regulation can be conceptually classified in two classes (Figure 17):

- RNA-RNA interaction-based RNA repression or activation.
- Protein-based RNA repression or activation.

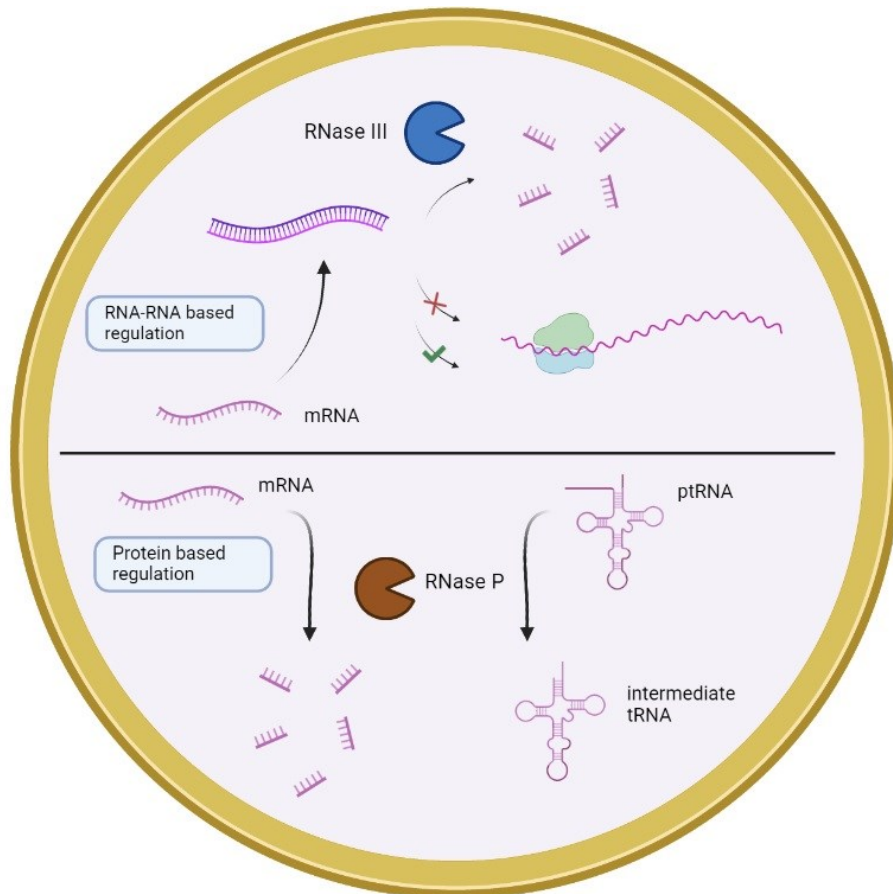


Figure 17: Mechanisms of post-transcriptional gene expression regulation: RNA-RNA interaction based, and Protein based regulation.

Within the first class, several small non-coding RNAs have been identified and characterized in *S. aureus*. For example, one of the most studied *S. aureus* RNA molecules able to govern virulence is RNAIII. RNAIII is a multifunctional small RNA molecule able to interact with SA1000 mRNA, which encodes for the fibrinogen-binding surface protein. This interaction completely inhibits ribosome binding and, consequently, the translation of the corresponding virulence factor (Liang *et al.*, 2006). Moreover, the double stranded RNA resulting from the interaction of RNAIII and SA1000 is attacked by RNase III, responsible for its degradation. Similarly, RNAIII is also able to bind *coa* mRNA, controlling its expression. In addition to the repressing, RNAIII can also activate mRNA through the formation of a duplex that permits translation (le Scornet and Redder, 2019). Subsequently to the

discovery of RNAlII and its roles, several other regulatory small RNAs were discovered in *S. aureus*, further underlying the importance of this mechanism of gene expression in this particular species.

Regarding the second class, it is known that the activity of various ribonucleases (RNases) is important in several bacterial species to control RNA turnover throughout bulk mRNA degradation and precursor tRNA maturation (Newman *et al.*, 2012). Nevertheless, the totality of the proteins involved into protein-based RNA repression or activation in bacteria can significantly differ in quality and function among bacterial species. For example, in *E. coli*, the essential ribonuclease (RNase) is RNase E, while in *B. subtilis* RNase J1, J2 and Y are the main actors (Newman *et al.*, 2012).

Within *S. aureus*, RNase Y was demonstrated to act differently compared to *B. subtilis*. In particular, RNase Y acts as an important degradosome protein for bulk mRNA degradation during mRNA turnover, while in *S. aureus* it was demonstrated to act as an activator of virulence gene expression at the promoter level and stabilizing the immature transcripts at different levels (Marincola *et al.*, 2012). Another example of important RNase in *S. aureus* is RNase III that, as aforementioned, is able to catalyse dsRNA degradation. Therefore, the main proteins involved in bulk mRNA degradation of *S. aureus* were not known yet.

***S. aureus* RNA decay, processing and maturation machinery: RnpA**

Discovery of S. aureus decay machinery

As anticipated before, most of the scientific community knowledge on RNA decay machineries relies on *E. coli*, which degrade RNA through a holoenzyme complex comprising RNase E (the ribonuclease), RNA helicase, enolase and PNPase A. Given the importance of RNase E in directly catalyse the bulk mRNA decay process, looking for RNase E orthologs in clinically significant bacteria, such as *S. aureus*, could represent the first step to start the target-based drug discovery process.

Nonetheless, *S. aureus* lacks a RNase E ortholog and, consequently, the RNA degradation machinery of this bacterium was less understood (Patrick D Olson *et al.*, 2011).

Presumably, also in *S. aureus*, the protein members of the organism's RNA degradation machinery had to be involved in the turnover of mRNA that governs the different expression of virulence factors in the exponential growth phase compared to the stationary

one. Thus, observing genes repressed during the stationary phase, it was noticed that the gene *rnpA* was less expressed. This gene codes for a component of the RNase P, named RnpA.

RnpA; the component of RNase P

RnpA (Figure 18) is a 14 kDa protein (Ha *et al.*, 2018) that possesses at least two physiological roles:

- RnpA is part of a ribonucleoprotein complex composed by the protein and *rnpB*, a single RNA molecule. This complex is able to catalyse the removal of the 5' leader sequence, promoting tRNA maturation.
- Moreover, RnpA alone, in complex with *rnpB* or with other elements, contributes to mRNA bulk degradation (Patrick D Olson *et al.*, 2011).



Figure 18: Structure of RnpA (PDB: 6D1R).

As a confirmation of the essentiality of this protein, by using an antisense mRNA technique, it was proved that the proliferation of *S. aureus* was significantly limited when RnpA was repressed.

These important insights on RnpA, demonstrated by Olson and colleagues in the same study of 2011, set the biological bases to start thinking of RnpA as a biological target for the drug discovery process.

At the same time, several information regarding the physiology of RnpA that are usually exploited while developing inhibitors are still lacking. It is known that within RNase P, RnpA

promotes the interaction within *rnpb* and its substrate, but how this occurs, and which is the site of the protein responsible for the effect is still unknown.

Despite the poor knowledge on this protein, given the essentiality of RnpA in modulating the virulence factors expression in *S. aureus* and the significant aminoacidic difference from human homologues, RnpA inhibitors can still potentially represent a novel class of anti-staphylococcal drugs with low toxicity for eukaryotic cells. This class would represent an important additional tool to fight *S. aureus* nosocomial infections, already identified as a present serious clinical problem.

RnpA inhibitors

RnpA, alone or as a component of complexes, participates in bulk mRNA degradation and in ptRNA maturation, regulating the expression of *S. aureus* virulence factors. Moreover, RnpA is well conserved among Gram-positive bacteria but significantly differs from mammalian homologues. All these data suggest that RnpA inhibitors could indeed represent a viable tool as anti-staphylococcal compounds, characterized by low toxicity. Therefore, after the discovery of the protein and of its role, four main classes of RnpA inhibitors were identified, mainly by screening commercial libraries of compounds (Patrick D. Olson *et al.*, 2011; Lounsbury *et al.*, 2018; Colquhoun *et al.*, 2019).

RNPA1000

The very first derivative able to express an antimicrobial activity through the inhibition of RnpA was **RNPA1000** (Figure 19), discovered shortly after the essentiality of the protein.

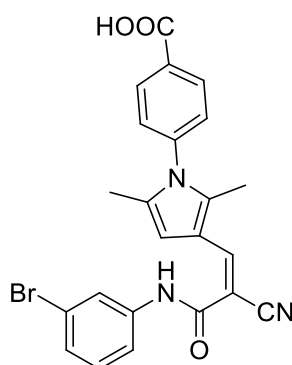


Figure 19: Structure of **RNPA1000**, the very first RnpA inhibitor.

In the first screening, this compound showed the ability to inhibit *in vitro* RnpA-mediated RNA degradation, without interacting with *E. coli* RNases or *S. aureus* RNase J1, which could

suggest a partial specificity for RnpA. Moreover, this compound showed moderate *in vitro* antimicrobial activity versus completely sensitive *S. aureus* strains, Methicillin- and Vancomycin resistant strains (with MICs ranging from 16 to 32 $\mu\text{g}/\text{mL}$) and towards other bacteria such as *Staphylococcus epidermidis*, *Streptococcus pneumoniae*, *Streptococcus pyogenes*, *Streptococcus agalactiae*, with bacteriostatic effect. The activities on these germs could be related to the aminoacidic similarity between *S. aureus* RnpA and RnpAs of these species. 24h exposure of human HepG2 cells to **RNPA1000** did not elicit toxicity at any concentration, while 48 hours exposure led to mild toxicity.

Subsequently to this initial *in vitro* characterization, **RNPA1000** was tested *in vivo*, on mouse infection model, in which the animal was inoculated with wild type *S. aureus* in the intraperitoneal cavity. This injection resulted in 100% death within 4 hours, while RNPA1000 showed an outstanding dose-dependent protection.

Nevertheless, the cytotoxicity on Hep2G cells of **RNPA1000** excluded its direct use as medication (Patrick D Olson *et al.*, 2011), as well as the further development of the class.

RNPA2000

Parallely to **RNPA1000**, a second important compound, **RNPA2000** (Figure 20), was discovered in the same screening in which derivatives able to reduce RnpA-mediated RNA degrading activity were evaluated.

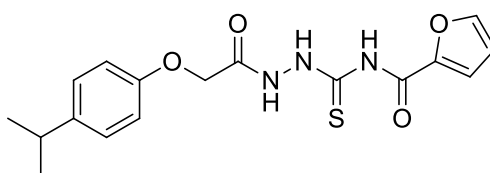


Figure 20: Structure of **RNPA2000**.

Conversely to **RNPA1000**, this compound showed bactericidal effect, with MICs towards several *S. aureus* strains ranging from 8 to 16 $\mu\text{g}/\text{mL}$. To evaluate whether the target of **RNPA2000** was indeed RnpA, its capability to interfere with both the RnpA-mediated cellular function: bulk mRNA degradation and ptRNA maturation.

For the first process, an *in vitro* gel-based RNA degradation assay was performed (Figure 21): **RNPA2000** was found to be able to mildly inhibit *spa* RNA degradation with apparent

IC₅₀ of 125 μM, displaying specificity towards RnpA, since no interaction with *E. coli* RNase III or *S. aureus* RNase J1 or J2 was observed.

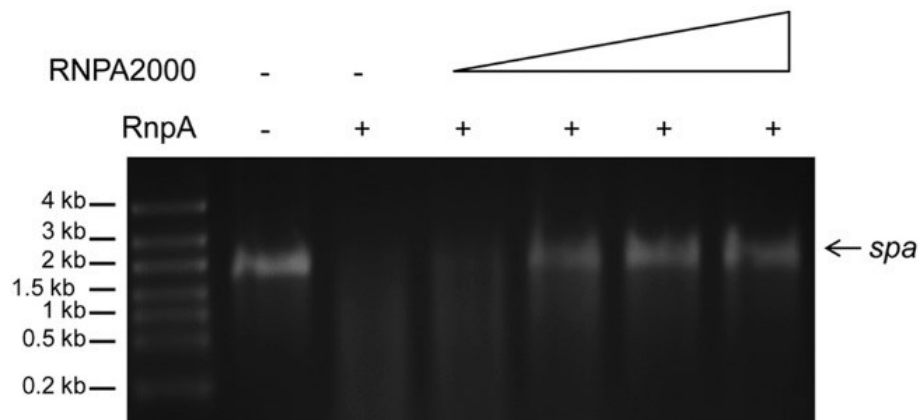


Figure 21: **RNPA2000** *in vitro* mRNA degradation assay: as shown in figure, increasing concentrations of **RNPA2000** gradually reduce RnpA-mediated *spa* RNA degradation. Image adapted from Eidem et al., 2015.

In addition to the participation in bulk mRNA degradation, as aforementioned, RnpA is a part of RNase P, which catalyse the removal of the 5' leader sequences from precursor tRNA, promoting tRNA maturation. Thus, **RNPA2000** was also tested *in vitro* to evaluate its capability to interact with this second physiological function of RnpA (Figure 22).

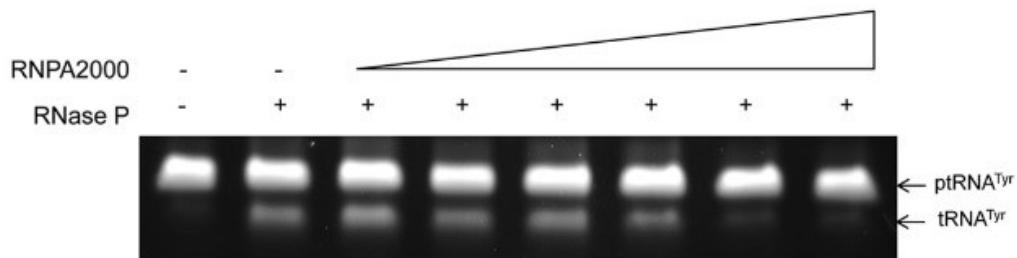


Figure 22: **RNPA2000** *in vitro* ptRNA degradation assay: Also in this case, increasing concentration of **RNPA2000** reduce ptRNA maturation. Image adapted from Eidem et al., 2015.

As clearly observable in Figure 22, when **RNPA2000** is incubated with the protein, ptRNA^{tyr} accumulates, with no conversion to mature tRNA observed, exactly as in absence of RNase P. This result shows that **RNPA2000** can inhibit also this second RnpA-mediated process, with a IC₅₀ of 130 μM.

These first *in vitro* evaluations raised the odds that RnpA-mediated processes were indeed the targets of **RNPA2000** and were, therefore, correlated with the antimicrobial activity of the compound. Nevertheless, the *in vitro* conditions of these assays significantly differ from

the complicate *S. aureus* cellular environment. Consequently, the evaluation of the same abilities in cellular assays was designed and carried out to strengthen the hypothesis of RnpA being the target of **RNPA2000**.

In a first cellular assay, RnpA-depleted cells (produced through antisense RNA fragment expression) showed hypersusceptibility to **RNPA2000**, while other antibiotics such as vancomycin, mupirocin, rifampin etc. did not exhibit increased activity. This further underlying how RnpA seem to represent the target of **RNPA2000**.

In parallel, microarrays have been used to evaluate mRNA degradation properties of a cellular line, in presence or absence of xenobiotics. Briefly, *de novo* transcripts synthesis is arrested in control cells and 0.5XMIC **RNPA2000**-30 minutes-treated cells and mRNA is quantified as specific time points, to measure the degradation properties. Again, **RNPA2000** treated cells showed a reduce degradation profile compared to the control, demonstrating how **RNPA2000** is also able to interfere with this process within the cell.

Lastly, the cellular evaluation of ptRNA maturation levels in presence of **RNPA2000** was carried out, to understand if this second RnpA-mediated process, already demonstrated to be affected by the compound *in vitro*, maintained its susceptibility in cellular assays. Also in this case, a Northern blot-based assay demonstrated how **RNPA2000**-treated cell showed a 160-fold concentration of polycistronic tRNA compared to the control. This accumulation seems to be correlated with the inhibition of the maturation catalytic activity of RNase P.

All these data underlined how **RNPA2000** is a strong inhibitor of RnpA, with good antimicrobial activity. This compound can represent a better starting point compared to **RNPA1000**, as shown by its capability to interfere with both RnpA-mediated cellular processes and serve as an initial point to guide the research on this promising family of potential antibiotics (Eidem *et al.*, 2015).

Nevertheless, several structural characteristics of **RNPA2000**, such as the 2-furanyl moiety and the thiosemicarbazide are suboptimal due to their known toxicity.

The last discovered classes: Phenylcarbamoyl cyclic thiophenes and Piperidine carboxamides

During the characterization of **RNPA2000**, Eidem and collaborators developed a mupirocin-synergistic assay to analyse RnpA inhibitors. This assay is based on the principle that agents able to inhibit two steps of the same biological process show a synergistic effect. RnpA, as component of RNase P, catalyse the progressing of polycistronic and precursor tRNA to mature tRNA that is immediately processed by the tRNA synthetases. Since Mupirocin shows antimicrobial activity through the inhibition of tRNA synthetases, RnpA inhibitors are expected to show a synergistic effect with this drug, improving its potency. **RNPA2000** proved a fractional inhibitory concentration (FIC) of 0.44, showing indeed the anticipated cooperative effect, where no significant synergisms were observed among **RNPA2000** and other known antibiotics (vancomycin, daptomycin etc.) (Eidem *et al.*, 2015).

After this evaluation, the mupirocin-synergistic assay was used to screen a 53000 small-molecule library with the goal to identify new chemical classes as RnpA inhibitors (Colquhoun *et al.*, 2019). Among all the evaluated compounds, 67 compounds were able to inhibit bacterial growth in presence of mupirocin. Nevertheless, when their capability of interfere *in vitro* with ptRTA maturation were assessed, to validate RnpA as target, only twelve showed this ability with IC₅₀ values below 250 µM.

Among these twelve compounds, seven had no significant effect on bulk mRNA degradation and two were highly toxic. The remaining compounds, **JC1**, **JC2** and **JR1**, characterized by good IC_{50s} versus both the RnpA-mediated processes and by low toxicity, were structurally classifiable in two chemical classes: Phenylcarbamoyl cyclic thiophenes and Piperidine carboxamides (Figure 23).

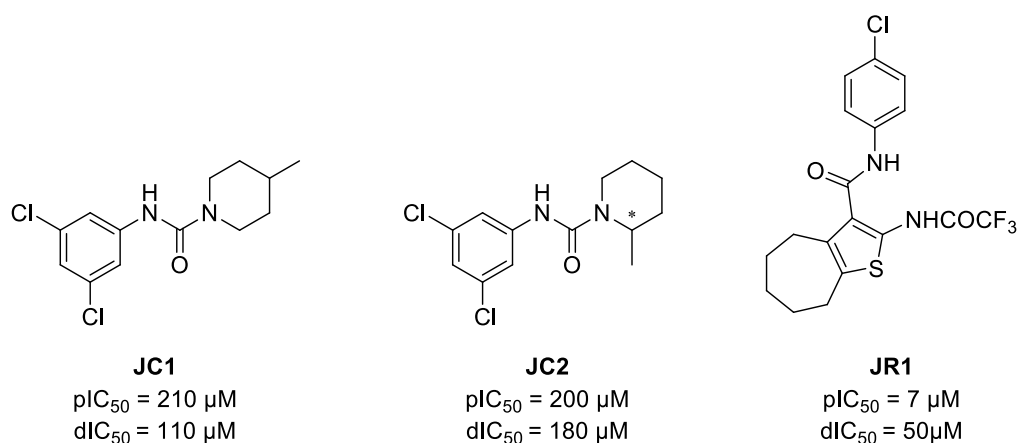


Figure 23: Structures of **JC1**, **JC2** and **JR1**, lead compounds of piperidine carboxamides and phenylcarbamoyl cyclic thiophenes. pIC₅₀=processing IC₅₀; dIC₅₀=degradation IC₅₀.

Given the promising activities of these three derivatives, phenylcarbamoyl cyclic thiophenes and piperidine carboxamides could represent two novel classes of inhibitors of RnpA able to overcome the limitations of **RNPA1000** and **RNPA2000** (Colquhoun *et al.*, 2019).

Structure-activity evaluation of the novel classes of RnpA inhibitors

In order to better understand the structural determinants of these molecules' ability to interact with RnpA, ten compounds belonging to the phenylcarbamoyl cyclic thiophenes class and twenty-one belonging to the piperidine carboxamides class were purchased and tested in the same assays, to evaluate their capability to interact with both RnpA-mediated processes and to assess their toxicity. These evaluations allowed to start the exploration of the structure-activity relationship (SAR) of these classes of compounds.

The structural modifications of **JR1** (Figure 24) were mainly focused on the aromatic group of the amide portion, with a few exceptions. As we can see, variations on this portion are generally well tolerated in terms of antimicrobial activity, even if the capability to interfere with mRNA degradation drastically drops when the 4-Cl is substituted by a methoxy group (**JR6**, dIC₅₀ > 250 μM). Surprisingly, the 2-Cl derivative maintains its activity when the cycloheptyl ring is untouched but presents complete inactivity when the cycloheptyl is reduced to a cyclohexyl (**JR2** vs **JR2b**). Conversely, the 3-Cl derivative shows good antimicrobial activity and RnpA-inhibition profile in both cases (**JR3** vs **JR3b**). Lastly, every change in the trifluoroacetamide moiety led to a complete loss of the activity (**JR1b**, **JR1c**).

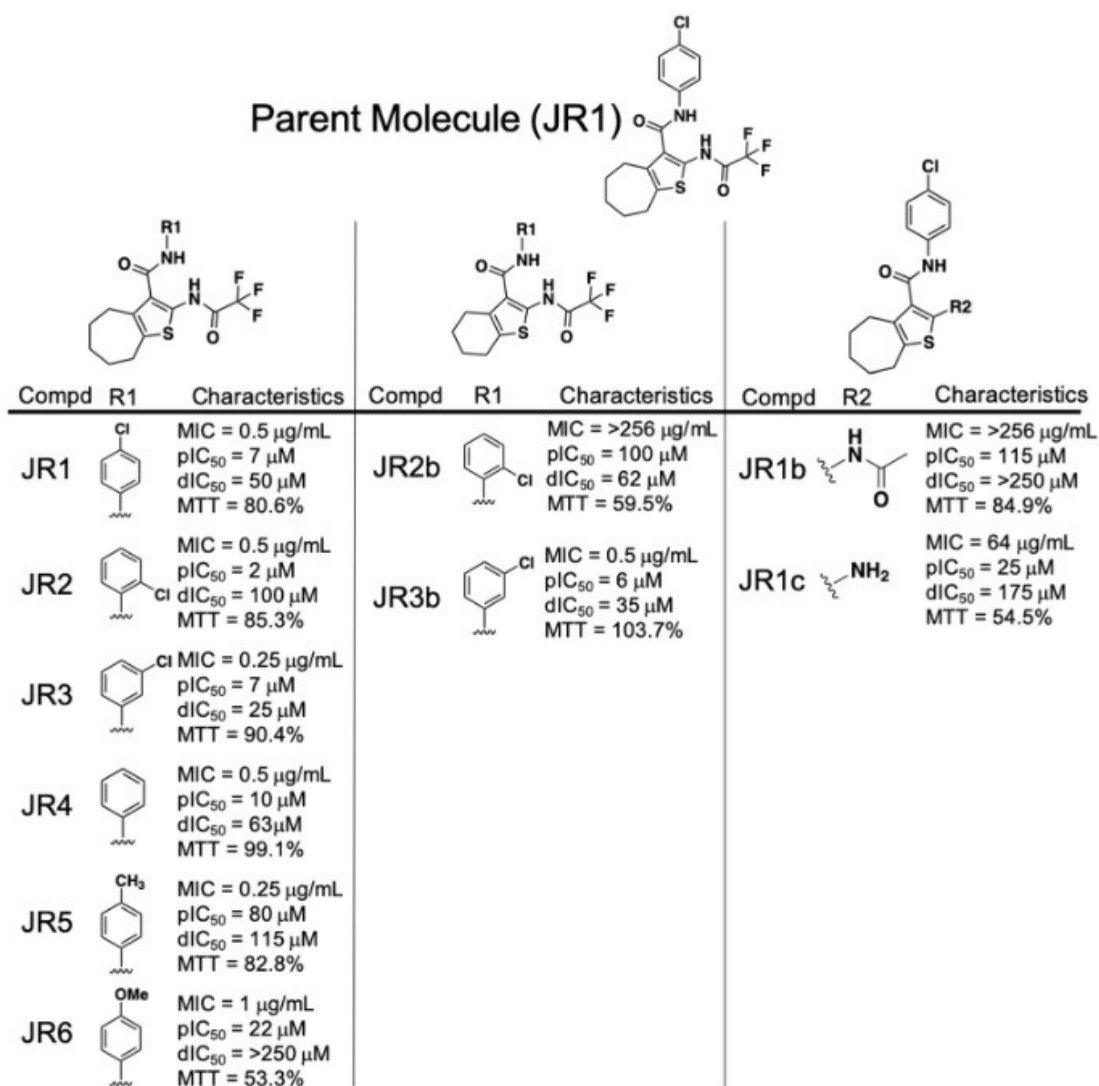


Figure 24: Initial SAR investigation of phenylcarbamoyl cyclic thiophenes RnpA inhibitors. pIC₅₀ = processing IC₅₀; dIC₅₀ = degradation IC₅₀. Adapted from Colquhoun et al., 2019.

In the case of piperidine carboxamides (Figure 25), the structural modifications concerned mainly the aromatic moiety and the piperidine group. Regarding the former, any modification of the 3,5-dichlorophenyl ring led to a loss of activity due to missed activity on both RnpA-mediated processes (**JC1-8 b-d**), while for the latter small modifications in nature and position of the methyl group were tolerated (**JC1**, **JC2** and **JC3**), whereas the substitution of the piperidine ring with a morpholine or a piperazine ring drastically nullified the activity.

Following this preliminary SAR evaluation, **JC1**, **JC2**, **JC3** and **JC3b** were selected for cellular assays, in a similar fashion to **RNPA2000**. Among them, **JC2** showed good antimicrobial activity, *in vitro* RnpA inhibition and reduced RnpA-associated cellular mRNA turnover,

synergistic effect with mupirocin and *in vivo* activity in *Galleria mellonella* model of *S. aureus* infection (Colquhoun *et al.*, 2019).

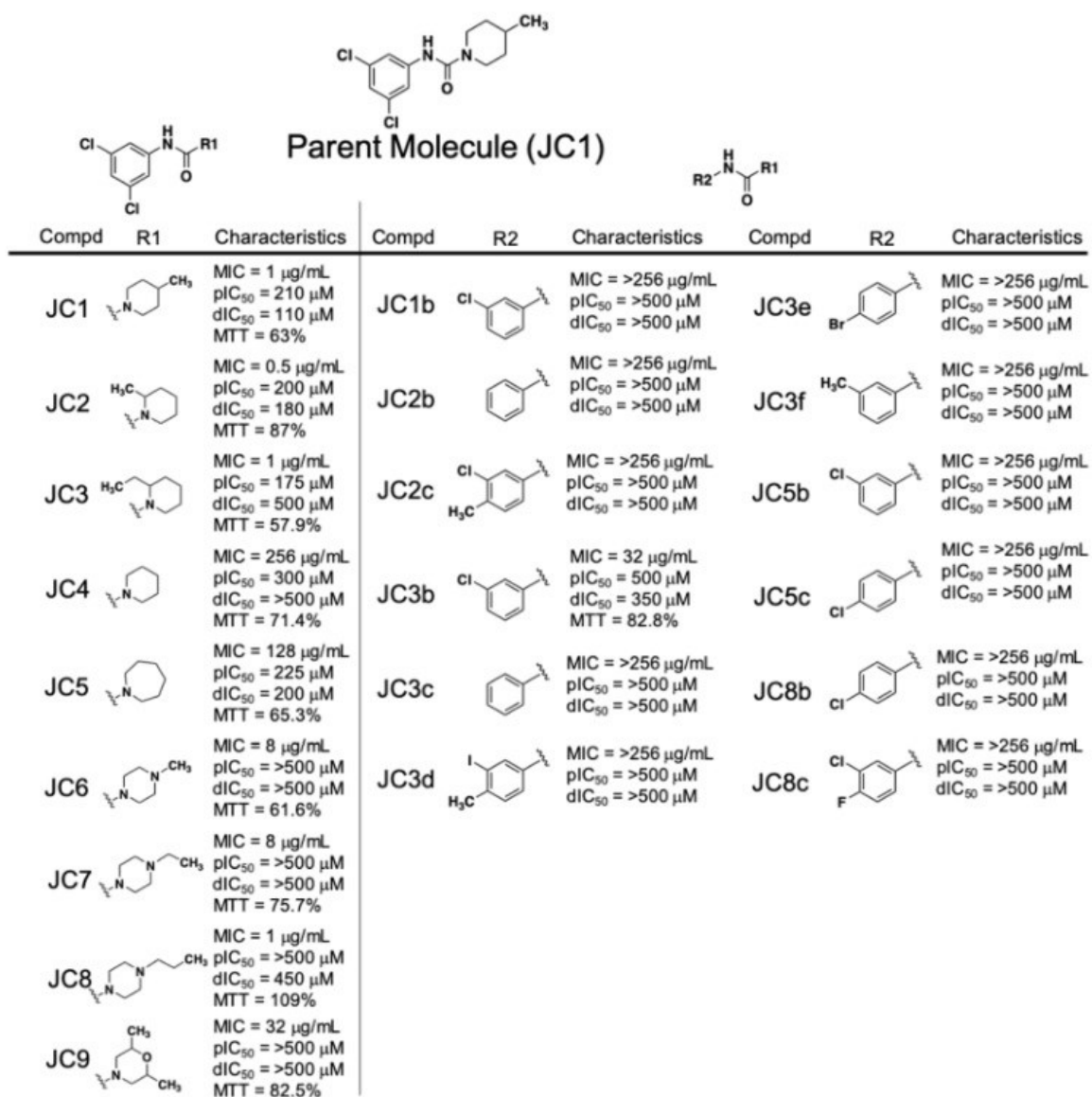


Figure 25: Initial SAR investigation of piperidine carboxamides RnpA inhibitors. pIC₅₀=processing IC₅₀; dIC₅₀=degradation IC₅₀. Adapted from Colquhoun *et al.*, 2019.

CHAPTER 4 – AIM OF THE WORK

As clearly explained in the “Global Action Plan on Antimicrobial Resistance” from WHO, the discovery of new chemical entities is an essential tool to treat several MDR-bugs related pathologies. Nevertheless, the drug discovery process can last many years from the beginning to the commercialization and is therefore associated with significant financial investments. This matter, from the pharmaceutical company point of view, is sustainable only if the expected money income can at least compensate the initial investment. The temporary and non-chronical nature of antibiotic treatments, as well as the fear of a rapid development of resistance to the new drug, makes antimicrobials drug discovery less appealing, when compared to chronical diseases drugs, such as the ones for heart illnesses.

In this context, the academic research, aiming at identifying new molecular targets and developing initial modulators as antimicrobials, became an important tool to speed up the antimicrobial drug discovery process.

As extensively explained in the previous chapters, both FtsZ and RnpA emerged as potential targets to be exploited for antimicrobial therapy for different reasons:

- Both FtsZ and RnpA are not targeted by marked antibiotics, therefore no resistance is currently present in circulating bacteria.
- RnpA lacks a human orthologue while FtsZ structure significantly differs from human β -tubulin one (especially in the C-terminal domain), therefore both FtsZ and RnpA inhibitors are expected to possess low to no toxicity.
- FtsZ is highly conserved among bacteria, making FtsZ inhibitors potential broad-spectrum agents. RnpA is peculiar of *S. aureus*, a very important bacteria from a clinical point of view, therefore RnpA inhibitors would be helpful in facing MDR-*S. aureus* mediated infections.

Starting from these considerations and from what previously discussed, the main objectives of the present work are the design, the synthesis, the purification, the characterization and the biological evaluation of new molecules as inhibitors of FtsZ or RnpA.

Inhibitors of FtsZ

The preliminary structure-activity relationship (SAR) exploration of the benzodioxane-benzamides proved the goodness of this class as very important potential tools to fight antimicrobial resistance and represents a promising starting point for the development of novel compounds able to overcome the problems related to PC190723 and derivatives. Nonetheless, several key steps must be faced and overcome to boost the development of this very promising family of antimicrobials:

- Further enhance the activity vs Gram-positive bacteria, both sensitive and resistant to the most used marketed antibiotics.
- Expand the spectrum of activity, towards other bacterial strains, especially Gram-negative, which represents an important limit for FtsZ benzamide inhibitors class.
- Deeply investigate the mechanism of action of these molecules.
- Improve the pharmacokinetic properties of this class of compounds.

To predict which modifications would more likely achieve these goals, a computational model was set up, in collaboration with Dr. Victor Sebastián-Pérez. To validate the model, TXA707 and PC190723, two well-known inhibitors of FtsZ that were also co-crystallized with *S. aureus* FtsZ, were docked and the docking poses almost perfectly resembled the ones encountered in the crystal structure.

Through the docking of compound **47**, it was demonstrated how, in addition to sharing the fundamental interactions achieved by the benzamide portion of the molecule with TXA707 and PC190723, the 1,2,4-oxadiazole moiety was inserted in a narrow and lipophilic cleft within the binding site, composed of several lipophilic residues such as Met98, Phe100, Val129, Ile162, Gly193, Ile197, Val214, Met218, Met226, Leu261 and Ile311 (Figure 26).

Moreover, the *in-silico* evaluation pointed out how more flexible derivatives, characterized by longer or differently branched linker between the scaffolds, could be better tolerated by the target.

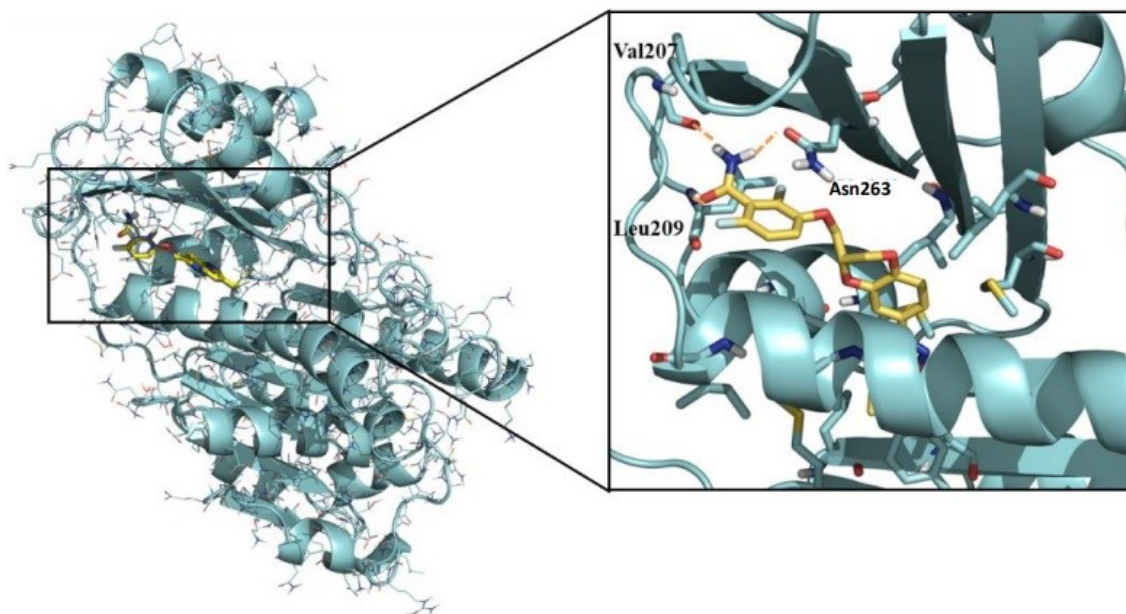


Figure 26: Docking pose of compound **47**.

For these reasons, starting from compound **47**, the structure was initially modified in 3 different directions (Figure 27):

- 1) Modifications of the 1,2,4-oxadiazole ring.
- 2) Modifications of the linker between the two main moieties.
- 3) Replacement of the oxygen of the benzodioxane ring with its lipophilic bioisoster sulphur, in different oxidation states.

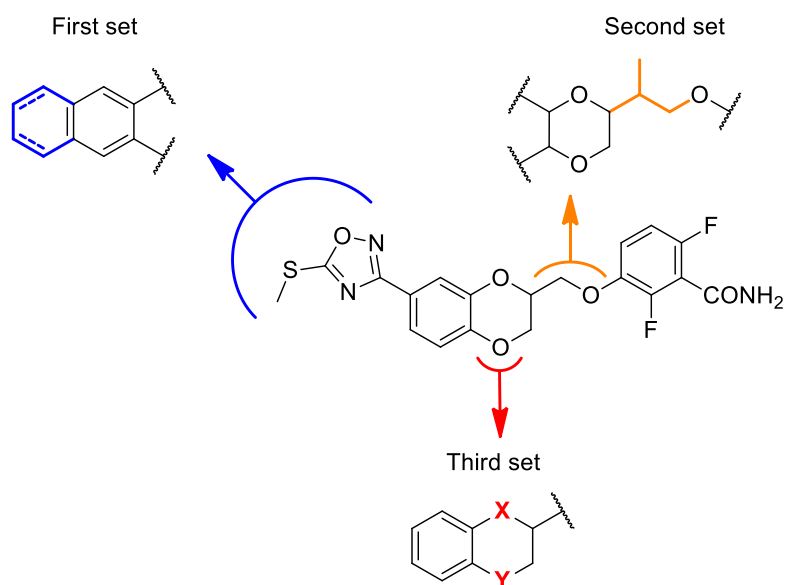


Figure 27: Modifications of the structure of derivative **47**; design of the three first sets of compounds object of the present work.

First set: modifications of the 1,2,4-oxadiazole ring

In previous studies, the activity data of derivatives **2** and **3** suggested that both positions 6 and 7 could bear substituents without compromising activity. Further studies, based on the developed computational model, showed that 1,2,4-oxadiazole is inserted in a narrow lipophilic cleft. On this basis, we wondered whether further elongation of the lipophilic portion of the benzodioxane axis could promote an optimal insertion into the FtsZ subpocket by establishing further hydrophobic interactions. Therefore, we decided to evaluate the naphthodioxane (compound **I**) and 5,6,7,8-tetrahydronaphthodioxane (compound **II**) (Figure 28), which could be tolerated given the hydrophobic residues present in the environment.

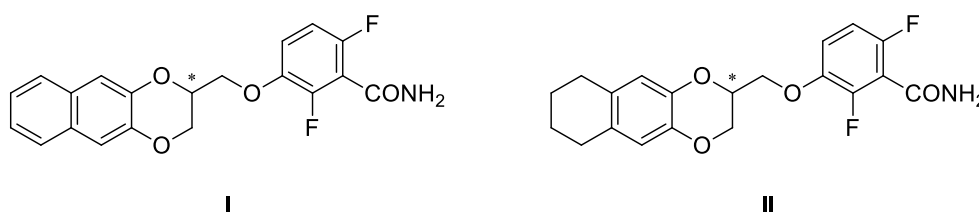


Figure 28: Structures of compounds **I-II**, aim of the present work.

Second set: modifications of the linker between the two main moieties

The docking studies performed on compound **47** demonstrated how the linker between the two main moieties does not directly achieve any crucial interaction with the target protein. Nevertheless, the linker allows the correct accommodation of the benzodioxane ring, opportunely substituted, into the narrow lipophilic subpocket.

For these reasons, a longer or differently branched linker should allow an even better accommodation of the benzodioxane, significantly improving the affinity for the protein. Therefore, a second set of derivatives, in which the linker was modified in different fashions, was designed and synthesized (compounds **III – VIII**; Figure 29).

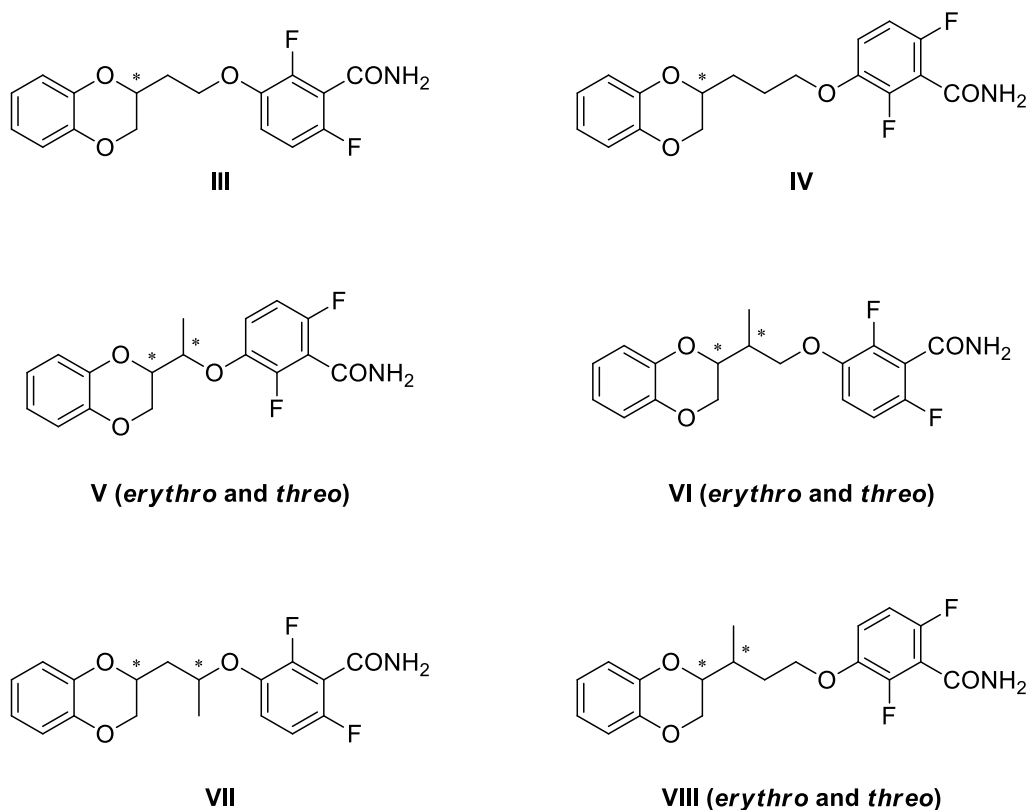


Figure 29: Structures of compounds III-VIII, aim of the present work.

Third set: modifications of the oxygen of the benzodioxane scaffold

During the initial evaluation of the SAR of the benzodioxane-benzamides, it was demonstrated how the substitution of one or both the oxygens of the benzodioxane scaffold, with a carbon or a nitrogen, was always detrimental for the antimicrobial potency of this class of compounds.

In this set of derivatives, the sulphur was introduced in lieu of the oxygens of the benzodioxane moiety, to evaluate the influence of this lipophilic heteroatom in the interaction with FtsZ (compounds IX – XIII; Figure 30).

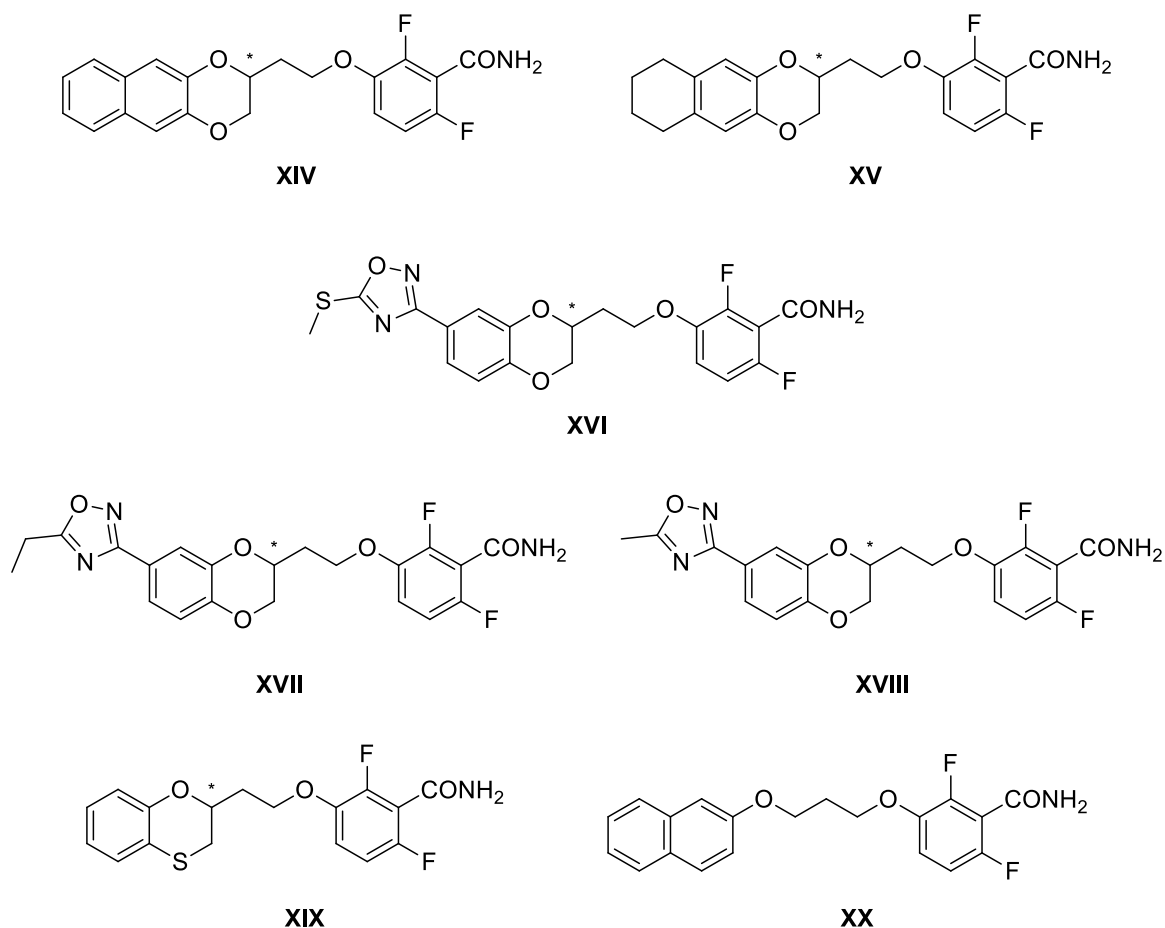


Figure 31: Structures of compound **XIV-XX**, aim of the present work.

Compounds **XIV** and **XV** keep the naphthalene and 5,6,7,8-tetrahydronaphthalene moiety, derivatives **XVI** to **XVIII** retain the 1,2,4-oxadiazole moiety typical of **47**, **48** and **49** and **XIX** is characterized by a 2-substituted 1,4-benzoxathiane moiety in place of the classic 1,4-benzodioxane one. Differently from the corresponding inferior homologues, these compounds present a 2 carbon atoms linker between the two main moieties, which proved to enhance the activity. Lastly, compound **XX** was designed to evaluate the effect of the drastic simplification of the naphthodioxane scaffold of compound **XIV**.

All the compounds belonging to these four sets were designed to further increase the activity versus Gram-positive bacteria and, potentially, acquire activity versus Gram-negative bacteria, both defined as key steps for the development of the benzodioxane-benzamides class of FtsZ inhibitors.

Therefore, after the obtainment of all the derivatives **I – XX**, they were tested on MSSA, MRSA, MDR-*S. aureus*, *B. subtilis* and wt-*E. coli*. While this evaluation led to the

development of very potent compounds vs *S. aureus* and *B. subtilis*, all these compounds showed again complete inactivity versus wt-*E. coli*.

In-vitro evaluation of the binding to *E. coli* FtsZ

The benzamide class is quite well-characterized in terms of *B. subtilis* and *S. aureus* antimicrobial activity and relative FtsZ inhibition: PC190723 is able to promote polymers assembly by stabilizing a high-affinity FtsZ conformation competent for the assembly (Elsen *et al.*, 2012), with consequent antimicrobial activity. Moreover, the co-crystal of FtsZ and PC190723, correctly accommodated within the Interdomain Site, was obtained and used to identify the main interactions driving FtsZ binding (Tan *et al.*, 2012). At the same time, PC190723 and all the most known benzamide FtsZ inhibitors are reported to be inactive versus wt-*E. coli* and unable to evoke any significant effect *in vitro* with purified *E. coli* FtsZ (Andreu *et al.*, 2010). Similarly, some of the compounds here reported showed a significantly higher activity, versus both *S. aureus* and *B. subtilis*, when compared to PC190723, but once again they seemed to be unable to evoke any antimicrobial effect versus *E. coli*.

Since the aminoacidic sequences of *E. coli* FtsZ and *S. aureus/B. subtilis* FtsZs are not so different to justify a very strong activity on the Gram-positive strains and a complete inactivity versus *E. coli*, we hypothesized that other non-target related factors could determine the inactivity of benzodioxane-benzamides on wt- *E. coli*.

For this reason, during the second year of my PhD, I spent 9 months in the laboratory of Prof. Rivas in Madrid, aiming at evaluating the ability of our derivatives to bind purified *E. coli* FtsZ and, hopefully, to interfere with its polymerization/depolymerization ability and/or the GTPase activity.

This would allow us to confirm or reject the hypothesis that benzodioxane-benzamides are indeed able to bind and interfere with *E. coli* FtsZ and that the *in vivo* inactivity versus wt-*E. coli* is attributable to other factors.

Fifth set: hydroxylated and methylated derivatives

The results obtained from the *in vitro* evaluation, as well as several *in vivo* tests, moved us to hypothesize that the presence of efflux pumps and the scarce membrane penetration are two important factors responsible of the inactivity of these compounds versus wt-*E.*

coli. Nonetheless, the insights coming from the previous computational data, in which it was shown how the 1,4-naphthodioxane or 5,6,7,8-tetrahydro-1,4-naphthodioxane moieties bind in the narrow and lipophilic cleft of the binding site, underline how the modification of these two moieties to increase the polarity would lead to a drastic lowering of the antimicrobial activity (Straniero, Sebastián-Pérez, *et al.*, 2020; Straniero, Suigo, *et al.*, 2020; Straniero *et al.*, 2021). At the same time, also the benzamide portion of the molecule can not be modified since it is responsible for crucial interactions that drive the binding. Conversely, the linker between the two main moieties, which should be responsible to allow the better accommodation of the scaffolds, without achieving additional interactions, could represent the suitable portion for introducing polar groups. Indeed, basing on similar principles, Stokes and collaborators exploited the linker between the benzamide portion of PC190723 and its phenyl-bromoxazole scaffold, to introduce a polar group with the final goal of designing prodrugs (Figure 32) (Stokes *et al.*, 2013).

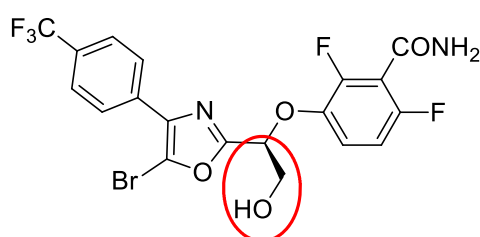


Figure 32: Structure of the lead compound of phenyl-bromoxazole benzamide FtsZ inhibitors.

As a result, trying to improve the membrane permeability, I designed a final fifth set of derivatives (Figure 33).

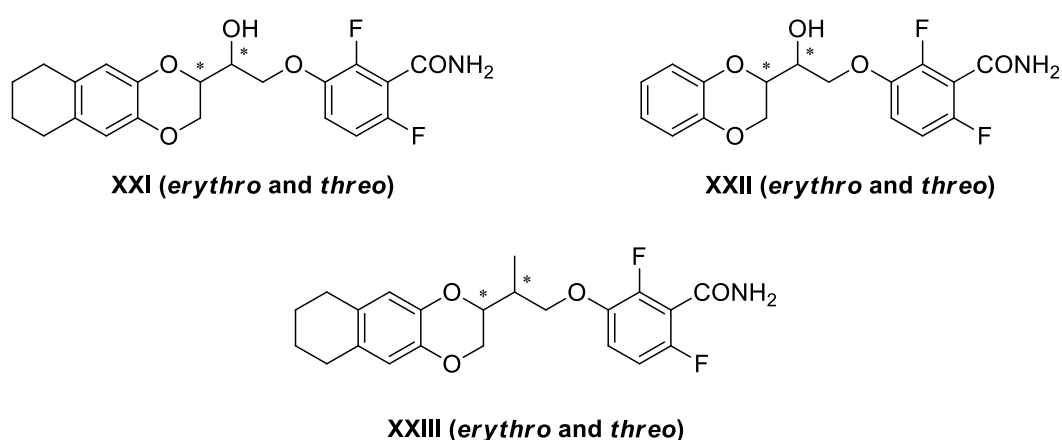


Figure 33: Structures of compounds **XXI** – **XXIII**, aim of the present work.

Compound **XXI** was designed to enhance the polarity and the membrane permeability of compound **XV**, one of the best derivatives versus both *S. aureus* and *B. subtilis*. Moreover,

the OH could be exploited for the obtainment of prodrugs or fluorescent probes. Compound **XXII** bears the same substitution on the structure of compound **III**. Lastly, in the structure of derivative **XXIII**, the same methyl substitution of derivative **VI** was used in place of the hydroxy group, to evaluate the influence of a substituent having a completely different nature.

Inhibitors of RnpA

The discovery of the key role of RnpA within *S. aureus* elevated the protein to a very promising target for the development of potential anti-staphylococcal compounds, which would represent a very important implement to fight *S. aureus* related MDR infections. Nonetheless, the research of potential classes of RnpA inhibitors generated only a few exploitable scaffolds, with some of them quickly abandoned due to the undesirable structure. Obviously, the reason behind the scarce number of known hits could be related to the novelty of the target and, consequently, to the low number of research groups working on this topic. As a result, in this moment the knowledge behind RnpA inhibitors is still poor.

To rationalize the design of RnpA inhibitors, a computational model was set up for the first time in literature, to the best of our knowledge. This was possible in collaboration with Dr. Victor Sebastián-Pérez, to understand which could be the potential binding site of known RnpA inhibitors **RNPA2000** and **JC1/2** and to evaluate the main interactions achieved between ligand and target.

Using *S. aureus* RnpA protein (Ha *et al.*, 2018), a hotspots maps analysis was performed. This unveiled how RnpA is less druggable than other proteins, but a main hotspot emerged as the most probable binding site (Figure 34).

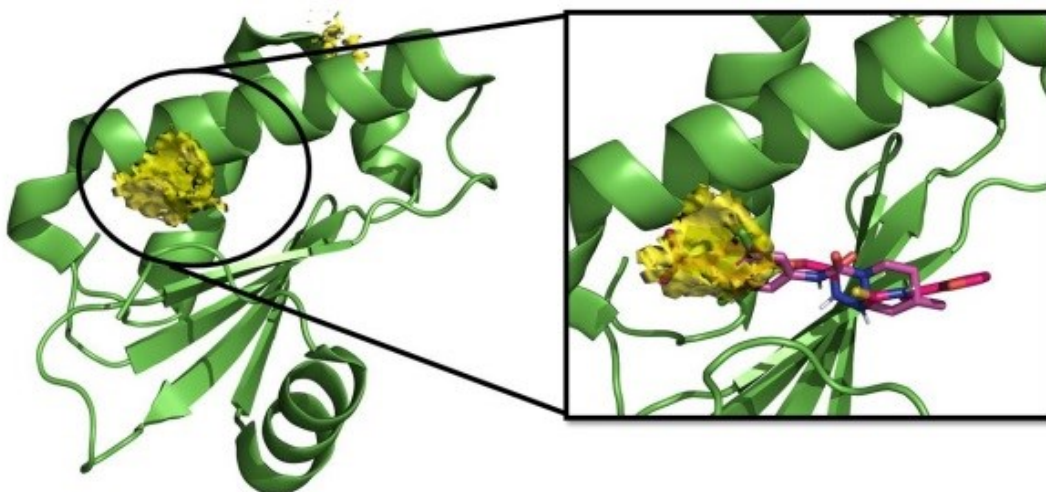


Figure 34: Hotspot maps analysis performed on RnpA. Both RNPA1000 and JC1/2 were successively docked within the identified binding site.

Both **RNPA2000** and **JC1/2** were docked and proved to be able to bind this putative binding site. In this cleft, several subareas were identified, in which the single moieties of the known inhibitors might achieve key interactions. For instance:

- Tyr7 and Phe43 generate a lipophilic cleft in which aromatic systems, such as the *i*-propylphenyl group of **RNPA2000**, can bind through π interactions.
- The central part of the binding cleft is surrounded by several residues such as Ile9, Leu45, Ile47 and Arg67. Linear linkers, like the ureidic moiety of **JC1/2** or the thiosemicarbazide of **RNPA2000**, can achieve hydrogen bonds with the backbone of the abovementioned aminoacids.
- In a different side, two residues, Phe15 and Lys63, seem to be suitable for π interaction or π -cation interactions. The 2-furanyl moiety of **RNPA2000** is predicted to bind within this region.

First set: modifications of JC1/JC2

Using the information gained from the computational docking studies, a first set of **JC2** derivatives was designed and synthesized (Figure 35 and Figure 36).

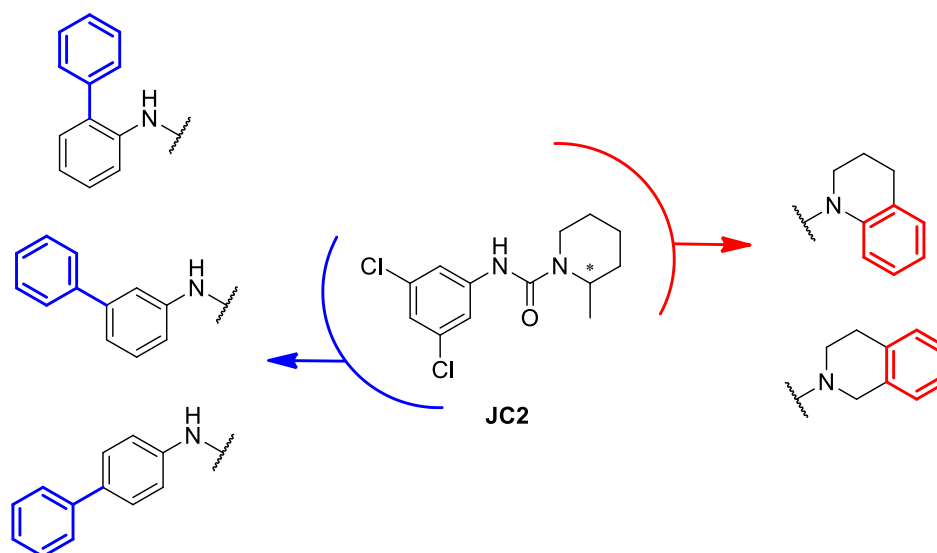


Figure 35: Modifications of the structure of the known RnpA inhibitor **JC2**; design of the first set of compounds object of the present work.

Derivatives **XXIV** to **XXVI** were designed to achieve extra interactions with the aromatic residues Tyr7, Phe43, Leu45 and Phe70, while compounds **XXVII** and **XXVIII** should engage interactions with the residues at the opposite side of the putative binding cleft, Phe15 and Lys63.

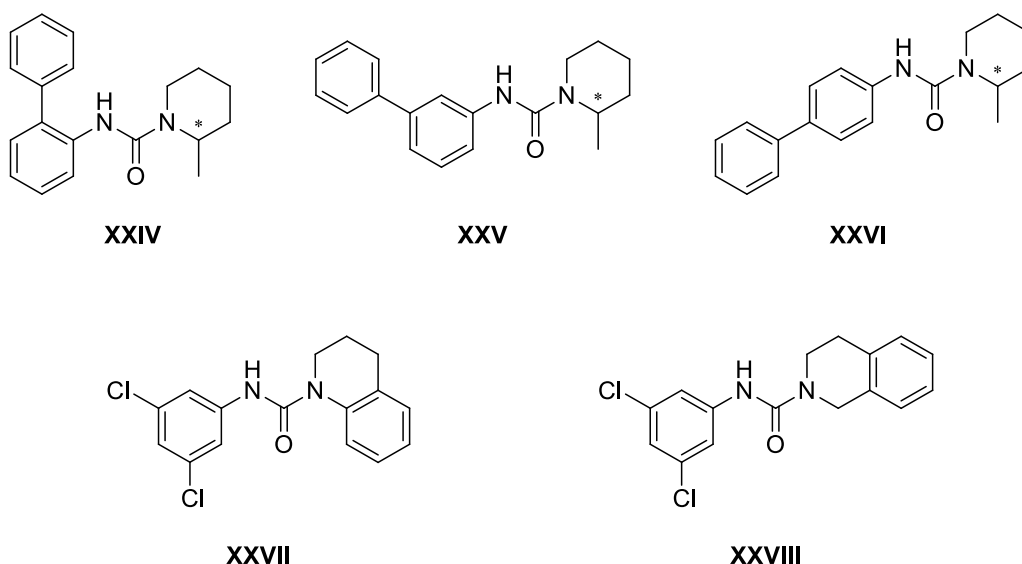


Figure 36: Structures of compounds **XXIV** and **XXVIII**.

Second set: modifications of the 2-furanyl moiety of RNPA2000

While the derivatives of the first class were designed basing on the structure of **JC1** and **JC2**, known RnpA inhibitors belonging to the piperidine carboxamides class of compounds, the derivatives of the second, the third and the fourth classes are modifications of **RNPA2000**, another known RnpA inhibitor, and their rationale is depicted in Figure 37.

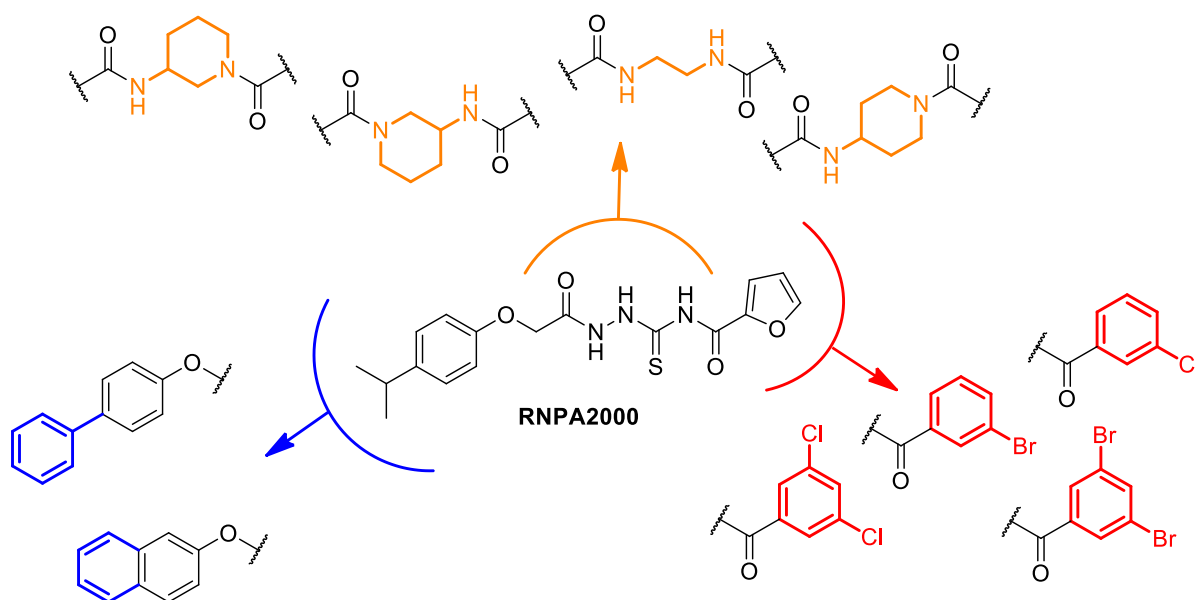


Figure 37: Modifications of the structure of the known RnpA inhibitor **RNPA2000**; design of the second, third and fourth sets of compounds object of the present work.

Specifically, the 2-furanyl moiety included in **RNPA2000** structure is known to be metabolized to toxic species *in vivo*, therefore, in compounds **XXIX** to **XXXII** (Figure 38), it

was replaced by several mono- or di-halogenated phenyl rings, which could resemble the same lipophilic nature, while exploring the effect of these different halogen atoms.

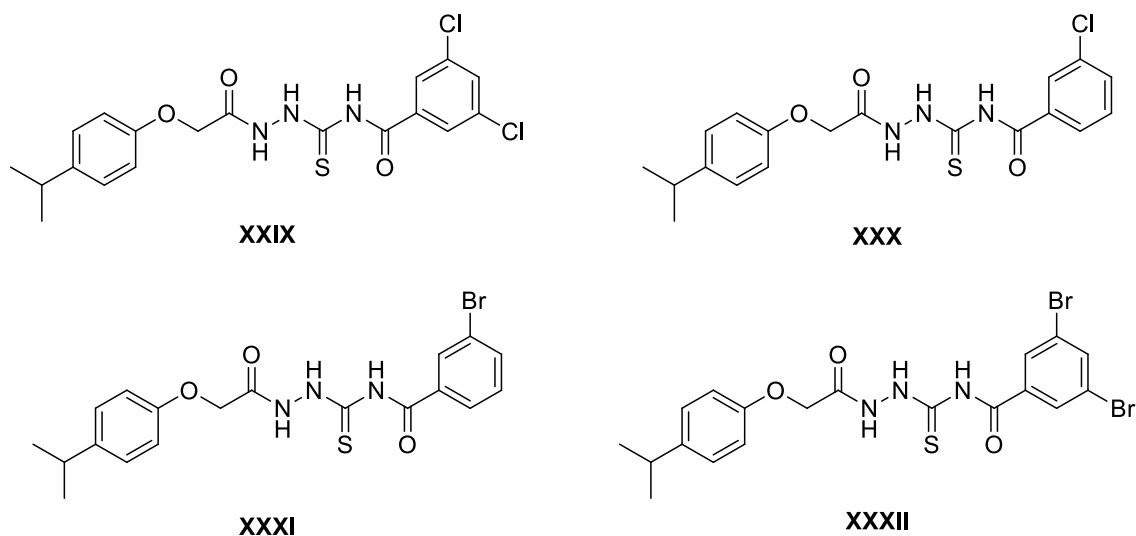


Figure 38: Structures of compounds **XXIX** – **XXXII**.

Third set: modifications of the *i*-propyl moiety of RNPA2000

Resembling the modifications applied to **JC1/2** to achieve the derivatives of the first set, the *i*-propyl moiety of **RNPA2000** was replaced by a 4-biphenyl and a 2-naphthyl scaffold, trying to establish further interactions with the aromatic moieties deeply set within the cavity, achieving compounds **XXXIII** and **XXXIV** (Figure 39). Considering the toxicity of the 2-furanyl moiety, in these and in all the following compounds, we decided to keep the 3,5-dichlorophenyl ring.

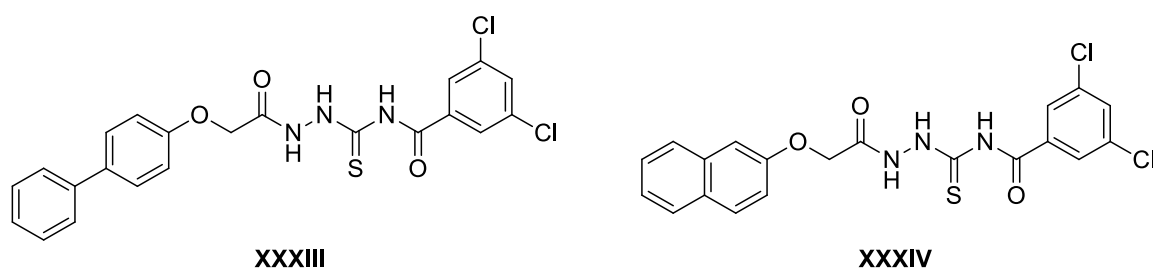


Figure 39: Structures of compounds **XXXIII** and **XXXIV**.

Fourth set: modifications of the thiosemicarbazide moiety of RNPA2000

The last evaluation for RnpA inhibitors was studying the importance of the thiosemicarbazide moiety of **RNPA2000**, which is related to poor *in vivo* stability. In particular, the computational studies pointed out how the simplification of the thiosemicarbazide to a diamide structure should not significantly impede the achievement

of the fundamental interactions within the binding site. Nonetheless, the removal of the thiosemicarbazide, a highly conjugated system, could strongly affect the tridimensionality of the molecule, therefore both linear and rigid systems have been considered during the design of these compounds. As said before, the 3,5-dichlorophenyl ring was kept.

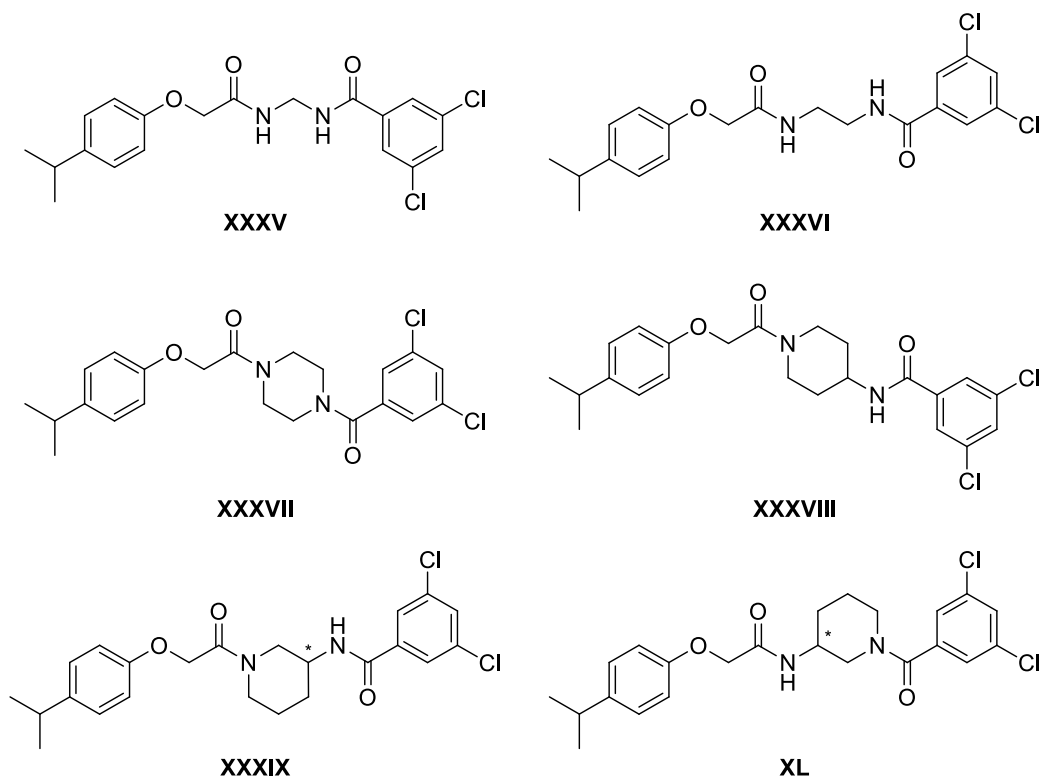


Figure 40: Structures of compounds **XXXV-XL**.

Derivatives **XXXV** and **XXXVI** (Figure 40) show a linear diamide moiety, while in derivatives **XXXVII** to **XL** the diamide portion was rigidified in different fashions, to observe and understand the importance of conformational rigidity within the system.

CHAPTER 5 – RESULTS AND DISCUSSION

Inhibitors of FtsZ

Structure-activity relationship exploration

The SAR exploration of benzodioxane-benzamides as FtsZ inhibitors conceptually started from the structure of compound **47** (Figure 41), which represented the best compound from several points of view (activity, stability etc.) at the beginning of the present thesis.

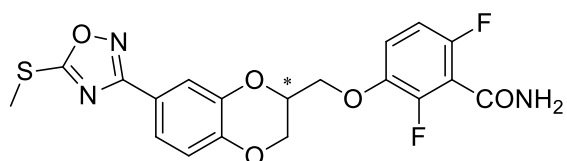


Figure 41: Structure of derivative **47**, the FtsZ inhibitors reference compound.

In addition, as anticipated before, compound **47**, as well as other previously developed compounds, possesses several sub-optimal features:

- The MIC versus *S. aureus* of 0.6 µg/mL (1.4 µM) is higher when compared to some other reference benzamide compounds, such as derivative 8j reported by Haydon (MIC vs *Aureus* = 0.7 µM) (Haydon et al., 2010).
- The activity is completely restricted to Gram-positive strains.
- The very low cytotoxicity on human MRC-5 cells should be further confirmed in animal models.
- The overall high lipophilicity of the molecule is positive for membrane penetration, but it is related to poor pharmacokinetic properties.

Therefore, starting from the structure of **47** and using the information achieved through the docking studies, the structure has been modified preparing the first three set of derivatives, previously elucidated.

Compounds **I – XIII**, soon after their characterization, were tested firstly on *S. aureus* for their antimicrobial activity, as previously done for their precursors. In particular, we first determined the minimal inhibitory concentration (MIC), i.e., the lowest compound dose (µg/mL) arresting bacterial growth, and the minimal bactericidal concentration (MBC), i.e., the minimal dose (µg/mL) of the compound required for an irreversible block, even after drug removal. They were firstly tested on Methicillin-sensitive *S. aureus* (MSSA) and

Methicillin-resistant *S. aureus* (MRSA), in collaboration with Dr. Zanotto at the Department of Medical Biotechnologies and Translational Medicine of the Università degli Studi di Milano. Moreover, part of these compounds was also examined on clinical Multi-drug Resistant *S. aureus* strains (MDRSA 12.1 and MRSA 11.7) by Dr. Hrast, at the University of Ljubljana. MDRSA 12.1 is a specific MDR strain that shows resistance towards gentamicin, kanamycin, rifampicin, streptomycin, sulfamethoxazole and tetracycline, while MDRSA 11.7 shows resistance towards ciprofloxacin, clindamycin, erythromycin, quinupristin and dalfopristin in association, tetracycline, tiamulin and trimethoprim. In addition, the cytotoxicity of part of these compounds has been evaluated on human MRC-5 cells and quantified as TD90, defined as the concentration ($\mu\text{g}/\text{mL}$) able to reduce the viability of MRC-5 cells by 90%.

Cpd	MSSA ATCC 29213			MRSA ATCC 43300			MDR-SA 12.1	MDR-SA 11.7	MRC-5
	MIC ($\mu\text{g/mL}$)	MBC ($\mu\text{g/mL}$)	MIC/ MBC	MIC ($\mu\text{g/mL}$)	MBC ($\mu\text{g/mL}$)	MIC/ MBC	MIC ($\mu\text{g/mL}$)	MIC ($\mu\text{g/mL}$)	TD90 ($\mu\text{g/mL}$)
47	0.6	0.6	1	0.6	0.6	1	/	/	740
<i>I</i>	2	5	2.5	2	5	2.5	4	4	>750
<i>II</i>	1.25	1.25	1	1.25	1.25	1	2	4	75
<i>III</i>	5	5	1	5	5	1	4	4	380
<i>IV</i>	10	100	10	10	100	10	16	32	/
<i>V (e)</i>	8	8	1	8	8	1	8	16	/
<i>V (t)</i>	64	64	1	64	64	1	64	128	/
<i>VI (e)</i>	32	32	1	32	32	1	32	64	/
<i>VI (t)</i>	128	128	1	128	128	1	128	>128	/
<i>VII</i>	20	40	2	20	40	2	128	>128	/
<i>VIII (e)</i>	16	16	1	16	16	1	16	32	/
<i>VIII (t)</i>	32	32	1	32	32	1	32	32	/
<i>IX</i>	1	1	1	1	1	1	2	2	>800
<i>X</i>	20	20	1	20	20	1	32	32	200
<i>XI</i>	5	10	2	5	10	2	8	8	200
<i>XII</i>	>100	>100	/	>100	>100	/	/	/	/
<i>XIII</i>	>100	>100	/	>100	>100	/	/	/	/

Table 6: Results of the biological evaluation of derivatives I-XIII.

The results, summarized in Table 6, revealed several important and interesting information:

- Derivatives **I** and **II**, in which the 1,2,4-oxadiazole ring of **47** was replaced by a Naphthalene or a 5,6,7,8-Tetrahydronaphthalene moiety, retain a strong activity. Moreover, both these functions can be derivatised, hoping for further antimicrobial improvements. Nonetheless, compound **II** presents a significant 10-fold increase of the cytotoxicity compared to **47**.
- The 2-carbon atoms linear linker (compound **III**) is confirmed to be the preferred, when compared to the 3-carbon atoms one (compound **IV**).
- Branching the linker seems to be detrimental for the antimicrobial activity. However, the *erythro* isomers always show a stronger activity, when compared to their relative *threo* isomers.
- Unlike previous work, in which the complete or partial substitution of the oxygen atoms in the benzodioxane system with carbon or nitrogen atoms led to a loss of activity, replacement with sulphur is not always detrimental for the antimicrobial

activity. Indeed, as clearly pointed out by the high antimicrobial activity of compound **IX**, the replacement of the oxygen in position 4 with a sulphur lead to 5-fold increase of the antimicrobial activity, without raising the cytotoxicity of the molecule. Conversely, the substitution of the oxygen in position 1 (compound **X**) or of both oxygens (compound **XI**) do not produce the same positive effect, leading to less active and more toxic compounds. Similarly, the oxidation of the sulphur atom, in both positions, is completely damaging for the antimicrobial activity (compounds **XII** and **XIII**).

From this initial evaluation it was possible to observe how the 2-carbon atom linker is indeed better tolerated and that the sulphur, the naphthalene or a 5,6,7,8-tetrahydronaphthalene moieties exerted a positive effect.

The positive results achieved with compounds **I**, **II**, **III** and **IX**, moved us to design the fourth set of compounds explained in the previous chapter.

Also in this case, after the synthesis and purification, all these compounds were evaluated on Gram-positive bacterial strains, and the results are summarized in Table 7:

<i>Cpd</i>	MSSA ATCC 29213			MRSA ATCC 43300			MDR- SA 12.1	MDR- SA 11.7	MRC-5
	MIC ($\mu\text{g/mL}$)	MBC ($\mu\text{g/mL}$)	MIC/ MBC	MIC ($\mu\text{g/mL}$)	MBC ($\mu\text{g/mL}$)	MIC/ MBC	MIC ($\mu\text{g/mL}$)	MIC ($\mu\text{g/mL}$)	TD90 ($\mu\text{g/mL}$)
XIV	0.25	0.25	1	0.25	0.25	1	0.25	0.5	360
XV	0.1	0.1	1	0.1	0.1	1	0.125	0.125	>800
XVI	0.25	0.25	1	0.25	0.25	1	0.5	0.5	380
XVII	0.25	0.25	1	0.25	0.25	1	0.25	0.25	/
XVIII	0.5	0.5	1	0.5	0.5	1	0.5	0.5	>800
XIX	2.5	5	2	2.5	5	2	4	8	/
XX	5	5	1	5	5	1	4	4	/

Table 7: Results of the biological evaluation of derivatives **XIV-XX**.

The results of the evaluation of this second set of compounds were really promising:

- Passing from 1-carbon atom linker to 2-carbons atom linker the antimicrobial activity is always enhanced; only derivative **XIX** shows a worsening of the activity compared to derivative **IX**. In particular, compound **XV** shows the outstanding capability to evoke a bactericidal effect at the surprisingly low concentration of 0.1 $\mu\text{g/mL}$ versus both MSSA and MRSA. Interestingly, while this elongation of the linker

raised the cytotoxicity of the Naphthodioxane derivative (**XIV**), completely cancelled the one of the 5,6,7,8-Tetrahydronaphthodioxane; indeed, compound **XV** does not show any significant effect on human MRC-5 cells.

- Simplifying the ring, and consequently reducing the rigidity of the system, lead to a significant lowering of the antimicrobial activity, as shown by the results of compound **XX** versus compound **XIV**.

Since all these compounds belong to the benzodioxane-benzamide class of FtsZ inhibitors and originate from derivative **47**, for which the inhibition of FtsZ was already demonstrated (Straniero *et al.*, 2021), we hypothesized that also for these compounds FtsZ remains to be the target. Nonetheless, to verify this hypothesis, we proceeded by evaluating the morphological changes of bacterial cells in presence and in absence of our compounds, as usually done to study the capability of a molecule to interfere with the bacterial division system.

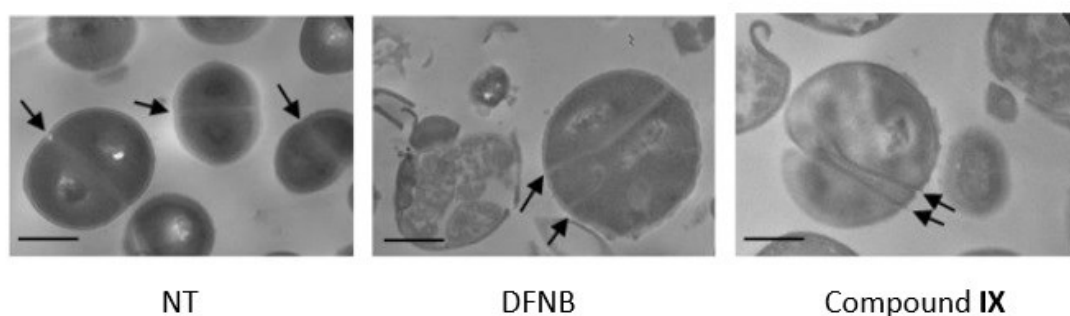


Figure 42: Target validation: the effects of compound **IX** were compared to a known FtsZ inhibitors, the 2,6-difluoro-3-nonyloxybenzamide, and to non-treated cells through TEM.

In this case, compound **IX** was used as reference. As we can see in Figure 42, in presence of both DFNB, the well-known inhibitor of FtsZ, and compound **IX** alterations in the formation of the septum are clearly visible, which are evident symptom of FtsZ inhibition.

After this evaluation of the antimicrobial activity versus *S. aureus*, which represents a model of Gram-positive bacteria as well as a clinically relevant problem, followed by the target validation, we proceeded evaluating some of the best derivatives (**XIV**, **XV** and **XVIII**) on *B. subtilis* as well, to assess the width of the spectrum of action of these compounds. Compounds **XIV** and **XV** proved to possess a MIC of 0.06 and 0.03 $\mu\text{g}/\text{mL}$ respectively, confirming their very high antimicrobial activity versus Gram-positive strains. Moreover,

also in this case, FtsZ was validated as the target of these compounds within *B. subtilis* (Straniero *et al.*, 2021).

Then we moved to evaluate the totality of the compounds on *wt-E. coli*, as a model of Gram-negative bacteria. All the above-mentioned derivatives showed an apparent complete inactivity. Nevertheless, since bacterial FtsZs are 40 to 50% identical in sequence among all the bacterial species (Erickson, 2007), the simultaneous ability possessed by some compounds to strongly inhibit *S. aureus* or *B. subtilis* FtsZ and complete inability to evoke any visible effect on *E. coli* FtsZ is counterintuitive and scarcely plausible.

More likely, we could hypothesise the benzodioxane-benzamides should bind and interfere with *E. coli* FtsZ, but other factors within the complex biological environment interfere and hamper the antimicrobial activity of this family versus *wt-E.coli*.

Therefore, to verify this hypothesis, two parallel investigations were performed:

- On one side, the antimicrobial activity of several benzodioxane-benzamides was evaluated on mutated strains of *E. coli*. In particular, *E. coli* D22 bears a mutation in the LpxC gene that enhance the outer-membrane permeability and *E. coli* N43 that is knocked out for AcrAB cell membrane efflux pump.
- On the other side, the binding of these compounds with the isolated *E. coli* FtsZ was evaluated.

The first task gave a hint on which could be factors intervening in determining the inactivity of this class of compounds and the results are reported in Table 8.

	<i>Wt-E. coli</i>	<i>E. coli D22</i>	<i>E. coli N43</i>
	MIC (µg/mL)	MIC (µg/mL)	MIC (µg/mL)
<i>I</i>	>128	>128	>128
<i>II</i>	>128	>128	8
<i>III</i>	>128	>128	8
<i>IV</i>	>128	>128	>128
<i>V (e)</i>	>128	>128	/
<i>V (t)</i>	>128	>128	/
<i>VI (e)</i>	>128	>128	64
<i>VI (t)</i>	>128	>128	>128
<i>VII</i>	>128	>128	>128
<i>VIII (e)</i>	>128	>128	32
<i>VIII (t)</i>	>128	>128	64
<i>IX</i>	>128	>128	64
<i>X</i>	>128	>128	128
<i>XI</i>	>128	>128	>128
<i>XII</i>	>128	>128	/
<i>XIII</i>	>128	>128	/
<i>XIV</i>	>128	8	>128
<i>XV</i>	>128	>128	>128
<i>XVI</i>	>128	>128	/
<i>XVII</i>	>128	>128	/
<i>XVIII</i>	>128	>128	/
<i>XIX</i>	>128	>128	64
<i>XX</i>	>128	>128	/

Table 8: Antimicrobial evaluation on *E. coli*: the results for both wild type and mutated strains are reported.

Interestingly, while all the compounds share a complete inactivity versus *wt-E. coli*, many of them are able to evoke an antimicrobial activity versus *E. coli* N43, KO for AcrAB efflux pump. From this first evaluation, the membrane efflux pumps of this germ seem to play an important role in determining the inactivity of 1,4-benzodioxane benzamides as antimicrobials, while the capability to interact with FtsZ is retained also within *E. coli*, as initially hypothesised. In this case, the co-administration of these inhibitors with efflux pump inhibitors (EPIs) would represent a viable therapeutic option to expand the spectrum of these compounds towards *E. coli* and other Gram-negative bacteria, which would represent an important achievement for this class of antimicrobials.

Figure 43: Compounds included in the *in vitro* study on purified *E. coli* FtsZ.

- Compounds **I** and **II** belong to the first set of compounds, object of the present work.
- Compounds **XIV**, **XV** and **XVI** belong to the fourth set of this thesis.
- Compounds **1**, **15**, **42**, **47** and **49** are benzodioxane-benzamides developed before the beginning of the present work.

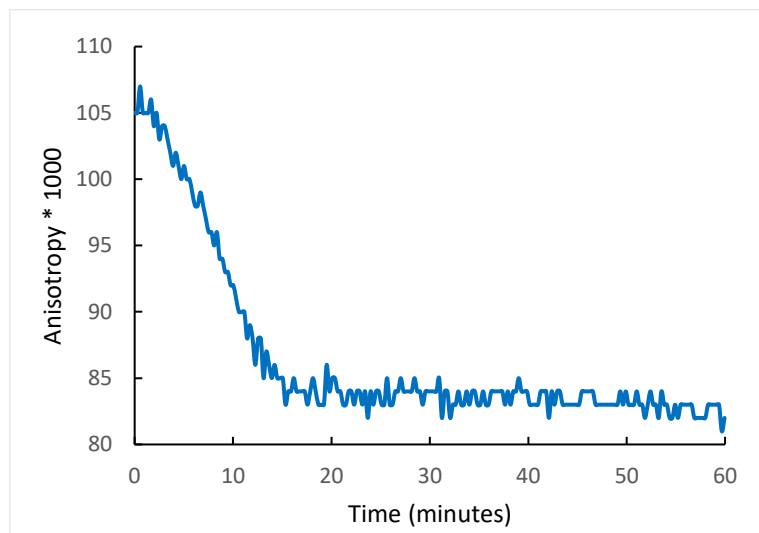
Within the bacterial cell division cycle of *E. coli*, the role of FtsZ, as well as of several molecular partners involved in the process, have been extensively studied and reported over the last years (Dai and Lutkenhaus, 1991; Margolin, 2005; Du and Lutkenhaus, 2019; Zorrilla *et al.*, 2021). Therefore, to evaluate the goodness of a putative FtsZ inhibitor, it is possible to observe drug capability to interfere with, at least, one essential function of FtsZ within the cell division cycle. One example is FtsZ GTP-dependent polymerization/depolymerization, which could be promoted, prevented or inhibited by a putative inhibitor.

As anticipated in the Introduction chapter, in bacterial physiological conditions, FtsZ is freely distributed as oligomers in the cytoplasm, bound to a molecule of GDP. Through GTP binding polymerization occurs, forming linear structures named protofilaments that represent the base for the progress of the process. The formed protofilaments show GTPase activity, allowing GTP to be hydrolysed and inducing the consequent disassembly of the protofilaments. The capability of the protofilaments to rapidly depolymerize after GTP hydrolysis confers them a dynamic nature that is very important for the bacterial cell.

Time-dependent disassembling of protofilaments in dilute conditions can be observed through fluorescent anisotropy. This technique, which can be applied on samples containing a certain amount of fluorescently labelled protein as tracer, is based on the unequal intensity of the emitted light from a fluorophore along different axis of polarization. The higher is the size or the rigidity of the fluorescent molecule, the higher is the value of its anisotropy.

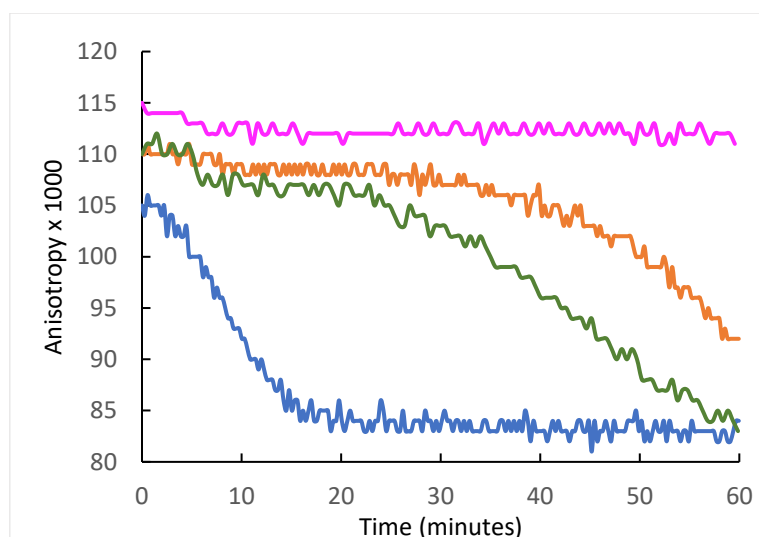
The addition of GTP to FtsZ, using FtsZ-Alexa488 as fluorescent tracer, results in the increase of the fluorescence anisotropy compared to the value of the unassembled protein, which reflects the formation of protofilaments (Reija *et al.*, 2011). Overtime, in absence of any compound, anisotropy decreases to the initial value upon GTP consumption and

consequent polymers disassembling. Indeed, as we can see from Graphic 1, 2 mM GTP induced polymerization disassembles in about 15 minutes.



Graphic 1: Kinetics of depolymerization of FtsZ in absence of inhibitors upon 2 mM GTP addition.

Starting from this, as a first sub aim, we wanted to investigate if and how this kinetics is modified by our compounds, as a consequence of the interaction of the inhibitor with the protein. To do so, and to also have a potency comparison, we screened all the compounds by incubating them at 40, 20 and 10 μM with FtsZ and by evaluating the anisotropy profile.



Graphic 2: Kinetics of depolymerization of FtsZ in presence of 40 μM (pink trace), 20 μM (orange trace) and 10 μM (green trace) compound XIV, compared to the absence of the inhibitor (blue trace), upon 2 mM GTP addition.

The results for compound **XIV** are shown in Graphic 2. As we can see, this compound is able to strongly delay protofilaments disassembly, following a concentration-dependent magnitude of effect. In particular, in presence of 40 μM **XIV**, no depolymerization is

observable throughout the duration of the analysis, as indicated by the almost constant value of anisotropy over time.

Most of the evaluated compounds showed the capability to delay FtsZ polymers disassembling, even if with different extents (Data not shown). Among all the derivatives, compounds **XIV** and **XV** resulted to induce the strongest stabilization effect.

Furthermore, since the FtsZ GTPase activity is a key feature of this protein, we also evaluated the effects of the same compounds on it, as a second index of molecule-protein interaction and perturbation.

	FtsZ GTPase activity	%Inhibition
FtsZ	9.4 ± 1.2	/
15	6.1 ± 0.7	40.8 ± 6.8
42	4.4 ± 0.9	56.8 ± 8.9
47	5.8 ± 1.8	43.7 ± 17.8
49	6.5 ± 0.3	35.6 ± 2.8
I	8.1 ± 0.8	16.0 ± 8.0
II	8.4 ± 0.1	16.8 ± 1.4
XIV	1.3 ± 0.7	84.2 ± 9.3
XV	1.9 ± 0.07	76.5 ± 0.8
XVI	5.3 ± 1.3	30.3 ± 16.7

Table 9: *E. coli* FtsZ GTPase activity: FtsZ alone or in co-presence of 20 μ M compounds.

As observable in Table 9, data suggest how *E. coli* FtsZ GTPase activity is lowered in presence of the benzodioxane-benzamides, if compared to their absence, keeping the same experimental conditions. Interestingly, the strongest effects are observable in presence of derivatives **XIV** and **XV**, which considerably reduce the GTPase activity by ~80%. All the compounds showed the capability, even if at different intensity, to evoke an inhibition effect of the GTPase activity, which is generally well related to the magnitude of stabilizing effect observed through fluorescence anisotropy. This suggests a good correlation between the two effects. The reduction of the GTPase activity, promoted by the compounds, could be related to a conformational change of the FtsZ protofilaments upon binding with the inhibitor, thus causing stabilization of the polymer itself.

To evaluate how the crowded *E. coli* cytoplasmatic environment could modulate the just described effects, the time dependent depolymerization of FtsZ polymers was also observed through turbidity measurements in solutions containing dextran as macromolecular crowder, in presence or absence of the putative inhibitors (Figure 44).

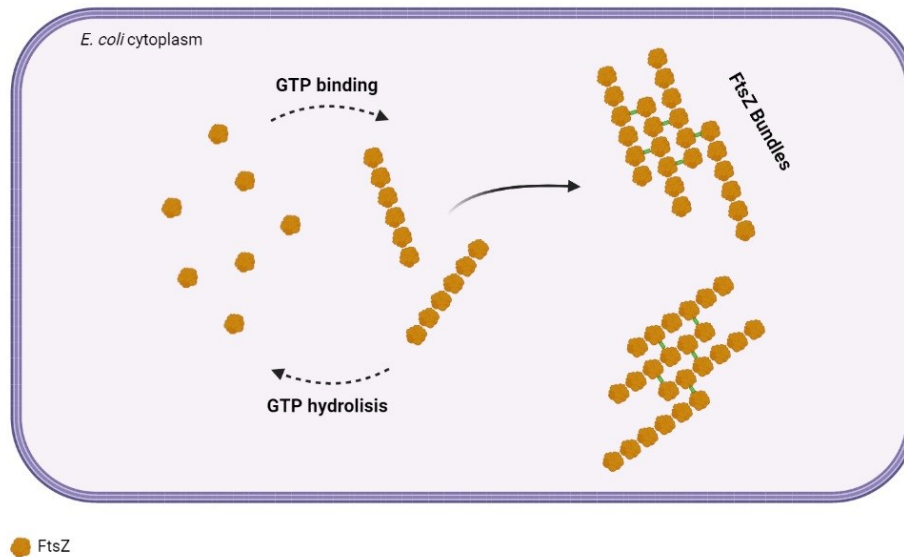
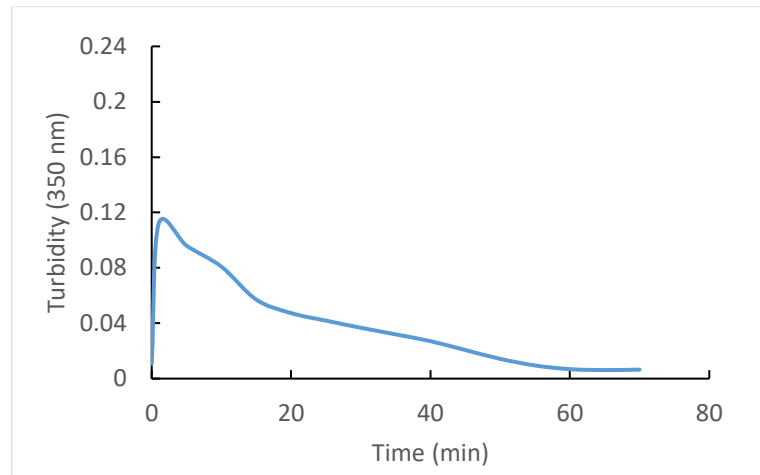


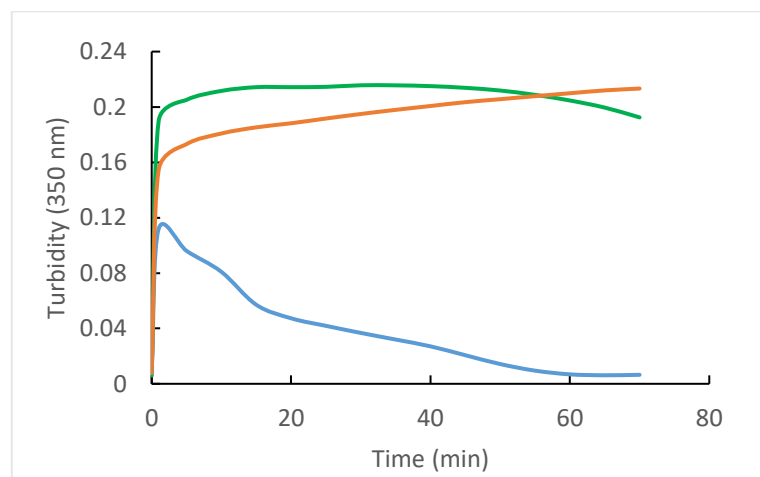
Figure 44: FtsZ bundling in E. coli: The linear polymerization, that represents the first step of the cell division process, is rapidly followed by the formation of bundles through lateral interactions, promoted by the crowded cytoplasmatic environment.

In these crowded conditions, following 1 mM GTP addition, FtsZ filaments require 40 to 50 minutes to completely depolymerize. In this time the turbidity value reached the basal level (Graphic 3). In this second evaluation, this time was longer compared to the one observed in diluted solution, despite of the half amount of GTP, because of the achievement of lateral interactions of single stranded FtsZ polymers to form bundles in crowded conditions.



*Graphic 3: Turbidity measurement of *E. coli* FtsZ alone upon 1 mM GTP addition in crowded conditions. Over time, upon GTP consumption, bundles depolymerize and the turbidity value lowers.*

In presence of 20 μM **XIV** or **XV** (Graphic 4), the turbidity values achieved through triggering polymerization with GTP remained stable for over 60 minutes, with only a slight decrease for **XV**. This is again compatible with a hyper-stabilizing effect on the FtsZ bundles mediated by the compounds, as previously observed for the single stranded protofilaments in diluted conditions.



*Graphic 4: Turbidity measurement of *E. coli* FtsZ in presence of 20 μM **XIV** (orange trace) or **XV** (green trace) upon 1 mM GTP addition in crowded conditions, compared to the measurement in absence of inhibitors (blue trace).*

Moreover, in addition to the turbidity measurements, the hyper-stabilization of *E. coli* FtsZ bundles was also studied through confocal microscopy, which allowed visualization of these structures and observation of their disassembly over time, in the same experimental conditions used in turbidity assays.

As shown in Figure 45, confocal images obtained with FtsZ (containing FtsZ-Alexa488 as tracer) showed that addition of GTP triggered the formation of bundles (as previously observed in turbidity measurements). In absence of our compounds, 60 minutes after GTP addition the complete bundle depolymerization occurs, due to GTP consumption.

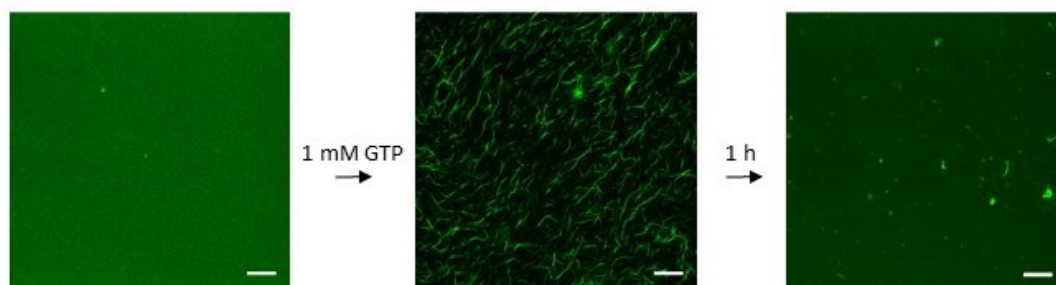


Figure 45: Confocal microscopy assay of FtsZ in absence of any inhibitor in crowded conditions. The white bar corresponds to 25 μm .

Conversely, when in presence of 20 μM **XIV** (Figure 46) or **XV** (Data not shown), *E. coli* FtsZ bundles remained abundant in the sample, even 60 minutes after GTP addition, as a consequence of the hyper-stabilizing effect mediated by the inhibitor.

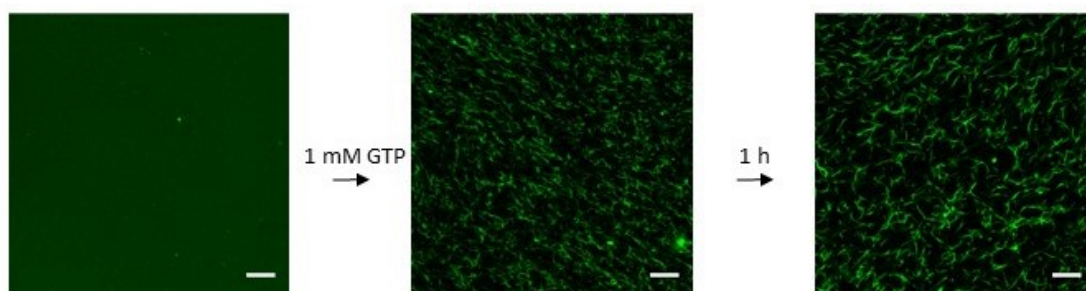


Figure 46: Confocal microscopy assay of FtsZ in presence of 20 μM **XIV** in crowded conditions. The white bar corresponds to 25 μm .

In conclusion, evaluating all this wide set of *in vitro* data, we could say the capability of benzodioxane-benzamides to interact also with *E. coli* FtsZ was satisfactory demonstrated. Moreover, it was shown how this interaction leads to the inhibition of the GTPase activity and to a reduction of the depolymerization process.

Considering that FtsZ rapid switching from the unassembled to the polymeric form is crucial for the correct development of the division process, this compound-mediated perturbation could represent the mechanism for a potential antimicrobial activity on *E. coli* and, hopefully, on other Gram-negative bacteria.

Structure-activity relationship exploration: fifth set of compounds

After having confirmed that benzodioxane-benzamides are capable of binding and productively interfere with crucial FtsZ properties and activities, the presence of efflux pumps on *E. coli* seem to represent the main limiting factor. Nonetheless, derivatives **XIV** and **XV** that showed the strongest activity *in vitro* do not show any significant antimicrobial activity on *E. coli* N43. Since this peculiar strain is characterized by being KO for AcrAB efflux pump, this inactivity suggests that more than one factor could be responsible for the inactivity of these compounds, such as the combination of poor permeability and being substrates of these efflux pumps. Indeed, keeping in mind also the hydrophilic nature of Gram-negative bacteria membrane, derivatives **XIV** and **XV** are characterized by a significant lipophilic structure (Figure 47). Moreover, this translates in poor water solubility that represents a strong limiting factor during the development of drugs.

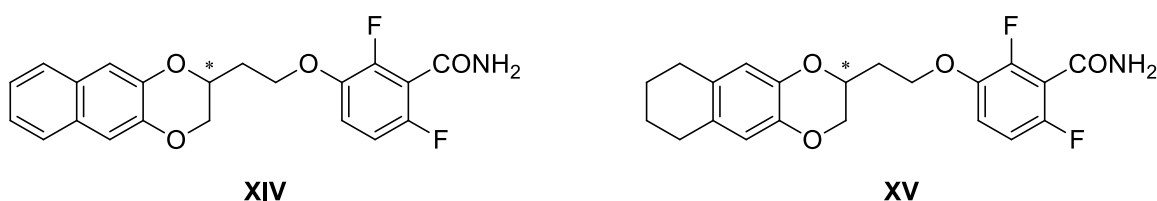


Figure 47: Structures of compounds **XIV** and **XV**, the derivatives that showed the strongest activity versus *S. aureus* as well as the best inhibition profile versus *E. coli*.

Therefore, a new set of derivatives characterized by a slight increased polarity could show a better Gram-negative membrane permeability profile, as well as better pharmacokinetic properties.

After the synthesis, purification and characterization, compounds **XXI**, **XXII** and **XXIII**, were tested as antimicrobials on MSSA and MRSA, thanks to the collaboration with Dr. Zanotto. In parallel, their antimicrobial activity versus *E. coli* N43 has been assessed, thanks to the collaboration with Prof. William Margolin from the University of Texas Health. Nonetheless, the antimicrobial evaluation now is still preliminary. Indeed, only compounds **Erythro-XXI** and **Threo-XXI** have been completely evaluated both on Gram-positive and Gram-negative bacteria. Their results, compared with the parent compound **XV**, are reported in Table 10.

Cpd	MSSA ATCC 29213			MRSA ATCC 43300			E. Coli N43
	MIC (µg/mL)	MBC (µg/mL)	MIC/MBC	MIC (µg/mL)	MBC (µg/mL)	MIC/MBC	MIC (µg/mL)
XV	0.1	0.1	1	0.1	0.1	1	>100
Erythro-XXI	5 < x < 10	5 < x < 10	1	5 < x < 10	5 < x < 10	1	1.8
Threo-XXI	10	10	1	10	10	1	7.5

Table 10: Biological evaluation of compound **XXI**, erythro and threo, as antimicrobial on both *S. aureus* and *E. coli*.

As clearly observable, while the introduction of the hydroxy group seems to be detrimental for the antimicrobial activity versus *S. aureus*, the results on *E. coli* N43 are outstanding. In the same conditions in which compound **XV** showed complete inactivity, both **Erythro-XXI** and **Threo-XXI** show high antimicrobial activity.

The completion of the biological evaluation of compounds **XXII** and **XXIII** will allow the further understanding of the role of the -OH in affecting the antimicrobial activity on both Gram-positive bacteria and Gram-negative bacteria, the toxicity and the pharmacokinetic properties of this class of compounds.

Inhibitors of RnpA

Structure-activity relationship exploration

As previously in-depth described, only a few molecular classes of compounds acting as RnpA inhibitors are so far known, mainly due to the novelty of the target. Moreover, all these classes were discovered through screening, and as a result their structure-activity relationship has been only scarcely explored.

Starting from these premises, the present work began with the development of a computational model, completely innovative for this protein. The computational work aimed at the identification of the possible binding site as well as of the main interaction achieved by the few known RnpA inhibitors. This information was exploited to design derivatives, hoping for higher antimicrobial potencies, higher synthetic accessibility, better pharmacokinetic properties, and lower toxicity.

Therefore, using the crystallographic information of the protein, the computational model was set up and a main potential binding site was identified, as previously described. The insights coming from the docking of the known inhibitors **RNPA2000** and **JC1/2** let us to modify their structures as previously described.

As fully detailed in the previous chapter, the structure of **JC2** has been modified in both the aromatic and the aliphatic moieties. In particular, the di-chlorophenyl ring has been replaced by 2-biphenyl, 3-biphenyl and 4-biphenyl one (Compounds **XXIV – XXVI**). The 2-methylpiperidine, which constitutes the ureidic portion, have been replaced by a tetrahydroquinoline and a tetrahydroisoquinoline (Derivatives **XXVII – XXVIII**).

Moreover, several modifications of **RNPA2000** were performed:

- The 2-furanyl moiety has been replaced with several mono and di-halogenated phenyl rings (Compounds **XXIX – XXXII**).
- The *p*-isopropyl moiety has been modified with a 4-biphenyl and a 2-naphthyl ones (Derivatives **XXXIII** and **XXXIV**).
- The thiosemicarbazide portion has been simplified and rigidified in different fashions (Compounds **XXXV – XL**).

In order to evaluate how the structural modifications affect the biological activity of these classes of compounds, derivatives **XXIV** to **XL** were firstly evaluated by the research group of Dr. Carlo Zanotto on two *S. aureus* strains: MSSA (ATCC 29213) and MRSA (ATCC 43300) by determining the minimum inhibitory concentration (MIC) and the results are reported in Table 11:

	MSSA ATCC 29213	MRSA ATCC 43300
	MIC (μM)	MIC (μM)
RNPA2000	44	44
XXIV	>500	>500
XXV	>500	>500
XXVI	>500	>500
XXVII	311	311
XXVIII	>500	>500
XXIX	21.1	21.1
XXX	24.7	24.7
XXXI	22.2	22.2
XXXII	>500	18.9
XXXIII	21.1	21.1
XXXIV	/	/
XXXV	>500	>500
XXXVI	>500	>500
XXXVII	>500	>500
XXXVIII	>500	>500
XXXIX	<i>Tbd</i>	<i>Tbd</i>
XL	<i>Tbd</i>	<i>Tbd</i>

Table 11: Results of the biological evaluation of derivatives **XXIV-XL**. *Tbd* = To be determined.

The results obtained from this first evaluation pointed out several insights:

- As shown by the activities of derivatives **XXIV**, **XXV**, **XXVI**, **XXVII** and **XXVIII**, any modification of **JC2**, already characterized by a low antimicrobial activity, lead to the complete loss of the effect.
- The modification of the 2-furanyl moiety of **RNPA2000** with a 3,5-chlorophenyl (**XXIX**), 3-chlorophenyl (**XXX**) and a 3-bromophenyl (**XXXI**) moiety led to a slight increase of the antimicrobial activity. Moreover, since the 2-furanyl moiety is known to be metabotoxic, these compounds are expected to possess a lower *in vivo*

toxicity than **RNPA2000**. Strangely, the 3,5-dibromophenylic derivative (**XXXII**) showed strong activity versus MRSA and complete inactivity versus MSSA. This discrepancy will surely deserve a deeper investigation.

- The modification of the *i*-propyl moiety of **RNPA2000** with a 4-biphenyl (**XXXIII**) one led to a similar increase of the activity, while the biological evaluation of derivative **XXXIV** was significantly hampered by the very low water solubility of the compound.
- Lastly, any simplification of the thiosemicarbazide moiety led to a complete loss of the antimicrobial activity. This suggests how, conversely to what predicted by the docking studies, this entire moiety is crucial for the activity versus RnpA.

Although none of the evaluated compounds shows a sub-micromolar antimicrobial activity, it is worthy to underline how derivatives **XXIX**, **XXX** and **XXXI** showed a 2-fold increase of the activity on both MSSA and MRSA, if compared to the reference compound. This enhancement in potency was achieved by productively replacing the undesired 2-furanyl moiety, hoping for a better tolerated structure. The cytotoxicity assays will confirm us this hypothesis.

In-vitro evaluation of the binding and inhibition of RnpA

This initial SAR exploration surely helped in increasing the knowledge behind these two classes of compounds. Nonetheless, we would like to confirm that the antimicrobial activities were indeed related to the desired inhibition of RnpA.

To do so and thanks to the collaboration with Prof. Paul M. Dunman, we resulted in evaluating the capability of these compounds to *in-vitro* inhibit both RnpA-mediated processes: ptRNA maturation and mRNA degradation.

For the first process, RNase P (RnpA + *rnpb*) was reconstituted and combined with the putative inhibitors. The relative quantities of ptRNA and mature tRNA were evaluated *via* Urea-PAGE. In Figure 48, the results of compounds **XXIX** and **XXX** are reported.

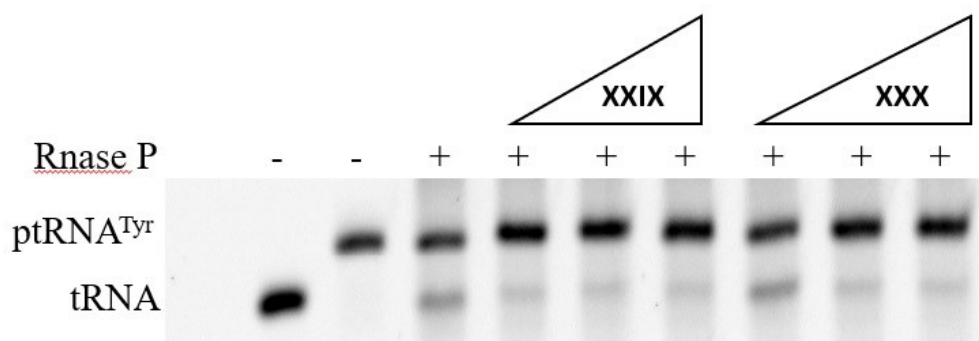


Figure 48: *in vitro* ptRNA maturation inhibition promoted by compounds **XXIX** and **XXX**.

As we can see, growing concentration (62.5 μ M, 250 μ M and 500 μ M) of **XXIX** or **XXX** are able to progressively diminish the maturation of ptRNA (second line) and, as a result, to mediate the accumulation of precursor tRNA (first line), clear symptom of RnpA inhibition.

For the second RnpA-mediated process, RnpA was incubated with the putative inhibitors in presence of fluorescently labelled mRNA substrates, which express fluorescence upon quencher removal through degradation. As we can see, RnpA efficiently degrades mRNA in presence of DMSO (negative control), while a certain degree of inhibition is observed in presence of the **XXX** and **XXXI** as putative inhibitors (Figure 49).

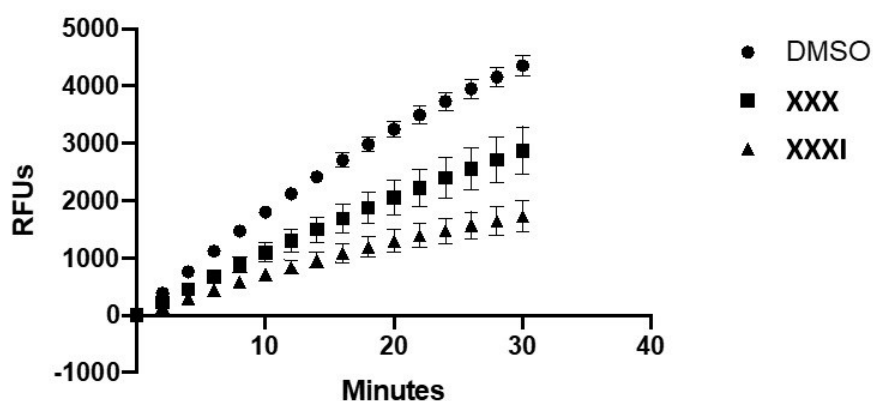


Figure 49: *in vitro* mRNA degradation inhibition promoted by compounds **XXX** and **XXXI**, both at 62.5 μ M.

These assays were performed for all the compounds, independently from the antimicrobial activity, and the results, described as IC_{50} , are showed in Table 12.

	Degradation IC ₅₀ (μM)	Processing IC ₅₀ (μM)
RNPA2000	275	140
JC2	180	200
XXIV	324	>500
XXV	233	37
XXVI	72.5	36
XXVII	66	50
XXVIII	>500	75
XXIX	53	59
XXX	77	28
XXXI	49	76
XXXII	/	/
XXXIII	188	33
XXXIV	/	/
XXXV	31	153
XXXVI	165	423
XXXVII	198	>500
XXXVIII	174	25
XXXIX	<i>Tbd</i>	<i>Tbd</i>
XL	<i>Tbd</i>	<i>Tbd</i>

Table 12: Degradation and processing IC₅₀ values of RnpA inhibition for all the compounds. *Tbd* = to be determined.

Interestingly, we noticed that the majority of our derivatives show a compound-dependent inhibition of the *in vitro* activity toward RnpA, even if, probably, for the most of them this inhibition is not enough to evoke a bactericidal effect.

These results underline how only compounds **XXXVI** and **XXXVII** show a better RnpA inhibition profile than **JC1**, but surprisingly only compound **XXXVII** possesses a weak antimicrobial activity, while the *in vitro* activity of **XXXVI**, unexpectedly, does not induce a similar promising antimicrobial potency.

Nonetheless it is important to notice how compounds **XXIX**, **XXX**, and **XXXI**, which showed a 2-fold increase of the antimicrobial activity of **RNPA2000**, also show a better *in vitro* inhibition profile, confirming and validating RnpA as the target of these compounds.

Cellular evaluation of RnpA inhibition

Finally, as a last step, the same evaluation performed *in vitro* on isolated RnpA was directly applied on clinically isolated *S. aureus* strains, checking also in this case the two RnpA-mediated processes individually.

To do so, starting from the evaluation of the ptRNA maturation inhibition potential, *S. aureus* cells were treated with 0,5X or 1X MIC for 1 hour and the quantity of ptRNA^{tyr} was measured *via* qRT-PCR. The results are reported in Figure 50 and compared with DMSO as negative control.

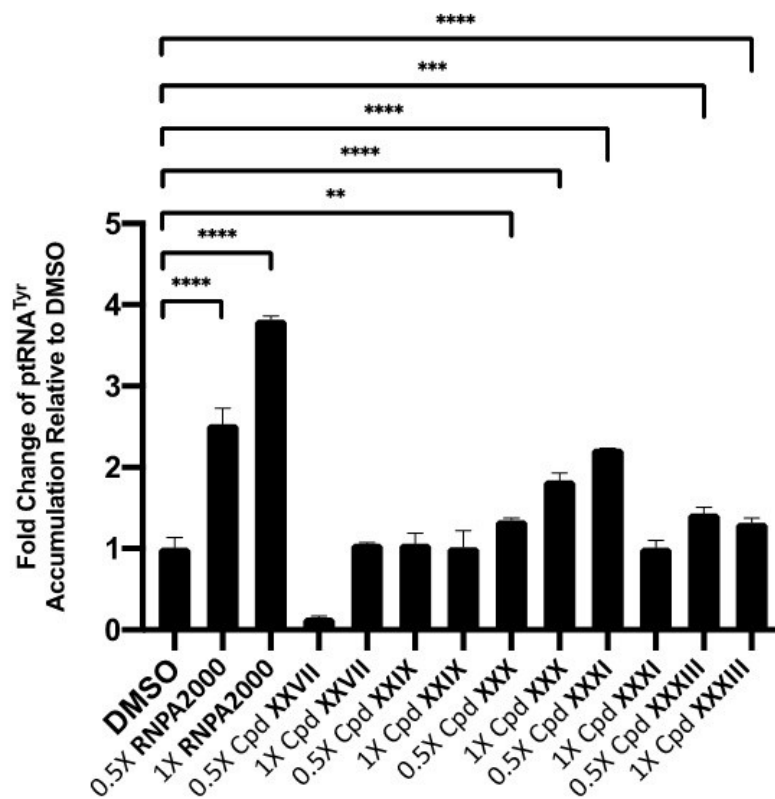


Figure 50: ptRNA accumulation cellular assay. Each compound was evaluated in replicates. One-way ANOVA test was performed: ** p -value<0.01, *** p -value=0.0001, **** p -value<0.0001.

In this assay, only compounds **XXX** and **XXXI** are able to promote ptRNA accumulation and none of them with a potency comparable to the reference compound **RNPA2000**.

The capability to inhibit the RnpA mediated mRNA degradation was also evaluated in cellular assays. *S. aureus* cells were treated with DMSO or 0.5X MIC of each tested inhibitor for 30 minutes before post-transcriptional arrest (PTA) with rifampin. *Spa* mRNA, a natural RnpA substrate, was therefore quantified via RT-PCR at 0- and 5-min PTA (Figure 51).

Conversely to what seen for ptRNA maturation, in this case both compounds **XXX** and **XXXI** reached potencies comparable to **RNPA2000**, suggesting that they rely mostly on inhibiting RnpA-mediated mRNA degradation, rather than ptRNA maturation, to evoke the antimicrobial activity.

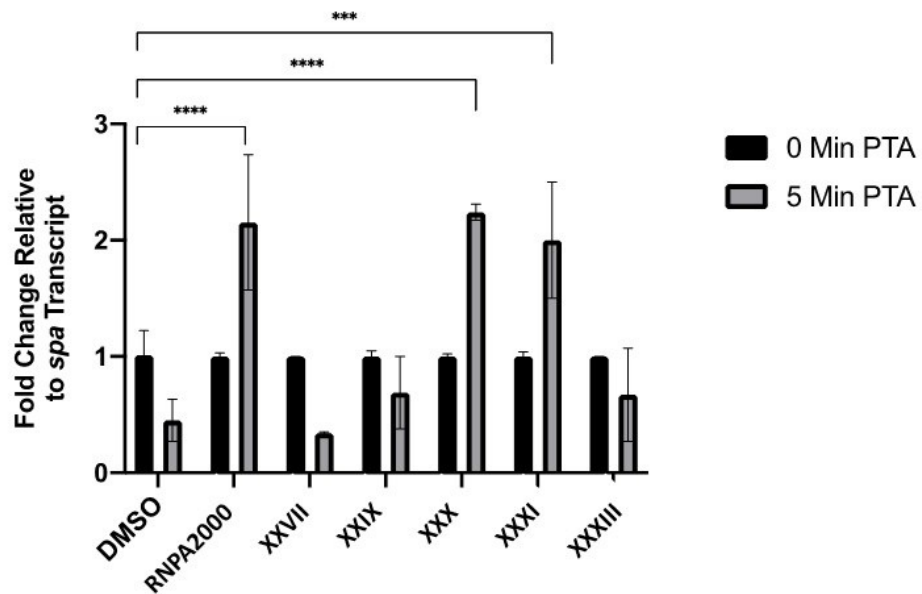


Figure 51: mRNA degradation cellular assay. Each compound was evaluated in replicates. One-way ANOVA test was performed: *** p -value <0.0005 , **** p -value <0.0001 .

CHAPTER 6 – CONCLUSIONS AND FUTURE WORK

Inhibitors of FtsZ

The present doctorate work on benzodioxane-benzamide allowed the obtainment of several insights on this class of compounds:

- High activities versus Gram-positive bacteria *S. aureus* and *B. subtilis* were achieved: derivatives **XIV** and **XV** are strong inhibitors of *Sa*-FtsZ and *Bs*-FtsZ and their potencies are up to 5-fold higher than the ones of previously known derivatives.
- Compound **XV**, which is one of the stronger compounds, is also characterized by a positive safety profile, with no evident toxicity *versus* human MRC-5 cells.
- The *in-vitro* evaluation on *E. coli* allowed to understand and demonstrate the capability of these derivatives to inhibit *E. coli* FtsZ in addition to *S. aureus* and *B. subtilis* FtsZs.
- The newest derivative **XXI**, more polar than its precursor, gained activity versus *E. coli* N43.

The obtainment of compound **XXI**, characterized by a significant activity versus *E. coli* N43, *S. aureus* and *B. subtilis*, as well as the *in vitro* demonstration of these derivatives to interact and to inhibit *E. coli* FtsZ, pave the way to FtsZ inhibitors as antibiotic agents having a broad spectrum of action. This non-limitation to only Gram-positive bacteria represents an important innovation for benzamides FtsZ inhibitors, since these last have been always considered as anti-staphylococcal agents with no activity on *E. coli*. We demonstrated our benzamide derivatives are able to affect *E. coli* FtsZ, even if they seem to be substrate of the efflux-pumps. If efflux-pumps will be confirmed to be the only limiting factor for the antimicrobial activity on this train, we could work on the co-administration of our compounds with Efflux-pumps inhibitors (EPIs), as a viable therapeutic tool.

Considering the outstanding activities presented by some of the developed compounds on Gram-positive strains, we aimed at assessing their pharmacokinetic properties, as well as testing them on animal models of drug-resistant infections. Moreover, since most of the presented compounds have been developed as racemates, the evaluation of the activity of the single enantiomers of the most interesting compounds will be performed, aiming at possibly identify the eutomers.

Inhibitors of RnpA

RnpA arose as potential target for the development of antimicrobials in the last decade, upon the discovery and definition of the role of RnpA within *Staphylococcus Aureus*, as well as its essentiality for the aggressive phenotype of the bacterium in exponential phase growth. For this reason, with the present work, we surely contributed to expand the knowledge about these important potential antibiotics, through the design of a novel computational model and of several molecules to expand the SAR. At the end of this work, it was possible to demonstrate, through the development of **XXX** and **XXXI**, how the substitution of 2-furanyl moiety with a mono-chlorophenyl or a mono-bromophenyl ring could achieve derivatives characterized by a higher antimicrobial activity, as well as better *in vitro* inhibition profile. Parallely, the activity of compound **XXXIII** also underlines how the *i*-propylphenoxy could also be replaced by the bigger 4-biphenyloxy moiety.

None of the obtained RnpA inhibitors still possess optimal characteristics or very high activities. Nonetheless, we aimed at further design and development of compounds showing both the 2-furanyl and the *i*-propyl moieties, to further study the SAR and potentially enhance the antimicrobial activity.

Overall conclusions

The design and development of new chemical entities able to act as antimicrobials on new molecular targets is considered one of the essential strategies, to fight antimicrobial resistance and, consequently, preserve the efficacy of the antibiotic therapy. The present PhD thesis contributed to the development of inhibitors of two essential bacterial proteins. FtsZ inhibitors have been deeply investigated, achieving strong compounds, potentially ready for a pre-clinical investigation and development. RnpA inhibitors, conceived as anti-staphylococcal agents, are promising and underdeveloped antimicrobials. The results obtained in the present work let the enhancement and the speed up of novel classes of compounds. We hope, one day, both these classes of inhibitors could really fight the worrying problem of antimicrobial resistance.

CHAPTER 7 – MATERIAL AND METHODS

Chemistry

The materials and synthetic methods are in-depth explained in the following chapter “Chemistry”.

FtsZ inhibitors: computation

Ligand preparation

The preparation of the compounds synthesized in this work was performed before carrying out further computational studies. The preparation, together with the two-dimensional-to-three-dimensional conversion, was performed using LigPrep, included in the Schrödinger software package. In the preparation, we generated different steps such as the addition of hydrogens, the calculation of the ionization state of the molecules at a specific pH or the generation of potential tautomers. Additionally, low-energy ring conformations were generated for every molecule, followed by a final energy minimization step using the OPLS-2005 force (Jorgensen, Maxwell and Tirado-Rives, 1996; Banks *et al.*, 2005). With the aim of mimicking cell conditions, physiological pH states were used to prepare the molecules, all of them were desalted and the compounds were minimized as default in the last step.

Protein preparation

The FtsZ crystal structure of *S. aureus* (PDB code: 5XDT) was used as the protein structure for the computational studies. The protein was prepared for docking studies following a protocol described in our previous study (Straniero, Sebastián-Pérez, *et al.*, 2020).

Docking studies

Docking studies were performed by employing the Glide module included in the Schrödinger software package. Once the protocol was validated in our previous studies (Straniero, Sebastián-Pérez, *et al.*, 2020), the FtsZ structure from *S. aureus* and the compounds synthesized in this work were used as a starting point for the analysis. Docking studies were performed applying the same protocol in terms of conformational search and evaluation parameters for all the molecules, considering the centre of the grid the centre of the previously crystallized ligand in the catalytic pocket. In the grid generation, a scaling factor of 1.0 in van der Waals radius scaling and a partial charge cut-off of 0.25 were used.

The extra precision (XP) mode with no constraints was applied during the docking (Friesner *et al.*, 2006). The ligand sampling was flexible, epik state penalties were added to the docking score and an energy window of 2.5 kcal/mol was utilized for ring sampling. In the energy minimization step, distance dependent dielectric constant was 4.0 with a maximum number of minimization steps of 100,000. In the clustering, poses were discarded as duplicates if both the RMS deviation was less than 0.5 Å and the maximum atomic displacement was less than 1.3 Å.

FtsZ inhibitors: *in vivo* evaluation

Antimicrobial activity evaluation on MSSA, MRSA and wt-*E. coli*

The antibacterial activity was tested on both a methicillin-sensitive and a methicillin-resistant *S. aureus* strain, and an ESBL *E. coli* clinical isolate. All the compounds were dissolved at the final concentration of 20 mg/mL in dimethyl sulfoxide (DMSO) and serially diluted in LB. Fresh cell cultures were used at 10⁵ cells/mL in a final volume of 2 mL. Each bacterial sample was grown with different compound concentrations that ranged from 100 to 0.1 µg/mL. After incubation at 37 °C for 16 h in aerobic culture tubes, the concentration of prokaryotic cells was determined by optical density measurement, at 600 nm (OD₆₀₀) in a SmartSpec™ 3000 spectrophotometer (Bio-Rad, Oceanside, CA, USA) to determine the MIC. To determine the MBC, the bacteria were then washed three times with LB, centrifuged at 900× g for 10 min at 4 °C, and the pellet resuspended in fresh LB. After overnight incubation at 37 °C, the absence of growth was confirmed by OD measurement. The presence of antibacterial activity, at any concentration tested, was established for values of absorbance < 0.1 OD₆₀₀. All tests were performed in quadruplicate and for each series of experiments, both positive (no compounds) and negative (no bacteria) controls were included.

Antimicrobial activity evaluation on MDRSA, *E. coli* N43 and *E. coli* D22

Antibacterial activities of compounds were determined by the broth microdilution method against MDRSA 11.7, MDRSA 12.1 and *E. coli* N43 following the European Committee on Antimicrobial Susceptibility Testing (EUCAST) recommendations and Clinical and Laboratory Standards Institute (CLSI) guidelines. Strains MDRSA ST-11.7 and ST-12.1 were obtained through the interlaboratory control organized by the EU Reference Laboratory—

Antimicrobial Resistance. Only data on their resistance to antibiotics are known, but other data are not available. Bacterial suspension of specific bacterial strain equivalent to 0.5 McFarland turbidity standard was diluted with cation-adjusted Mueller Hinton broth with TES (Thermo Fisher Scientific), to obtain a final inoculum of 10^5 CFU/mL. Compounds dissolved in DMSO and inoculum were mixed together and incubated for 20 h at 37 °C. After incubation, the minimal inhibitory concentration (MIC) values were determined by visual inspection as the lowest dilution of compounds showing no turbidity. Tetracycline was used as a positive control on every assay plate.

Antimicrobial activity evaluation on *B. subtilis*

The two *B. subtilis* strains used were WM3612 (JH642 amyE::Pxyl-gfp-gp56), described in Bhambhani et al. (Bhambhani *et al.*, 2021), and WM5126 (JH642 amyE::Pxyl-gfp-zapA), which is the same as strain FG347 (Gueiros-Filho and Losick, 2002). For spot viability assays on plates, compounds were diluted from DMSO stocks into molten LB agar as described above and mixed well before solidifying. WM3612 cultures were grown to early exponential phase in LB broth at 37 °C, then spotted directly or after 1:10 dilution into LB onto LB plates containing various concentrations of compounds. After allowing spots to air dry, plates were then incubated overnight at 34 °C and photographed. For fluorescence microscopy, overnight cultures of WM5126 were grown at 33 °C (after 1:200 dilution of overnight and addition of 0.1% xylose to induce expression of GFP-ZapA) for ~2 h until reaching a OD600 of ~0.2, then treated with no drug or with compounds **XIV** or **XV** diluted in water from stock solutions of 40 mg/mL (**XV**) or 27 mg/mL (**XIV**) in DMSO. Those dilutions (40 µg/mL in water) were then added at 1:100 or 1:50 to the cultures and grown for 1 h shaking at 33 °C prior to spotting on a thin layer of 1% agarose in phosphate buffered saline. Cells were imaged with differential interference contrast (DIC) and fluorescence using an Olympus BX100 fitted with a 100 × Plan Apochromat objective (N.A. 1.4) and a GFP filter set (Chroma). Images were acquired with CellSens software (Olympus) and DIC, and fluorescent images of the same field were overlaid using ImageJ.

Thiazolyl Blue Tetrazolium Bromide (MTT) Cytotoxicity Assay

Compounds showing an antibacterial activity at a concentration lower than 10 µg/mL were serially diluted in DMEM and tested on MRC-5 cells by the MTT cytotoxicity assay (Sigma, St Louis, MO, USA). Cells (10^4 cells/well) were tested in a 96-well plate, in quadruplicate,

using serially two-fold-diluted concentrations of the compound in 100 μ L DMEM medium. After a 24-h incubation, the compound was removed, and the cells were overlaid with 1 mg/mL MTT in 100 μ L serum-free DMEM for 3 h at 37 °C. The MTT solution was then replaced with DMSO for 10 min, and the absorbance was measured at 570 nm. The percentage of cytotoxicity was calculated by the formula $[100 - (\text{sample OD}/\text{untreated cells OD}) \times 100]$. The compound concentration reducing cell viability by 90% was defined as the TD90 cytotoxic dose. The “therapeutic index” (TI) was also determined and defined as the ratio between TD90 and the MBC values.

Transmission electron microscopy (TEM)

S. aureus ATCC 43300 (10^9 cells/mL) were cultured in the presence of **IX** and **DFNB** (positive control), at the same concentrations used for optical microscopy and, after 16 h incubation at 37 °C, the cells were harvested and processed for transmission electron microscopy. Untreated *S. aureus* was used as negative control. After centrifugation at 3100 \times g for 5 min at room temperature, pelleted bacteria were fixed in 2.5% glutaraldehyde (Polysciences, Warrington, PA) in 0.1 M Na cacodylate buffer, pH 7.4, for 1 h at 4 °C, rinsed twice and post-fixed in Na cacodylate-buffered 1% OsO₄ for 1 h at 4 °C. The samples were dehydrated through a series of graded ethanol solutions and propylene oxide and embedded in Poly/Bed 812 resin mixture. Ultrathin sections were obtained using a Reichert-Jung ultramicrotome equipped with a diamond knife. Samples were then stained with water-saturated uranyl acetate and 0.4% lead citrate in 0.1 M NaOH. The specimens were viewed under a Philips CM10 electron microscope.

FtsZ inhibitors: *in vitro* evaluation

E. coli FtsZ protein purification

Wild-type *E. coli* FtsZ was purified following the procedure previously described (Rivas *et al.*, 2000). FtsZ was overproduced in BL21 cells transformed with the plasmid pMFV56 by induction with 1 mM IPTG at 37 °C for 3 hours. The cells were lysed through sonication and centrifuged to obtain the soluble fraction containing FtsZ. The protein was then isolated through two calcium-induced precipitation cycles by addition of 20 mM CaCl₂ and 1 mM GTP at 30 °C followed by centrifugation and resuspension in buffer without calcium. Then, the protein was further purified by ionic exchange chromatography using a HiTrap Q HP

column and stored in aliquots at -80 °C. FtsZ obtained through this protocol was bound to GDP (Rivas *et al.*, 2000). Protein purity was verified by SDS-PAGE and its GTPase activity was determined by quantification of the inorganic phosphate released using BIOMOL® GREEN assay. The concentration of FtsZ was experimentally calculated from its molar absorption coefficients at 280 nm ($14000 \text{ M}^{-1} \text{ cm}^{-1}$).

Fluorescent labelling of FtsZ

FtsZ was covalently labelled in the amino groups with Alexa Fluor 488 succinimidyl ester dye as hereafter described. The polymerization of FtsZ was induced by addition of 2 mM GTP and 20 mM CaCl_2 prior to incubation with the reactive dye in order to avoid binding of the dye with regions involved in the polymerization. The mixture was incubated for 15 minutes at 30°C followed by centrifugation. Polymers were resuspended in buffer without CaCl_2 and the remaining free dye was removed through size-exclusion chromatography using a Hi-Trap desalting column. The degree of labeling, determined through spectroscopic quantification, ranged between 0.3 and 0.8 mol of fluorophore per mole of protein. The fractions with the labeled protein were pooled and stored at -80 °C in aliquots.

Fluorescent anisotropy binding experiments

Anisotropy experiments were conducted in a Spark® Multimode microplate reader (Tecan) at 25 °C with 485 and 530 nm excitation and emission filters, respectively, using 384 or 96 black polystyrene (non-binding surface), flat bottom microplates (Corning). To monitor the time-dependent FtsZ depolymerization, the anisotropy of the solution containing a tracer amount of FtsZ-alexa488 (50 nM), unlabeled FtsZ up to 10 μM (freshly dialyzed in 50 mM Tris-HCl, 300 mM KCl, 5 mM MgCl_2) and 40, 20 or 10 μM of the tested compound was recorded with time, after 2 mM GTP addition. Moreover, the anisotropy value was recorded in triplicates before GTP addition.

Turbidity measurements

The turbidity of samples (125 μl solutions) containing 10 μM FtsZ (freshly dialyzed in 50 mM Tris*HCl, 300 mM KCl, 5 mM MgCl_2), 20 μM of the tested compound, with dextran 500 (150 g/l) was determined at room temperature using a Varioskan Flash plate reader (Thermo). To monitor the time dependent FtsZ depolymerization, the absorbance at 350 nm was measured every 5 min for 70 min upon 1 mM GTP addition.

FtsZ inhibitors: confocal microscopy imaging

Preparation of bulk samples

The bulk samples to observe the depolymerization kinetics were prepared by simply adding freshly dialyzed FtsZ (1 μ M FtsZ-Alexa488 and unlabelled FtsZ up to 10 μ M) in 50 mM Tris*HCl, 300 mM KCl, 5 mM MgCl₂ in the buffer solution containing 150 g/L of dextran 500 as macromolecular crowder, with or without 20 μ M of the tested compound. The polymerization of GTP was achieved by addition of 1 mM GTP directly over the mixture.

Confocal microscopy measurements and data analysis

Bulk samples were visualized in silicone chambers (Molecular probes/Invitrogen) glued to coverslips. Image acquisition was performed with Leica TCS-SP2 or TCS-SP5 inverted confocal microscopes equipped with a HCX PL APO 63 \times oil immersion objective (N.A. = 1.4; Leica, Mannheim, Germany). 488 nm laser excitation lines were used to excite Alexa 488 dye. Multiple images were registered across each sample, corresponding to different observation fields. Brightfield and fluorescence images were taken simultaneously. Production of images was carried out with ImageJ (National Institutes of Health, USA).

RnpA inhibitors: computation

Hotspot maps

The Fragment Hotspot maps software identifies the location and environment of binding sites on the protein by first calculating atomic hotspots and then producing Fragment Hotspot maps while using simple molecular probes. These maps specifically highlight fragment-binding sites and their corresponding pharmacophores. For this reason and given the limited knowledge about ligand binding in this target, we applied hotspot maps to decipher the potential binding site for the set of molecules synthesized in this work. For this study, we used the crystal structure of *S. aureus* RNase P protein already available as 6D1R in the Protein Data Bank.

Computational studies

Automated docking was used to assess the potential binding pocket of the set of molecules together with their binding conformations. A Lamarckian genetic algorithm method that was implemented in the program, AutoDock 4.2 (Morris *et al.*, 2009), was employed. For

docking calculations, Gasteiger charges were added, rotatable bonds were set using AutoDock tools (ADT), and all of the torsions were allowed to rotate for the ligand. As a first approach, blind docking was carried out with the reference compounds **RNPA2000** and **JC1**, including all the receptor as part of the grid to assess the potential binding site of these compounds. For docking the compounds that were synthesized in this work, we used grid maps with a grid box size of 60-by-60-by-60 Å³ points and a grid-point spacing of 0.375 Å. The docking protocol consisted of 100 independent Genetic Algorithm (GA) runs, a population size of 200, and a maximum of 250,000 evaluations, while the other parameters were set as default. The final best-docked clusters, within the default 2.0-Å root mean square deviation (RMSD), according to the binding energies and relative population data provided by Autodock, were analyzed by visual inspection.

RnpA inhibitors: biological study

Bacterial growth conditions

Staphylococcus aureus strains UAMS-1 is a well-characterized antibiotic-susceptible osteomyelitis clinical isolate (Blevins Infect. Immun 2003). It was cultured in Mueller Hinton (MH) broth and processed. as described below. *Escherichia coli* strain BL21 (DE3) was cultured in Luria–Bertani (LB) and supplemented with ampicillin (50 µg mL⁻¹).

Antimicrobial susceptibility testing ATCC 29213 and ATCC 43300

The antibacterial activity was tested on both a methicillin-sensitive *S. aureus* strain (MSSA, ATCC 29213) and a methicillin-resistant *S. aureus* strain (MRSA, ATCC 43300). All of the compounds were dissolved in dimethyl sulfoxide (DMSO). Fresh cell cultures were used at 10⁵ cells/mL in a final volume of 2 mL. Each bacterial sample was grown with different compound concentrations at 37 °C for 16 h in aerobic culture tubes. The concentration of bacterial cells was then determined by optical density measurement, at 600 nm (OD₆₀₀) in a SmartSpec™ 3000 spectrophotometer (Bio-Rad, Oceanside, CA, USA). The presence of antibacterial activity, at any concentration tested, was established for values of absorbance.

RnpA protein purification

His-tagged RnpA was purified, as previously described (Eidem AAC 2015). *E. coli* BL21 (DE3) cells harboring plasmid pEXP5-nt containing a hexahistidine tag fused to the N-terminus of

S. aureus RnpA coding region were grown in LB supplemented with 50 µg mL⁻¹ ampicillin to OD₆₀₀ = 0.6 and then induced with 1 mM isopropyl β-d-1- Thiogalactopyranoside (IPTG) for 3 h to induce protein expression. *E. coli* cells were subjected to centrifugation at 3.488× g for 20 min at 4 °C and the cell pellet was resuspended in 20 mL buffer A (300 mM NaCl, 50 mM Na₂HPO₄, pH 7.4) containing a mini EDTA-free protease inhibitor tablet (Roche; Bradford, CT, USA) and 20 mM imidazole. Cells were mechanically lysed by three passes at 18,000 psi through a French Pressure Cell Press (SLM-Aminco; Pittsford, NY, USA) and cell debris was removed by centrifugation at 17,000× g for 10 min at 4 °C. Supernatants were collected, filtered through a 0.2 µM syringe filter, and then loaded onto a 5 mL HisPur cobalt column (ThermoFisher Scientific) using the BioRad Maximizer Duo-Flow Medium Pressure Chromatography System. The protein was eluted using an imidazole gradient (80 mM to 500 mM). Fractions were assessed for RnpA presence and purity via SDS-PAGE analysis, Coomassie staining, and Western blotting using an anti-His antibody (Invitrogen; Grand Island, NY, USA). His-RnpA was eluted off the column at imidazole concentrations ranging between 200–300 mM. Fractions that only contained bands corresponding to His-RnpA were pooled and stored at 4 °C. No additional dialysis or concentration protocols were implemented. ptRNA processing assays were performed with RnpA and ptRNA substrate in the absence of rnpB, as controls to eliminate the possibility that the protein preparation contained undetected contaminating RNase proteins. Because ptRNA processing requires the RNase P enzyme (RnpA+rnpB), no processing activity was detected with RnpA alone, which confirmed the absence of contaminating RNases (data not shown).

In-Vitro transcription of RNA

RnpB and RNA substrates (*spa*, ptRNATyr) for RnpA functional assays, as well as mature tRNA, were synthesized in vitro, as previously described (Eidem AAC 2015). Each gene was PCR amplified using *S. aureus* UAMS-1 chromosomal DNA as a template and the corresponding oligonucleotide primer pairs, in which the forward primers contained an RNA polymerase T7 promoter sequence. The following primer pairs were used in this study (T7 promoter underlined): T7-rnpB forward—GAT TAC ATA ATA CGA CTC ACT ATA GGG TGA TAT TTC GGG TAA TCG CTA TA and rnpB reverse—ACT AGT AGT GAT ATT TCT ATA AGC CAT G; T7-ptRNATyr forward—GAT TAC ATA A TA CGA CTC ACT ATA GGG CAC CAT TTA TGG AGG GGT AGC G and ptRNATyr reverse—TGGTGGAG GGGGGCAGATTC; T7-*spa* forward—GAT TAC ATA ATA CGA CTC ACT ATA GGG TTA TAG TTC GCG ACG ACG TCC AG and *spa* reverse—

TTG AAA AAG AAA AAC ATT TAT TCA ATT CGT AAA CTA GG. The resulting PCR products were analyzed on a 0.8% agarose gel and then purified using the Qiagen QIAquick Gel Extraction kit, according to the manufacturer's instructions. In-vitro transcription was performed using the TranscriptAid T7 High Yield Transcription kit (Fermentas; Burlington, ON, Canada) following the manufacturer's instructions. Following in-vitro transcription, the RNA was treated with DNase I for 90 min and then re-purified using the Qiagen RNeasy Mini kit. RNA was quantified using a NanoDrop2000 spectrophotometer.

In vitro ptRNA processing assays

S. aureus RNase P activity assays were performed as previously described (Eidem AAC 2015). Briefly, ptRNATyr and rnpB RNA was denatured by heating at 95 °C for 5 min and then slowly cooled to RT. RNA species were then combined with 2 × low salt buffer (50 mM Tris-HCl pH 8.0, 5 mM MgCl₂) and incubated for 5 min at 37 °C. RNase P was reconstituted by mixing an equal molar ratio of His-RnpA and rnpB for 15 min at 37 °C. Precursor tRNA processing inhibition reactions were performed by combining 5 pmol of reconstituted RNase P with DMSO (negative control) or compound and incubating for 5 min at 37 °C. 5 pmol ptRNATyr was added to each reaction and incubated for an additional 30 min at 37 °C. Reactions were stopped with 2 × RNA loading dye (Thermo Scientific) and heating at 65 °C for 10 min. The samples were electrophoresed on a 7 M urea/8% polyacrylamide gel and then stained with 0.5 µg mL⁻¹ ethidium bromide. The BioRad EZ Gel Doc imaging system was used to visualize the RNA and the relative abundance of mature tRNATyr in the DMSO control or in the samples containing the compound. Samples were analyzed using the BioRad Image Lab densitometry software. The percent inhibitory activity of each compound was calculated using the following equation: (% experimental processing/% processing negative control) × 100.

In vitro mRNA degradation assays

RnpA-mediated degradation was assessed using the RNase Alert QC System (ThermoFisher Scientific). His-RnpA (20 pmol) was combined with 0.4 µM (final concentration) FRET substrate and either DMSO (negative control) or compound (≤500 µM in 1 × RNase Alert Buffer). Reactions were assembled in 96-well PCR plates (BioRad) and incubated at 37 °C for 30 min in the BioRad CFX 96 Connect Real Time instrument, measuring fluorescence every 2 min at 490 nm excitation/520 nm emission. Percent inhibition of each compound

was calculated at the 30 min time-point based on the following formula: (RFU of compound treated RnpA/RFU of DMSO-treated RnpA) × 100.

Cellular tRNA^{Tyr} population measures

Cellular *S. aureus* tRNA^{Tyr} pools were measured, as previously described (Colquhoun Antibiotics 2019). Briefly, *S. aureus* was grown to OD₆₀₀ = 0.18 in MHB and then treated with DMSO (negative control), 0.5× or 1× MIC of the indicated compound for 1 h with shaking at 37 °C. The culture was removed, combined with an equal volume of acetone:ethanol (1:1 v/v), and stored at –80 °C.

Cellular mRNA turnover assays

S. aureus RNA half-life determinations were performed, as described (Eidem AAC 2015). Briefly, *S. aureus* UAMS-1 was grown to an optical density of 0.18 at 600nm in MHB and then treated with DMSO (negative control) or 0.5× MIC of the indicated compound for 30 min with shaking at 37 °C. To inhibit de novo RNA synthesis, rifampin (Alfa Aesar, Haverhill, MA, USA) was added to the culture at a final concentration of 200 µg mL⁻¹. Half of the culture was immediately removed and combined with an equal volume of ice-cold acetone:ethanol (1:1 v/v). The remainder of the culture was returned to the 37 °C incubator for an additional 5 min and then combined with an equal volume of ice-cold acetone: ethanol (1:1 v/v) and stored at –80 °C.

Bacterial RNA Isolation and Quantitative Reverse Transcription Polymerase Chain Reaction (qRT-PCR)

Cell suspensions in acetone:ethanol were thawed on ice and centrifuged at 1560× g for 10 min at 4 °C. Acetone:ethanol was decanted and the pellets were air-dried for 5 min. Cell pellets were resuspended in 500 µL ice-cold TE buffer (10 mM Tris-HCl, pH 8.0, 1 mM EDTA) and transferred to FastPrep Lysing Matrix B tubes (MP Biomedicals, Santa Ana, CA, USA). Mixtures were homogenized at 5 m·s⁻¹ for 20 s, rested on ice for 5 min, then homogenized again at 4.5 m·s⁻¹ for 20 s in a FastPrep-24 instrument. Cell lysates were centrifuged at 16,200× g for 15 min at 4 °C to remove cell debris. The total bacterial RNA and tRNA^{Tyr} populations were isolated from the supernatant using Qiagen RNeasy Mini kits and miRNeasy kits, respectively, following the manufacturer's recommendations (Germantown, MD, USA). For qRT-PCR, 2 µg of RNA substrate was treated with two units

of DNaseI (New England Biolabs, Ipswich, MA, USA) for 1 h at 37 °C and then re-purified using Qiagen RNeasy Mini kits, following the manufacturer's instructions. RNA was measured for concentration and quality using a NanoDrop spectrophotometer. Quantabio (Beverly, MA, USA) qScript cDNA Supermix was used to convert 200 ng of RNA into cDNA, following the manufacturer's instructions, which was subsequently amplified using Quantabio SYBR Green Fast Mix following the manufacturer's instructions. Fluorescence was read on the BioRad (Hercules, CA, USA) CFX 96 Connect Real Time Machine. The transcript levels were compared to the internal control 16S rRNA ($\Delta\Delta C_t$) and plotted as fold change compared to the control. The following primer pairs were used in this study for qRT-PCR: spa forward—GCA GAT AAC AAA TTA GCT GAT AAA AAC AT; spa reverse—CTA ACG CTA ATG ATA ATC CAC CAA ATA C; -15 ptRNATyr forward—TTA ACT GAA TAA GCT GGA GGG G; tRNATyr reverse—TGG TGG AGG GGG GCA GAT TC; 16S rRNA forward—TAA CCT ACC TAT AAG ACT GGG ATA A; 16S rRNA reverse—GCT TTC ACA TCA GAC TTA AAA A.

CHAPTER 8 – CHEMISTRY

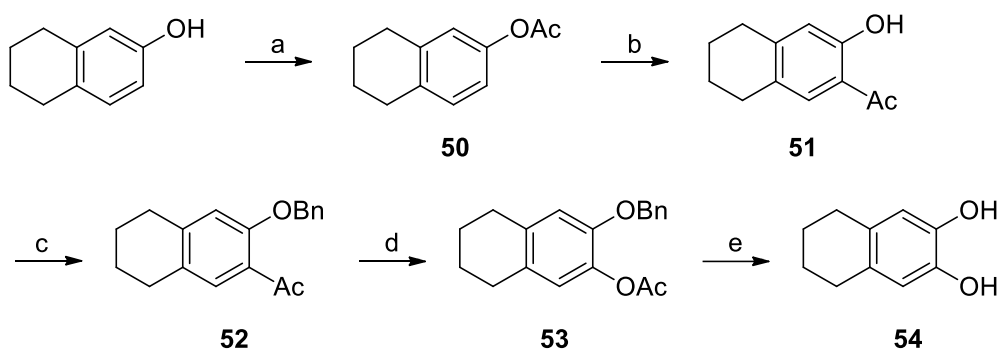
All the reagents and solvents were purchased from commercial suppliers (Merck, Fluorochem and TCI) and used without further purifications. Silica gel matrix, with fluorescent indicator 254 nm, was used in analytical thin-layer chromatography (TLC on aluminum foils), and silica gel (particle size 40–63 μm , Merck) was used in flash chromatography on Sepachrom Puriflash XS 420. Visualizations were accomplished with UV light (λ 254 or 280 nm). The ^1H -NMR spectra were measured by Varian Mercury 300 NMR spectrometer/Oxford Narrow Bore superconducting magnet operating at 300 MHz. The ^{13}C -NMR spectra were acquired operating at 75 MHz. Chemical shifts (δ) are reported in ppm relative to residual solvent as the internal standard. Signal multiplicity is used according to the following abbreviations: s = singlet, d = doublet, dd = doublet of doublets, t = triplet, q = quadruplet, dq = doublet of quadruplets, m = multiplet, bs = broad singlet, and set = septuplet. Melting points were measured with on a TA Q20 DSC system; Chromatographic purifications were performed, in normal phase, using PuriFlash xs 420 Interchim over different disposable chromatography cartridges; HPLC analysis were performed using VWR-Hitachi LaChrom Elite[®] HPLC System, with Diode Array Detector (190-400 nm), using a Water XBridgeTM C18 column (5 μm , 4.6x150 mm).

Considering the noticeable number of compounds evaluated in the present work, several synthetic schemes have been developed and applied. When appropriated, a flexible synthetic way was designed and used for the obtainment of several derivatives (for instance compounds **XXIX** to **XXXII**). Nonetheless, the majority of the compounds required a peculiar synthetic pathway for their obtainment.

Inhibitors of FtsZ

Synthesis of 5,6,7,8-Tetrahydronaphthalen-2,3-diol

For the obtainment of compounds **II**, **XV**, **XXI** and **XXIII**, the synthesis required the 5,6,7,8-Tetrahydronaphthalen-2,3-diol (**54**) as starting material, not commercially available.

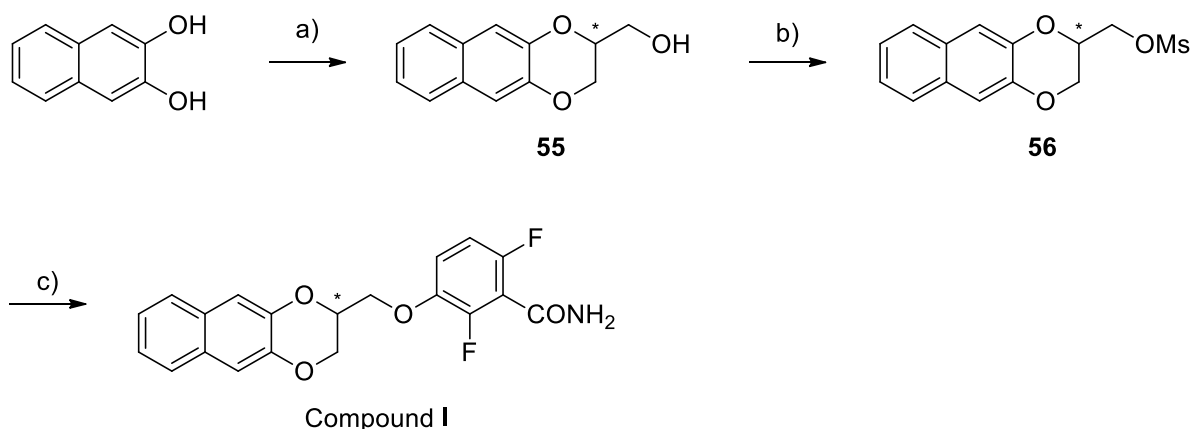
Scheme 1 | Synthesis of intermediate **54**: 5,6,7,8-Tetrahydronaphthalen-2,3-diol.

Reagents and conditions: a) CH_3COCl , Pyridine, DCM, RT; b) AlCl_3 , 1,2-dichlorobenzene, 100°C ; c) BnBr, TBAB, DCM, 2,5N aq. NaOH, RT; d) *m*-CPBA, DCM, RT; e) 1) 2,5N aq. NaOH, MeOH, RT; 2) H_2 , 10% Pd/C, MeOH, RT.

The obtainment of intermediate **54** (Scheme 1) started from the commercially available 5,6,7,8-Tetrahydronaphthalen-2-ol and partially resembled the synthesis described by Bolchi and co-workers (Bolchi *et al.*, 2004). The phenolic function was firstly acylated (**50**) and subsequently underwent to Fries transposition to achieve intermediate **51**. This intermediate was then protected through benzylation (**52**) and later oxidated to give **53**. Complete deprotection of both the phenolic functions led to intermediate **54**.

Synthesis of first set compounds: derivatives I and II

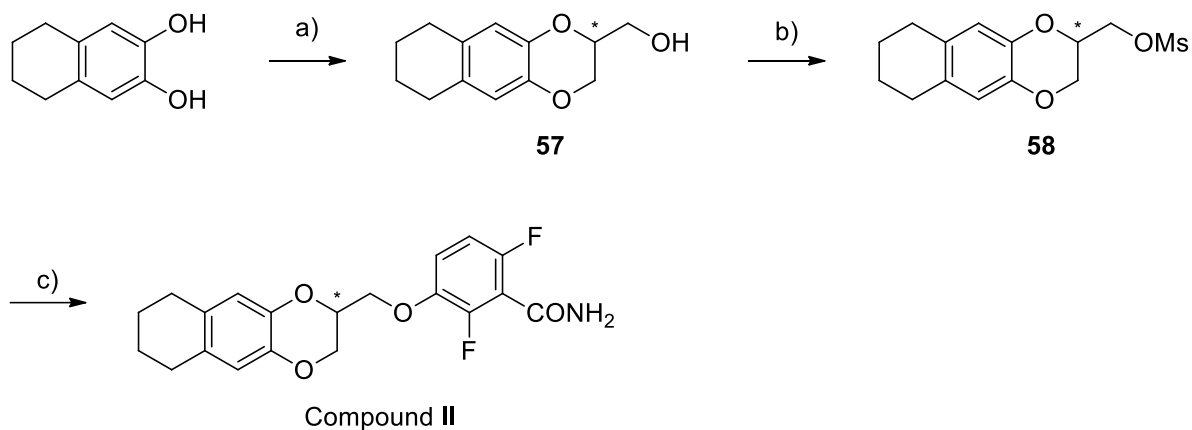
The synthesis of compounds **I** and **II** proceed with the same steps. For compound **I** (Scheme 2), the synthetic pathway starts from the commercially available Naphthalen-2,3-diol, reacting with Epibromohydrin, in order to obtain the 1,4-naphthodioxane ring (**55**). This first intermediate has been mesylated (**56**) and successively substituted by the 2,6-difluoro-3-hydroxybenzamide, which represents the pharmacophoric group.

Scheme 2 | Synthesis of compound **I**.

Reagents and conditions: a) Epibromohydrin, K_2CO_3 , Acetone, RT; b) MsCl, TEA, DCM, RT; c) 2,6-difluoro-3-hydroxybenzamide, K_2CO_3 , DMF, $80^\circ C$.

Compound **II** (Scheme 3) was achieved following the same synthetic scheme just described for derivative **I** but starting from intermediate **54**, described above.

Scheme 3 | Synthesis of compound **II**.

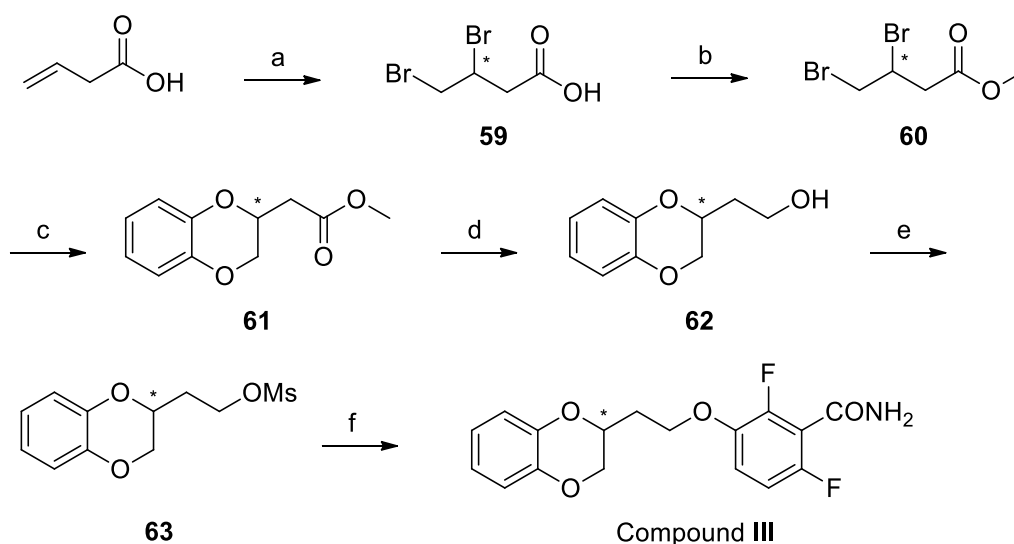


Reagents and conditions: a) Epibromohydrin, K_2CO_3 , Acetone, RT; b) MsCl, TEA, DCM, RT; c) 2,6-difluoro-3-hydroxybenzamide, K_2CO_3 , DMF, $80^\circ C$.

Synthesis of second set compounds: derivatives **III** to **VIII**

For the obtainment of derivative **III** (Scheme 4), the commercially available Catechol was reacted with the *ad-hoc* synthesized Methyl 3,4-dibromobutirrate (**60**), obtained in two steps starting from the 3-Butenoic acid. The resulting intermediate **61** was then reduced with $LiAlH_4$ (**62**), mesylated (**63**) and substituted with the 2,6-difluoro-3-hydroxybenzamide to give compound **III**.

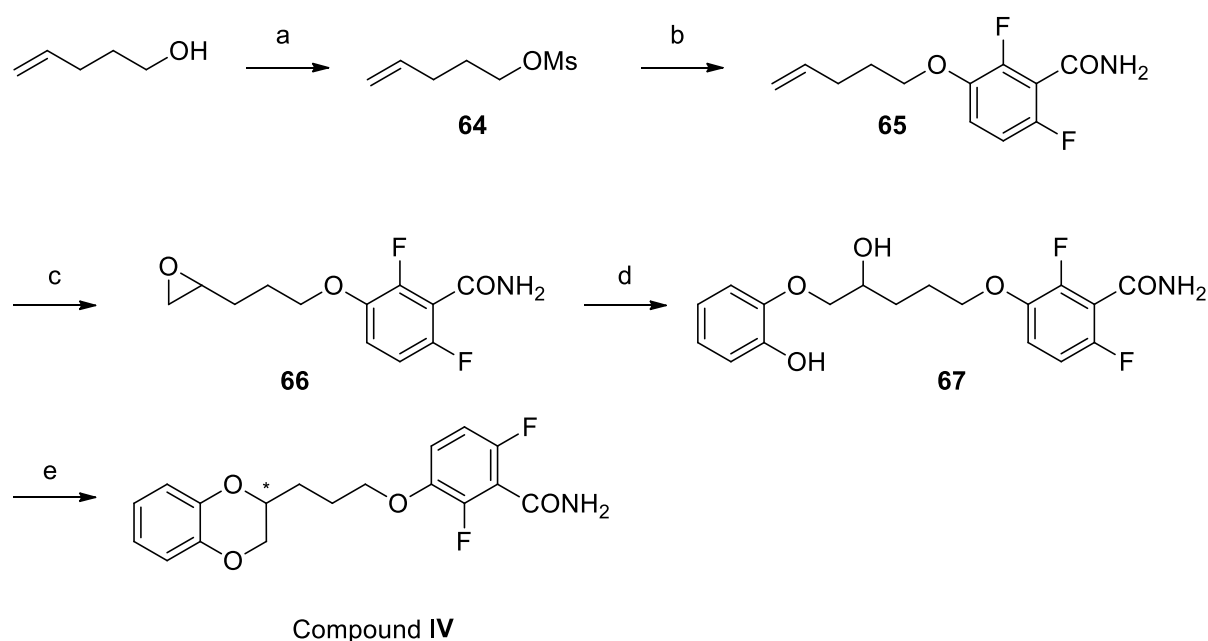
Scheme 4 | Synthesis of compound **III**.



Reagents and conditions: a) Br₂, DCM, RT; b) Trimethylorthoformate, MeOH, H₂SO₄, Reflux; c) Catechol, K₂CO₃, Acetone, Reflux; d) LiAlH₄, THF, RT; e) MsCl, TEA, DCM, RT; f) 2,6-difluoro-3-hydroxybenzamide, K₂CO₃, DMF, 80°C.

The synthesis of compound **IV** (Scheme 5) starts from the 4-Penten-1-ol, commercially available, that underwent through mesylation (**64**) and substitution with the pharmacophoric group (**65**). Successively, the double bond was epoxidated (**66**) with *m*-CPBA and the oxirane opened with Catechol (**67**). Lastly, the intramolecular Mitsunobu reaction allowed the obtainment of the final compound **IV**.

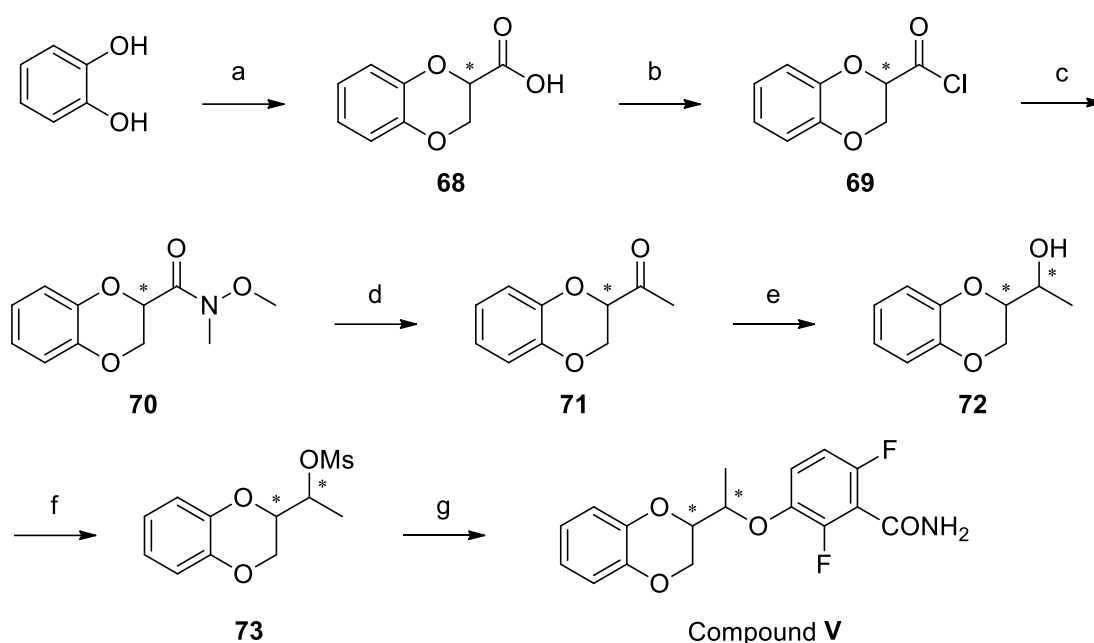
Scheme 5 | Synthesis of compound **IV**.



Reagents and conditions: a) MsCl, TEA, DCM, RT; b) 2,6-difluoro-3-hydroxybenzamide, K₂CO₃, DMF, 80°C c) *m*-CPBA, DCM, RT; d) Catechol, NaH, DMF, 100°C; e) Triphenylphosphine, DEAD, THF, 60°C.

The obtainment of compound **V** (Scheme 6) starts with the achievement of the 1,4-benzodioxane ring from the reaction between Catechol and Ethyl 2,3-dibromopropionate, followed by ester hydrolysis (**68**). The carboxylic function was then converted into a Weinreb amide through acyl chloride formation (**69, 70**). The amide group was then converted into a methyl ketone (**71**), reduced (**72**), mesylated (**73**) and substituted with the pharmacophoric group, achieving derivative **V**. The separation of the *Erythro* and the *Threo* diastereomers was achieved through flash chromatography on silica gel.

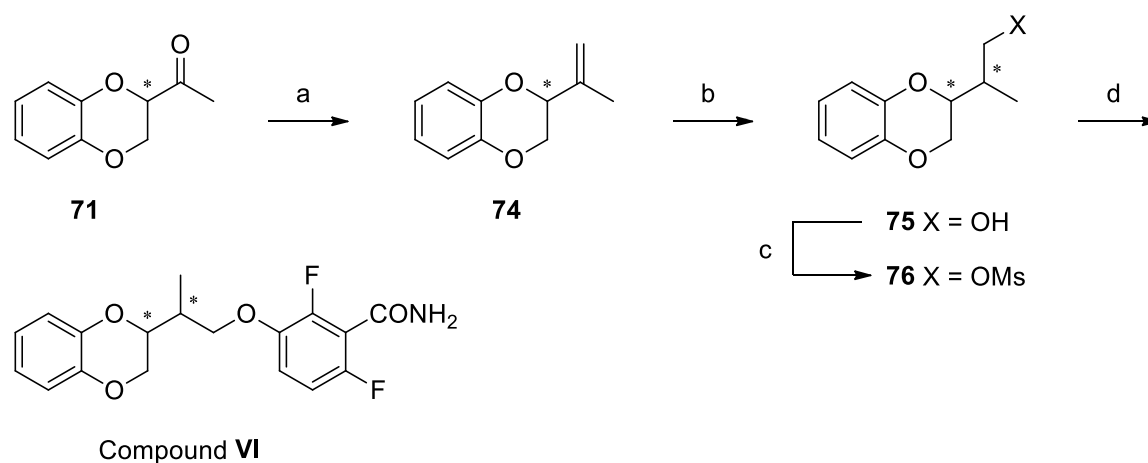
Scheme 6 | Synthesis of compound V.



Reagents and conditions: a) Ethyl 2,3-Dibromopropionate, K_2CO_3 , Acetone, NaOH 10%, MeOH, $60^\circ C$; (b) $SOCl_2$, DCM, $40^\circ C$; (c) *N,O*-dimethylhydroxyl amine hydrochloride, DCM, RT; (d) CH_3MgBr , THF, RT; (e) $NaBH_4$, MeOH, $0-5^\circ C$; (f) TEA; MsCl, DCM, RT; (g) 2,6-difluoro-3-hydroxybenzamide, K_2CO_3 , DMF, $80^\circ C$.

The synthesis of compound **VI** (Scheme 7) begins with the intermediate **71** described for the obtainment of compound **V** and undergoes into a similar synthetic pathway. The initial Wittig reaction allows the conversion of the ketone group into an olefinic group, which has been successfully anti-Markovnikov hydrated *via* hydroboration-oxidation. As mentioned before, this alcoholic intermediate (**75**) yields to the desired compound through the same reactions described for compound **V**. In this case, the two diastereomers have been separated *via* HPLC.

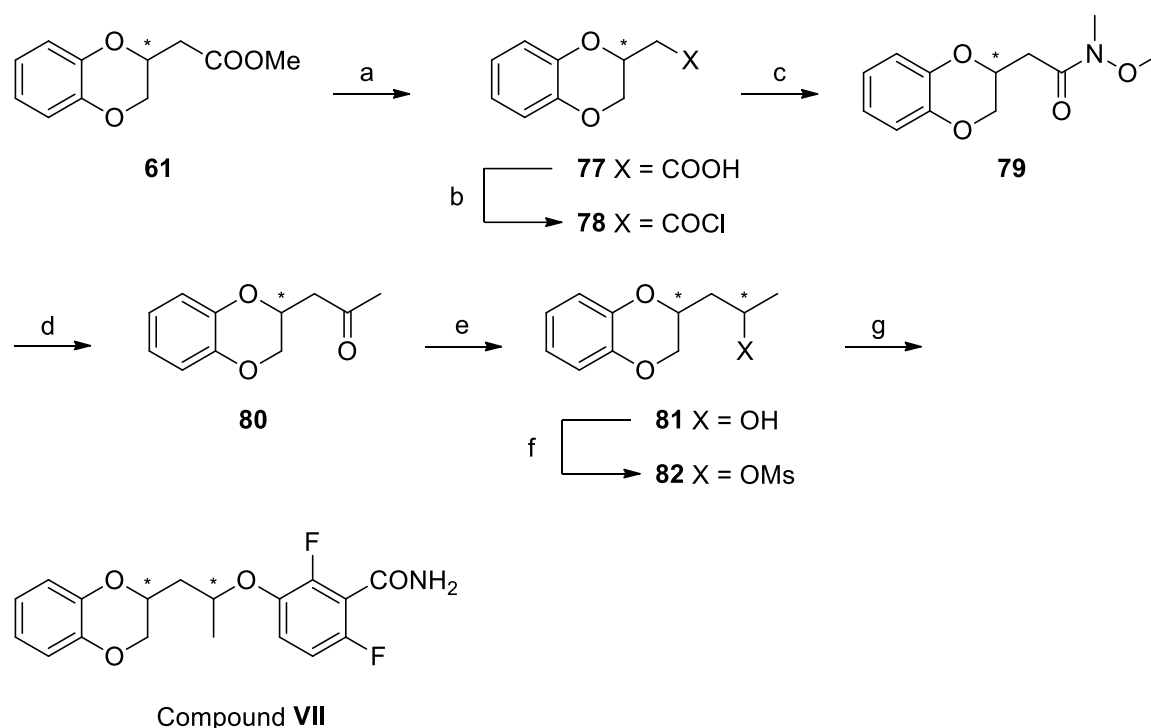
Scheme 7 | Synthesis of compound VI.



Reagents and conditions: a) Methyltriphenylphosphonium bromide, *t*-BuOK, THF, RT; b) 1M BH₃/THF, H₂O, NaOH, H₂O₂, THF, RT; c) MsCl, TEA, DCM, RT; d) 2,6-difluoro-3-hydroxybenzamide, K₂CO₃, DMF, 80°C.

The initial reaction for compound **VII** (Scheme 8) is the conversion of intermediate **61** into the corresponding methyl ketone *via* hydrolysis of the ester group followed by the Weinreb ketones synthesis (**80**). The ketone undergoes through reduction (**81**), mesylation (**82**) and nucleophilic substitution in order to introduce the pharmacophoric group. In this case the separation of the two diastereomers was not possible using the same conditions described before.

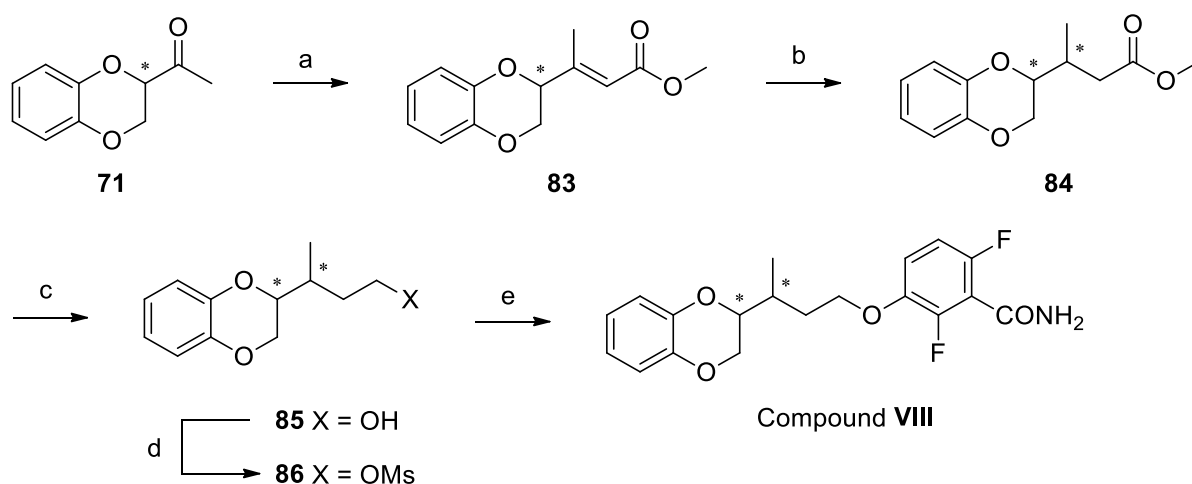
Scheme 8 | Synthesis of compound **VII**.



Reagents and conditions: a) 10% aq. NaOH, MeOH; b) SOCl₂, DCM, reflux; c) *N,O*-Dimethylhydroxylamine hydrochloride, DCM, RT; d) CH₃MgBr, THF, RT; e) NaBH₄, MeOH, 0°C; f) MsCl, TEA, DCM, RT; g) 2,6-difluoro-3-hydroxybenzamide, K₂CO₃, DMF, 80°C.

The synthetic scheme applied for the obtainment of compound **VIII** (Scheme 9) starts from the intermediate **71**, whose synthesis was previously described. This derivative undergoes Wittig-Horner reaction to afford the α,β -unsaturated methyl ester (**83**). The following hydrogenation of the unsaturation (**84**), reduction of the ester group (**85**), mesylation (**86**) and condensation with the pharmacophoric benzamide allowed the obtainment of the desired compound. Also in this case, the two diastereomers have been separated *via* HPLC.

Scheme 9 | Synthesis of compound VIII.

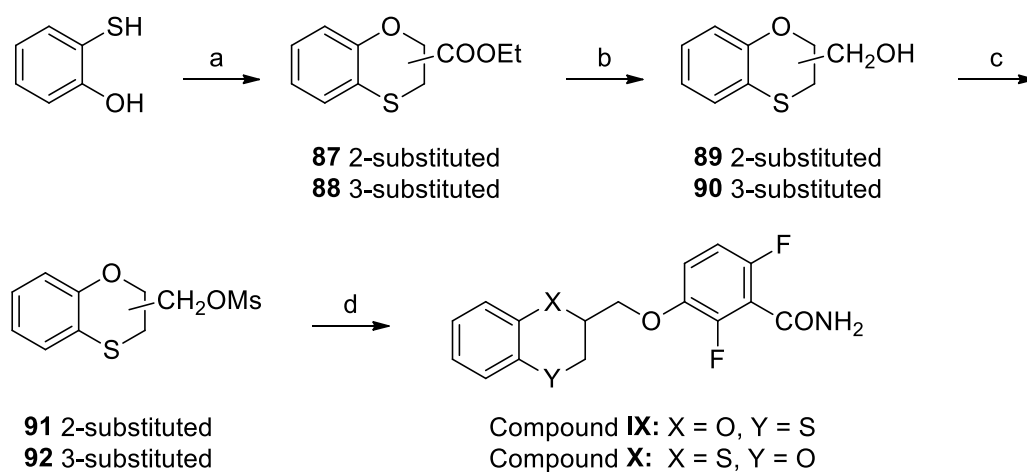


Reagents and conditions: a) Methyl (2-methoxyphosphoryl)acetate, NaH, THF, RT; b) H₂, Pd/C, MeOH, RT; c) LiAlH₄, THF, RT; d) MsCl, TEA, DCM, RT; e) 2,6-difluoro-3-hydroxybenzamide, K₂CO₃, DMF, 80°C.

Synthesis of third set compounds: derivatives IX to XIII

The obtainment of compounds **IX** and **X** (Scheme 10) starts with the reaction between the 1,2-Mercaptophenol with the Ethyl 2,3-dibromopropionate that gives a mixture of Ethyl 1,4-benzoxathian-2-carboxylate and Ethyl 1,4-benzoxathian-3-carboxylate (**87**, **88**). The whole mixture underwent through reduction (**89**, **90**), mesylation (**91**, **92**) and substitution with the pharmacophoric group to give the desired compounds, isolated through flash chromatography on silica gel.

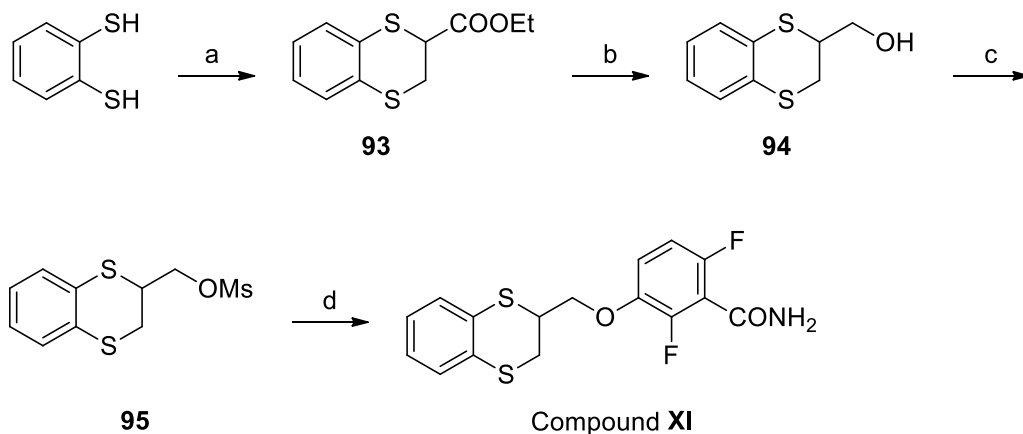
Scheme 10 | Syntheses of compounds IX and X.



Reagents and conditions: a) Ethyl 2,3-Dibromopropionate, TEA, DMF, RT; b) LiAlH₄, THF, RT; c) MsCl, TEA, DCM, RT; f) 2,6-difluoro-3-hydroxybenzamide, K₂CO₃, DMF, 80°C.

The synthesis of compound **XI** (Scheme 11) starts from the commercially available Benzene-1,2-dithiol, which underwent to the same reaction described for derivatives **IX** and **X**.

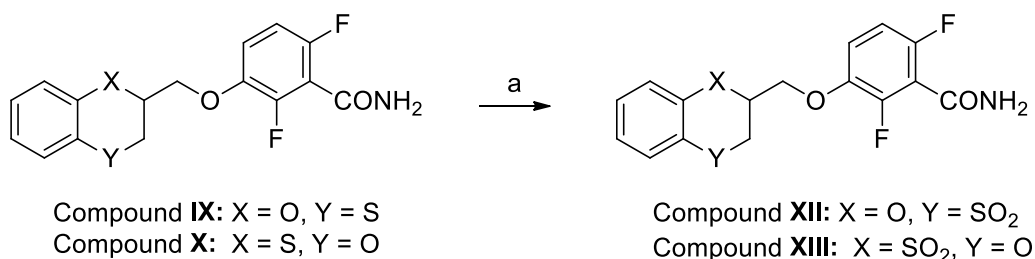
Scheme 11 | Synthesis of compound **XI**.



Reagents and conditions: a) Ethyl 2,3-Dibromopropionate, TEA, ACN/H₂O, RT; b) LiAlH₄, THF, RT; c) MsCl, TEA, DCM, RT; f) 2,6-difluoro-3-hydroxybenzamide, K₂CO₃, DMF, 80°C.

Lastly, for the obtainment of the two last derivatives belonging to the third set, **XII** and **XIII**, the synthesis starts from the final compounds **IX** and **X** that were simply oxidated with *m*-CPBA (Scheme 12).

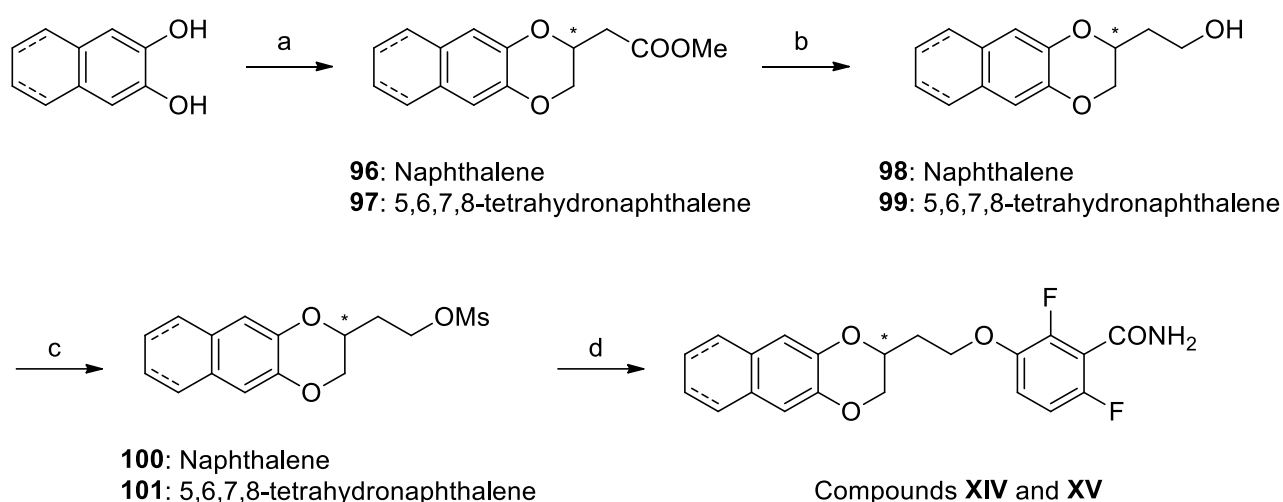
Scheme 12 | Syntheses of compounds **XII** and **XIII**.



Reagents and conditions: a) *m*-CPBA, DCM, RT.

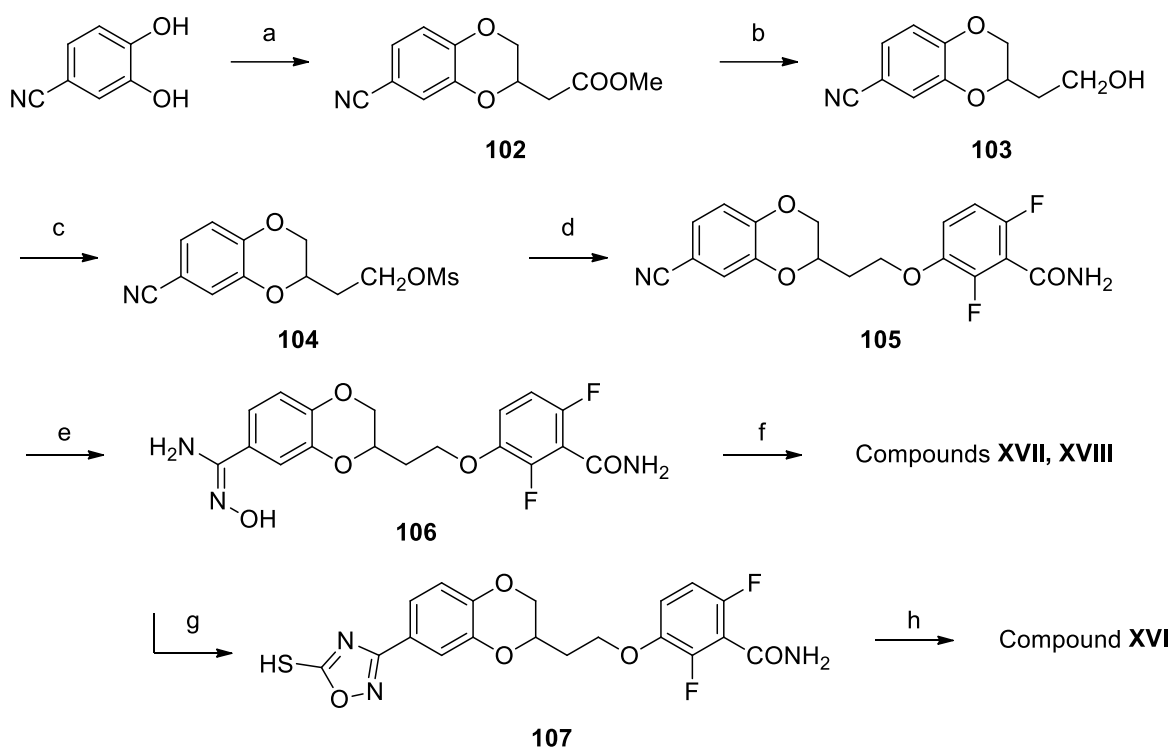
Synthesis of fourth set compounds: derivatives **XIV** to **XX**

For the obtainment of derivatives **XIV** and **XV** (Scheme 13), the synthesis resembles the one applied for the obtainment of compound **III**, starting from Naphthalen-2,3-diol and 5,6,7,8-Tetrahydronaphthalen-2,3-diol respectively. Indeed, also in this case Methyl 3,4-dibromobutanoate was reacted with the corresponding diol, achieving the ring closure (**96**, **97**). Then, the ester group was reduced (**98**, **99**), mesylated (**100**, **101**), and substituted with the pharmacophoric benzamide.

Scheme 13 | Syntheses of compounds **XIV** and **XV**.

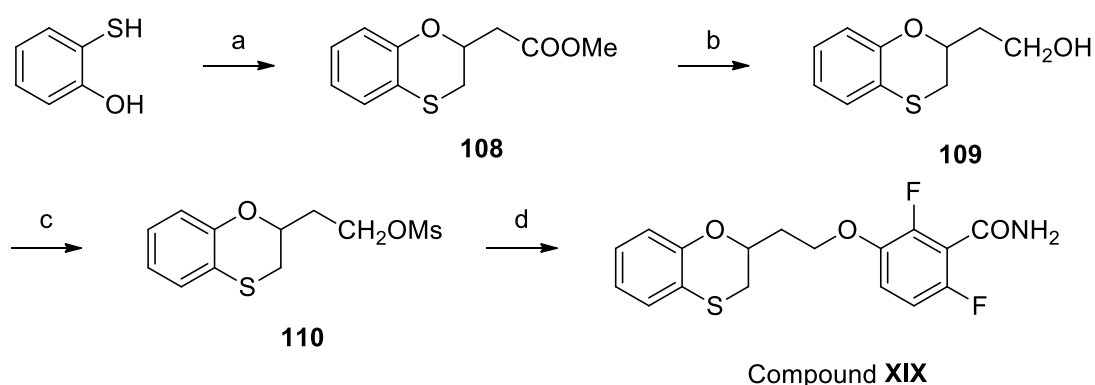
Reagents and conditions: a) Methyl 3,4-dibromobutanoate, K_2CO_3 , acetone, reflux; b) $LiAlH_4$, THF, RT; c) MsCl, TEA, DCM, RT; d) 2,6-difluoro-3-hydroxybenzamide, K_2CO_3 , DMF, $80^\circ C$.

The syntheses of compounds **XVI**, **XVII** and **XVIII** (Scheme 14) share several steps; the commercially available 4-Cyano-1,2-dihydroxybenzene was reacted with Methyl 3,4-dibromobutanoate to achieve ring closure (**102**), then the ester group was reduced (**103**), mesylated (**104**), and condensed with the pharmacophoric benzamide (**105**). The cyano group was successively converted into the corresponding amidoxime (**106**) that was reacted with Acetic or Propionic anhydride to give the desired compounds **XVII** and **XVIII**. The same amidoxime was used also for the ring closure with 1,1'-Thiocarbonyldiimidazole (**107**) and subsequent methylation to achieve final compound **XVI**.

Scheme 14 | Syntheses of compounds **XVI**, **XVII** and **XVIII**.

Reagents and conditions: a) Methyl 3,4-dibromobutanoate, K_2CO_3 , acetone, reflux; b) $LiAlH_4$, THF, RT; c) MsCl, TEA, DCM, RT; d) 2,6-difluoro-3-hydroxybenzamide, K_2CO_3 , DMF, 80°C; e) Hydroxylamine hydrochloride, K_2CO_3 , water, DMF, 80°C; f) 1- Acetic or propionic anhydride, Py, DMF, $CHCl_3$, reflux; 2- 2.5 N aqueous NaOH, RT; g) 1,1'-thiocarbonyldiimidazol, DBU, dioxane, RT; h) Methyl iodide, K_2CO_3 , ACN, DMF, 50°C.

The obtainment of compound **XIX** (Scheme 15) is achieved with the same strategy applied for compounds **XIV** and **XV**, starting from the commercially available 2-Mercatophenol.

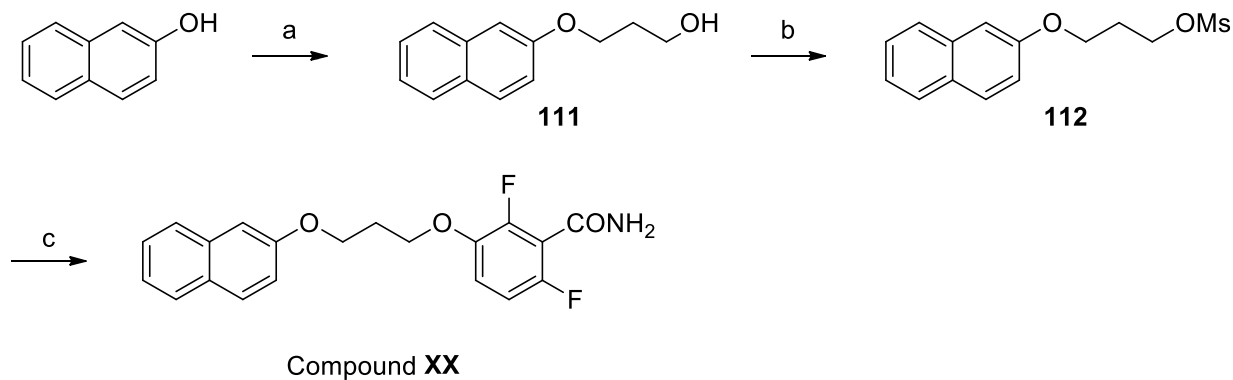
Scheme 15 | Synthesis of compound **XIX**.

Reagents and conditions: a) Methyl 3,4-dibromobutanoate, TEA, ACN/ H_2O , RT; b) $LiAlH_4$, THF, RT; c) MsCl, TEA, DCM, RT; d) 2,6-difluoro-3-hydroxybenzamide, K_2CO_3 , DMF, 80°C.

Lastly, the obtainment of compound **XX** (Scheme 16), last derivative belonging to the fourth set, was easily achieved starting from the β -Naphthol. This was reacted with 3-

Chloropropan-1-ol (**111**), the alcoholic function mesylated (**112**) and quickly substituted with the pharmacophoric benzamide.

Scheme 16 | Synthesis of compound **XX**.

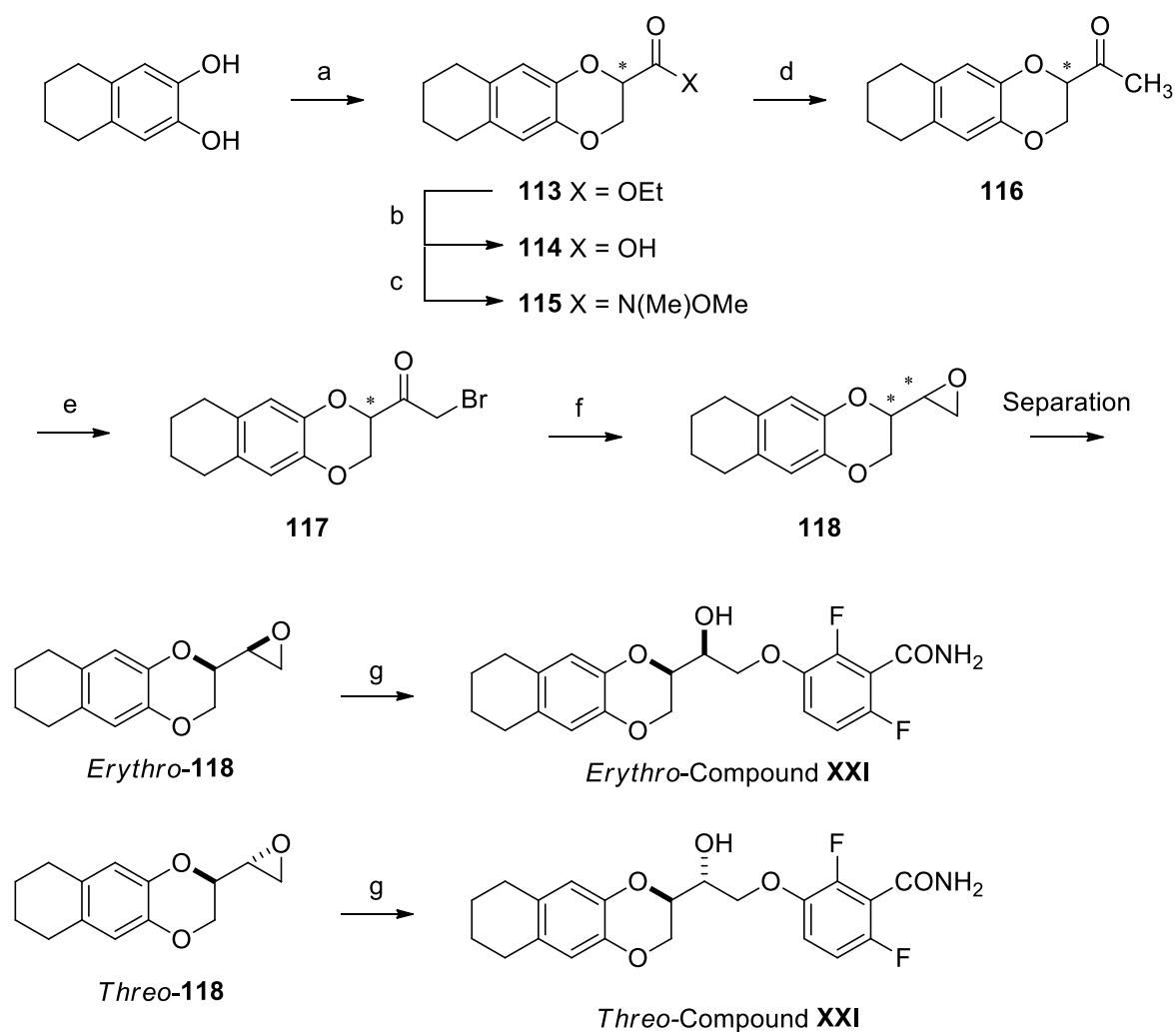


Reagents and conditions: a) 3-Chloropropan-1-ol, K_2CO_3 , Acetone, Reflux; b) MsCl, TEA, DCM, RT; c) 2,6-difluoro-3-hydroxybenzamide, K_2CO_3 , DMF, 80°C.

Synthesis of fifth set compounds: derivatives XXI to XXIII

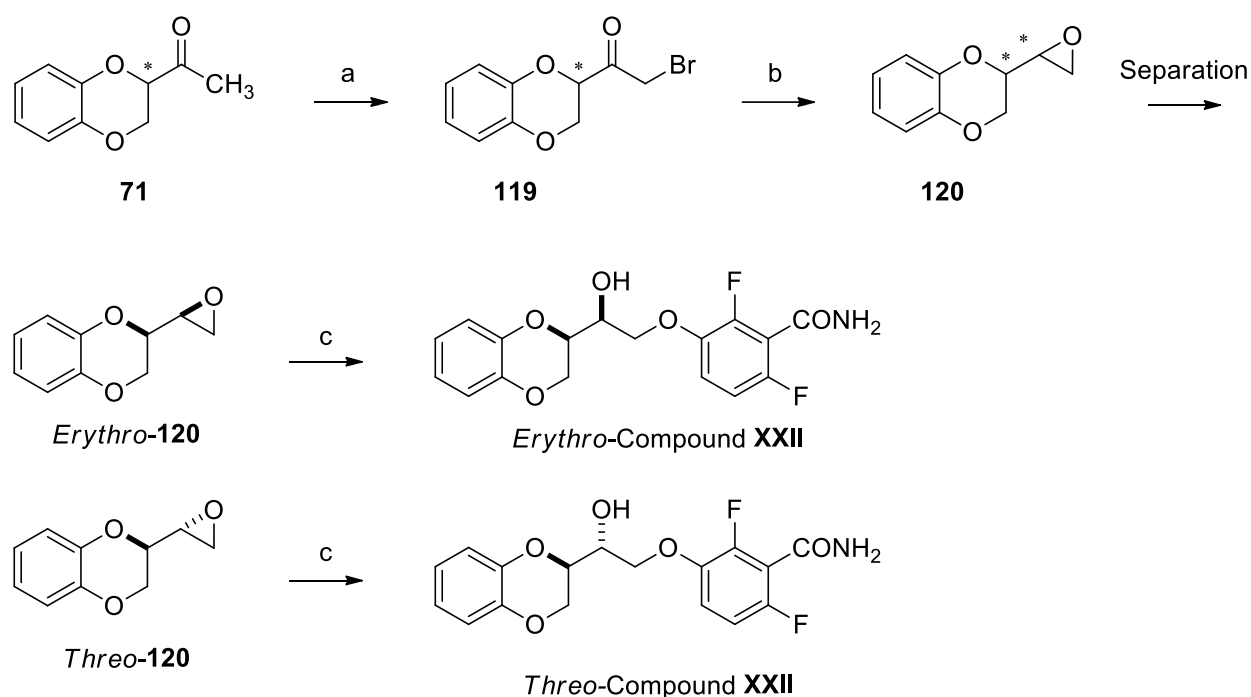
The syntheses of the compounds belonging to the fifth set have to take in considerations the separation of the diastereomers. Therefore, for each compound, a specific strategy to separate them was designed and applied.

For the obtainment of compound **XXI** (Scheme 17), erythro and threo, the synthesis starts from the previously described 5,6,7,8-Tetrahydronaphthalen-2,3-diol. This was reacted with Ethyl 2,3-dibromopropionate to achieve ring closure (**113**), hydrolysed (**114**), and converted into methyl ketone through Weinreb ketone synthesis (**115**, **116**). Then, this was brominated (**117**), reduced and converted into the corresponding mixture of epoxides (**118**). The rigidity of the system allowed the isolation of the *erythro* couple from the *threo* couple of epoxides, that were separately used for the obtainment of the final compound through direct ring opening.

Scheme 17 | Synthesis of compound **XXI**, *Erythro* and *Threo*.

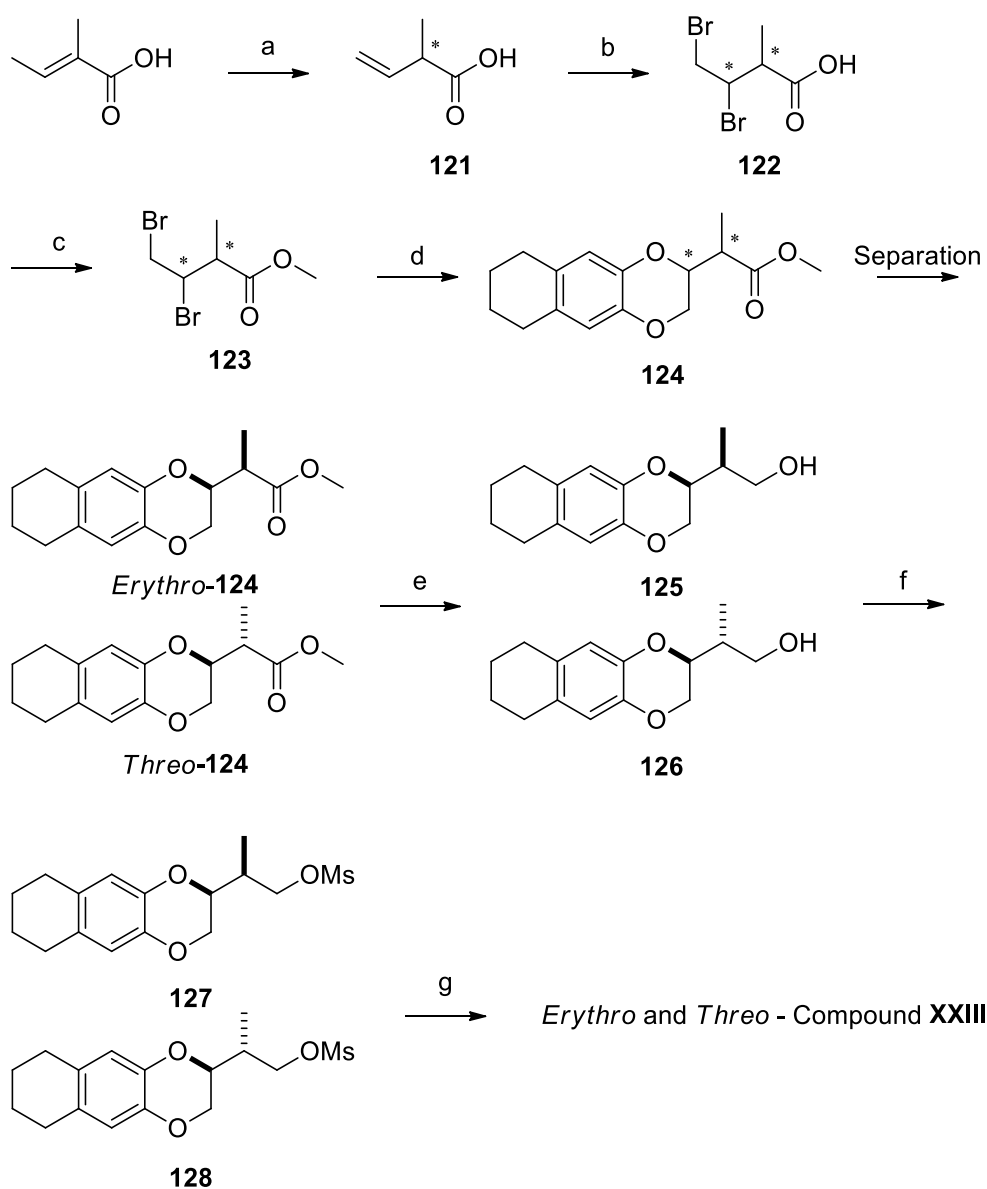
Reagents and conditions: a) 2,3-dibromopropionate, K₂CO₃, DMF, 70°C; b) 2.5 N aqueous NaOH, MeOH, RT; c) 1-SOCl₂, 2-*N,O*-dimethylhydroxylamine, DCM, RT; d) MeMgBr, Et₂O, RT; e) Br₂, Et₂O, 0°C; f) 1-NaBH₄, MeOH, RT; 2- NaH, THF, RT; g) 2,6-difluoro-3-hydroxybenzamide, K₂CO₃, DMF, 70°C.

Similarly, compound **XXII**, erythro and threo, was obtained starting from intermediate **71**, previously described, following the same strategy just described for derivative **XXI** (Scheme 18).

Scheme 18 | Synthesis of compound **XXII**, *Erythro* and *Threo*.

Reagents and conditions: a) Br_2 , Et_2O , 0°C ; b) 1- NaBH_4 , MeOH , RT ; 2- NaH , THF , RT ; c) 2,6-difluoro-3-hydroxybenzamide, K_2CO_3 , DMF , 70°C .

Lastly, for the achievement of derivative **XXIII** (Scheme 19), *threo* and *erythro*, a slightly different synthetic method was applied. Briefly, the 5,6,7,8-Tetrahydronaphthalen-2,3-diol was reacted with Methyl 3,4-dibromo-2-methylbutanoate (**123**), obtained through deconjugative transposition (**121**), bromination (**122**) and esterification of the commercially available Tiglic acid. The nature of the derivative obtained (**124**) allowed the separation of the *erythro* couple from the *threo* one, which proceed individually through reduction (**125**, **126**), mesylation (**127**, **128**) and condensation with the pharmacophoric benzamide to achieve compound **XXIII**.

Scheme 19 | Synthesis of compound **XXIII**, *Erythro* and *Threo*.

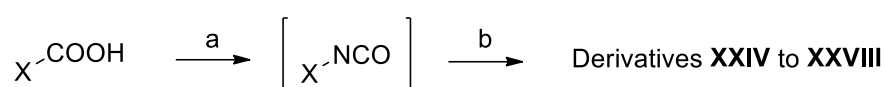
Reagents and conditions: a) LDA, THF, -78°C ; b) Br_2 , DCM, RT; c) Trimethylorthoformate, MeOH, Reflux; d) 5,6,7,8-Tetrahydronaphthodioxane, K_2CO_3 , DMF, 70°C ; e) LiAlH_4 , THF, RT; f) MsCl, TEA, DCM, RT; g) 2,6-difluoro-3-hydroxybenzamide, K_2CO_3 , DMF, 70°C .

Inhibitors of RnpA

Synthesis of first set compounds: derivatives XXIV and XXVIII

The syntheses of derivatives **XXIV** – **XXVIII** share the same strategy (Scheme 20). Starting from the appropriate carboxylic acid, this was converted into the corresponding isocyanate through reaction with DPPA. Then, the facile conversion into urea was achieved by reaction with the corresponding amine: 2-Methyl piperidine for compounds **XIV**, **XV** and **XVI** and Tetrahydroquinoline or Tetrahydroisoquinoline for compounds **XVII** and **XVIII**, respectively.

Scheme 20 | Syntheses of derivatives XXIV to XXVIII.

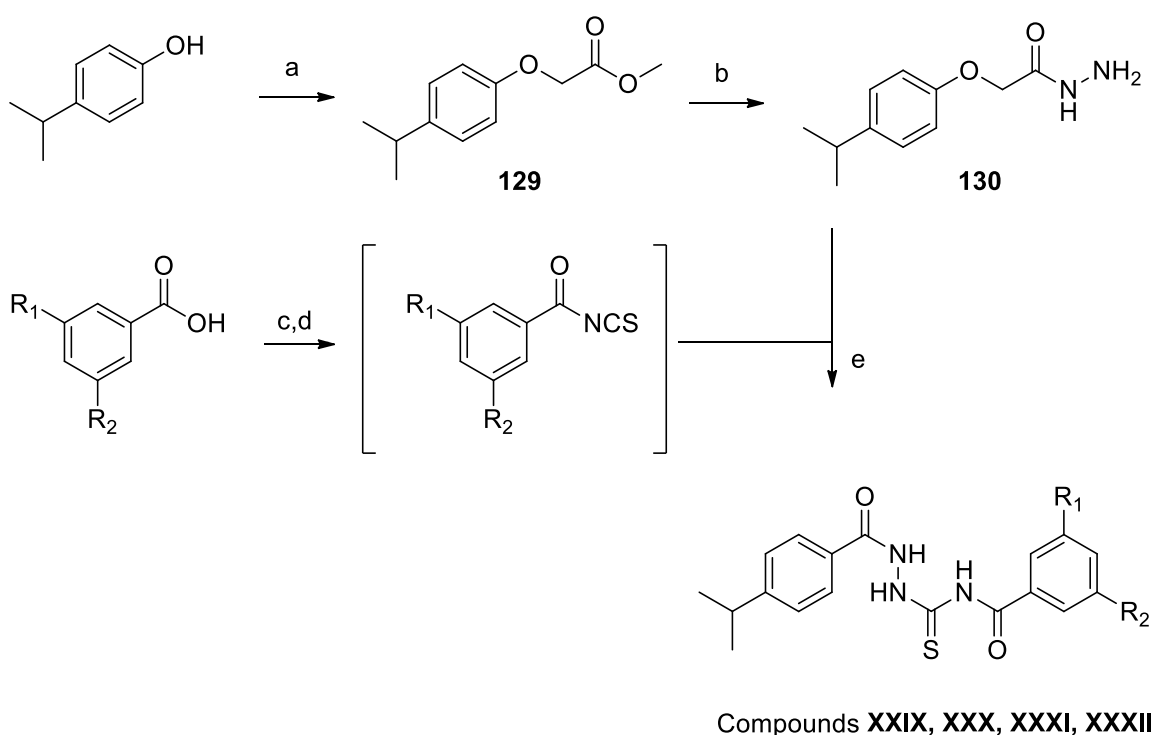


Reagents and conditions: a) DPPA, TEA, toluene, 95°C; b) appropriate amine, 95°C.

Synthesis of second set compounds: derivatives XXIX and XXXII

The synthetic strategy for the obtainment of compounds **XXIX** – **XXXII** (Scheme 21) took the cue from the work of Lounsbury and co-workers (Lounsbury *et al.*, 2018).

Scheme 21 | Syntheses of derivatives XXIX to XXXII.



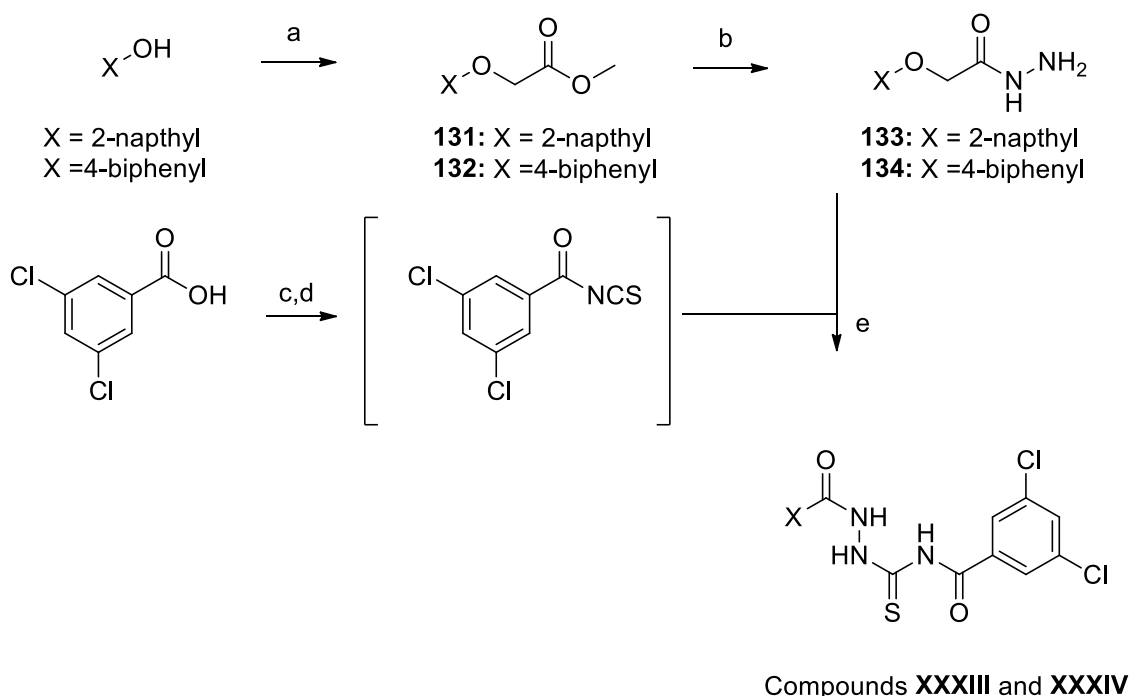
Reagents and conditions: a) Methyl 2-chloroacetate, K_2CO_3 , DMF, 50 °C; b) Hydrazine hydrate, Methanol, Reflux; c) $SOCl_2$, Reflux; d) Potassium thiocyanate, ACN, RT; e) ACN, RT.

Briefly, the commercially available 4-*i*-Propylphenol was converted into the Methyl 4-*i*-propylphenoxyacetate through reaction with Methyl 2-chloroacetate (**129**), and subsequently converted into the corresponding hydrazide (**130**). As a last step, the appropriate mono or di-halogenphenylacyl isothiocyanate reacts with the hydrazide achieving the corresponding final compound.

Synthesis of third set compounds: derivatives XXXIII and XXXIV

Similarly, compounds **XXXIII** and **XXXIV** were achieved applying the same strategy but with the appropriate phenol, 4-Phenyl-phenol or 2-Naphthol respectively (Scheme 22).

Scheme 22 | Syntheses of derivatives **XXXIII** and **XXXIV**.



Reagents and conditions: a) Methyl 2-chloroacetate, K_2CO_3 , DMF, 50 °C; b) Hydrazine hydrate, Methanol, Reflux; c) $SOCl_2$, Reflux; d) Potassium thiocyanate, ACN, RT; e) ACN, RT.

Synthesis of fourth set compounds: derivatives XXXV to XL

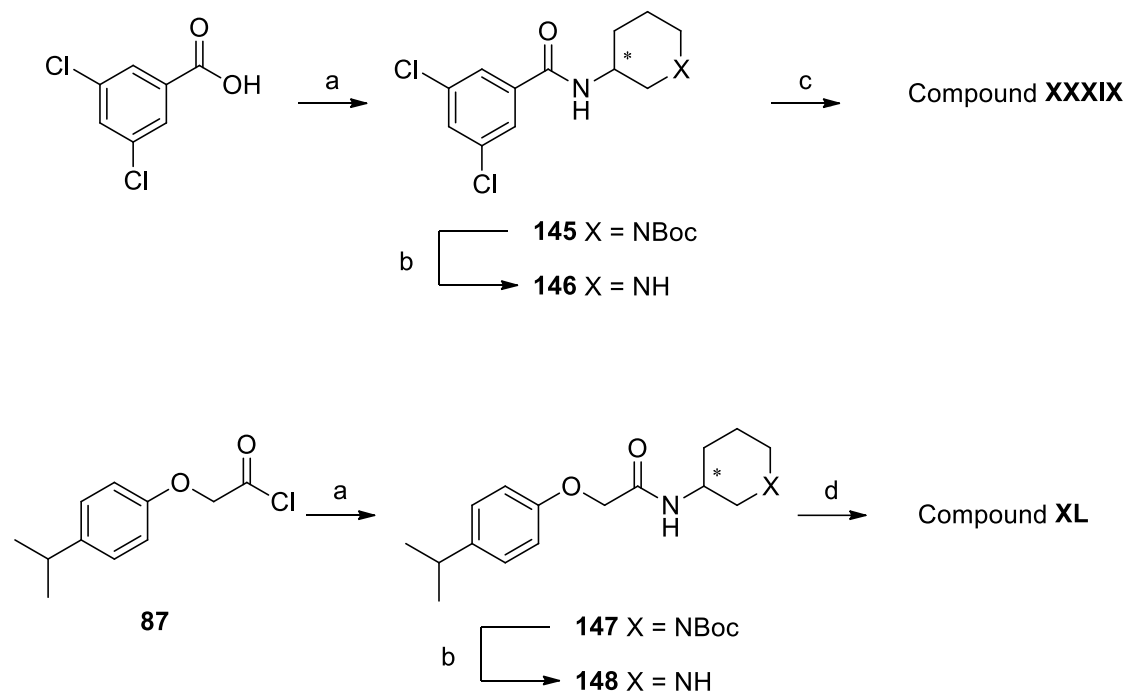
All the compounds belonging to fourth set possess a diamide structure, achieved in several ways.

For compounds **XXXV** and **XXXVI** (Scheme 23), the two moieties were reacted with the appropriate monoprotected amine, generating the first amide group. Thus, deprotection and reaction with the second moiety followed and led to the obtainment of the final desired compounds.

Reagents and conditions: a) 4-*N*-Boc-aminopiperidine or *N*-Boc-piperazine, TEA, DCM, RT; (b) TFA, DCM, RT; (c) 3,5-dichlorobenzoyl chloride, TEA, DCM, RT.

Lastly the synthesis of compounds **XXXIX** and **XL** (Scheme 25) exploit the same 3-*N*-Boc-aminopiperidine, reacted in one case firstly with intermediate **136** (**145**, **147**) and, post deprotection (**146**, **148**), with 3,5-Dichlorobenzoyl chloride and in the other case in the opposite way.

Scheme 25 | Syntheses of compounds **XXXIX** and **XL**.

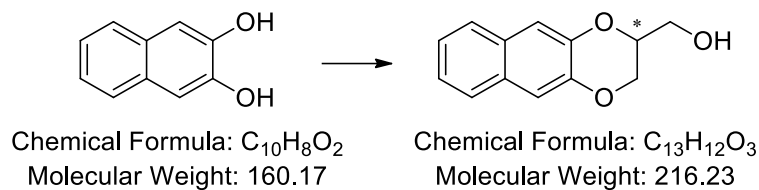


Reagents and conditions: (a) 3-*N*-Boc-aminopiperidine, TEA, DCM, RT; (b) TFA, DCM, RT; (c) Intermediate **136**, TEA, DCM, RT; d) 3,5-dichlorobenzoyl chloride, TEA, DCM, RT.

CHAPTER 9 – EXPERIMENTAL

Abbreviations used: ACN: Acetonitrile, CDI: carbonyldiimidazole DCE: dichloroethane; DCM: dichloromethane; DIAD: diisopropylazodicarboxyate; DIPEA: diisopropylethylamine; DIPA: diisopropylamine; DMF: dimethylformamide; DMSO: dimethylsulfoxide; mp: melting point; MW: molecular weight; Py: Pyridine, RT: room temperature; TBAB: tetrabutylammonium bromide; TEA: triethylamine; THF: tetrahydrofuran.

(1,4-naphthodioxan-2-yl)methanol

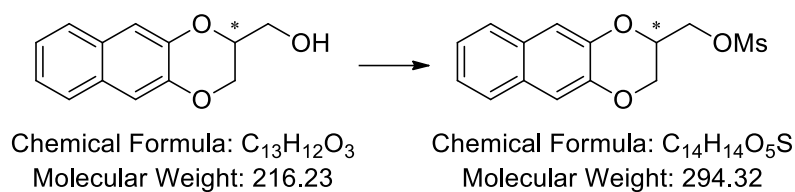


Potassium carbonate (1.9 g, 13.73 mmol) was added to a solution of Naphthalen-2,3-diol (1.00 g, 6.24 mmol) in acetone (10 mL). After stirring for 30 minutes, Epibromohydrin (0.59 mL, 6.9 mmol) was added dropwise. The reaction mixture was stirred at RT for 72 hours, concentrated under vacuum, diluted with Ethyl acetate (35 mL), washed with 10% aqueous NaOH (15 mL) and 10% aqueous NaCl (15 mL), dried with Na_2SO_4 , filtered and concentrated under vacuum to yield 1.01 g of (1,4-naphthodioxan-2-yl)methanol as a viscous oil.

Yield = 75.0%

1H NMR ($CDCl_3$): δ 7.66 (m, 2H), 7.30 (m, 4H), 4.37 (m, 2H), 4.15 (m, 1H), 3.91 ppm (m, 2H).

(1,4-naphthodioxan-2-yl)methanesulfonate

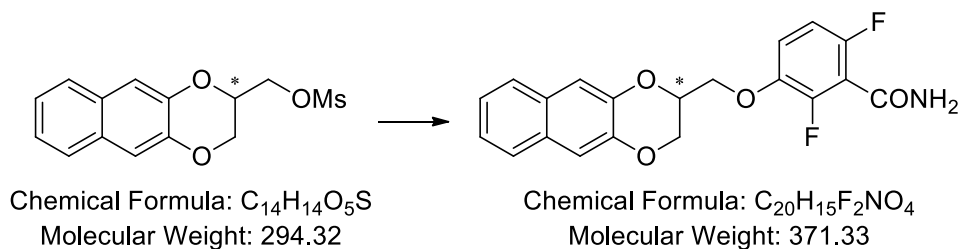


Mesyl chloride (0.43 mL, 5.60 mmol) was added dropwise to a solution of (1,4-naphthodioxan-2-yl)methanol (1.01 g, 4.67 mol) and TEA (0.78 mL, 5.60 mmol) in DCM (10 mL) at 0°C. The reaction mixture was stirred at room temperature for 2.5 hours, diluted with DCM (15 mL), washed firstly with 10% aqueous NaHCO₃ (5 mL), secondly with 10% aqueous HCl (5 mL) and finally with 10% aqueous NaCl (10 mL), dried with Na₂SO₄, filtered and concentrated under vacuum to give 1.53 g of (1,4-naphthodioxan-2-yl)methanesulfonate as a yellowish oil.

Yield = 98.5%

¹H NMR (CDCl₃): δ 7.66 (m, 2H), 7.32 (m, 4H), 4.59 (m, 1H), 4.49 (d, *J* = 5.3 Hz, 2H), 4.40 (dd, *J* = 11.7, 2.4 Hz, 1H), 4.22 (dd, *J* = 11.7, 6.6 Hz, 1H), 3.11 ppm (s, 3H).

(I) 3-(1,4-Naphthodioxan-2-yl)methoxy)-2,6-difluorobenzamide



Potassium carbonate (0.21 g, 1.50 mmol) was added to a solution of 2,6-Difluoro-3-hydroxybenzamide (0.25 g, 1.43 mmol) in dry DMF (5 mL) under N_2 atmosphere. After stirring at room temperature for 30 minutes, a solution of 2-Mesyloxymethyl-1,4-naphthodioxane (0.40 g, 1.36 mmol) in dry DMF (5 mL) was added. The reaction mixture was stirred at $60^\circ C$ for 24 hours, concentrated under vacuum, diluted with Ethyl acetate (15 mL), washed with 10% aqueous NaCl (4 x 10 mL), dried over Na_2SO_4 , filtered and concentrated to give a residue which was purified by flash chromatography on silica gel. Elution with 1/1 Cyclohexane/Ethyl acetate on silica gel gave 0.20 g of 3-(1,4-Naphthodioxan-2-yl)methoxy)-2,6-difluorobenzamide as a white solid.

Yield = 40.0%

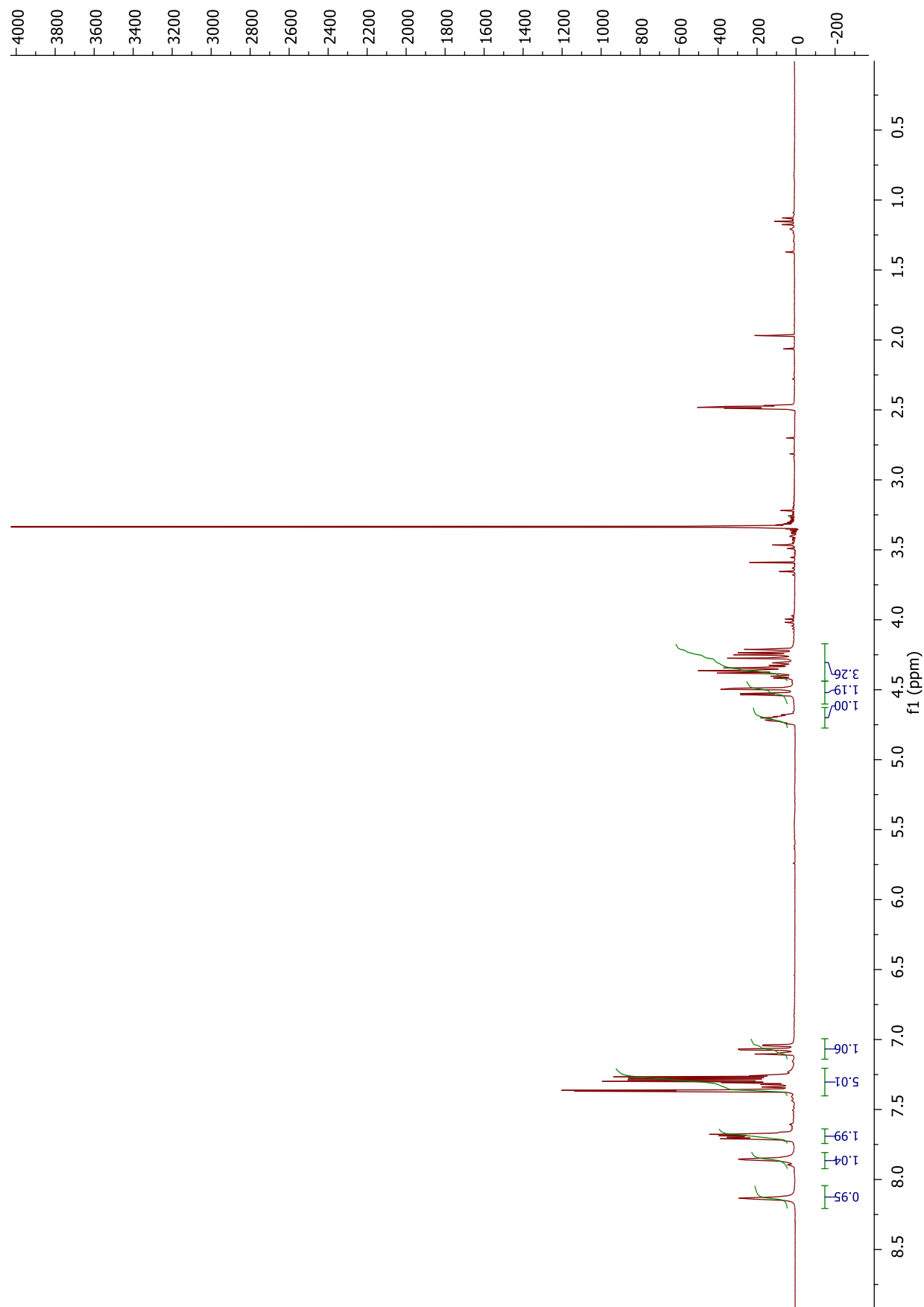
M.p. = $157.4^\circ C$

Tr (HPLC, gradient, 90% H_2O with 0.10% TFA to 10% acetonitrile with 0.10% TFA in 25 min with 35 min run time. Flow rate: 1 mL/min) = 14.5 min, Purity = 97.0%

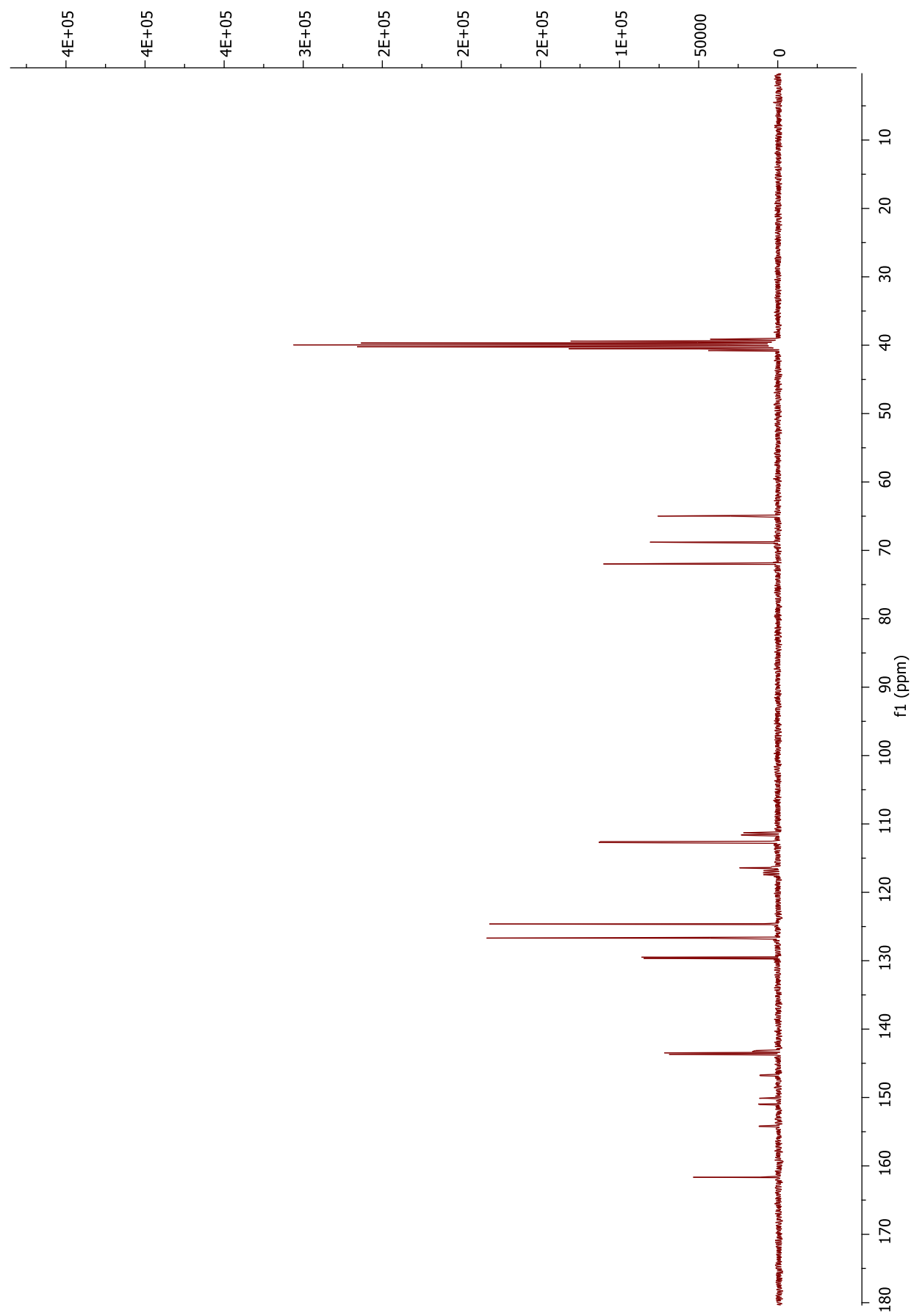
1H NMR (d_6 -DMSO): δ 8.13 (bs, 1H), 7.86 (bs, 1H), 7.53 (m, 2H), 7.30 (m, 5H), 7.07 (td, J = 9.0, 1.9 Hz, 1H), 4.73 (m, 1H), 4.51 (dd, J = 11.6, 2.5 Hz, 1H), 4.39 (dd, J = 11.4, 4.6 Hz, 1H), 4.34 (dd, J = 11.4, 5.8 Hz, 1H), 4.24 ppm (dd, J = 11.6, 7.3 Hz, 1H).

^{13}C NMR (d_6 -DMSO): δ 161.66, 152.60 (dd, J = 240.0, 6.8 Hz), 148.40 (dd, J = 247.1, 8.6 Hz), 148.68, 143.47, 143.20 (dd, J = 10.9, 3.4 Hz), 129.66, 129.49, 126.69, 124.63, 117.10 (dd, J = 25.1, 20.6 Hz), 116.40 (dd, J = 9.0, 2.3 Hz), 112.72, 112.58, 111.50 (dd, J = 22.5, 3.7 Hz) 71.98, 68.80, 64.99 ppm.

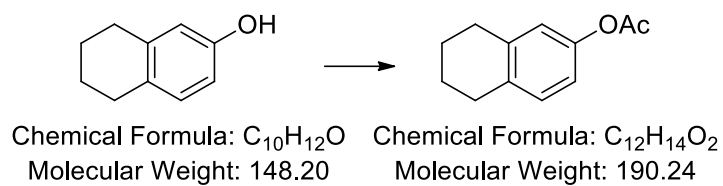
Experimental



Experimental



5,6,7,8-Tetrahydronaphthalen-2-yl acetate

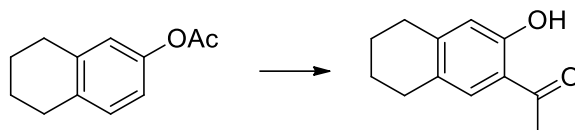


Acetyl chloride (2.52 mL, 35.43 mmol) was added dropwise to a solution of 5,6,7,8-Tetrahydro-2-naphthol (5.0 g, 33.74 mmol) in DCM (25 mL) at 0°C. After stirring at room temperature for 2 hours, the reaction mixture was washed with 10% aqueous HCl (25 mL), 10% aqueous NaCl, dried with Na_2SO_4 , filtered and concentrated under vacuum giving 6.16 g of 5,6,7,8-Tetrahydronaphthalen-2-yl acetate as a colourless oil.

Yield = 95.9%

1H NMR ($CDCl_3$): 7.07 (m, 1H), 6.82 (m, 1H), 5.28 (m, 1H), 2.77 (m, 4H), 2.29 (s, 3H), 1.80 ppm (m, 4H).

3-Acetyl-5,6,7,8-tetrahydro-2-naphthol



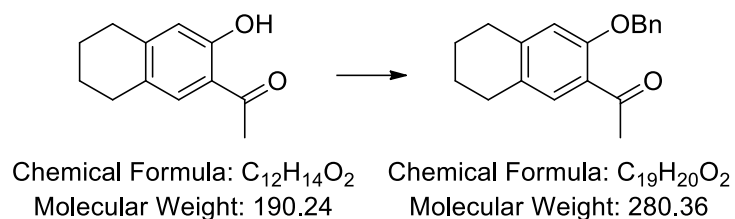
Chemical Formula: C₁₂H₁₄O₂ Chemical Formula: C₁₂H₁₄O₂
Molecular Weight: 190.24 Molecular Weight: 190.24

Aluminium chloride (4.32 g, 32.38 mmol) was added to a solution of 5,6,7,8-Tetrahydronaphthalen-2-yl acetate (6.16 g, 32.38 mmol) in 1,2-Dichlorobenzene (30 mL). The reaction mixture was heated at 100°C and stirred for 5 hours, monitoring the reaction *via* NMR. The mixture was then allowed to return at room temperature, diluted with DCM (80 mL) and poured in frozen 10% aqueous HCl. The organic phase was then dried with Na₂SO₄, filtered and concentrated under vacuum to give a residue which was purified by flash chromatography on silica gel. Elution with Cyclohexane/Ethyl Acetate 95:5 to 9:1 on silica gel gave 4.91 g of 3-Acetyl-5,6,7,8-tetrahydro-2-naphthol as a colourless oil.

Yield = 80.0%

¹H NMR (CDCl₃): δ 7.40 (s, 1H), 6.67 (s, 1H), 2.74 (m, 4H), 2.58 (s, 3H), 1.77 ppm (m, 4H).

2-Acety-3-benzyloxy-5,6,7,8-tetrahydronaphthalene



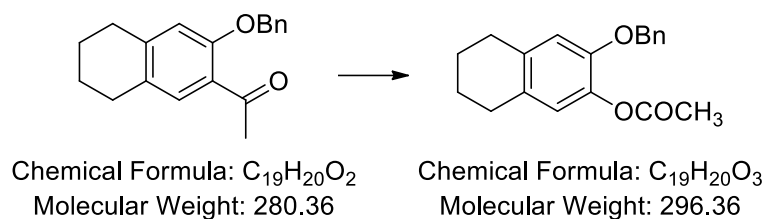
Tetrabutylammonium bromide (1.25 g, 3.87 mmol), Benzyl bromide (4.60 mL, 38.71 mmol) and 2,5 N aqueous NaOH (50 mL) were added to a solution of 3-Acetyl-5,6,7,8- tetrahydro-2-naphthol (4.91 g, 25.81 mmol) in DCM (50 mL). The reaction mixture was warmed at room temperature and stirred for 6 hours. The organic and aqueous phases were then separated, and the aqueous one extracted twice with DCM (2 x 30mL). The organic phase was then washed with 10% aqueous HCl (20 mL) and 10% aqueous NaCl (20 mL), dried with Na₂SO₄, filtered and concentrated under vacuum to give a dark solid which was purified by crystallization from Methanol (3 volumes) to give 5.3 g of 2-Acety-3-benzyloxy-5,6,7,8-tetrahydronaphthalene as a white solid.

Yield = 73.2%

M.p. = 95.2°C

¹H NMR (CDCl₃): δ 7.50 (s, 1H), 7.38 (m, 5H), 6.72 (s, 1H), 5.11 (s, 2H), 2.75 (m, 4H), 2.57 (s, 3H), 1.78 ppm (m, 4H).

2-Acetoxy-3-benzyloxy-5,6,7,8-tetrahydronaphthalene

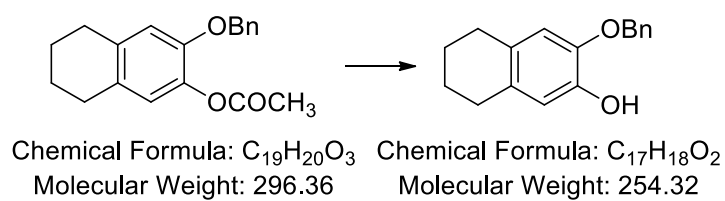


m-Chloroperbenzoic acid (3.83 g, 22.20 mmol) was added to a solution of 2-Acetyl-3-benzyloxy-5,6,7,8-tetrahydronaphthalene (4.15 g, 14.80 mmol) in DCM (42 mL) at 0°C. The reaction mixture was then allowed to warm at room temperature and stirred for 18 hours, monitoring the reaction *via* NMR. The mixture was then washed with $NaHCO_3$ (3 x 25 mL), dried with Na_2SO_4 , filtered and concentrated under vacuum to give 1.03 g of 2-Acetoxy-3-benzyloxy-5,6,7,8-tetrahydronaphthalene as a yellowish oil.

Yield = 97.1%

1H NMR ($CDCl_3$): δ 7.41 (m, 5H), 6.76 (s, 1H), 6.71 (s, 1H), 5.04 (s, 2H), 2.70 (m, 4H), 2.26 (s, 3H), 1.78 ppm (m, 4H).

2-Benzyloxy-5,6,7,8-tetrahydro-2-naphthol

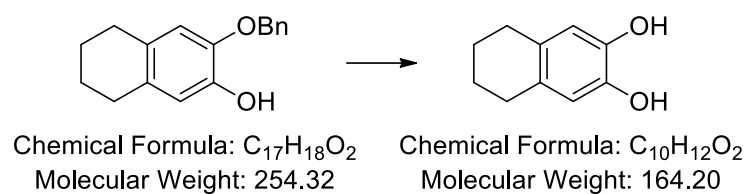


2,5 N aqueous NaOH (10 mL) was added to a solution of 2-Benzyloxy-3-acetoxy-5,6,7,8-tetrahydronaphthalene (5.32 g, 17.95 mmol) in Methanol (25 mL) and the reaction mixture was stirred at room temperature for 18 hours. The pH of the mixture was then lowered to 1 with conc. HCl, the precipitate was collected by filtration and used in the next step without further purification.

Yield = 97.0%

$^1\text{H NMR (CDCl}_3\text{): } \delta$ 7.41 (m, 5H), 6.66 (s, 1H), 6.63 (s, 1H), 5.06 (s, 2H), 2.68 (m, 4H), 1.78 ppm (m, 4H)

5,6,7,8-Tetrahydronaphthalene-2,3-diol

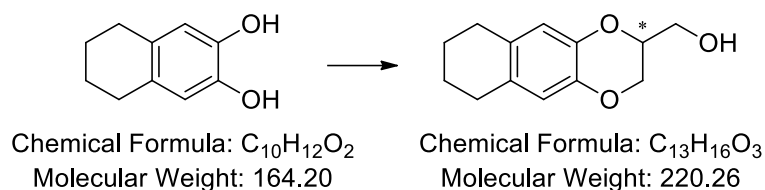


10% palladium on carbon was added to a solution of 2-Benzyloxy-5,6,7,8-tetrahydro-2-naphthol (2.86 g, 11.24 mmol) in MeOH (35 mL). The reaction mixture was vigorously stirred under H_2 (1 atm) for 18 hours, filtered on a celite pad and concentrated under vacuum to give 1.68 g of 5,6,7,8-Tetrahydronaphthalene-2,3-diol as a dark oil.

Yield = 91.0%

1H NMR ($CDCl_3$): δ 6.57 (s, 2H), 2.62 (m, 4H), 1.75 ppm (m, 4H).

(5,6,7,8-tetrahydro-1,4-naphthodioxan-2-yl)methanol

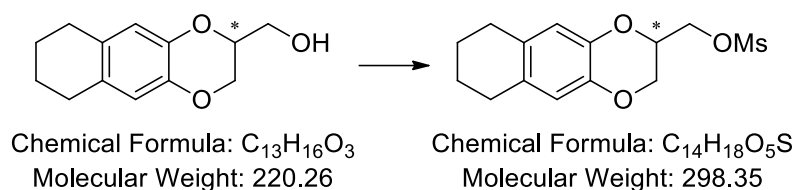


Potassium carbonate (1.26 g, 9.11 mmol) was added to a solution of 5,6,7,8-Tetrahydronaphthalen-2,3-diol (0.68 g, 4.14 mmol) in Acetone (8 mL). After stirring at room temperature for 30 minutes, Epibromohydrin (0.78 mL, 9.10 mmol) was added. The reaction mixture was stirred at reflux for 18 hours, concentrated under vacuum, diluted with Ethyl acetate (25 mL), washed with 10% aqueous NaCl (15 mL), dried with Na_2SO_4 , filtered and concentrated under vacuum to yield a dark oil, which was purified by flash chromatography on silica gel. Elution with 6/4 Cyclohexane/Ethyl acetate on silica gel gave 0.12 g of (5,6,7,8-tetrahydro-1,4-naphthodioxan-2-yl)methanol as a colourless oil.

Yield = 13.0%

1H NMR ($CDCl_3$): δ 6.61 (s, 1H), 6.59 (s, 1H) 4.22 (m, 2H), 4.05 (m, 1H), 3.85 (m, 2H), 2.65 (m, 4H), 1.77 ppm (m, 4H).

(5,6,7,8-tetrahydro-1,4-naphthodioxan-2-yl)methanesulfonate

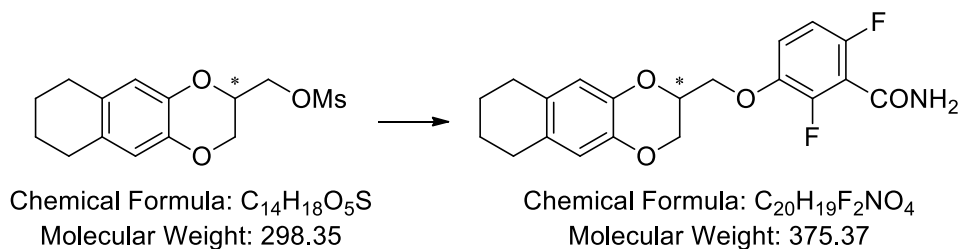


Mesyl chloride (0.055 mL, 0.71 mmol) was added dropwise to a solution of (5,6,7,8-tetrahydro-1,4-naphthodioxan-2-yl)methanol (0.12 g, 0.54 mmol) and TEA (0.098 mL, 0.71 mmol) in DCM (5 mL) at 0°C. The reaction mixture was stirred at room temperature for 3 hours, diluted with DCM (15 mL), washed firstly with 10% aqueous NaHCO₃ (5 mL), secondly with 10% aqueous HCl (5 mL) and finally with 10% aqueous NaCl (10 mL), dried with Na₂SO₄, filtered and concentrated under vacuum to give 0.15 g of (5,6,7,8-tetrahydro-1,4-naphthodioxan-2-yl)methanesulfonate as a yellow oil.

Yield = 92.6%

¹H NMR (CDCl₃): δ 6.59 (s, 2H), 4.42 (m, 1H), 4.42 (m, 2H), 4.26 (dd, *J* = 11.6, 2.0 Hz, 1H), 4.09 (dd, *J* = 11.6, 6.0 Hz, 1H), 3.08 (s, 3H), 2.68 (m, 4H), 1.75 ppm (m, 4H).

(II) 3-(5,6,7,8-Tetrahydro-1,4-naphthodioxan-2-yl)methoxy)-2,6-difluorobenzamide



Potassium carbonate (0.077 g, 0,55 mmol) was added to a solution of 2,6-Difluoro-3-hydroxybenzamide (0.091 g, 0,53 mmol) in dry DMF (2 mL) under N_2 atmosphere. After stirring at room temperature for 30 minutes, a solution of 2-Mesyloxymethyl-5,6,7,8-tetrahydro-1,4-naphthodioxane (0.15 g,0,50 mmol) in dry DMF (5 mL) was added. The reaction mixture was stirred at $80^\circ C$ for 4 hours, concentrated under vacuum, diluted with Ethyl acetate (15 mL), washed with 10% aqueous NaCl (4 x 10 mL), dried over Na_2SO_4 , filtered and concentrated to give a residue which was purified by flash chromatography on silica gel. Elution with 1/1 Cyclohexane/Ethyl acetate on silica gel and subsequent treatment with DCM lets the precipitation of 0.04 g of 3-(5,6,7,8-Tetrahydro-1,4-naphthodioxan-2-yl)methoxy)-2,6-difluorobenzamide as a white solid.

Yield = 22.0%

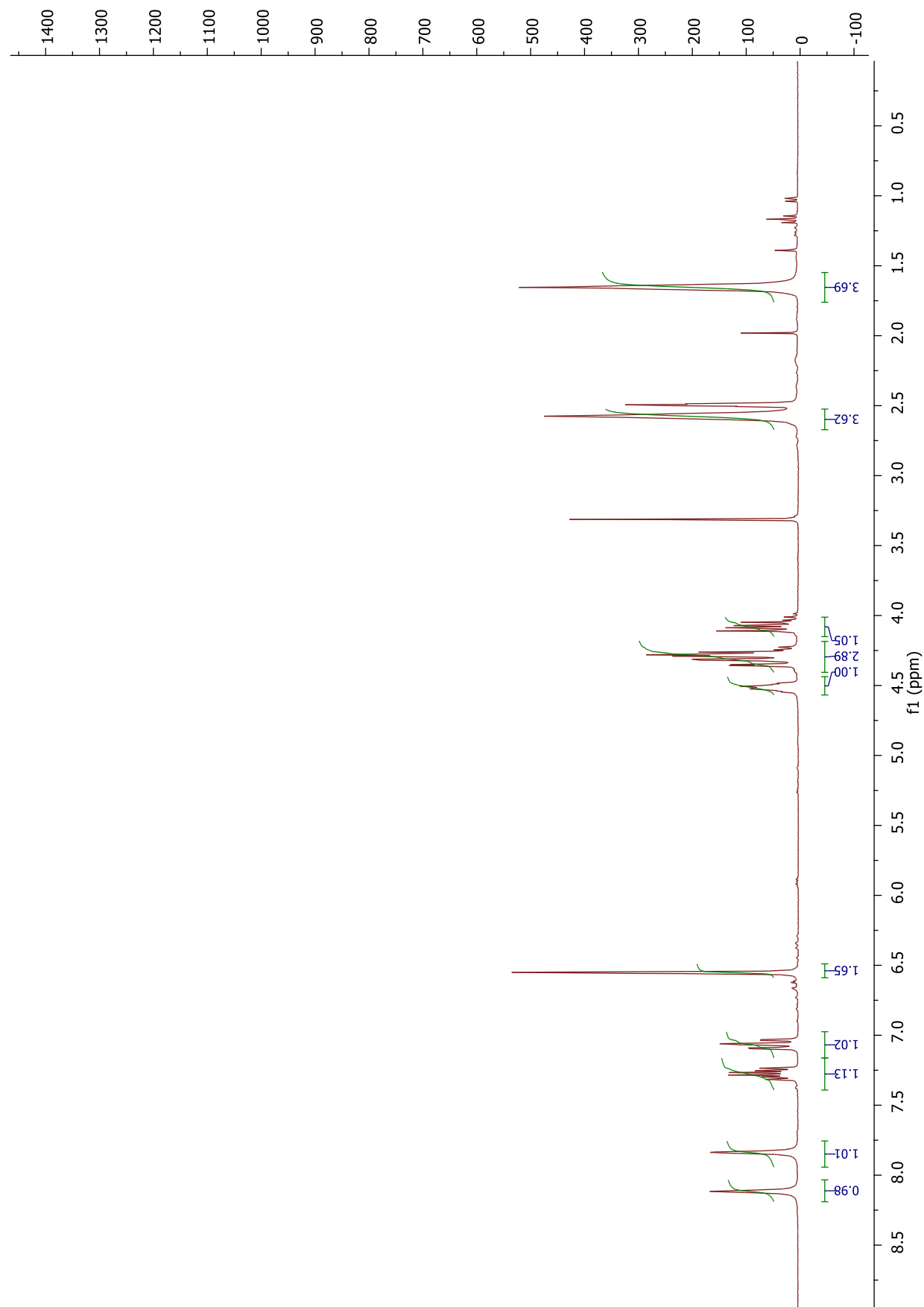
M.p. = $156.6^\circ C$

Tr (HPLC, gradient, 90% H_2O with 0.10% TFA to 10% acetonitrile with 0.10% TFA in 25 min with 35 min run time. Flow rate: 1 mL/min) = 15.3 min, Purity = 95.1%

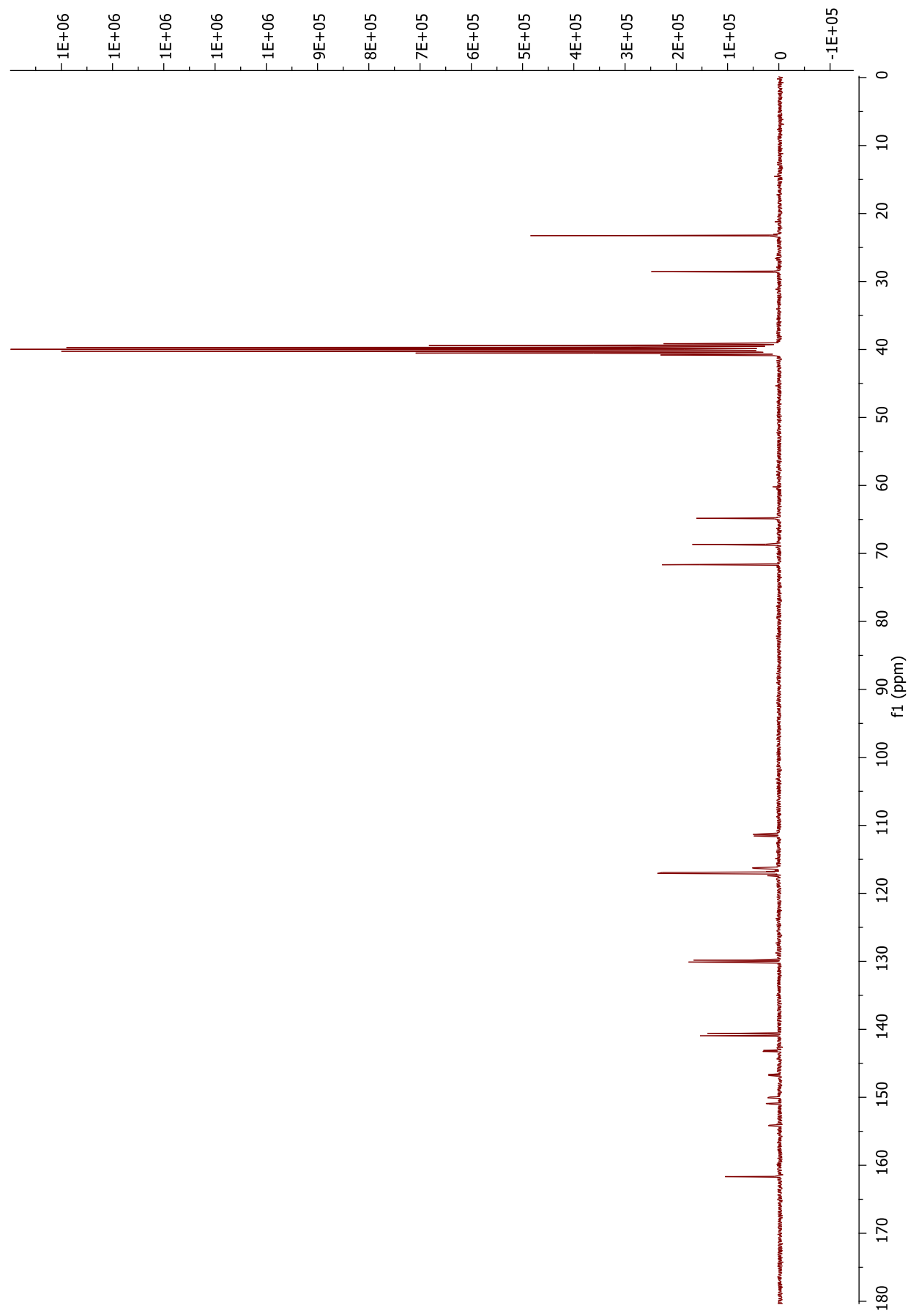
1H NMR (d_6 -DMSO): δ 8.12 (s, 1H), 7.84 (s, 1H), 7.28 (td, J = 9.1, 5.3 Hz, 1H), 7.06 (td, J = 9.1, 1.8 Hz, 1H), 6.55 (s, 2H), 4.52 (m, 1H), 4.28 (m, 2H), 4.27 (m, 1H) 4.08 (dd, J = 11.5, 6.8 Hz, 1H), 2.58 (s, 4H), 1.65 ppm (s, 4H).

^{13}C NMR (d_6 -DMSO): δ 161.7, 152.5 (dd, J = 240.0, 6.8 Hz), 148.4 (dd, J = 247.1, 8.6 Hz), 143.2 (dd, J = 10.9, 3.4 Hz), 141.0, 140.6, 130.1, 129.8, 117.1 (dd, J = 24.8, 20.3 Hz), 117.1, 116.9, 116.3 (dd, J = 9.4, 1.9 Hz), 111.4 (dd, J = 22.9, 4.1 Hz), 71.7, 68.7, 64.8, 28.5, 23.3 ppm.

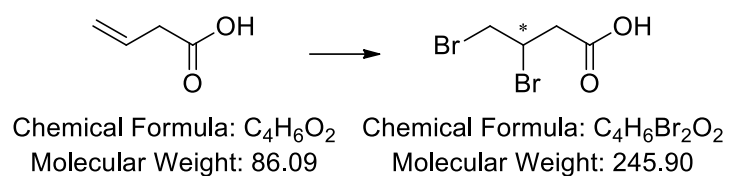
Experimental



Experimental



3,4-Dibromobutanoic acid

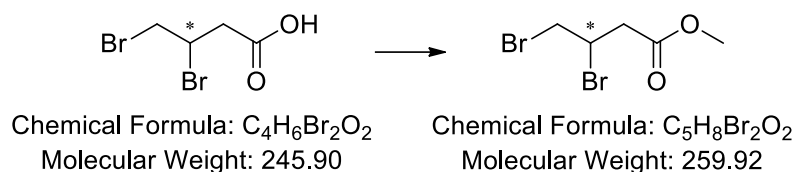


Bromine (2.98 mL, 58.1 mmol) was added dropwise to a solution of 3-Butenoic acid (5.0 g, 58.1 mmol) in DCM (50 mL) at 0°C. Once added, the reaction mixture was warmed to RT and kept stirring for 16 h. The reaction mixture was then quenched with aqueous 10% sodium thiosulfate solution, dried over Na_2SO_4 , filtered and concentrated under reduced pressure, affording 13.25 g of 3,4-Dibromobutanoic acid as a yellowish oil.

Yield = 93.0%

1H NMR ($CDCl_3$): δ 9.58 (bs, 1H); 4.48 (m, 1H), 3.92 (dd, $J = 10.4, 4.3$ Hz, 1H), 3.72 (t, $J = 10.4$ Hz, 1H), 3.44 (dd, $J = 17.1, 3.8$ Hz, 1H), 2.93 ppm (dd, $J = 17.1, 9.2$ Hz, 1H).

Methyl 3,4-dibromobutanoate

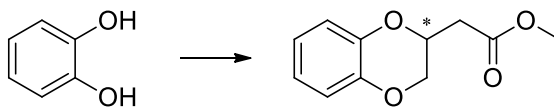


0.5 mL of H_2SO_4 conc. was added dropwise to a solution of 3,4-Dibromobutanoic acid (13.25 g, 53.8 mmol) and Trimethyl orthoformate (11.35 g, 107.0 mmol) in Methanol (150 mL) at $0^\circ C$. Once added, the reaction mixture was warmed to RT and then refluxed, keeping stirring, for 16 h. The reaction mixture was then concentrated under reduced pressure, resumed with Ethyl acetate (150 mL), washed with aqueous 10% $NaHCO_3$ (2×100 mL) and brine (100 mL), dried over Na_2SO_4 , filtered and concentrated under vacuum, affording 10.9 g of Methyl 3,4-dibromobutanoate as a yellowish oil.

Yield = 78.0%

1H NMR ($CDCl_3$): δ 4.50 (m, 1H), 3.91 (dd, $J = 10.4, 4.3$ Hz, 1H), 3.76 (s, 3H), 3.72 (dd, $J = 10.2, 2.7$ Hz, 1H), 3.34 (dd, $J = 17.1, 3.8$ Hz, 1H), 2.87 ppm (dd, $J = 16.7, 9.2$ Hz, 1H).

Methyl 2-(1,4-benzodioxan-2-yl)-acetate



Chemical Formula: $C_6H_6O_2$
Molecular Weight: 110.11

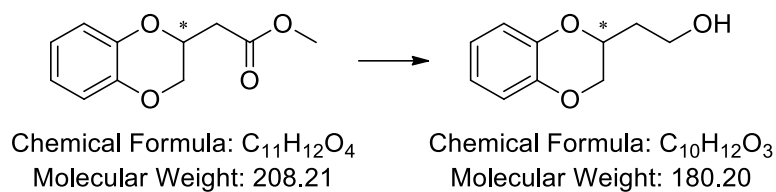
Chemical Formula: $C_{11}H_{12}O_4$
Molecular Weight: 208.21

Potassium carbonate (18.82 g, 136.2 mmol) was added to a solution of Catechol (5.00 g, 45.4 mmol) and Methyl 3,4-dibromobutanoate (11.80 g, 45.4 mmol) in Acetone (50 mL) at room temperature. The reaction mixture was heated at reflux, stirred for 3 hours, concentrated under vacuum, diluted with Ethyl Acetate (50 mL), washed with brine (50 mL), dried over Na_2SO_4 , filtered and concentrated under vacuum to give 8.59 g of Methyl 2-(1,4-benzodioxan-2-yl)-acetate as a yellowish oil.

Yield = 91.0%

1H NMR ($CDCl_3$): δ 6.82 (m, 4H), 4.63 (dq, $J = 6.7, 2.3$ Hz, 1H), 4.31 (dd, $J = 11.3, 2.3$ Hz, 1H), 4.00 (dd, $J = 11.3, 6.7$ Hz, 1H), 3.75 (s, 3H), 2.79 (dd, $J = 16.1, 6.7$ Hz, 1H), 2.65 ppm (dd, $J = 16.1, 6.7$ Hz, 1H).

2-(1,4-Benzodioxane-2-yl)-ethanol

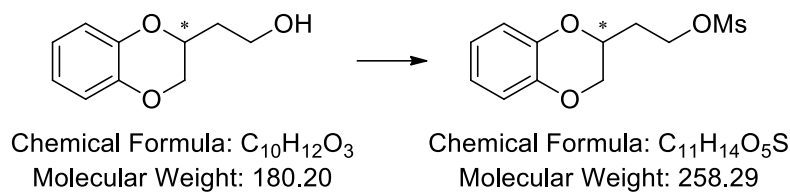


$LiAlH_4$ (0.37 g, 10.00 mmol) was suspended in dry THF (2 mL) at $0^\circ C$ under nitrogen atmosphere. A solution of Methyl 1,4-benzodioxane-2-yl-acetate (1.98 g, 9.5 mmol) in THF (5 mL) was added dropwise to the mixture; once added, the reaction was warmed to RT and stirred for 1 h; at completion, it was cooled to $0^\circ C$ and slowly quenched with Ethyl acetate (10 mL). Further ethyl acetate (10 mL) was added, the organic layer was washed with brine (3×20 mL), dried over Na_2SO_4 and concentrated under vacuum to give 1.60 g of 2-(1,4-Benzodioxane-2-yl)-ethanol as a colourless oil.

Yield = 93.0%

1H NMR ($CDCl_3$): δ 6.87 (m, 4H), 4.38 (m, 1H), 4.28 (dd, $J = 11.3, 2.2$ Hz, 1H), 3.94 (m, 3H), 1.91 ppm (m, 2H)

2-(1,4-Benzodioxane-2-yl)-ethyl methanesulfonate

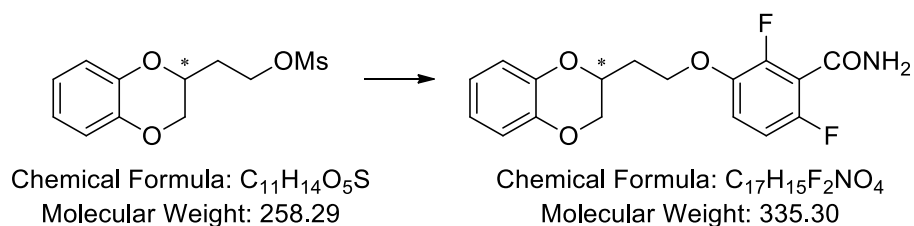


Mesyl chloride (1.00 mL, 13.32 mmol) was added dropwise to a solution of 2-(1,4-Benzodioxane-2-yl)-ethanol (1.60 g, 8.88 mmol) and TEA (1.80 mL, 13.32 mmol) in DCM (20 mL) at 0°C. The mixture was warmed to RT and stirred at that temperature for 2 h, diluted with further DCM (20 mL), washed firstly with 10% aqueous NaHCO₃ (30 mL), secondly with 10% aqueous HCl (30 mL) and finally with brine (30 mL), dried over Na₂SO₄, filtered and concentrated under vacuum to yield 2.10 g of 2-(1,4-Benzodioxane-2-yl)-ethyl methanesulfonate as yellowish oil.

Yield = 91.0%

¹H NMR (CDCl₃): δ 6.87 (m, 4H), 4.48 (ddd, J = 10.2, 7.0, 5.1 Hz, 2H), 4.34 (m, 1H), 4.27 (dd, J = 11.4, 2.3 Hz, 1H), 3.96 (dd, J = 11.4, 7.0 Hz, 1H), 3.05 (s, 3H), 2.09 ppm (m, 2H).

(III) 3-(1,4-Benzodioxane-2-yl)ethoxy)-2,6-difluorobenzamide



Potassium carbonate (0.42 g, 3.01 mmol) was added to a solution of 2,6-Difluoro-3-hydroxybenzamide (0.50 g, 2.88 mmol) in dry DMF (5 mL). After stirring at room temperature for 30 min, a solution of 2-(1,4-Benzodioxane-2-yl)-ethyl methanesulfonate (0.71 g, 2.75 mmol) in DMF (5 mL) was added. The reaction mixture was stirred at 60°C for 16 h, concentrated under vacuum, diluted with Ethyl acetate (30 mL), washed with brine (3 × 20 mL), dried over Na_2SO_4 , filtered and concentrated, to give a residue which was crystallized from 3/2 Cyclohexane/Ethyl acetate, accomplishing 0.50 g of 3-(1,4-Benzodioxane-2-yl)ethoxy)-2,6-difluorobenzamide as a white solid.

Yield = 54.0%

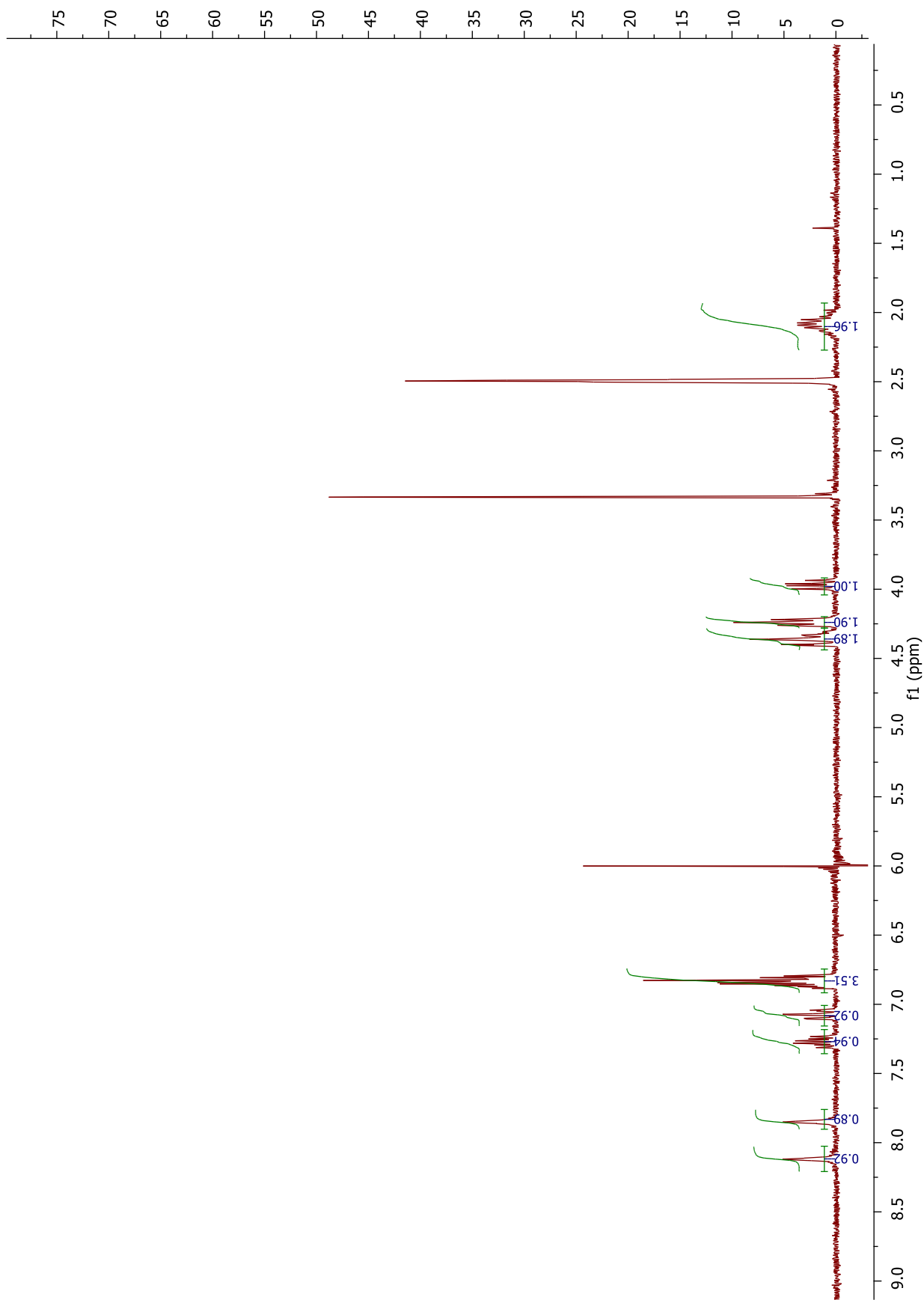
M.p. = 96.0°C

Tr (HPLC, gradient, 90% H_2O with 0.10% TFA to 10% acetonitrile with 0.10% TFA in 25 min with 35 min run time. Flow rate: 1 mL/min) = 13.2 min, Purity = 98.0%

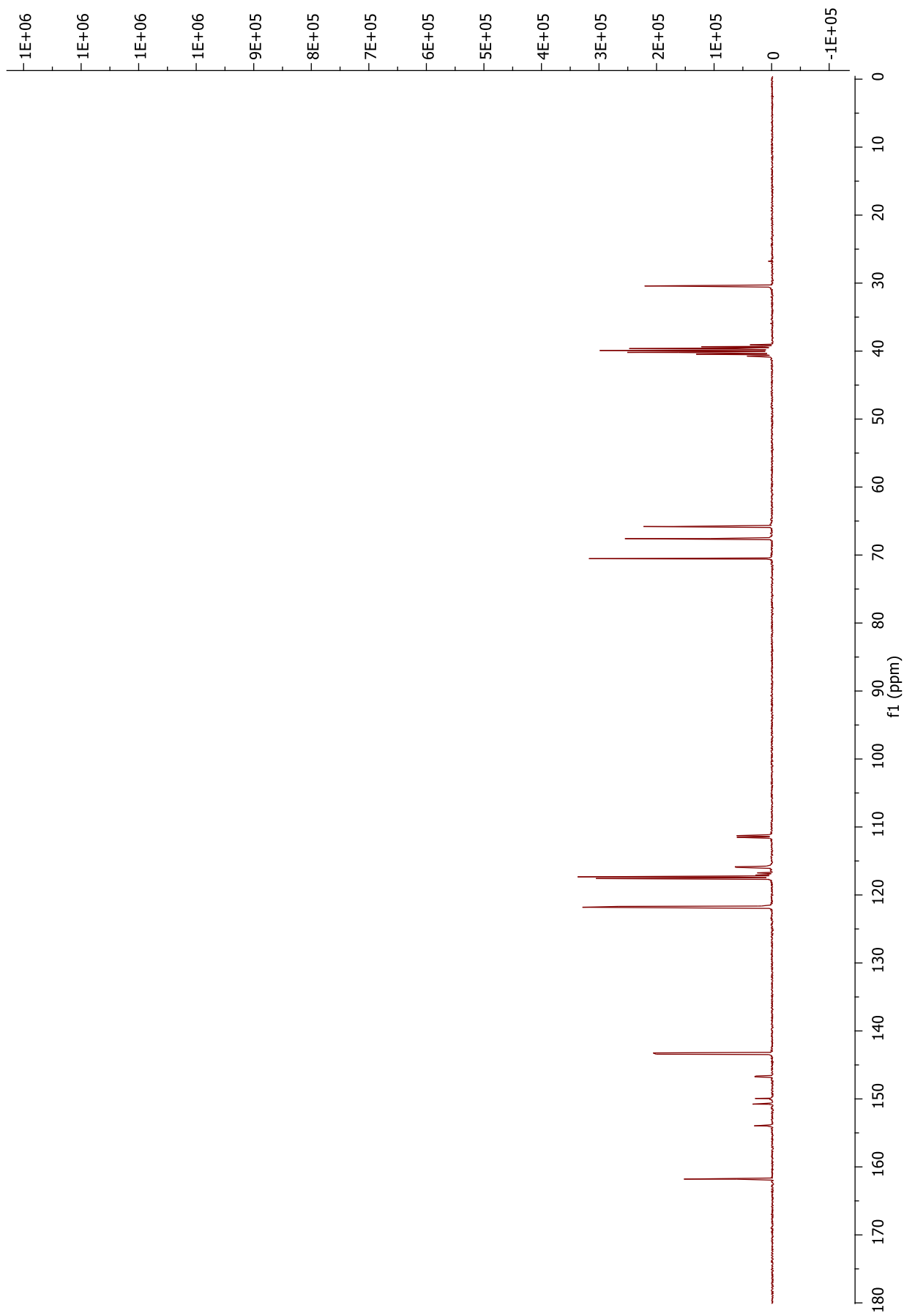
1H NMR (d_6 -DMSO): δ 8.12 (bs, 1H), 7.85 (bs, 1H), 7.27 (td, $J = 9.4, 5.3$ Hz, 1H), 7.07 (t, $J = 8.9$ Hz, 1H), 6.84 (m, 4H), 4.37 (dd, $J = 16.8, 5.7$ Hz, 2H), 4.24 (t, $J = 6.1$ Hz, 2H), 3.97 (dd, $J = 11.2, 7.2$ Hz, 1H), 2.08 ppm (dd, $J = 11.0, 6.2$ Hz, 2H).

^{13}C NMR (d_6 -DMSO): δ 161.8, 152.3 (dd, $J = 239.9, 6.8$ Hz), 148.3 (dd, $J = 246.9, 8.4$ Hz), 143.4, 143.3 (d, $J = 10.8$ Hz), 143.2, 121.8, 121.7, 117.6, 117.3, 117.1 (dd, $J = 25.6, 21.0$ Hz), 115.9 (d, $J = 7.1$ Hz), 111.4 (dd, $J = 22.8, 3.9$ Hz), 70.5, 67.6, 66.8, 30.4 ppm.

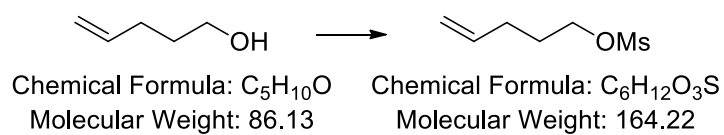
Experimental



Experimental



Pent-4-en-1-yl methanesulfonate

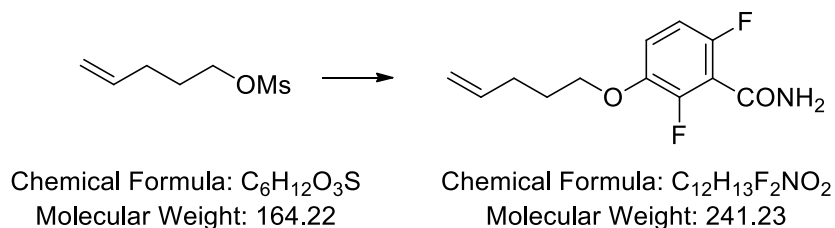


Mesyl chloride (1.08 mL, 13.93 mmol) was added dropwise to a solution of 4-Penten-1-ol (1.00 g, 11.61 mmol) and TEA (1.90 mL, 13.93 mmol) in DCM (10 mL) at $-15\text{ }^\circ\text{C}$. The mixture was stirred at that temperature for 3 h, diluted with DCM (20 mL), washed firstly with 10% aqueous NaHCO_3 (10 mL), secondly with 10% aqueous HCl (10 mL) and finally with brine (10 mL), dried over Na_2SO_4 , filtered and concentrated under vacuum to yield 1.52 g of Pent-4-en-1-yl methanesulfonate as a colourless oil.

Yield = 80.0%

$^1\text{H NMR}$ (CDCl_3): δ 5.78 (ddt, $J = 16.9, 10.2, 6.7$ Hz, 1H), 5.05 (m, 2H), 4.23 (t, $J = 6.5$ Hz, 2H), 3.00 (s, 3H), 2.18 (m, 2H), 1.86 ppm (m, 2H).

2,6-Difluoro-3-(pent-4-en-1-yloxy)benzamide

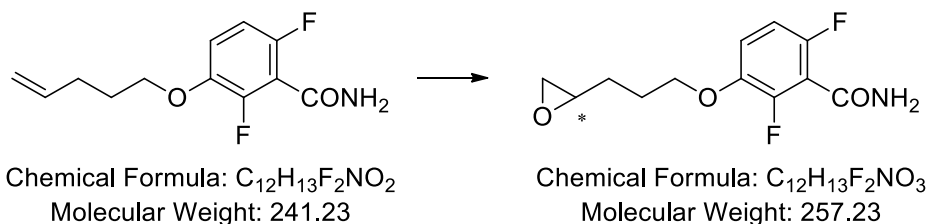


Potassium carbonate (0.48 g, 3.48 mmol) was added to a solution of 2,6-Difluoro-3-hydroxybenzamide (0.57 g, 3.32 mmol) in dry DMF (5 mL). After stirring at room temperature for 30 min, a solution of Pent-4-en-1-yl methanesulfonate (0.52 g, 3.17 mmol) in DMF (5 mL) was added. The reaction mixture was stirred at 80°C for 16 h, concentrated under vacuum, diluted with ethyl acetate (30 mL), washed firstly with 10% aqueous $NaHCO_3$ (10 mL), secondly with 10% aqueous HCl (10 mL) and finally with brine (10 mL), dried over Na_2SO_4 , filtered and concentrated, to give 0.71 g of 2,6-Difluoro-3-(pent-4-en-1-yloxy)benzamide as a brown oil.

Yield = 93.0%

1H NMR ($CDCl_3$): δ 6.99 (td, $J = 9.1, 5.2$ Hz, 1H), 6.86 (td, $J = 9.1, 1.9$ Hz, 1H), 5.98 (bs, 2H), 5.83 (ddt, $J = 16.9, 10.2, 7.0$ Hz, 1H), 5.02 (m, 2H), 4.01 (t, $J = 6.4$ Hz, 2H), 2.24 (dd, $J = 14.1, 7.0$ Hz, 2H), 1.89 ppm (m, 2H)

2,6-Difluoro-3-(3-(oxiran-2-yl)propoxy)benzamide

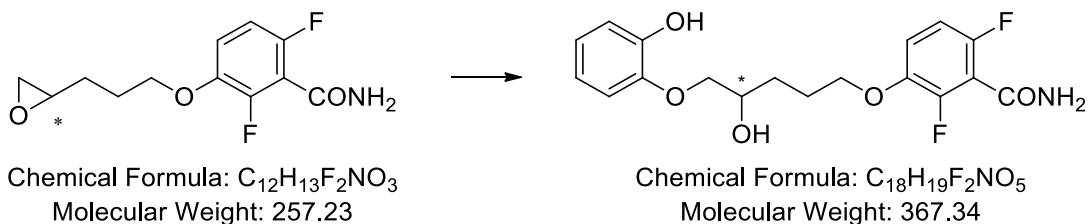


m-CPBA (0.31 g, 1.78 mmol) was added to a solution of 2,6-Difluoro-3-(pent-4-en-1-yloxy)benzamide (0.43 g, 1.78 mmol) in DCM (5 mL) at 0°C. The reaction mixture was stirred at room temperature for 18 h, diluted with DCM, washed with 10% aqueous $NaHCO_3$ (2 × 15 mL) dried over Na_2SO_4 , filtered and concentrated to give 0.42 g of 2,6-Difluoro-3-(3-(oxiran-2-yl)propoxy)benzamide as a colourless oil.

Yield = 91.0%

1H NMR ($CDCl_3$): δ 7.00 (td, J = 9.1, 5.2 Hz, 1H), 6.86 (td, J = 9.1, 1.9 Hz, 1H), 6.16 (bs, 1H), 6.03 (bs, 1H), 4.06 (m, 2H), 2.98 (m, 1H), 2.78 (dd, J = 4.8, 4.1 Hz, 1H), 2.51 (dd, J = 4.8, 2.7 Hz, 1H), 1.88 (m, 2H), 1.58 ppm (m, 2H).

2,6-Difluoro-3-((4-hydroxy-5-(2-hydroxyphenoxy)pentyl)oxy)benzamide

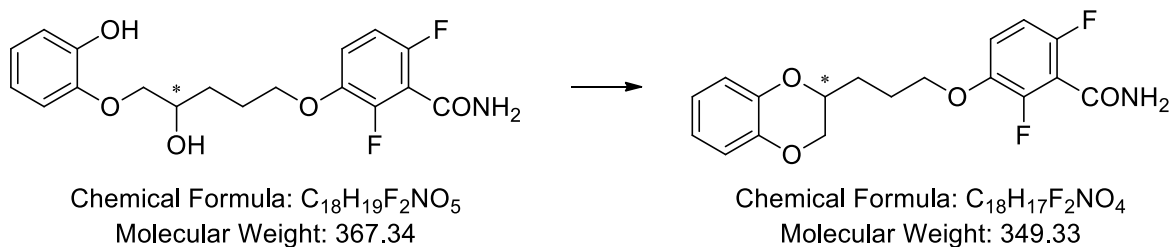


NaH (0.04 g, 1.63 mmol) was suspended in dry DMF (5 mL) at 0°C under nitrogen atmosphere. A solution of Catechol (0.18 g, 1.63 mmol) in DMF (5 mL) was added dropwise and, after stirring at room temperature for 30 minutes, a solution of 2,6-Difluoro-3-(3-(oxiran-2-yl)propoxy)benzamide (0.42 g, 1.63 mmol) in DMF (5 mL) was then added dropwise. The reaction mixture is heated at 100°C and stirred for 72 h. The mixture was then cooled to RT and slowly quenched with 1/1 ethyl acetate and 10% aqueous HCl (40 mL). The phases were separated and the organic one was washed with brine (10 mL), dried over Na_2SO_4 , filtered and concentrated to yield 0.46 g of 2,6-Difluoro-3-((4-hydroxy-5-(2-hydroxyphenoxy)pentyl)oxy)benzamide as a reddish oil.

Yield = 77.0%

1H NMR ($CDCl_3$): δ 7.00 (td, $J = 9.1, 5.2$ Hz, 1H), 6.86 (td, $J = 9.1, 1.9$ Hz, 1H), 6.16 (bs, 1H), 6.03 (bs, 1H), 4.06 (m, 2H), 2.98 (m, 1H), 2.78 (dd, $J = 4.8, 4.1$ Hz, 1H), 2.51 (dd, $J = 4.8, 2.7$ Hz, 1H), 1.88 (m, 2H), 1.58 ppm (m, 2H).

(IV) 3-(1,4-Benzodioxane-2-yl)propoxy)-2,6-difluorobenzamide



Under nitrogen atmosphere, to a solution of Triphenylphosphine (0.48 g, 1.84 mmol) in THF (2 mL), DIAD (0.36 mL, 1.84 mmol) and a solution of 2,6-Difluoro-3-((4-hydroxy-5-(2-hydroxyphenoxy)pentyl)oxy)benzamide (0.45 g, 1.23 mmol) in THF (1 mL) were added dropwise at 0°C. The reaction mixture was stirred at reflux for 24 h, concentrated under vacuum, diluted with Ethyl acetate (10 mL), washed firstly with brine (10 mL), secondly with 10% aqueous NaOH (10 mL) and lastly with brine (10 mL), dried over Na_2SO_4 , filtered and concentrated, to give a residue which was purified by flash chromatography on silica gel. Elution with 1/1 Cyclohexane/Ethyl acetate on silica gel gave 0.05 g of 3-(1,4-Benzodioxane-2-yl)propoxy)-2,6-difluorobenzamide as a white wax.

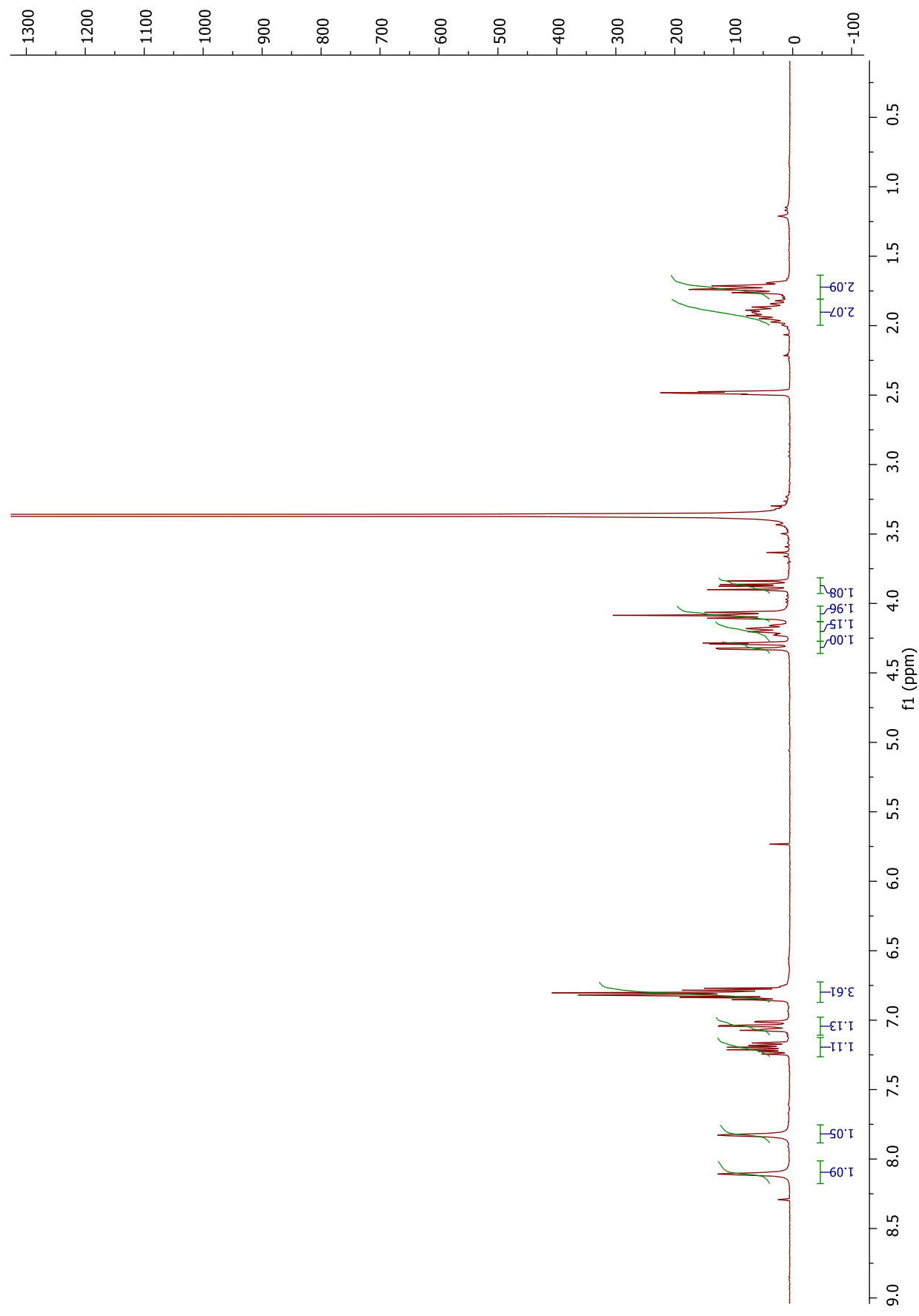
Yield = 11.0%

Tr (HPLC, gradient, 90% H_2O with 0.10% TFA to 10% acetonitrile with 0.10% TFA in 25 min with 35 min run time. Flow rate: 1 mL/min) = 13.7 min, Purity = 99.2%

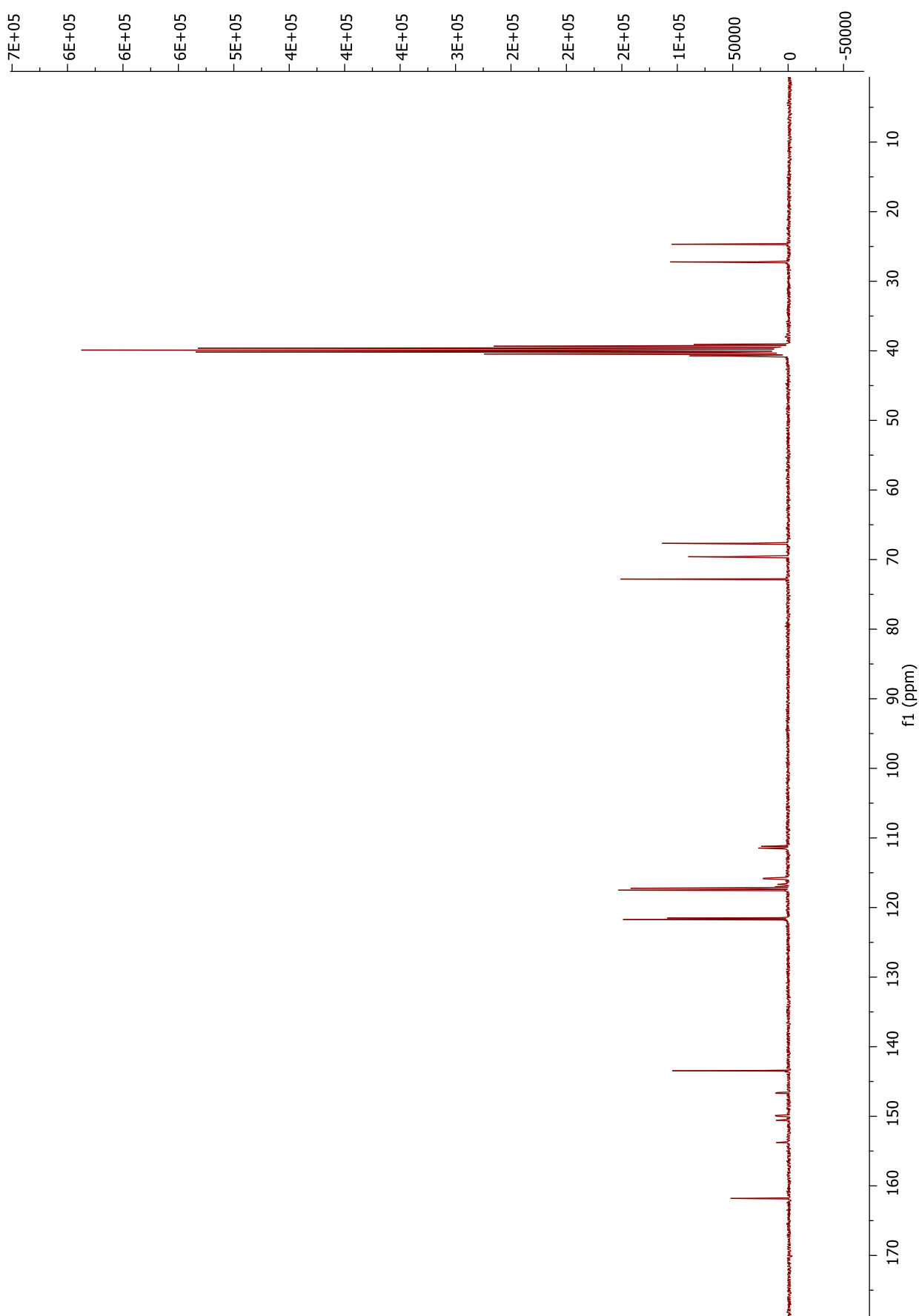
1H NMR (d_6 -DMSO): δ 8.11 (bs, 1H), 7.83 (bs, 1H), 7.20 (td, $J = 9.3, 5.3$ Hz, 1H), 7.04 (td, $J = 9.0, 1.8$ Hz, 1H), 6.78 (m, 4H), 4.31 (dd, $J = 11.4, 2.2$ Hz, 1H), 4.20 (m, 1H), 4.08 (t, $J = 6.3$ Hz, 2H), 3.87 (dd, $J = 11.4, 7.5$ Hz, 1H), 1.90 (m, 2H), 1.69 ppm (m, 2H).

^{13}C NMR (d_6 -DMSO): δ 161.81, 152.13 (dd, $J = 240.8, 6.8$ Hz), 148.29 (dd, $J = 248.2, 8.5$ Hz), 143.46, 143.50 (dd, $J = 10.6, 3.2$ Hz), 143.45, 121.72, 121.51, 117.51, 117.23, 117.0 (dd, $J = 23.0, 18.6$ Hz), 115.83 (dd, $J = 9.3, 2.5$ Hz), 111.33 (dd, $J = 22.8, 4.0$ Hz), 72.80, 69.59, 67.67, 27.22, 24.68 ppm.

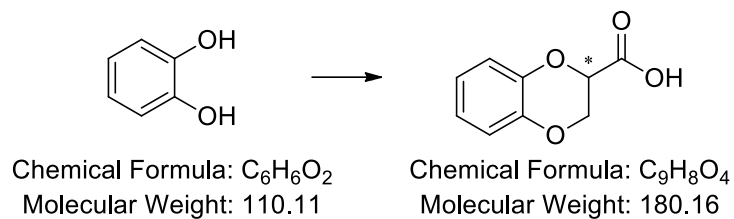
Experimental



Experimental



(1,4-Benzodioxan-2-yl)-carboxylic acid



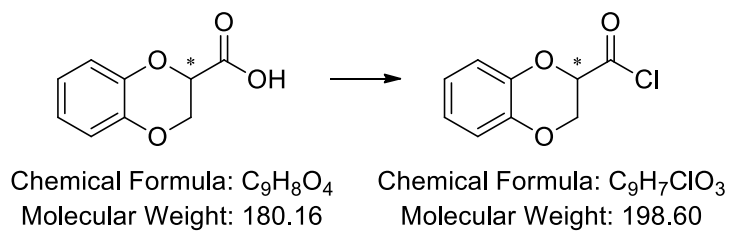
A suspension of Catechol (11.01 g, 100 mmol) and K_2CO_3 (41.46 g, 300 mmol) in Acetone (110 mL) was stirred at room temperature for 30 minutes. Ethyl 2,3-dibromopropionate (24.60 g, 100 mmol) was added dropwise and the reaction mixture was stirred at $60^\circ C$ for 18 hours, concentrated under vacuum, diluted with Methanol (100 mL), added with 10% aqueous NaOH (80 mL) and stirred for 18 hours. The reaction mixture was then acidified with 10% aqueous HCl, extracted with Ethyl Acetate (3 x 50 mL), washed with 10% aqueous NaCl, dried with Na_2SO_4 , filtered and concentrated under vacuum to give 14.43 g of (1,4-Benzodioxan-2-yl)-carboxylic acid as a brownish solid.

Yield = 80.0%

M.p. = $125.4^\circ C$

1H NMR ($CDCl_3$): δ 6.95 (m, 4H), 4.90 (dd, $J = 4.2, 3.5$ Hz, 1H), 4.44 (dd, $J = 11.5, 4.2$ Hz, 1H), 4.40 ppm (dd, $J = 11.5, 3.5$ Hz, 1H).

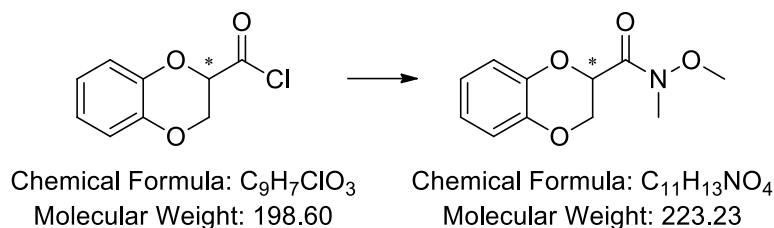
(1,4-Benzodioxan-2-yl) carbonyl chloride



$SOCl_2$ (5.28 g, 44.40 mmol) was added dropwise to a solution of Ethyl 2,3-dihydrobenzo[b][1,4]dioxine-2-carboxylate (4.00 g, 22.2 mmol) in DCM (40 mL) at $0^\circ C$. The reaction mixture was stirred at reflux for 18 hours and concentrated under vacuum to give 4.40 g of (1,4-Benzodioxan-2-yl) carbonyl chloride as a brown oil.

Yield = Quantitative

1H NMR ($CDCl_3$): δ 6.95 (m, 4H), 5.09 (t, $J = 2.9$ Hz, 1H), 4.73 (dd, $J = 11.8, 2.9$ Hz, 1H), 4.34 ppm (dd, $J = 11.8, 2.9$ Hz, 1H).

N-Methoxy-*N*-methyl-(1,4-benzodioxan-2-yl)carboxamide

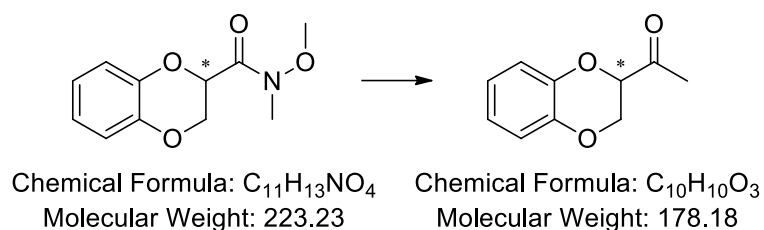
N,O-Dimethylhydroxylamine hydrochloride (4.10 g, 41.1 mmol) was added to a solution of (1,4-Benzodioxan-2-yl) carbonyl chloride (4.40 g, 20.54 mmol) in DCM (44 mL) at 0°C. The reaction mixture was allowed to warm at room temperature and stirred for 18 hours, diluted with DCM (40 mL), washed firstly with 10% aqueous HCl, secondly with 10% aqueous $NaHCO_3$, lastly with 10% aqueous NaCl, dried over Na_2SO_4 , filtered and concentrated under vacuum to give 4.05 g of *N*-Methoxy-*N*-methyl-(1,4-benzodioxan-2-yl)carboxamide as a yellowish solid.

Yield = 89.0%

M.p. = 68.6°C

1H NMR ($CDCl_3$): δ 6.93 (m, 4H), 5.05 (dd, J = 7.0, 2.5 Hz, 1H), 4.43 (dd, J = 11.4, 2.5 Hz, 1H), 4.25 (dd, J = 11.4, 7.0 Hz, 1H), 3.79 (s, 3H), 3.26 ppm (s, 3H).

1-(1,4-Benzodioxan-2-yl)-ethanone



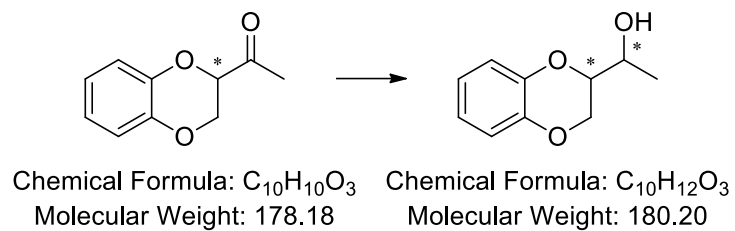
Methyl magnesium bromide (27.21 mmol, 9.07 mL) was added dropwise to a solution of *N*-Methoxy-*N*-methyl-(1,4-benzodioxan-2-yl)carboxamide (4.05 g, 18.14 mmol) in dry THF (73 mL) at 0°C under N_2 . The reaction mixture was stirred at room temperature for 1,5 hours and poured into a 1/1 mixture of Ethyl acetate and 10% aqueous HCl (50 + 50 mL). The organic phase was then washed twice with 10% aqueous NaCl, dried over Na_2SO_4 , filtered and concentrated under vacuum to give 2.97 g of 1-(1,4-Benzodioxan-2-yl)ethanone as a brownish solid.

Yield = 92.0%

M.p. = 32.4°C

1H NMR ($CDCl_3$): δ 6.84 (m, 4H), 4.61 (dd, J = 6.2, 3.9 Hz, 1H), 4.33 (dd, J = 12.9, 3.9 Hz, 1H), 4.30 (dd, J = 12.9, 6.2 Hz, 1H), 2.30 ppm (s, 3H).

1-(1,4-Benzodioxan-2-yl)-ethanol

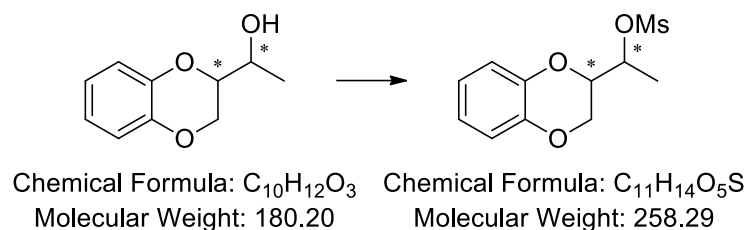


$NaBH_4$ (0.21 g, 5.61 mmol) was added to a solution of 1-(1,4-Benzodioxan-2-yl)ethanone (2.00 g, 11.22 mmol) in Methanol (20 mL) at 0°C. The reaction mixture was stirred at the same temperature for 0.5 hours and then concentrated under vacuum to give 2.02 g of 1-(1,4-Benzodioxan-2-yl)-ethanol as a brown oil, which was used for the subsequent step without further purification.

Yield = Quantitative

1H NMR ($CDCl_3$) mixture of 4 isomers: δ 6.89 (m, 4H), 4.32 (ddd, $J = 12.8, 11.3, 2.0$ Hz, 1H), 4.04 (m, 2H), 4.05 (m, 1H), 1.34 ppm (d, $J = 6.5$ Hz, 3H).

1-(1,4-Benzodioxan-2-yl)-ethyl methanesulfonate

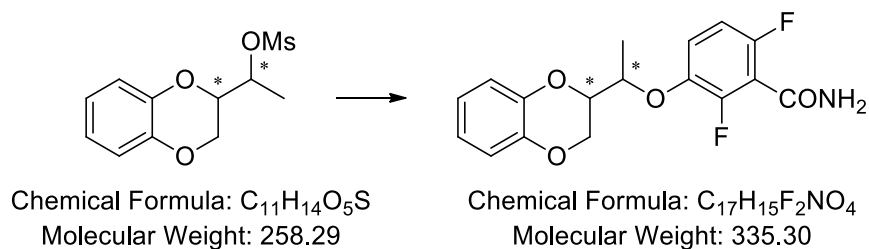


Methanesulfonyl chloride (1.54 g, 13.4 mmol) was added dropwise to a solution of 1-(1,4-Benzodioxan-2-yl)-ethanol (2.02 g, 11.2 mmol) and TEA (1.48 g, 14.6 mmol) in DCM (40 mL) at 0°C. The reaction mixture was stirred at room temperature for 1 hour, washed firstly with 10% aqueous HCl (20 mL), with 10% aqueous NaCl (20 mL), dried over Na_2SO_4 , filtered and concentrated under vacuum to give 2.65 g of 1-(1,4-Benzodioxan-2-yl)-ethyl methanesulfonate as a brownish oil.

Yield = 92.0%

1H NMR ($CDCl_3$) mixture of 4 isomers: δ 6.86 (m, 4H), 4.96 (m, 1H), 4.25 (m, 2H), 4.24 (m, 1H) 3.08 and 3.06 (s, 3H), 1.57 and 1.56 ppm (d, $J = 6.6$ Hz, 3H).

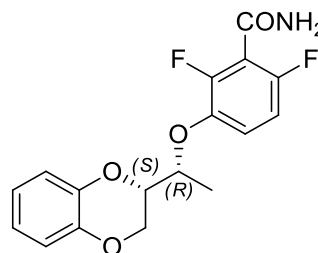
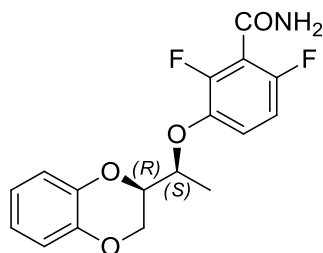
(V) 3-(1-(1,4-Benzodioxan-2-yl)-ethoxy)-2,6-difluorobenzamide



Potassium carbonate (0.84 g, 6.1 mmol) was added to a solution of 2,6-Difluoro-3-hydroxybenzamide (1.00 g, 5.8 mmol) in dry DMF (5 mL). After stirring at room temperature for 30 minutes, a solution of 1-(1,4-Benzodioxan-2-yl)-ethyl methanesulfonate (1.49 g, 5.8 mmol) in dry DMF (5 mL) was added. The reaction mixture was stirred at 80°C for 16 hours, concentrated under vacuum, diluted with Ethyl Acetate (15 mL), washed with brine (3 x 10 mL), dried over Na₂SO₄, filtered and concentrated under vacuum. Elution with 6/4 Cyclohexane/Ethyl Acetate on silica gel gave 0.2 g of 3-(1-(1,4-Benzodioxan-2-yl)-ethoxy)-2,6-difluorobenzamide as a yellowish oil. 0.14 g corresponded to one enantiomeric couple and 0.06 g to the other.

Yield = 10.0%

(S,R) and *(R,S)* – Erythro couple:

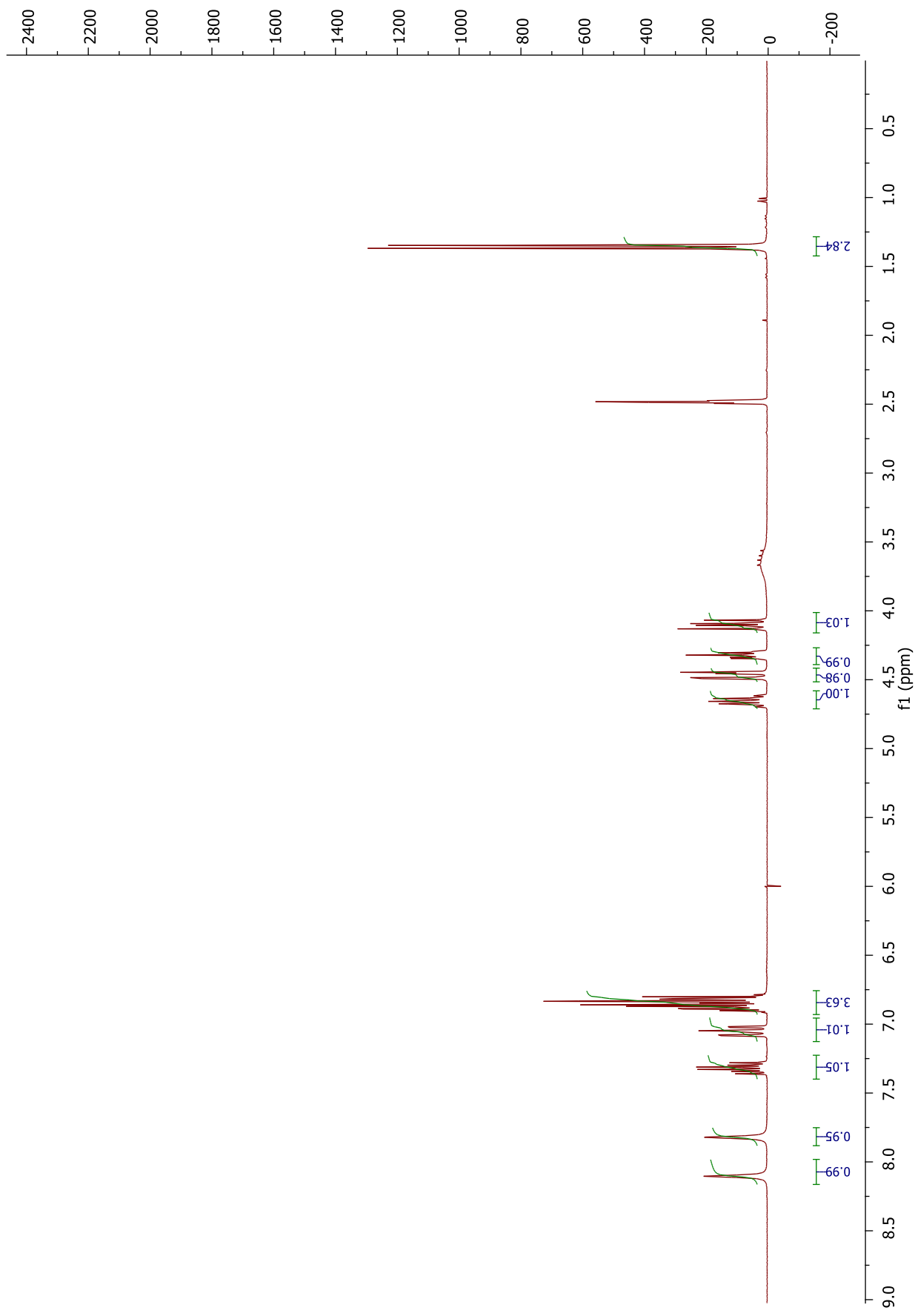


¹H NMR (d₆-DMSO): δ 8.10 (bs, 1H), 7.82 (bs, 1H), 7.32 (dt, *J* = 9.2, 5.3 Hz, 1H), 7.05 (dt, *J* = 9.2, 1.9 Hz, 1H), 6.83 (m, 4H), 4.66 (dq, *J* = 6.3, 5.1 Hz, 1H), 4.47 (dd, *J* = 11.5, 2.2 Hz, 1H), 4.32 (ddd, *J* = 7.3, 5.1, 2.2 Hz, 1H), 4.10 (dd, *J* = 11.5, 7.3 Hz, 1H), 1.36 ppm (d, *J* = 6.3 Hz, 3H).

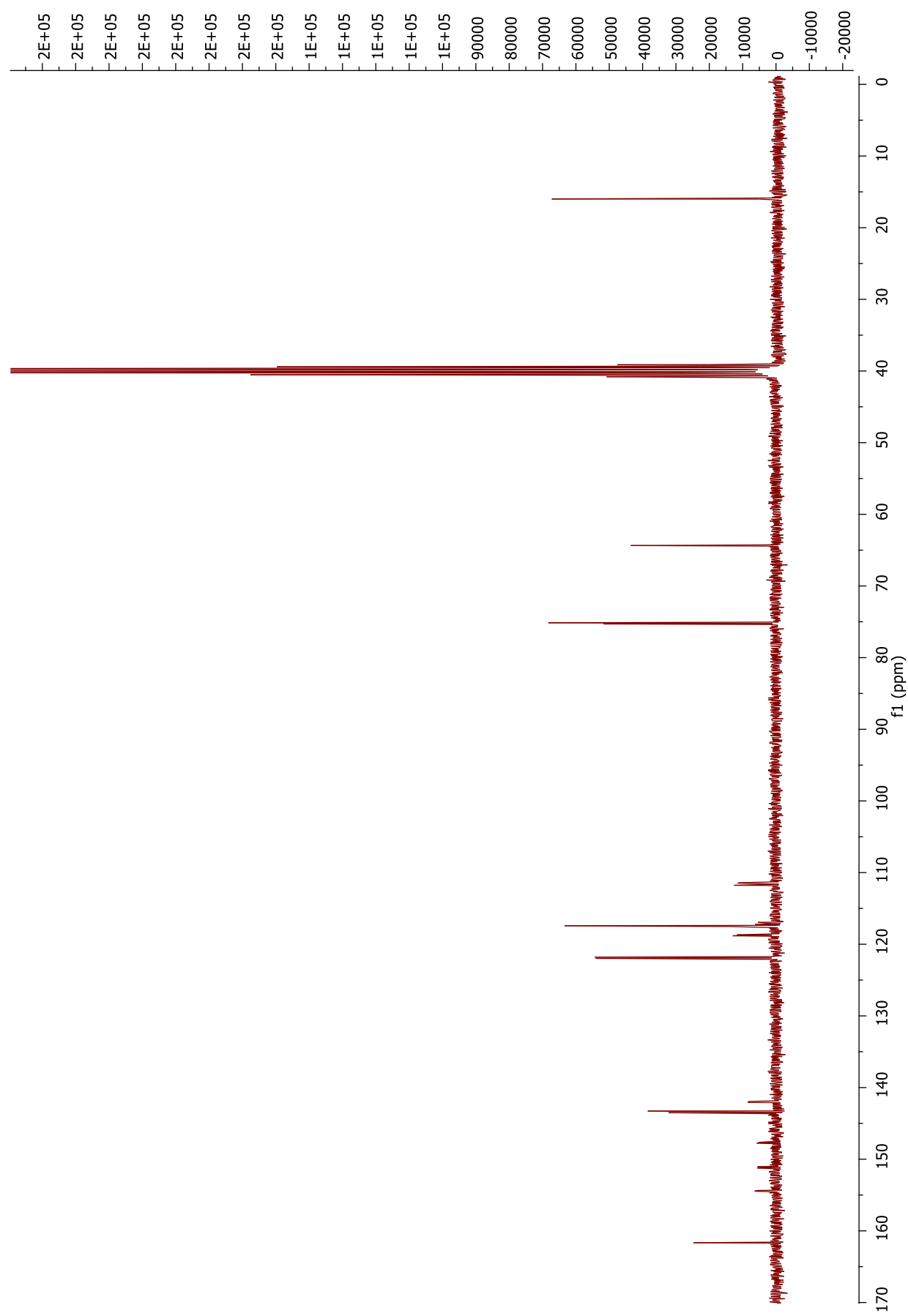
¹³C NMR (d₆-DMSO): δ 161.7, 152.8 (dd, *J* = 242.2, 6.8 Hz), 149.4 (dd, *J* = 248.6, 8.6 Hz), 143.5, 143.3, 142.0 (dd, *J* = 11.0, 3.3 Hz), 122.0, 121.8, 118.7 (dd, *J* = 9.4, 2.2 Hz), 117.5, 117.4, 117.2 (dd, *J* = 24.8, 20.9 Hz), 111.6 (dd, *J* = 23.0, 4.0 Hz), 75.3, 75.1, 64.4, 16.0 ppm.

Tr (HPLC, Isocratic, H₂O with 0.10% TFA / Acetonitrile with 0.10% TFA 60/40. 30 min run time. Flow rate: 1 mL/min) = 7.48 min, Purity = 99.0%

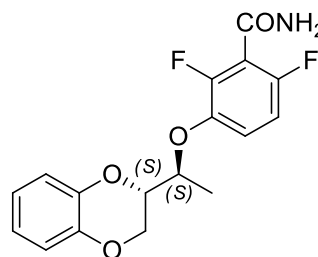
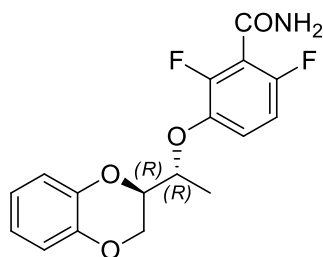
Experimental



Experimental



(S,S) and *(R,R)* – Threo couple:

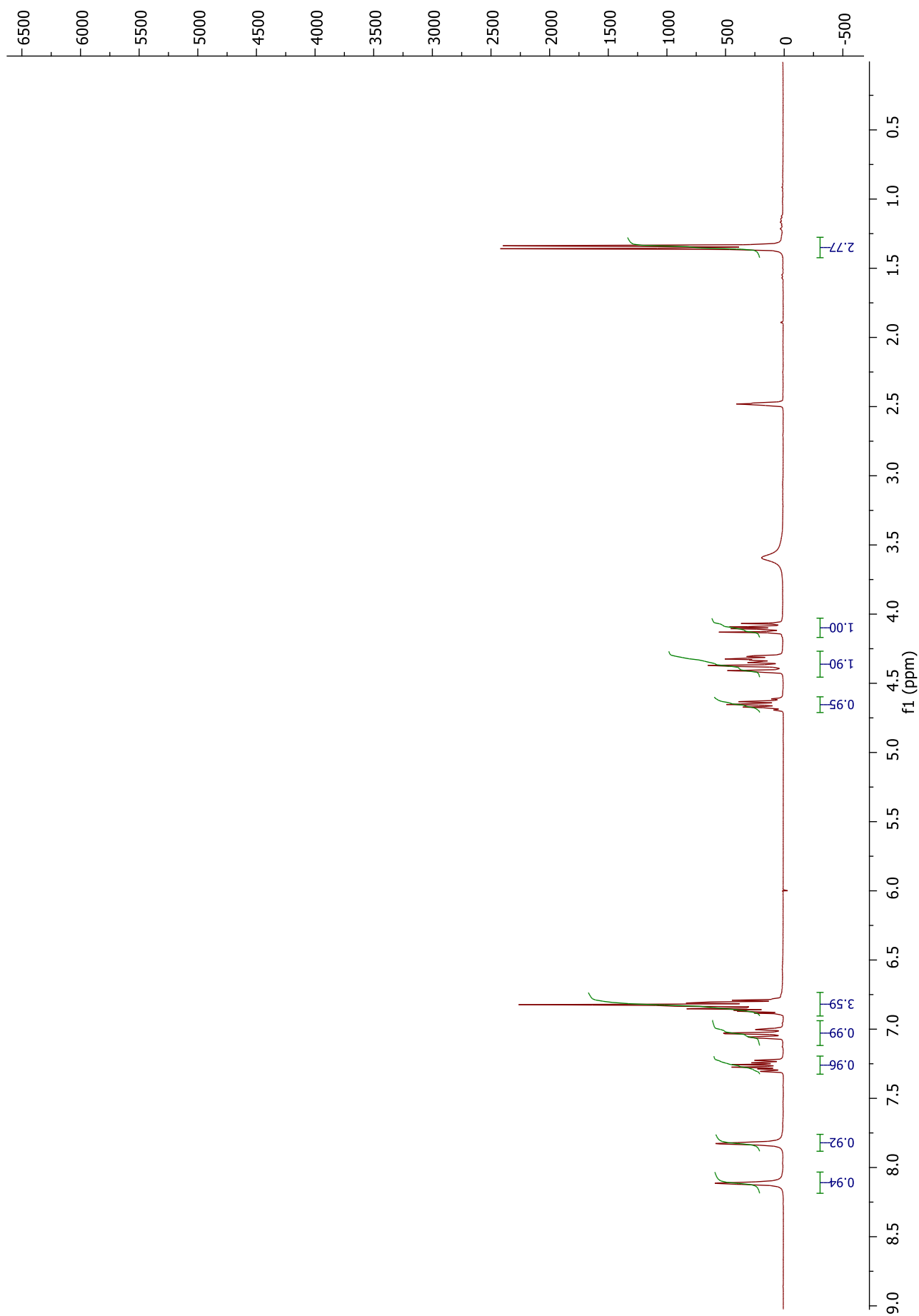


¹H NMR (d₆-DMSO): δ 8.11 (bs, 1H), 7.83 (bs, 1H), 7.27 (dt, J = 9.1, 5.4 Hz, 1H), 7.03 (dt, J = 9.1, 1.6 Hz, 1H), 6.85 (m, 4H), 4.65 (dq, J = 6.3, 5.2 Hz, 1H), 4.39 (dd, J = 11.3, 2.1 Hz, 1H), 4.3 (ddd, J = 7.4, 5.2, 2.1 Hz, 1H), 4.10 (dd, J = 11.3, 7.4 Hz, 1H), 1.35 ppm (d, J = 6.3 Hz, 3H).

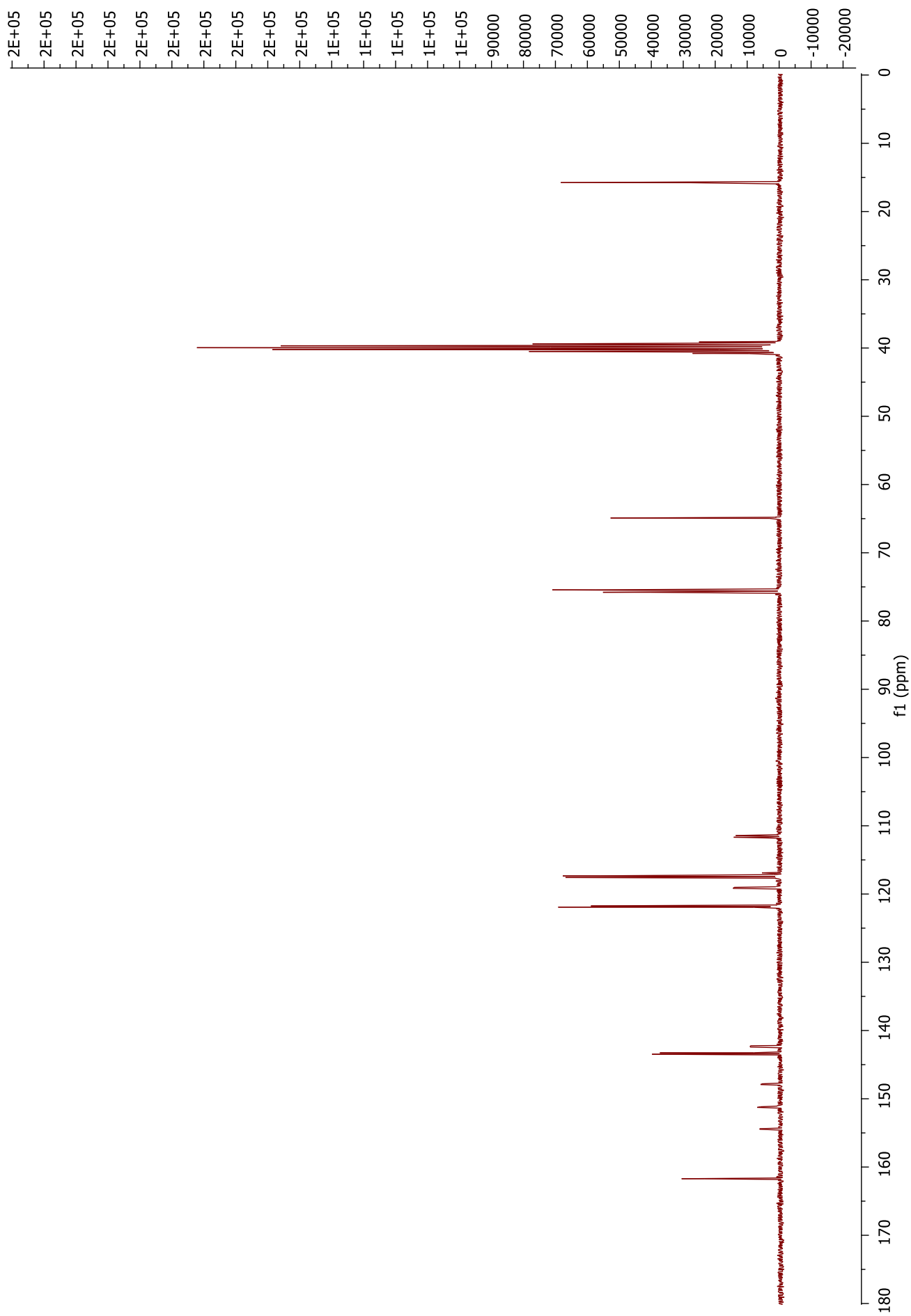
¹³C NMR (d₆-DMSO): δ 161.7, 152.8 (dd, J = 242.1, 6.9 Hz), 149.5 (dd, J = 248.6, 8.6 Hz), 143.5, 143.3, 142.3 (dd, J = 11.0, 3.4 Hz), 121.9, 121.7, 119.1 (dd, J = 9.4, 2.1 Hz), 117.6, 117.3, 117.2 (dd, J = 24.9, 20.9 Hz), 111.6 (dd, J = 23.0, 3.9 Hz), 75.8, 75.4, 64.9, 15.8 ppm.

Tr (HPLC, Isocratic, H₂O with 0.10% TFA / Acetonitrile with 0.10% TFA 60/40. 30 min run time. Flow rate: 1 mL/min) = 5.58 min, Purity = 99.0%

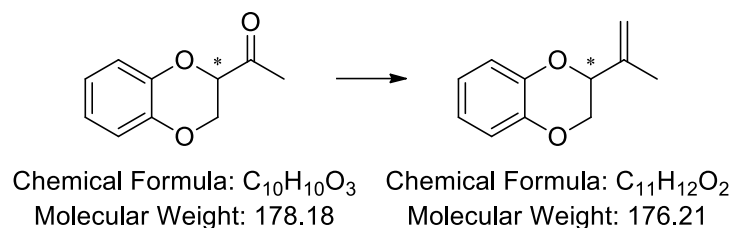
Experimental



Experimental



2-(1,4-Benzodioxan-2-yl)-propene

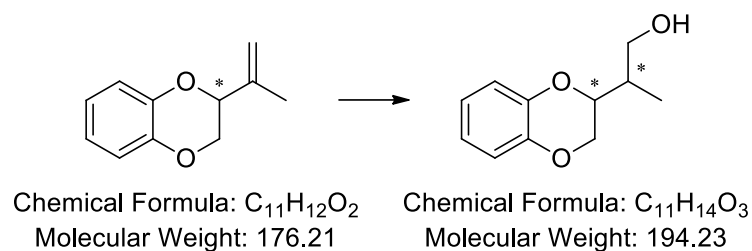


Potassium *t*-butoxide (0.30 g, 2.7 mmol) was added to a solution of Methyltriphenyl Phosphonium Bromide (1.28 g, 2.7 mmol) in Toluene (10 mL) under N₂. After stirring at room temperature for 20 minutes, a solution of 1-(1,4-Benzodioxan-2-yl)ethanone (0.27 g, 1.5 mmol) in Toluene (5 mL) was added dropwise. The reaction mixture was stirred at 80°C for 5 hours, concentrated under vacuum, diluted with Ethyl acetate (20 mL), washed twice with brine (10 + 10 mL), dried over Na₂SO₄, filtered and concentrated under vacuum. Elution with 8/2 Cyclohexane/Ethyl Acetate on silica gel gave 0.18 g of 2-(1,4-Benzodioxan-2-yl)-propene as a yellowish oil.

Yield = 69.0%

¹H NMR (CDCl₃): δ 6.92 (m, 4H), 5.19 (s, 1H), 5.10 (s, 1H), 4.53 (dd, J = 8.1, 2.4 Hz, 1H), 4.30 (dd, J = 11.3, 2.4 Hz, 1H), 3.95 (dd, J = 11.3, 8.1 Hz, 1H), 1.85 ppm (s, 3H).

2-(1,4-Benzodioxan-2-yl)-1-propanol

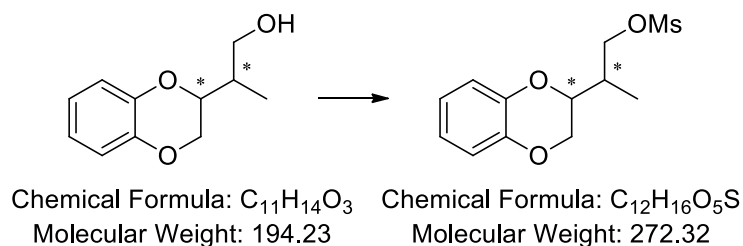


A 1M solution of BH_3 in THF (3 mL) was added to 2-(1,4-Benzodioxan-2-yl)-propene (0.18 g, 1 mmol) under N_2 . After stirring for 2 hours, H_2O (1.8 mL), 10% aqueous NaOH (4 mL) and 30% H_2O_2 (3.6 mL) were added. The reaction mixture was stirred at room temperature for 18 hours, diluted with H_2O (10 mL) and extracted with Ethyl Acetate (3 x 25 mL). The organic phase was then dried over Na_2SO_4 , filtered and concentrated under vacuum to give 0.13 g of 2-(1,4-Benzodioxan-2-yl)-1-propanol as a yellowish oil.

Yield = 68.0%

1H NMR ($CDCl_3$) mixture of 4 isomers: δ 6.85 (m, 4H), 4.19 (m, 2H), 4.21 (m, 1H), 3.74 (m, 2H), 2.05 (m, 1H), 1.07 and 1.05 ppm (d, $J = 7.0$ Hz, 3H).

2-(1,4-Benzodioxan-2-yl)-1-propyl methanesulfonate

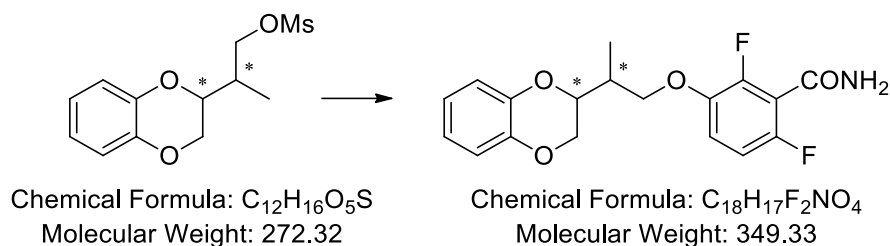


Methanesulfonyl chloride (0.06 g, 0.54 mmol) was added dropwise to a solution of 2-(1,4-Benzodioxan-2-yl)-1-propanol (0.08 g, 0.4 mmol) and TEA (0.05 g, 0.54 mmol) in DCM (1,6 mL) at 0°C. The reaction mixture was stirred at room temperature for 3 hours, washed firstly with 10% aqueous HCl (3 mL), with 10% aqueous NaCl (2 mL), dried over Na_2SO_4 , filtered and concentrated under vacuum to give 0.11 g of 2-(1,4-Benzodioxan-2-yl)-1-propyl methanesulphonate as a yellowish oil.

Yield = 92.0%

1H NMR ($CDCl_3$) mixture of 4 isomers: δ 6.81 (m, 4H), 4.44 (m, 1H), 4.26 (m, 2H), 4.23 (m, 1H), 4.02 (m, 2H), 3.03 (s, 3H), 1.16 and 1.11 ppm (d, $J = 7.0$ Hz, 3H).

(VI) 3-[2-(1,4-Benzodioxan-2-yl)-1-propiloxy]-2,6-difluorobenzamide

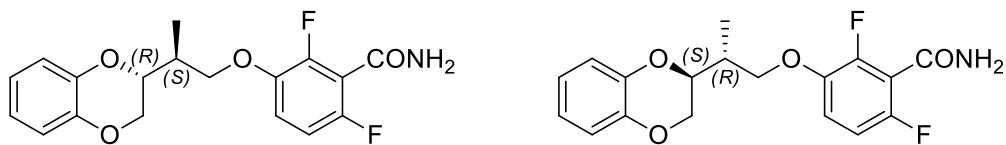


Potassium carbonate (0.06 g, 0.44 mmol) was added to a solution of 2,6-Difluoro-3-hydroxybenzamide (0.07 g, 0.4 mmol) in dry DMF (3 mL). After stirring at room temperature for 30 minutes, a solution of 2-(1,4-Benzodioxan-2-yl)-1-propyl methanesulphonate (0.11 g, 0.4 mmol) in dry DMF (3 mL) was added. The reaction mixture was stirred at 80°C for 16 hours, concentrated under vacuum, diluted with Ethyl Acetate (15 mL), washed with brine (3 x 10 mL), dried over Na_2SO_4 , filtered and concentrated under vacuum. Elution with 3/7 Cyclohexane/Ethyl Acetate on silica gel gave 0.06 g of 3-[2-(1,4-Benzodioxan-2-yl)-1-propiloxy]-2,6-difluorobenzamide, as a mixture of stereoisomers, as a yellowish oil.

The mixture of stereoisomers was further purified via preparative HPLC.

Yield = 43.0%

(*S,R*) and (*R,S*) – Threo couple:

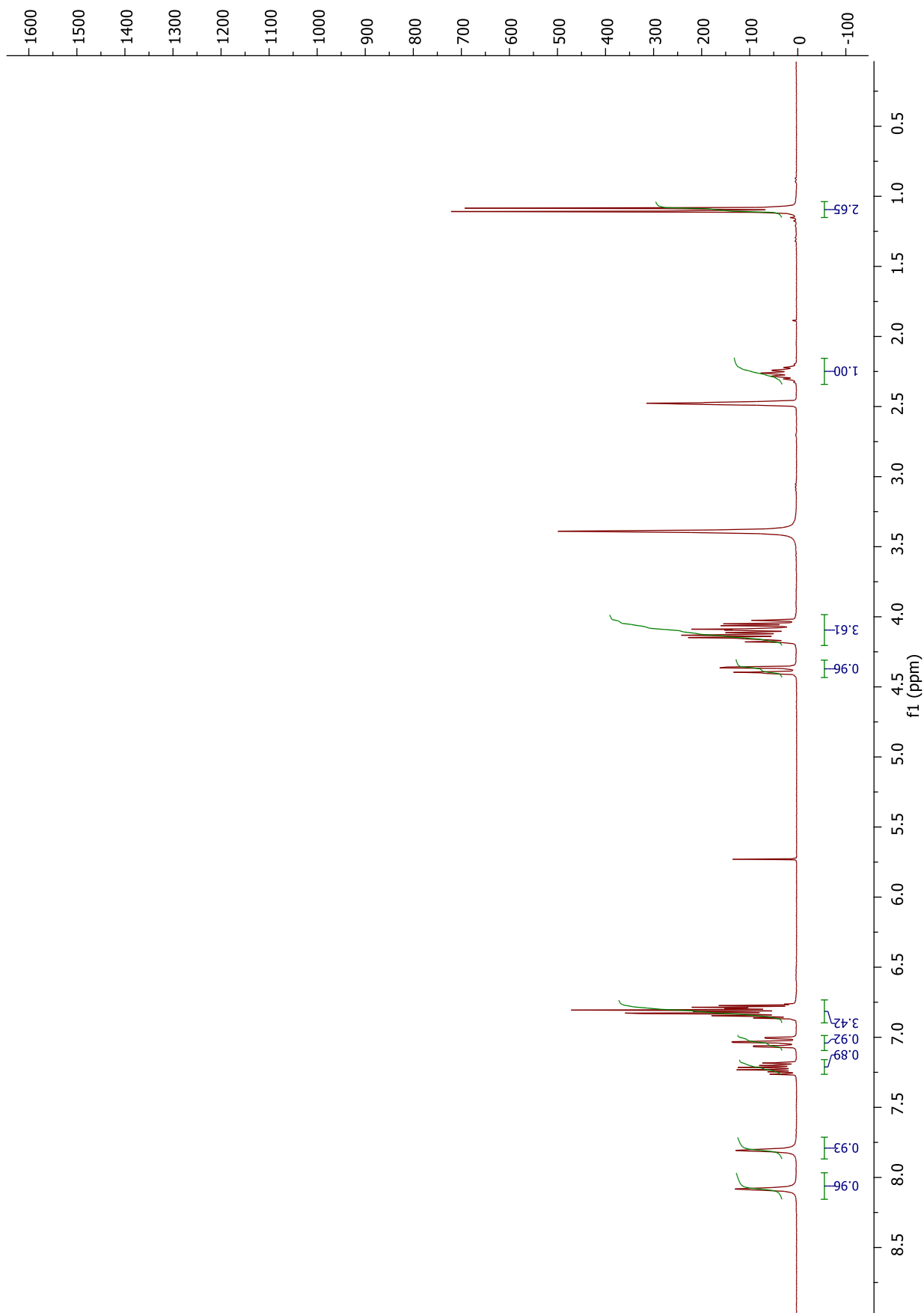


¹H NMR (d₆-DMSO): δ 8.08 (bs, 1H), 7.80 (bs, 1H), 7.22 (dt, *J* = 9.2, 5.3 Hz, 1H), 7.03 (dt, *J* = 9.2, 1.9 Hz, 1H), 6.80 (m, 4H), 4.38 (dd, *J* = 11.3, 1.8 Hz, 1H), 4.14 (m, 3H), 4.06 (dd, *J* = 10.4, 6.6 Hz, 1H), 2.20 (m, 1H), 1.10 ppm (d, *J* = 7.0 Hz, 3H).

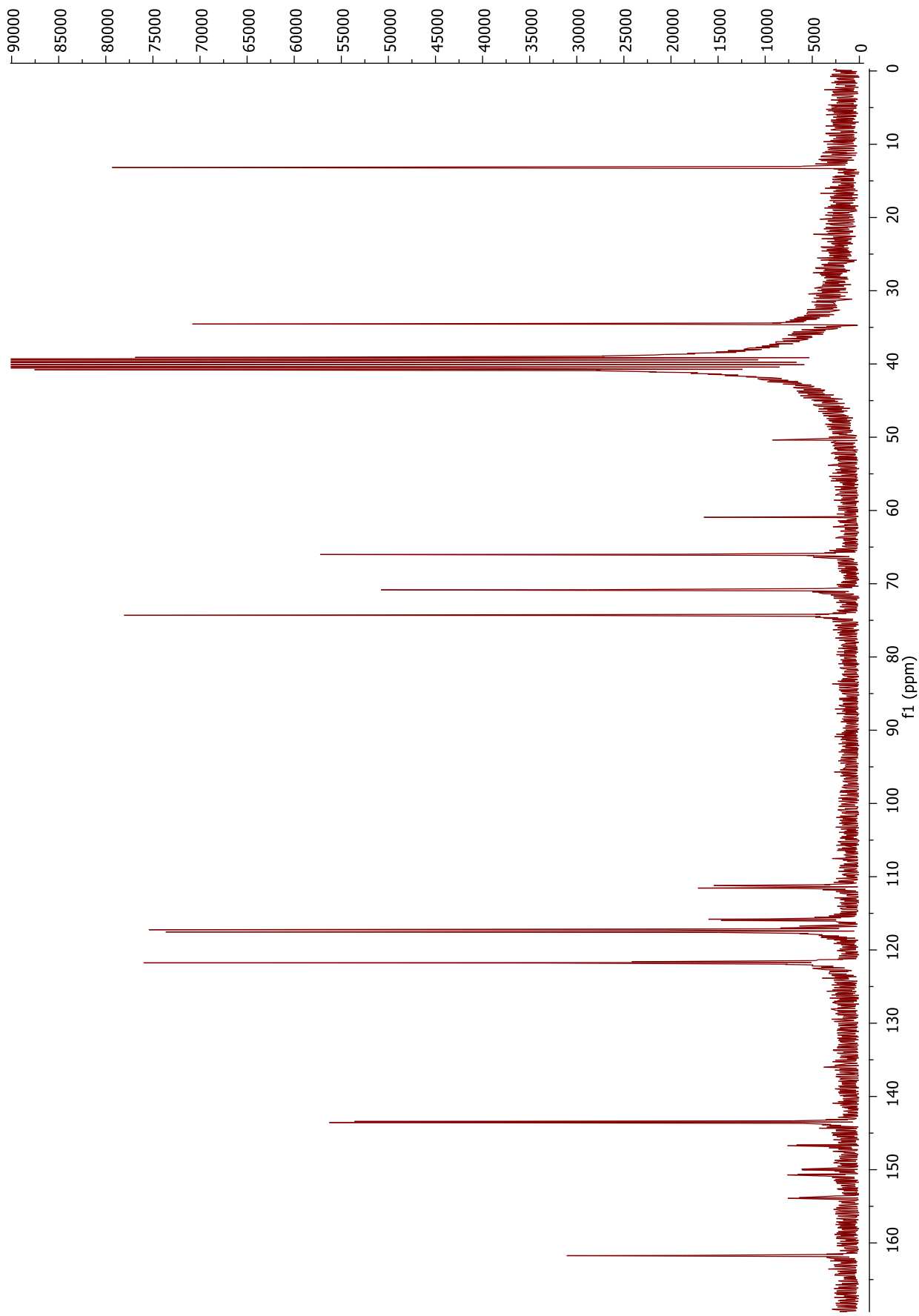
¹³C NMR (d₆-DMSO): δ 161.7, 152.3 (dd, *J* = 241.1, 6.9 Hz), 148.3 (dd, *J* = 248.4, 8.6 Hz), 143.6, 143.5 (dd, *J* = 11.0, 3.0 Hz), 143.4, 121.8, 121.6, 117.6, 117.3, 117.04 (dd, *J* = 25.3, 20.6 Hz), 115.9 (dd, *J* = 9.6, 3.0 Hz), 111.4 (dd, *J* = 22.9, 4.5 Hz), 74.3, 70.8, 66.0, 34.6, 13.2 ppm.

Tr (HPLC, Isocratic, H₂O with 0.10% TFA / Acetonitrile with 0.10% TFA 60/40. 30 min run time. Flow rate: 1.2 mL/min) = 10.15 min, Purity = 99.1%

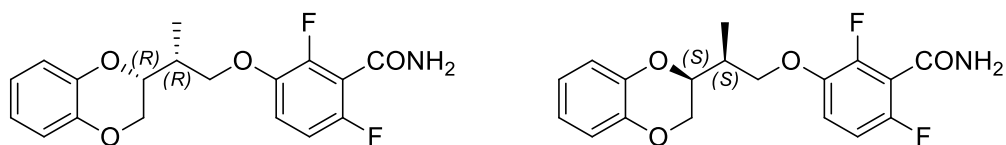
Experimental



Experimental



(R,R) and *(S,S)* – Erythro couple:

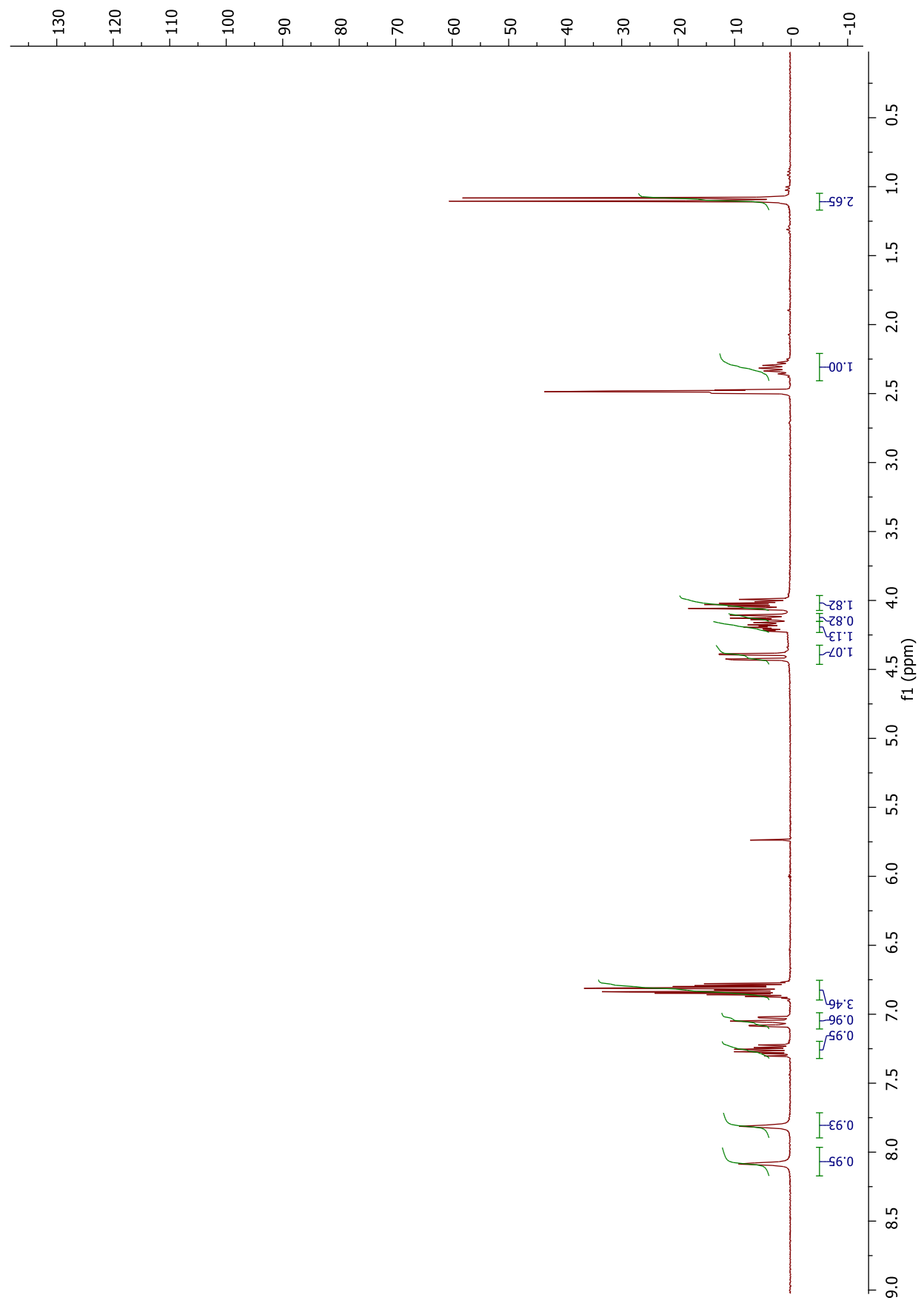


$^1\text{H NMR}$ (d_6 -DMSO): δ 8.09 (bs, 1H), 7.81 (bs, 1H), 7.26 (dt, $J = 9.3, 5.3$ Hz, 1H), 7.05 (dt, $J = 9.3, 1.9$ Hz, 1H), 6.81 (m, 4H), 4.41 (dd, $J = 11.4, 2.1$ Hz, 1H), 4.20 (ddd, $J = 8.4, 5.4, 2.1$ Hz, 1H), 4.13 (dd, $J = 9.7, 6.5$ Hz, 2H), 4.04 (dd, $J = 9.7, 6.0$ Hz, 1H), 4.04 (dd, $J = 11.4, 8.4$ Hz, 1H), 1.09 ppm (d, $J = 7.0$ Hz, 3H).

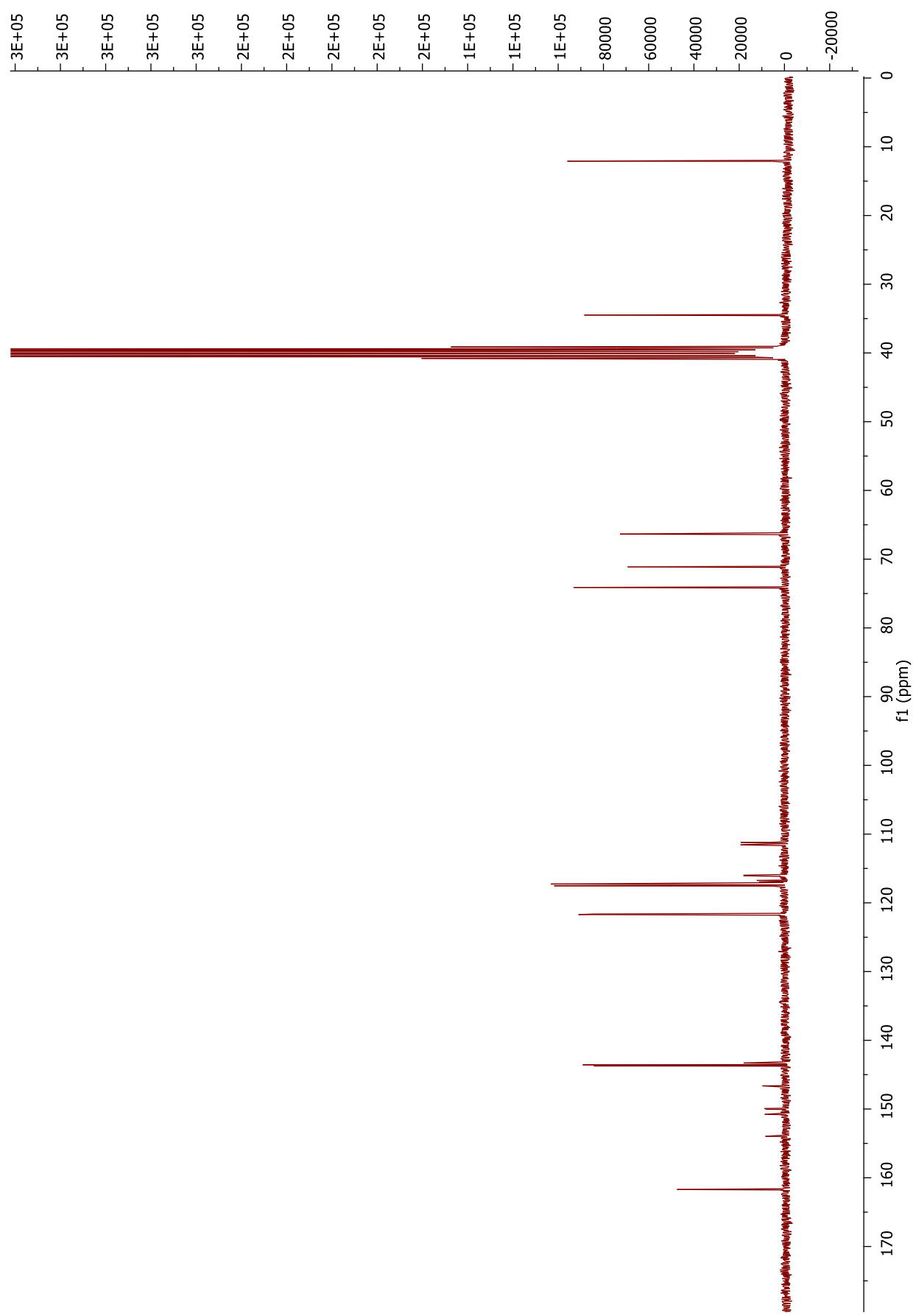
$^{13}\text{C NMR}$ (d_6 -DMSO): δ 161.7, 152.3 (dd, $J = 241.1, 6.8$ Hz), 148.3 (dd, $J = 248.4, 8.5$ Hz), 143.7, 143.6, 143.4 (dd, $J = 11.0, 3.2$ Hz), 121.7, 121.6, 117.5, 117.3, 117.04 (dd, $J = 25.0, 20.4$ Hz), 116.0 (dd, $J = 9.6, 2.4$ Hz), 111.4 (dd, $J = 22.9, 4.0$ Hz), 74.1, 71.1, 66.4, 34.5, 12.1 ppm.

Tr (HPLC, Isocratic, H_2O with 0.10% TFA / Acetonitrile with 0.10% TFA 60/40. 30 min run time. Flow rate: 1.2 mL/min) = 10.99 min, Purity = 99.3%

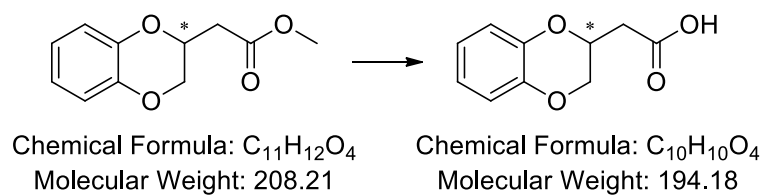
Experimental



Experimental



2-(1,4-Benzodioxan-2-yl)-acetic acid

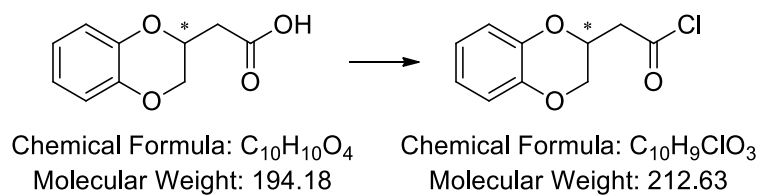


10% aqueous NaOH (48 mmol) was added to a solution of Methyl 2-(1,4-benzodioxan-2-yl)-acetate (5.00 g, 24 mmol) in Methanol (50 mL). The reaction mixture was stirred at 18 hours, concentrated under vacuum, diluted with Ethyl Acetate (50 mL), washed with 10% aqueous HCl (2 x 25 mL), dried over Na_2SO_4 , filtered and concentrated under vacuum to give 4.36 g of 2-(1,4-Benzodioxan-2-yl)-acetic acid as a brownish oil.

Yield = 94.0%

1H NMR ($CDCl_3$): δ 6.87 (m, 4H), 4.64 (dq, $J = 6.7, 2.2$ Hz, 1H), 4.33 (dd, $J = 11.3, 2.2$ Hz, 1H), 4.02 (dd, $J = 11.3, 6.7$ Hz, 1H), 2.84 (dd, $J = 16.5, 6.7$ Hz, 1H), 2.71 ppm (dd, $J = 16.5, 6.7$ Hz, 1H).

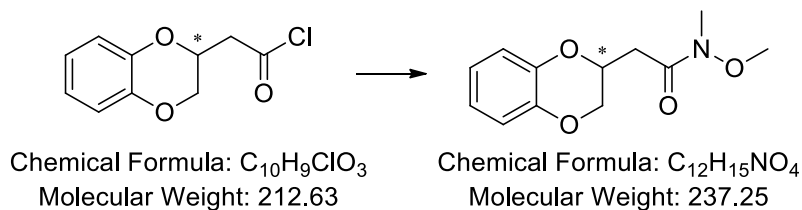
2-(1,4-Benzodioxan-2-yl)-acetyl chloride



$SOCl_2$ (2.17 g, 18.3 mmol) was added dropwise to a solution of 2-(1,4-Benzodioxan-2-yl)-acetic acid (1.18 g, 6.1 mmol) in DCM (12 mL) at 0°C. The reaction mixture was heated at reflux, stirred for 5 hours and then concentrated under vacuum to give 1.09 g of 2-(1,4-Benzodioxan-2-yl)-acetyl chloride as a yellow oil.

Yield = 83.0%

1H NMR ($CDCl_3$): δ 6.85 (m, 4H), 4.72 (m, 1H), 4.28 (dd, $J = 11.5, 2.3$ Hz, 1H), 4.03 (dd, $J = 11.5, 6.0$ Hz, 1H), 3.33 (dd, $J = 17.2, 7.1$ Hz, 1H), 3.21 ppm (dd, $J = 17.2, 5.8$ Hz, 1H).

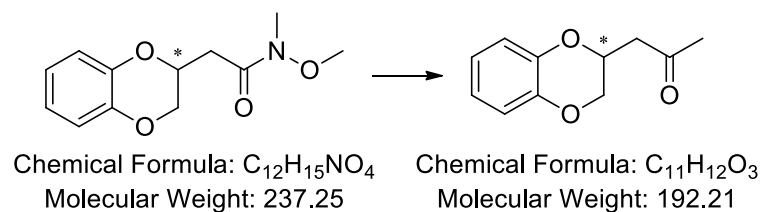
2-(1,4-Benzodioxan-2-yl)-*N*-methoxy-*N*-methyl-acetamide

N,O-dimethylhydroxylamine was added to a solution of 2-(1,4-Benzodioxan-2-yl)-acetyl chloride (4.80 g, 22.6 mmol) in DCM (50 mL) at 0°C. The reaction mixture was stirred at room temperature for 3 hours, diluted with DCM, washed with 10% aqueous NaHCO₃ and brine (25 + 25 mL), dried over Na₂SO₄, filtered and concentrated under vacuum to give 4.06 g of 2-(1,4-Benzodioxan-2-yl)-*N*-methoxy-*N*-methyl-acetamide as a brown oil.

Yield = 76.0%

¹H NMR (CDCl₃): δ 6.85 (m, 4H), 4.71 (dddd, *J* = 7.2, 6.4, 6.0, 2.2 Hz, 1H), 4.36 (dd, *J* = 11.3, 2.2 Hz, 1H), 4.03 (dd, *J* = 11.3, 6.4 Hz, 1H), 3.68 (s, 3H), 3.22 (s, 3H), 2.99 (dd, *J* = 16.2, 6.0, Hz, 1H), 2.70 ppm (dd, *J* = 16.2, 7.2 Hz, 1H).

1-(1,4-Benzodioxan-2-yl)-propan-2-one



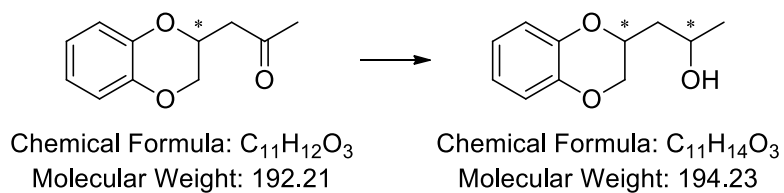
Methyl magnesium bromide (4.62 mmol, 1.54 mL) was added dropwise to a solution of 2-(1,4-Benzodioxan-2-yl)-*N*-methoxy-*N*-methyl-acetamide (0.49 g, 2.1 mmol) in dry THF (9 mL) at 0°C under N_2 , The reaction mixture was stirred at room temperature for 18 hours and poured into a 1/1 mixture of Ethyl acetate and 10% aqueous HCl (10 + 10 mL). The organic phase was then washed twice with 10% aqueous NaCl, dried over Na_2SO_4 , filtered and concentrated under vacuum to give 0.24 g of 1-(1,4-Benzodioxan-2-yl)-propan-2-one as a brownish solid.

Yield = 60.0%

M.p. = 32.5°C

1H NMR ($CDCl_3$): δ 7.86 (m, 4H), 4.66 (dq, J = 6.4, 2.3 Hz, 1H), 4.28 (dd, J = 11.3, 2.3 Hz, 1H), 3.95 (dd, J = 11.3, 6.4 Hz, 1H), 2.92 (dd, J = 17.1, 6.4 Hz, 1H), 2.71 (dd, J = 17.1, 6.4 Hz, 1H), 2.24 ppm (s, 3H).

1-(1,4-Benzodioxan-2-yl)-propan-2-ol

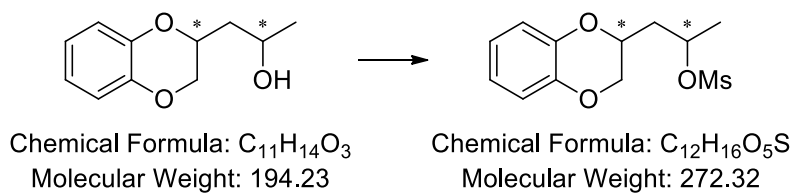


NaBH₄ (0.02 g, 0.5 mmol) was added to a solution of 1-(1,4-Benzodioxan-2-yl)-propan-2-one (0.19 g, 0.99 mmol) in Methanol (2 mL) at 0°C. The reaction mixture was stirred at the same temperature for 0.5 hours and then concentrated under vacuum to give 0.19 g of 1-(1,4-Benzodioxan-2-yl)-propan-2-ol as a brown oil, which was used for the subsequent step without further purification.

Yield = Quantitative

¹H NMR (CDCl₃) mixture of 4 isomers: δ 6.85 (m, 4H), 4.43 (m, 1H), 4.22 (m, 2H), 3.96 and 3.92 (dd, J = 7.6, 4.7 Hz, 1H), 2.77 (m, 2H), 1.28 and 1.29 ppm (d, J = 6.2 Hz, 3H).

1-(1,4-Benzodioxan-2-yl)-propan-2-yl methanesulfonate

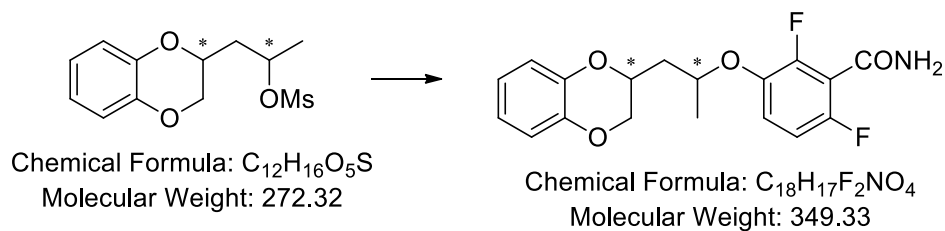


Methanesulfonyl chloride (0.14 g, 1.18 mmol) was added dropwise to a solution of 1-(1,4-Benzodioxan-2-yl)-propan-2-ol (0.19 g, 0.98 mmol) and TEA (0.13 g, 1.27 mmol) in DCM (4 mL) at 0°C. The reaction mixture was stirred at room temperature for 2 hours, washed firstly with 10% aqueous HCl (5 mL), with 10% aqueous NaCl (5 mL), dried over Na₂SO₄, filtered and concentrated under vacuum to give 0.22 g of 1-(1,4-Benzodioxan-2-yl)-propan-2-yl methanesulfonate as a brownish oil.

Yield = 76.0%

¹H NMR (CDCl₃) mixture of 4 isomers: δ 6.90 (m, 4H), 5.07 (m, 1H), 4.32 (m, 1H), 3.94 (m, 2H), 3.03 and 3.02 (s, 3H), 2.20 and 2.15 (dd, J = 8.2, 6.3 Hz, 1H), 1.91 (m, 1H), 1.55 and 1.53 ppm(d, J = 6.2 Hz, 3H).

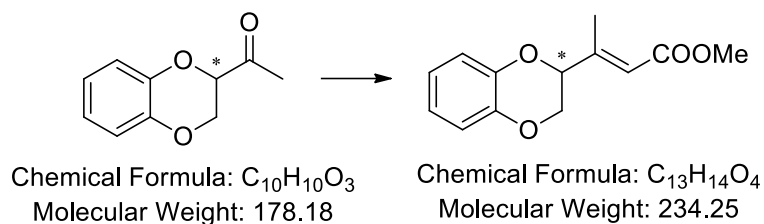
(VII) 3-[2-(1,4-Benzodioxan-2-yl)propan-2-yl]oxy)-2,6-difluorobenzamide



Potassium carbonate (0.19 g, 1.40 mmol) was added to a solution of 2,6-Difluoro-3-hydroxybenzamide (0.2 g, 1.2 mmol) in dry DMF (3 mL). After stirring at room temperature for 30 minutes, a solution of 1-(1,4-Benzodioxan-2-yl)-propan-2-yl methanesulfonate (0.37 g, 1.2 mmol) in dry DMF (3 mL) was added. The reaction mixture was stirred at 80°C for 2 hours, concentrated under vacuum, diluted with Ethyl Acetate (15 mL), washed with brine (3 x 10 mL), dried over Na_2SO_4 , filtered and concentrated under vacuum. Elution with 3/7 Cyclohexane/Ethyl Acetate on silica gel gave 0.08 g of 3-[2-(1,4-Benzodioxan-2-yl)propan-2-yl]oxy)-2,6-difluorobenzamide, as a mixture of stereoisomers, as a brownish oil.

Yield = 20.0%

Methyl 3-(1,4-benzodioxan-2-yl)-buten-2-onate



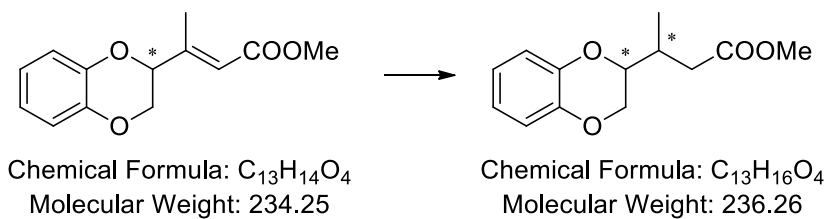
Methyl 2-(dimethoxyphosphoryl) acetate (1.60 g, 9.0 mmol) was added dropwise to a suspension of 60% NaH on mineral oil (0.19 g, 8.1 mmol) in dry THF (2 mL) at 0°C under N_2 . The reaction mixture was stirred at 0°C for 1 hour, added with 1-(1,4-Benzodioxan-2-yl)ethanone (0.80 g, 4.5 mmol) and stirred at room temperature for 1 hour. The reaction was then quenched with H_2O (2 mL), concentrated under vacuum, diluted with Ethyl acetate (5 mL), washed with brine (5 mL), dried over Na_2SO_4 , filtered and concentrated under vacuum. Elution with 97/3 Cyclohexane/Ethyl acetate on silica gel gave 0.56 g of Methyl 3-(1,4-benzodioxan-2-yl)-buten-2-onate as a colourless oil, as a mixture of E and Z isomers.

Yield = 51.0%

1H NMR ($CDCl_3$): δ 6.90 (m, 4H), 5.87 (m, 2H), 4.36 (dd, $J = 10.9, 2.6$ Hz, 1H), 3.94 (dd, $J = 10.9, 7.9$ Hz, 1H), 3.71 (s, 3H), 2.00 ppm (s, 3H).

1H NMR ($CDCl_3$): δ 6.90 (m, 4H), 6.12 (s, 1H), 4.57 (dd, $J = 7.9, 2.4$ Hz, 1H), 4.36 (dd, $J = 11.4, 2.4$ Hz, 1H), 3.89 (dd, $J = 11.4, 7.9$ Hz, 1H), 3.73 (s, 3H), 2.24 ppm (s, 3H).

Methyl 3-(1,4-benzodioxan-2-yl)-butanonate

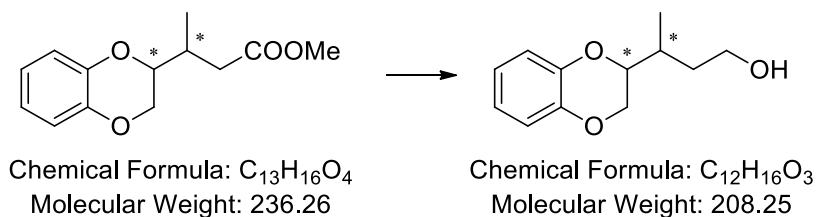


Pd/C (10% w/w) was added to a solution of Methyl 3-(1,4-benzodioxan-2-yl)-buten-2-onate (0.33 g, 1.4 mmol) at room temperature under H₂. The reaction mixture was stirred at room temperature for 3 hours, filtered through celite and concentrated under vacuum to give 0.33 g of Methyl 3-(1,4-benzodioxan-2-yl)-butanonate as a brownish oil.

Yield = Quantitative

¹H NMR (CDCl₃) mixture of 4 isomers: δ 6.85 (m, 4H), 4.12 (m, 4H), 4.15 (m, 1H), 3.70 and 3.69 (s, 3H), 2.34 (m, 1H), 1.10 and 1.07 (s, 3H).

3-(1,4-Benzodioxan-2-yl)-butan-1-ol

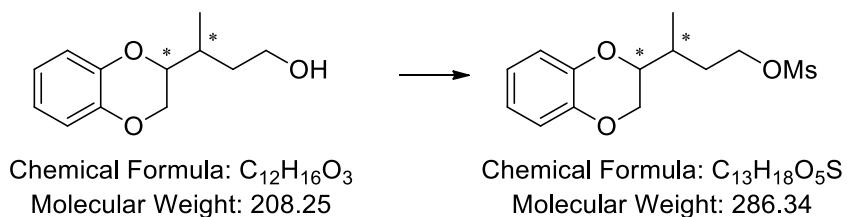


A solution of Methyl 3-(1,4-benzodioxan-2-yl)-butanoate (0.33 g, 1.4 mmol) in dry THF (1 mL) was added dropwise to a suspension of $LiAlH_4$ (0.05 g, 1.4 mmol) in dry THF (2 mL) at $0^\circ C$ under N_2 . The reaction mixture was stirred at room temperature for 1 hour, diluted with Ethyl acetate (3 mL) and H_2O (2 mL), washed with 10% aqueous HCl (2 mL), brine (2 mL), dried over Na_2SO_4 , filtered and concentrated under vacuum to give 0.23 g of 3-(1,4-Benzodioxan-2-yl)-butan-1-ol as a colourless oil.

Yield = 79.3%

1H NMR ($CDCl_3$) mixture of 4 isomers: δ 6.85 (m, 4H), 4.31 (m, 1H), 3.99 (m, 2H), 3.77 (m, 2H), 1.93 (m, 2H), 1.58 (m, 1H), 1.07 and 1.05 (d, $J = 6.8$ Hz, 3H).

3-(1,4-Benzodioxan-2-yl)-butan-1-yl methanesulfonate

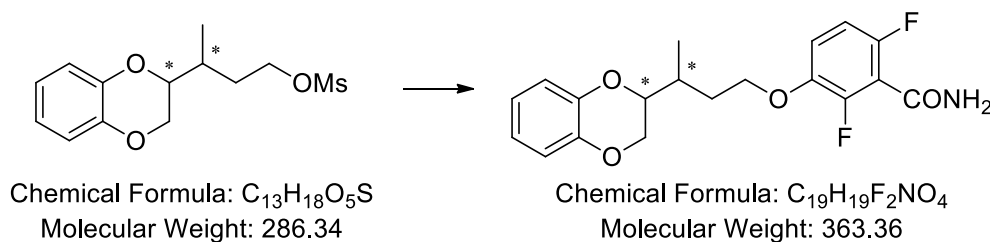


Methanesulfonyl chloride (0.3 g, 2.60 mmol) was added dropwise to a solution of 3-(1,4-Benzodioxan-2-yl)-butan-1-ol (0.41 g, 2.00 mmol) and TEA (0.28 g, 2.80 mmol) in DCM (8 mL) at 0°C. The reaction mixture was stirred at room temperature for 3 hours, washed firstly with 10% aqueous HCl (5 mL), with 10% aqueous NaCl (5 mL), dried over Na_2SO_4 , filtered and concentrated under vacuum to give 0.45 g of 3-(1,4-Benzodioxan-2-yl)-butan-1-yl methanesulfonate as a yellowish oil.

Yield = 79.0%

1H NMR ($CDCl_3$) mixture of 4 isomers: δ 6.86 (m, 4H), 4.15 (m, 5H), 3.03 and 2.99 (s, 3H), 2.05 (m, 2H), 1.75 (m, 1H), 1.09 and 1.08 (d, $J = 6.9$ Hz, 3H).

(VIII) 3-[2-(1,4-Benzodioxan-2-yl)butan-1-yl]oxy)-2,6-difluorobenzamide

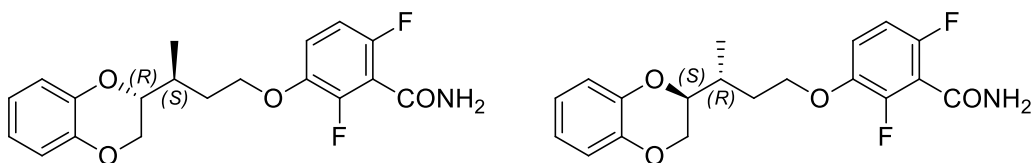


Potassium carbonate (0.23 g, 1.80 mmol) was added to a solution of 2,6-Difluoro-3-hydroxybenzamide (0.28 g, 1.6 mmol) in dry DMF (3 mL). After stirring at room temperature for 30 minutes, a solution of -(1,4-Benzodioxan-2-yl)-butan-1-yl methanesulfonate (0.45 g, 1.6 mmol) in dry DMF (3 mL) was added. The reaction mixture was stirred at 80°C for 2 hours, concentrated under vacuum, diluted with Ethyl Acetate (15 mL), washed with brine (3 x 10 mL), dried over Na_2SO_4 , filtered and concentrated under vacuum. Elution with 6/4 Cyclohexane/Ethyl Acetate on silica gel gave 0.11 g of 3-[2-(1,4-Benzodioxan-2-yl)butan-1-yl]oxy)-2,6-difluorobenzamide, as a mixture of stereoisomers, as a brownish oil.

The mixture of stereoisomers was further purified *via* preparative HPLC.

Yield = 19.0%

(S,R) and *(R,S)* – Threo couple:

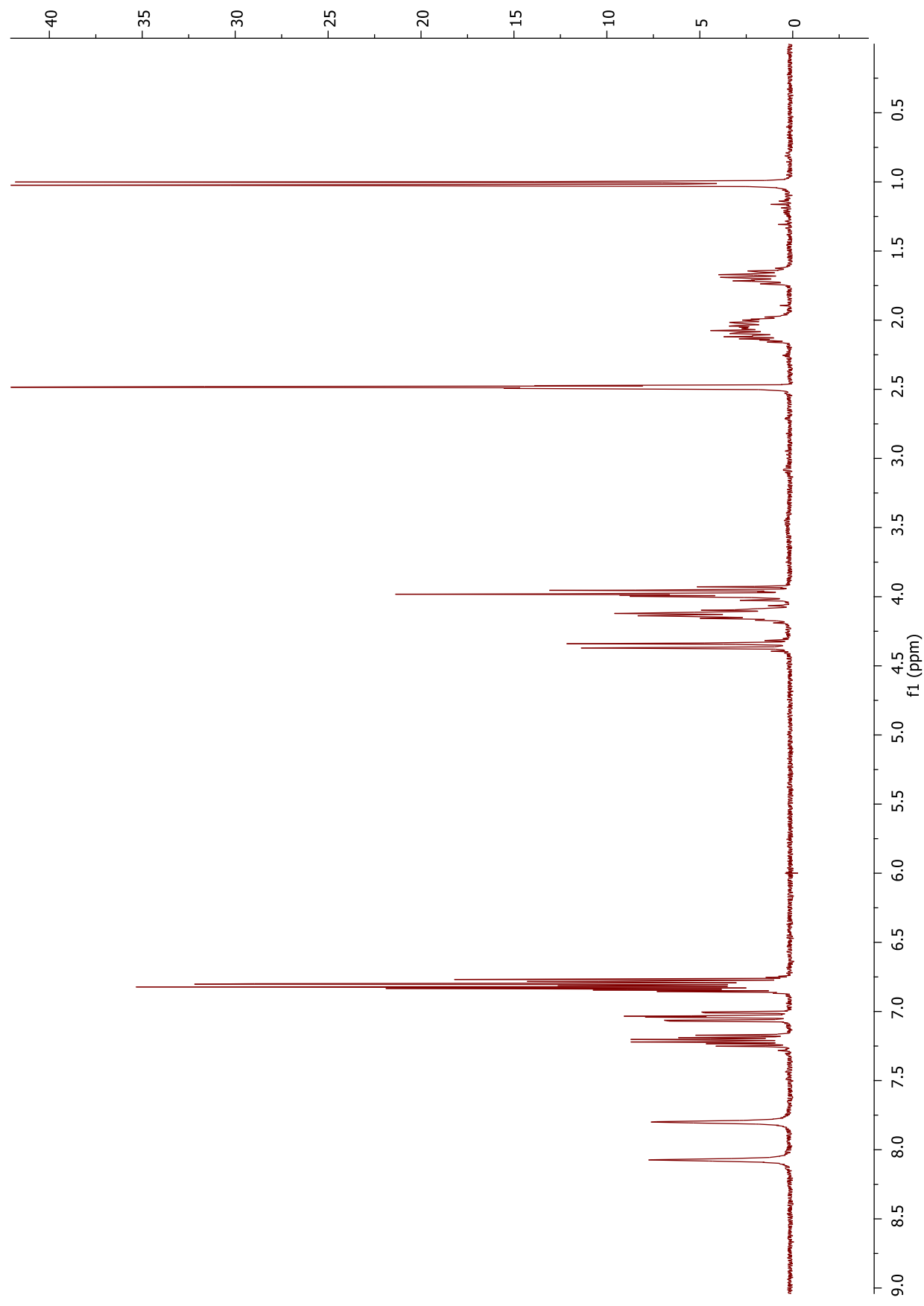


¹H NMR (d₆-DMSO): δ 8.07 (bs, 1H), 7.80 (bs, 1H), 7.21 (dt, *J* = 9.2, 5.3 Hz, 1H), 7.04 (dt, *J* = 9.2, 1.9 Hz, 1H), 6.78 (m, 4H), 4.36 (dd, *J* = 7.0, 16.5 Hz, 1H), 4.12 (m, 2H), 4.00 (m, 1H), 3.97 (dd, *J* = 8.3, 16.5 Hz, 1H), 2.05 (m, 2H), 1.68 (m, 1H), 1.01 (d, *J* = 6.8 Hz, 3H).

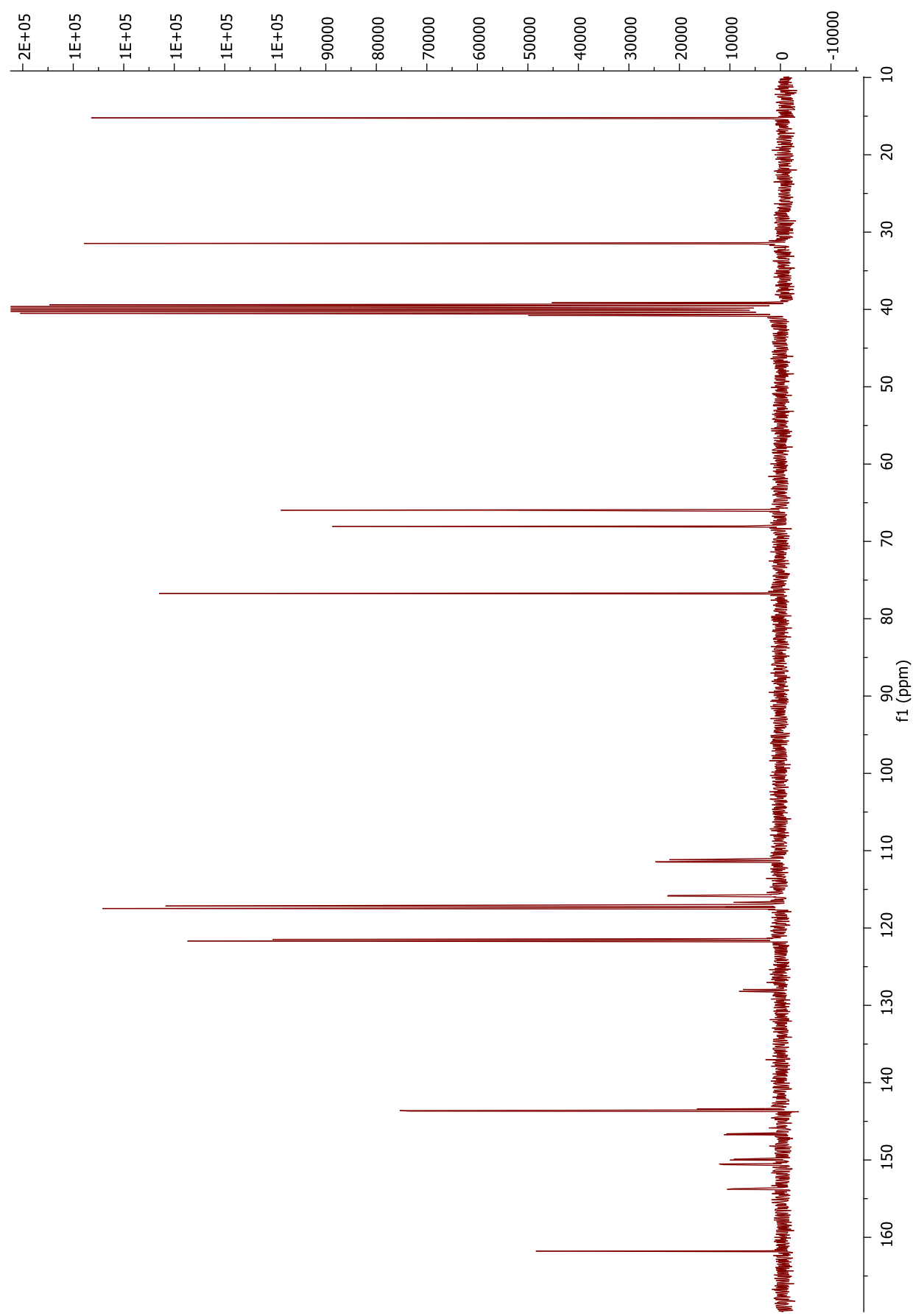
¹³C NMR (d₆-DMSO): δ 161.8, 152.15 (dd, *J* = 240.9, 6.8 Hz), 148.31 (dd, *J* = 248.3, 8.5 Hz), 143.7, 143.6, 143.5 (dd, *J* = 10.2, 2.4 Hz), 121.7, 121.5, 117.5, 117.2, 117.0 (dd, *J* = 24.9, 20.5 Hz), 115.8 (dd, *J* = 9.3, 2.6 Hz), 111.3 (dd, *J* = 22.9, 4.0 Hz), 76.7, 68.1, 66.0, 31.5, 34.4, 15.22.

T.r. HPLC (M.P. H₂O + TFA 0.1% / ACN + TFA 0.1% 60/40; 1 mL/min): 10.15 min

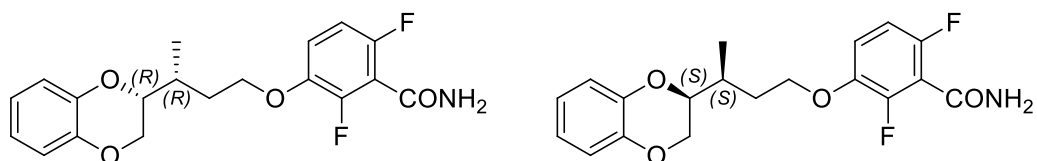
Experimental



Experimental



(R,R) and *(S,S)* – Erythro couple:

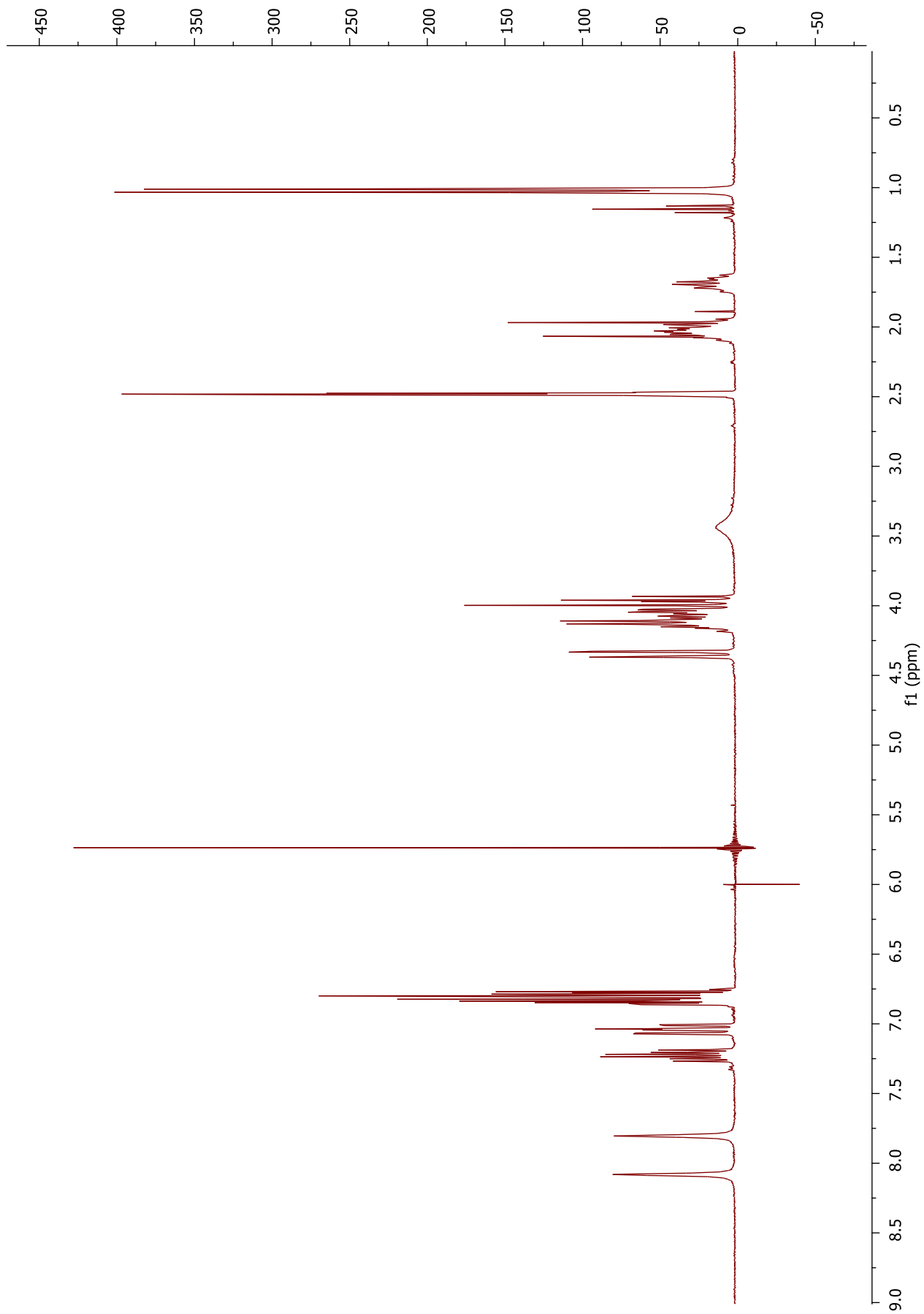


¹H NMR (d₆-DMSO): δ 8.08 (bs, 1H), 7.80 (bs, 1H), 7.23 (dt, *J* = 9.2, 5.3 Hz, 1H), 7.04 (dt, *J* = 9.2, 1.8 Hz, 1H), 6.80 (m, 4H), 4.35 (dd, *J* = 11.0, 1.8 Hz, 1H), 4.14 (m, 2H), 4.05 (m, 1H), 3.97 (dd, *J* = 11.1, 8.2 Hz, 1H), 2.01 (m, 2H), 1.69 (m, 1H), 1.02 (d, *J* = 6.8 Hz, 3H).

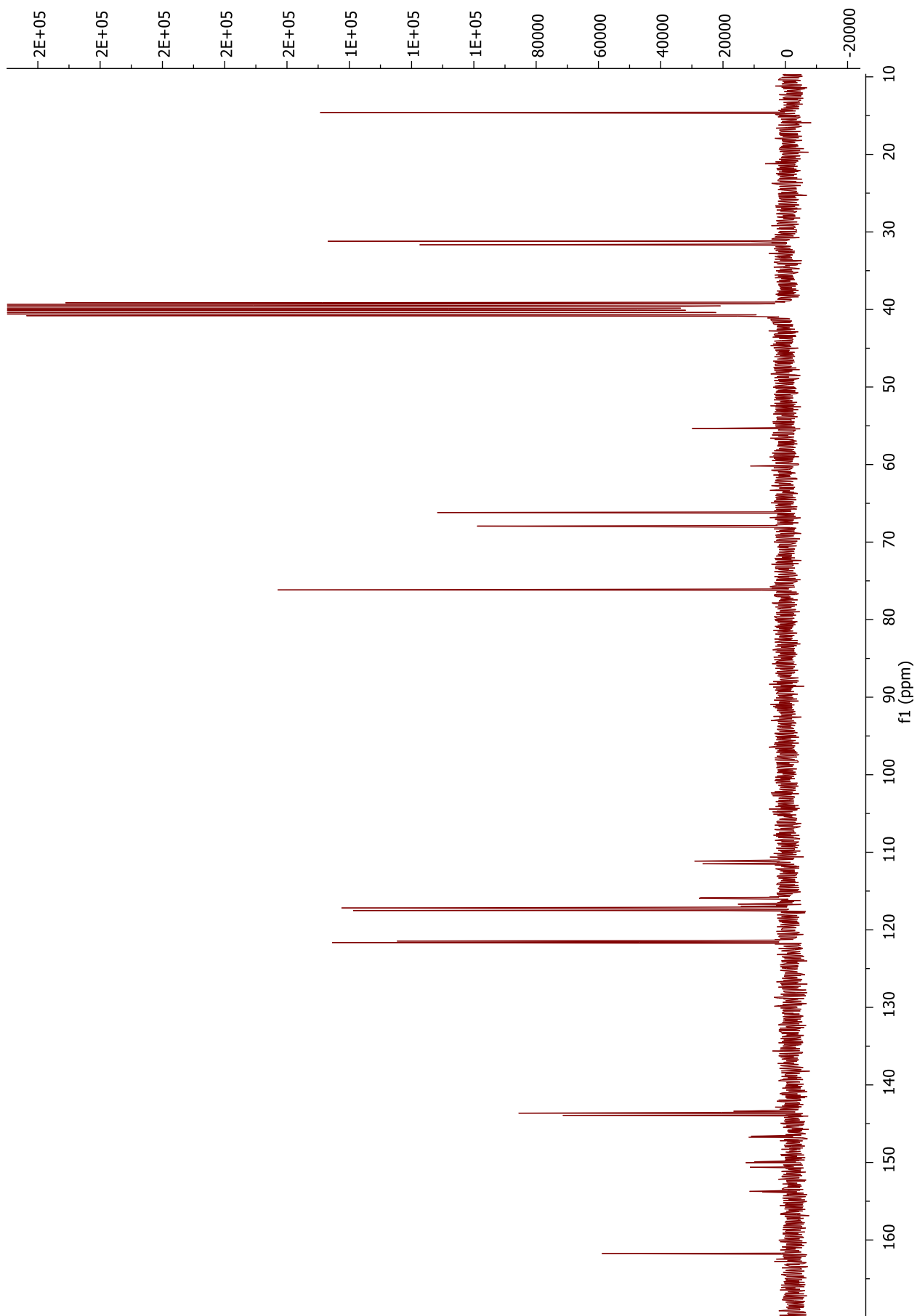
¹³C NMR (d₆-DMSO): δ 161.8, 152.2 (dd, *J* = 240.8, 6.7 Hz), 148.33 (dd, *J* = 248.2, 8.5 Hz), 143.9, 143.6, 143.5 (dd, *J* = 11.0, 3.2 Hz), 121.6, 121.5, 117.5, 117.2, 117.0 (dd, *J* = 24.8, 20.7 Hz), 115.9 (dd, *J* = 9.4, 2.5 Hz), 111.31 (dd, *J* = 22.8, 4.0 Hz), 76.2, 67.9, 66.23, 31.7, 31.21, 14.61.

T.r. HPLC (M.P. H₂O + TFA 0.1% / ACN + TFA 0.1% 60/40; 1 mL/min): 11.54 min

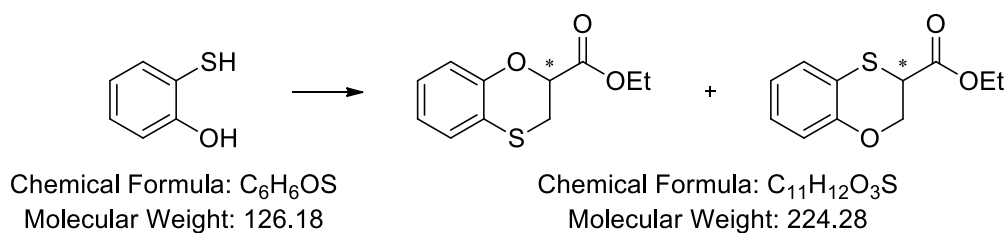
Experimental



Experimental



Ethyl 1,4-benzoxathian-2-carboxylate and Ethyl 1,4-benzoxathian-3-carboxylate



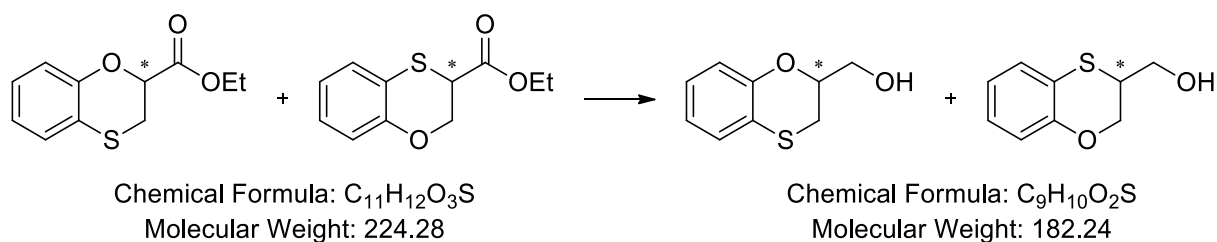
TEA (0.50 mL, 3.52 mmol) was added dropwise to a solution of Ethyl-2,3-dibromopropionate (0.44 g, 1.76 mmol) into a mixture 1/1 of ACN and water (10 mL). After stirring at room temperature for 30 min, 1,2-Mercaptophenol (0.22 g, 1.76 mmol) was slowly added. The reaction mixture was stirred at RT for 72 h, and then, it was diluted with diethyl ether and water. The organic phase was dried over Na₂SO₄, filtered and concentrated to give a yellow oil as the residue. The crude was purified by flash chromatography on silica gel, using Cyclohexane/Ethyl acetate 95/5 as the elution solvent; the yielded ratio between 9 and 10 was quantified by ¹H NMR and resulted in 60% for Ethyl 1,4-benzoxathian-2-carboxylate and of 40% for Ethyl 1,4-benzoxathian-3-carboxylate.

Yield = 65.0%

¹H NMR (CDCl₃) Ethyl 1,4-benzoxathian-2-carboxylate: δ 7.04 (m, 2H), 6.96 (d, J = 7.7 Hz, 1H), 6.87 (t, J = 7.4 Hz, 1H), 4.99 (dd, J = 5.3, 3.8 Hz, 1H), 4.27 (q, J = 7.1 Hz, 2H), 3.29 (d, J = 3.8 Hz, 1H), 3.28 (d, J = 5.3 Hz, 1H), 1.28 ppm (t, J = 7.1 Hz, 3H).

¹H NMR (CDCl₃) Ethyl 1,4-benzoxathian-3-carboxylate: δ 7.06 (m, 1H), 7.00 (dd, J = 7.6, 2.0 Hz, 1H), 6.88 (t, J = 7.4 Hz, 2H), 4.56 (dd, J = 11.5, 3.0 Hz, 1H), 4.46 (dd, J = 11.5, 6.5 Hz, 1H), 4.25 (q, J = 7.1 Hz, 2H), 4.12 (dd, J = 6.5, 3.0 Hz, 1H), 1.30 ppm (t, J = 7.1 Hz, 3H).

2-(1,4-Benzoxathiane-2-yl)-ethanol and 2-(1,4-Benzoxathiane-3-yl)-ethanol



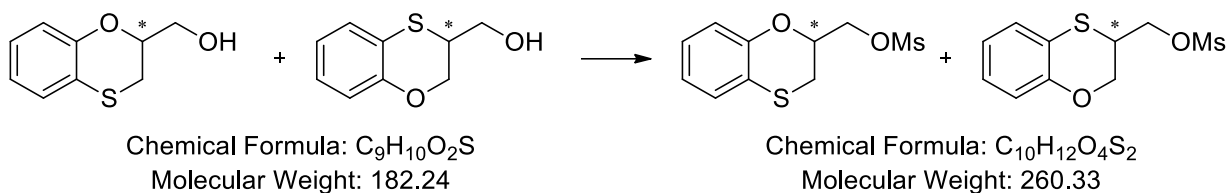
$LiAlH_4$ (0.085 g, 2.23 mmol) was suspended in dry THF (5 mL) at $0^\circ C$ under nitrogen atmosphere. The mixture of Ethyl 1,4-benzoxathian-2-carboxylate and Ethyl 1,4-benzoxathian-3-carboxylate (0.5 g, 2.23 mmol) was dissolved in THF (5 mL) and was added to the reaction. The mixture was warmed to RT and stirred for 30 minutes; at completion, it was cooled to $0^\circ C$ and slowly quenched with Ethyl acetate (5 mL). Further Ethyl acetate (10 mL) was added, the organic layer was washed with brine (3×10 mL), dried over Na_2SO_4 and concentrated under vacuum to give 0.38 g as a mixture of 60% 2-(1,4-Benzoxathiane-2-yl)-ethanol and 40% 2-(1,4-Benzoxathiane-3-yl)-ethanol as a colourless oil

Yield = 81.0%

1H NMR ($CDCl_3$) 2-(1,4-Benzoxathiane-2-yl)-ethanol: δ 7.03 (m, 2H), 6.86 (m, 2H), 4.32 (m, 1H), 3.90 (dd, $J = 11.7, 4.2$ Hz, 1H), 3.84 (dd, $J = 11.7, 5.6$ Hz, 1H), 3.14 (dd, $J = 13.0, 9.0$ Hz, 1H), 2.97 ppm (dd, $J = 13.0, 2.1$ Hz, 1H).

1H NMR ($CDCl_3$) 2-(1,4-Benzoxathiane-3-yl)-ethanol: δ 7.02 (m, 2H), 6.86 (m, 2H), 4.50 (dd, $J = 11.7, 4.2$ Hz, 1H), 4.34 (dd, $J = 11.7, 2.1$ Hz, 1H), 3.88 (m, 2H), 3.42 ppm (ddd, $J = 7.2, 4.2, 2.1$ Hz, 1H).

2-(1,4-Benzoxathiane-2-yl)-ethyl methanesulfonate and 2-(1,4-Benzoxathiane-3-yl)-ethyl methanesulfonate



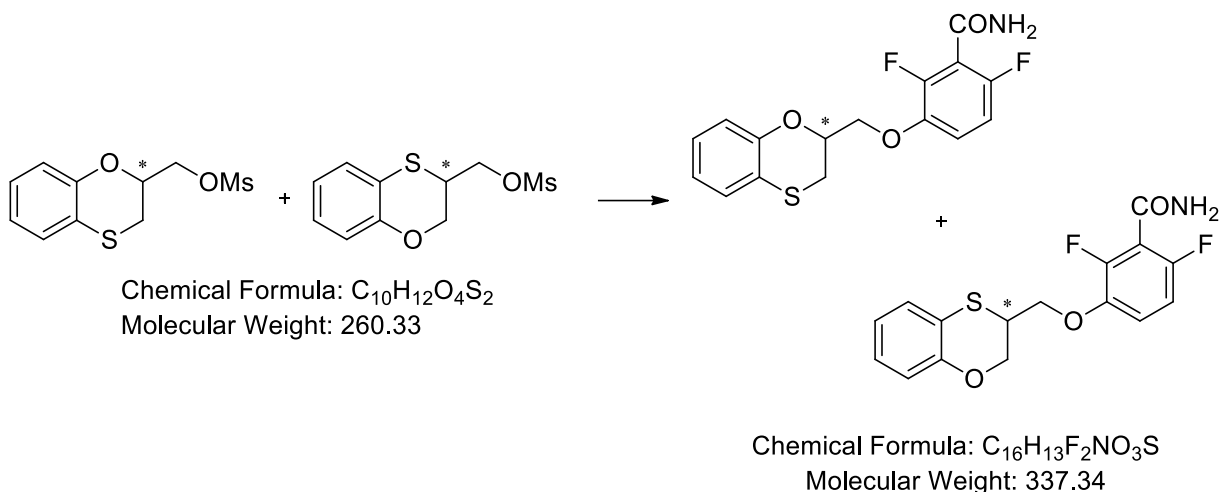
Mesyl chloride (0.55 mL, 7.13 mmol) was added dropwise to a solution of 2-(1,4-Benzoxathiane-2-yl)-ethanol and 2-(1,4-Benzoxathiane-3-yl)-ethanol (1.0 g, 5.49 mmol) and TEA (1.0 mL, 7.13 mmol) in DCM (5 mL) at 0°C. The mixture was stirred at room temperature for 3 h, diluted with DCM (20 mL), washed firstly with 10% aqueous $NaHCO_3$ (10 mL), secondly with 10% aqueous HCl (10 mL) and finally with brine (10 mL), dried over Na_2SO_4 , filtered and concentrated under vacuum to yield 1.58 g of 2-(1,4-Benzoxathiane-2-yl)-ethyl methanesulfonate and 2-(1,4-Benzoxathiane-3-yl)-ethyl methanesulfonate as an oil residue.

Yield = 80.0%

1H NMR ($CDCl_3$) 2-(1,4-Benzoxathiane-2-yl)-ethyl methanesulfonate: δ 7.04 (m, 2H), 6.88 (ddd, $J = 14.2, 7.7, 1.2$ Hz, 2H), 4.57 (m, 1H), 4.45 (m, 2H), 3.10 (s, 3H), 3.10 ppm (m, 2H).

1H NMR ($CDCl_3$) 2-(1,4-Benzoxathiane-3-yl)-ethyl methanesulfonate: δ 7.03 (m, 2H), 6.89 (m, 2H), 4.63 (ddd, $J = 11.8, 3.2, 1.5$ Hz, 1H), 4.42 (m, 2H), 4.24 (m, 1H), 3.59 (dddd, $J = 9.5, 6.4, 3.2, 1.7$ Hz, 1H), 3.07 ppm (s, 3H).

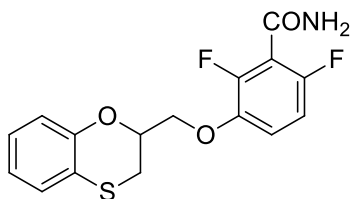
(IX) and (X) 3-(1,4-Benzoxathiane-2-yl)methoxy)-2,6-difluorobenzamide and 2-(1,4-Benzoxathiane-3-yl)methoxy)-2,6-difluorobenzamide



Potassium carbonate (0.42 g, 3.01 mmol) was added to a solution of 2,6-Difluoro-3-hydroxybenzamide (0.50 g, 2.88 mmol) in dry DMF (2 mL). After stirring at room temperature for 30 min, a solution of 2-(1,4-Benzoxathiane-2-yl)-ethyl methanesulfonate and 2-(1,4-Benzoxathiane-3-yl)-ethyl methanesulfonate (0.71 g, 2.74 mmol) in DMF (2 mL) was added. The reaction mixture was stirred at 60°C for 16 h, concentrated under vacuum, diluted with Ethyl Acetate (20 mL), washed with brine (3 × 10 mL), dried over Na_2SO_4 , filtered and concentrated, to give a residue, which was purified by flash chromatography on silica gel. Elution with 9/1 Cyclohexane/Ethyl Acetate gave 3-(1,4-Benzoxathiane-2-yl)methoxy)-2,6-difluorobenzamide (35%) and 3-(1,4-Benzoxathiane-2-yl)methoxy)-2,6-difluorobenzamide (20%) as white solids.

Yield = 55.0%

3-(1,4-Benzoxathiane-2-yl)methoxy)-2,6-difluorobenzamide:



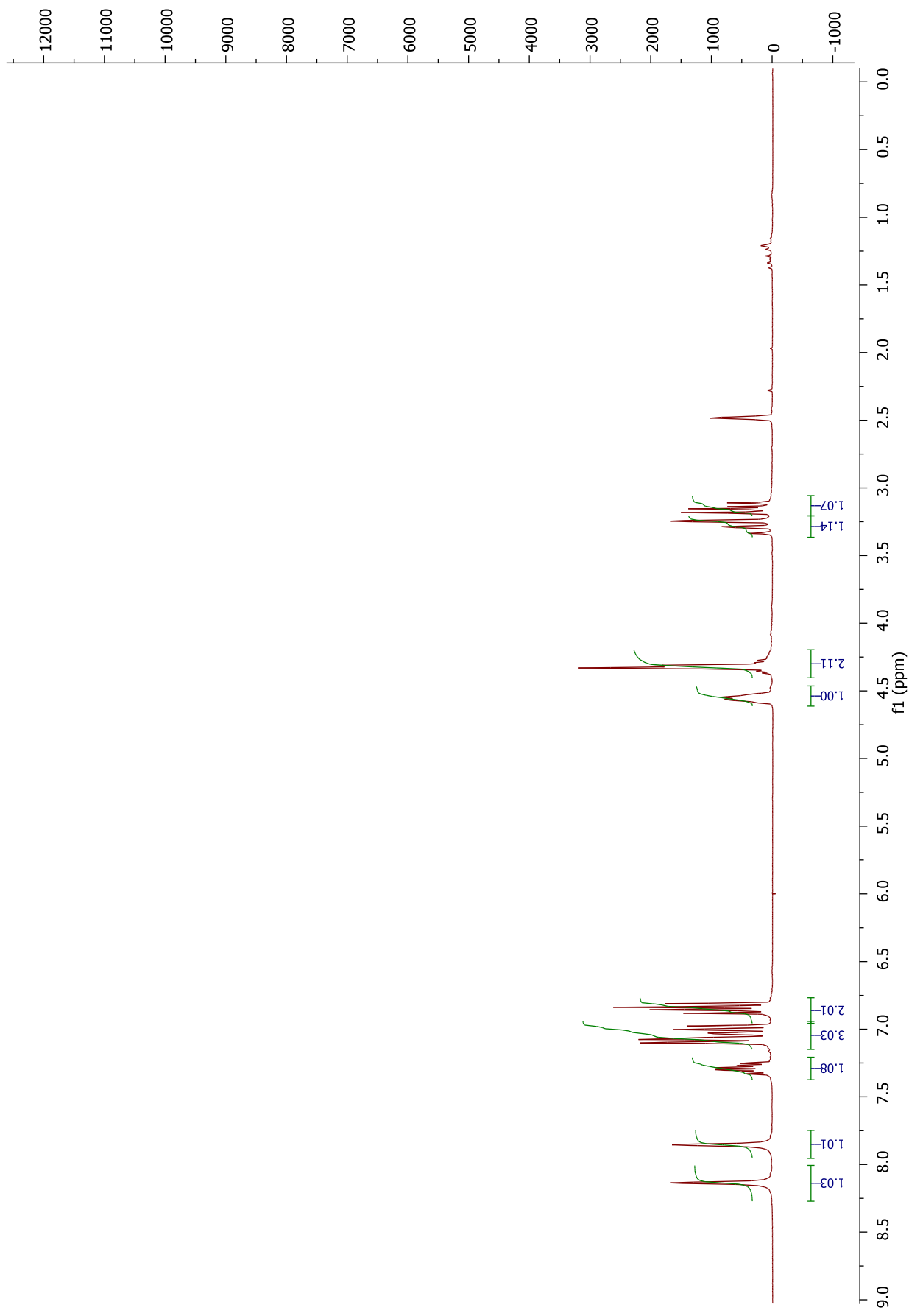
¹H NMR (d₆-DMSO): δ 8.14 (bs, 1H), 7.85 (bs, 1H), 7.29 (m, 1H), 7.04 (m, 3H), 6.85 (m, 2H), 4.56 (m, 1H), 4.31 (m, 2H), 3.29 (dd, J = 14.1, 13.1 Hz, 1H), 3.15 ppm (dd, J = 13.1, 8.4 Hz, 1H).

¹³C NMR (d₆-DMSO): δ 161.7, 152.6 (dd, J = 240.5, 6.9 Hz), 151.2, 148.4 (dd, J = 247.4, 9.1 Hz), 143.2 (dd, J = 10.9, 2.8 Hz), 127.7, 126.2, 122.1, 118.8, 117.5, 117.1 (dd, J = 24.0, 20.6 Hz), 116.5 (d, J = 9.1 Hz), 111.5 (dd, J = 22.9, 3.4 Hz), 73.1, 71.2, 26.1 ppm.

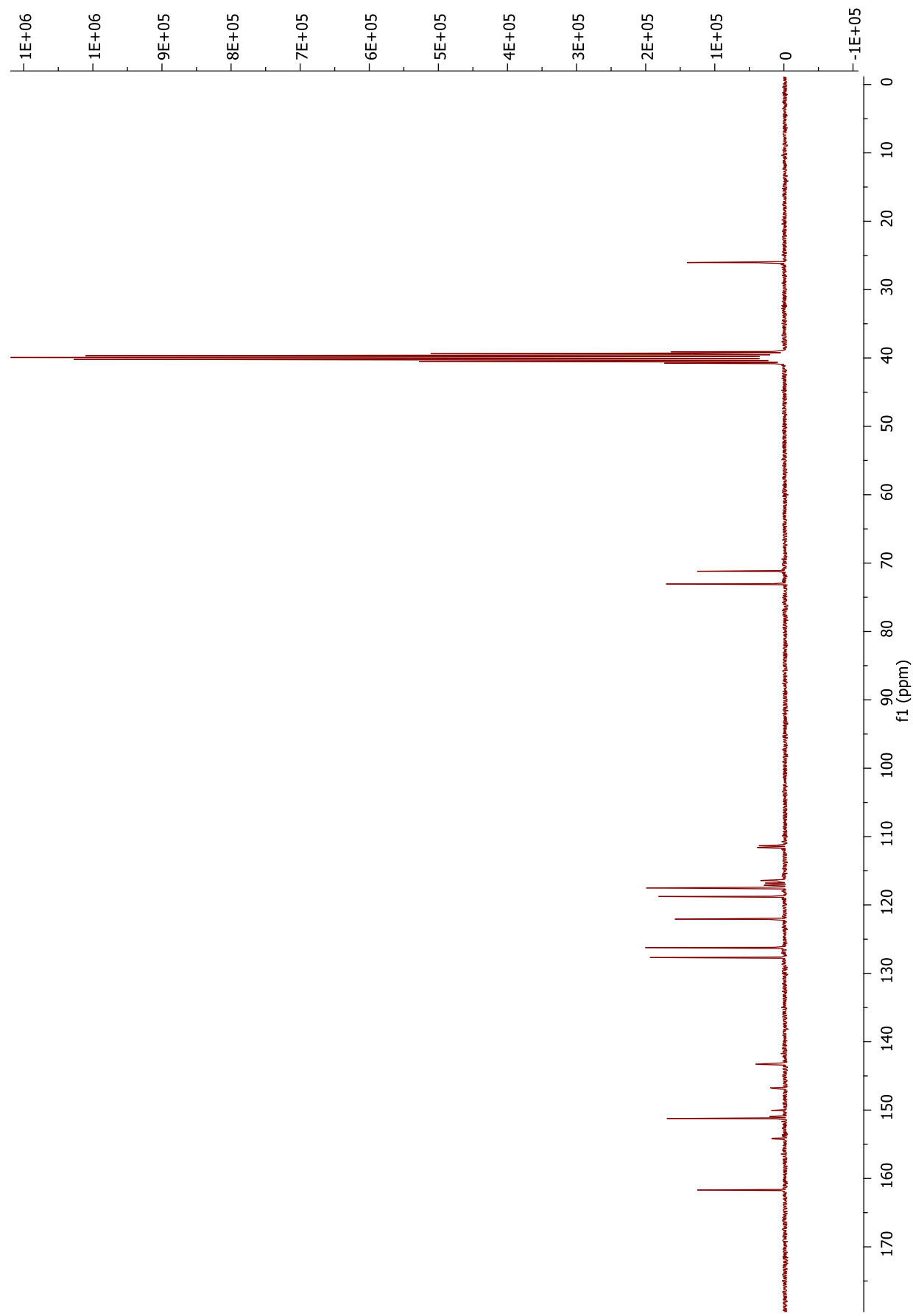
M.p. = 117.0°C

Tr (HPLC, gradient, 90% H₂O with 0.10% TFA to 10% acetonitrile with 0.10% TFA in 25 min with 35 min run time. Flow rate: 1 mL/min) = 13.3 min, Purity = 98.0%

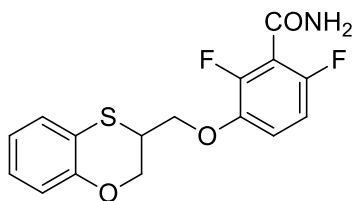
Experimental



Experimental



3-(1,4-Benzoxathiane-3-yl)methoxy)-2,6-difluorobenzamide:



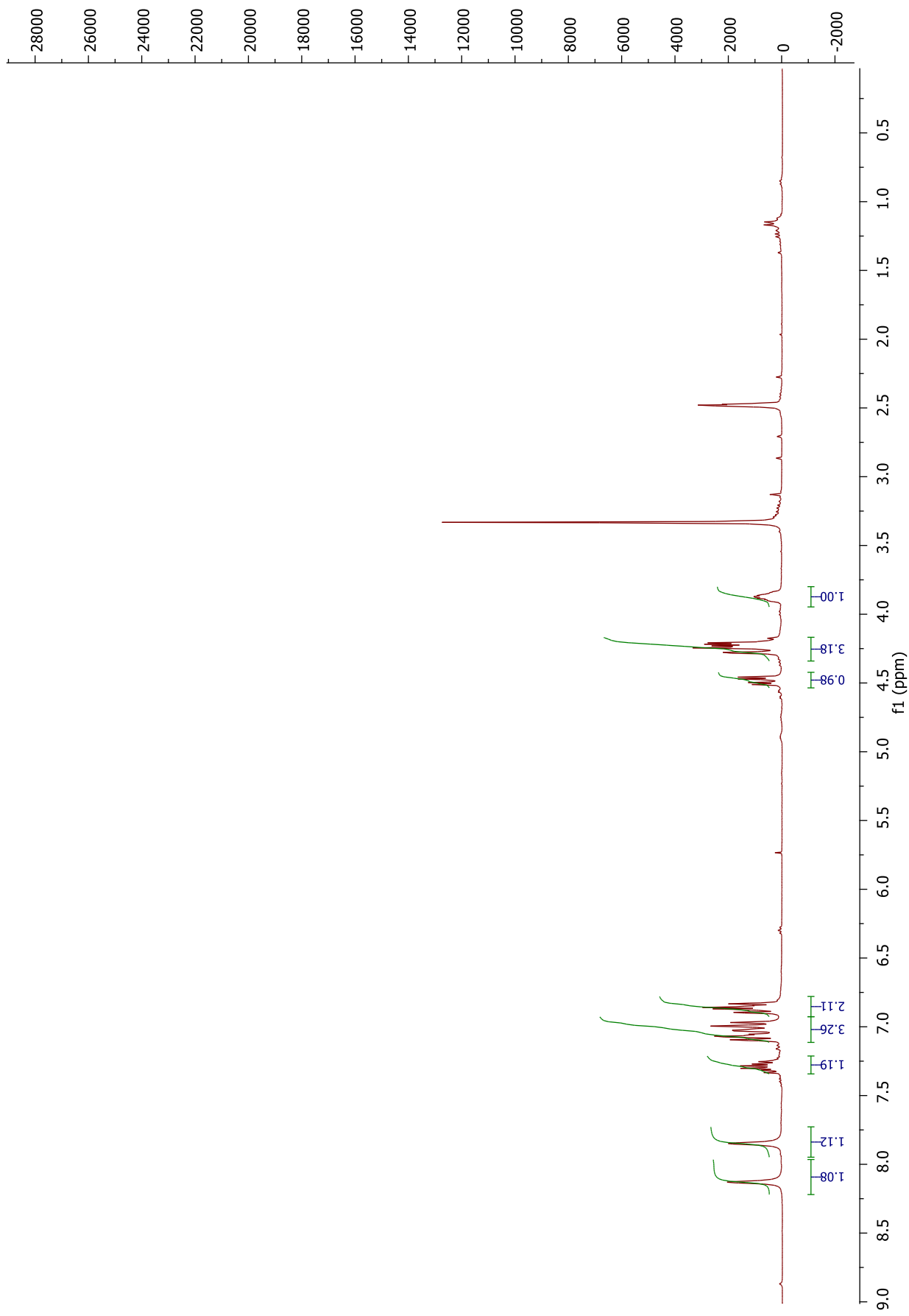
¹H NMR (d₆-DMSO): δ 8.13 (bs, 1H), 7.85 (bs, 1H), 7.27 (m, 1H), 7.03 (m, 3H), 6.86 (m, 2H), 4.48 (dd, J = 11.8, 4.3 Hz, 1H), 4.24 (m, 3H), 3.88 ppm (m, 1H).

¹³C NMR (d₆-DMSO): δ 161.7, 152.6 (dd, J = 240.5, 6.8 Hz), 151.5, 148.3 (dd, J = 247.3, 8.0 Hz), 143.0 (dd, J = 10.9, 2.8 Hz), 127.7, 126.0, 122.5, 118.7, 117.3, 117.1 (dd, J = 24.6, 20.0 Hz), 116.4 (d, J = 9.2 Hz), 111.5 (dd, J = 22.9, 4.6 Hz), 69.3, 65.3, 37.4 ppm.

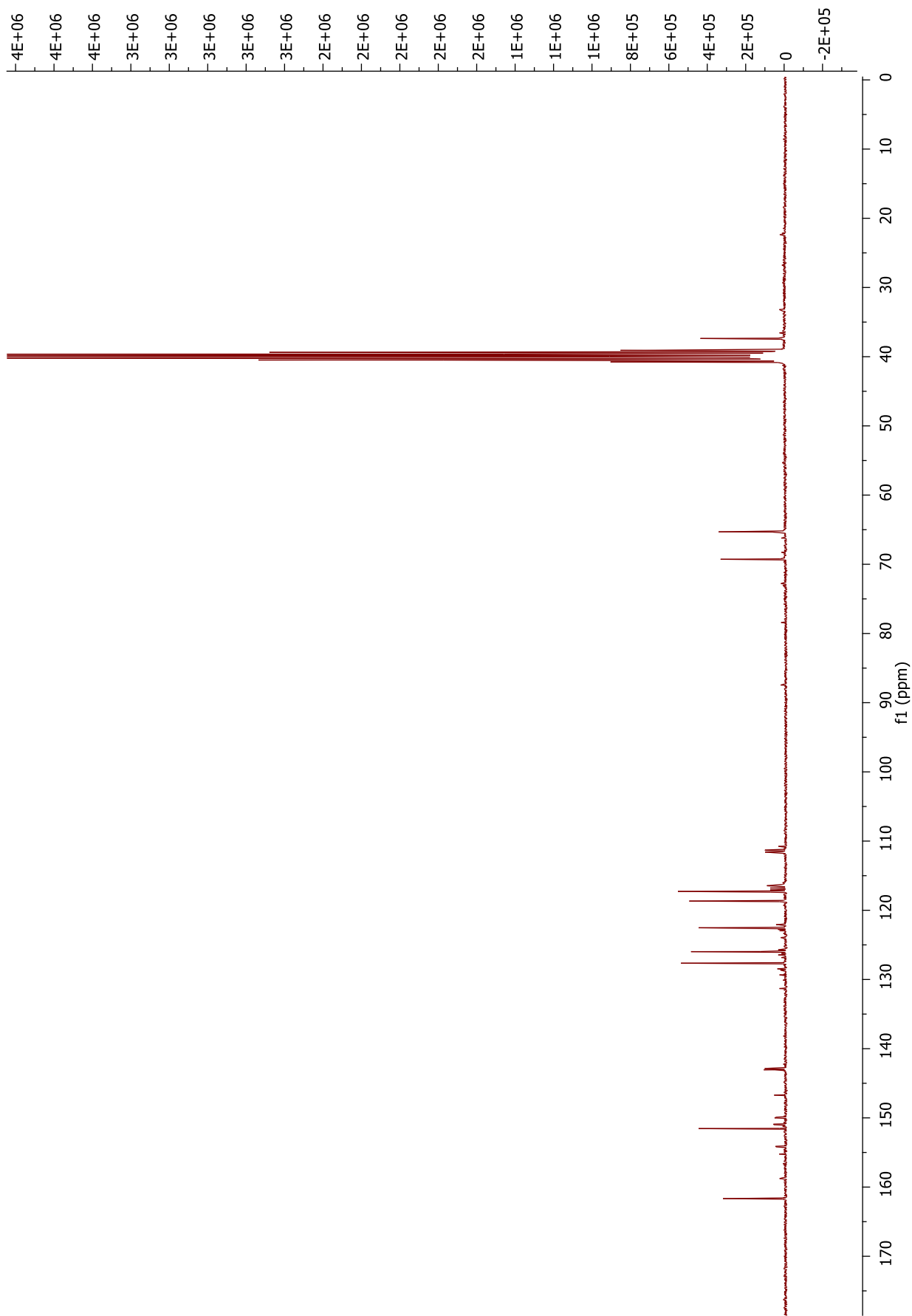
M.p. = 111.0°C

Tr (HPLC, gradient, 90% H₂O with 0.10% TFA to 10% acetonitrile with 0.10% TFA in 25 min with 35 min run time. Flow rate: 1 mL/min) = 13.5 min, Purity = 95.1%

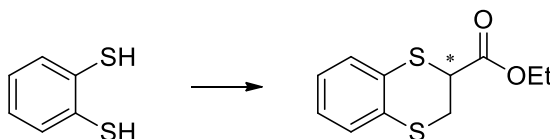
Experimental



Experimental



Ethyl 1,4-benzodithian-2-carboxylate



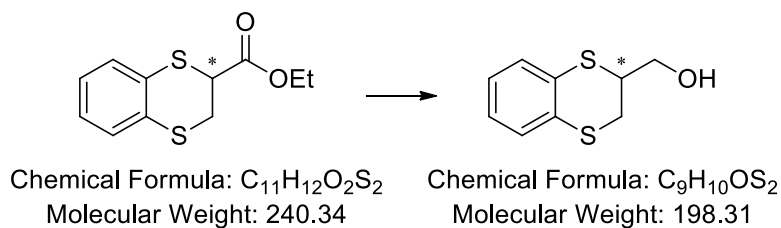
Chemical Formula: $C_6H_6S_2$ Chemical Formula: $C_{11}H_{12}O_2S_2$
 Molecular Weight: 142.24 Molecular Weight: 240.34

TEA (0.56 mL, 4.03 mmol) was added dropwise to a solution of Ethyl-2,3-dibromopropionate (0.52 g, 2.01 mmol) in DMF (5 mL). After stirring at room temperature for 20 min; therefore, 1,2-Benzenedithiol (0.26 g, 1.83 mmol) in 2 mL of DMF was slowly added. The reaction mixture was stirred at RT for 2 h, and then it was concentrated under vacuum and then diluted with 15 mL of ethyl acetate. The organic phase was washed with brine (3×10 mL), dried over Na_2SO_4 , filtered, and concentrated to give 0.38 g of Ethyl 1,4-benzodithian-2-carboxylate as a yellow oil.

Yield = 86.0%

1H NMR ($CDCl_3$): δ 7.26 (m, 2H), 7.06 (m, 2H), 4.30 (t, $J = 6.5$ Hz, 1H), 4.23 (q, $J = 7.2$ Hz, 2H), 3.32 (d, $J = 6.5$ Hz, 2H), 1.28 ppm (t, $J = 7.2$ Hz, 3H).

2-(1,4-Benzodithian-2-yl)-ethanol

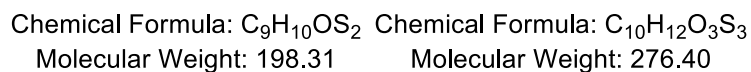


$LiAlH_4$ (0.060 g, 1.58 mmol) was suspended in dry THF (2 mL) at $0^\circ C$ under nitrogen atmosphere. The solution of Ethyl 1,4-benzodithian-2-carboxylate (0.38 g, 1.58 mmol) in THF (5 mL) was slowly added to the reaction. The mixture was then warmed to RT and stirred for 1 h; at completion, it was cooled to $0^\circ C$ and slowly quenched with Ethyl acetate (5 mL). Further Ethyl acetate (10 mL) was added, the organic layer was washed with brine (3×10 mL), dried over Na_2SO_4 and concentrated under vacuum to give 0.26 g of 2-(1,4-Benzodithian-2-yl)-ethanol as a brown oil.

Yield = 84.0%

1H NMR ($CDCl_3$): δ 7.20 (m, 2H), 7.02 (m, 2H), 3.90 (dd, $J = 11.1, 7.3$ Hz, 1H), 3.81 (dd, $J = 11.1, 6.0$ Hz, 1H), 3.70 (m, 1H), 3.27 (dd, $J = 13.4, 3.7$ Hz, 1H), 3.10 ppm (dd, $J = 13.4, 6.4$ Hz, 1H).

2-(1,4-Benzodithian-2-yl)-ethyl methanesulfonate

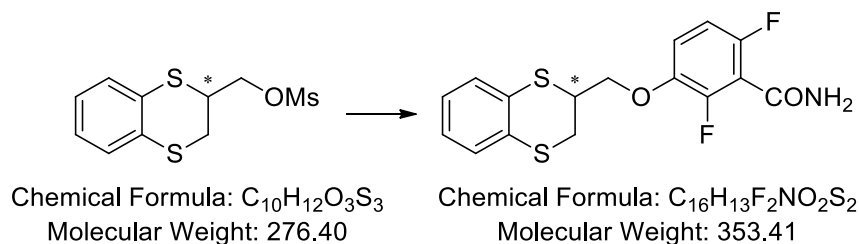


Mesyl chloride (0.14 mL, 1.76 mmol) was added dropwise to a solution of 2-(1,4-Benzodithian-2-yl)-ethanol (0.25 g, 1.26 mmol) and TEA (0.25 mL, 1.76 mmol) in DCM (4 mL) at 0°C. The mixture was stirred at that temperature for 3 h, diluted with DCM (20 mL), washed firstly with 10% aqueous $NaHCO_3$ (10 mL), secondly with 10% aqueous HCl (10 mL) and finally with brine (10 mL), dried over Na_2SO_4 , filtered and concentrated under vacuum to yield 0.34 g of 2-(1,4-Benzodithian-2-yl)-ethyl methanesulfonate as a pink oil

Yield = Quantitative

1H NMR ($CDCl_3$): δ 7.18 (ddd, $J = 9.4, 4.8, 2.3$ Hz, 2H), 7.04 (m, 2H), 4.57 (t, $J = 10.0$ Hz, 1H), 4.40 (dd, $J = 10.3, 5.1$ Hz, 1H), 3.91 (m, 1H), 3.29 (dd, $J = 14.0, 3.5$ Hz, 1H), 3.19 (dd, $J = 14.0, 5.1$ Hz, 1H), 3.07 ppm (s, 3H).

(XI) 3-(1,4-Benzodithian-2-yl)methoxy)-2,6-difluorobenzamide



Potassium carbonate (0.19 g, 1.35 mmol) was added to a solution of 2,6-Difluoro-3-hydroxybenzamide (0.22 g, 1.29 mmol) in dry DMF (2 mL). After stirring at room temperature for 30 min, a solution of 2-(1,4-Benzodithian-2-yl)-ethyl methanesulfonate (0.34 g, 1.23 mmol) in DMF (2 mL) was added. The reaction mixture was stirred at 60°C for 16 h, concentrated under vacuum, diluted with Ethyl Acetate (15 mL), washed with brine (3 × 10 mL), dried over Na_2SO_4 , filtered and concentrated, to give a residue, which was purified by flash chromatography on silica gel. Elution with 6/4 Cyclohexane/Ethyl Acetate on silica gel and further crystallization from Chloroform gave 0.22 g of 3-(1,4-Benzodithian-2-yl)methoxy)-2,6-difluorobenzamide as a white solid.

Yield = 50.0%

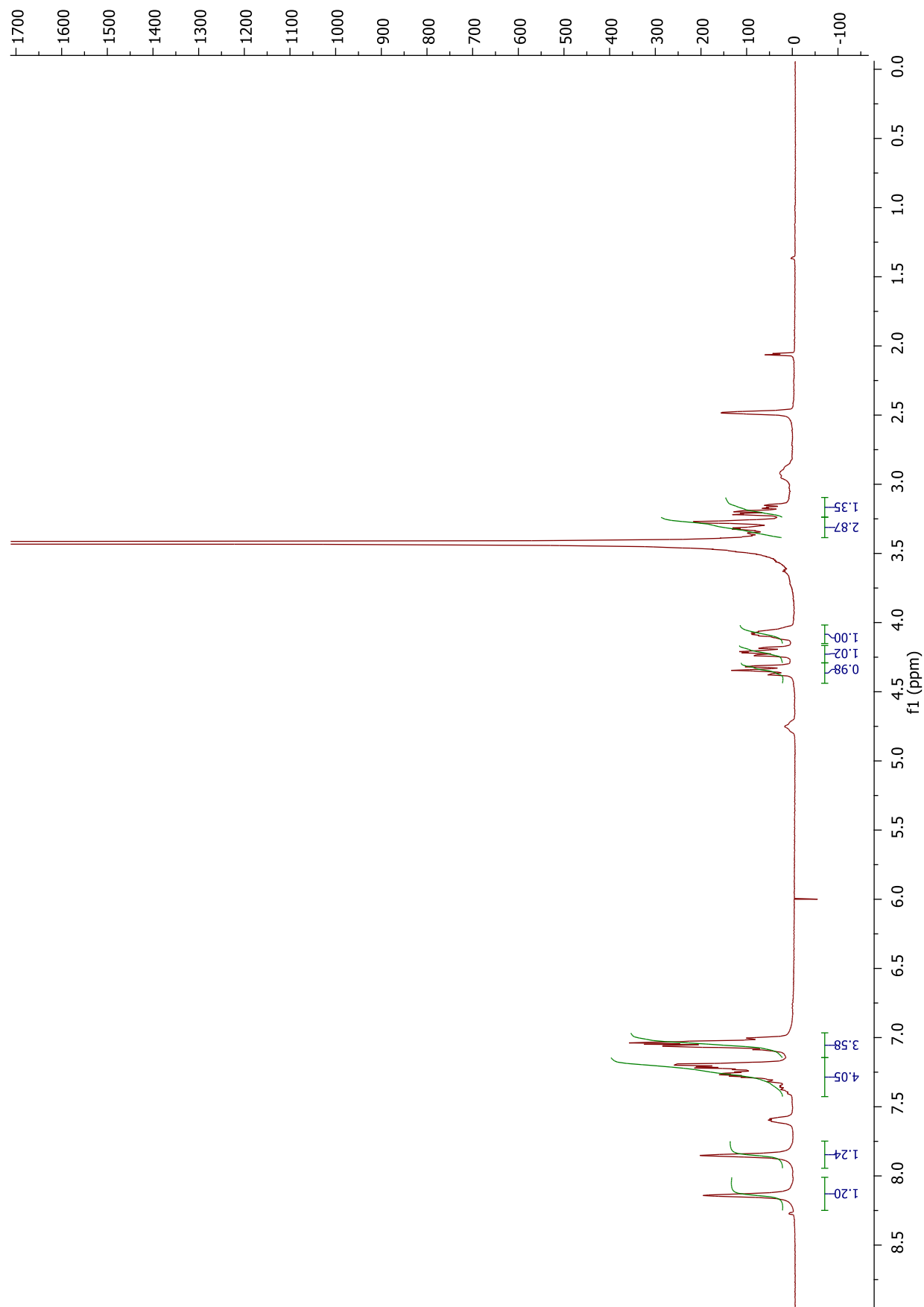
M.p. = 96.0°C

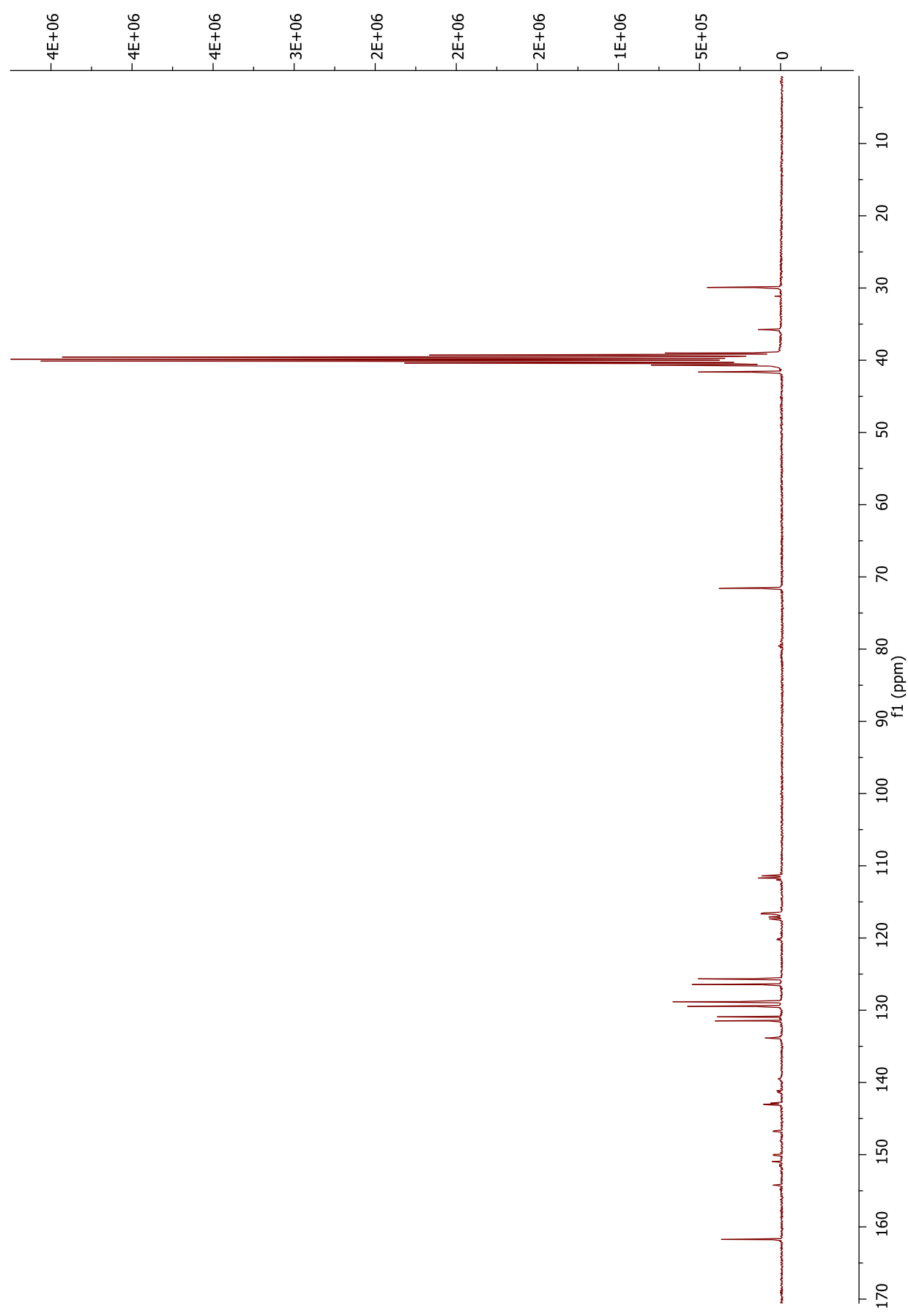
Tr (HPLC, gradient, 90% H_2O with 0.10% TFA to 10% acetonitrile with 0.10% TFA in 25 min with 35 min run time. Flow rate: 1 mL/min) = 14.3 min, Purity = 98.8%

1H NMR (d_6 -DMSO): δ 8.14 (bs, 1H), 7.85 (bs, 1H), 7.26 (m, 1H), 7.21 (m, 2H), 7.05 (m, 3H), 4.35 (m, 1H), 4.21 (m, 1H), 4.09 (m, 1H), 3.30 (dd, $J = 13.6, 3.0$ Hz, 1H), 3.18 ppm (dd, $J = 13.6, 6.1, 2.5$ Hz, 1H).

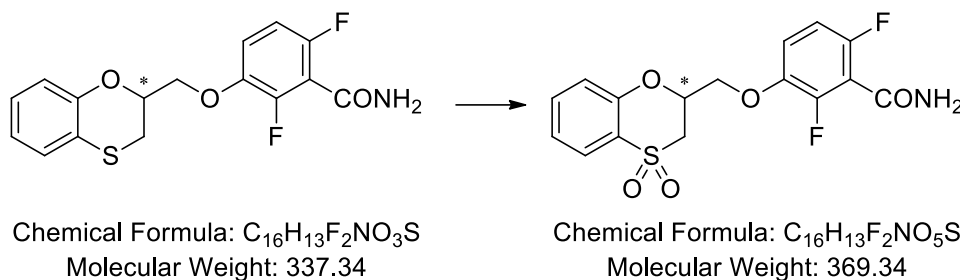
^{13}C NMR (d_6 -DMSO): δ 161.6, 152.6 (dd, $J = 240.4, 6.8$ Hz), 148.4 (dd, $J = 247.2, 8.3$ Hz), 143.0 (dd, $J = 10.8, 3.2$ Hz), 131.5, 131.0, 129.5, 128.8, 126.4, 125.6, 117.1 (dd, $J = 24.9, 20.4$ Hz), 116.6 (dd, $J = 9.3, 2.1$ Hz), 111.5 (dd, $J = 22.8, 3.9$ Hz), 71.6, 41.6, 29.9 ppm.

Experimental





(XII) 3-(1,4-Benzoxathiane-4,4-dioxide-2-yl)methoxy)-2,6-difluorobenzamide



m-CPBA (0.10 g, 0.59 mmol) was added to a cooled solution of 3-(1,4-Benzoxathiane-2-yl)methoxy)-2,6-difluorobenzamide (0.10 g, 0.30 mmol) in Acetone (5 mL) at 0°C. The reaction mixture was warmed to RT and stirred for 2 h, then 10 mL of 10% aqueous $NaHCO_3$ was added, followed by 15 mL of Ethyl acetate. The organic phase was dried over Na_2SO_4 , filtered, and concentrated to give an oily residue. The further treatment with DCM lets the precipitation of 0.03 g of 3-(1,4-Benzoxathiane-4,4-dioxide-2-yl)methoxy)-2,6-difluorobenzamide as a white solid.

Yield = 28.0%

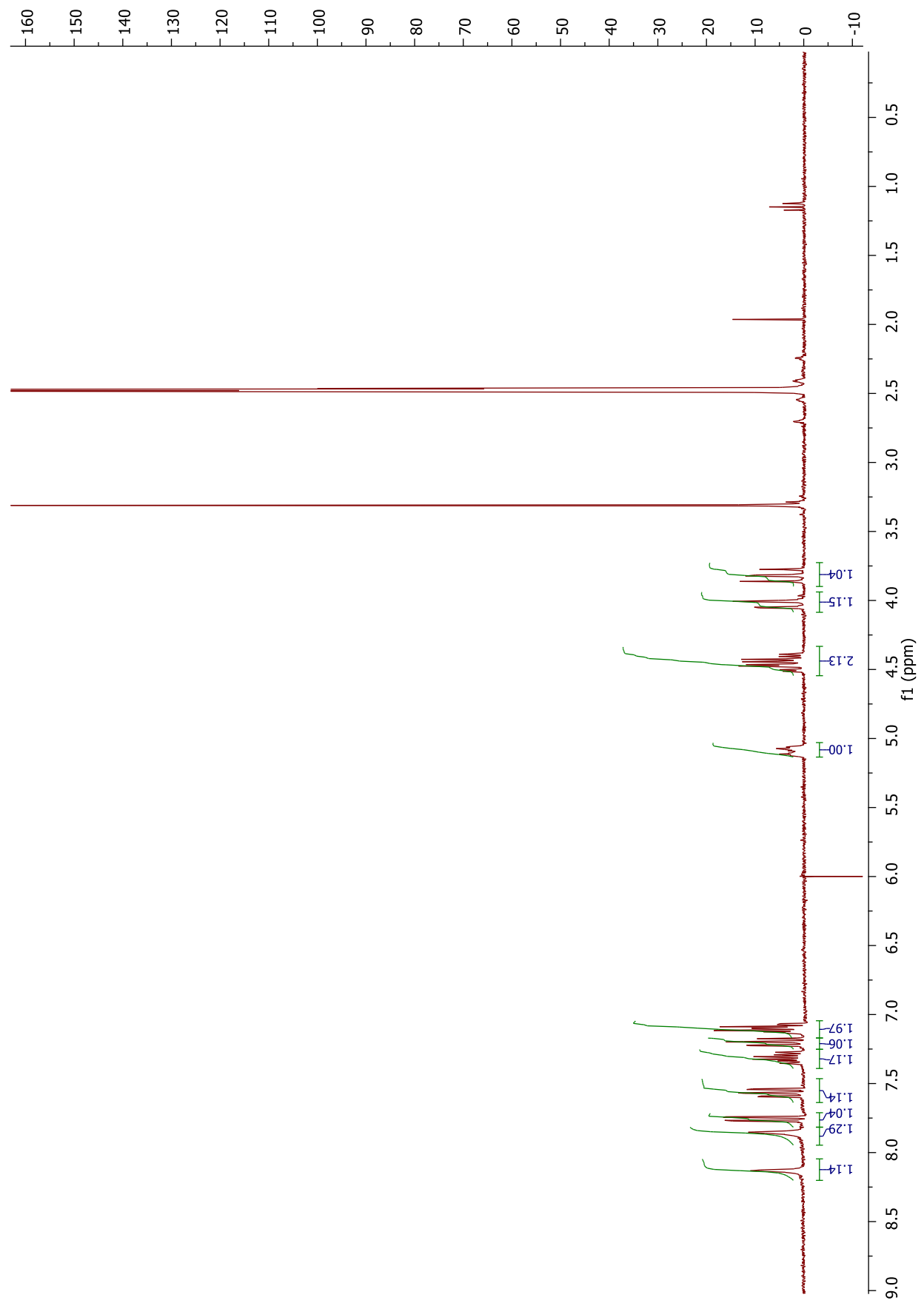
M.p. = 192.0°C

Tr (HPLC, gradient, 90% H_2O with 0.10% TFA to 10% acetonitrile with 0.10% TFA in 25 min with 35 min run time. Flow rate: 1 mL/min) = 10.1 min, Purity = 95.9%

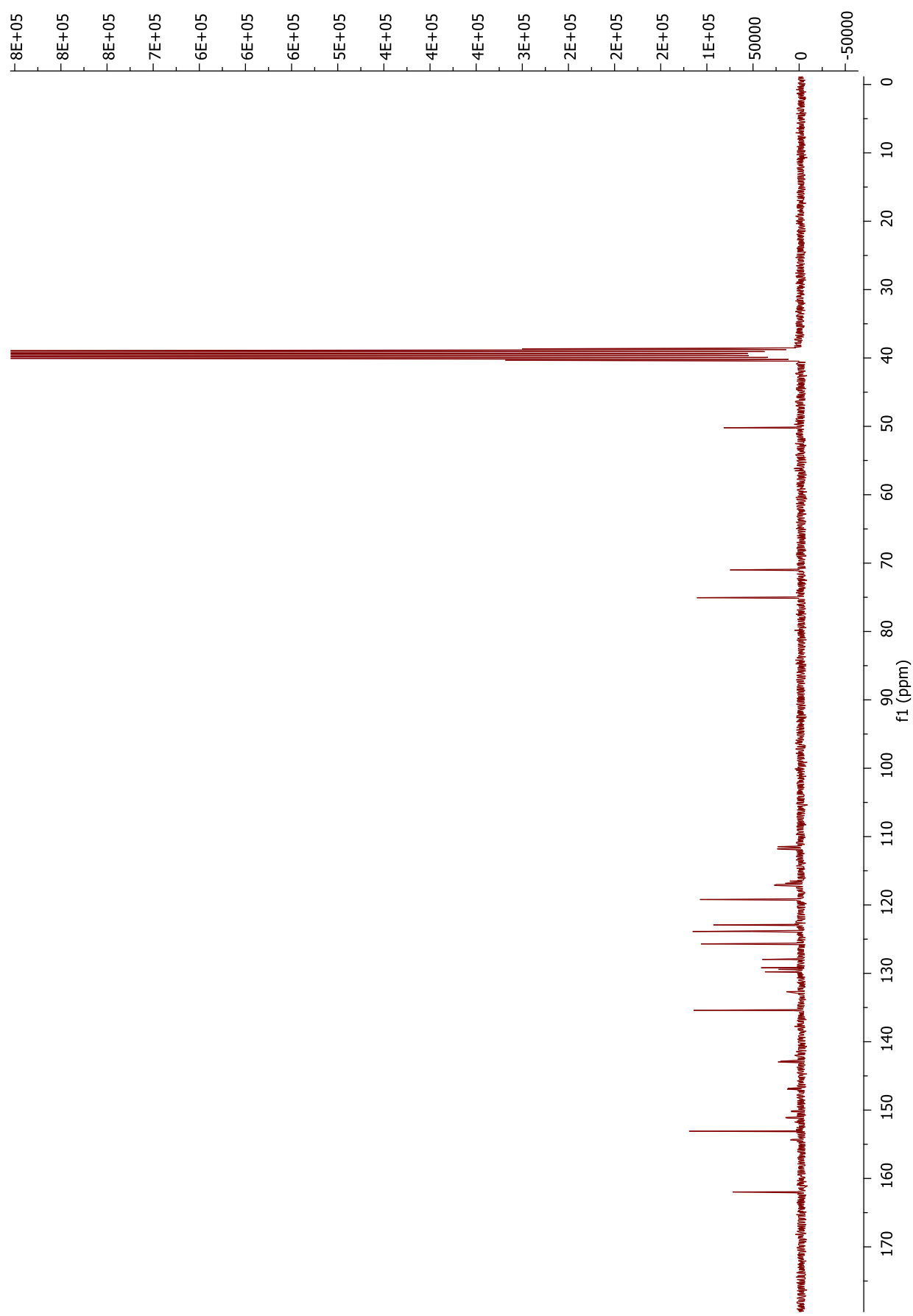
1H NMR (d_6 -DMSO): δ 8.13 (bs, 1H), 7.85 (bs, 1H), 7.76 (dd, J = 8.0, 1.6 Hz, 1H), 7.57 (m, 1H), 7.31 (td, J = 9.3, 5.3 Hz, 1H), 7.20 (m, 1H), 7.10 (m, 2H), 5.10 (m, 1H), 4.49 (dd, J = 11.3, 3.2 Hz, 1H), 4.42 (dd, J = 11.3, 5.1 Hz, 1H), 4.03 (dd, J = 14.2, 1.6 Hz, 1H), 3.82 ppm (dd, J = 14.2, 12.0 Hz, 1H).

^{13}C NMR (d_6 -DMSO): δ 162.0, 153.1, 152.7 (dd, J = 240.8, 6.7 Hz), 148.5 (dd, J = 247.5, 9.0 Hz), 142.9 (dd, J = 10.9, 3.4 Hz), 135.4, 125.7, 123.9, 122.9, 119.2, 117.1 (dd, J = 7.9, 1.9 Hz), 116.8 (dd, J = 24.7, 20.2 Hz), 111.7 (dd, J = 23.3, 3.7 Hz), 75.1, 71.0, 50.2 ppm.

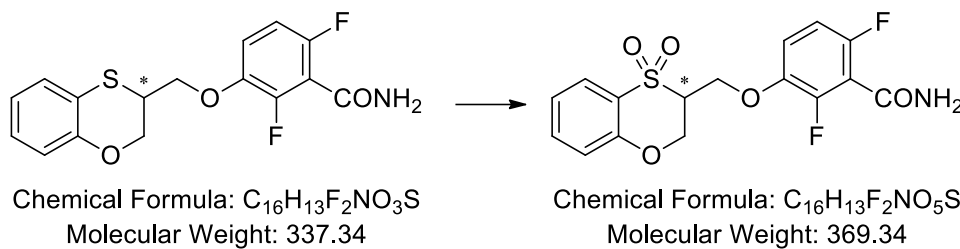
Experimental



Experimental



(XIII) 3-(1,4-Benzoxathiane-4,4-dioxide-3-yl)methoxy)-2,6-difluorobenzamide



m-CPBA (0.06 g, 0.36 mmol) was added to a cooled solution of 3-(1,4-Benzoxathiane-3-yl)methoxy)-2,6-difluorobenzamide (0.06 g, 0.18 mmol) in Acetone (5 mL) at 0°C. The reaction mixture was warmed to RT and stirred for 2 h, then 10 mL of 10% aqueous $NaHCO_3$ was added, followed by 15 mL of Ethyl acetate. The organic phase was dried over Na_2SO_4 , filtered, and concentrated to give an oily residue. The further treatment with DCM lets the precipitation of 0.03 g of 3-(1,4-Benzoxathiane-4,4-dioxide-2-yl)methoxy)-2,6-difluorobenzamide as a white solid.

Yield = 50.0%

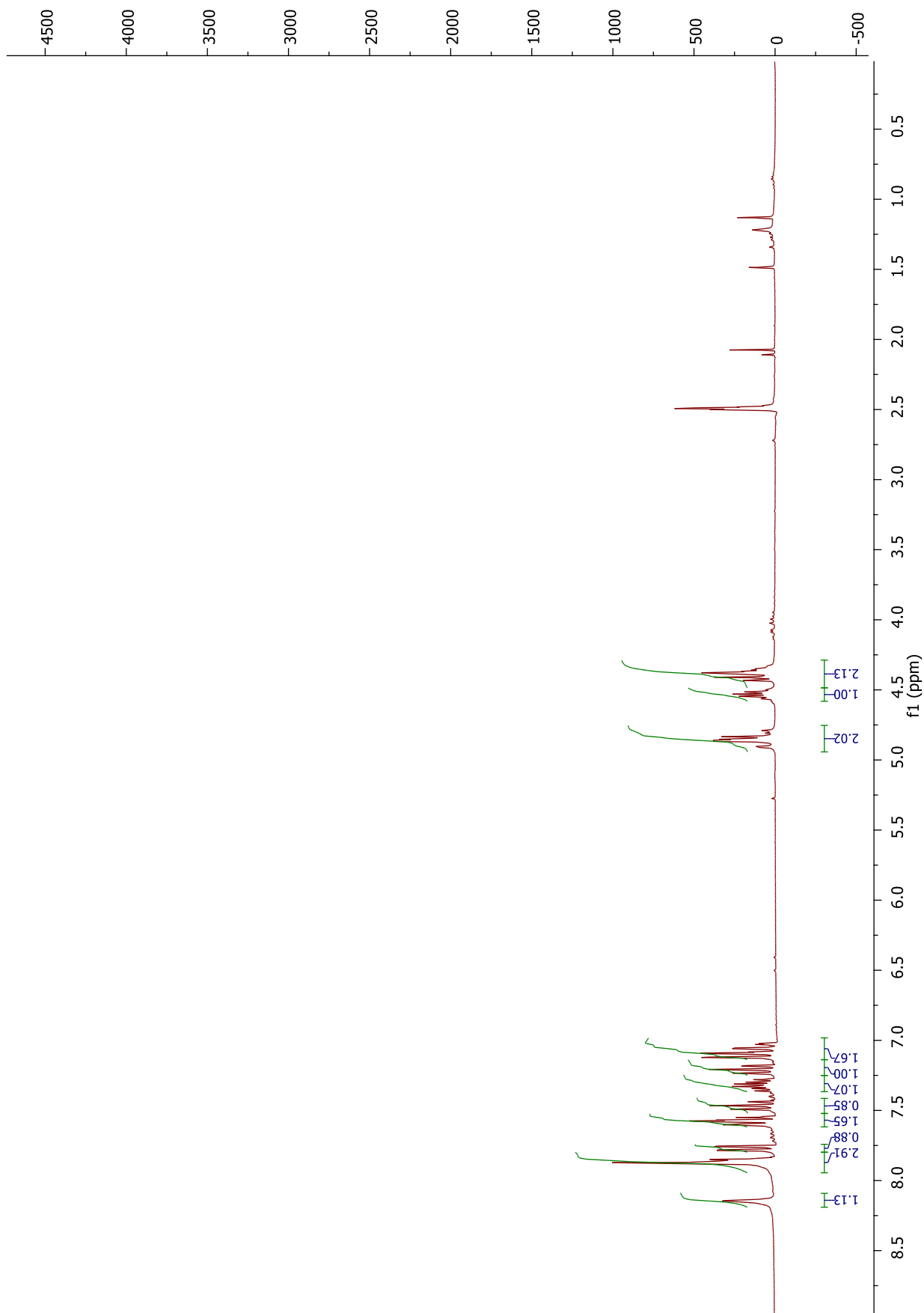
M.p. = 184.0°C

Tr (HPLC, gradient, 90% H_2O with 0.10% TFA to 10% acetonitrile with 0.10% TFA in 25 min with 35 min run time. Flow rate: 1 mL/min) = 10.3 min, Purity = 97.9%

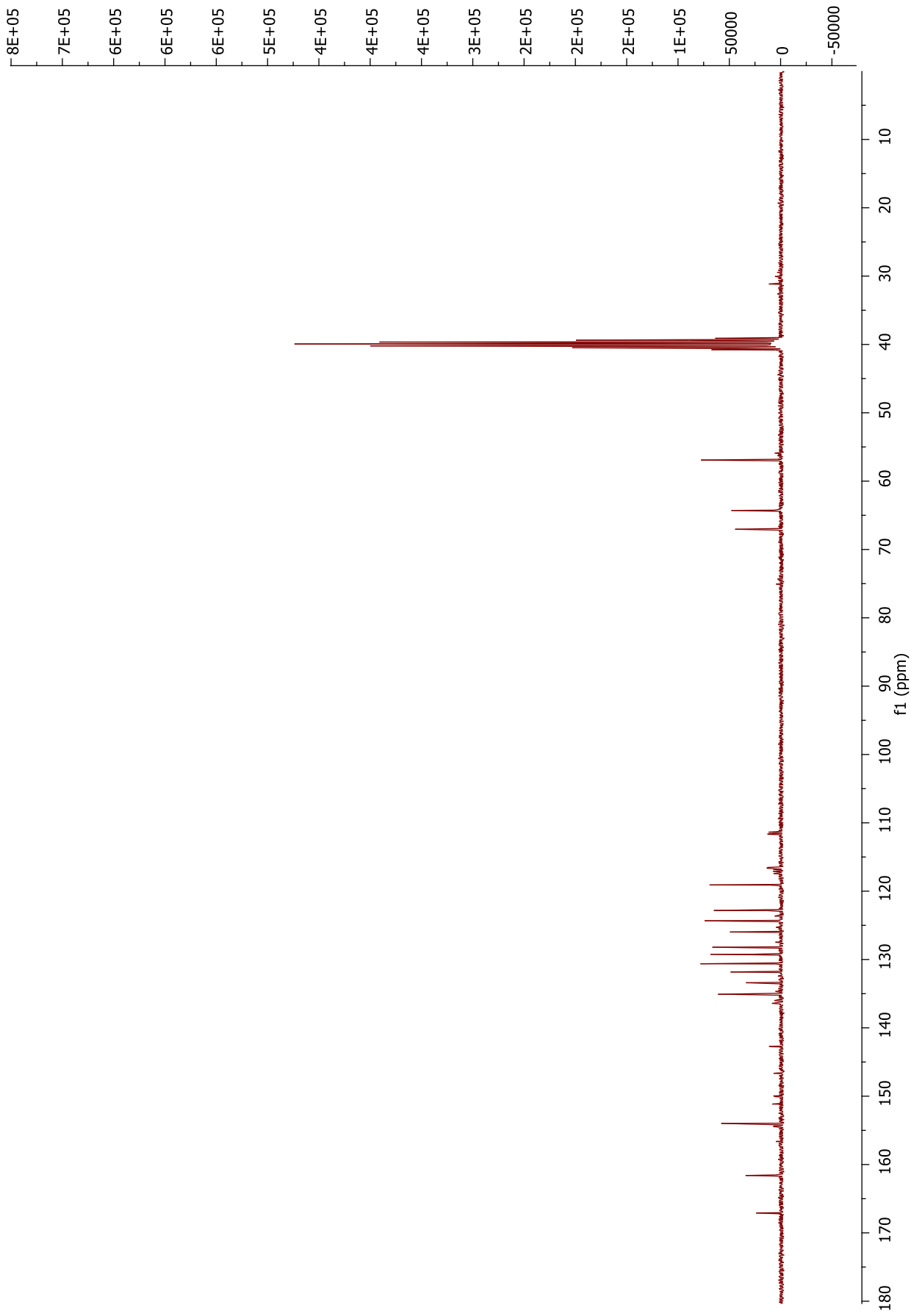
1H NMR (d_6 -DMSO): δ 8.11 (bs, 1H), 7.82 (bs, 1H), 7.76 (dd, J = 8.0, 1.6 Hz, 1H), 7.56 (ddd, J = 8.9, 7.3, 1.6 Hz, 1H 1H), 7.31 (td, J = 9.3, 5.3 Hz, 1H), 7.20 (m, 1H), 7.07 (m, 2H), 4.87 (dd, J = 13.1, 2.0 Hz, 1H), 4.81 (dd, J = 13.1, 5.6 Hz, 1H), 4.53 (m, 1H), 4.35 ppm (m, 2H).

^{13}C NMR (d_6 -DMSO): δ 161.5, 154.0, 152.8 (dd, J = 242.2, 6.7 Hz), 148.4 (dd, J = 249.8, 8.6 Hz), 142.7 (dd, J = 11.4, 3.4 Hz), 135.0, 126.0, 124.3, 122.8, 119.1, 117.1 (dd, J = 24.9, 19.9 Hz), 116.7 (d, J = 10.4 Hz), 111.5 (dd, J = 23.0, 4.0 Hz), 67.1, 64.3, 57.0 ppm.

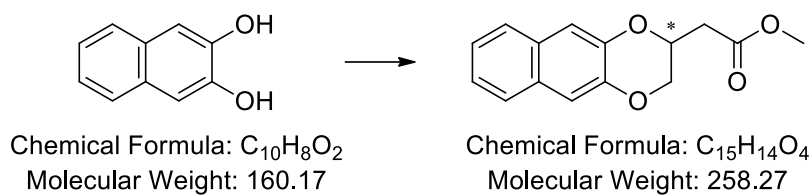
Experimental



Experimental



Methyl-(1,4-naphthodioxan-2-yl) acetate

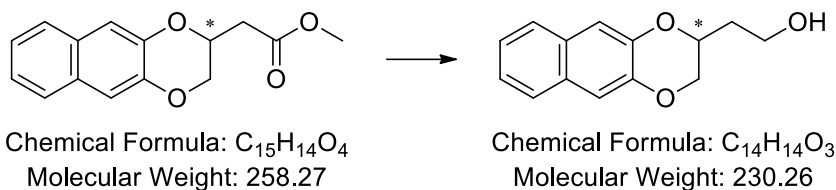


Potassium carbonate (1.9 g, 13.73 mmol) was added to a solution of Naphthalen-2,3-diol (1.00 g, 6.24 mmol) in Acetone (10 mL). After stirring for 30 minutes, Methyl 3,4-dibromobutirrate (1.79 mL, 6.90 mmol) was added dropwise. The reaction mixture was stirred at reflux for 72 hours, concentrated under vacuum, diluted with Ethyl acetate (35 mL), washed with 10% aqueous NaOH (15 mL) and 10% aqueous NaCl (15 mL), dried with Na₂SO₄, filtered and concentrated under vacuum to yield 1.42 g of Methyl-(1,4-naphthodioxan-2-yl) acetate as a dark oil.

Yield = 94.0%

¹H NMR (CDCl₃) δ 7.64 (m, 2H), 7.29 (m, 4H), 4.73 (m, 1H), 4.41 (dd, *J* = 11.4, 2.2 Hz, 1H), 4.09 (dd, *J* = 11.4, 6.9 Hz, 1H), 3.76 (s, 3H), 2.85 (dd, *J* = 16.1, 6.8 Hz, 1H), 2.70 ppm (dd, *J* = 16.1, 6.5 Hz, 1H).

2-Hydroxyethyl-1,4-naphthodioxane

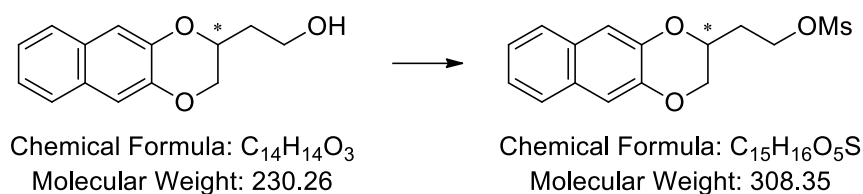


A solution of Methyl-(1,4-naphthodioxan-2-yl) acetate (1.42 g, 5.86 mmol) in dry THF (5 mL) was added dropwise to a suspension of $LiAlH_4$ (0.24 g, 6.45 mmol) was suspended in dry THF (5 mL) at $0^\circ C$ under N_2 atmosphere. The reaction mixture was stirred at room temperature for 1 hour, diluted with Ethyl acetate (15 mL), washed with 10% aqueous HCl, water and 10% aqueous NaCl (10 + 10 + 10 mL), dried over Na_2SO_4 , filtered and concentrated to give 1.14 g of 2-Hydroxyethyl-1,4-naphthodioxane as a brownish oil.

Yield = 85.0%

1H NMR ($CDCl_3$): δ 7.63 (m, 2H), 7.28 (m, 4H), 4.47 (m, 1H), 4.35 (dd, $J = 11.4, 2.3$ Hz, 1H), 4.05 (dd, $J = 11.4, 7.8$ Hz, 1H), 3.95 (m, 2H), 1.92 ppm (m, 2H).

2-Mesyloxyethyl-1,4-naphthodioxane

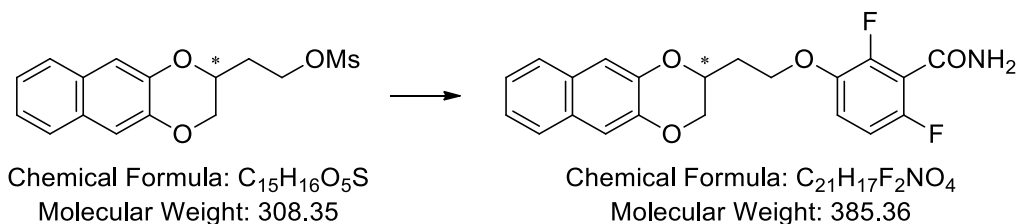


Mesyl chloride (0.2 mL, 2.60 mmol) was added dropwise to a solution of 2-Hydroxyethyl-5,6,7,8-tetrahydro-1,4-naphthodioxane (0.50 g, 2.17 mmol) and TEA (0.36 mL, 3.22 mmol) in DCM (10 mL) at 0°C. The reaction mixture was stirred at room temperature for 3 hours, diluted with DCM (15 mL), washed firstly with 10% aqueous $NaHCO_3$ (5 mL), secondly with 10% aqueous HCl (5 mL) and finally with 10% aqueous NaCl (10 mL), filtered and concentrated under vacuum to give 0.15 g of 2-Mesyloxyethyl-1,4-naphthodioxane as a yellowish oil.

Yield = 93.0%

1H NMR ($CDCl_3$): δ 7.65 (m, 2H), 7.30 (m, 4H), 4.51 (m, 3H), 4.36 (dd, $J = 11.4, 2.3$ Hz, 1H), 4.06 (dd, $J = 11.4, 7.2$ Hz, 1H), 3.06 (s, 3H), 2.14 ppm (m, 2H).

(XIV) 3-(1,4-Naphthodioxan-2-yl)ethoxy)-2,6-difluorobenzamide



Potassium carbonate (0.21 g, 1.50 mmol) was added to a solution of 2,6-Difluoro-3-hydroxybenzamide (0.25 g, 1.43 mmol) in dry DMF (5 mL) under N_2 atmosphere. After stirring at room temperature for 30 minutes, a solution of 2-Mesyloxyethyl-1,4-naphthodioxane (0.40 g, 1.36 mmol) in dry DMF (5 mL) was added. The reaction mixture was stirred at $60^\circ C$ for 24 hours, concentrated under vacuum, diluted with Ethyl acetate (15 mL), washed with 10% aqueous NaCl (4 x 10 mL), dried over Na_2SO_4 , filtered and concentrated to give a residue which was purified by flash chromatography. Elution with 1/1 Cyclohexane/Ethyl acetate on silica gel gave 0.12 g of 3-(1,4-Naphthodioxan-2-yl)ethoxy)-2,6-difluorobenzamide as a white solid.

Yield = 23.0%

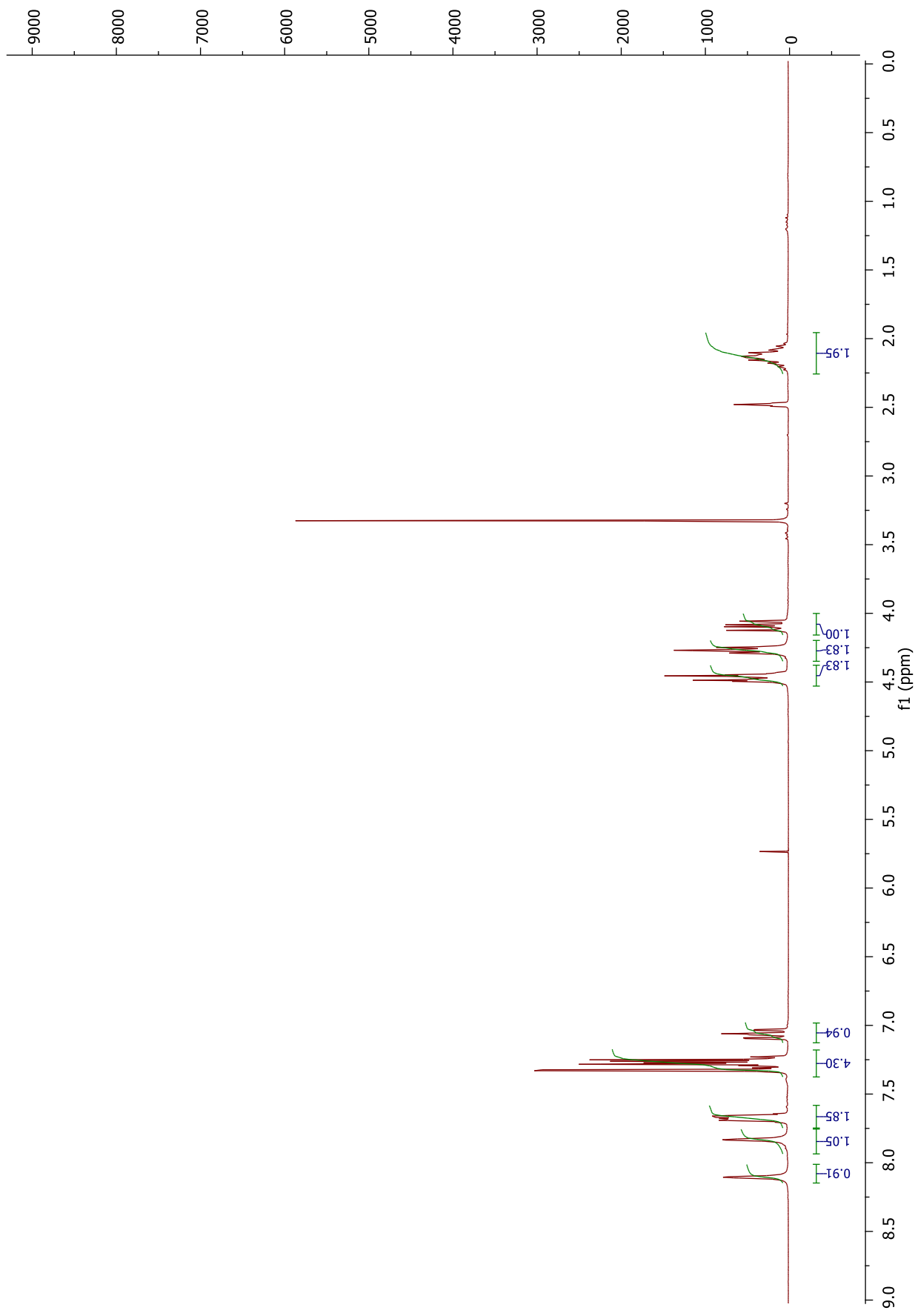
M.p. = $140.9^\circ C$

Tr (HPLC, gradient, 90% H_2O with 0.10% TFA to 10% acetonitrile with 0.10% TFA in 25 min with 35 min run time. Flow rate: 1 mL/min) = 15.2 min, Purity = 99.3%

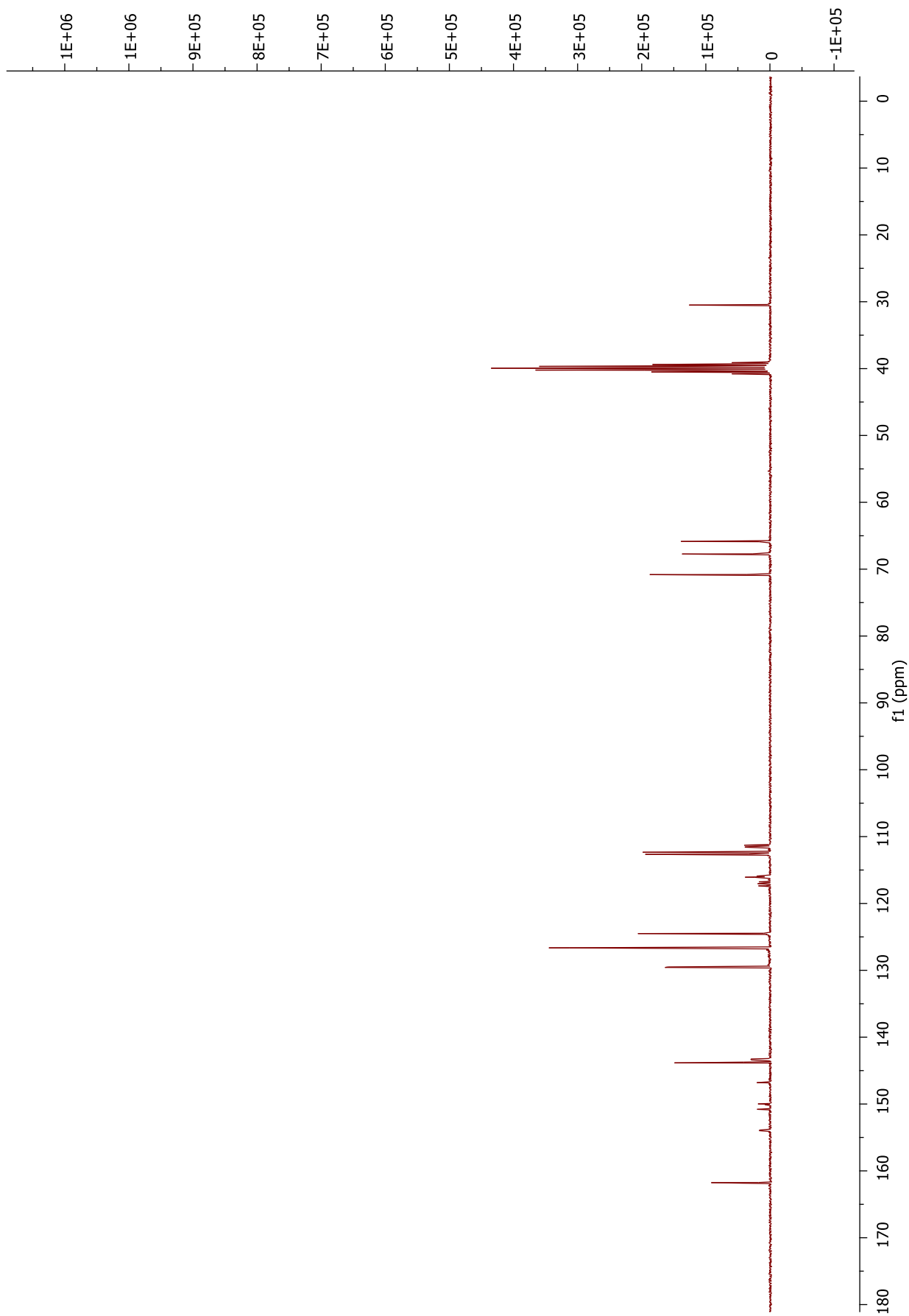
1H NMR (d_6 -DMSO): δ 8.11 (bs, 1H), 7.83 (bs, 1H), 7.68 (m, 2H), 7.33 (d $J=1.9$ Hz, 1H), 7.31–7.22 (m, 4H), 7.06 (td, $J = 9.0, 1.9$ Hz, 1H), 4.47 (m, 2H), 4.27 (t, $J = 6.2$ Hz, 2H), 4.09 (dd, $J = 12.0, 7.9$ Hz, 1H), 2.12 ppm (m, 2H).

^{13}C NMR (d_6 -DMSO): δ 161.76, 152.35 (dd, $J = 238.8, 6.8$ Hz), 148.39 (dd, $J = 246.9, 8.4$ Hz), 143.84, 143.74, 143.31 (dd, $J = 10.9, 3.1$ Hz), 129.57, 129.49, 126.64, 124.53, 117.07 (dd, $J = 24.9, 20.4$ Hz), 116.00 (dd, $J = 9.3, 2.3$ Hz), 112.65, 112.34, 111.41 (dd, $J = 22.7, 4.0$ Hz), 70.82, 67.73, 65.86, 30.49 ppm.

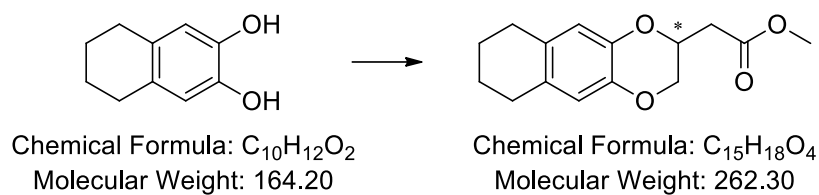
Experimental



Experimental



Methyl-(5,6,7,8-tetrahydro-1,4-naphthodioxan-2-yl) acetate

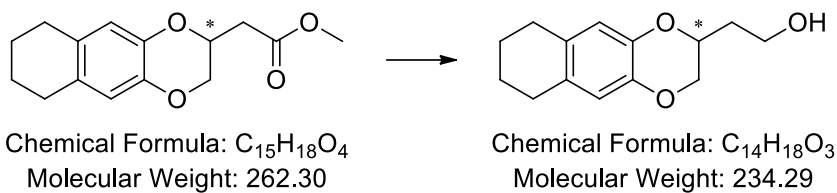


Potassium carbonate (1.74 g, 13.40 mmol) was added to a solution of 5,6,7,8-Tetrahydronaphthalen-2,3-diol (1.00 g, 6.09 mmol) in acetone (15 mL). After stirring at room temperature for 30 minutes, Methyl 3,4-dibromobutirrate (1.85 g, 6.70 mmol) was added. The reaction mixture was stirred at reflux for 18 hours, concentrated under vacuum, diluted with Ethyl acetate (25 mL), washed with 10% aqueous NaCl (15 mL), dried with Na_2SO_4 , filtered and concentrated under vacuum to yield an orange oil, which was purified by flash chromatography on silica gel. Elution with 9/1 Cyclohexane/Ethyl acetate on silica gel gave 0.85 g of Methyl-(5,6,7,8-tetrahydro-1,4-naphthodioxan-2-yl) acetate as a colourless oil.

Yield = 52.5%

1H NMR ($CDCl_3$): δ 6.58 (s, 2H), 4.59 (qd, $J = 6.6, 2.3$ Hz, 1H), 4.26 (dd, $J = 11.3, 2.3$ Hz, 1H), 3.96 (dd, $J = 11.3, 6.6$ Hz, 1H), 3.74 (s, 3H), 2.77 (dd, $J = 16.1, 6.6$ Hz, 1H), 2.64 (m, 4H), 2.63 (dd, $J = 16.1, 6.6$ Hz, 1H), 1.73 ppm (m, 4H).

2-(2-Hydroxyethyl)-5,6,7,8-tetrahydro-1,4-naphthodioxane

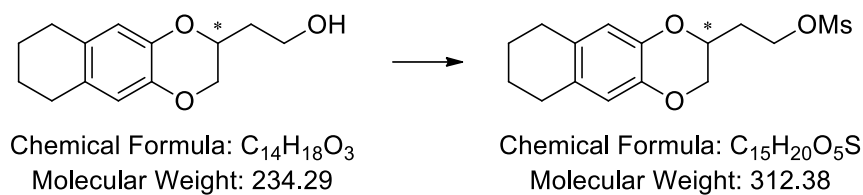


A solution of Methyl-(5,6,7,8-tetrahydro-1,4-naphthodioxan-2-yl) acetate (0.85 g, 3.24 mmol) in dry THF (5 mL) was added dropwise to a suspension of $LiAlH_4$ (0.12 g, 3.24 mmol) was suspended in dry THF (5 mL) at $0^\circ C$ under N_2 atmosphere. The reaction mixture was stirred at room temperature for 1 hour, diluted with Ethyl acetate (15 mL), washed with 10% aqueous HCl, water and 10% aqueous NaCl (10+10+10 mL), dried over Na_2SO_4 , filtered and concentrated to give 0.59 g of 2-(2-Hydroxyethyl)-5,6,7,8-tetrahydro-1,4-naphthodioxane as a yellowish oil.

Yield = 77.6%

1H NMR ($CDCl_3$): δ 6.57 (s, 2H), 4.33 (m, 1H), 4.21 (dd, $J = 11.3, 2.2$ Hz, 1H), 3.91 (m, 3H) 2.64 (m, 4H), 1.89 (m, 2H), 1.72 ppm (m, 4H).

2-(2-Mesyloxyethyl)-5,6,7,8-tetrahydro-1,4-naphthodioxane



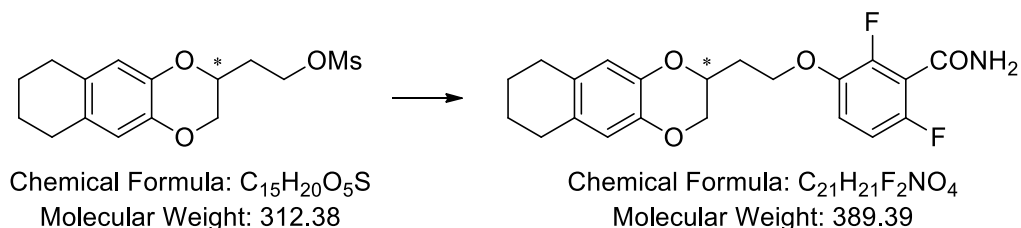
Mesyl chloride (0.25 mL, 3.22 mmol) was added dropwise to a solution of 2-(2-Hydroxyethyl)-5,6,7,8-tetrahydro-1,4-naphthodioxane (0.58 g, 2.47 mmol) and TEA (0.45 mL, 3.22 mmol) in DCM (10 mL) at 0°C. The reaction mixture was stirred at room temperature for 3 hours, diluted with DCM (15 mL), washed firstly with 10% aqueous $NaHCO_3$ (5 mL), secondly with 10% aqueous HCl (5 mL) and finally with 10% aqueous NaCl (10 mL), filtered and concentrated under vacuum to give 0.15 g of 2-(2-Mesyloxyethyl)-5,6,7,8-tetrahydro-1,4-naphthodioxane as a white solid

Yield = 87.0%

M.p. = 87.3°C

1H NMR ($CDCl_3$): δ 6.57 (s, 2H), 4.46 (m, 2H), 4.31 (ddd, $J = 13.4, 6.8, 2.2$ Hz, 1H), 4.22 (dd, $J = 11.3, 2.2$ Hz, 1H), 3.91 (dd, $J = 11.3, 6.8$ Hz, 1H), 3.04 (s, 3H), 2.65 (m, 4H), 2.04 (m, 2H), 1.75 ppm (m, 4H).

(XV) 3-(5,6,7,8-Tetrahydro-1,4-naphthodioxan-2-yl)ethoxy)-2,6-difluorobenzamide



Potassium carbonate (0.19 g, 1.41 mmol) was added to a solution of 2,6-Difluoro-3-hydroxybenzamide (0.23 g, 1.34 mmol) in dry DMF (5 mL) under N_2 atmosphere. After stirring at room temperature for 30 minutes, a solution of 2-Mesyloxyethyl-5,6,7,8-tetrahydro-1,4-naphthodioxane (0.40 g, 1.28 mmol) in dry DMF (5 mL) was added. The reaction mixture was stirred at $80^\circ C$ for 4 hours, concentrated under vacuum, diluted with Ethyl acetate (15 mL), washed with 10% aqueous NaCl (4 x 10 mL), dried over Na_2SO_4 , filtered and concentrated to give a residue. Crystallization from IPA (20 vol.) gave 0.24 g of 3-(5,6,7,8-Tetrahydro-1,4-naphthodioxan-2-yl)ethoxy)-2,6-difluorobenzamide as a white solid.

Yield = 50.0%

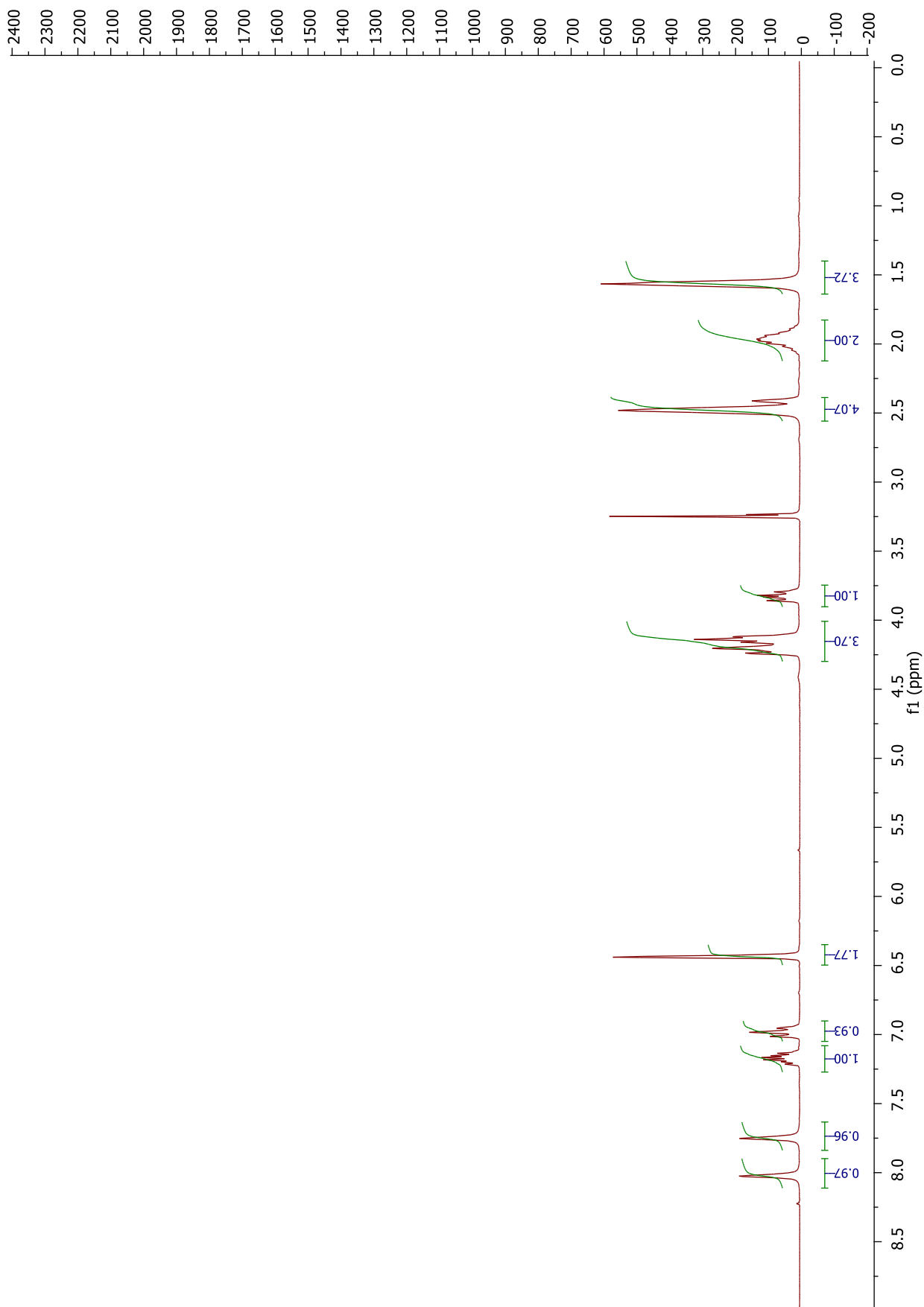
M.p. = $166.5^\circ C$

Tr (HPLC, gradient, 90% H_2O with 0.10% TFA to 10% acetonitrile with 0.10% TFA in 25 min with 35 min run time. Flow rate: 1 mL/min) = 16.7 min, Purity = 95.0%

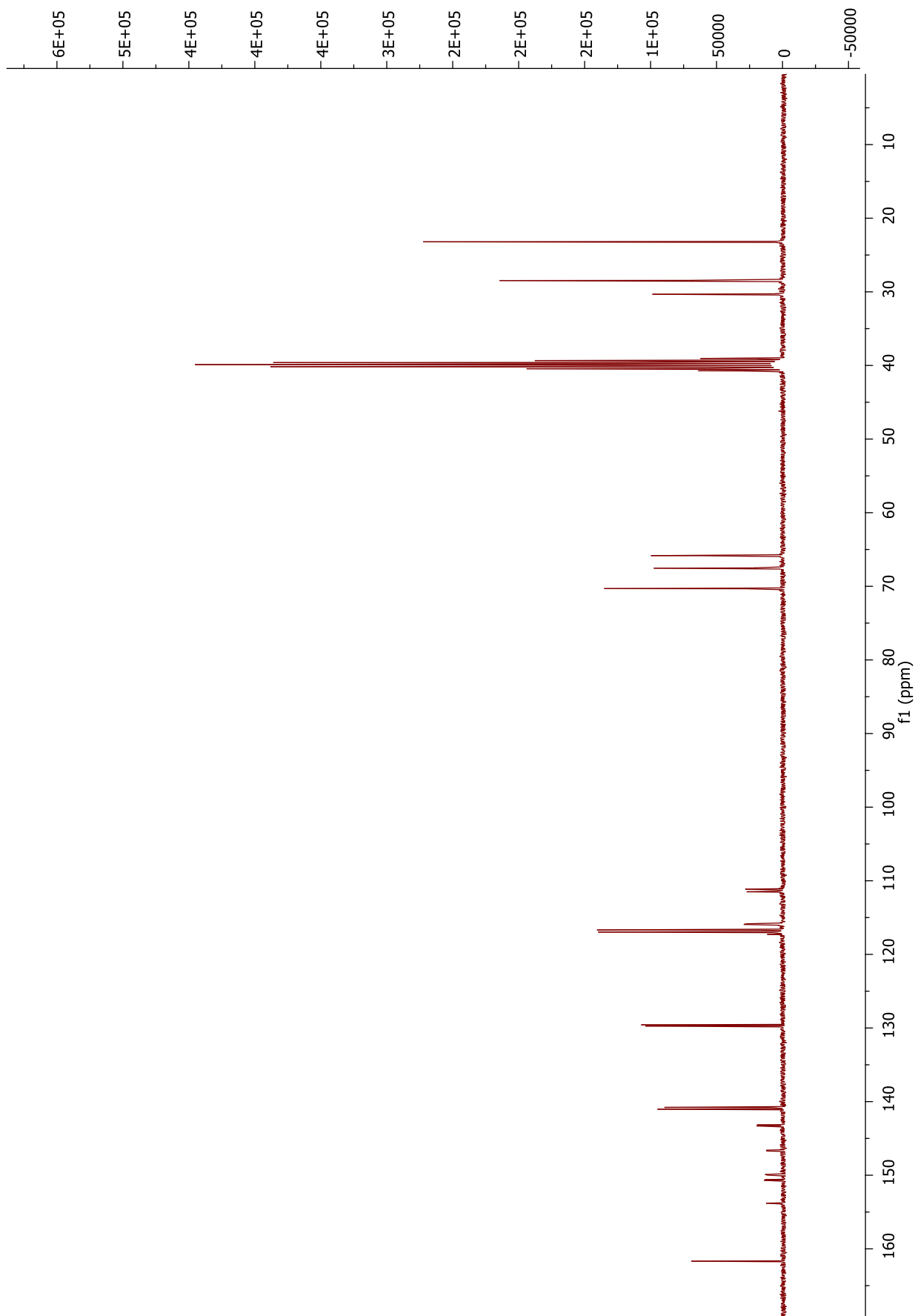
1H NMR (d_6 -DMSO): δ 8.03 (s, 1H), 7.75 (s, 1H), 7.17 (tt, J = 9.0, 4.5 Hz, 1H), 6.98 (t, J = 9.0 Hz, 1H), 6.44 (s, 2H), 4.17 (m, 4H), 3.82 (m, 1H), 2.48 (m, 4H), 1.96 (m, 2H), 1.56 ppm (m, 4H).

^{13}C NMR (d_6 -DMSO): 161.7, 152.2 (dd, J = 240.0, 6.7 Hz), 148.3 (dd, J = 246.7, 9.0 Hz), 143.3 (dd, J = 10.5, 3.0 Hz), 141.0, 140.8, 129.7, 129.6, 117.0 (dd, J = 25.4, 20.7 Hz), 117.0, 116.7, 115.9 (dd, J = 9.4, 1.9 Hz), 111.3 (dd, J = 22.5, 4.5 Hz), 70.3, 67.5, 65.8, 30.3, 28.5, 23.2 ppm.

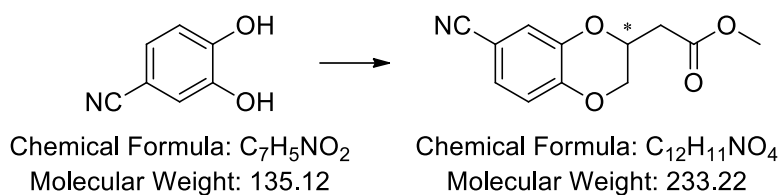
Experimental



Experimental



Methyl (7-cyano-1,4-benzodioxan-2-yl)-acetate



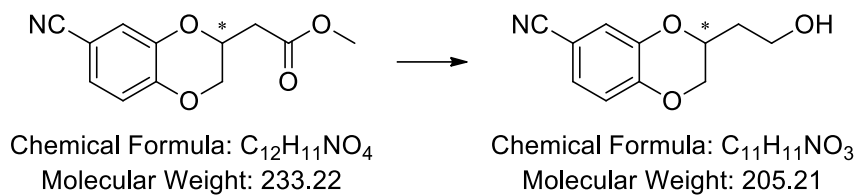
A solution of 3,4-Dihydroxybenzonitrile (2.00 g, 14.80 mmol) in acetone (20 mL) was added of potassium carbonate (4.91 g, 35.52 mmol). The reaction mixture was kept stirring at room temperature for 30 min, then Methyl 3,4-dibromobutyrate (4.23 g, 16.68 mmol) was added dropwise, and the medium was heated at reflux. The reaction mixture was then stirred at that temperature for 3 h, letting the completion of the reaction. After concentration under vacuum, the crude was diluted with ethyl acetate (50 mL), washed with 10% aqueous NaOH, and 10% aqueous NaCl (2 × 20 mL), dried over Na₂SO₄, filtered, and concentrated to give a residue. Crystallization from Methanol (3 vol) gave 1.40 g of Methyl (7-cyano-1,4-benzodioxan-2-yl)-acetate as a white solid.

Yield = 41.0%

M.p. = 143.2°C

¹H NMR (CDCl₃): δ 7.14 (m, 2H), 6.92 (d, J = 9.0 Hz, 1H), 4.62 (dq, J = 6.6, 2.2 Hz, 1H), 4.39 (dd, J = 11.5, 2.2 Hz, 1H), 4.04 (dd, J = 11.5, 6.6 Hz, 1H), 3.75 (s, 3H), 2.78 (dd, J = 16.3, 6.6 Hz, 1H), 2.64 ppm (dd, J = 16.3, 6.6 Hz, 1H).

2-(2-Hydroxyethyl)-7-cyano-1,4-benzodioxane

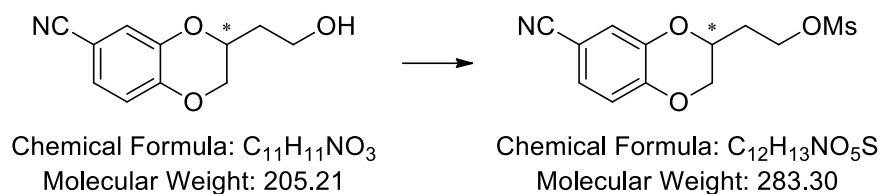


A solution of Methyl (7-cyano-1,4-benzodioxan-2-yl)-acetate (1.40 g, 6.00 mmol) in dry THF (10 mL) was added dropwise to a suspension of $LiAlH_4$ (0.21 g, 6.00 mmol) in dry THF (5 mL) at $-40^\circ C$ under N_2 atmosphere. The reaction mixture was stirred at $-35^\circ C$ for 30 min, then diluted with ethyl acetate (15 mL), washed with 10% aqueous HCl, water and 10% aqueous NaCl (3×10 mL), dried over Na_2SO_4 , filtered, and concentrated to give 0.95 g of 2-(2-Hydroxyethyl)-7-cyano-1,4-benzodioxane as a yellowish oil.

Yield = 82.0%

1H NMR ($CDCl_3$): δ 7.13 (m, 2H), 6.92 (m, 1H), 4.37 (m, 2H), 3.95 (m, 3H), 1.94 ppm (m, 2H).

2-(2-Mesyloxyethyl)-7-cyano-1,4-benzodioxane

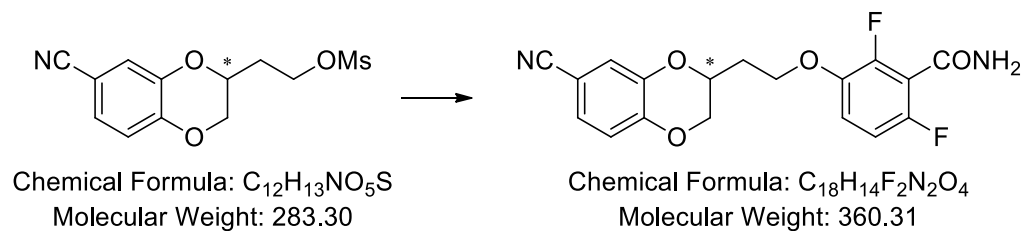


2-(2-Hydroxyethyl)-7-cyano-1,4-benzodioxane (0.95 g, 4.63 mmol) was dissolved in DCM (10 mL) and TEA (0.97 mL, 6.94 mmol), then added of Mesyl chloride (0.54 mL, 6.94 mmol), dropwise, at 0°C. The reaction mixture was stirred at room temperature for 3.5 h, until reaction completion. Then diluted with DCM (15 mL), washed firstly with 10% aqueous $NaHCO_3$ (5 mL), secondly with 10% aqueous HCl (5 mL) and finally with 10% aqueous NaCl (10 mL), filtered, and concentrated under vacuum to give 1.18 g of 2-(2-Mesyloxyethyl)-7-cyano-1,4-benzodioxane as yellowish oil.

Yield = 90.0%

1H NMR ($CDCl_3$): δ 7.17 (m, 2H), 6.93 (d, $J = 8.9$ Hz, 1H), 4.47 (m, 2H), 4.35 (m, 2H), 3.99 (dd, $J = 11.6, 7.5$ Hz, 1H), 3.05 (s, $J = 1.9$ Hz, 3H), 2.09 ppm (m, 2H).

3-[2-(7-Cyano-1,4-benzodioxan-2-yl)ethoxy]-2,6-difluorobenzamide



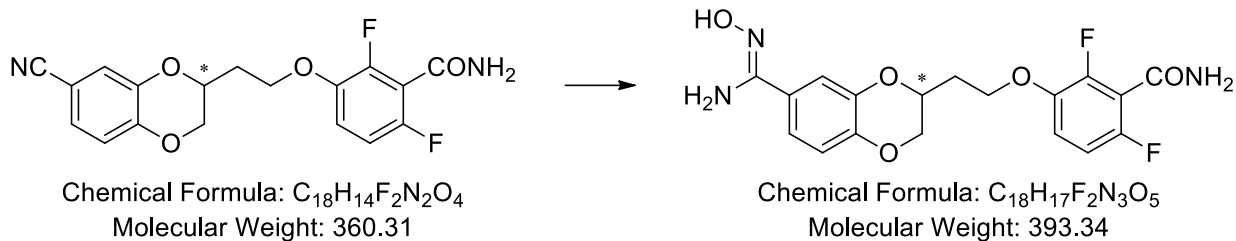
A solution of 3-Hydroxy-2,6-difluorobenzamide (0.76 g, 4.37 mmol) in dry DMF (5 mL) under N_2 atmosphere was amount of potassium carbonate (0.63 g, 4.58 mmol). After stirring at room temperature for 30 min, a solution of 2-Methansulfonyloxyethyl-7-cyano-1,4-benzodioxane (1.18 g, 4.16 mmol) in dry DMF (5 mL) was added. The reaction mixture was stirred at $80^\circ C$ for 4 h, until reaction completion, and then concentrated under vacuum, diluted with Ethyl acetate (15 mL), washed with 10% aqueous NaCl (4×10 mL), dried over Na_2SO_4 , filtered, and concentrated to give a residue which was purified by flash chromatography. Elution with 55/45 Cyclohexane/Ethyl acetate on silica gel gave 1.02 g of 3-[2-(7-Cyano-1,4-benzodioxan-2-yl)ethoxy]-2,6-difluorobenzamide as a white solid.

Yield = 68.0%

M.p. = $172.1^\circ C$

1H NMR ($CDCl_3$): δ 7.15 (m, 2H), 7.02 (m, 1H), 6.89 (m, 2H), 6.21 (bs, 1H), 6.05 (bs, 1H), 4.45 (m, 2H), 4.25 (m, 2H), 4.05 (m, 1H), 2.16 ppm (m, 2H).

3-[2-(7-*N'*-Hydroxycarbamimidoyl-1,4-benzodioxan-2-yl)ethoxy]-2,6-difluorobenzamide

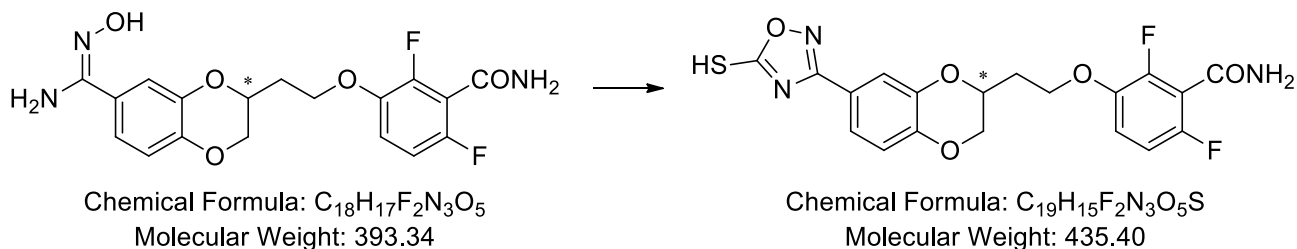


A solution of 3-[2-(7-Cyano-1,4-benzodioxan-2-yl)ethoxy]-2,6-difluorobenzamide (1.00 g, 2.77 mmol) and Hydroxylamine hydrochloride (0.96 g, 13.87 mmol) in dry DMF (10 mL) was added of a solution of Potassium carbonate (1.91 g, 13.87 mmol) in water (5 mL). The reaction mixture was stirred at 80°C for 18 h, concentrated under vacuum, diluted with Ethyl acetate (15 mL), washed with 10% aqueous NaCl (4 × 10 mL), dried over Na_2SO_4 , filtered, and concentrated to give a 1.01 g of 3-[2-(7-*N'*-Hydroxycarbamimidoyl-1,4-benzodioxan-2-yl)ethoxy]-2,6-difluorobenzamide as a yellowish oil.

Yield = 95.0%

1H NMR (CD_3OD): δ 7.21 (td, $J = 9.2, 5.2$ Hz, 1H), 7.12 (m, 2H), 6.96 (td, $J = 2.3, 0.7$ Hz, 1H), 6.85 (d, $J = 8.4$ Hz, 1H), 4.39 (m, 2H), 4.27 (m, 2H), 4.00 (dd, $J = 11.8, 7.7$ Hz, 1H), 2.14 ppm (m, 2H).

3-[2-(7-(5-Mercapto-1,2,4-oxadiazol-3-yl)-1,4-benzodioxan-2-yl)ethoxy-2,6-difluorobenzamide

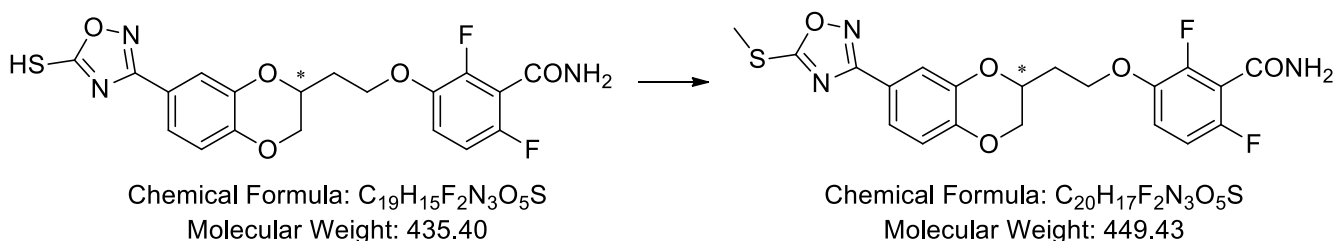


1,10 -Thiocarbonyldiimidazol (0.34 g, 1.91 mmol) was added to a solution of 3-[2-(7-N'-Hydroxycarbonylimidoyl-1,4-benzodioxan-2-yl)ethoxy]-2,6-difluorobenzamide (0.5 g, 1.27 mmol) and DBU (0.76 mL, 5.08 mmol) in Dioxane (10 mL) under N_2 atmosphere. The reaction mixture was stirred at room temperature for 3.5 h, then concentrated under vacuum, diluted with ethyl acetate and 10% aqueous HCl (2×15 mL), washed with 10% aqueous NaCl (3×10 mL), dried over Na_2SO_4 , filtered, and concentrated to give 0.47 g of 3-[2-(7-(5-Mercapto-1,2,4-oxadiazol-3-yl)-1,4-benzodioxan-2-yl)ethoxy]-2,6-difluorobenzamide as a yellow oil.

Yield = 85.0%

1H NMR (CD_3OD): δ 7.35 (m, 2H), 7.22 (m, 1H), 6.96 (m, 1H), 4.45 (m, 2H), 4.29 (m, 2H), 4.06 (dd, $J = 11.9, 7.9$ Hz, 1H), 2.11 ppm (m, 2H).

(XVI) 3-[2-(7-(5-Methylthio-1,2,4-oxadiazol-3-yl)-1,4-benzodioxan-2-yl)ethoxy-2,6-difluorobenzamide



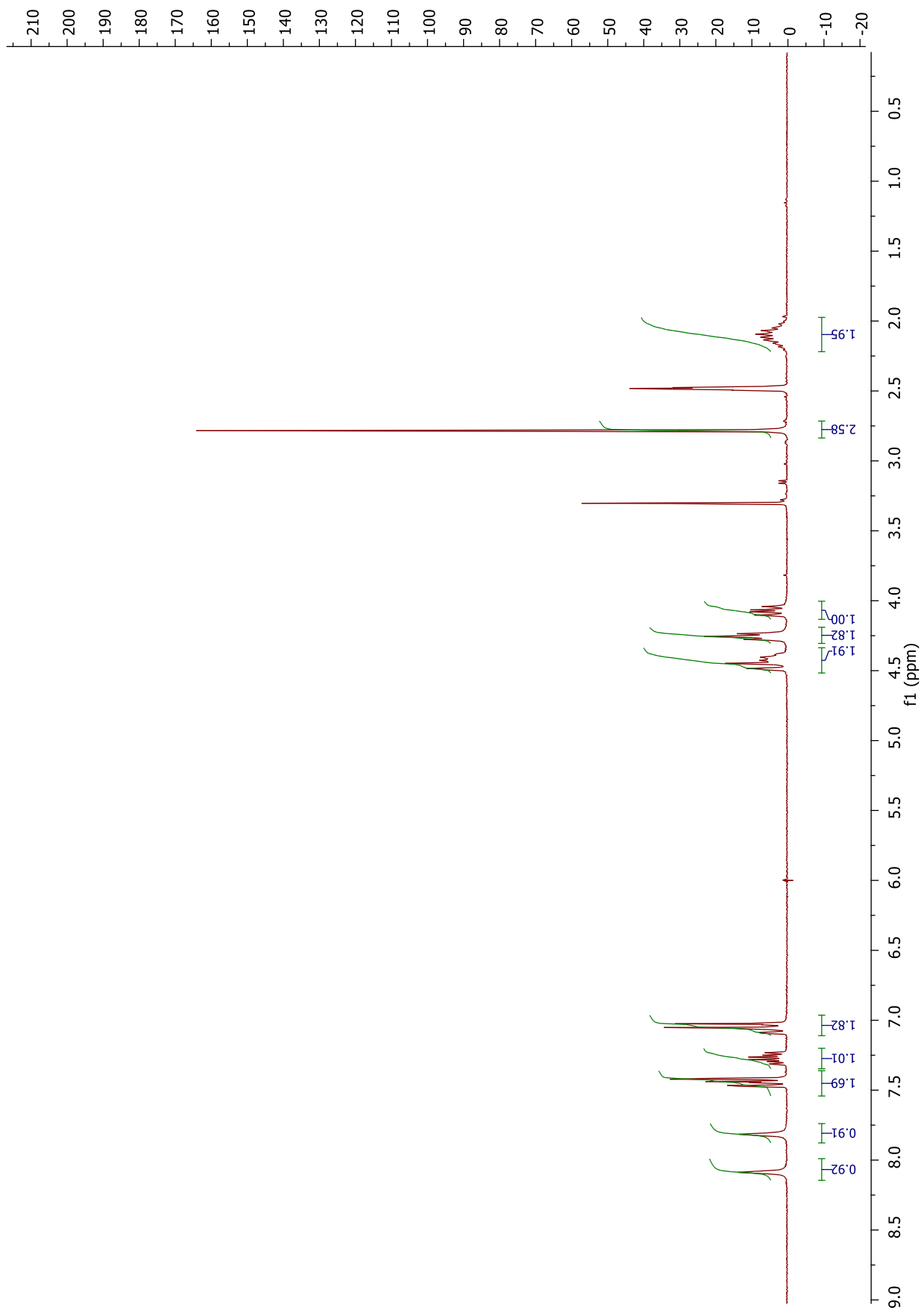
Potassium carbonate (0.17 g, 1.27 mmol) was added to a solution of 3-[2-(7-(5-Mercapto-1,2,4-oxadiazol-3-yl)-1,4-benzodioxan-2-yl)ethoxy-2,6-difluorobenzamide (0.46 g, 1.06 mmol) in ACN/DMF (10 + 2 mL) under N_2 atmosphere. After stirring at room temperature for 30 min, Methyl iodide (0.08 mL, 1.27 mmol) was added dropwise. The reaction mixture was stirred at 50°C for 1.5 h, then concentrated under vacuum, diluted with ethyl acetate and 10% aqueous NaCl (2 × 15 mL), washed with 10% aqueous $NaHCO_3$ and 10% aqueous NaCl (2 × 10 mL), dried over Na_2SO_4 , filtered, and concentrated to give a residue. Digestion with Methanol (20 vol.) gave 0.18 g of 3-[2-(7-(5-Methylthio-1,2,4-oxadiazol-3-yl)-1,4-benzodioxan-2-yl)ethoxy-2,6-difluorobenzamide as a yellowish solid.

Yield = 38.0%

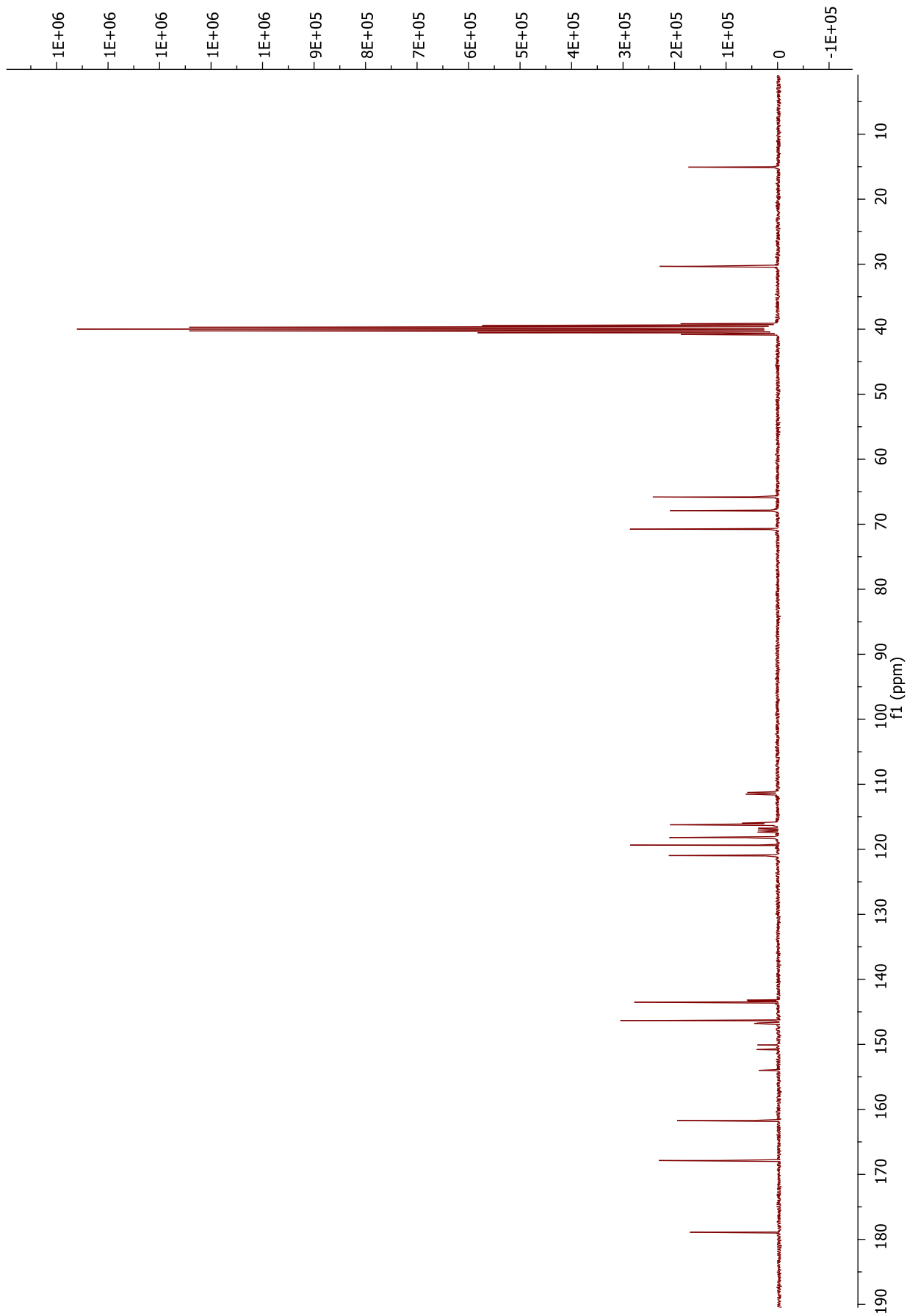
Tr (HPLC, gradient, 90% H_2O with 0.10% TFA to 10% acetonitrile with 0.10% TFA in 25 min with 35 min run time. Flow rate: 1 mL/min) = 15.0 min, Purity = 95.0%

1H NMR (d_6 -DMSO): δ 8.08 (s, 1H), 7.80 (s, 1H), 7.44 (m, 2H), 7.27 (td, $J = 9.3, 5.3$ Hz, 1H), 7.06 (m, 2H), 4.45 (m, 2H), 4.26 (m, 2H), 4.07 (dd, $J = 11.4, 7.2$ Hz, 1H), 2.78 (s, 3H), 2.11 ppm (m, 2H).

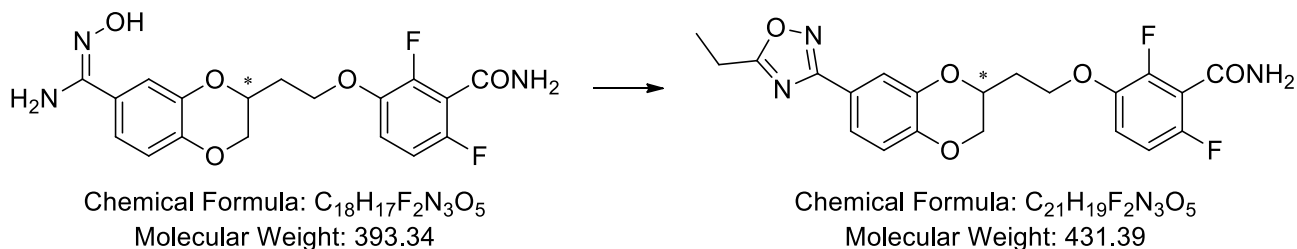
^{13}C NMR (d_6 -DMSO): δ 178.90, 167.87, 161.72, 152.40 (dd, $J = 240.0, 6.8$ Hz), 148.40 (dd, $J = 247.1, 8.6$ Hz), 146.34, 143.52, 143.30 (dd, $J = 10.5, 3.0$ Hz), 120.97, 119.35, 118.19, 117.10 (dd, $J = 24.7, 20.2$ Hz), 116.23, 116.10 (dd, $J = 9.7, 1.5$ Hz), 111.40 (dd, $J = 22.5, 3.8$ Hz) 70.75, 67.90, 65.81, 30.33, 15.08 ppm.



Experimental



(XVII) 3-[2-(7-(5-Ethyl-1,2,4-oxadiazol-3-yl)-1,4-benzodioxan-2-yl)ethoxy]-2,6-difluorobenzamide (VII)



Propionic anhydride (0.10 mL, 0.76 mmol) was added to a solution of 3-[2-(7-*N'*-Hydroxycarbamimidoyl-1,4-benzodioxan-2-yl)ethoxy]-2,6-difluorobenzamide (0.25 g, 0.63 mmol) and Pyridine (0.07 g, 0.95 mmol) in dry DMF and $CHCl_3$ (10 mL + 2 mL). After stirring at reflux for 2 h, 2.5 N aqueous NaOH (1 mL) was added and the reaction was stirred for 18 h. The reaction mixture was then concentrated under vacuum, diluted with Ethyl acetate (15 mL), washed with 10% aqueous NaCl (4 × 10 mL), dried over Na_2SO_4 , filtered, and concentrated to give a residue which was purified by flash Chromatography. Elution with 1/1 Cyclohexane/Ethyl acetate on silica gel and subsequent digestion with Methanol (20 vol.) gave 0.02 g of 3-[2-(7-(5-Ethyl-1,2,4-oxadiazol-3-yl))-1,4-benzodioxan-2-yl]ethoxy-2,6-difluorobenzamide as a white solid.

Yield = 7.0%

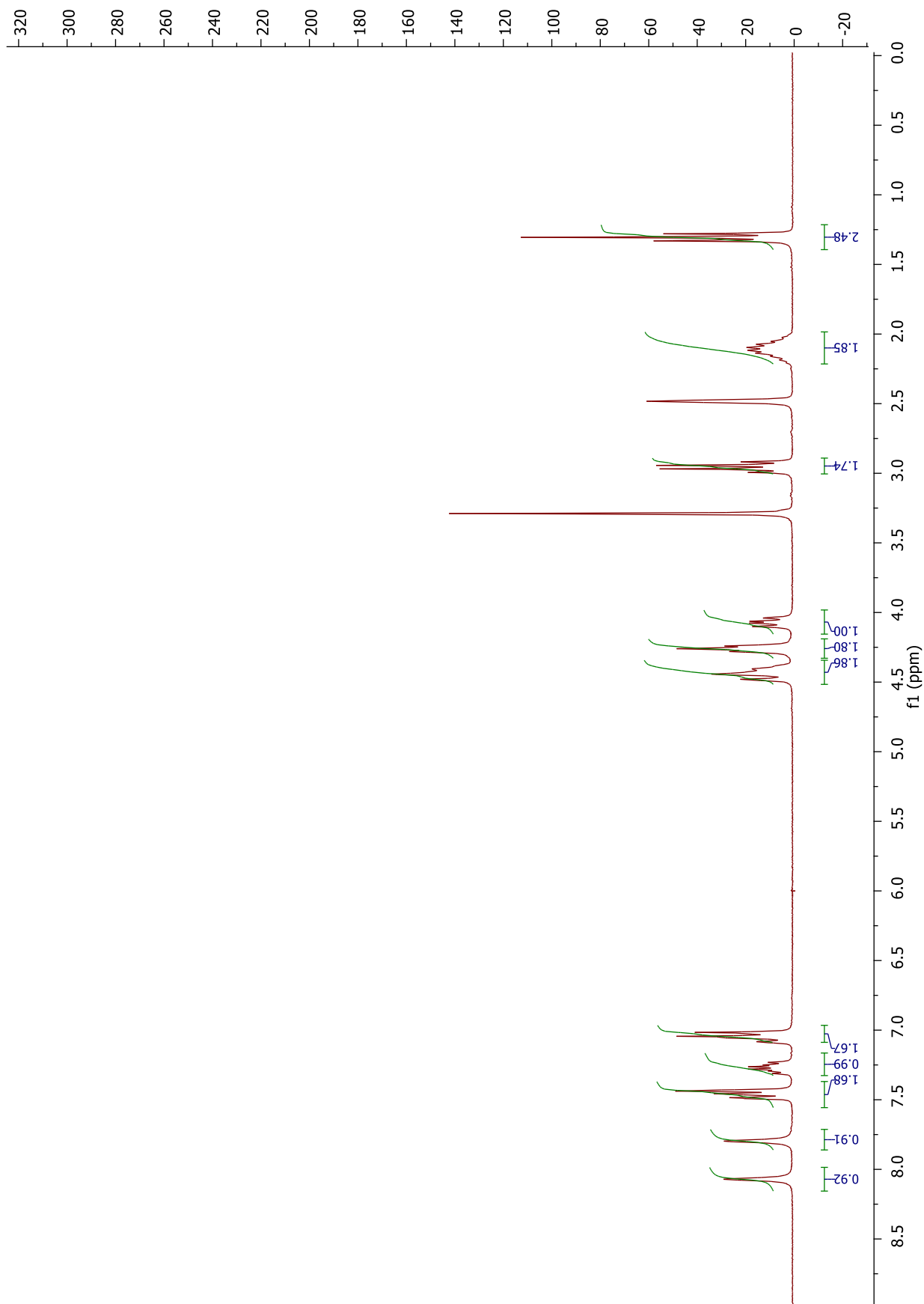
M.p. = 151.1°C

Tr (HPLC, gradient, 90% H_2O with 0.10% TFA to 10% acetonitrile with 0.10% TFA in 25 min with 35 min run time. Flow rate: 1 mL/min) = 9.9 min, Purity = 99.4%

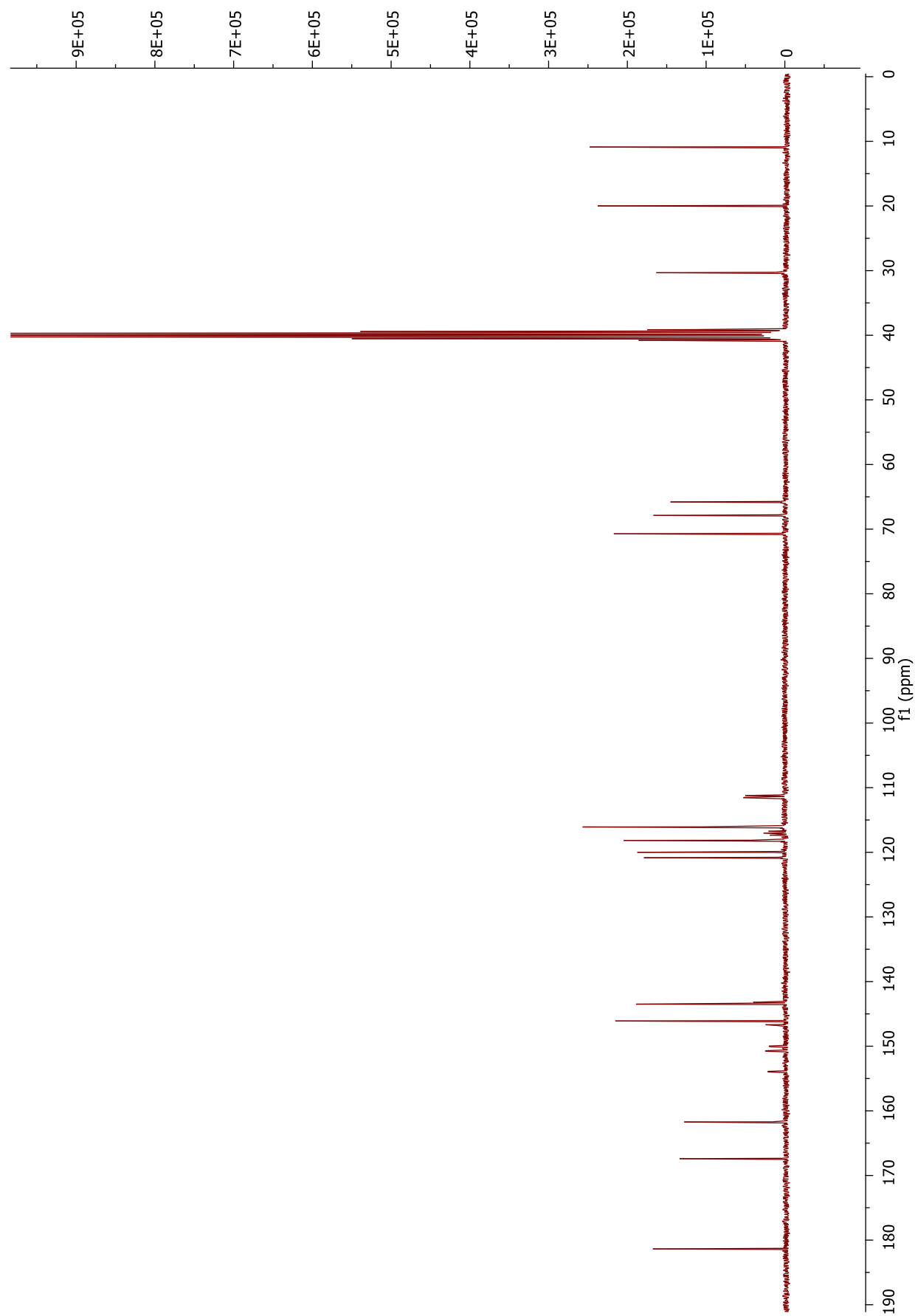
1H NMR (d_6 -DMSO): δ 8.09 (s, 1H), 7.82 (s, 1H), 7.46 (m, 2H), 7.28 (td, J = 9.3, 5.3 Hz, 1H), 7.06 (td, J = 9.1, 1.9 Hz, 1H), 7.03 (d, J = 8.4 Hz, 1H), 4.44 (m, 2H), 4.27 (m, 2H), 4.07 (dd, J = 11.4, 7.1 Hz, 1H), 2.96 (q, J = 7.6 Hz, 2H), 2.11 (m, 2H), 1.30 ppm (t, J = 7.6 Hz, 3H).

^{13}C NMR (d_6 -DMSO): δ 181.37, 167.40, 161.72, 152.30 (dd, J = 239.6, 7.1 Hz), 148.40 (dd, J = 246.8, 8.2 Hz), 146.10, 143.49, 143.30 (dd, J = 10.5, 3.0 Hz), 129.73, 120.84, 120.00, 118.16, 117.10 (dd, J = 24.7, 20.2 Hz), 116.08, 116.00, 111.40 (dd, J = 22.5, 3.8 Hz) 70.73, 67.88, 65.80, 30.32, 19.98, 10.88 ppm.

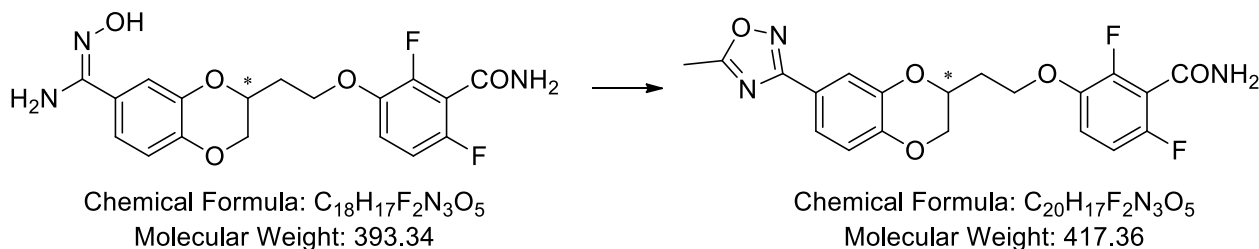
Experimental



Experimental



(XVIII) 3-[2-(7-(5-Methyl-1,2,4-oxadiazol-3-yl)-1,4-benzodioxan-2-yl)ethoxy]-2,6-difluorobenzamide



Acetic anhydride (0.07 mL, 0.76 mmol) was added to a solution of 3-[2-(7-*N'*-Hydroxycarbamimidoyl-1,4-benzodioxan-2-yl)ethoxy]-2,6-difluorobenzamide (0.25 g, 0.63 mmol) and Pyridine (0.07 g, 0.95 mmol) in dry DMF and $CHCl_3$ (10 mL + 2 mL). After stirring at reflux for 2 h, 2.5 N aqueous NaOH (1 mL) was added and the reaction was stirred for 18 h. The reaction mixture was then concentrated under vacuum, diluted with Ethyl acetate (15 mL), washed with 10% aqueous NaCl (4 × 10 mL), dried over Na_2SO_4 , filtered, and concentrated to give a residue. Digestion with Methanol (20 vol.) gave 0.09 g of 3-[2-(7-(5-Methyl-1,2,4-oxadiazol-3-yl)-1,4-benzodioxan-2-yl)ethoxy]-2,6-difluorobenzamide as a white solid.

Yield = 34.0%

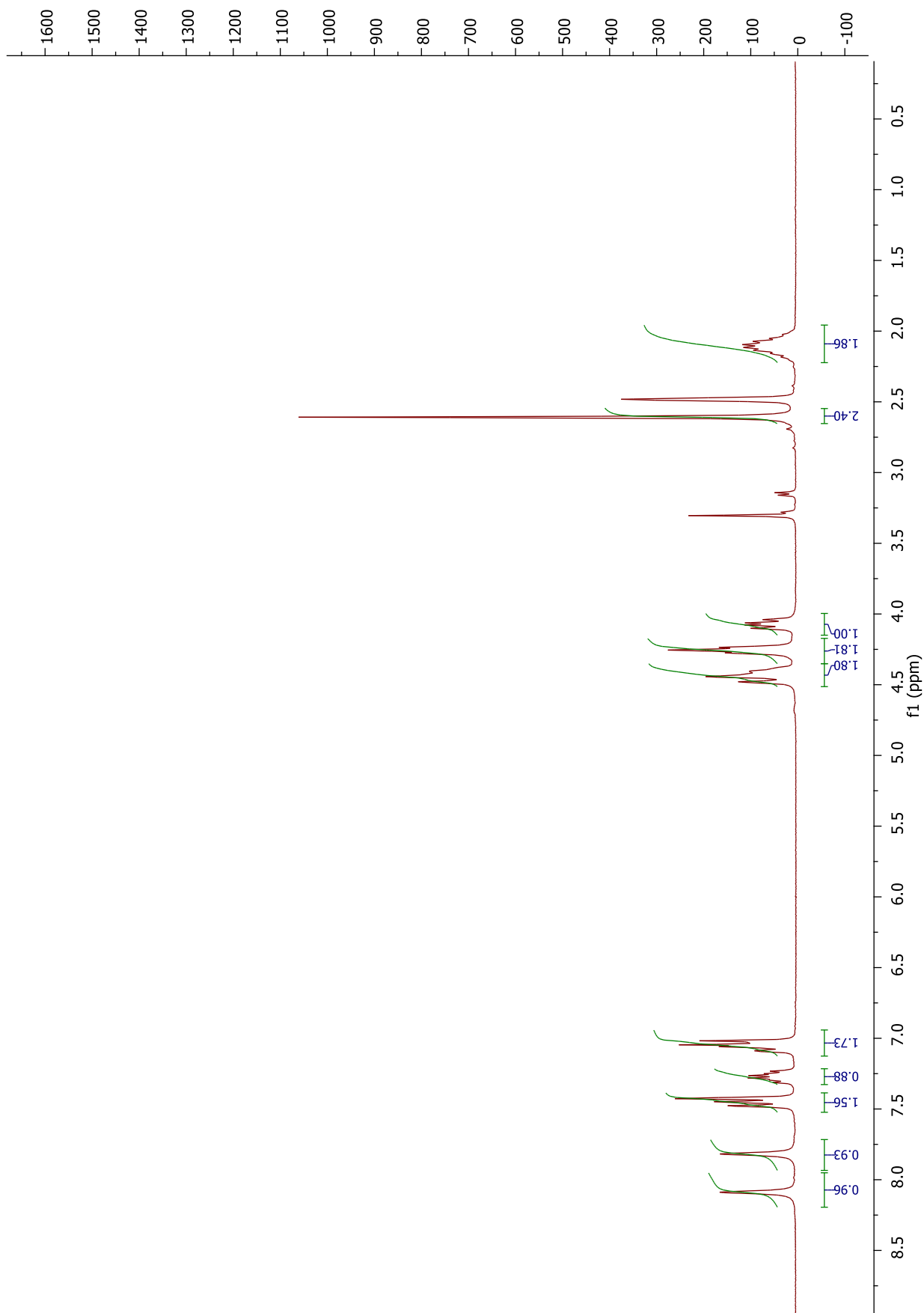
M.p. = 164.4°C

Tr (HPLC, gradient, 90% H_2O with 0.10% TFA to 10% acetonitrile with 0.10% TFA in 25 min with 35 min run time. Flow rate: 1 mL/min) = 12.9 min, Purity = 95.5%

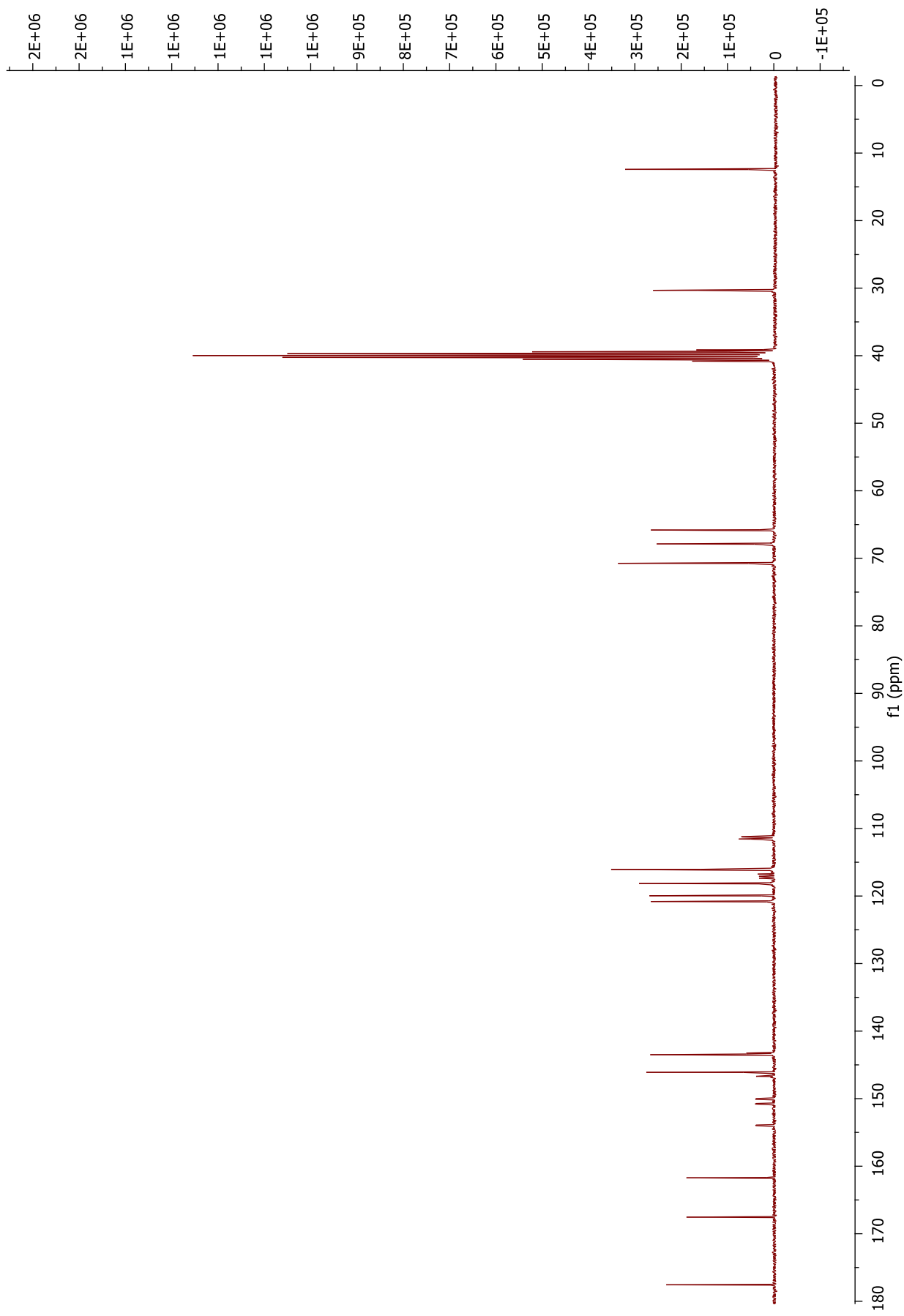
1H NMR (d_6 -DMSO): δ 8.09 (s, 1H), 7.82 (s, 1H), 7.45 (m, 2H), 7.27 (td, $J = 9.3, 5.3$ Hz, 1H), 7.05 (m, 2H), 4.43 (m, 2H), 4.26 (m, 2H), 4.07 (dd, $J = 11.4, 7.1$ Hz, 1H), 2.61 (s, 3H), 2.09 ppm (m, 2H).

^{13}C NMR (d_6 -DMSO): δ 176.56, 167.54, 161.73, 152.40 (dd, $J = 240.0, 6.8$ Hz), 148.40 (dd, $J = 247.1, 8.6$ Hz), 146.1, 143.5, 143.30 (dd, $J = 10.9, 3.4$ Hz), 120.81, 119.96, 118.15, 117.10 (dd, $J = 24.7, 20.2$ Hz), 116.70, 116.07, 111.40 (dd, $J = 22.5, 3.8$ Hz) 70.74, 67.87, 65.81, 20.32, 12.41 ppm.

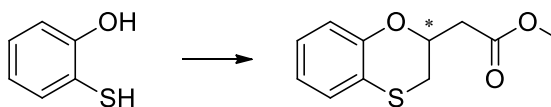
Experimental



Experimental



Methyl (1,4-benzoxathian-2-yl)-acetate



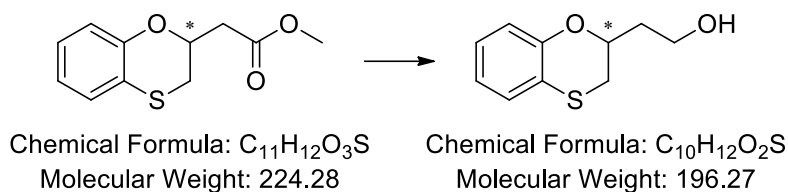
Chemical Formula: C_6H_6OS Chemical Formula: $C_{11}H_{12}O_3S$
 Molecular Weight: 126.18 Molecular Weight: 224.28

Methyl 3,4-dibromobutirrate (1.50 g, 5.77 mmol) was added dropwise to a solution of 1,2-Mercaptophenol (0.73 g, 5.77 mmol) and TEA (1.16 mL, 11.54 mmol) in acetonitrile/water 1:1 (15 mL) and stirred at room temperature for 18 h. The reaction mixture is then added with Ethyl acetate (15 mL), washed firstly with 10% aqueous NaOH (15 mL) and lastly with brine (15 mL). The organic phase is then dried over Na_2SO_4 , filtered and concentrated under vacuum, affording 1.01 g of Methyl (1,4-benzoxathian-2-yl)-acetate as a yellowish oil.

Yield = 78.0%

1H NMR ($CDCl_3$): δ 7.04 (m, 2H), 6.84 (m, 2H), 4.70 (m, 1H), 3.74 (s, 3H), 3.14 (dd, $J = 13.0, 2.3$ Hz, 1H), 3.04 (dd, $J = 13.0, 7.6$ Hz, 1H), 2.87 (dd, $J = 15.8, 6.7$ Hz, 1H), 2.74 ppm (dd, $J = 15.8, 6.5$ Hz, 1H).

2-(1,4- Benzoxathian-2-yl)-ethanol

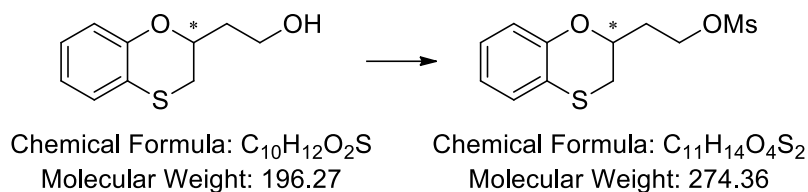


$LiAlH_4$ (0.030 g, 1.78 mmol) was suspended in dry THF (2 mL) at $0^\circ C$ under nitrogen atmosphere. The solution of Methyl (1,4-benzoxathian-2-yl)-acetate (0.18 g, 0.71 mmol) in THF (5 mL) was slowly added to the reaction. The mixture was then warmed to RT and stirred for 1 h; at completion, it was cooled to $0^\circ C$ and slowly quenched with Ethyl acetate (5 mL). Further Ethyl acetate (10 mL) was added, the organic layer was washed with brine (3×10 mL), dried over Na_2SO_4 and concentrated under vacuum to give 0.13 g of 2-(1,4-Benzoxathian-2-yl)-ethanol as an orange oil.

Yield = 92.0%

1H NMR ($CDCl_3$): δ 7.00 (m, 2H), 6.83 (m, 2H), 4.44 (m, 1H), 3.90 (m, 2H), 3.03 (m, 2H), 2.01 (m, 2H), 1.78 ppm (bs, 1H).

2-(1,4- Benzoxathian-2-yl)-ethyl methanesulfonate

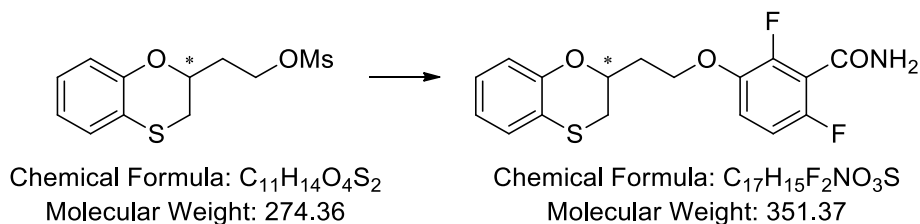


Mesyl chloride (0.24 mL, 3.12 mmol) was added dropwise to a solution of 2-(1,4-Benzoxathian-2-yl)-ethanol (0.51 g, 2.59 mmol) and TEA (0.44 mL, 3.12 mmol) in DCM (5 mL) at 0°C. The mixture was stirred at that temperature for 3 h, diluted with DCM (20 mL), washed firstly with 10% aqueous $NaHCO_3$ (10 mL), secondly with 10% aqueous HCl (10 mL) and finally with brine (10 mL), dried over Na_2SO_4 , filtered and concentrated under vacuum to yield 0.71 g of 2-(1,4- Benzoxathian-2-yl)-ethyl methanesulfonate as a yellowish oil.

Yield = Quantitative

1H NMR ($CDCl_3$): δ 7.02 (m, 2H), 6.85 (m, 2H), 4.48 (m, 3H), 3.04 (m, 2H), 3.03 (s, 3H), 2.18 ppm (m, 2H).

(XIX) 3-(1,4-Benzoxathian-2-yl)ethoxy)-2,6-difluorobenzamide



Potassium carbonate (0.40 g, 2.86 mmol) was added to a solution of 2,6-Difluoro-3-hydroxybenzamide (0.49 g, 2.73 mmol) in dry DMF (5 mL). After stirring at room temperature for 30 min, a solution of 2-(1,4-Benzoxathian-2-yl)-ethyl methanesulfonate (0.70 g, 2.55 mmol) in DMF (5 mL) was added. The reaction mixture was stirred at 60°C for 16 h, concentrated under vacuum, diluted with Ethyl acetate (30 mL), washed with brine (3 × 20 mL), dried over Na_2SO_4 , filtered and concentrated, to give a residue, which was purified by flash chromatography on silica gel. Elution with 1/1 Cyclohexane/Ethyl acetate on silica gel and further crystallization from IPA gave 0.36 g of 3-(1,4-Benzoxathian-2-yl)ethoxy)-2,6-difluorobenzamide as a white solid.

Yield = 39.0%

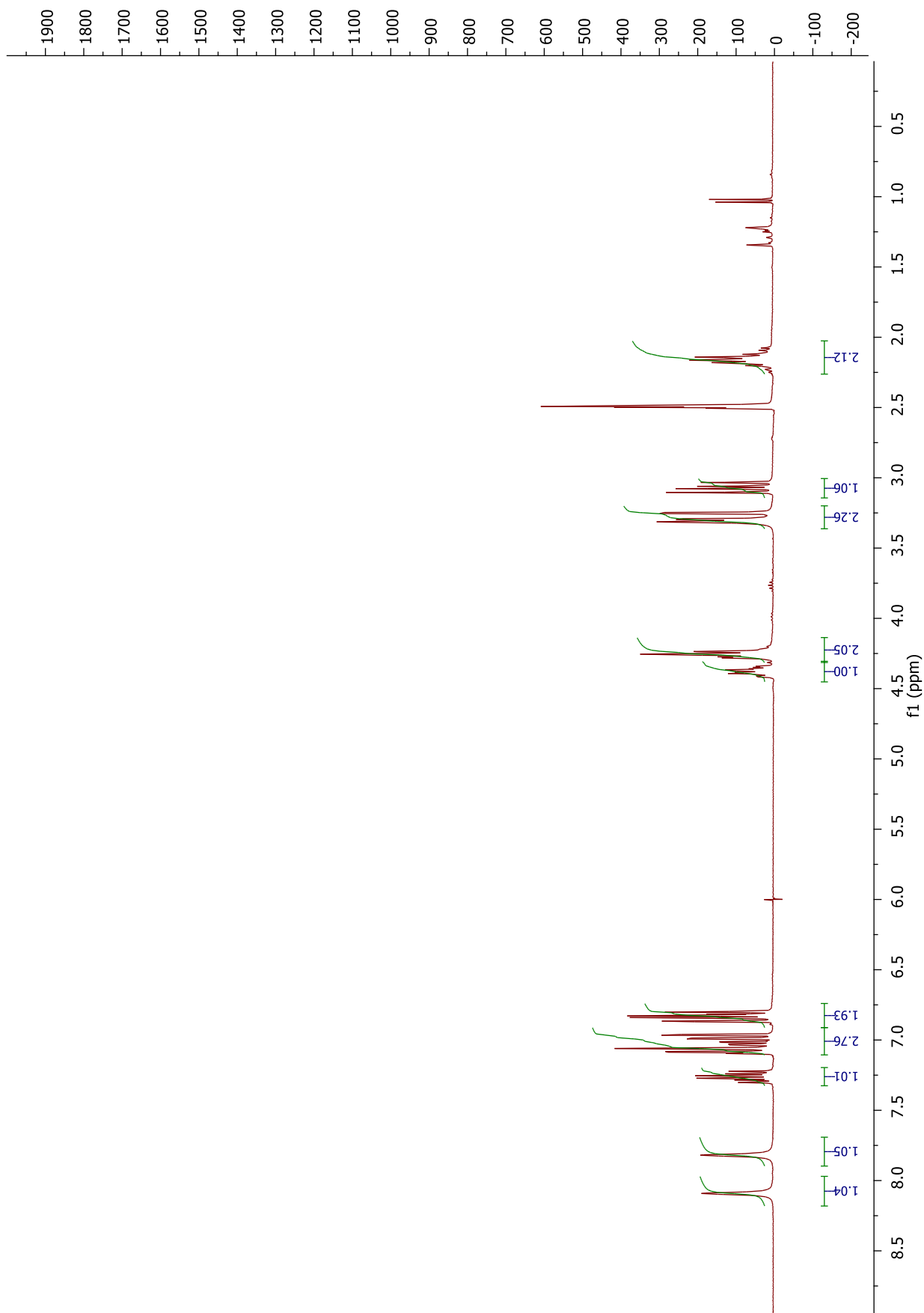
M.p. = 109.7°C

Tr (HPLC, gradient, 90% H_2O with 0.10% TFA to 10% acetonitrile with 0.10% TFA in 25 min with 35 min run time. Flow rate: 1 mL/min) = 14.1 min, Purity = 99.4%

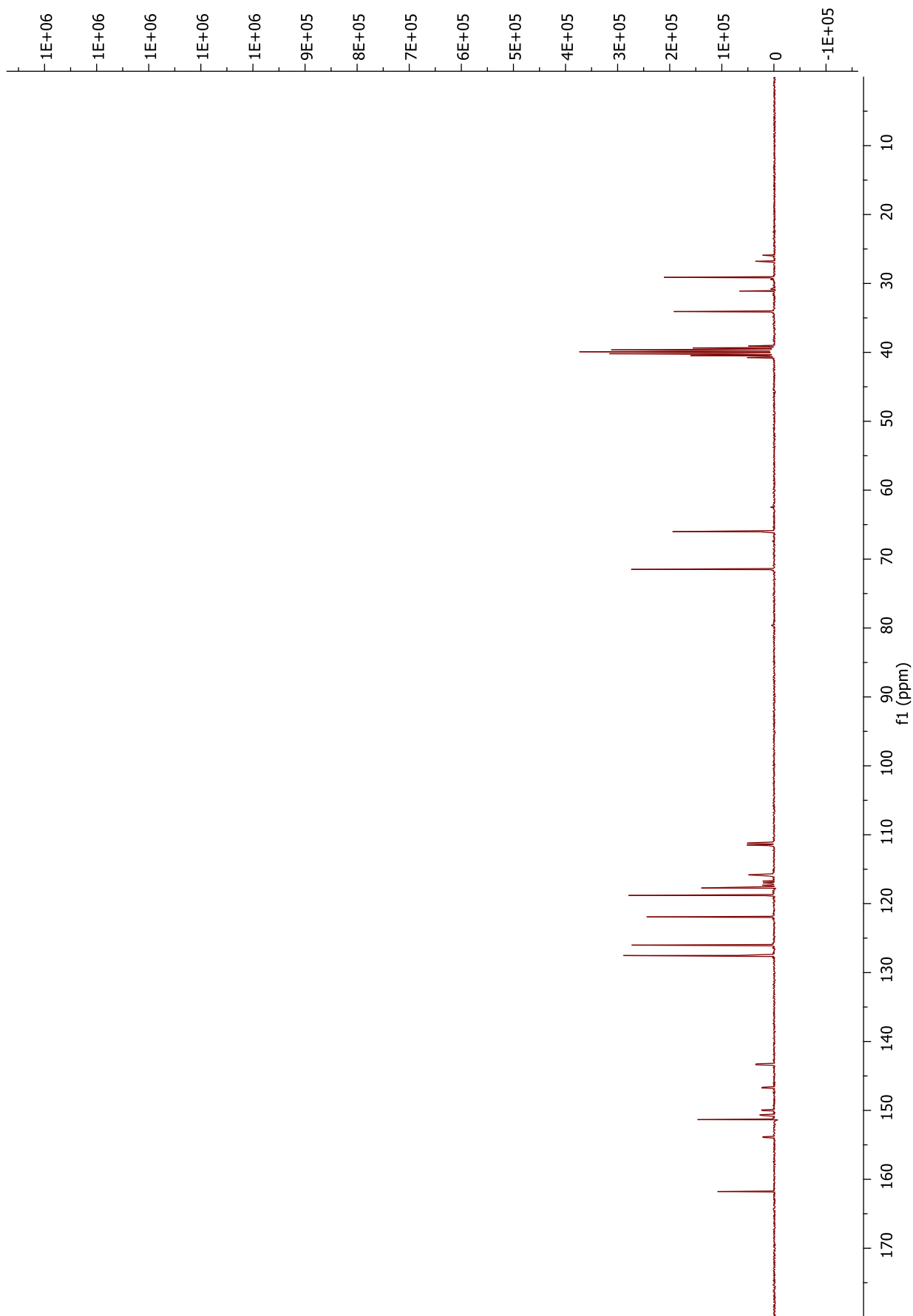
1H NMR (d_6 -DMSO): δ 8.09 (bs, 1H), 7.82 (bs, 1H), 7.26 (dt, J = 9.3, 5.3 Hz, 1H), 7.02 (m, 3H), 6.81 (m, 2H), 4.38 (tdd, J = 8.1, 5.2, 2.1 Hz, 1H), 4.24 (m, 2H), 3.27 (dd, J = 13.2, 2.1 Hz, 1H), 3.07 (dd, J = 13.2, 8.1 Hz, 1H), 2.16 ppm (m, 2H).

^{13}C NMR (d_6 -DMSO): δ 161.8, 152.3 (dd, J = 241.2, 6.8 Hz), 151.3, 148.3 (dd, J = 248.4, 8.4 Hz), 143.3 (dd, J = 10.9, 3.3 Hz), 127.5, 126.0, 121.9, 118.8, 117.7, 117.0 (dd, J = 24.9, 20.5 Hz), 115.9 (dd, J = 9.4, 2.5 Hz), 111.4 (dd, J = 22.9, 4.0 Hz), 71.5, 66.0, 34.1, 29.1 ppm.

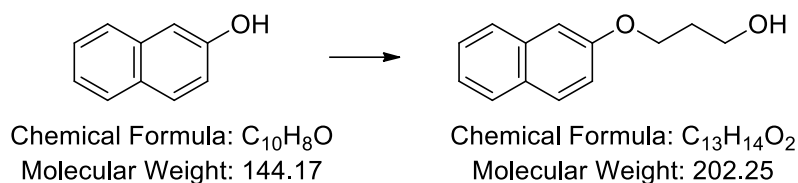
Experimental



Experimental



3-(Naphthalen-2-yloxy)-1-propanol



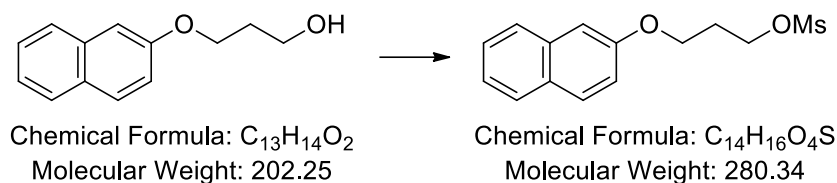
Potassium carbonate (5.75 g, 41.62 mmol) was added to a solution of 2-Naphthol (3.00 g, 20.81 mmol), and Potassium iodide (0.34 g, 2.08 mmol) in dry DMF (30 mL). After stirring at room temperature for 30 minutes, 3-Chloro-1-propanol (1.91 mL, 22.89 mmol) was added dropwise. The reaction mixture was stirred at 70°C for 24 hours, concentrated under vacuum, diluted with Ethyl acetate (50 mL), washed with 10% aqueous NaOH and 10% aqueous NaCl (2 x 20 mL), dried over Na₂SO₄, filtered and concentrated to give 4.21 g of 3-(Naphthalen-2-yloxy)-1-propanol as a white solid

Yield = Quantitative

M.p. = 99.0 °C (lit.)

¹H NMR (CDCl₃): δ 7.74 (m, 3H), 7.44 (t, J = 7.5 Hz, 1H), 7.33 (t, J = 8.0 Hz, 1H), 7.14 (m, 2H), 4.26 (t, J = 6.0 Hz, 1H), 3.92 (t, J = 6.0 Hz, 1H), 2.12 ppm (p, J = 6.0 Hz, 1H).

3-(Naphthalen-2-yloxy)propyl methansulfonate

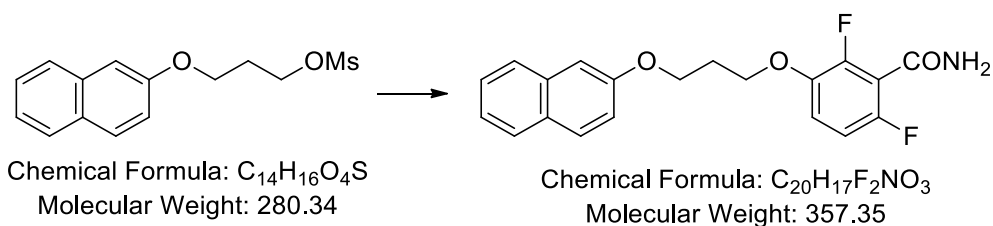


Mesyl chloride (2.1 mL, 27.07 mmol) was added dropwise to a solution of 3-(Naphthalen-2-yloxy)-1-propanol (4.21 g, 20.82 mmol) and TEA (3.77 mL, 27.07 mmol) in DCM (40 mL) at 0°C. The reaction mixture was stirred at room temperature for 1,5 hours, diluted with DCM (15 mL), washed firstly with 10% aqueous $NaHCO_3$ (5 mL), secondly with 10% aqueous HCl (5 mL) and finally with 10% aqueous NaCl (10 mL), filtered and concentrated under vacuum to give 5.84 g of 3-(Naphthalen-2-yloxy)propyl methansulfonate as a yellowish oil.

Yield = Quantitative

1H NMR ($CDCl_3$): δ 7.75 (m, 3H), 7.45 (t, $J = 7.5$ Hz, 1H), 7.35 (m, 1H), 7.13 (m, 2H), 4.50 (t, $J = 6.0$ Hz, 2H), 4.22 (t, $J = 6.0$ Hz, 2H), 2.99 (s, 3H), 2.30 ppm (p, $J = 6.0$ Hz, 2H).

(XX) 3-(3-(Naphthalen-2-yloxy)propoxy)-2,6-difluorobenzamide



Potassium carbonate (0.25 g, 1.81 mmol) was added to a solution of 2,6-Difluoro-3-hydroxybenzamide (0.30 g, 1.73 mmol) in dry DMF (5 mL) under N_2 atmosphere. After stirring at room temperature for 30 minutes, a solution of 3-(Naphthalen-2-yloxy)propyl methanesulfonate (0.46 g, 1.65 mmol) in dry DMF (5 mL) was added. The reaction mixture was stirred at $80^\circ C$ for 1 hour, concentrated under vacuum, diluted with Ethyl acetate (15 mL), washed with 10% aqueous NaCl (4 x 10 mL), dried over Na_2SO_4 , filtered and concentrated to give a residue which was purified by flash chromatography. Elution with 6/4 Cyclohexane/Ethyl acetate on silica gel and subsequent crystallization with chloroform (5 vol) gave 0.20 g of 3-(3-(Naphthalen-2-yloxy)propoxy)-2,6-difluorobenzamide as a white solid.

Yield = 33.8%

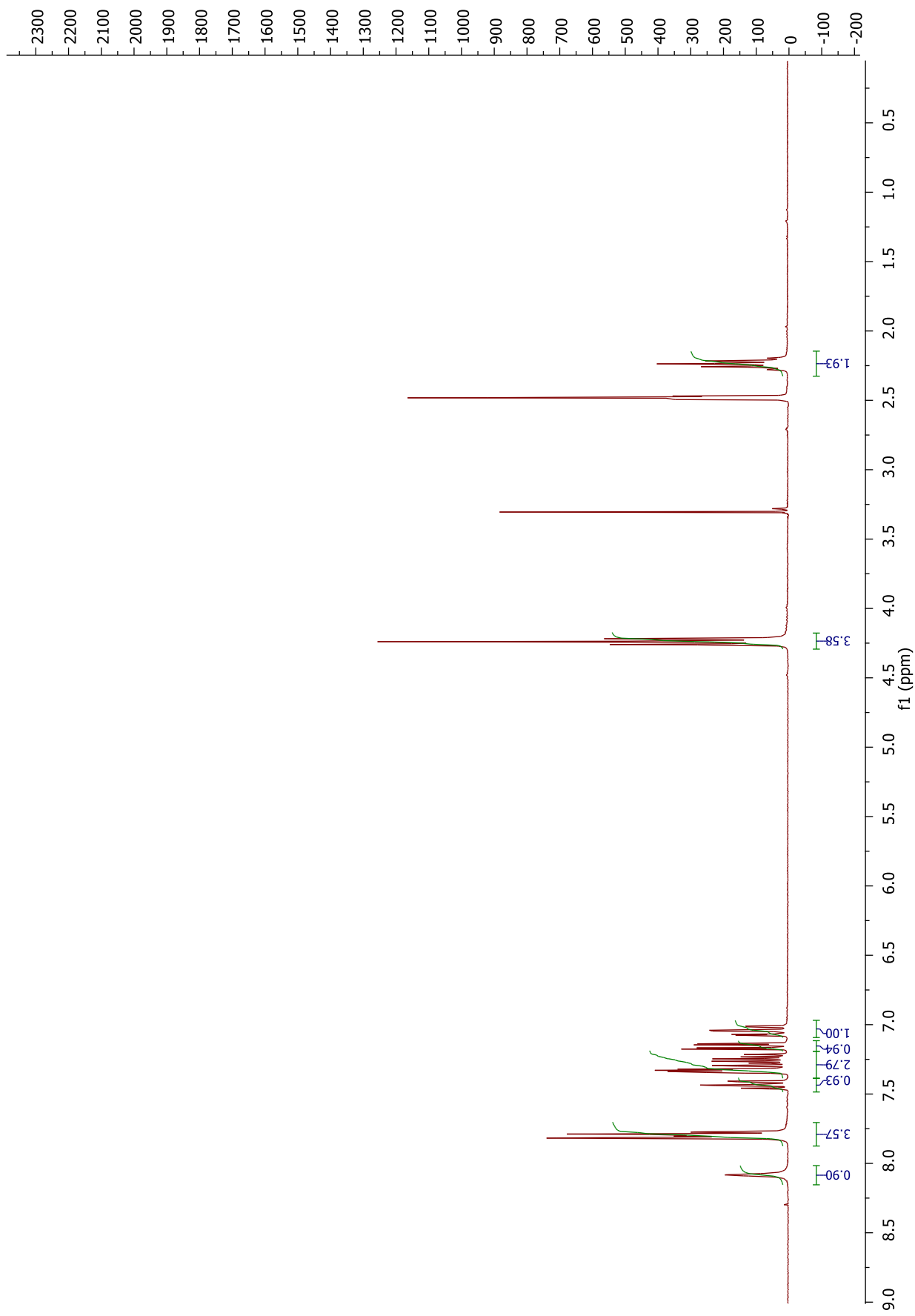
M.p. = $120.9^\circ C$

Tr (HPLC, gradient, 90% H_2O with 0.10% TFA to 10% acetonitrile with 0.10% TFA in 25 min with 35 min run time. Flow rate: 1 mL/min) = 14.8 min, Purity = 96.4%

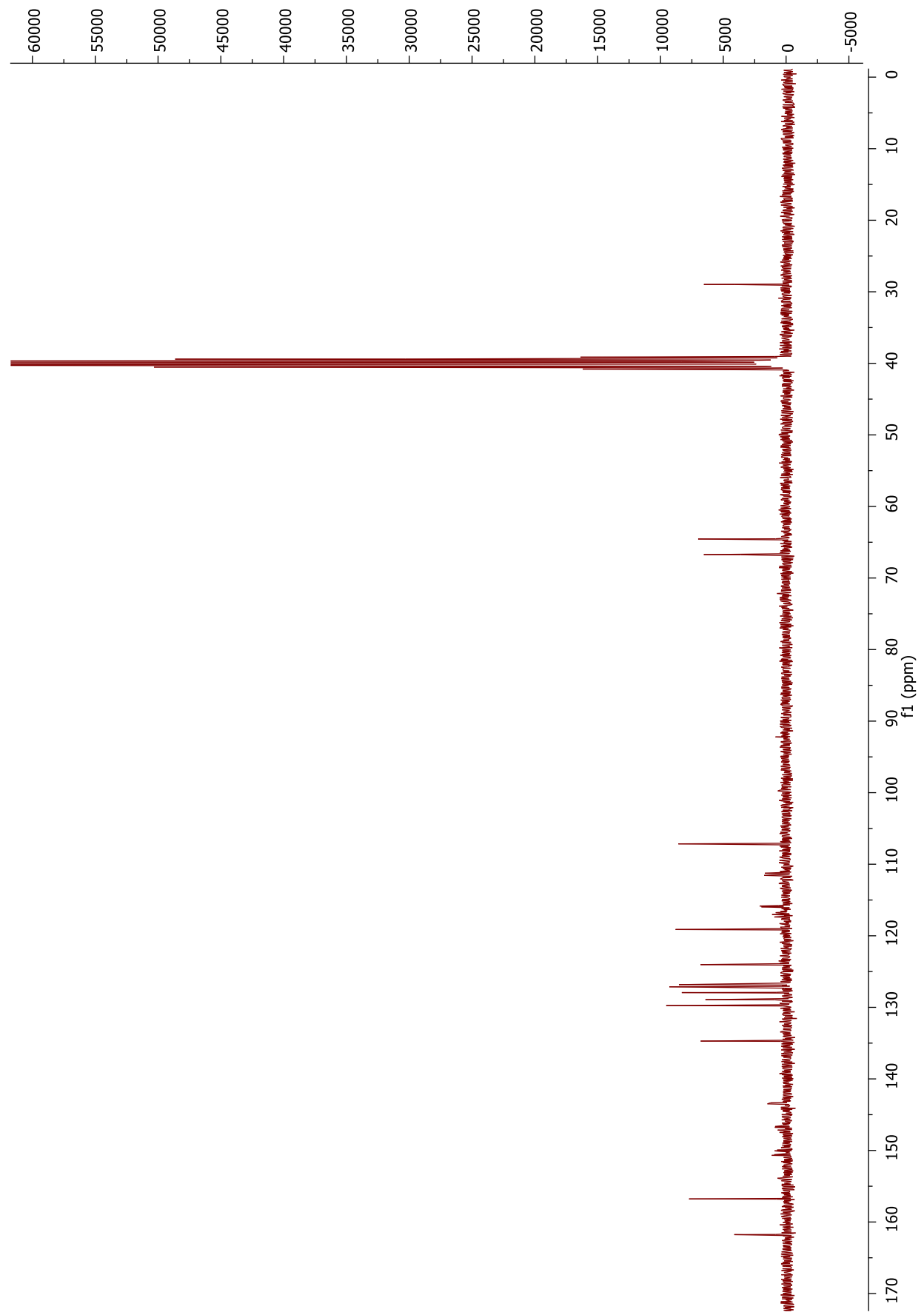
1H NMR (d_6 -DMSO): δ 8.08 (s, 1H), 7.80 (m, 4H), 7.43 (m, 1H), 7.31 (m, 2H), 7.24 (dd, J = 9.4, 5.3 Hz, 1H), 7.16 (dd, J = 9.0, 2.5 Hz, 1H), 7.04 (td, J = 9.0, 1.9 Hz, 1H), 4.24 (t, J = 6.2 Hz, 4H), 2.24 ppm (p, J = 6.2 Hz, 2H).

^{13}C NMR (d_6 -DMSO): δ 161.76, 156.78, 152.20 (dd, J = 239.3, 6.8 Hz), 148.39 (dd, J = 246.7, 8.3 Hz), 143.40 (dd, J = 11.3, 3.0 Hz), 134.72, 129.76, 128.93, 127.93, 127.13, 126.83, 124.03, 119.12, 117.10 (dd, J = 25.1, 20.6 Hz), 115.90 (dd, J = 9.0, 2.2 Hz), 111.40 (dd, J = 22.9, 4.1 Hz) 107.15, 66.74, 65.55, 28.98 ppm.

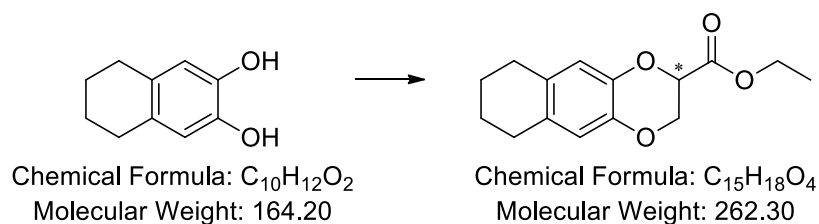
Experimental



Experimental



Ethyl (5,6,7,8-tetrahydro-1,4-naphthodioxane-2-yl)-carboxylate

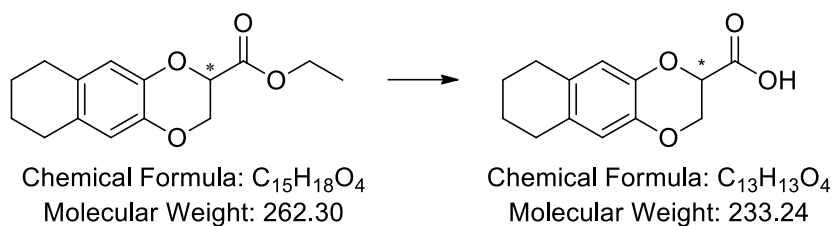


A suspension of 5,6,7,8-Tetrahydronaphthalen-2,3-diol (9.92 g, 60.41 mmol) and K_2CO_3 (20.04 g, 114.98 mmol) in DMF (100 mL) was stirred at room temperature for 30 minutes. Ethyl 2,3-dibromopropionate (17.27 g, 66.45 mmol) was added dropwise and the reaction mixture was stirred at 70°C for 1.5 hours, concentrated under vacuum, diluted with Ethyl acetate (100 mL), washed with 10% aqueous NaCl (5 x 25 mL), dried with Na_2SO_4 , filtered and concentrated under vacuum to give 11.71 g of Ethyl (5,6,7,8-tetrahydro-1,4-naphthodioxane-2-yl)-carboxylate as a yellowish oil.

Yield = 74.0%

1H NMR ($CDCl_3$): δ 6.70 (s, 1H), 6.56 (s, 1H), 4.77 (t, $J = 3.8$ Hz, 1H), 4.34 (m, 2H), 4.27 (q, $J = 7.1$ Hz, 2H), 2.67 (m, 4H), 1.75 (m, 4H), 1.29 (t, $J = 7.1$ Hz, 3H).

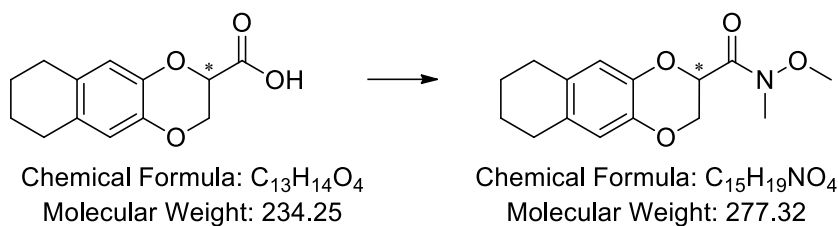
(5,6,7,8-Tetrahydro-1,4-naphthodioxane-2-yl)-carboxylic acid



Aqueous NaOH 2.5 N (55.0 mL) was added to a solution of Ethyl (5,6,7,8-tetrahydro-1,4-naphthodioxane-2-yl)-carboxylate (11.71 g, 44.64 mmol) in MeOH (110 mL) at 0°C. The reaction mixture was stirred at RT for 2 hours, concentrated under vacuum, diluted with Ethyl acetate (100 mL) and 10% aqueous HCl (80 mL). The organic phase was then washed with 10 % aqueous NaCl, dried with Na_2SO_4 , filtered and concentrated under vacuum to give 10.29 g of (5,6,7,8-Tetrahydro-1,4-naphthodioxane-2-yl)-carboxylic acid as a yellowish oil.

Yield = 98.0%

1H NMR ($CDCl_3$): δ 6.70 (s, 1H), 6.59 (s, 1H), 4.85 (dd, $J = 4.4, 3.1$ Hz, 1H), 4.36 (m, 2H), 2.71 (m, 4H), 1.76 (m, 4H).

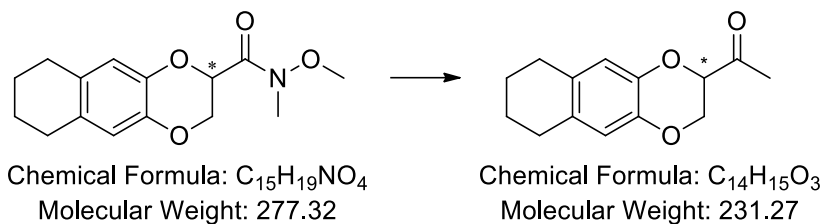
N-Methoxy-*N*-methyl-(5,6,7,8-tetrahydro-1,4-naphthodioxane-2-yl)-carboxamide

CDI (8.07 g, 48.33 mmol) was added to a solution of (5,6,7,8-Tetrahydro-1,4-naphthodioxane-2-yl)-carboxylic acid (10.29 g, 43.93 mmol) in DCM (100 mL) at 0°C. The reaction mixture was stirred at RT for 0.5 hours, added with *N,O*-dimethylhydroxylamine (4.49 g, 46.13 mmol), stirred for 3 hours, washed firstly with 10% aqueous NaHCO₃ (50 mL), secondly with 10% aqueous HCl (50 mL), and finally with 10% aqueous NaCl, dried with Na₂SO₄, filtered and concentrated under vacuum to give 9.36 g of *N*-Methoxy-*N*-methyl-(5,6,7,8-tetrahydro-1,4-naphthodioxane-2-yl)-carboxamide as a brownish oil.

Yield = 77.0%

¹H NMR (CDCl₃): δ 6.68 (s, 1H), 6.58 (s, 1H), 5.00 (m, 1H), 4.37 (dd, J = 11.4, 2.6 Hz, 1H), 4.24 (dd, J = 11.4, 6.7 Hz, 1H), 3.78 (s, 3H), 3.25 (s, 3H), 2.71 (m, 4H), 1.70 (m, 4H).

1-(5,6,7,8-Tetrahydro-1,4-naphthodioxane-2-yl)-ethanone

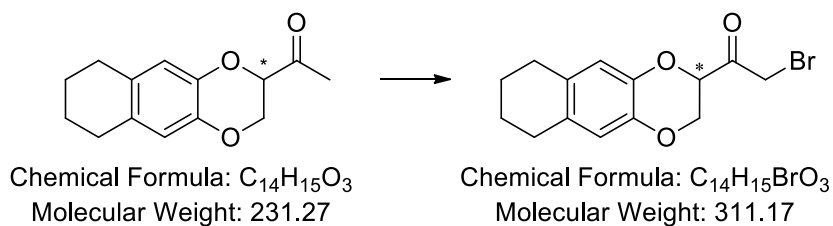


Methyl magnesium bromide (12.29 mL, 36.89 mmol) was added dropwise to a solution of *N*-Methoxy-*N*-methyl-(5,6,7,8-tetrahydro-1,4-naphthodioxane-2-yl)-carboxamide (6.82 g, 24.59 mmol) in dry THF (120 mL) at 0°C under N_2 . The reaction mixture was stirred at room temperature for 1.5 hours and poured into a 1/1 mixture of Ethyl acetate and 10% aqueous HCl (50 + 50 mL). The organic phase was then washed twice with 10% aqueous NaCl, dried over Na_2SO_4 , filtered and concentrated under vacuum to give 5.00 g of 1-(5,6,7,8-Tetrahydro-1,4-naphthodioxane-2-yl)-ethanone as a yellowish oil.

Yield = 88.0%

1H NMR ($CDCl_3$): δ 6.69 (s, 1H), 6.58 (s, 1H), 4.56 (dd, $J = 4.9, 3.5$ Hz, 1H), 4.28 (m, 1H), 4.26 (m, 1H), 2.68 (m, 4H), 2.29 (s, 3H), 1.75 (m, 4H).

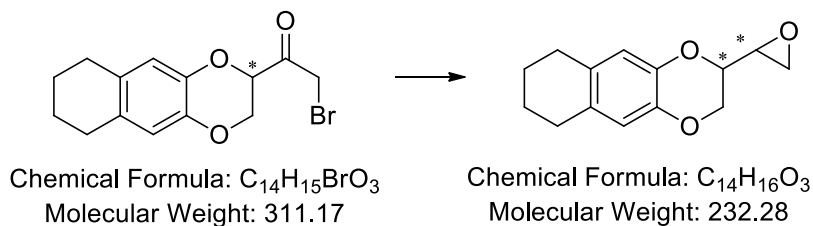
2-Bromo-1-(5,6,7,8-tetrahydro-1,4-naphthodioxane-2-yl)-ethanone



Bromine (1.26 mL, 24.54 mmol) was added dropwise to a solution 1-(5,6,7,8-Tetrahydro-1,4-naphthodioxane-2-yl)-ethanone (5.70 g, 24.54 mmol) in Et_2O (50 mL) at $-20^\circ C$. The mixture was stirred at that temperature for 3 h, washed $Na_2S_2O_5$ (10 mL), dried over Na_2SO_4 , filtered and concentrated under vacuum. Elution with 95/5 Cyclohexane/Ethyl acetate on silica gel gave 4.90 g of 2-Bromo-1-(5,6,7,8-tetrahydro-1,4-naphthodioxane-2-yl)-ethanone as a yellowish oil.

Yield = 64.0%

1H NMR ($CDCl_3$): δ 6.70 (s, 1H), 6.59 (s, 1H), 4.86 (dd, $J = 4.7, 3.3$ Hz, 1H), 4.40 (m, 2H), 4.33 (d, $J = 14.0$ Hz, 1H), 4.10 (d, $J = 14.0$ Hz, 1H), 2.70 (m, 4H), 1.76 (m, 4H).

Erythro and *Threo*-2-(5,6,7,8-tetrahydro-1,4-naphthodioxane-2-yl)-oxirane

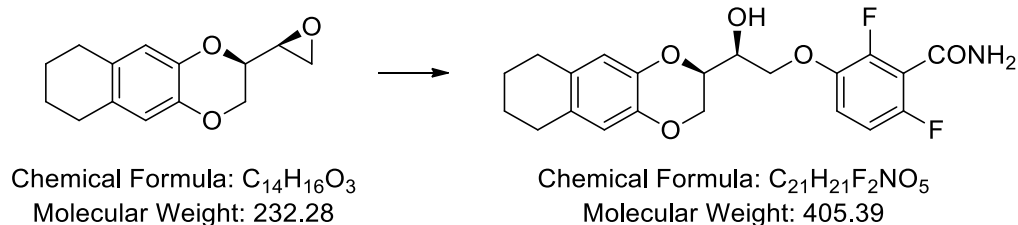
$NaBH_4$ (0.29 g, 7.85 mmol) was added to a solution of 2-Bromo-1-(5,6,7,8-tetrahydro-1,4-naphthodioxane-2-yl)-ethanone (4.90 g, 15.71 mmol) in MeOH (50 mL) at $0^\circ C$. The reaction mixture was stirred at $0^\circ C$ for 0.5 hours, concentrated under vacuum, diluted with THF (20 mL) and added dropwise to a suspension of NaH (0.75 g, 18.88 mmol) in THF (10 mL) at $0^\circ C$ under nitrogen atmosphere. The reaction mixture was stirred at room temperature for 2 hours, concentrated under vacuum, diluted with Ethyl Acetate (20 mL) and phosphate buffer pH = 7, washed with 10% aqueous NaCl, dried over Na_2SO_4 , filtered and concentrated under vacuum to give a brown residue. Elution with 9/1 Cyclohexane/Ethyl acetate on silica gel gave 0.65 g of *Erythro* 2-(5,6,7,8-tetrahydro-1,4-naphthodioxane-2-yl)-oxirane and 1.30 g of *Threo* 2-(5,6,7,8-tetrahydro-1,4-naphthodioxane-2-yl)-oxirane as colourless oils

Yield (sum) = 53.0%

1H NMR ($CDCl_3$) *Erythro*: δ 6.60 (s, 2H), 4.29 (dd, $J = 11.4, 2.4$ Hz, 1H), 4.12 (dd, $J = 11.4, 6.6$ Hz, 1H), 3.91 (td, $J = 6.6, 2.4$ Hz, 1H), 3.13 (ddd, $J = 6.5, 4.1, 2.6$ Hz, 1H), 2.90 (dd, $J = 4.9, 4.1$ Hz, 1H), 2.80 (dd, $J = 4.9, 2.6$ Hz, 1H), 2.67 (m, 4H), 1.73 (m, 4H).

1H NMR ($CDCl_3$) *Threo*: δ 6.63 (s, 1H), 6.58 (s, 1H), 4.26 (m, 1H), 4.07 (m, 2H), 3.19 (m, 1H), 2.85 (m, 2H), 2.66 (m, 4H), 1.74 (m, 4H).

Erythro (XXI) 3-(5,6,7,8-tetrahydro-1,4-naphthodioxane-2-yl)-2-hydroxyethoxy)-2,6-difluorobenzamide



A solution of 3-Hydroxy-2,6-difluorobenzamide (0.25 g, 1.45 mmol) in DMF (3 mL) was added to a solution of *Erythro* 2-(1,4-Benzodioxan-2-yl)-oxirane (0.32 g, 1.38 mmol) and K_2CO_3 (0.21 g, 1.52 mmol) in DMF (2 mL) at RT. The reaction mixture was stirred at 70°C for 2 hours, concentrated under vacuum, diluted with Ethyl Acetate (20 mL) washed with 10% aqueous NaCl (5 x 10 mL), dried over Na_2SO_4 , filtered and concentrated under vacuum to give a brown residue. The crude was quickly hydrogenated in MeOH to remove polybrominated impurities. Elution with 6/4 to 4/6 Cyclohexane/Ethyl acetate on silica gel and subsequent crystallization with $CHCl_3$ gave 0.11 g of *Erythro* 3-(5,6,7,8-tetrahydro-1,4-naphthodioxane-2-yl)-2,6-difluorobenzamide as a white solid

Yield = 20.0%

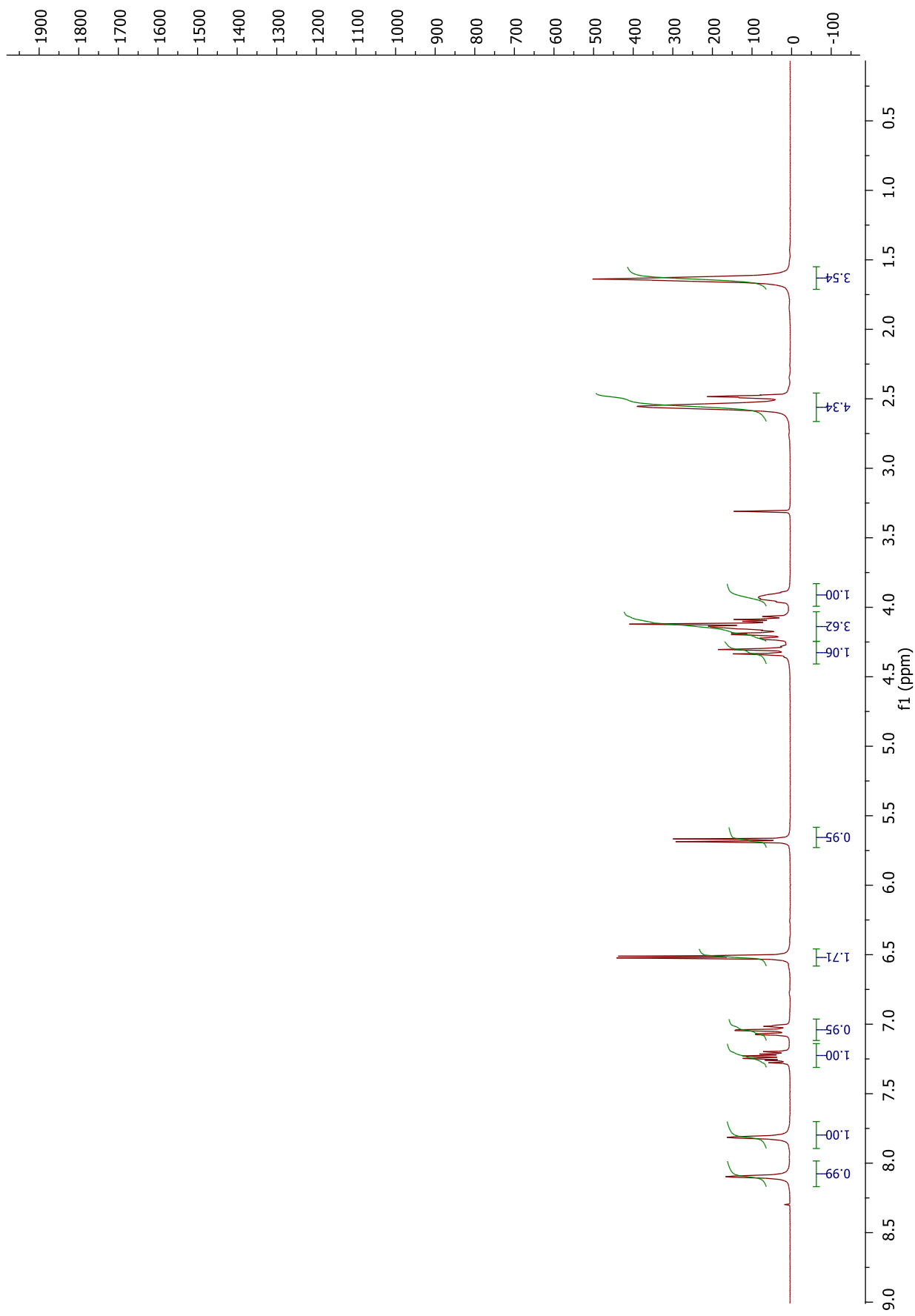
M.p. = 155.36°C

Tr HPLC, gradient, 90% H_2O with 0.10% TFA to 10% acetonitrile with 0.10% TFA in 25 min with 35 min run time. Flow rate: 1 mL/min) = 14.9 min, Purity = 98.6%

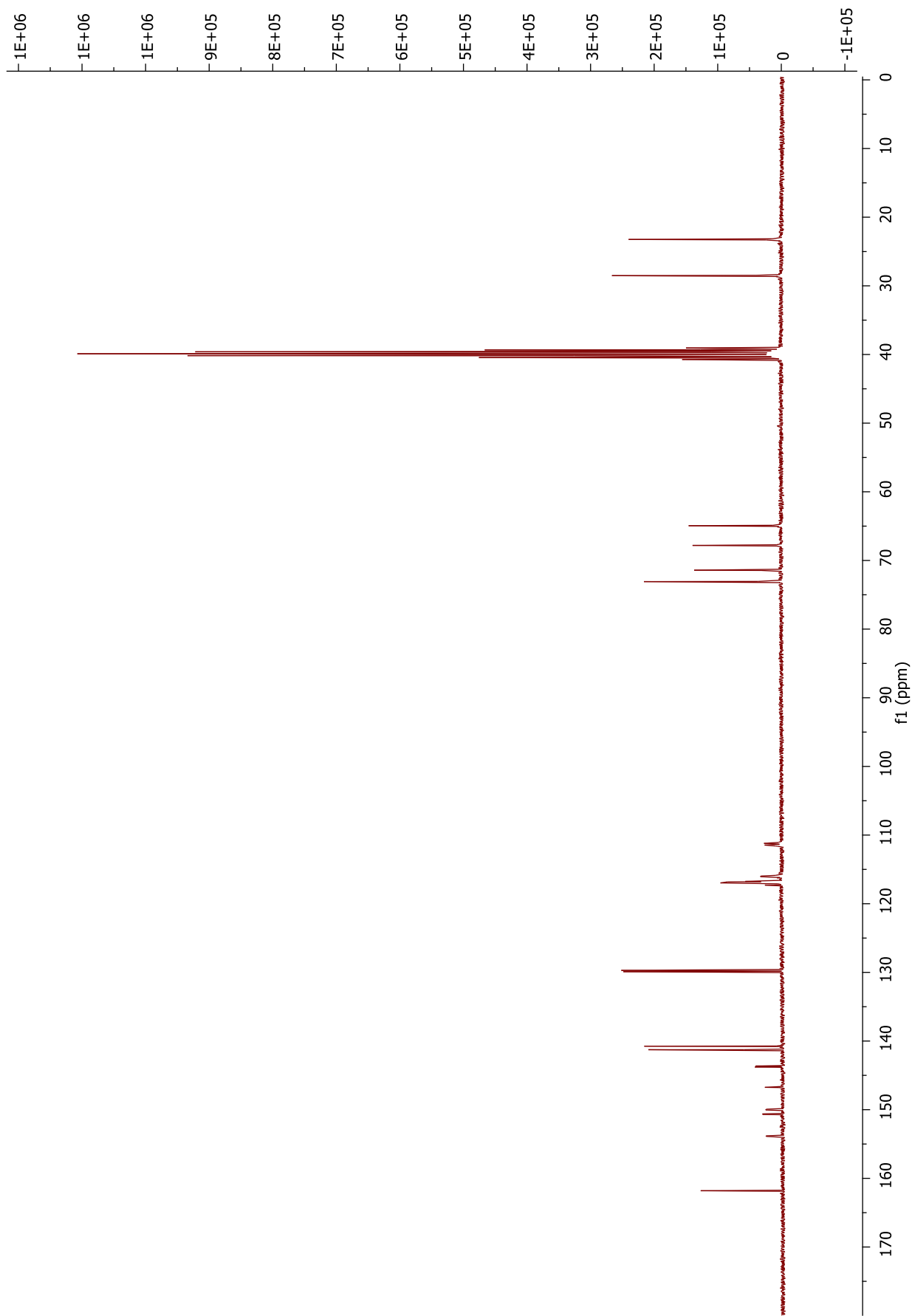
1H NMR (d_6 -DMSO): δ 8.10 (s, 1H), 7.81 (s, 1H), 7.24 (td, J = 9.3, 5.3 Hz, 1H), 7.04 (td, J = 9.0, 1.8 Hz, 1H), 6.52 (s, 1H), 6.51 (s, 1H), 5.68 (d, J = 5.9 Hz, 1H), 4.32 (d, J = 9.5 Hz, 1H), 4.15 (m, 4H), 3.94 (m, 1H), 2.55 (m, 4H), 1.64 (m, 4H).

^{13}C NMR (d_6 -DMSO): δ 161.8, 152.3 (dd, J = 239.3, 6.7 Hz), 148.3 (dd, J = 246.8, 8.2 Hz), 143.7 (dd, J = 10.5, 3.0 Hz), 143.3, 140.8, 129.9, 129.7, 117.0 (dd, J = 24.6, 20.3 Hz), 117.0, 116.9, 116.8, 116.7, 116.0 (dd, J = 8.5, 1.7 Hz), 111.3 (dd, J = 23.1, 3.0 Hz), 73.1, 71.4, 67.8, 64.9, 28.5, 23.2 ppm.

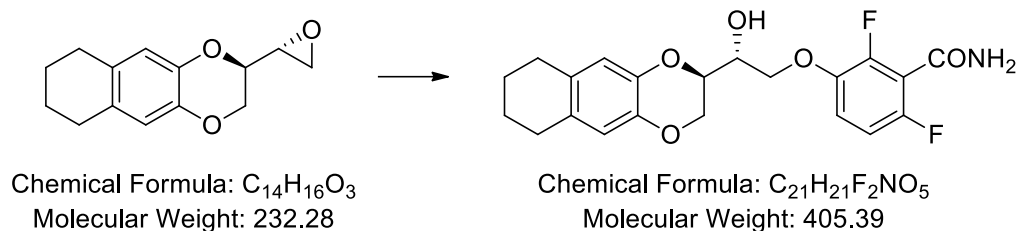
Experimental



Experimental



Threo (XXI) 3-(5,6,7,8-tetrahydro-1,4-naphthodioxane-2-yl)2-hydroxyethoxy)-2,6-difluorobenzamide



A solution of 3-Hydroxy-2,6-difluorobenzamide (0.10 g, 0.59 mmol) in DMF (3 mL) was added to a solution of *Threo* 2-(1,4-Benzodioxan-2-yl)-oxirane (0.13 g, 0.56 mmol) and K₂CO₃ (0.085 g, 0.62 mmol) in DMF (2 mL) at RT. The reaction mixture was stirred at 70°C for 2 hours, concentrated under vacuum, diluted with Ethyl Acetate (20 mL) washed with 10% aqueous NaCl (5 x 10 mL), dried over Na₂SO₄, filtered and concentrated under vacuum to give a brown residue. The crude was quickly hydrogenated in MeOH to remove polybrominated impurities. Elution with 6/4 to 4/6 Cyclohexane/Ethyl acetate on silica gel and subsequent crystallization with CHCl₃ gave 0.11 g of *Threo* 3-(5,6,7,8-tetrahydro-1,4-naphthodioxane-2-yl)-2,6-difluorobenzamide as a white solid

Yield = 31.0%

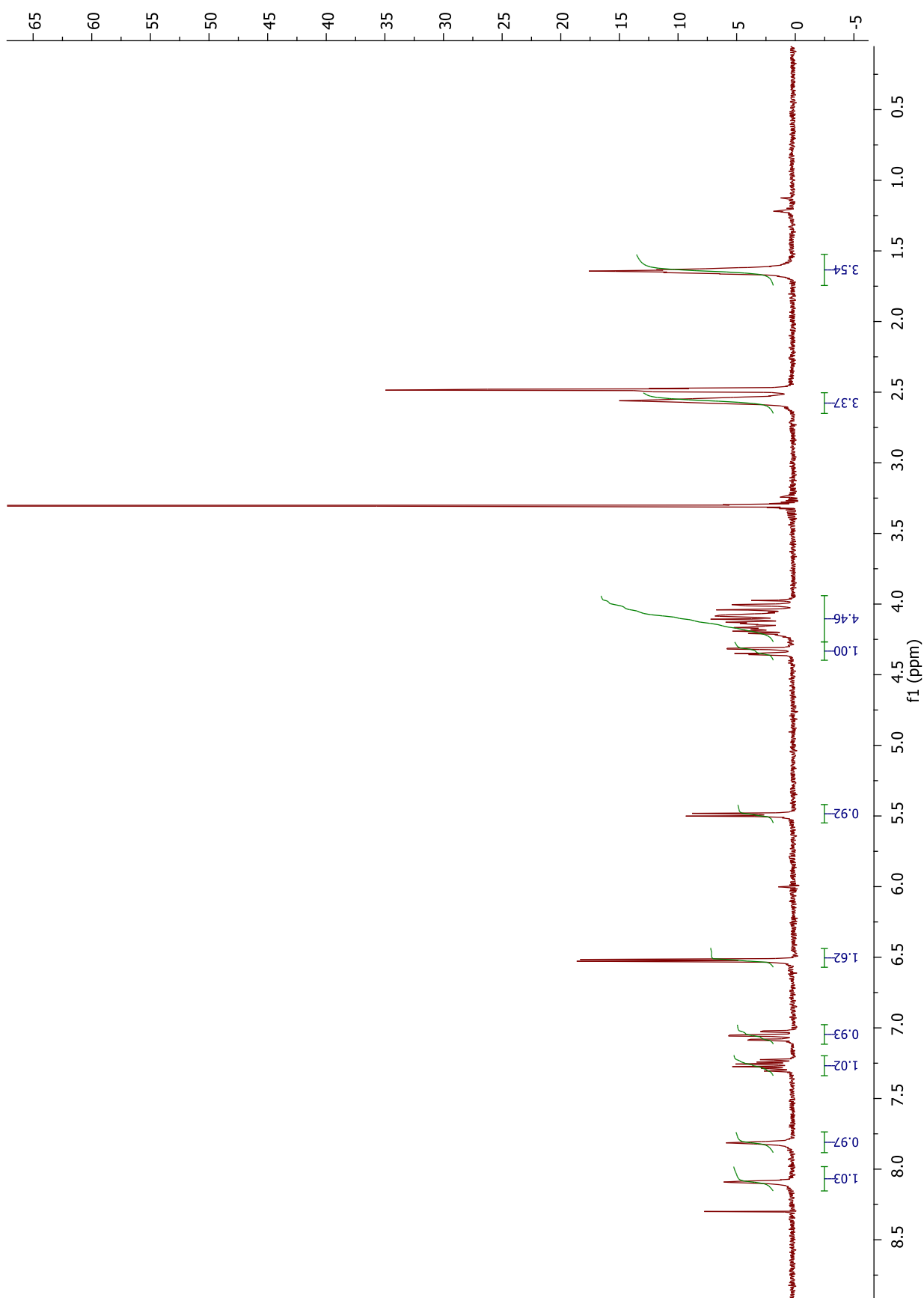
M.p. = 147.38°C

Tr HPLC, gradient, 90% H₂O with 0.10% TFA to 10% acetonitrile with 0.10% TFA in 25 min with 35 min run time. Flow rate: 1 mL/min) = 14.6 min, Purity = 98.5%

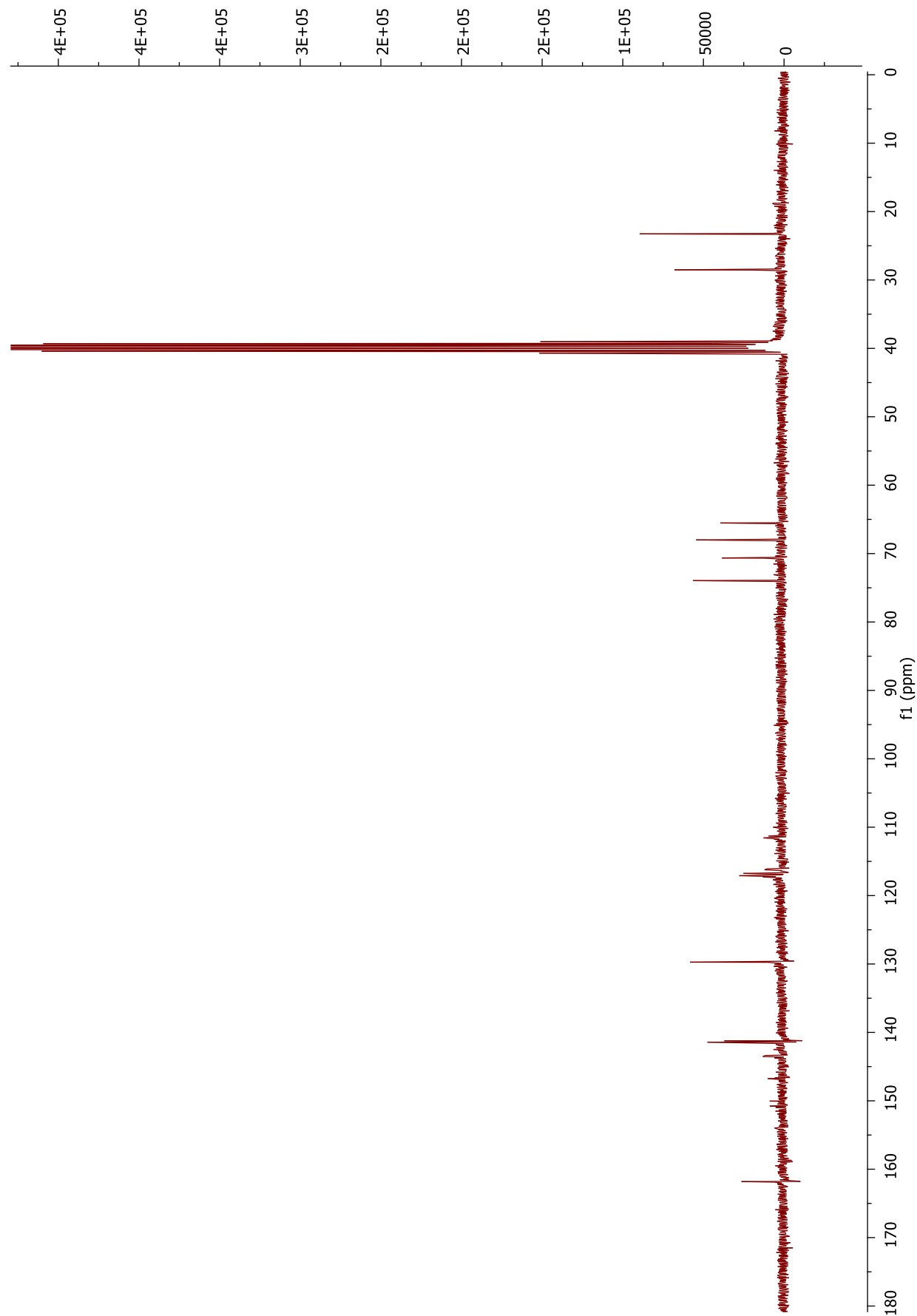
¹H NMR (d₆-DMSO): δ 8.09 (s, 1H), 7.81 (s, 1H), 7.27 (td, *J* = 9.4, 5.3 Hz, 1H), 7.05 (td, *J* = 9.0, 1.9 Hz, 1H), 6.53 (s, 1H), 6.52 (s, 1H), 5.49 (d, *J* = 5.8 Hz, 1H), 4.33 (dd, *J* = 11.2, 2.0 Hz, 1H), 4.09 (m, 5H), 2.56 (m, 4H), 1.64 (m, 4H).

¹³C NMR (d₆-DMSO): δ 161.8, 152.3 (dd, *J* = 239.3, 6.7 Hz), 148.3 (dd, *J* = 246.8, 8.2 Hz), 143.7 (dd, *J* = 10.5, 3.0 Hz), 143.3, 140.8, 129.9, 129.7, 117.0 (dd, *J* = 24.6, 20.3 Hz), 117.0, 116.9, 116.8, 116.7, 116.0 (dd, *J* = 8.5, 1.7 Hz), 111.3 (dd, *J* = 23.1, 3.0 Hz), 73.1, 71.4, 67.8, 64.9, 28.5, 23.2 ppm.

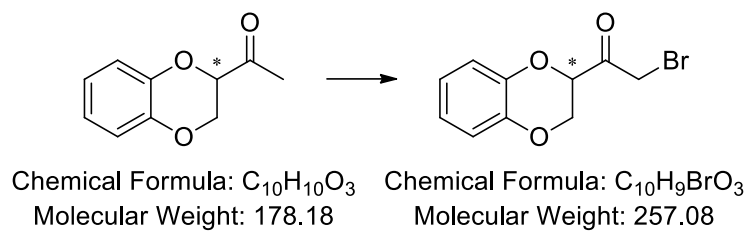
Experimental



Experimental



2-Bromo-1-(1,4-benzodioxan-2-yl)-ethanone

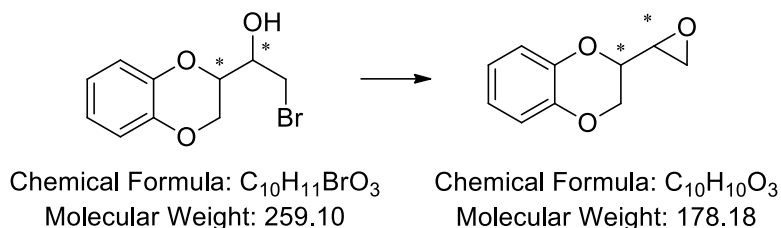


Bromine (0.24 mL, 3.12 mmol) was added dropwise to a solution of 1-(1,4-Benzodioxan-2-yl)-ethanone (0.55 g, 3.12 mmol) in Et₂O (5 mL) at -20°C. The mixture was stirred at that temperature for 3 h, washed Na₂S₂O₅ (10 mL), dried over Na₂SO₄, filtered and concentrated under vacuum to yield 0.8 g of 2-Bromo-1-(1,4-benzodioxan-2-yl)-ethanone as a yellowish oil.

Yield = Quantitative

¹H NMR (CDCl₃): δ 7.05 (m, 1H), 6.92 (m, 3H), 4.90 (m, 1H), 4.39 (m, 2H), 4.33 (dd, J = 13.8, 1.3 Hz, 1H), 4.12 ppm (dd, J = 13.8, 1.3 Hz, 1H)

Erythro and *Threo*-2-(1,4-Benzodioxan-2-yl)-oxirane

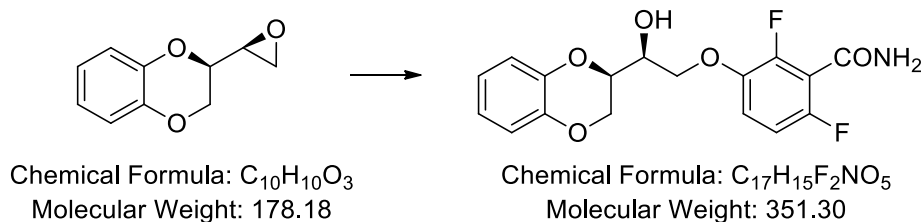


NaBH₄ (0.14 g, 3.69 mmol) was added to a solution of 2-Bromo-1-(1,4-benzodioxan-2-yl)-ethanone (1.9 g, 7.39 mmol) in MeOH (19 mL) at 0°C. The reaction mixture was stirred at 0°C for 0.5 hours, concentrated under vacuum, diluted with THF (20 mL) and added dropwise to a suspension of NaH (0.21 g, 8.87 mmol) in THF (10 mL) at 0°C under nitrogen atmosphere. The reaction mixture was stirred at room temperature for 2 hours, concentrated under vacuum, diluted with Ethyl Acetate (20 mL) and phosphate buffer pH = 7, washed with 10% aqueous NaCl, dried over Na₂SO₄, filtered and concentrated under vacuum to give a brown residue. Elution with 9/1 Cyclohexane/Ethyl acetate on silica gel gave 0.3 g of *Erythro* 2-(1,4-Benzodioxan-2-yl)-oxirane and 0.18 g of *Threo* 2-(1,4-Benzodioxan-2-yl)-oxirane as colourless oils

Yield (sum) = 36.0%

¹H NMR (CDCl₃) *Erythro*: δ 6.87 (m, 4H), 4.34 (dd, J = 11.4, 2.4 Hz, 1H), 4.15 (dd, J = 11.4, 6.7 Hz, 1H), 3.96 (m, 1H), 3.14 (ddd, J = 6.2, 3.9, 2.5 Hz, 1H), 2.92 (dd, J = 5.0, 3.9 Hz, 1H), 2.81 ppm (dd, J = 5.0, 2.5 Hz, 1H).

¹H NMR (CDCl₃) *Threo*: δ 6.85 (m, 4H), 4.32 (dd, J = 9.1, 2.3 Hz, 1H), 4.10 (m, 2H), 3.22 (m, 1H), 2.85 ppm (m, 2H).

Erythro (XXII) 3-(1,4-Benzodioxane-2-yl)2-hydroxyethoxy)-2,6-difluorobenzamide

A solution of 3-Hydroxy-2,6-difluorobenzamide (0.18 g, 1.06 mmol) in DMF (3 mL) was added to a solution of *Erythro* 2-(1,4-Benzodioxan-2-yl)-oxirane (0.18 g, 1.01 mmol) and K₂CO₃ (0.15, 1.11 mmol) in DMF (2 mL) at RT. The reaction mixture was stirred at 70°C for 2 hours, concentrated under vacuum, diluted with Ethyl Acetate (20 mL) washed with 10% aqueous NaCl (5 x 10 mL), dried over Na₂SO₄, filtered and concentrated under vacuum to give a brown residue. Elution with 6/4 Cyclohexane/Ethyl acetate on silica gel and subsequent elution with 7/3 water/ACN on C18 gave 0.05 g of *Erythro* 3-(1,4-Benzodioxane-2-yl)2-hydroxyethoxy)-2,6-difluorobenzamide as a white solid

Yield = 14.0%

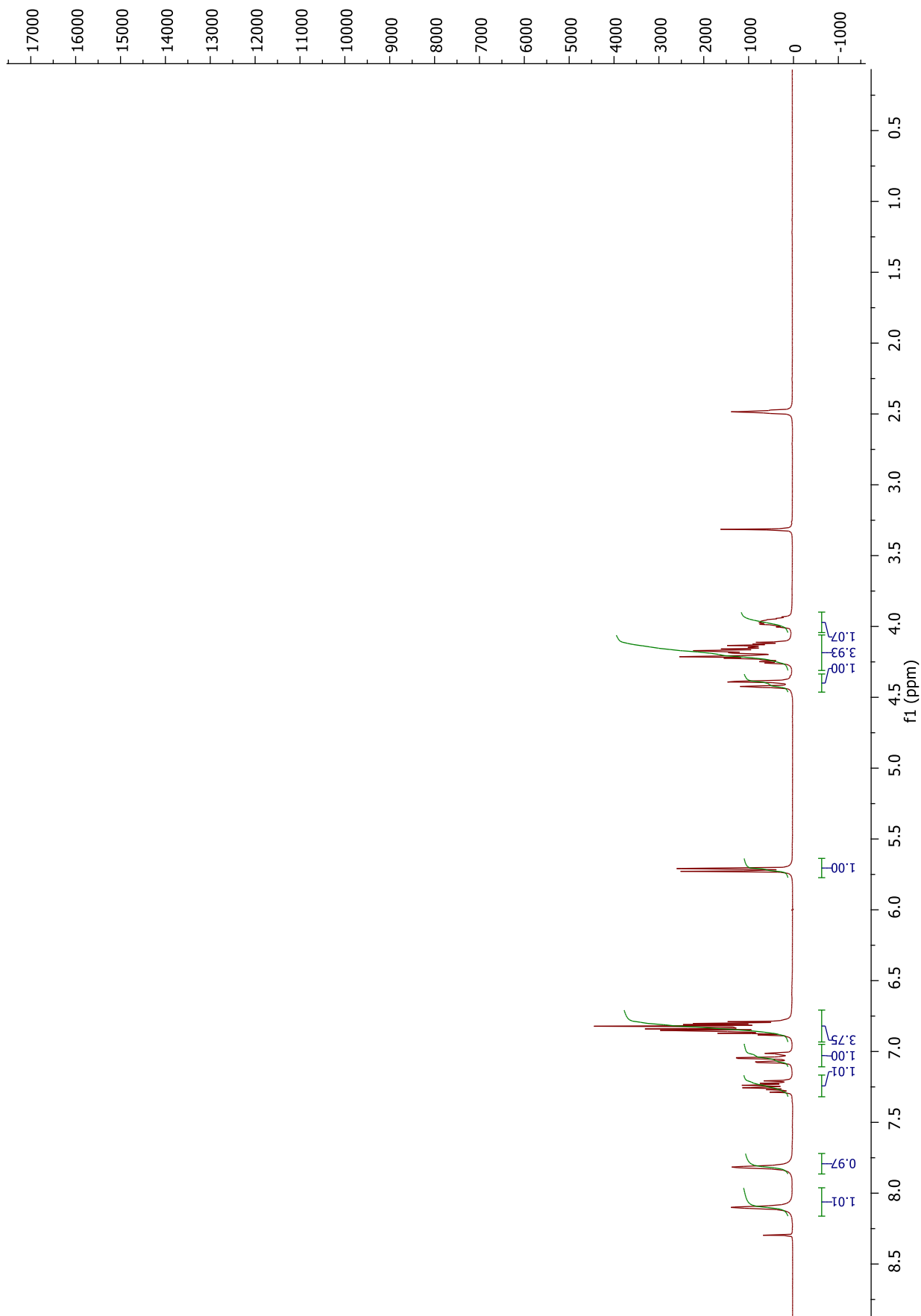
M.p. = 92.32°C

Tr (HPLC, Isocratic, H₂O/Acetonitrile 60/40. 15 min run time. Flow rate: 1 mL/min) = 3.9 min, Purity = 98.7%

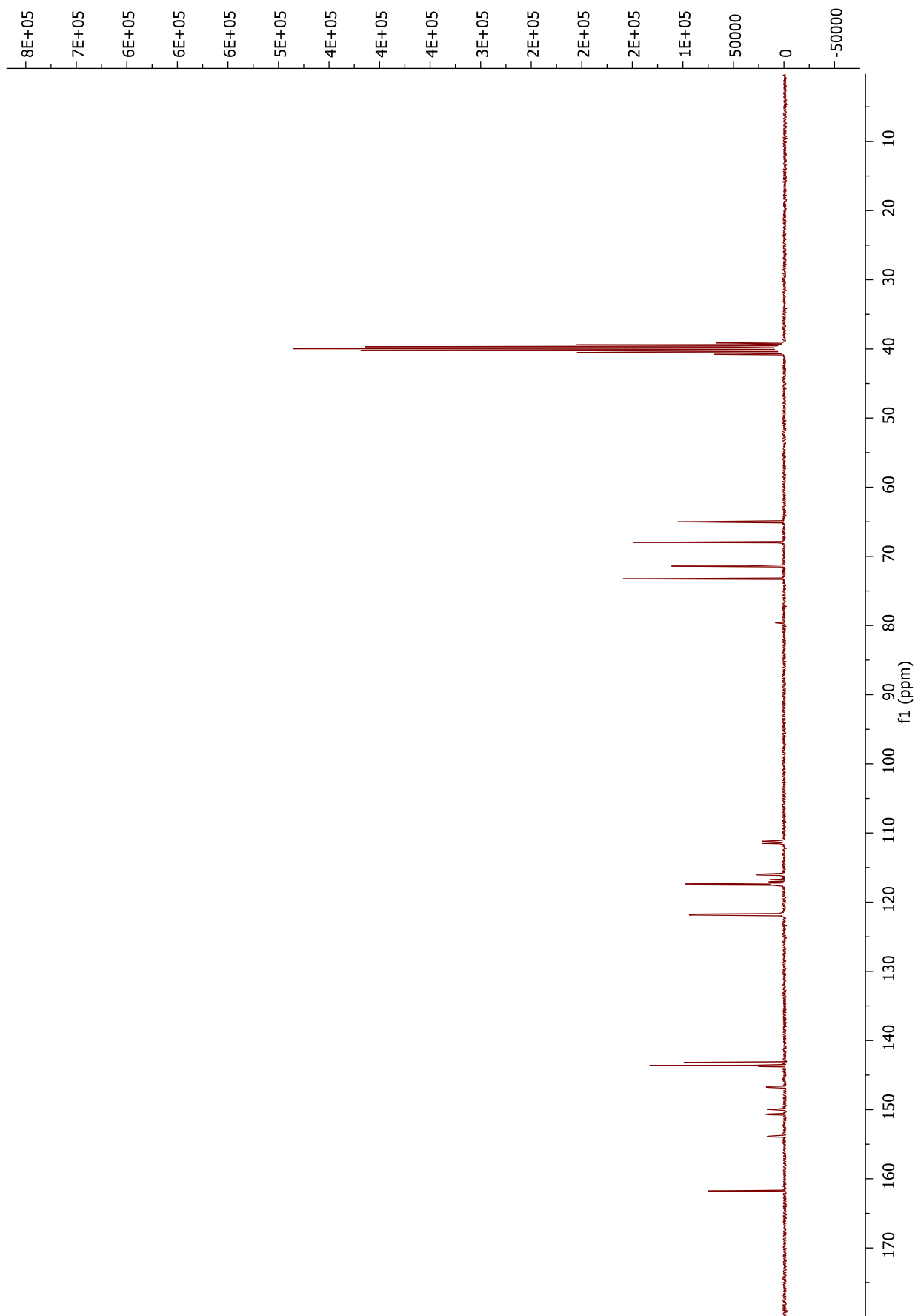
¹H NMR (d₆-DMSO): δ 8.10 (s, 1H), 7.82 (s, 1H), 7.25 (td, J = 9.3, 5.3 Hz, 1H), 7.05 (td, J = 9.0, 1.8 Hz, 1H), 6.83 (m, 4H), 5.72 (d, J = 5.8 Hz, 1H), 4.41 (dd, J = 10.9, 1.6 Hz, 1H), 4.24 (m, 2H), 4.14 (m, 2H), 3.97 ppm (m, 1H).

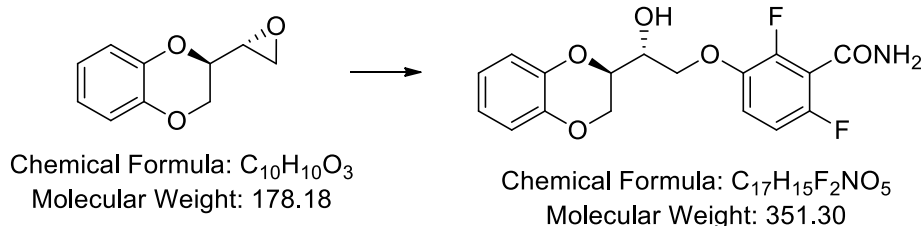
¹³C NMR (d₆-DMSO): δ 161.8, 152.3 (dd, J = 239.9, 6.7 Hz), 148.4 (dd, J = 246.7, 8.3 Hz), 143.7 (dd, J = 10.8, 3.0 Hz), 143.6, 143.2, 121.9, 121.7, 117.5, 117.4, 117.1 (dd, J = 25.0, 20.5 Hz), 116.0 (dd, J = 8.7, 1.0 Hz), 111.3 (dd, J = 22.9, 3.5 Hz), 73.3, 71.4, 68.0, 65.0 ppm.

Experimental



Experimental



Threo (XXII) 3-(1,4-Benzodioxane-2-yl)2-hydroxyethoxy)-2,6-difluorobenzamide

A solution of 3-Hydroxy-2,6-difluorobenzamide (0.18 g, 1.06 mmol) in DMF (3 mL) was added to a solution of *Threo* 2-(1,4-Benzodioxan-2-yl)-oxirane (0.18 g, 1.01 mmol) and K₂CO₃ (0.15, 1.11 mmol) in DMF (2 mL) at RT. The reaction mixture was stirred at 70°C for 2 hours, concentrated under vacuum, diluted with Ethyl Acetate (20 mL) washed with 10% aqueous NaCl (5 x 10 mL), dried over Na₂SO₄, filtered and concentrated under vacuum to give a brown residue. Elution with 6/4 Cyclohexane/Ethyl acetate on silica gel and subsequent elution with 7/3 water/ACN on C18 gave 0.15 g of *Threo* 3-(1,4-Benzodioxane-2-yl)2-hydroxyethoxy)-2,6-difluorobenzamide as a white solid

Yield = 36.0%

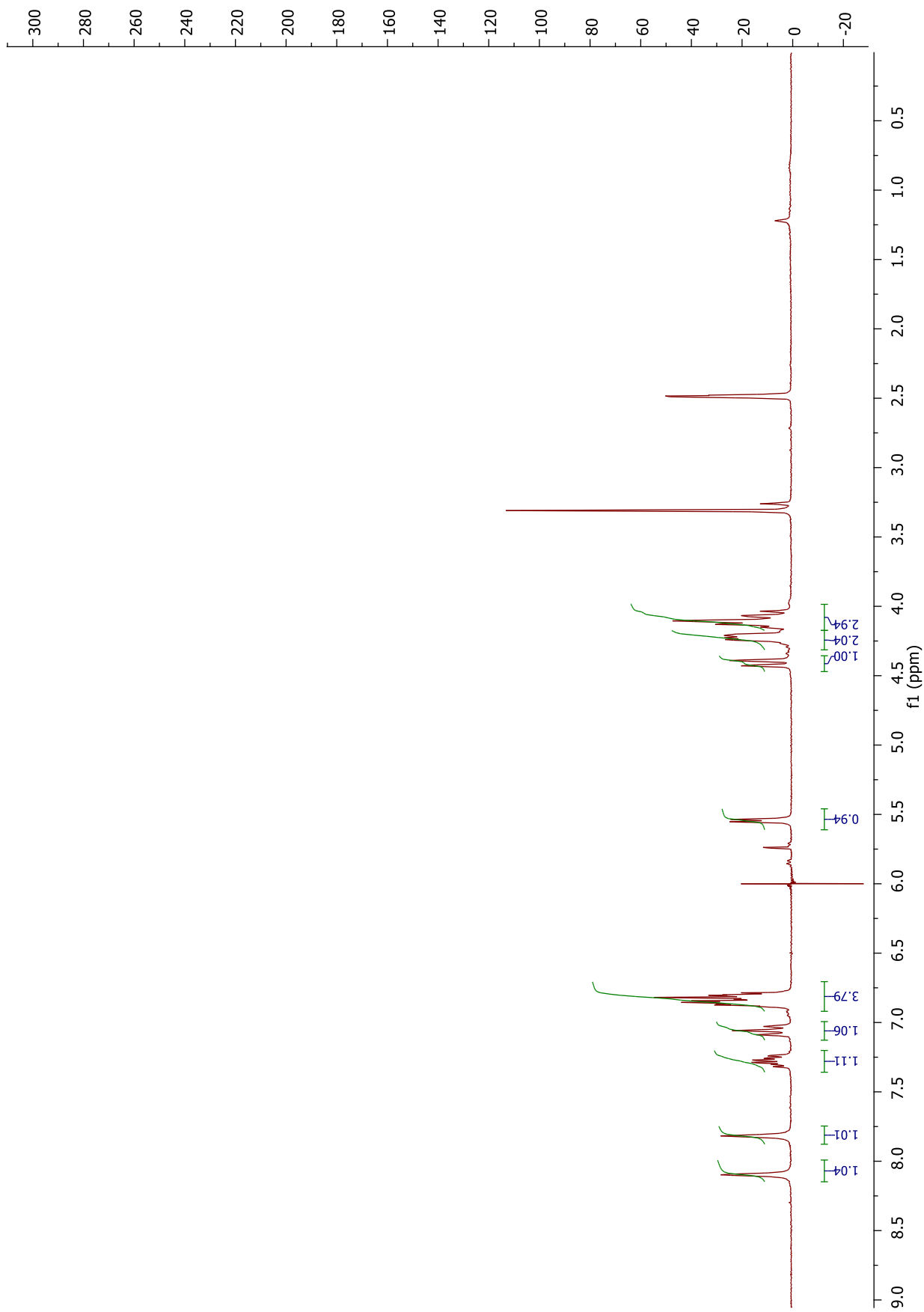
M.p. = 117.42°C

(HPLC, Isocratic, H₂O/Acetonitrile 60/40. 15 min run time. Flow rate: 1 mL/min) = 3.6 min,
Purity = 97.5%

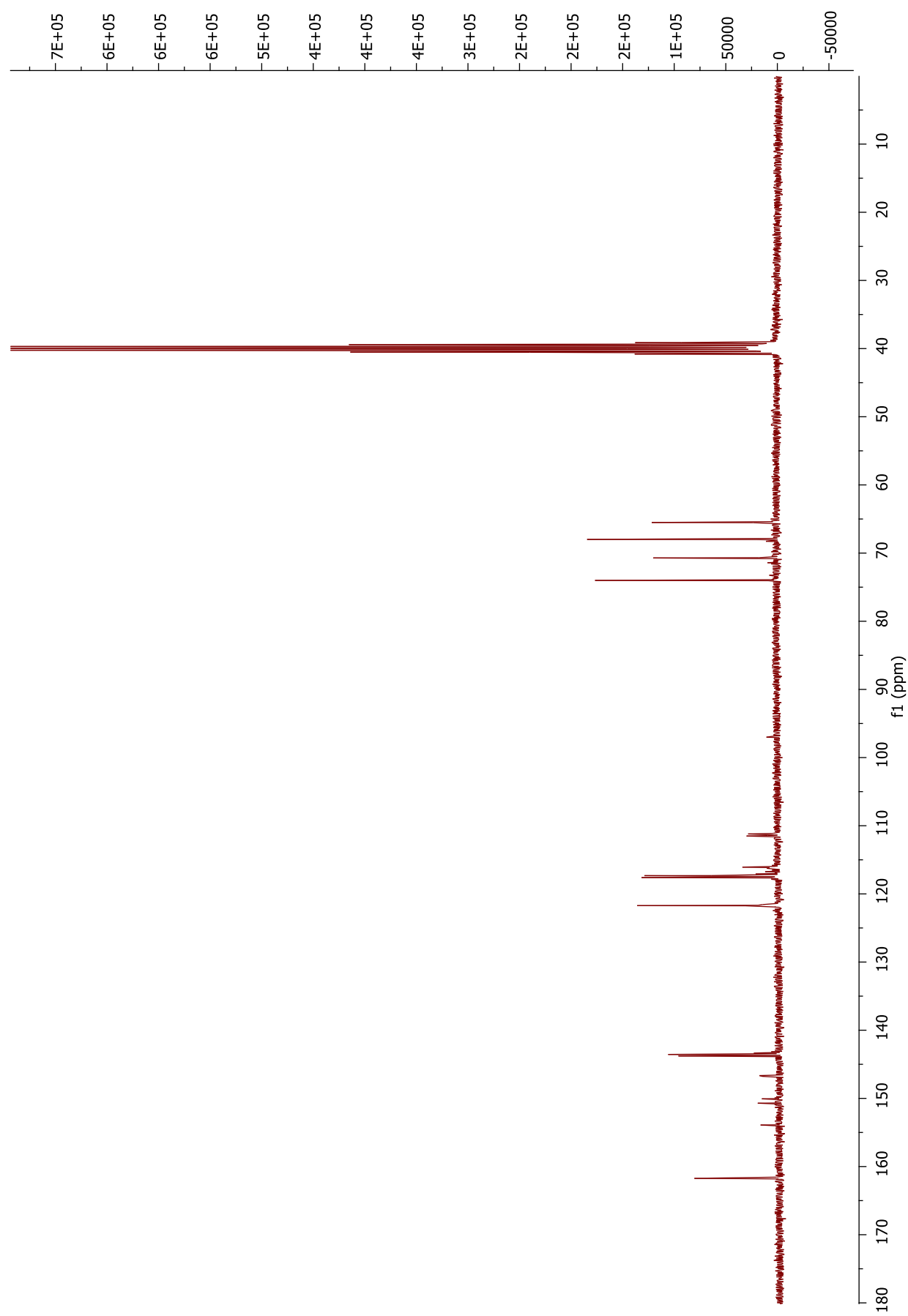
¹H NMR (d₆-DMSO): δ 8.10 (s, 1H), 7.82 (s, 1H), 7.28 (td, J = 9.0, 5.4 Hz, 1H), 7.06 (t, J = 8.9 Hz, 1H), 6.82 (m, 3H), 5.54 (d, J = 4.9 Hz, 1H), 4.41 (d, J = 11.2 Hz, 1H), 4.22 (m, 2H), 4.07 ppm (m, 3H).

¹³C NMR (d₆-DMSO): δ 161.7, 152.4 (dd, J = 239.9, 6.6 Hz), 148.4 (dd, J = 247.1, 8.4 Hz), 143.8, 143.6, 143.4 (dd, J = 9.5, 4.9 Hz), 121.7, 121.2, 117.6, 117.3, 117.1 (dd, J = 25.0, 20.4 Hz), 116.1 (dd, J = 11.0, 2.1 Hz), 111.4 (dd, J = 22.9, 3.7 Hz), 74.0, 70.7, 68.0, 65.5 ppm.

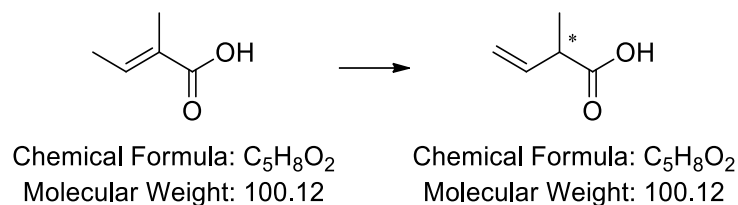
Experimental



Experimental



2-Methyl-3-butenic acid

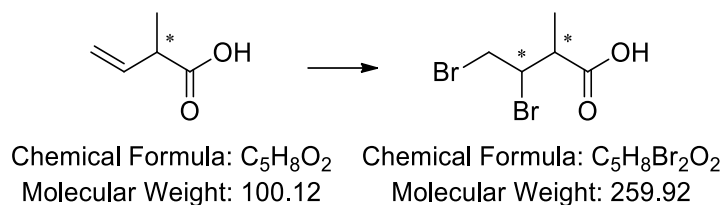


2.7 M *n*-BuLi (9.26 mL, 25 mmol) in heptane was added dropwise to a solution of DIPA (3.85 mL, 27.5 mmol) in THF (15 mL) at -78°C. The reaction mixture was stirred for 1 hour at -78°C, added with 2-Methyl-2-butenoic acid (1 g, 10 mmol) in THF (5 mL), stirred at RT for 2 hours and poured into 20 mL of 10% aqueous HCl at 0°C and extracted with Ethyl acetate (2 x 20 mL). The organic phase was washed with brine (2 x 10 mL), dried over Na₂SO₄, filtered and concentrated under vacuum, affording 0.85 g of 2-Methyl-3-butenic acid as a colourless oil.

Yield = 85.0%

¹H NMR (CDCl₃): δ 5.94 (ddd, *J* = 18.5, 10.2, 7.4 Hz, 1H), 5.17 (m, 2H), 3.18 (m, 1H), 1.31 (d, *J* = 7.1 Hz, 3H).

3,4-Dibromo-2-methylbutanoic acid



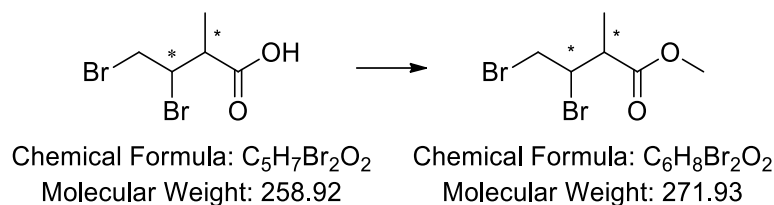
Bromine (0.43 mL, 8.49 mmol) was added dropwise to a solution of 2-Methyl-3-butenoic acid (0.85 g, 8.49 mmol) in DCM (10 mL) at 0°C. The reaction mixture was stirred for 18 hours at RT, quenched with $Na_2S_2O_5$ (2 x 10 mL), was washed with brine (10 mL), dried over Na_2SO_4 , filtered and concentrated under vacuum, affording 1.72 g of 3,4-Dibromo-2-methylbutanoic acid as a colourless oil, used as a mixture of 4 stereoisomers in the next step without further purification.

Yield = 78.0%

1H NMR ($CDCl_3$): δ 4.29 (m, 1H), 3.89 (dd, $J = 10.6, 4.9$ Hz, 1H), 3.85 (dd, $J = 10.8, 5.0$ Hz, 1H), 3.33 (m, 1H), 1.35 (d, $J = 7.0$ Hz, 3H).

1H NMR ($CDCl_3$): δ 4.76 (ddd, $J = 11.3, 8.6, 3.2$ Hz, 1H), 4.07 (dd, $J = 10.7, 8.6$ Hz, 1H), 3.62 (dd, $J = 11.0, 10.7$, 1H), 3.33 (m, 1H), 1.26 (d, $J = 6.8$ Hz, 3H).

Methyl 3,4-dibromo-2-methylbutanoate



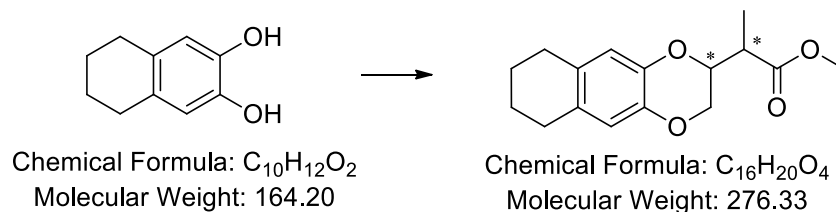
Trimethylorthoformate (1.37 mL, 12.56 mmol) and a catalytic amount of conc. H_2SO_4 were added to a solution of 3,4-Dibromo-2-methylbutanoic acid (1.72 g, 6.62 mmol) in MeOH (20 mL) at $0^\circ C$. The reaction mixture was stirred at reflux for 18 hours, concentrated under vacuum, diluted with Ethyl acetate (20 mL), washed with phosphate buffer pH = 7 (10 mL), dried over Na_2SO_4 , filtered and concentrated under vacuum, affording 1.38 g of Methyl 3,4-dibromo-2-methylbutanoate as a yellowish oil, used as a mixture of 4 stereoisomers in the next step without further purification.

Yield = 78.0%

1H NMR ($CDCl_3$): δ 4.74 (ddd, $J = 10.9, 6.5, 3.5$ Hz, 1H), 4.01 (dd, $J = 10.8, 6.5$ Hz, 1H), 3.62 (dd, $J = 10.9, 10.8$ Hz, 1H), 3.25 (m, 1H), 1.24 (d, $J = 6.8$ Hz, 3H).

1H NMR ($CDCl_3$): δ 4.31 (dt, $J = 8.2, 4.9$ Hz, 1H), 3.87 (dd, $J = 10.5, 4.9$ Hz, 1H), 3.83 (dd, $J = 10.5, 4.9$ Hz, 1H), 3.23 (m, 1H), 1.31 (d, $J = 7.0$ Hz, 3H).

Erythro and *Threo* Methyl 2-(5,6,7,8-tetrahydro-1,4-naphthodioxan-2-yl)-2-methylacetate

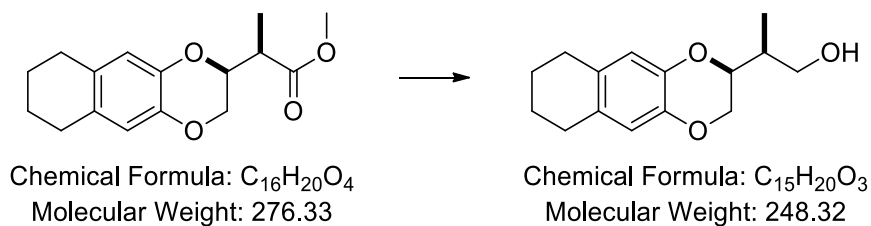


A solution of Methyl 3,4-dibromo-2-methylbutanoate (1.38 g, 5.04 mmol) in DMF (5 mL) was added to a solution of 5,6,7,8-Tetrahydronaphthalen-2,3-diol (0.75 g, 4.58 mmol) and K_2CO_3 in DMF (10 mL) at RT. The reaction mixture was stirred at 70°C for 18 hours, concentrated under vacuum, diluted with Ethyl acetate (20 mL), washed with brine (5 x 10 mL), dried over Na_2SO_4 , filtered and concentrated under vacuum. Elution with 97/3 Cyclohexane/Ethyl acetate gave 0.38 g of Methyl 2-(5,6,7,8-tetrahydro-1,4-naphthodioxan-2-yl)-2-methylacetate, 0.25 g corresponding at the *Erythro* couple and 0.13 g corresponding to the *Threo* one.

Yield = 30.0%

1H NMR ($CDCl_3$) *Erythro*: δ 6.59 (s, 1H), 6.57 (s, 1H), 4.28 (ddd, $J = 9.0, 6.5, 2.2$ Hz, 1H), 4.21 (dd, $J = 11.4, 2.2$ Hz, 1H), 3.98 (dd, $J = 11.4, 6.5$ Hz, 1H), 3.72 (s, 3H), 2.82 (m, 1H), 2.64 (m, 4H), 1.74 (m, 4H), 1.33 (d, $J = 7.1$ Hz, 3H).

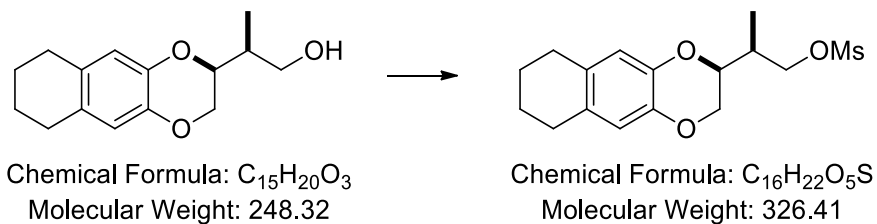
1H NMR ($CDCl_3$) *Threo*: δ 6.56 (s, 2H), 4.32 (ddd, $J = 9.0, 6.9, 2.1$ Hz, 1H), 4.24 (dd, $J = 11.4, 2.1$ Hz, 1H), 4.00 (dd, $J = 11.4, 6.9$ Hz, 1H), 3.73 (s, 3H), 2.86 (m, 1H), 2.65 (m, 4H), 1.73 (m, 4H), 1.24 (d, $J = 7.1$ Hz, 3H).

Erythro 2-(5,6,7,8-tetrahydro-1,4-naphthodioxan-2-yl)propan-1-ol

$LiAlH_4$ (0.035 g, 0.905 mmol) was suspended in dry THF (2 mL) at $0^\circ C$ under nitrogen atmosphere. The solution of *Erythro* Methyl 2-(5,6,7,8-tetrahydro-1,4-naphthodioxan-2-yl)-2-methylacetate (0.25 g, 0.91 mmol) in THF (3 mL) was slowly added to the reaction. The mixture was then warmed to RT and stirred for 1 h; at completion, it was cooled to $0^\circ C$ and slowly quenched with Ethyl acetate (5 mL). Further Ethyl acetate (10 mL) was added, the organic layer was washed with brine (3×10 mL), dried over Na_2SO_4 and concentrated under vacuum to give 0.19 g of *Erythro*-2-(5,6,7,8-Tetrahydro-1,4-naphthodioxan-2-yl)propan-1-ol as a colourless oil.

Yield = 85.0%

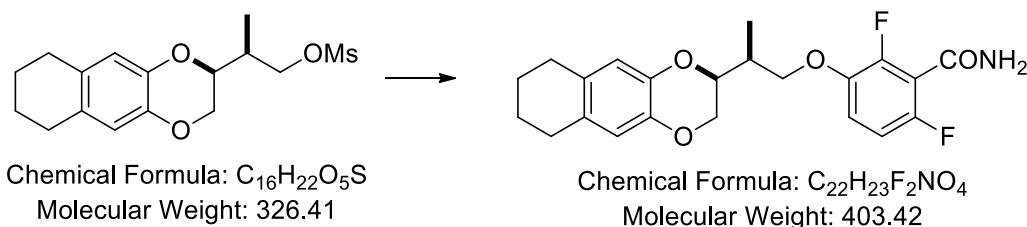
1H NMR ($CDCl_3$): δ 6.58 (s, 1H), 6.57 (s, 1H), 4.24 (dd, $J = 10.8, 2.0$ Hz, 1H), 4.17 (m, 1H), 4.03 (dd, $J = 10.8, 8.0$ Hz, 1H), 3.72 (m, 2H), 2.64 (m, 4H), 2.04 (m, 1H), 1.73 (m, 4H), 1.05 (d, $J = 7.0$ Hz, 3H).

Erythro 2-(5,6,7,8-Tetrahydro-1,4-naphthodioxan-2-yl)prop-1-yl methanesulfonate

Mesyl chloride (0.09 mL, 1.15 mmol) was added dropwise to a solution of *Erythro*-2-(5,6,7,8-Tetrahydro-1,4-naphthodioxan-2-yl)propan-1-ol (0.19 g, 0.76 mmol) and TEA (0.16 mL, 1.15 mmol) in DCM (10 mL) at 0°C. The reaction mixture was stirred at room temperature for 3 hours, diluted with DCM (15 mL), washed firstly with 10% aqueous $NaHCO_3$ (5 mL), secondly with 10% aqueous HCl (5 mL) and finally with 10% aqueous NaCl (10 mL), filtered and concentrated under vacuum to give 0.19 g of *Erythro* 2-(5,6,7,8-Tetrahydro-1,4-naphthodioxan-2-yl)prop-1-yl methanesulfonate as a yellowish oil.

Yield = 76.0%

1H NMR ($CDCl_3$): δ 6.59 (s, 2H), 4.33 (dd, J = 9.0, 7.2 Hz, 1H), 4.26 (dd, J = 9.5, 4.3 Hz, 1H), 4.20 (m, 2H), 4.01 (dd, J = 11.7, 8.8 Hz, 1H), 3.03 (s, 3H), 2.66 (m, 4H), 2.30 (m, 1H), 1.75 (m, 4H), 1.10 (d, J = 7.0 Hz, 3H).

(XXIII) *Erythro* 3-(2-(5,6,7,8-Tetrahydro-1,4-naphthodioxan-2-yl)prop-1-yloxy)-2,6-difluorobenzamide

A solution of 3-Hydroxy-2,6-difluorobenzamide (0.11 g, 0.61 mmol) in DMF (2 mL) was added to a solution of *Erythro* 2-(5,6,7,8-Tetrahydro-1,4-naphthodioxan-2-yl)prop-1-yl methanesulfonate (0.19 g, 0.58 mmol) and K₂CO₃ (0.088 g, 0.64 mmol) in DMF (2 mL) at RT. The reaction mixture was stirred at 70°C for 2 hours, concentrated under vacuum, diluted with Ethyl Acetate (20 mL) washed with 10% aqueous NaCl (5 x 10 mL), dried over Na₂SO₄, filtered and concentrated under vacuum to give a brown residue. Elution with 6/4 Cyclohexane/Ethyl acetate on silica gel and subsequent treatment with IPE (2 mL) gave 0.06 g of *Erythro* 3-(2-(5,6,7,8-Tetrahydro-1,4-naphthodioxan-2-yl)prop-1-yloxy)-2,6-difluorobenzamide as a white solid

Yield = 26.0%

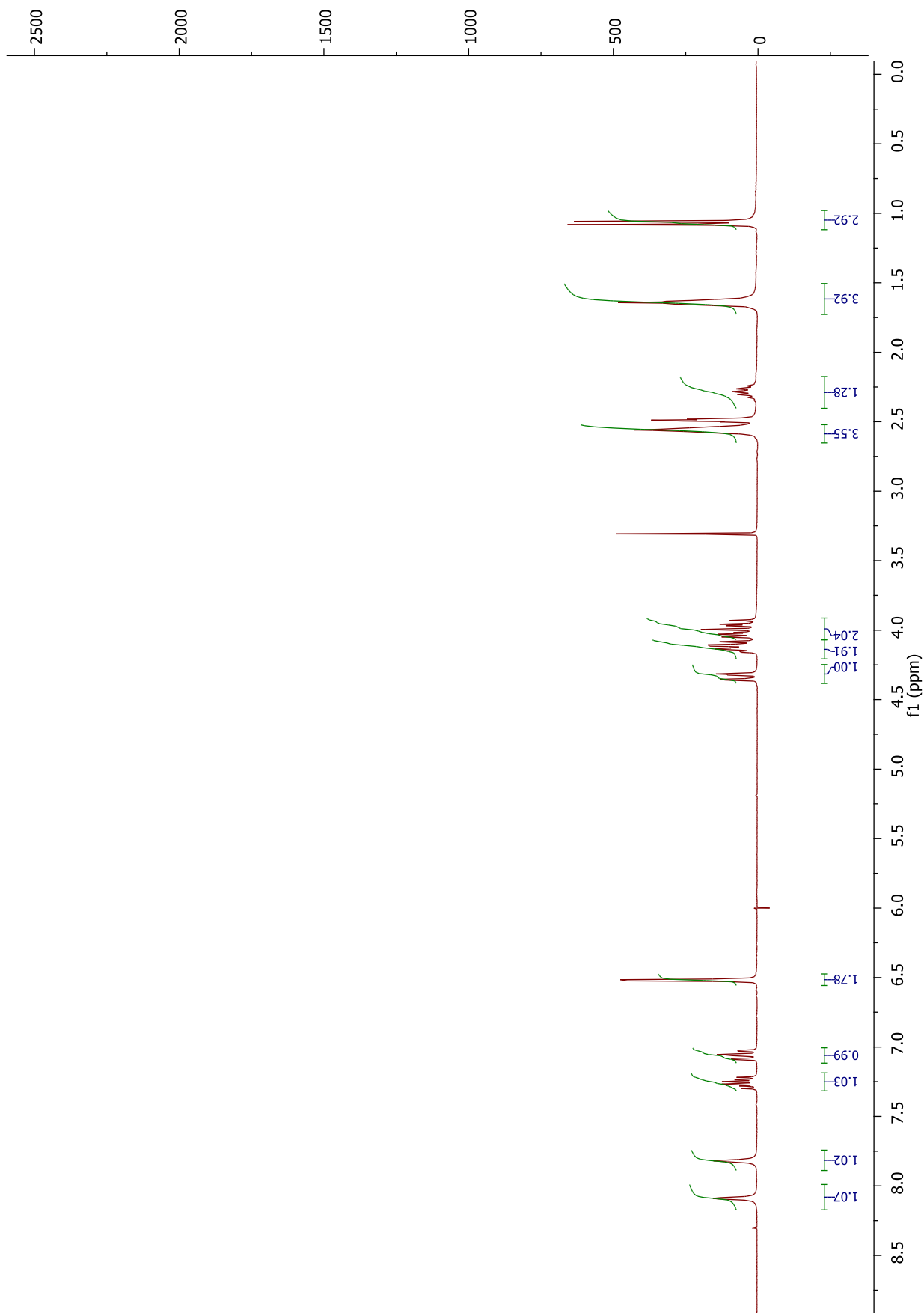
M.p. = 169.82°C

Tr HPLC, gradient, 90% H₂O with 0.10% TFA to 10% acetonitrile with 0.10% TFA in 25 min with 35 min run time. Flow rate: 1 mL/min) = 17.9 min, Purity = 95.4%

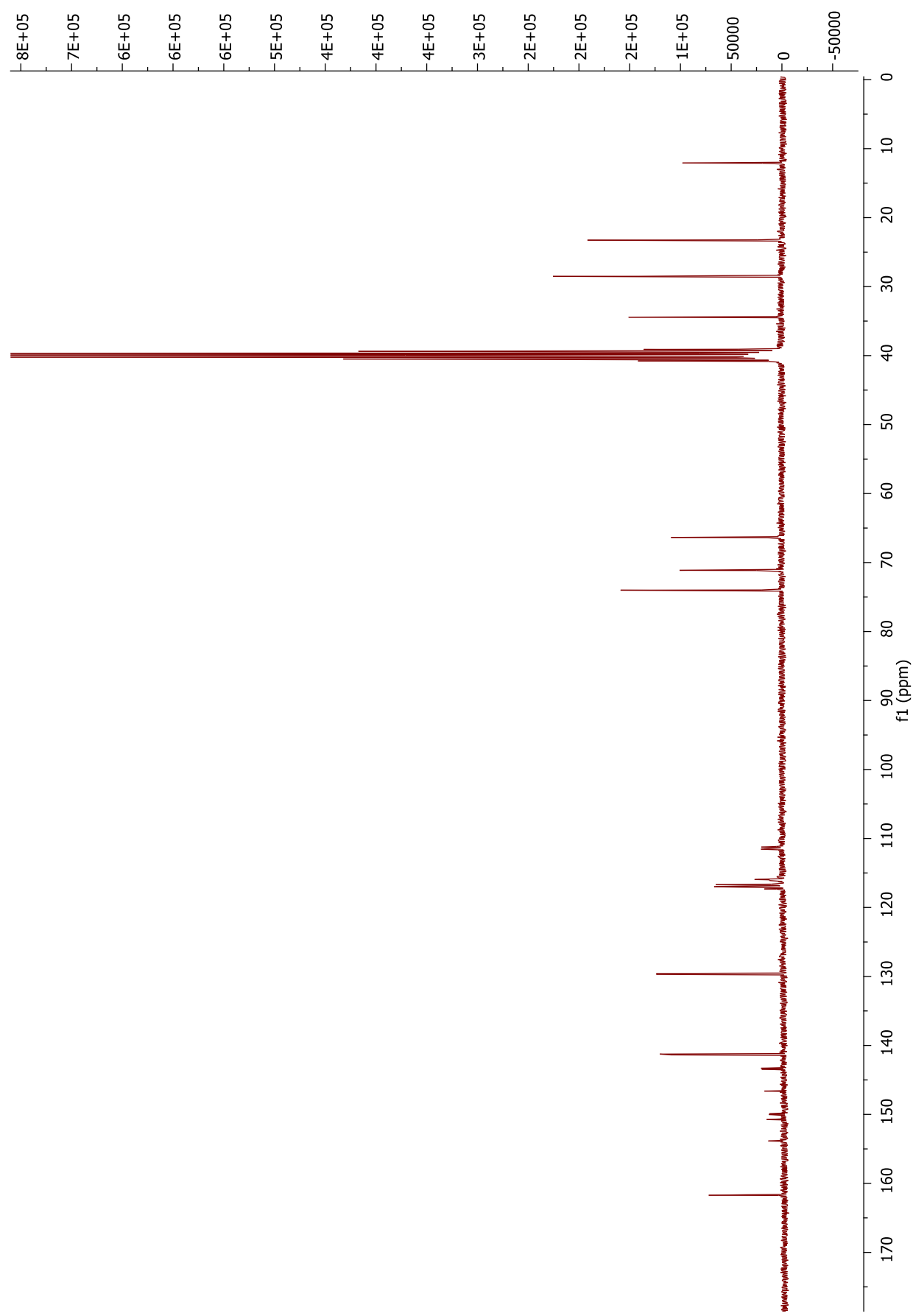
¹H NMR (d₆-DMSO): δ 8.09 (s, 1H), 7.82 (s, 1H), 7.26 (td, *J* = 9.3, 5.3 Hz, 1H), 7.06 (td, *J* = 9.0, 1.8 Hz, 1H), 6.52 (s, 1H), 6.51 (s, 1H), 4.34 (dd, *J* = 11.4, 1.9 Hz, 1H), 4.13 (m, 2H), 3.99 (m, 2H), 2.56 (m, 4H), 2.28 (m, 1H), 1.64 (m, 4H), 1.07 (d, *J* = 6.9 Hz, 3H).

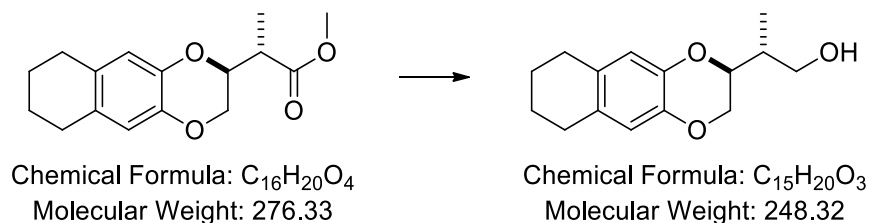
¹³C NMR (d₆-DMSO): δ 161.7, 152.3 (dd, *J* = 240.0, 6.7 Hz), 148.3 (dd, *J* = 246.8, 8.2 Hz), 143.4 (dd, *J* = 11.2, 3.0 Hz), 141.4, 141.3, 129.7, 129.6, 117.0 (dd, *J* = 21.2, 20.1 Hz), 117.0, 116.97, 116.7, 116.66, 116.0 (dd, *J* = 9.4, 1.9 Hz), 111.4 (dd, *J* = 22.9, 3.4 Hz), 74.0, 71.1, 66.4, 34.4, 28.5, 23.3, 12.1 ppm.

Experimental



Experimental

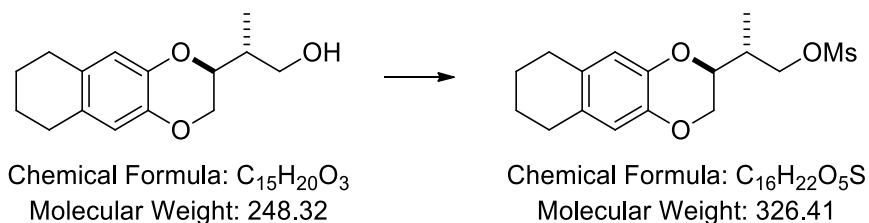


Threo 2-(5,6,7,8-tetrahydro-1,4-naphthodioxan-2-yl)propan-1-ol

LiAlH₄ (0.018 g, 0.47 mmol) was suspended in dry THF (2 mL) at 0°C under nitrogen atmosphere. The solution of *Threo* Methyl 2-(5,6,7,8-tetrahydro-1,4-naphthodioxan-2-yl)-2-methylacetate (0.13 g, 0.47 mmol) in THF (3 mL) was slowly added to the reaction. The mixture was then warmed to RT and stirred for 1 h; at completion, it was cooled to 0°C and slowly quenched with Ethyl acetate (5 mL). Further Ethyl acetate (10 mL) was added, the organic layer was washed with brine (3 × 10 mL), dried over Na₂SO₄ and concentrated under vacuum to give 0.12 g of *Threo*-2-(5,6,7,8-Tetrahydro-1,4-naphthodioxan-2-yl)propan-1-ol as a colourless oil.

Yield = Quantitative

¹H NMR (CDCl₃): δ 6.57 (s, 2H), 4.26 (dd, *J* = 9.3, 1.2 Hz, 1H), 4.01 (m, 2H), 3.75 (m, 2H), 2.64 (m, 4H), 2.01 (m, 1H), 1.71 (m, 4H), 1.03 (d, *J* = 7.0 Hz, 3H).

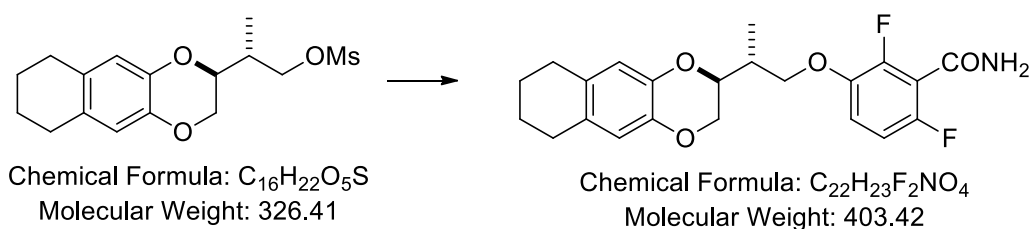
Threo 2-(5,6,7,8-Tetrahydro-1,4-naphthodioxan-2-yl)prop-1-yl methanesulfonate

Mesyl chloride (0.056 mL, 0.72 mmol) was added dropwise to a solution of *Threo*-2-(5,6,7,8-Tetrahydro-1,4-naphthodioxan-2-yl)propan-1-ol (0.12 g, 0.48 mmol) and TEA (0.10 mL, 0.72 mmol) in DCM (10 mL) at 0°C. The reaction mixture was stirred at room temperature for 3 hours, diluted with DCM (15 mL), washed firstly with 10% aqueous NaHCO₃ (5 mL), secondly with 10% aqueous HCl (5 mL) and finally with 10% aqueous NaCl (10 mL), filtered and concentrated under vacuum to give 0.12 g of *Threo* 2-(5,6,7,8-Tetrahydro-1,4-naphthodioxan-2-yl)prop-1-yl methanesulfonate as a yellowish oil.

Yield = 75.0%

¹H NMR (CDCl₃): δ 6.57 (s, 2H), 4.42 (dd, *J* = 9.7, 4.9 Hz, 1H), 4.32 (dd, *J* = 9.7, 3.8 Hz, 1H), 4.25 (m, 1H), 4.01 (m, 2H), 3.03 (s, 3H), 2.65 (m, 4H), 2.20 (m, 1H), 1.72 (m, 4H), 1.14 (d, *J* = 7.0 Hz, 3H).

(XXIII) *Threo* 3-(2-(5,6,7,8-Tetrahydro-1,4-naphthodioxan-2-yl)prop-1-yloxy)-
2,6-difluorobenzamide



A solution of 3-Hydroxy-2,6-difluorobenzamide (0.067 g, 0.386 mmol) in DMF (2 mL) was added to a solution of *Threo* 2-(5,6,7,8-Tetrahydro-1,4-naphthodioxan-2-yl)prop-1-yl methanesulfonate (0.12 g, 0.37 mmol) and K₂CO₃ (0.056 g, 0.41 mmol) in DMF (2 mL) at RT. The reaction mixture was stirred at 70°C for 2 hours, concentrated under vacuum, diluted with Ethyl Acetate (20 mL) washed with 10% aqueous NaCl (5 x 10 mL), dried over Na₂SO₄, filtered and concentrated under vacuum to give a brown residue. Elution with 6/4 Cyclohexane/Ethyl acetate on silica gel and subsequent treatment with IPE (1 mL) gave 0.025 g of *Threo* 3-(2-(5,6,7,8-Tetrahydro-1,4-naphthodioxan-2-yl)prop-1-yloxy)-2,6-difluorobenzamide as a white solid

Yield = 16.0%

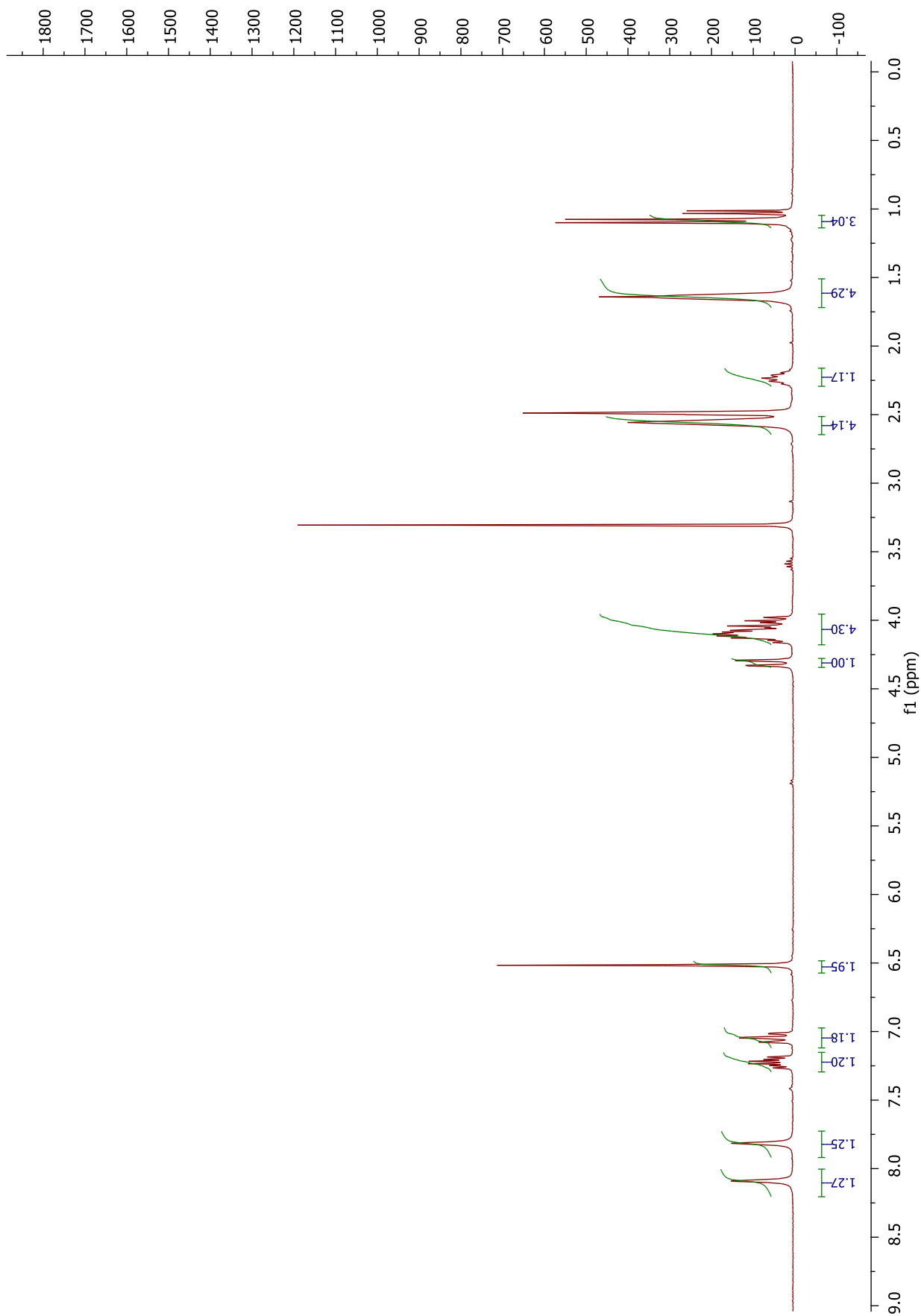
M.p. = 159.48°C

Tr HPLC, gradient, 90% H₂O with 0.10% TFA to 10% acetonitrile with 0.10% TFA in 25 min with 35 min run time. Flow rate: 1 mL/min) = 17.8 min, Purity = 96.7%

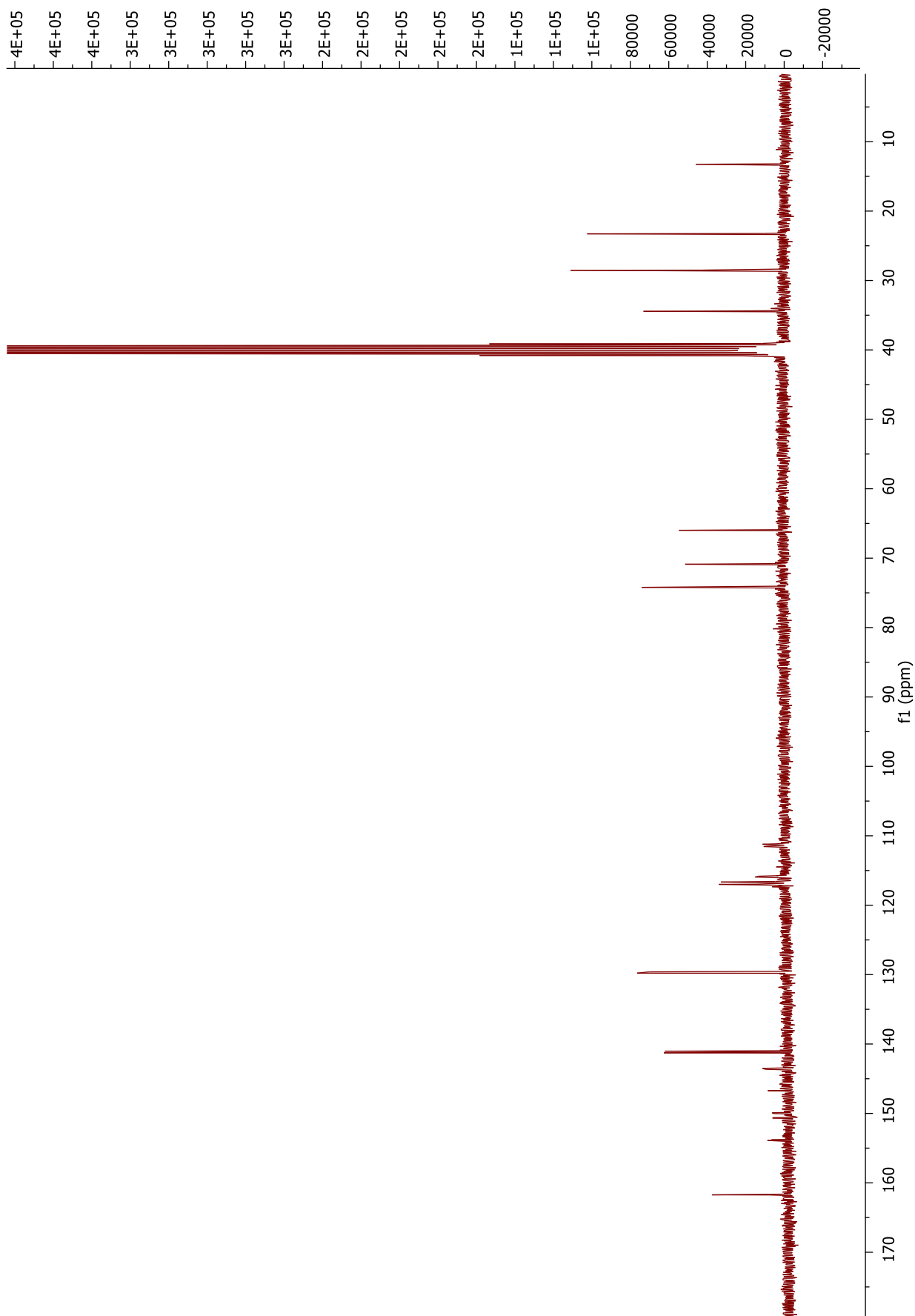
¹H NMR (d₆-DMSO): δ 8.09 (s, 1H), 7.82 (s, 1H), 7.23 (td, *J* = 9.3, 5.3 Hz, 1H), 7.04 (td, *J* = 9.0, 1.7 Hz, 1H), 6.52 (s, 2H), 4.31 (dd, *J* = 11.2, 1.5 Hz, 1H), 4.08 (m, 4H), 2.56 (m, 4H), 2.23 (m, 1H), 1.64 (m, 4H), 1.09 (d, *J* = 7.0 Hz, 3H).

¹³C NMR (d₆-DMSO): δ 161.7, 152.2 (dd, *J* = 240.0, 6.7 Hz), 148.3 (dd, *J* = 246.7, 8.2 Hz), 143.6 (dd, *J* = 10.8, 3.3 Hz), 141.3, 141.0, 129.8, 129.6, 117.0 (dd, *J* = 24.2, 21.3 Hz), 117.0, 116.99, 116.7, 116.66, 115.9 (dd, *J* = 9.0, 2.0 Hz), 111.4 (dd, *J* = 22.3, 2.8 Hz), 74.2, 70.9, 66.0, 34.4, 28.5, 23.3, 13.3 ppm.

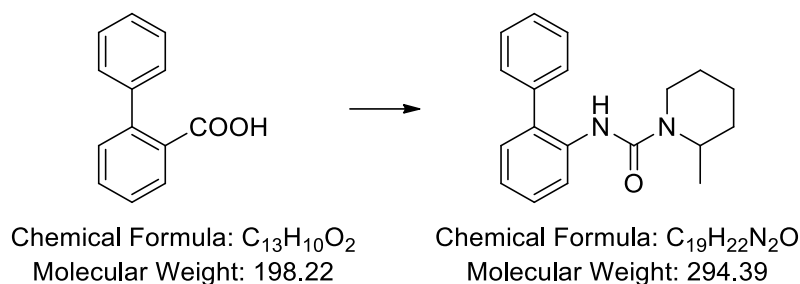
Experimental



Experimental



(XXIV) 1-(2-Biphenyl)-3-(2-methylpiperdin-1-yl)urea



Diphenyl phosphoryl azide (DPPA) (2.71 mL, 12.10 mmol) was added dropwise to a solution of Biphenyl-2-carboxylic acid (2.00 g, 10.09 mmol) and TEA (1.69 mL, 12.10 mmol) in Toluene (20 mL). The reaction mixture was stirred at RT for 20 min, heated at 95°C, and then stirred again for 20 min. The mixture was cooled at RT, added with 2-Methylpiperidine (1.25 mL, 10.59 mmol), heated again at 95°C and stirred overnight. Then, the mixture was diluted with Ethyl acetate (30 mL), washed twice with 10% aqueous $NaHCO_3$, dried over Na_2SO_4 , filtered, and concentrated under vacuum to give a residue, which was purified by flash chromatography. Elution with Cyclohexane/Ethyl acetate 80/20 and subsequent crystallization from IPA (4 vol) gave 1.02 g of 1-(2-Biphenyl)-3-(2-methylpiperdin-1-yl)urea as a white solid.

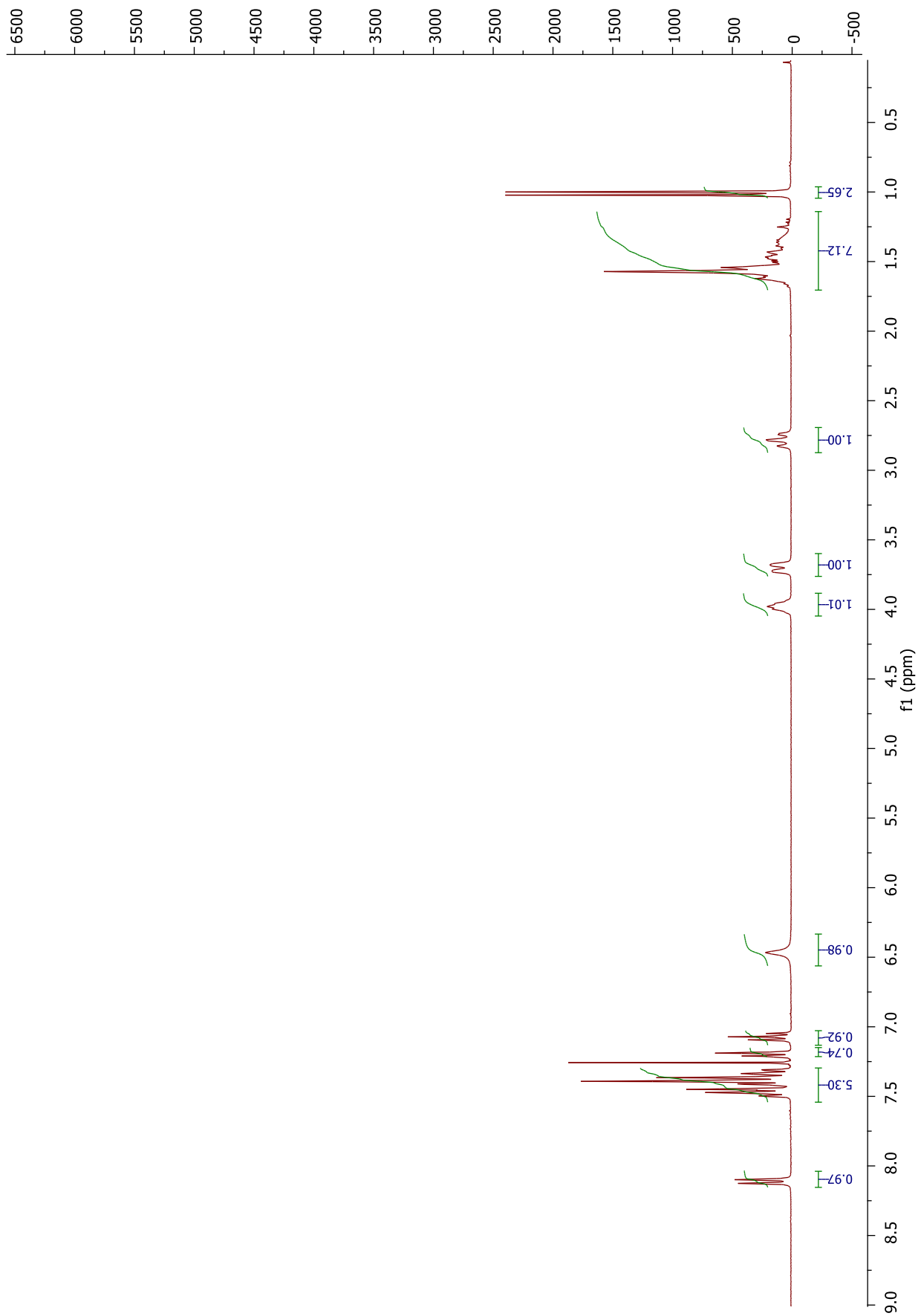
Yield = 35.0%

M.p. = 104.0°C

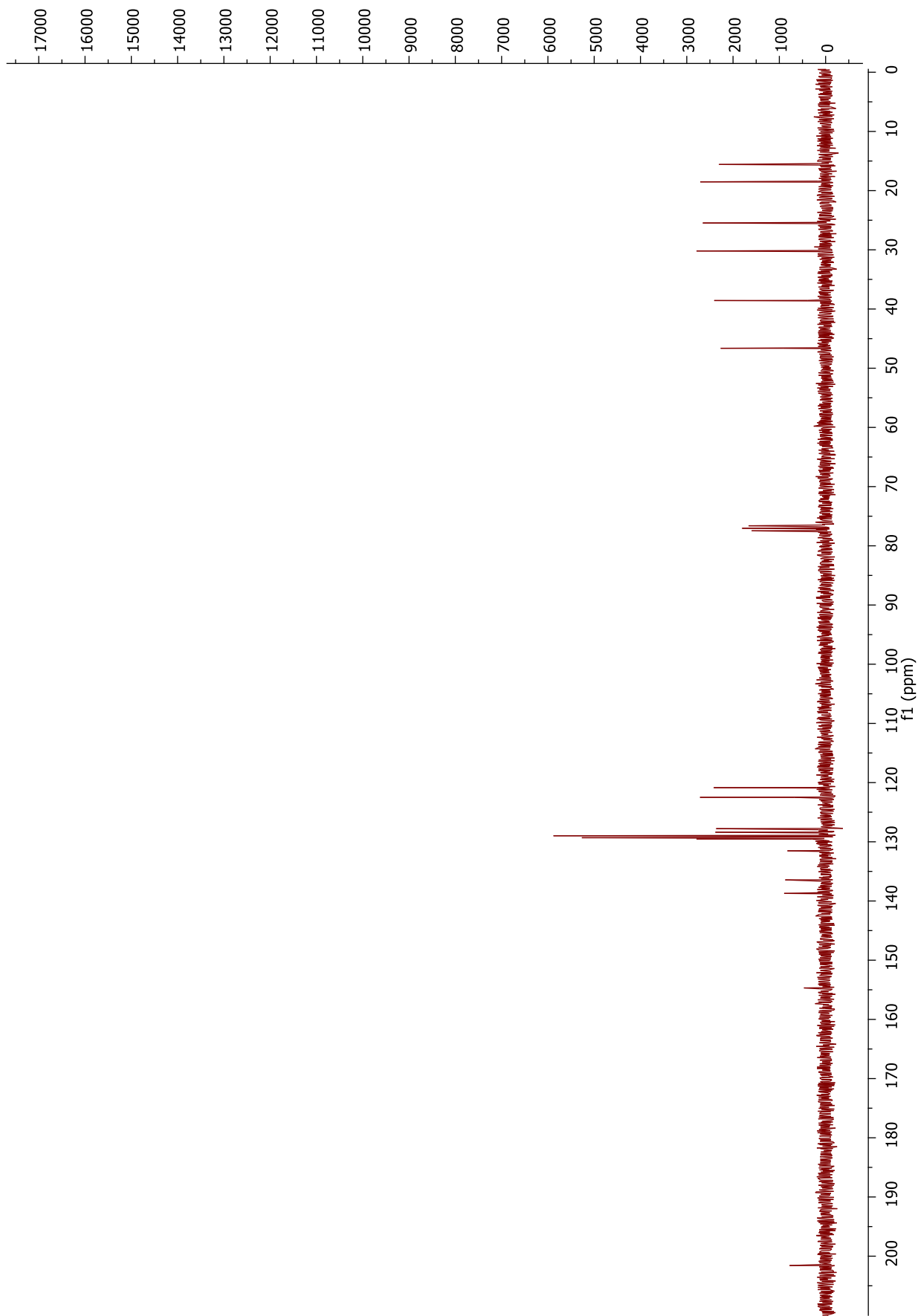
Tr (HPLC, Isocratic, H_2O with 0.10% TFA / Acetonitrile with 0.10% TFA 55/45. 30 min run time. Flow rate: 1 mL/min) = 10.67 min, Purity = 96.4%

1H NMR ($CDCl_3$): δ 8.11 (d, $J = 8.1$ Hz, 1H), 7.41 (m, 6H), 7.20 (dd, $J = 7.6, 1.6$ Hz, 1H), 7.07 (td, $J = 7.6, 0.9$ Hz, 1H), 6.47 (bs, 1H), 3.98 (m, 1H), 3.70 (d, $J = 12.6$ Hz, 1H), 2.78 (t, $J = 12.6$ Hz, 1H), 1.44 (m, 6H), 1.01 ppm (d, $J = 6.9$ Hz, 3H).

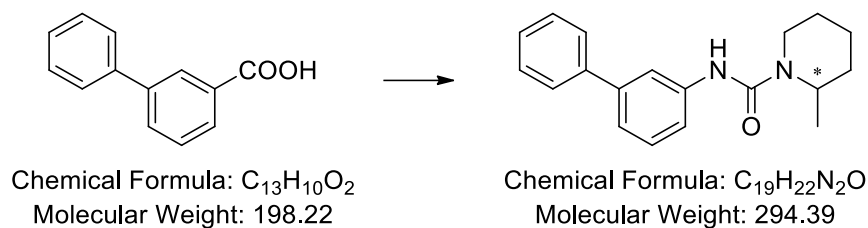
^{13}C NMR ($CDCl_3$): δ 154.68, 138.72, 136.43, 131.52, 129.52, 129.32, 128.98, 128.38, 127.77, 122.49, 120.85, 46.62, 38.57, 30.19, 25.46, 18.52, 15.58 ppm.



Experimental



(XXV) 1-(3-Biphenyl)-3-(2-methylpiperidin-1-yl)urea



Diphenyl phosphoryl azide (DPPA) (2.71 mL, 12.10 mmol) was added dropwise to a solution of Biphenyl-3-carboxylic acid (2.00 g, 10.09 mmol) and TEA (1.69 mL, 12.10 mmol) in Toluene (20 mL). The reaction mixture was stirred at RT for 20 min, heated at 95°C, and then stirred again for 20 min. The mixture was cooled at RT, added with 2-Methylpiperidine (1.25 mL, 10.59 mmol), heated again at 95°C and stirred overnight. Then, the mixture was diluted with Ethyl acetate (30 mL), washed twice with 10% aqueous $NaHCO_3$, dried over Na_2SO_4 , filtered, and concentrated under vacuum to give a residue, which was purified by flash chromatography. Elution with Cyclohexane/Ethyl acetate 80/20 and subsequent crystallization from IPA (4 vol) gave 0.52 g of 1-(3-Biphenyl)-3-(2-methylpiperidin-1-yl)urea as a white solid.

Yield = 17.0%

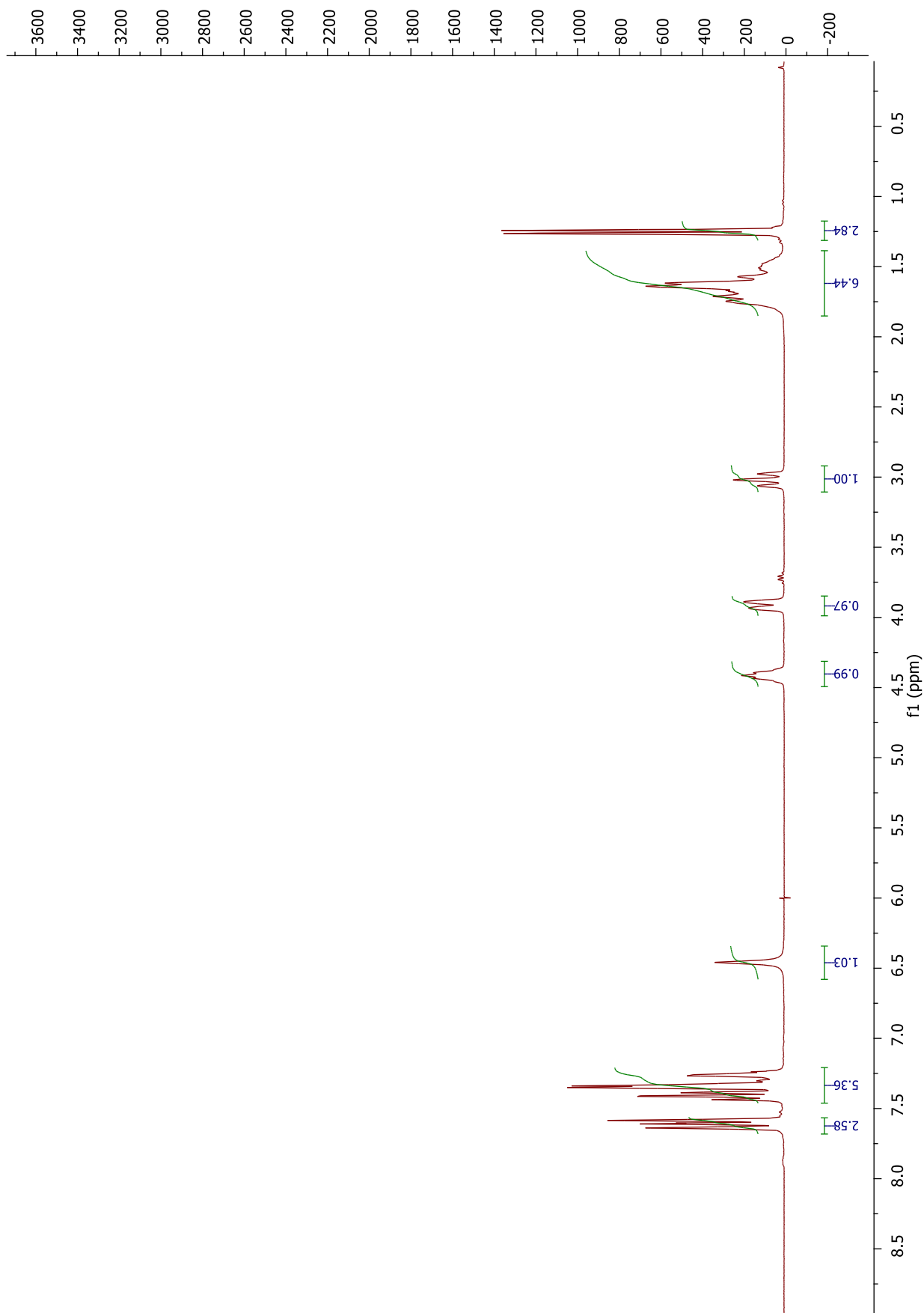
M.p. = 126.5°C

Tr (HPLC, Isocratic, H_2O with 0.10% TFA / Acetonitrile with 0.10% TFA 55/45. 30 min run time. Flow rate: 1 mL/min) = 12.67 min, Purity = 99.3%

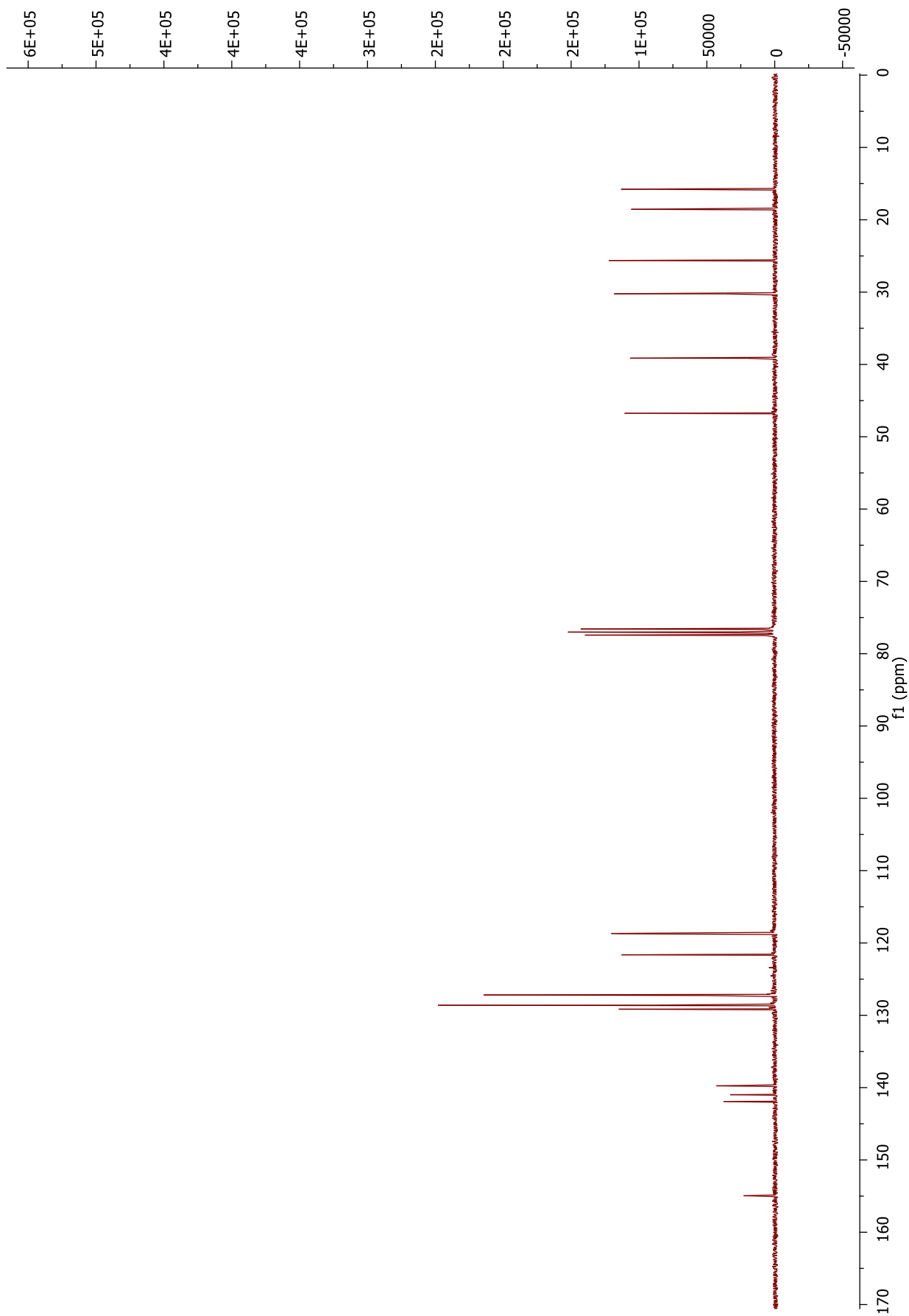
1H NMR ($CDCl_3$): δ 7.65 (m, 3H), 7.32 (m, 6H), 6.46 (bs, 1H), 4.41 (m, 1H), 3.91 (d, $J = 13.0$ Hz, 1H), 3.02 (t, $J = 13.0$ Hz, 1H), 1.64 (m, 6H), 1.25 ppm (d, $J = 6.9$ Hz, 3H).

^{13}C NMR ($CDCl_3$): δ 154.94, 141.91, 140.98, 139.75, 129.16, 128.61, 127.26, 127.18, 121.64, 118.72, 118.68, 46.76, 39.13, 30.23, 25.63, 18.55, 15.77 ppm.

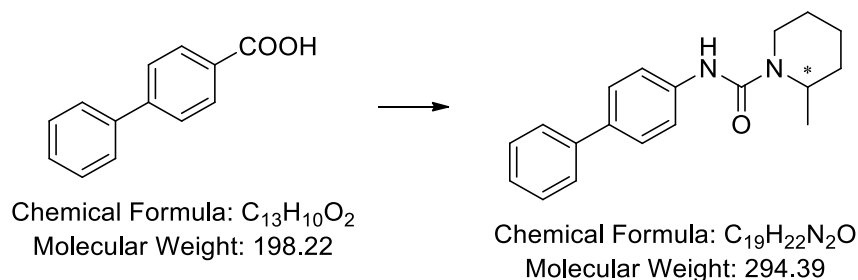
Experimental



Experimental



(XXVI) 1-(4-Biphenyl)-3-(2-methylpiperdin-1-yl)urea



Diphenyl phosphoryl azide (DPPA) (2.71 mL, 12.10 mmol) was added dropwise to a solution of Biphenyl-4-carboxylic acid (2.00 g, 10.09 mmol) and TEA (1.69 mL, 12.10 mmol) in Toluene (20 mL). The reaction mixture was stirred at RT for 20 min, heated at 95°C, and then stirred again for 20 min. The mixture was cooled at RT, added with 2-Methylpiperidine (1.25 mL, 10.59 mmol), heated again at 95°C and stirred overnight. Then, the mixture was diluted with Ethyl acetate (30 mL), washed twice with 10% aqueous $NaHCO_3$, dried over Na_2SO_4 , filtered, and concentrated under vacuum to give a residue, which was purified by flash chromatography. Elution with Cyclohexane/Ethyl acetate 80/20 and subsequent crystallization from EtOH (15 vol) gave 0.85 g of 1-(4-Biphenyl)-3-(2-methylpiperdin-1-yl)urea as a white solid.

Yield = 29.0%

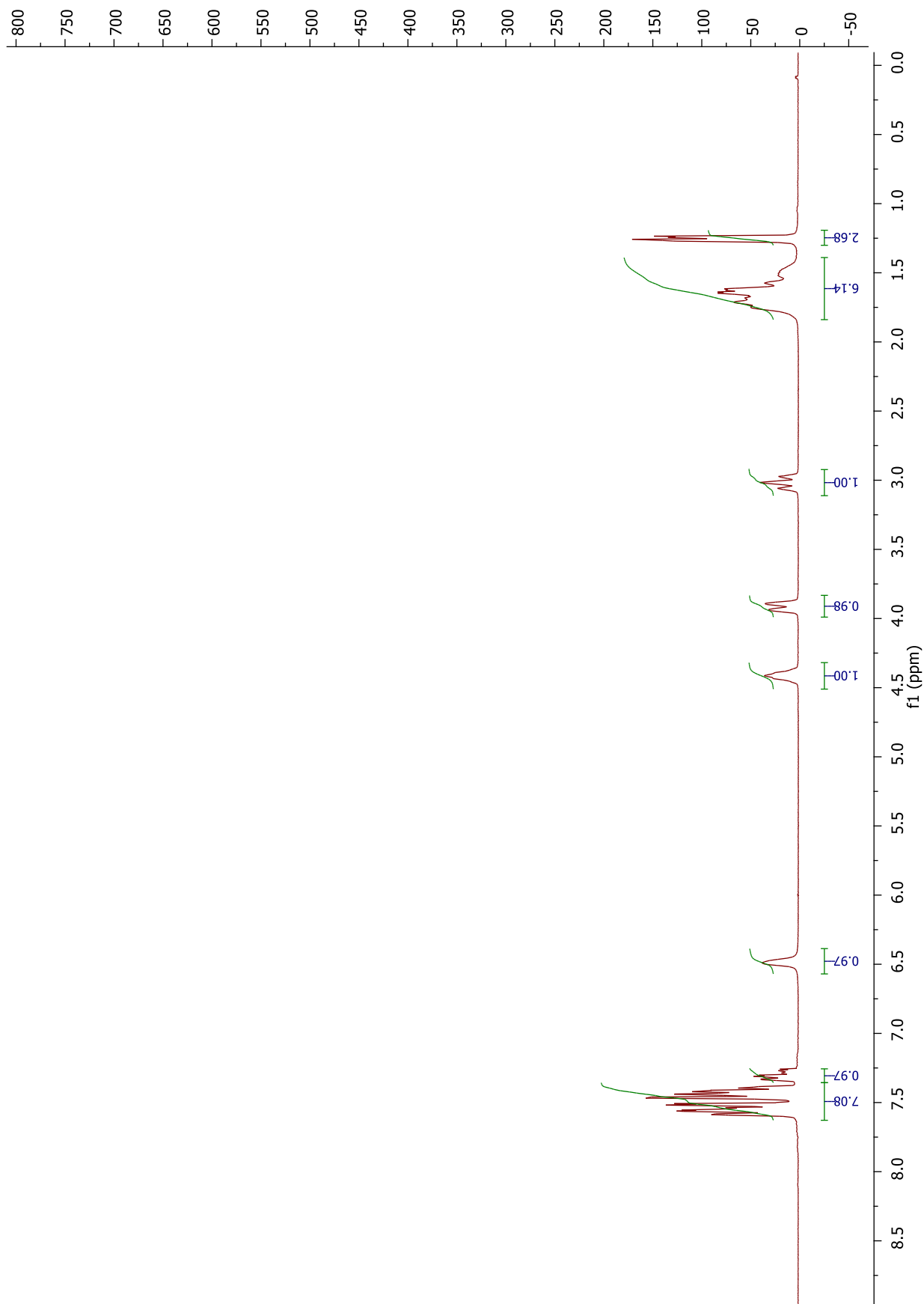
M.p. = 164.2°C

Tr (HPLC, Isocratic, H_2O with 0.10% TFA / Acetonitrile with 0.10% TFA 55/45. 30 min run time. Flow rate: 1 mL/min) = 12.65 min, Purity = 99.7%

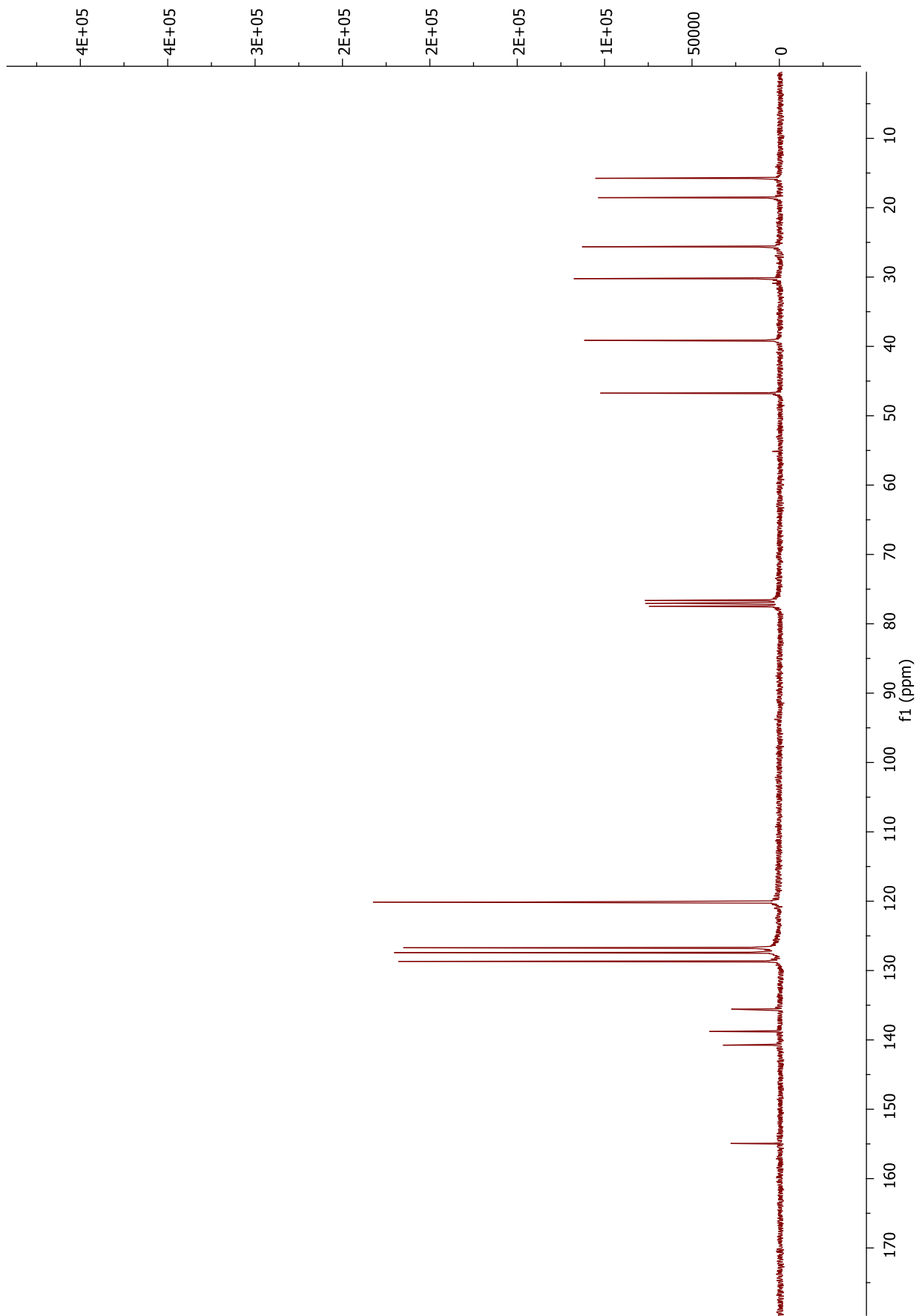
1H NMR ($CDCl_3$): δ 7.55 (m, 4H), 7.46 (m, 4H), 7.29 (m, 1H), 6.49 (bs, 1H), 4.39 (m, 1H), 3.91 (d, $J = 12.8$ Hz, 1H), 3.02 (t, $J = 12.8$ Hz, 1H), 1.62 (m, 6H), 1.25 ppm (d, $J = 6.8$ Hz, 3H).

^{13}C NMR ($CDCl_3$): δ 154.94, 140.76, 138.79, 135.57, 128.68, 127.41, 126.77, 126.71, 120.13, 46.74, 39.13, 30.23, 25.63, 18.55, 15.76 ppm.

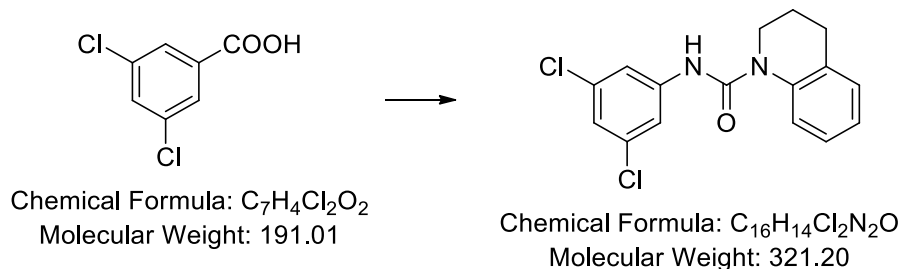
Experimental



Experimental



(XXVII) 1-(3,5-Dichlorophenyl)-3-(1,2,3,4-tetrahydroquinolin-1-yl)urea



Diphenyl phosphoryl azide (DPPA) (2.71 mL, 12.10 mmol) was added dropwise to a solution of 3,5-Dichlorobenzoic acid (2.00 g, 10.09 mmol) and TEA (1.69 mL, 12.10 mmol) in Toluene (20 mL). The reaction mixture was stirred at RT for 20 min, heated at 95°C, and then stirred again for 20 min. The mixture was cooled at RT, added with 1,2,3,4-Tetrahydroquinoline (1.25 mL, 10.59 mmol), heated again at 95°C and stirred overnight. Then, the mixture was diluted with Ethyl acetate (30 mL), washed twice with 10% aqueous $NaHCO_3$, dried over Na_2SO_4 , filtered, and concentrated under vacuum to give a residue, which was purified by flash chromatography. Elution with Cyclohexane/Ethyl acetate 80/20 and subsequent crystallization from EtOH (6 vol) gave 0.80 g of 1-(3,5-Dichlorophenyl)-3-(1,2,3,4-tetrahydroquinolin-1-yl)urea as a white solid.

Yield = 32.0%

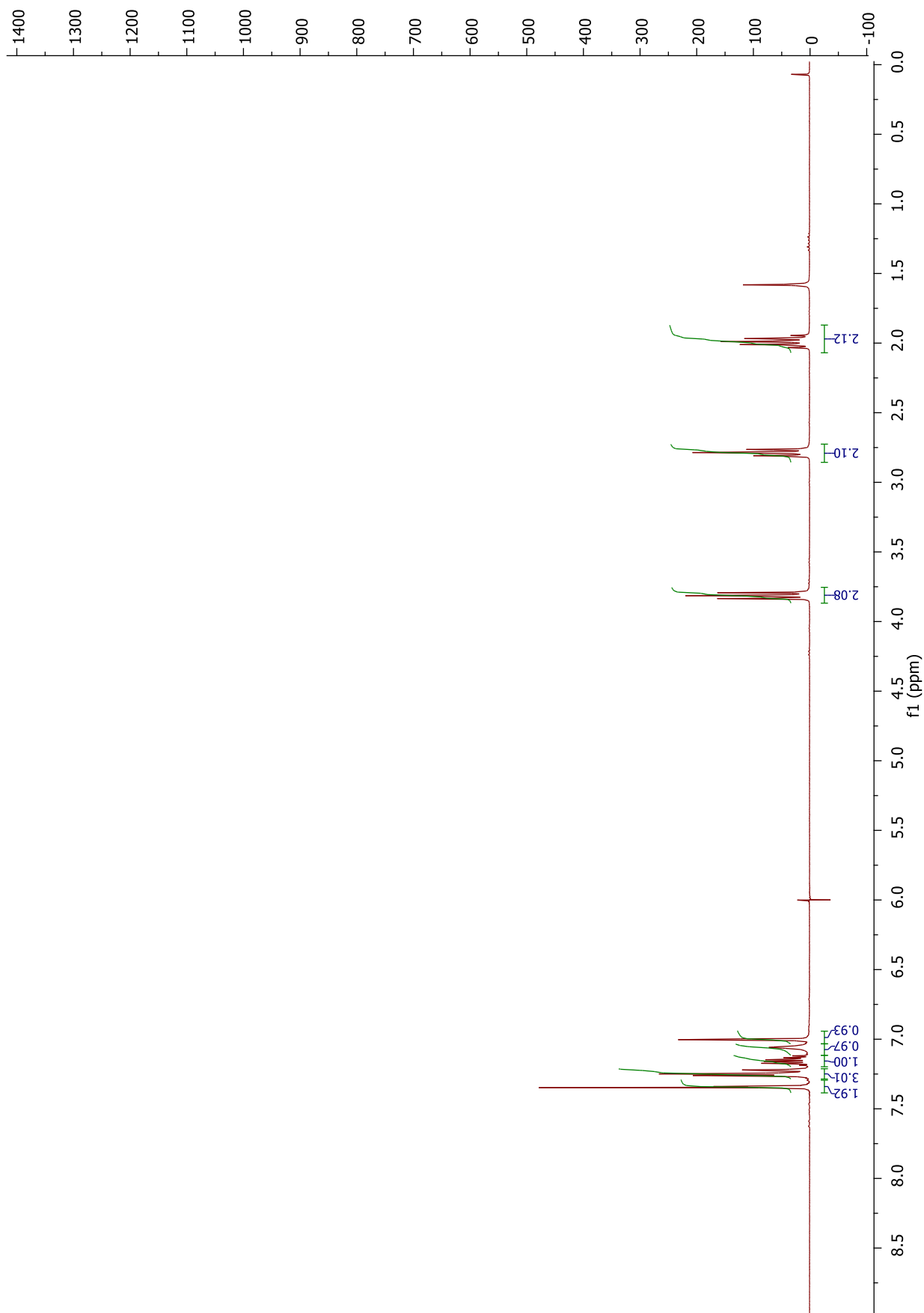
M.p. = 143.3°C

Tr (HPLC, Isocratic, H_2O with 0.10% TFA / Acetonitrile with 0.10% TFA 50/50. 30 min run time. Flow rate: 1.5 mL/min) = 12.47 min, Purity = 99.8%

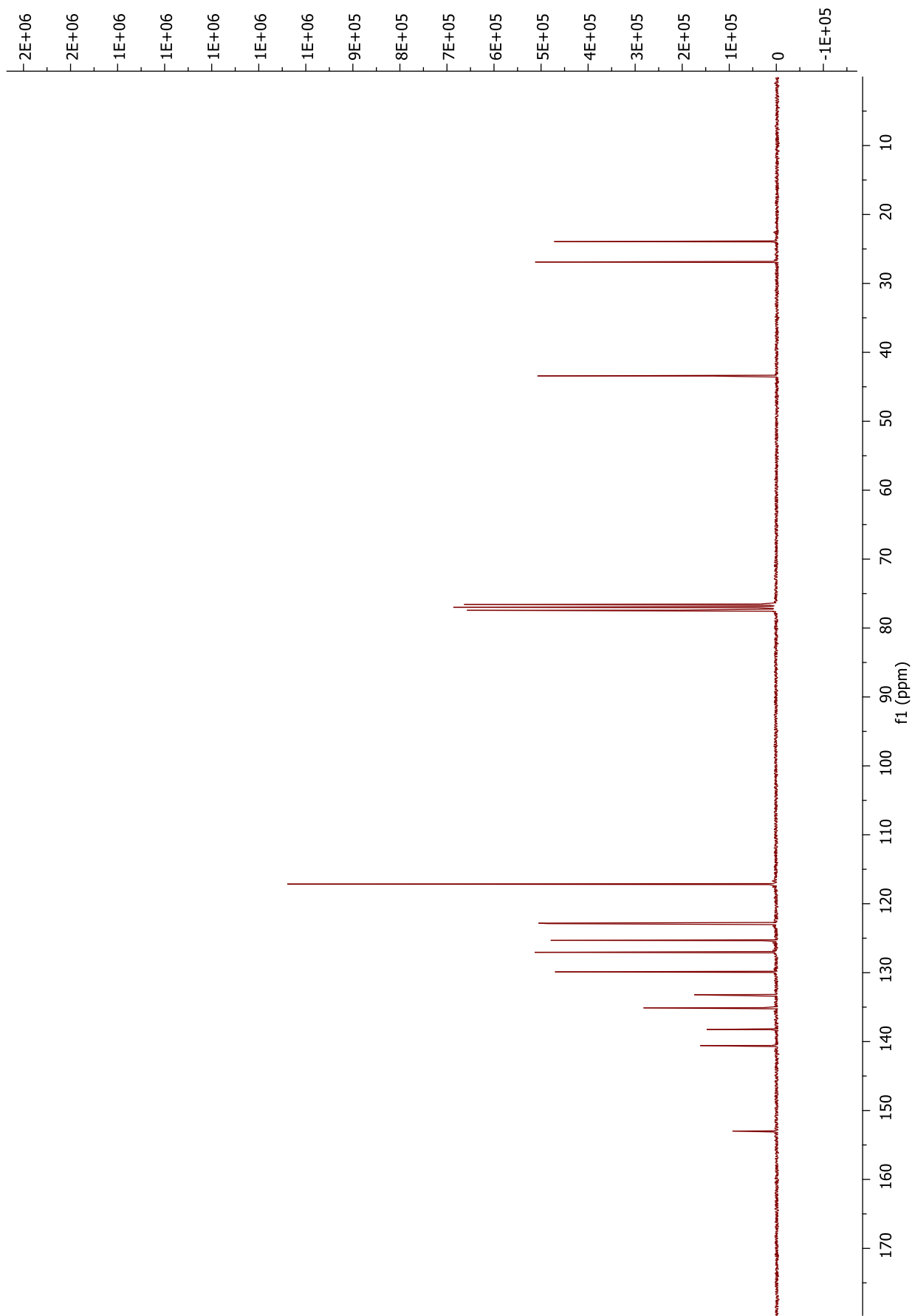
1H NMR ($CDCl_3$): δ 7.34 (d, $J = 1.9$ Hz, 2H), 7.25 (m, 3H), 7.15 (m, 1H), 7.06 (bs, 1H), 7.00 (t, $J = 1.8$ Hz, 1H), 3.81 (t, $J = 6.3$ Hz, 2H), 2.79 (t, $J = 6.7$ Hz, 2H), 1.98 ppm (m, 2H).

^{13}C NMR ($CDCl_3$): δ 152.98, 140.59, 138.25, 135.11, 133.21, 129.89, 127.05, 125.32, 122.88, 122.82, 117.15, 43.43, 26.90, 23.94 ppm.

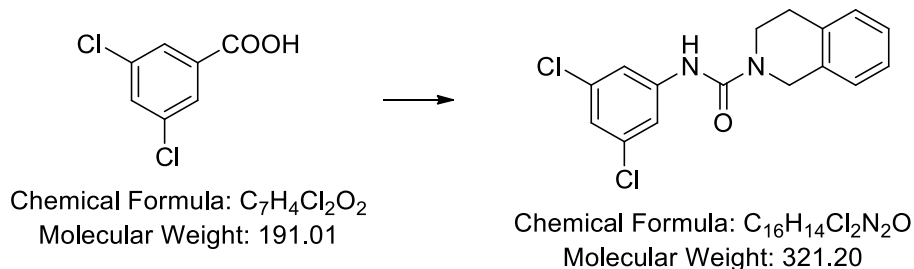
Experimental



Experimental



(XXVIII) 1-(3,5-Dichlorophenyl)-3-(1,2,3,4-tetrahydroisoquinolin-1-yl)urea



Diphenyl phosphoryl azide (DPPA) (2.71 mL, 12.10 mmol) was added dropwise to a solution of 3,5-Dichlorobenzoic acid (2.00 g, 10.09 mmol) and TEA (1.69 mL, 12.10 mmol) in Toluene (20 mL). The reaction mixture was stirred at RT for 20 min, heated at 95°C, and then stirred again for 20 min. The mixture was cooled at RT, added with 1,2,3,4-Tetrahydroisoquinoline (1.25 mL, 10.59 mmol), heated again at 95°C and stirred overnight. Then, the mixture was diluted with Ethyl acetate (30 mL), washed twice with 10% aqueous $NaHCO_3$, dried over Na_2SO_4 , filtered, and concentrated under vacuum to give a residue, which was purified by flash chromatography. Elution with Cyclohexane/Ethyl acetate 80/20 and subsequent crystallization from IPE (20 vol) gave 0.60 g of 1-(3,5-Dichlorophenyl)-3-(1,2,3,4-tetrahydroisoquinolin-1-yl)urea as a white solid.

Yield = 24.0%

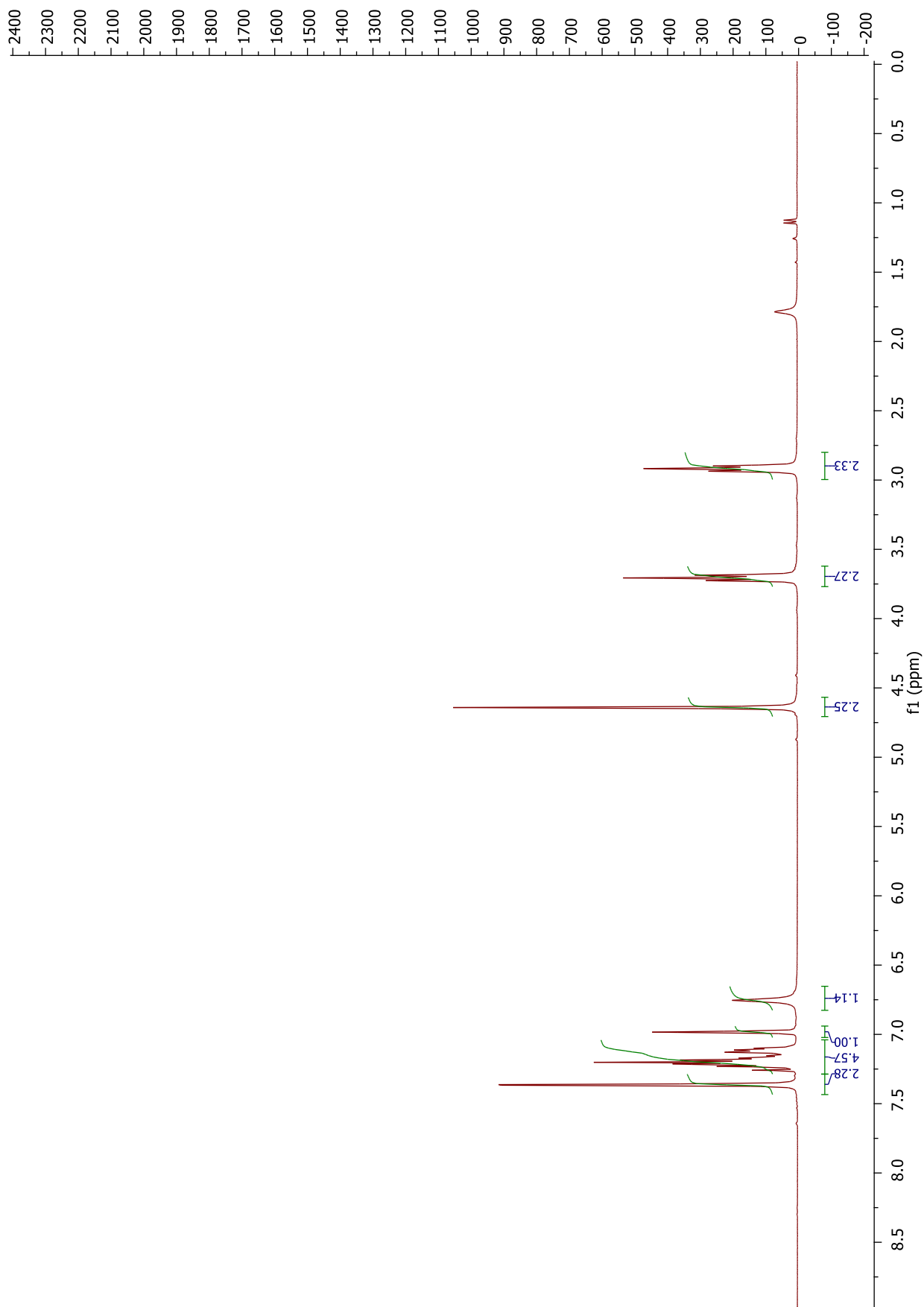
M.p. = 128.8°C

Tr (HPLC, Isocratic, H_2O with 0.10% TFA / Acetonitrile with 0.10% TFA 50/50. 30 min run time. Flow rate: 1.5 mL/min) = 9.00 min, Purity = 99.9%

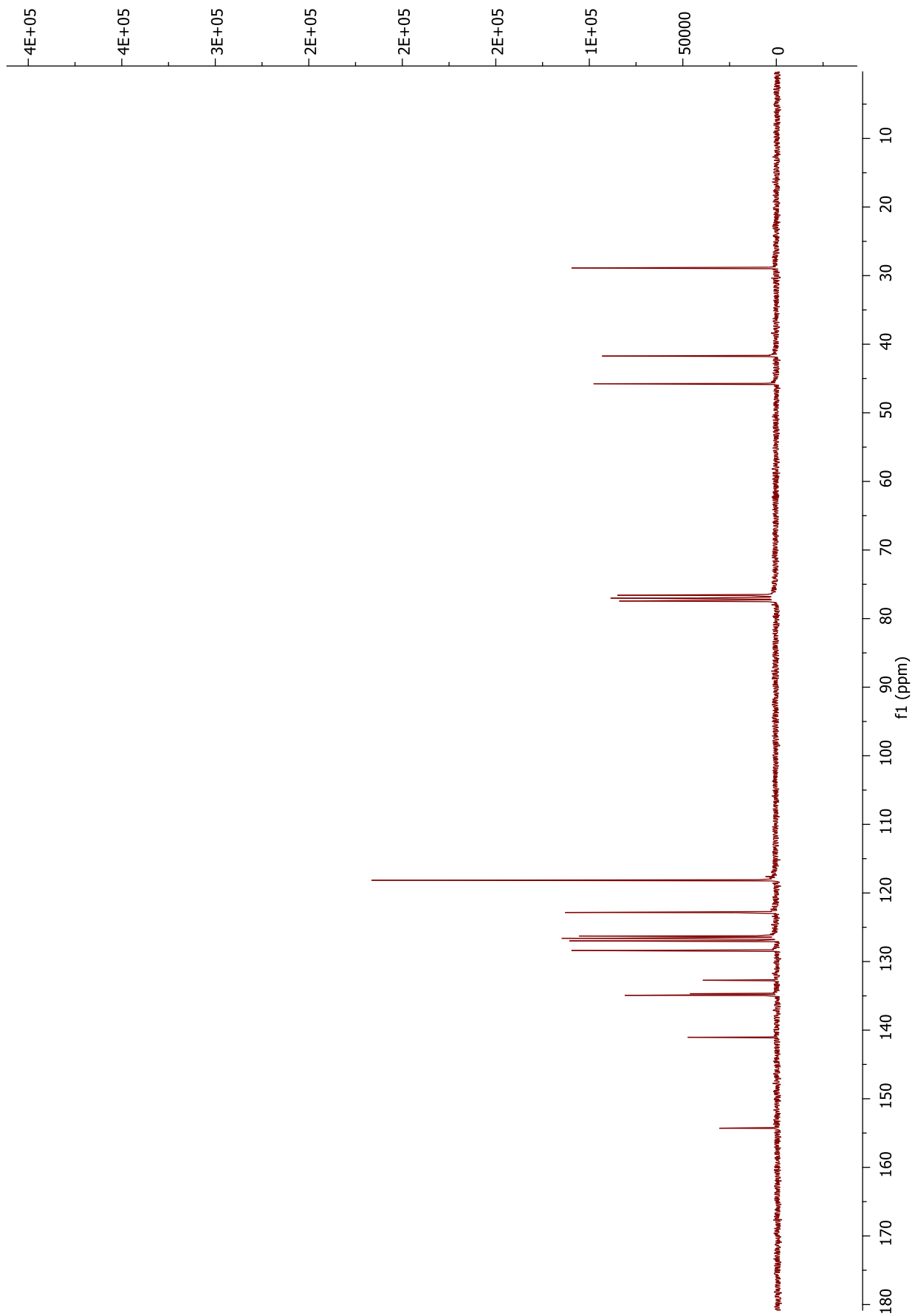
1H NMR ($CDCl_3$): δ 7.36 (d, J = 1.5 Hz, 2H), 7.18 (m, 4H), 6.98 (s, 1H), 6.75 (bs, 1H), 4.64 (s, 2H), 3.71 (t, J = 5.8 Hz, 2H), 2.92 ppm (t, J = 5.7 Hz, 2H).

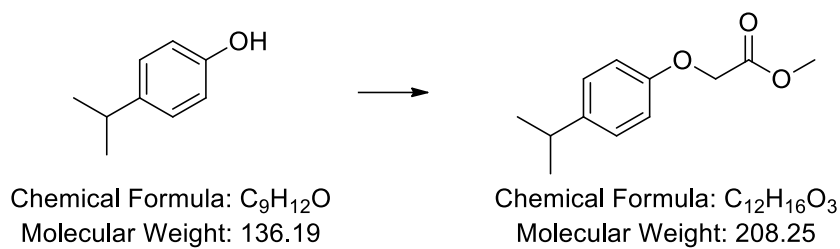
^{13}C NMR ($CDCl_3$): δ 154.29, 141.04, 134.92, 134.68, 132.73, 128.39, 126.99, 126.61, 126.29, 122.85, 118.15, 45.77, 41.73, 28.89 ppm.

Experimental



Experimental

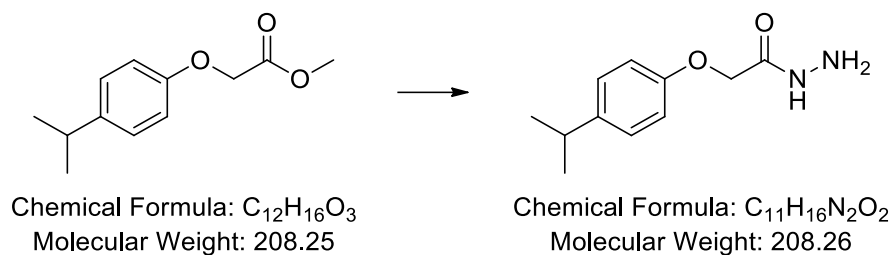


Methyl 4-*i*-propylphenoxyacetate

Methyl chloroacetate (0.71 mL, 8.01 mmol) was added to a solution of 4-Isopropylphenol (1.00 g, 7.34 mmol) and Potassium carbonate (1.12 g, 8.01 mmol) in DMF (10 mL). The reaction mixture was stirred at 50°C for 1.5 h, concentrated under vacuum, diluted with Ethyl acetate (30 mL), washed with brine (4 × 10 mL), dried over Na₂SO₄, filtered, and then concentrated under vacuum to give 1.4 g of Methyl 4-*i*-propylphenoxyacetate as a yellowish oil.

Yield = 92.0%

¹H NMR (CDCl₃): δ 7.14 (d, J = 8.7 Hz, 2H), 6.84 (d, J = 8.7 Hz, 2H), 4.61 (s, 2H), 3.80 (s, 3H), 2.86 (set, J = 6.9 Hz, 1H), 1.22 ppm (d, J = 6.9 Hz, 6H).

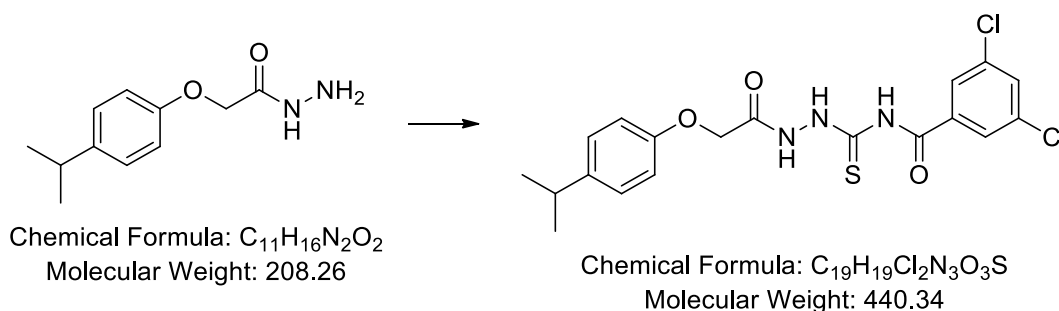
4-*i*-Propylphenoxyacetohydrazide

Hydrazine hydrate (2.1 mL, 33.60 mmol) was added to a solution of Methyl 4-*i*-propylphenoxyacetate (1.40 g, 6.72 mmol) in Methanol (15 mL). The reaction mixture was stirred at reflux for 16 h, concentrated under vacuum, diluted with Ethyl acetate (30 mL), washed with brine (10 mL), dried over Na_2SO_4 , filtered, and concentrated under vacuum to give 1.36 g of 4-*i*-Propylphenoxyacetohydrazide as a white solid.

Yield = 97.0%

M.p. = 105.2°C

1H NMR ($CDCl_3$): δ 7.16 (d, J = 8.2 Hz, 2H), 6.83 (d, J = 8.2 Hz, 2H), 4.55 (s, 2H), 2.87 (set, J = 6.9 Hz, 1H), 1.22 ppm (d, J = 6.9 Hz, 6H).

(XXIX) 1-(4-*i*-Propylphenoxyacetyl)-4-(3,5-dichlorobenzoyl)thiosemicarbazide

A solution of 3,5-Dichlorobenzoic acid (1.30 g, 6.8 mmol) in $SOCl_2$ (6.5 mL) was stirred at reflux for 1 h. Thus, the solution was concentrated under vacuum, diluted with Acetonitrile (15 mL), and then added with Potassium thiocyanate (1.12 g, 11.56 mmol). The reaction mixture was stirred at RT for 1 h, added with a solution of 4-*i*-Propylphenoxyacetohydrazide (1.40 g, 6.8 mmol) in DMF (5 mL), stirred at RT for 30 min, concentrated under vacuum, diluted with Ethyl acetate (50 mL), washed with brine (4×10 mL), dried over Na_2SO_4 , filtered, and then concentrated under vacuum to give a solid. Digestion firstly with MeOH (15 vol) at reflux and secondly with ACN (15 vol) at reflux gave 1.3 g of 1-(4-*i*-Propylphenoxyacetyl)-4-(3,5-dichlorobenzoyl)thiosemicarbazide as a yellowish solid.

Yield = 43.0%

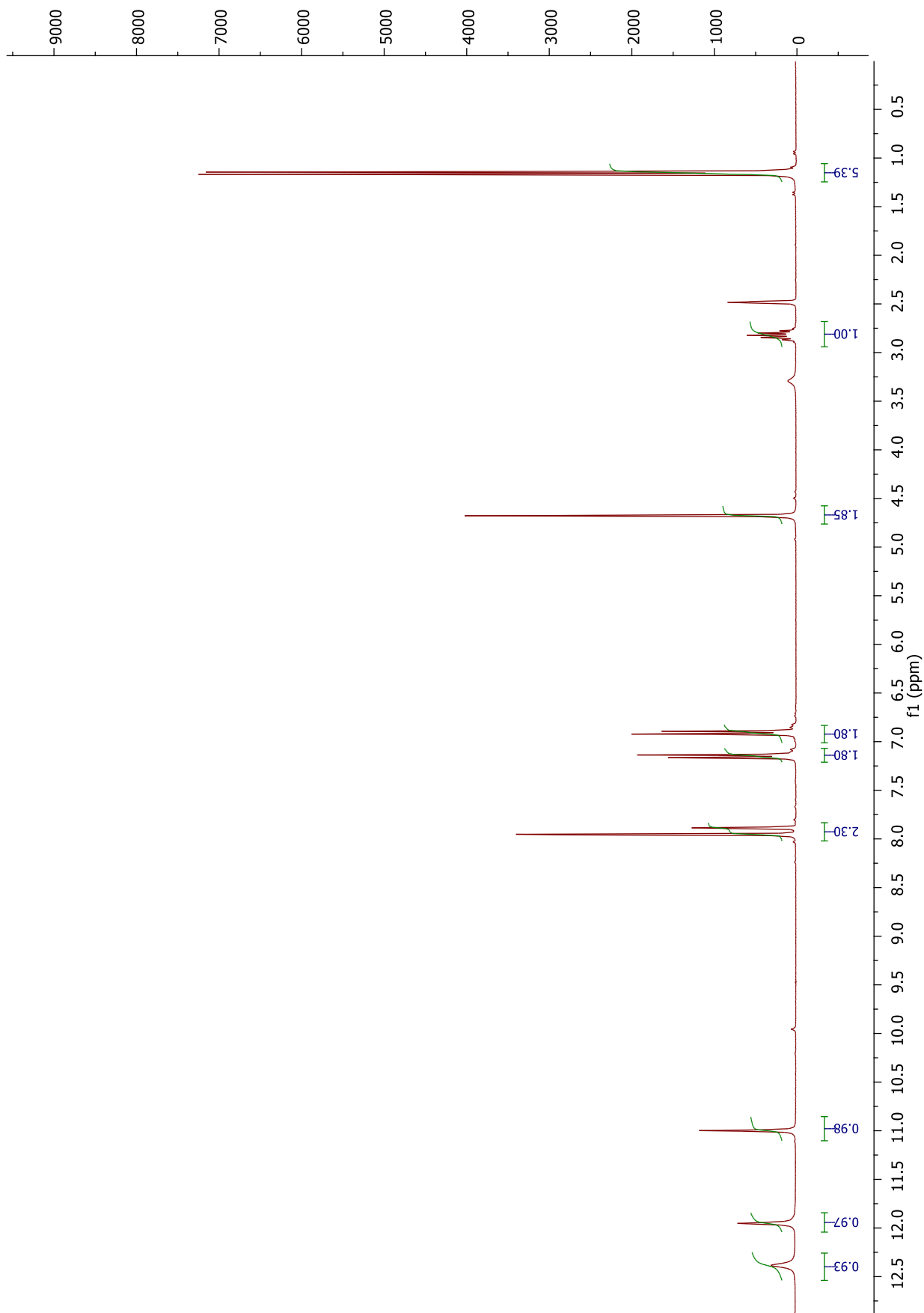
M.p. = 195.7°C

Tr (HPLC, Isocratic, H_2O with 0.10% TFA / Acetonitrile with 0.10% TFA 50/50. 30 min run time. Flow rate: 1.5 mL/min) = 17.60 min, Purity = 99.6%

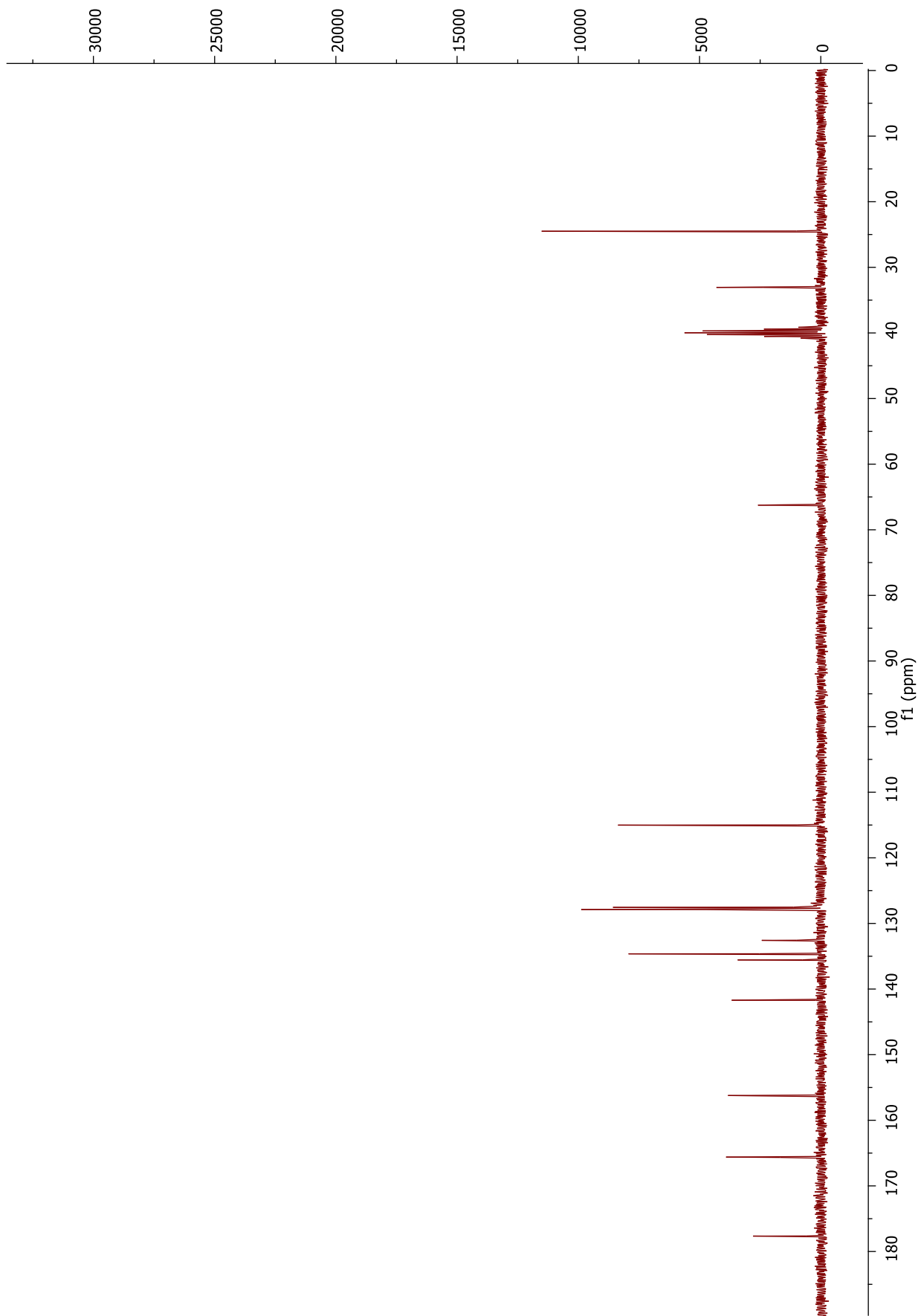
1H NMR (d_6 -DMSO): δ 12.38 (bs, 1H), 11.95 (bs, 1H), 11.00 (bs, 1H), 7.96 (d, $J = 1.8$ Hz, 2H), 7.89 (t, $J = 1.8$ Hz, 1H), 7.15 (d, $J = 8.6$ Hz, 2H), 6.91 (d, $J = 8.6$ Hz, 2H), 4.68 (s, 2H), 2.82 (set, $J = 6.9$ Hz, 1H), 1.16 ppm (d, $J = 6.9$ Hz, 6H).

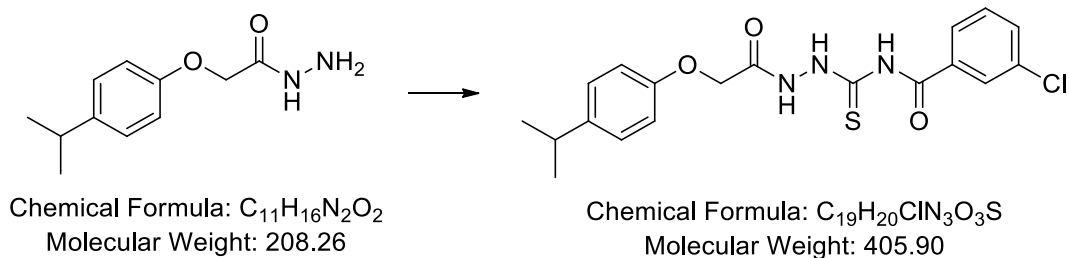
^{13}C NMR (d_6 -DMSO): δ 177.66, 165.66, 165.61, 156.23, 141.70, 135.56, 134.63, 132.58, 127.88, 127.55, 115.02, 66.24, 33.06, 24.50 ppm.

Experimental



Experimental



(XXX) 1-(4-*i*-Propylphenoxyacetyl)-4-(3-chlorobenzoyl)thiosemicarbazide

A solution of 3-Chlorobenzoic acid (1.30 g, 6.8 mmol) in $SOCl_2$ (6.5 mL) was stirred at reflux for 1 h. Thus, the solution was concentrated under vacuum, diluted with Acetonitrile (15 mL), and then added with Potassium thiocyanate (1.12 g, 11.56 mmol). The reaction mixture was stirred at RT for 1 h, added with a solution of 4-*i*-Propylphenoxyacetohydrazide (1.40 g, 6.8 mmol) in DMF (5 mL), stirred at RT for 30 min, concentrated under vacuum, diluted with Ethyl acetate (50 mL), washed with brine (4 × 10 mL), dried over Na_2SO_4 , filtered, and then concentrated under vacuum to give a solid. Digestion firstly with IPA (10 vol) at reflux gave 1.06 g of 1-(4-*i*-Propylphenoxyacetyl)-4-(3-chlorobenzoyl)thiosemicarbazide as a pale yellow solid.

Yield = 27.0%

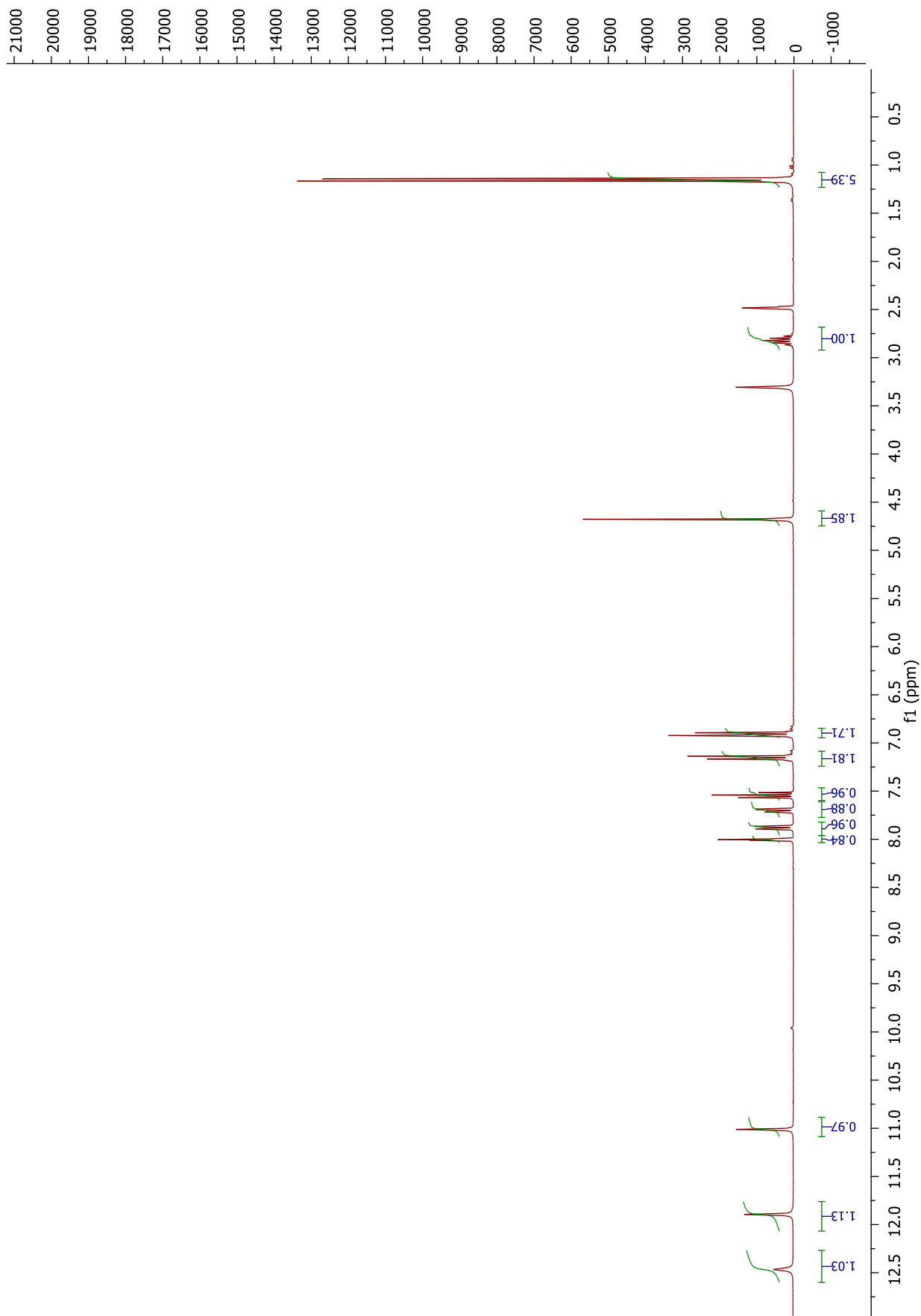
M.p. = 187.3°C

Tr (HPLC, Isocratic, H_2O with 0.10% TFA / Acetonitrile with 0.10% TFA 50/50. 30 min run time. Flow rate: 1.5 mL/min) = 9.38 min, Purity = 98.5%

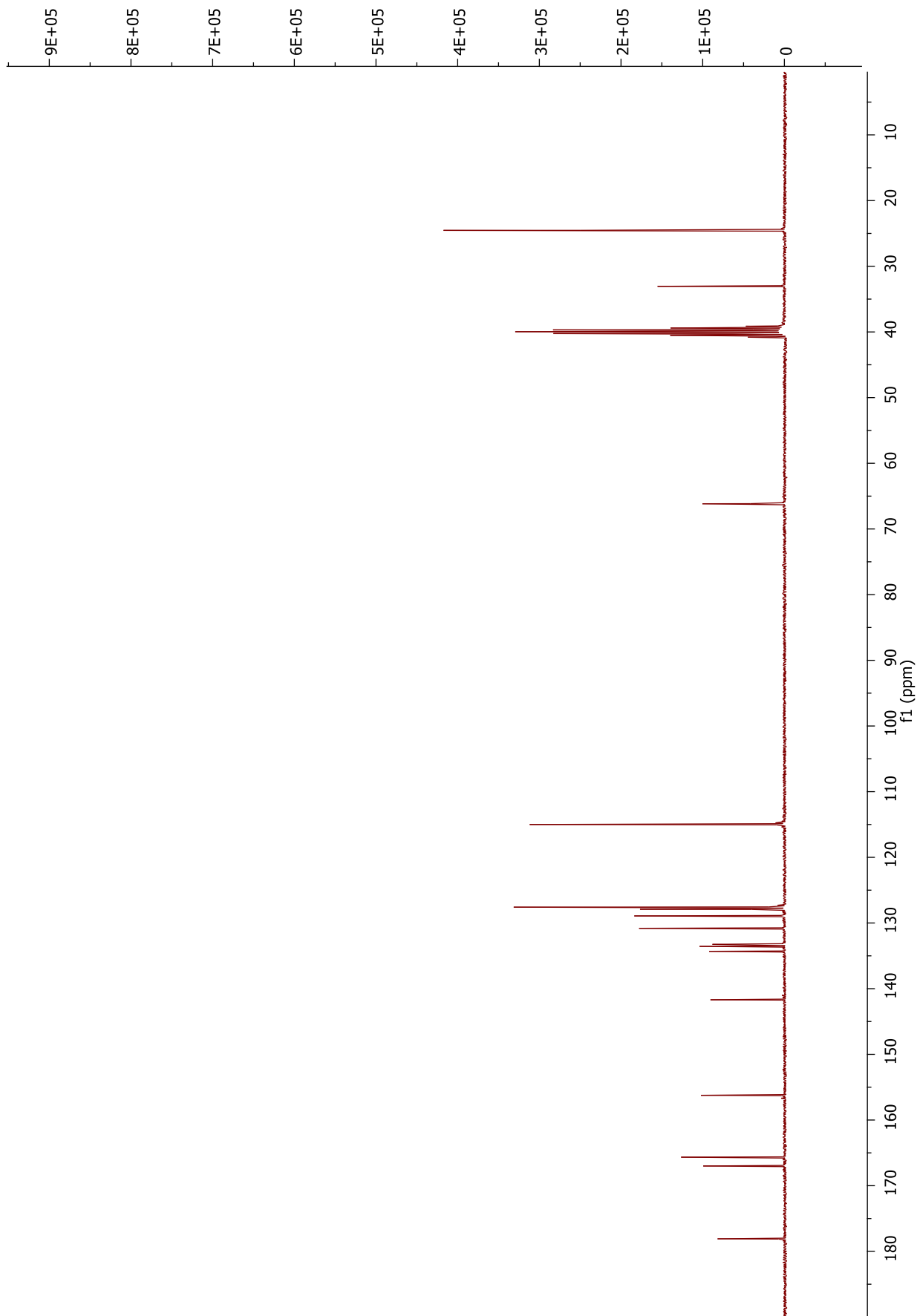
1H NMR (d_6 -DMSO): δ 12.47 (bs, 1H), 11.90 (bs, 1H), 11.01 (bs, 1H), 8.00 (t, J = 1.9 Hz, 1H), 7.86 (m, 1H), 7.70 (ddd, J = 8.0, 1.9, 1.0 Hz, 1H), 7.54 (t, J = 8.0 Hz, 1H), 7.15 (d, J = 8.7 Hz, 2H), 6.91 (d, J = 8.7 Hz, 2H), 4.68 (s, 2H), 2.82 (set, J = 6.9 Hz, 1H), 1.15 ppm (d, J = 6.9 Hz, 6H).

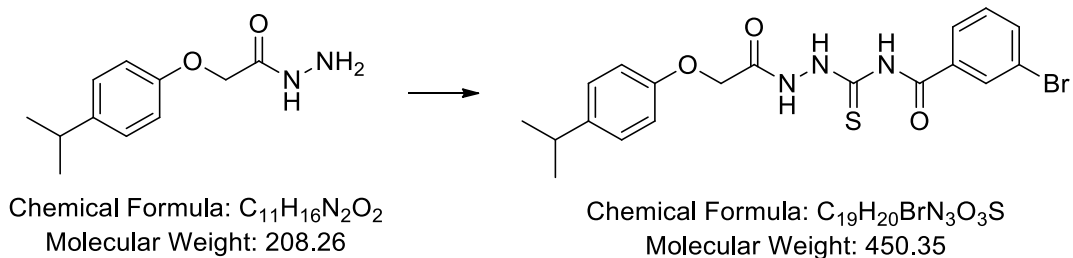
^{13}C NMR (d_6 -DMSO): δ 178.09, 167.00, 156.66, 156.24, 141.69, 134.31, 133.56, 133.25, 130.81, 128.92, 127.91, 127.59, 115.00, 66.16, 33.05, 24.54 ppm.

Experimental



Experimental



(XXXI) 1-(4-*i*-Propylphenoxyacetyl)-4-(3-bromobenzoyl)thiosemicarbazide

A solution of 3-Bromobenzoic acid (1.30 g, 6.8 mmol) in $SOCl_2$ (6.5 mL) was stirred at reflux for 1 h. Thus, the solution was concentrated under vacuum, diluted with Acetonitrile (15 mL), and then added with Potassium thiocyanate (1.12 g, 11.56 mmol). The reaction mixture was stirred at RT for 1 h, added with a solution of 4-*i*-Propylphenoxyacetohydrazide (1.40 g, 6.8 mmol) in DMF (5 mL), stirred at RT for 30 min, concentrated under vacuum, diluted with Ethyl acetate (50 mL), washed with brine (4×10 mL), dried over Na_2SO_4 , filtered, and then concentrated under vacuum to give a solid. Digestion with IPA (5 vol) at reflux gave 1.96 g of 1-(4-*i*-Propylphenoxyacetyl)-4-(3-bromobenzoyl)thiosemicarbazide as a pale yellow solid.

Yield = 62.0%

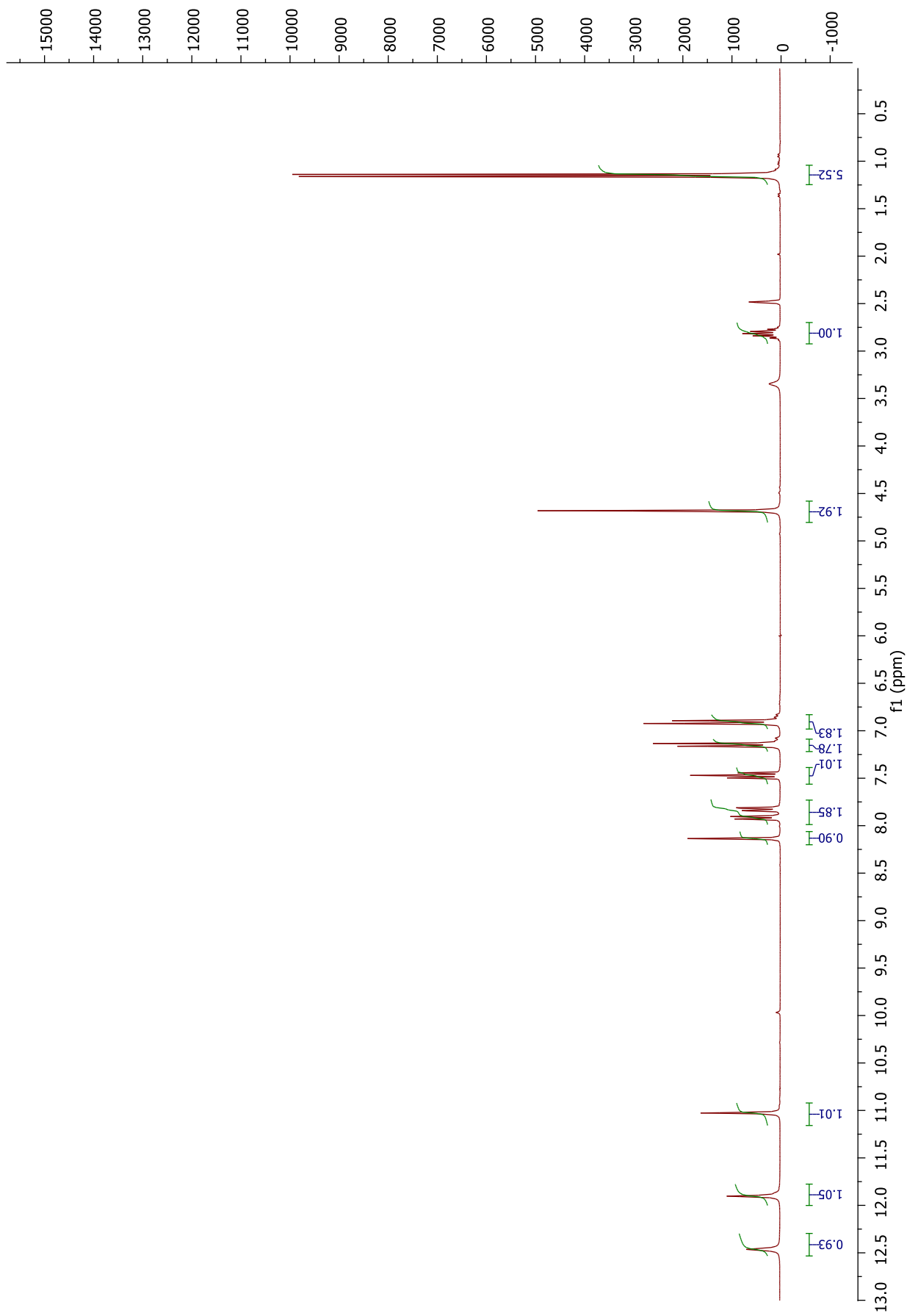
M.p. = 184.0°C

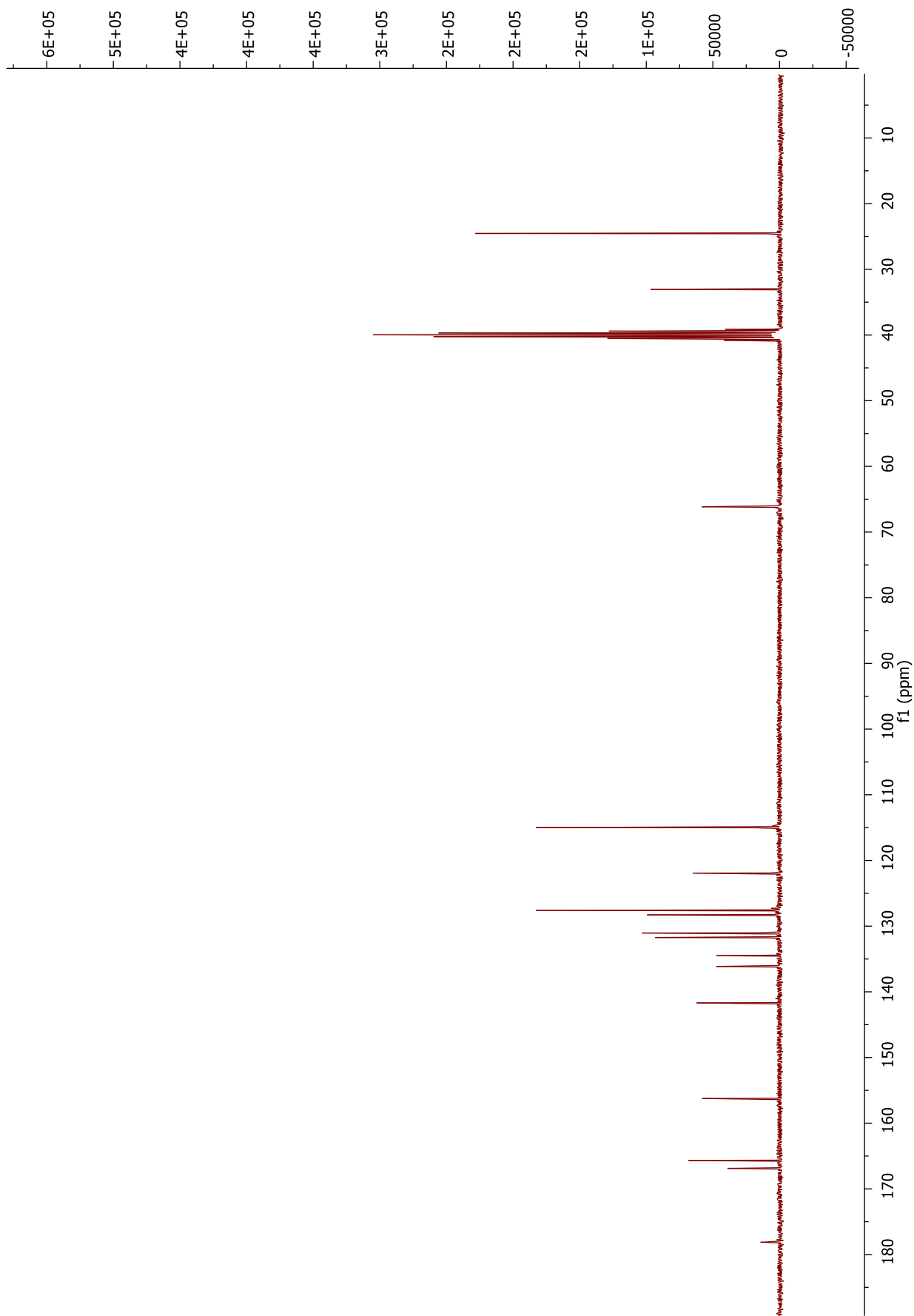
Tr (HPLC, Isocratic, H_2O with 0.10% TFA / Acetonitrile with 0.10% TFA 50/50. 30 min run time. Flow rate: 1.5 mL/min) = 10.13 min, Purity = 98.5%

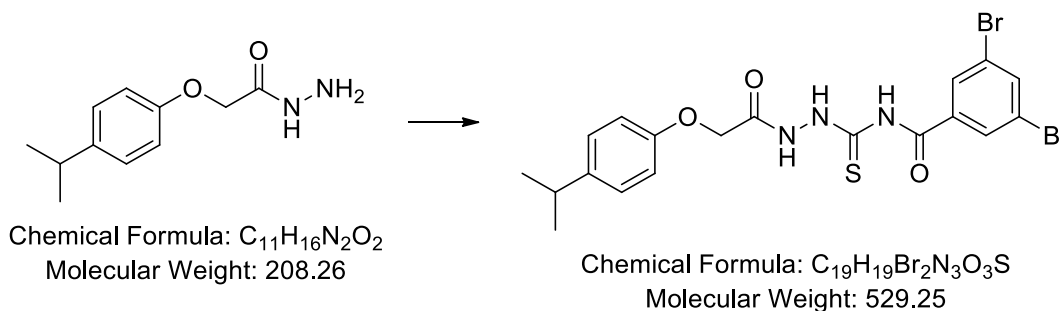
1H NMR (d_6 -DMSO): δ 12.46 (bs, 1H), 11.90 (bs, 1H), 11.03 (bs, 1H), 8.14 (t, $J = 1.7$ Hz, 1H), 7.92 (d, $J = 7.9$ Hz, 1H), 7.83 (m, 1H), 7.47 (t, $J = 7.9$ Hz, 1H), 7.15 (d, $J = 8.7$ Hz, 2H), 6.91 (d, $J = 8.7$ Hz, 2H), 4.68 (s, 2H), 2.81 (set, $J = 6.9$ Hz, 1H), 1.15 ppm (d, $J = 6.9$ Hz, 6H).

^{13}C NMR (d_6 -DMSO): δ 178.13, 166.89, 165.67, 156.24, 141.69, 136.13, 134.50, 131.73, 131.04, 128.28, 127.59, 121.92, 114.99, 66.15, 33.05, 24.54 ppm.

Experimental





(XXXII) 1-(4-*i*-Propylphenoxyacetyl)-4-(3,5-dibromobenzoyl)thiosemicarbazide

A solution of 3,5-Dibromobenzoic acid (1.30 g, 6.8 mmol) in $SOCl_2$ (6.5 mL) was stirred at reflux for 1 h. Thus, the solution was concentrated under vacuum, diluted with Acetonitrile (15 mL), and then added with Potassium thiocyanate (1.12 g, 11.56 mmol). The reaction mixture was stirred at RT for 1 h, added with a solution of 4-*i*-Propylphenoxyacetohydrazide (1.40 g, 6.8 mmol) in DMF (5 mL), stirred at RT for 30 min, concentrated under vacuum, diluted with Ethyl acetate (50 mL), washed with brine (4×10 mL), dried over Na_2SO_4 , filtered, and then concentrated under vacuum to give a solid. Digestion firstly with MeOH (10 vol) at reflux and secondly with IPA (15 vol) at reflux gave 2.0 g of 1-(4-*i*-Propylphenoxyacetyl)-4-(3,5-dibromobenzoyl)thiosemicarbazide as a white solid.

Yield = 62.0%

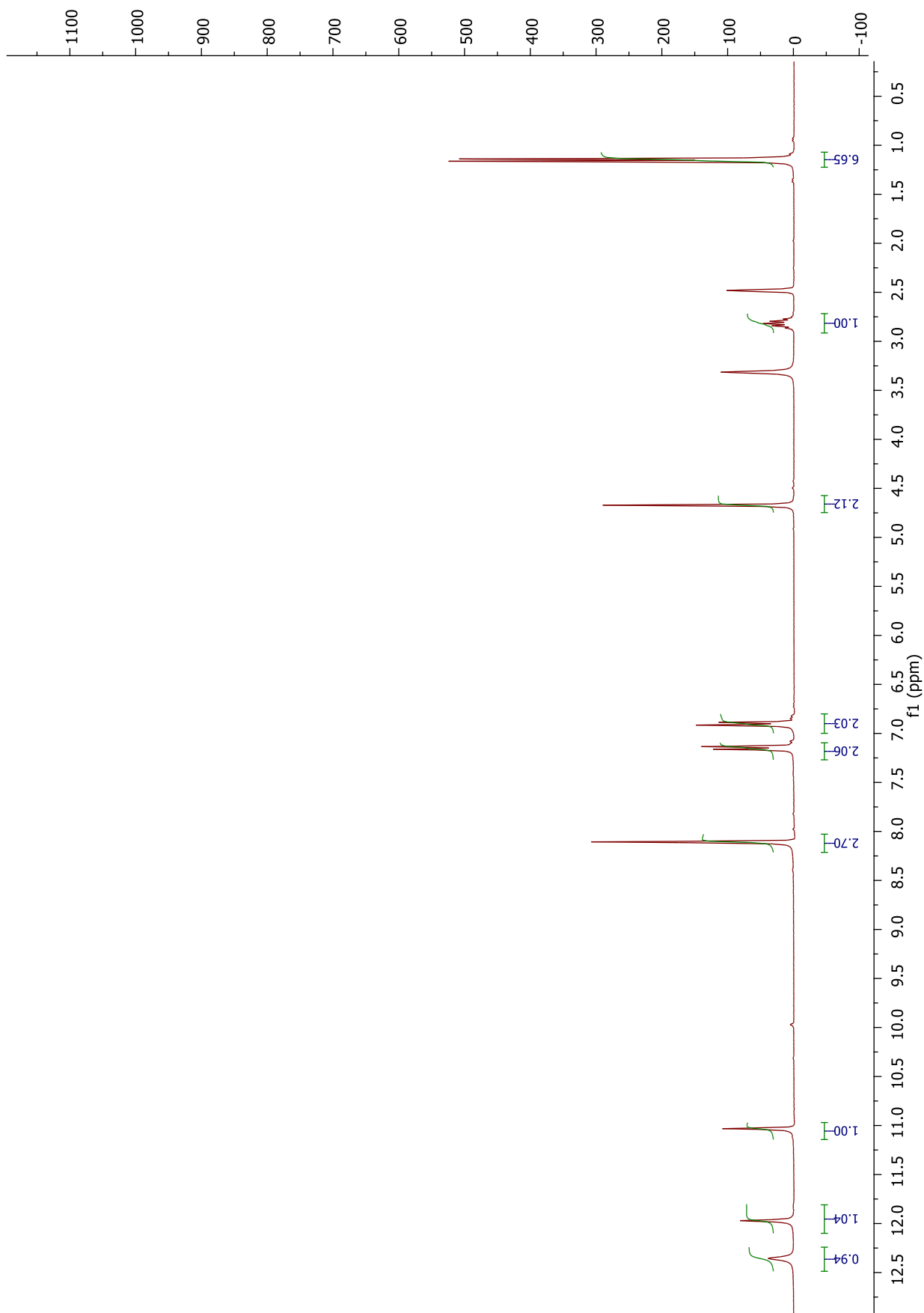
M.p. = 201.8°C

Tr (HPLC, Isocratic, H_2O with 0.10% TFA / Acetonitrile with 0.10% TFA 40/60. 30 min run time. Flow rate: 1.5 mL/min) = 6.19 min, Purity = 99.0%

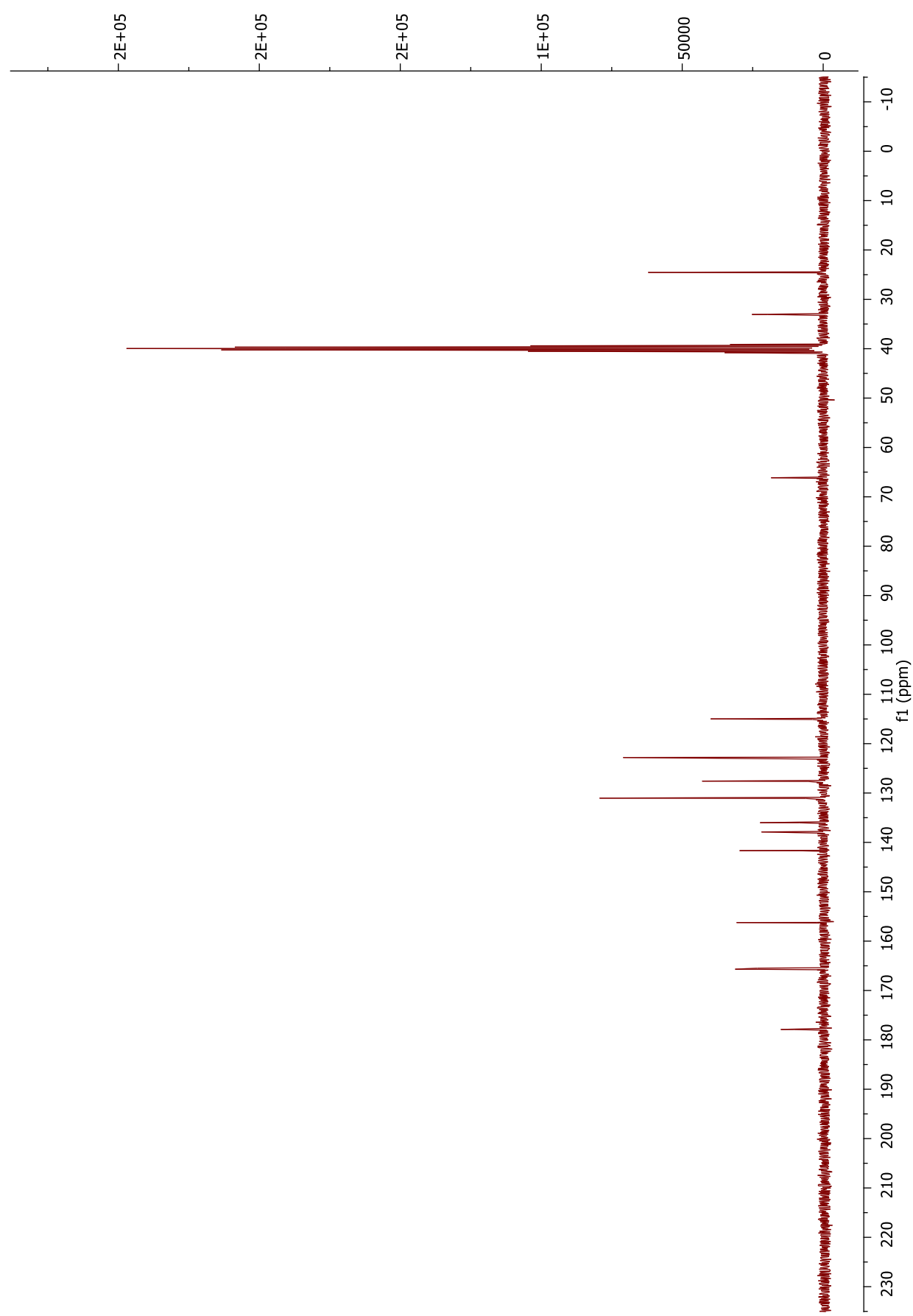
1H NMR (d_6 -DMSO): δ 12.36 (bs, 1H), 11.97 (bs, 1H), 11.03 (bs, 1H), 8.11 (s, 3H), 7.15 (d, J = 8.3 Hz, 2H), 6.87 (dd, J = 8.3 Hz, 2H), 4.67 (s, 2H), 2.82 (set, J = 6.9 Hz, 1H), 1.15 ppm (d, J = 6.9 Hz, 7H).

^{13}C NMR (d_6 -DMSO): δ 177.89, 165.68, 165.48, 156.24, 141.68, 137.88, 136.01, 131.04, 131.04, 127.59, 122.81, 114.99, 66.14, 33.05, 24.54 ppm.

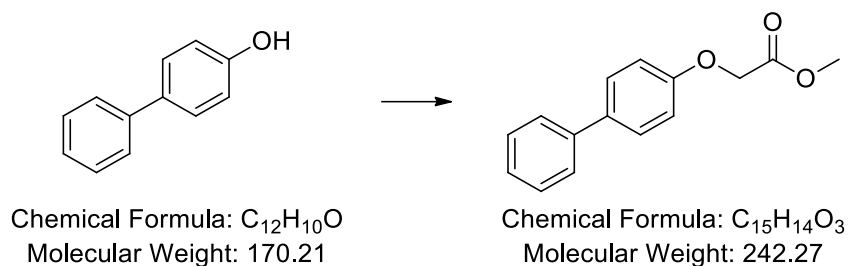
Experimental



Experimental



Methyl 4-biphenyloxyacetate



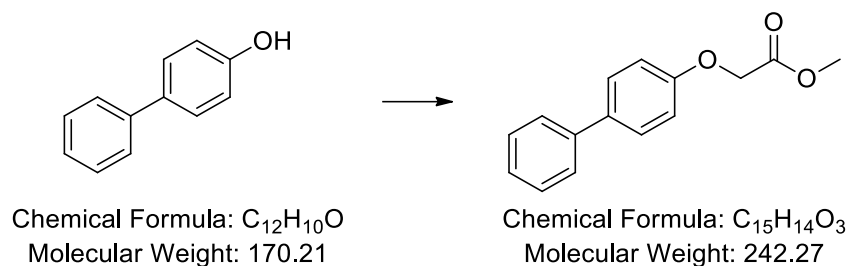
Methyl chloroacetate (1.71 mL, 15.81 mmol) was added to a solution of 4-Hydroxybiphenyl (2.15 g, 12.65 mmol) and Potassium carbonate (2.09 g, 15.18 mmol) in DMF (20 mL). The reaction mixture was stirred at 50°C for 1.5 h, concentrated under vacuum, diluted with Ethyl acetate (30 mL), washed with brine (4 × 10 mL), dried over Na₂SO₄, filtered, and then concentrated under vacuum to give 2.85 g of Methyl 4-biphenyloxyacetate as a white solid.

Yield = 93.0%

M.p. = 100.1°C

¹H NMR (CDCl₃): δ 7.53 (m, 4H), 7.41 (m, 2H), 7.31 (m, 1H), 6.99 (d, J = 8.8 Hz, 2H), 4.68 (s, 2H), 3.83 ppm (s, 3H).

4-Biphenyloxyacetohydrazide



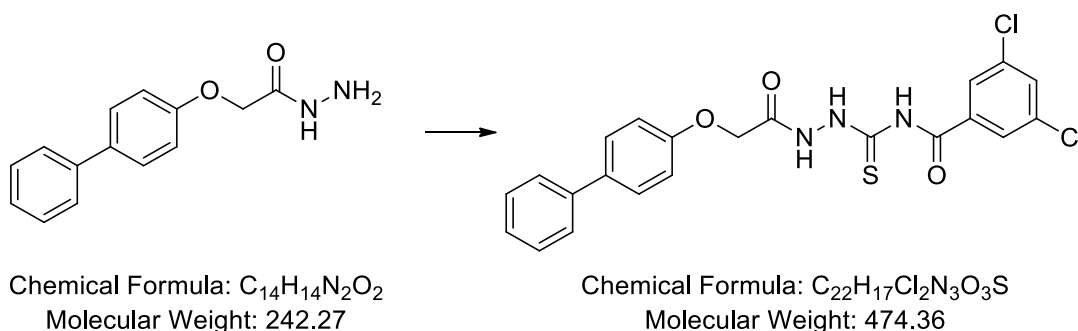
Hydrazine hydrate (2.1 mL, 33.60 mmol) was added to a solution of Methyl 4-biphenyloxyacetate (1.40 g, 6.72 mmol) in Methanol (15 mL). The reaction mixture was stirred at reflux for 16 h, concentrated under vacuum, diluted with Ethyl acetate (30 mL), washed with brine (10 mL), dried over Na_2SO_4 , filtered, and concentrated under vacuum to give 1.85 g of 4-Biphenyloxyacetohydrazide as a white solid.

Yield = 64.0%

M.p. = 112.9°C

1H NMR (d_6 -DMSO): δ 9.43 (bs, 1H), 7.58 (m, 4H), 7.41 (t, J = 7.4 Hz, 2H), 7.29 (t, J = 7.4 Hz, 1H), 7.02 (dd, J = 9.3, 2.4 Hz, 2H), 4.53 (s, 2H), 4.33 ppm (s, 2H).

(XXXIII) 1-(4-Biphenyloxyacetyl)-4-(3,5-dichlorobenzoyl)thiosemicarbazide



A solution of 3,5-Dichlorobenzoic acid (1.30 g, 6.8 mmol) in $SOCl_2$ (6.5 mL) was stirred at reflux for 1 h. Thus, the solution was concentrated under vacuum, diluted with Acetonitrile (15 mL), and then added with Potassium thiocyanate (1.12 g, 11.56 mmol). The reaction mixture was stirred at RT for 1 h, added with a solution of 4-Biphenyloxyacetohydrazide (1.40 g, 6.8 mmol) in DMF (5 mL), stirred at RT for 30 min, concentrated under vacuum, diluted with Ethyl acetate (50 mL), washed with brine (4×10 mL), dried over Na_2SO_4 , filtered, and then concentrated under vacuum to give a solid. Digestion with MeOH (15 vol) at reflux gave 2.77 g of 1-(4-biphenyloxyacetyl)-4-(3,5-dichlorobenzoyl)thiosemicarbazide as a white solid.

Yield = 73.0%

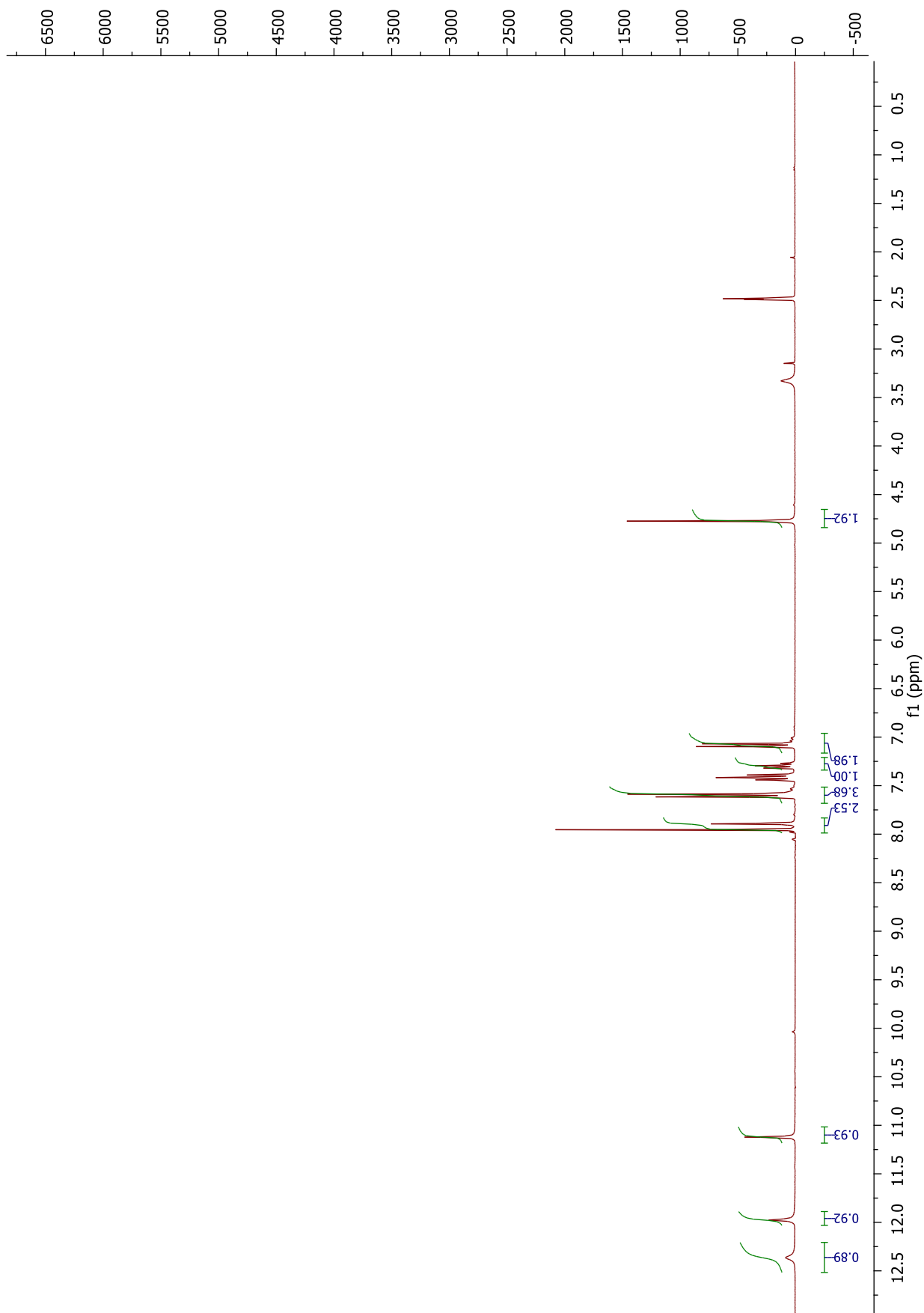
M.p. = 200.7°C

Tr (HPLC, Isocratic, H_2O with 0.10% TFA / Acetonitrile with 0.10% TFA 50/50. 30 min run time. Flow rate: 1.5 mL/min) = 13.80 min, Purity = 95.2%

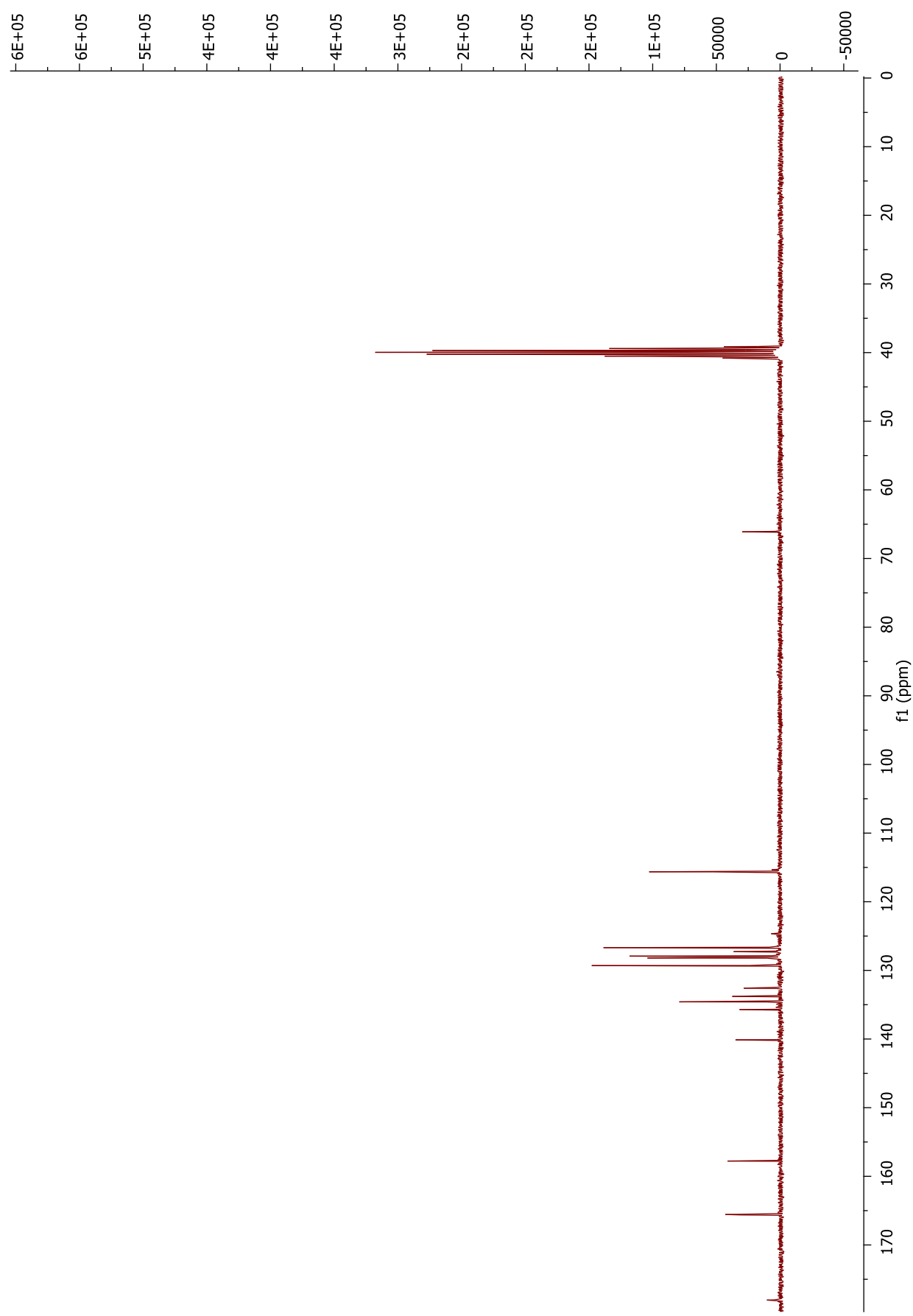
1H NMR (d_6 -DMSO): δ 12.37 (bs, 1H), 11.98 (bs, 1H), 11.12 (bs, 1H), 7.96 (d, $J = 1.9$ Hz, 2H), 7.89 (t, $J = 1.9$ Hz, 1H), 7.59 (m, 4H), 7.42 (t, $J = 7.6$ Hz, 2H), 7.29 (m, 1H), 7.08 (d, $J = 8.8$ Hz, 2H), 4.77 ppm (s, 2H).

^{13}C NMR (d_6 -DMSO): δ 178.03, 165.63, 165.56, 157.78, 140.12, 135.70, 134.58, 133.79, 132.60, 129.31, 128.20, 127.92, 127.27, 126.69, 115.64, 66.11 ppm.

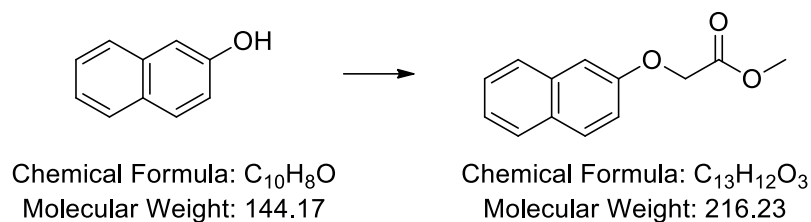
Experimental



Experimental



Methyl 2-naphthoxyacetate



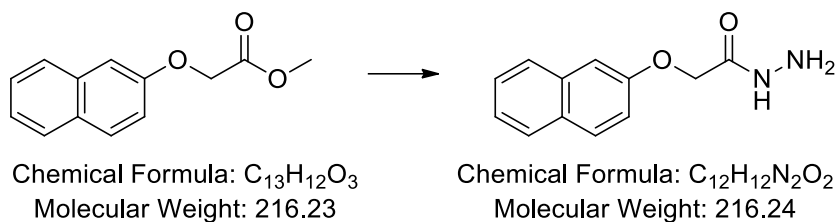
Methyl chloroacetate (1.65 mL, 15.81 mmol) was added to a solution of 2-naphthol (1.75 g, 12.17 mmol) and Potassium carbonate (2.01 g, 14.57 mmol) in DMF (17.5 mL). The reaction mixture was stirred at 50°C for 1.5 h, concentrated under vacuum, diluted with Ethyl acetate (30 mL), washed with brine (4 × 10 mL), dried over Na₂SO₄, filtered, and then concentrated under vacuum to give 2.63 g of Methyl 2-naphthoxyacetate as a white solid.

Yield = Quantitative

M.p. = 76.6°C

¹H NMR (CDCl₃): δ 7.78 (m, 1H), 7.73 (m, 1H), 7.45 (m, 1H), 7.37 (m, 1H), 7.26 (m, 1H), 7.24 (m, 1H), 7.09 (m, 1H), 4.76 (s, 2H), 3.83 (s, 3H).

2-Naphthoxyacetohydrazide



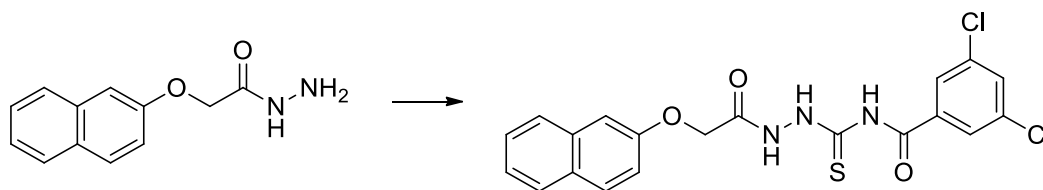
Hydrazine hydrate (3.31 mL, 56.65 mmol) was added to a solution of Methyl 2-naphthoxyacetate (2.45 g, 11.33 mmol) in Methanol (25 mL). The reaction mixture was stirred at reflux for 16 h, concentrated under vacuum, diluted with Ethyl acetate (30 mL), washed with brine (10 mL), dried over Na_2SO_4 , filtered, and concentrated under vacuum to give 1.78 g of 2-Naphthoxyacetohydrazide as a white solid.

Yield = 73.0%

M.p. = 121.7°C

1H NMR ($CDCl_3$): δ 9.40 (s, 1H), 7.83 (m, 1H), 7.76 (m, 1H), 7.45 (m, 1H), 7.34 (m, 1H), 7.28 (m, 1H), 7.25 (m, 1H), 7.22 (m, 1H), 4.60 (s, 2H), 4.36 (s, 2H).

(XXXIV) 1-(2-naphthoxyacetyl)-4-(3,5-dichlorobenzoyl)thiosemicarbazide



Chemical Formula: $C_{12}H_{12}N_2O_2$
Molecular Weight: 216.24

Chemical Formula: $C_{20}H_{15}Cl_2N_3O_3S$
Molecular Weight: 448.32

A solution of 3,5-Dichlorobenzoic acid (1.50 g, 7.85 mmol) in $SOCl_2$ (7.5 mL) was stirred at reflux for 1 h. Thus, the solution was concentrated under vacuum, diluted with Acetonitrile (15 mL), and then added with Potassium thiocyanate (1.18 g, 12.17 mmol). The reaction mixture was stirred at RT for 1 h, added with a solution of 2-Naphthoxyacetohydrazide (1.73 g, 7.16 mmol) in DMF (5 mL), stirred at RT for 30 min, concentrated under vacuum, diluted with Ethyl acetate (50 mL), washed with brine (4×10 mL), dried over Na_2SO_4 , filtered, and then concentrated under vacuum to give a solid. Digestion with MeOH (13 vol) at reflux gave 2.77 g of 1-(2-naphthoxyacetyl)-4-(3,5-dichlorobenzoyl)thiosemicarbazide as a white solid.

Yield = 72.6%

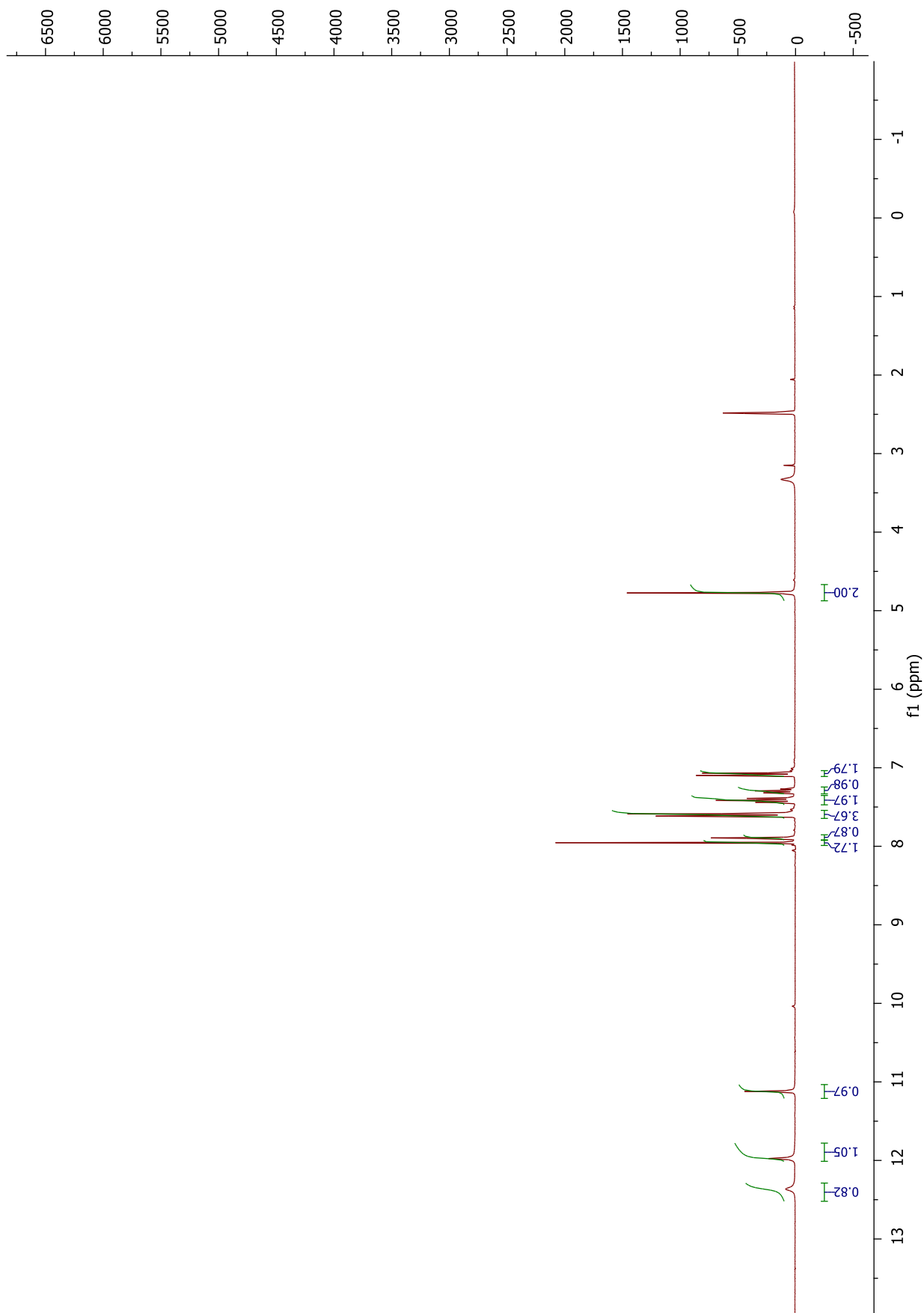
M.p. = 193.38°C

The HPLC purity evaluation was difficult due to the complete insolubility of the product.

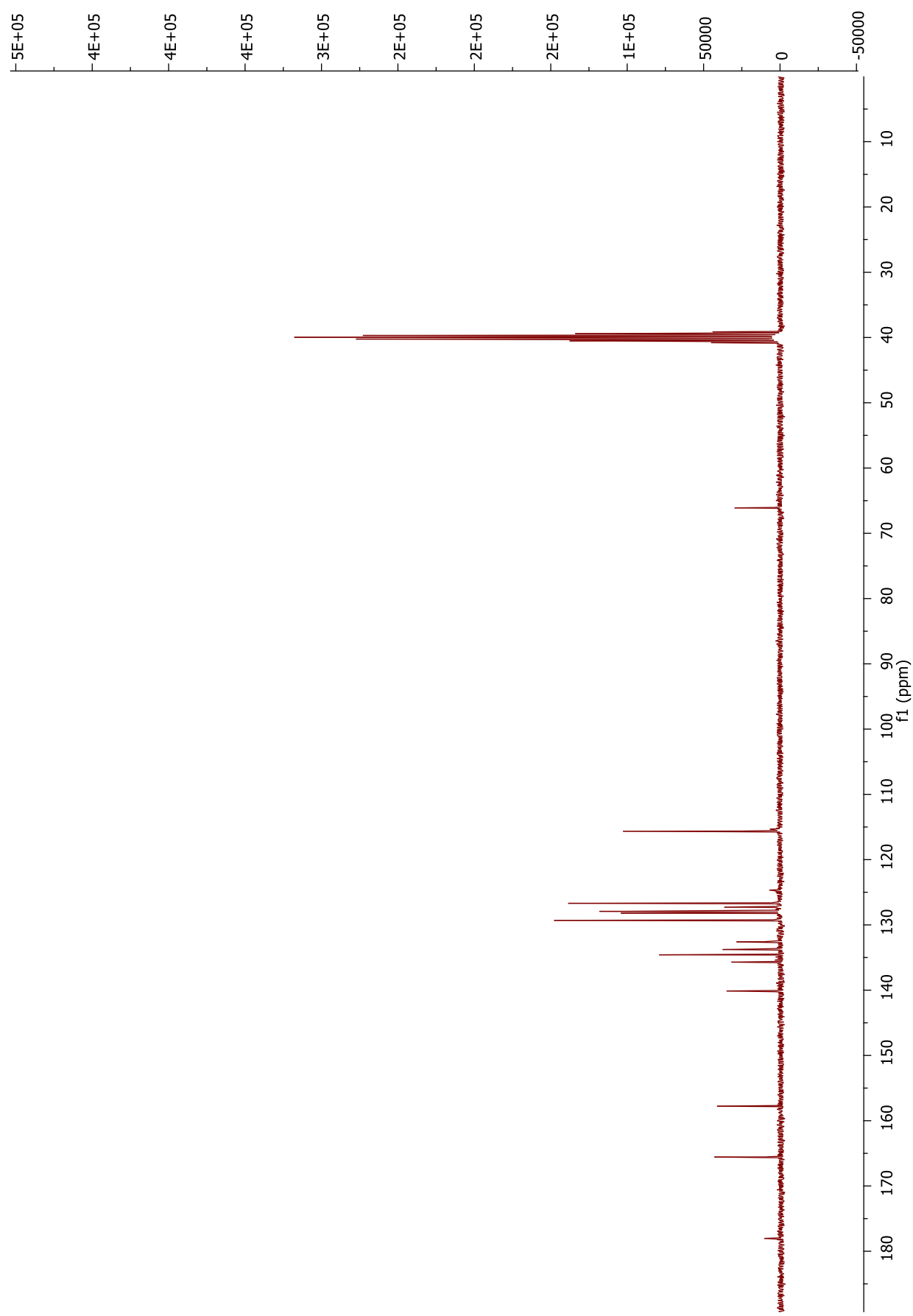
1H NMR (d_6 -DMSO): δ 12.37 (bs, 1H), 11.98 (bs, 1H), 11.12 (bs, 1H), 7.96 (d, J = 1.9 Hz, 2H), 7.89 (t, J = 1.9 Hz, 1H), 7.60 (d, J = 8.5 Hz, 2H), 7.42 (t, J = 7.6 Hz, 2H), 7.30 (m, 1H), 7.08 (d, J = 8.8 Hz, 2H), 4.77 (s, 2H).

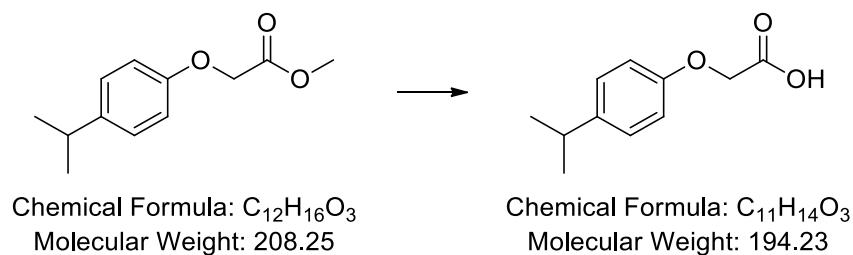
^{13}C NMR (d_6 -DMSO): δ 165.63, 157.78, 140.12, 135.70, 134.58, 133.79, 132.60, 129.31, 128.20, 127.92, 127.27, 126.69, 115.64, 66.11 ppm.

Experimental



Experimental



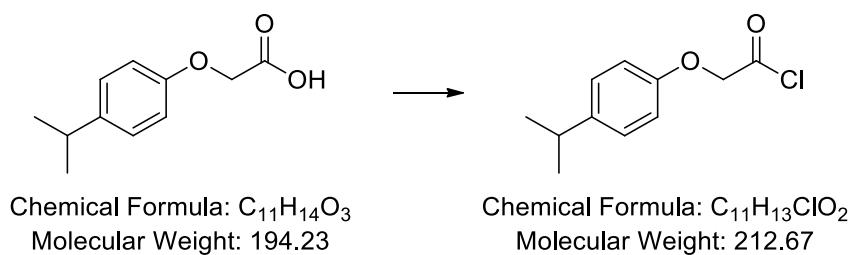
4-*i*-Propylphenoxyacetic acid

2.5 N aqueous NaOH (6 mL, 15 mmol) was added to a solution of Methyl 4-*i*-propylphenoxyacetate (3.00 g, 14.40 mmol) in MeOH (30 mL). The reaction mixture was stirred at RT for 1.5 h, concentrated under vacuum, diluted with water, acidified to pH = 1 with conc. HCl, extracted twice with Ethyl acetate (2 × 30 mL), dried over Na₂SO₄, filtered, and concentrated under vacuum to give 2.60 g of 4-*i*-Propylphenoxyacetic acid as a white solid.

Yield = 95.0%

M.p. = 82.1°C

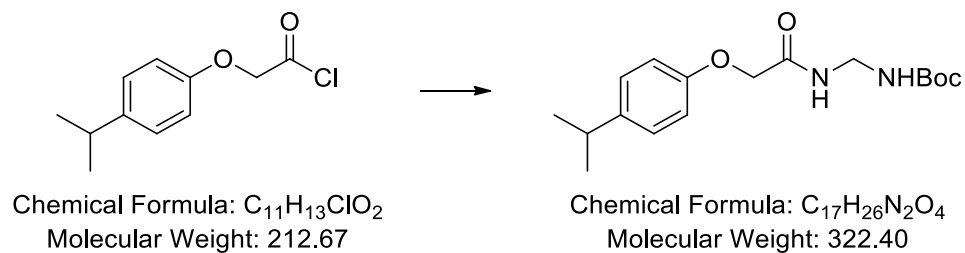
¹H NMR (CDCl₃): δ 7.16 (d, J = 8.6 Hz, 2H), 6.86 (d, J = 8.6 Hz, 2H), 4.66 (s, 2H), 2.86 (set, J = 6.9 Hz, 1H), 1.22 ppm (d, J = 6.9 Hz, 6H).

4-*i*-Propylphenoxyacetyl chloride

SOCl₂ (10 mL, 5 vol) was added to 4-*i*-Propylphenoxyacetic acid (2.00 g, 10.30 mmol). The reaction mixture was stirred at reflux for 1 h and concentrated under vacuum to give 2.15 g of 4-*i*-Propylphenoxyacetyl chloride as a dark oil.

Yield = 98.0%

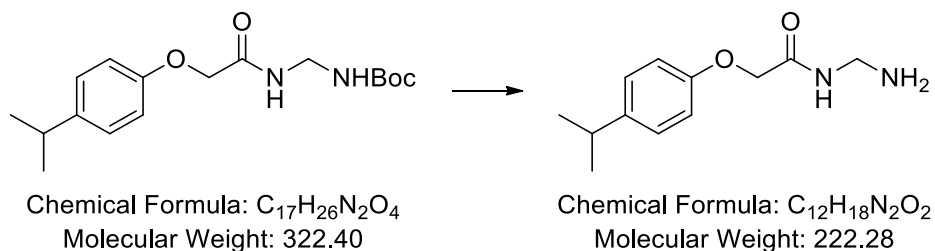
¹H NMR (CDCl₃): δ 7.17 (d, J = 8.6 Hz, 2H), 6.83 (d, J = 8.6 Hz, 2H), 4.92 (s, 2H), 2.87 (set, J = 6.9 Hz, 1H), 1.22 ppm (d, J = 6.9 Hz, 6H).

N-(*t*-Butoxycarbonylaminomethyl)-4-*i*-propylphenoxyacetamide

A solution of *N*-Boc methylendiamine (1.20 g, 8.21 mmol) in DCM (5 mL) was added to a solution of 4-*i*-Propylphenoxyacetyl chloride (1.6 g, 8.21 mmol) and TEA (1.37 mL, 9.85 mmol) in DCM (5 mL) at 0°C. The reaction mixture was stirred at RT for 3 h, diluted with DCM (20 mL), washed twice with 10% aqueous NaHCO₃ (2 × 10 mL) and once with brine (10 mL), dried over Na₂SO₄, filtered and concentrated under vacuum to give 2.17 g of *N*-(*t*-Butoxycarbonylaminomethyl)-4-*i*-propylphenoxyacetamide as a yellowish oil.

Yield = 82.0%

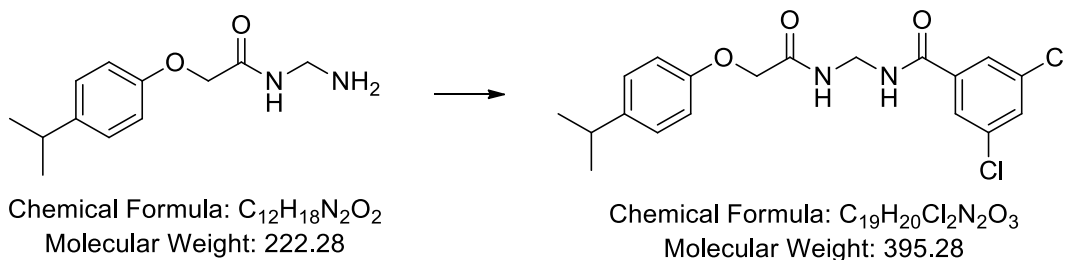
¹H NMR (CDCl₃): δ 7.50 (bs, 1H), 7.15 (d, J = 8.6 Hz, 2H), 6.83 (d, J = 8.6 Hz, 2H), 5.57 (bs, 1H), 4.62 (t, J = 6.4 Hz, 2H), 4.45 (s, 2H), 2.86 (set, J = 6.9 Hz, 1H), 1.43 (s, 9H), 1.22 ppm (d, J = 6.9 Hz, 6H).

N-(Aminomethyl)-4-*i*-propylphenoxyacetamide

10% aqueous HCl (2.5 mL, 7.5 mmol) was added to a solution of *N*-(*t*-Butoxycarbonylamino)methyl)-4-*i*-propylphenoxyacetamide (1.00 g, 3.10 mmol) in MeOH (10 mL) at RT. The reaction mixture was stirred at reflux for 0.5 h, concentrated under vacuum, diluted with Et₂O (30 mL) and extracted twice with 10% aqueous HCl (2 × 15 mL). The aqueous phase was thus basified to pH = 12 and extracted three times with Ethyl acetate (3 × 25 mL), dried over Na₂SO₄, filtered and concentrated under vacuum to give 0.40 g of *N*-(Aminomethyl)-4-*i*-propylphenoxyacetamide as a yellowish oil.

Yield = 58.0%

¹H NMR (CDCl₃): δ 7.26 (bs, 1H), 7.16 (d, J = 8.4 Hz, 1H), 6.84 (d, J = 8.4 Hz, 1H), 4.46 (s, J = 20.8 Hz, 2H), 4.30 (s, 2H), 2.86 (set, J = 6.9 Hz, 1H), 2.36 (bs, 2H), 1.24 ppm (dd, J = 14.8, 7.0 Hz, 6H).

(XXXV) 3,5-Dichloro-*N*-((2-(4-*i*-propylphenoxy)acetamido)methyl)benzamide

A solution of *N*-(Aminomethyl)-4-*i*-propylphenoxyacetamide (0.68 g, 3.07 mmol) in DCM (5 mL) was added to a solution of 3,5-Dichlorobenzoyl chloride (0.64 g, 3.07 mmol) and TEA (0.52 mL, 3.85 mmol) in DCM (5 mL) at 0°C. The reaction mixture was stirred at RT for 3 h, diluted with DCM (20 mL), washed twice with 10% aqueous $NaHCO_3$ (2 × 10 mL) and once with brine (10 mL), dried over Na_2SO_4 , filtered and concentrated under vacuum. Digestion with IPA (10 vol.) at reflux gave 0.85 g of 3,5-Dichloro-*N*-((2-(4-*i*-propylphenoxy)acetamido)methyl)benzamide as a white solid.

Yield = 70.0%

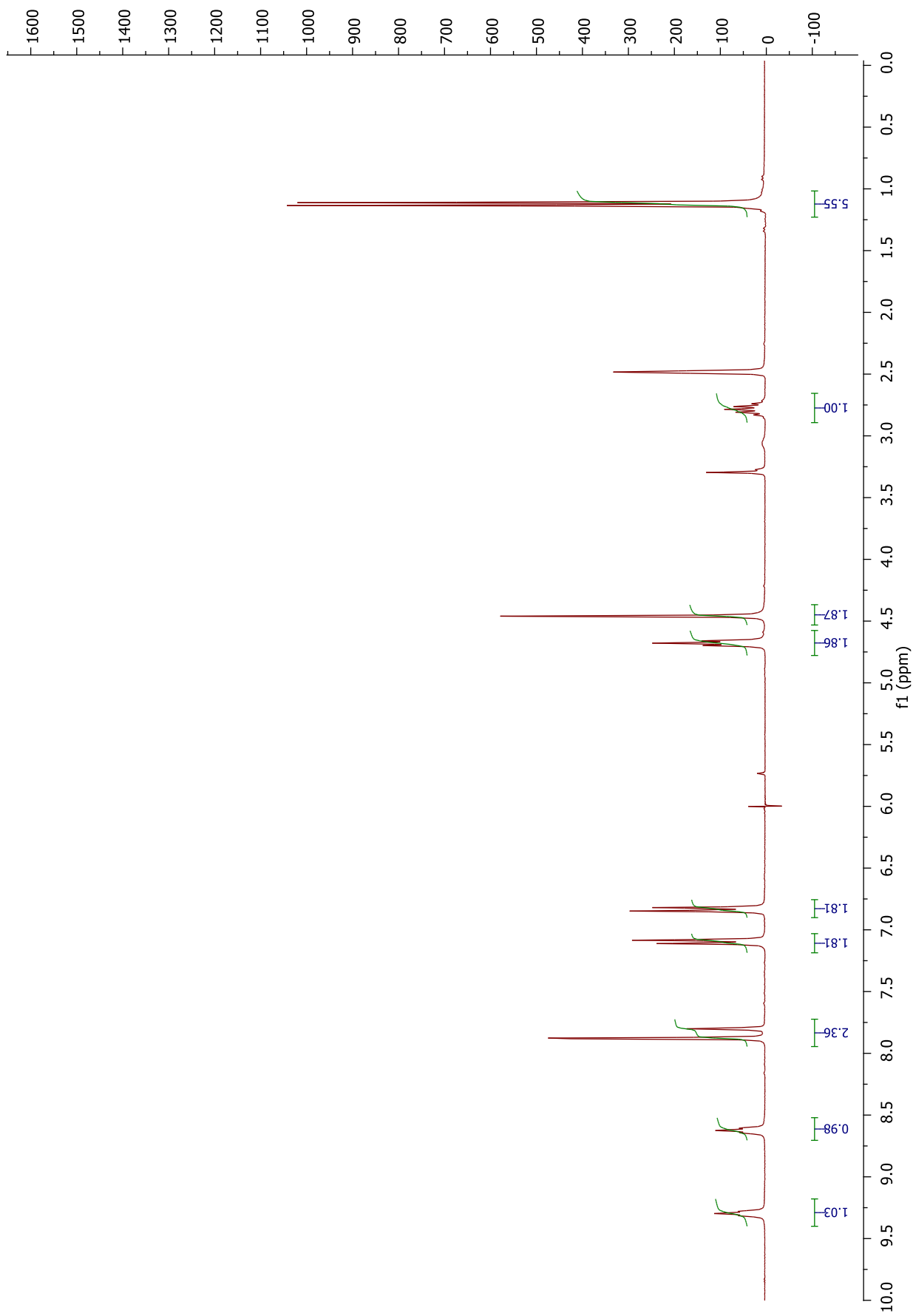
M.p. = 189.9°C

Tr (HPLC, Isocratic, H_2O with 0.10% TFA / Acetonitrile with 0.10% TFA 55/45. 30 min run time. Flow rate: 1.5 mL/min) = 9.94 min, Purity = 97.0%

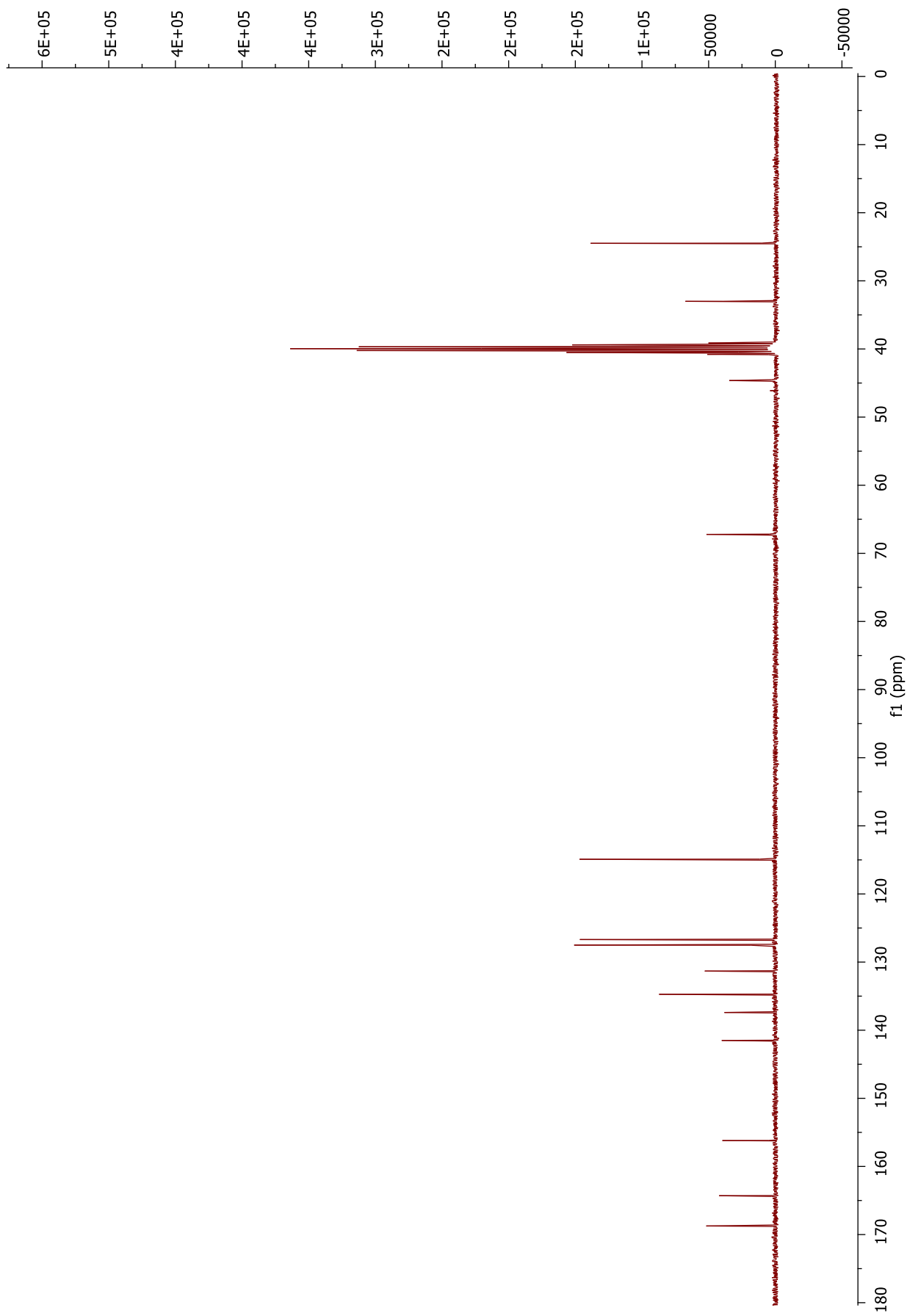
1H NMR (d_6 -DMSO): δ 9.30 (t, J = 5.4 Hz, 1H), 8.63 (t, J = 5.4 Hz, 1H), 7.88 (d, J = 1.7 Hz, 2H), 7.80 (s, 1H), 7.10 (d, J = 8.6 Hz, 2H), 6.83 (d, J = 8.6 Hz, 2H), 4.68 (t, J = 5.4 Hz, 2H), 4.46 (s, 2H), 2.79 (set, J = 6.9 Hz, 1H), 1.12 ppm (d, J = 6.9 Hz, 6H).

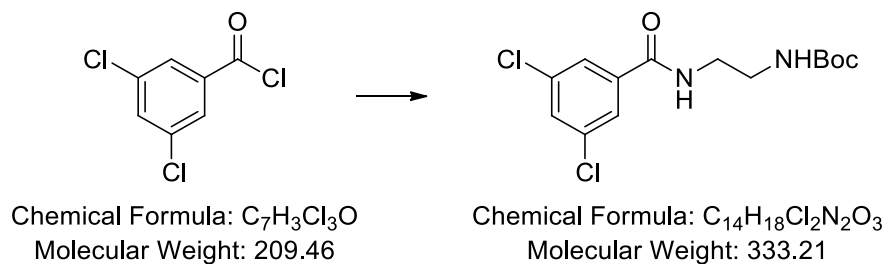
^{13}C NMR (d_6 -DMSO): δ 168.74, 164.30, 156.20, 141.50, 137.40, 134.73, 131.32, 127.51, 126.69, 114.91, 67.21, 44.63, 33.01, 24.49 ppm.

Experimental



Experimental

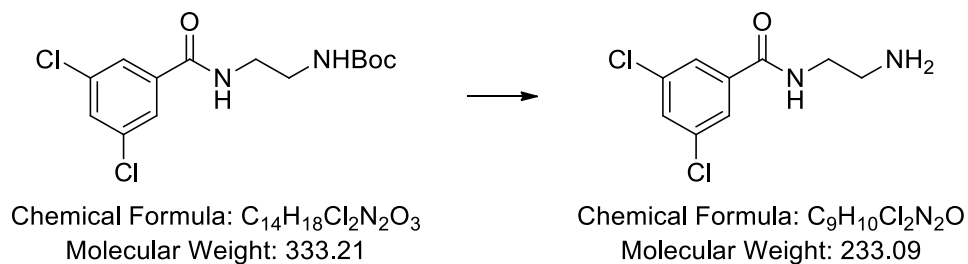


N-(*t*-Butoxycarbonylaminoethyl)-3,5-dichlorobenzamide

A solution of *N*-Boc ethylendiamine (2.54 g, 15.84 mmol) in DCM (5 mL) was added to a solution of 3,5-dichlorobenzoyl chloride (2.21 g, 10.56 mmol) and TEA (2.20 mL, 15.84 mmol) in DCM (5 mL) at 0°C. The reaction mixture was stirred at RT for 3 h, diluted with DCM (20 mL), washed twice with 10% aqueous NaHCO₃ (2 × 10 mL) and once with brine (10 mL), dried over Na₂SO₄, filtered and concentrated under vacuum to give 2.85 g of *N*-(*t*-Butoxycarbonylaminoethyl)-3,5-dichlorobenzamide as a yellowish oil.

Yield = 81.0%

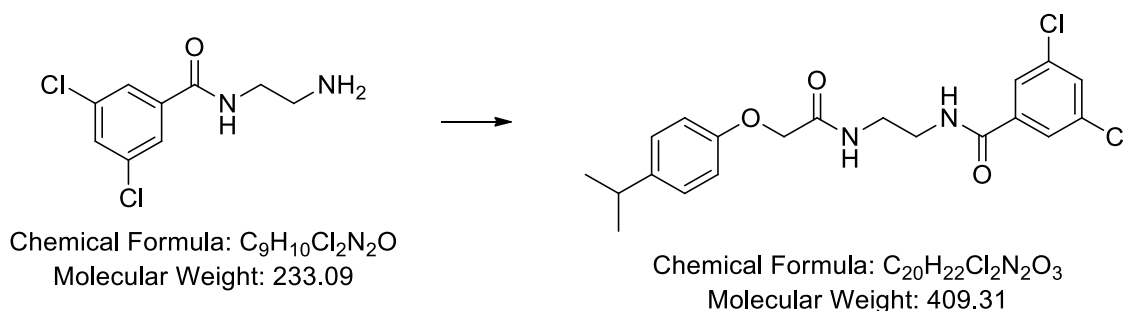
¹H NMR (CDCl₃): δ 7.71 (d, J = 1.7 Hz, 2H), 7.57 (bs, 1H), 7.45 (t, J = 1.7 Hz, 1H), 5.07 (bs, 1H), 3.52 (m, 2H), 3.40 (m, 2H), 1.44 ppm (s, 9H).

N-(Aminoethyl)-3,5-dichlorobenzamide

10% aqueous HCl (5.7 mL, 17.3 mmol) was added to a solution of *N*-(*t*-Butoxycarbonylaminoethyl)-3,5-dichlorobenzamide (2.85 g, 8.63 mmol) in MeOH (10 mL) at RT. The reaction mixture was stirred at reflux for 0.5 h, concentrated under vacuum, diluted with Et₂O (30 mL) and extracted twice with 10% aqueous HCl (2 × 15 mL). The aqueous phase was thus basified to pH = 12 and extracted three times with Ethyl acetate (3 × 25 mL), dried over Na₂SO₄, filtered and concentrated under vacuum to give 1.61 g of *N*-(Aminoethyl)-3,5-dichlorobenzamide as a brownish oil.

Yield = 80.0%

¹H NMR (CDCl₃): δ 7.64 (d, *J* = 1.6 Hz, 2H), 7.43 (t, *J* = 1.6 Hz, 1H), 7.14 (bs), 3.46 (dd, *J* = 10.9, 5.4 Hz, 2H), 2.93 (t, *J* = 5.7 Hz, 2H), 1.67 ppm (bs, 2H).

(XXXVI) 3,5-Dichloro-*N*-((2-(4-*i*-propylphenoxy)acetamido)ethyl)benzamide

A solution of *N*-(aminoethyl)-3,5-dichlorobenzamide (0.68 g, 6.96 mmol) in DCM (5 mL) was added to a solution of 4-*i*-Propylphenoxyacetyl chloride (0.64 g, 6.96 mmol) and TEA (1.16 mL, 8.35 mmol) in DCM (5 mL) at 0°C. The reaction mixture was stirred at RT for 3 h, diluted with DCM (20 mL), washed twice with 10% aqueous $NaHCO_3$ (2 × 10 mL) and once with brine (10 mL), dried over Na_2SO_4 , filtered and concentrated under vacuum. Digestion with IPA (10 vol.) at reflux gave 1.68 g of 3,5-Dichloro-*N*-((2-(4-*i*-propylphenoxy)acetamido)ethyl)benzamide as a white solid.

Yield = 59.0%

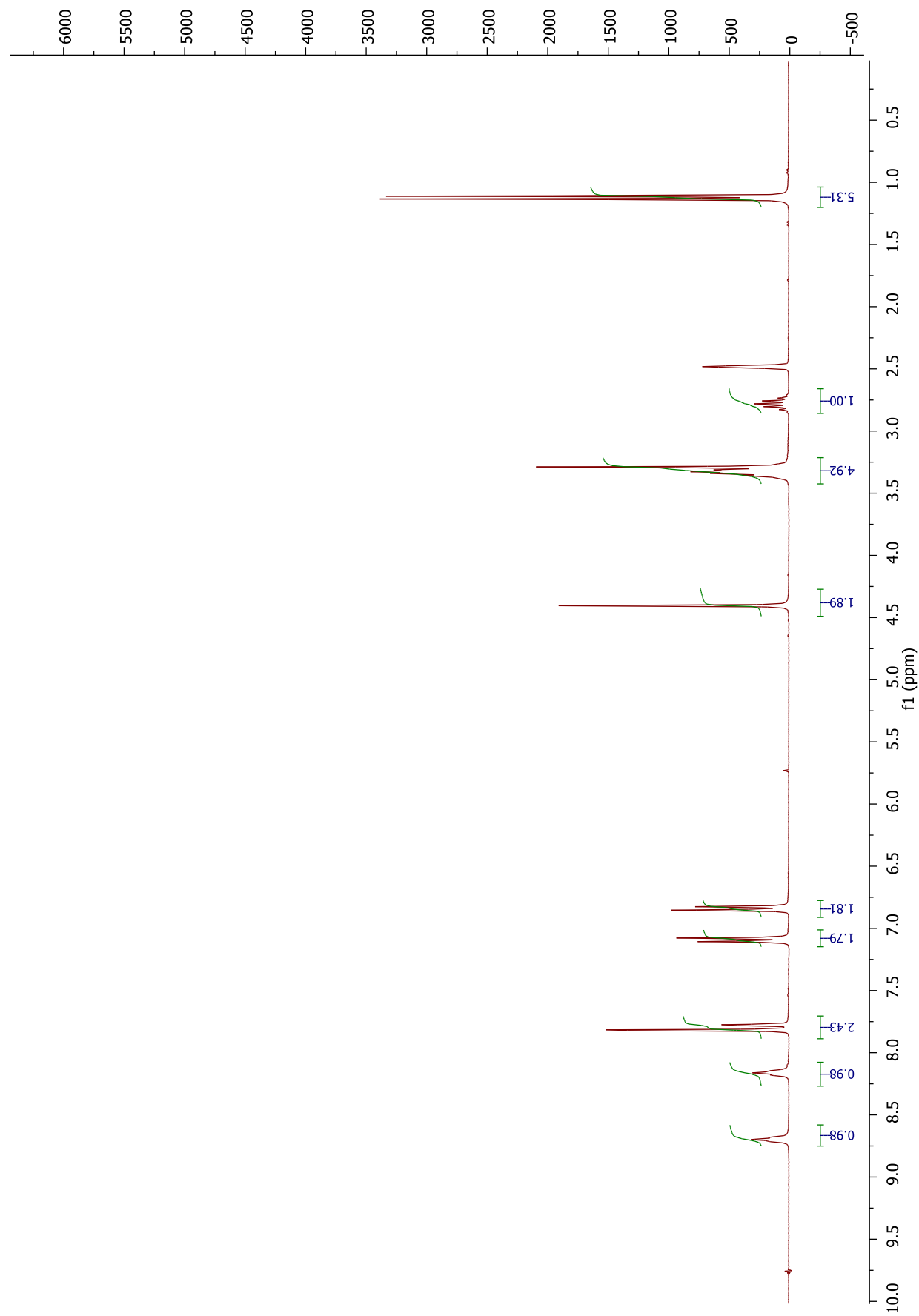
M.p. = 181.7°C

Tr (HPLC, Isocratic, H_2O with 0.10% TFA / Acetonitrile with 0.10% TFA 50/50. 30 min run time. Flow rate: 1.5 mL/min) = 7.21 min, Purity = 97.1%

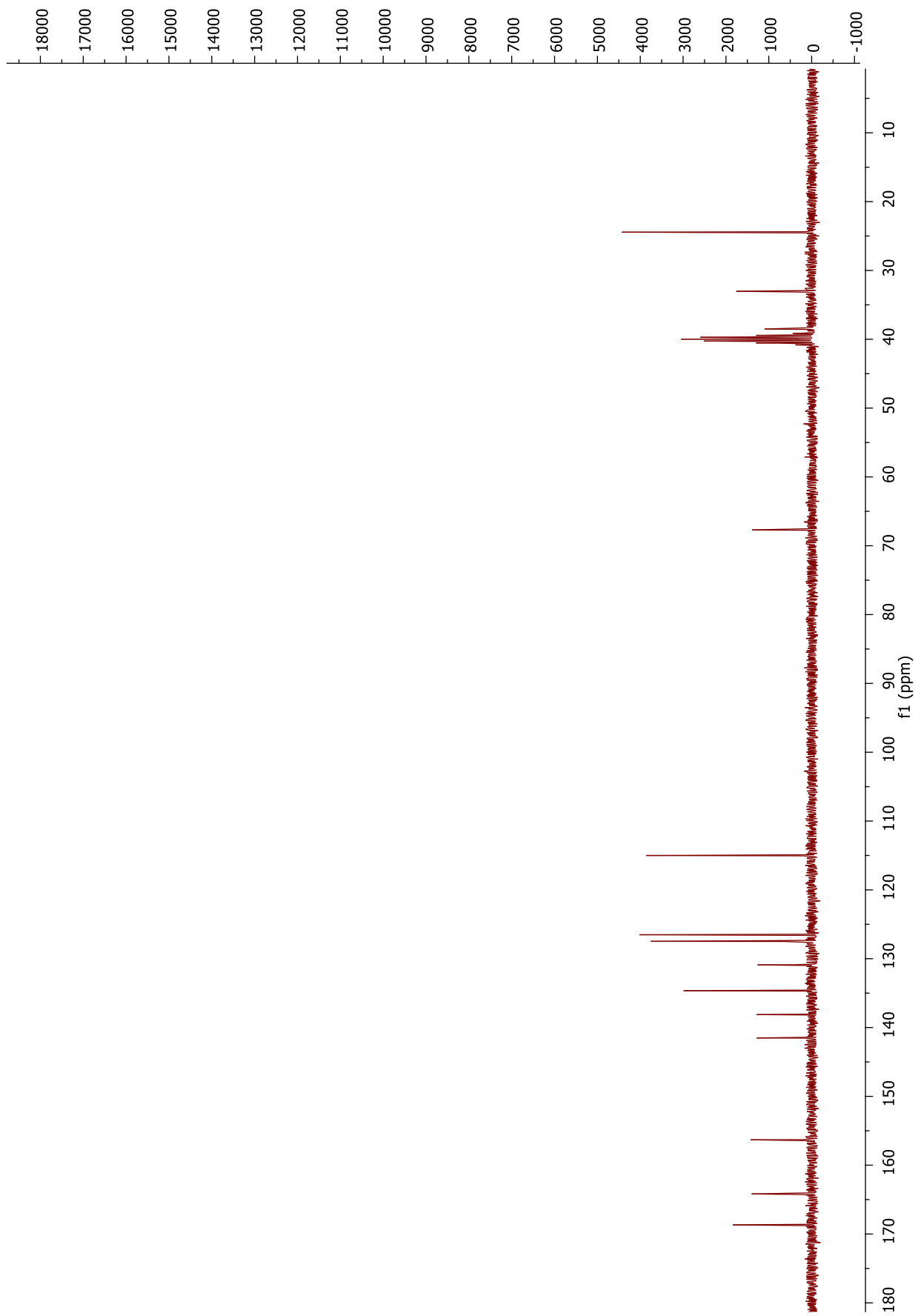
1H NMR (d_6 -DMSO): δ 8.70 (t, J = 4.6 Hz, 1H), 8.16 (t, J = 4.6 Hz, 1H), 7.82 (d, J = 1.7 Hz, 2H), 7.78 (t, J = 1.7 Hz, 1H), 7.09 (d, J = 8.6 Hz, 2H), 6.84 (d, J = 8.6 Hz, 2H), 4.40 (s, 2H), 3.33 (m, 4H), 2.77 (sec, J = 6.9 Hz, 1H), 1.12 ppm (d, J = 6.9 Hz, 6H).

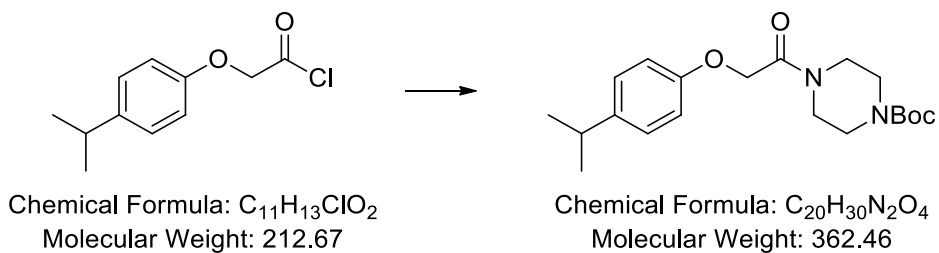
^{13}C NMR (d_6 -DMSO): δ 168.87, 164.17, 156.31, 141.52, 138.12, 134.65, 130.89, 127.41, 126.52, 115.01, 67.70, 38.51, 33.02, 24.44 ppm.

Experimental



Experimental

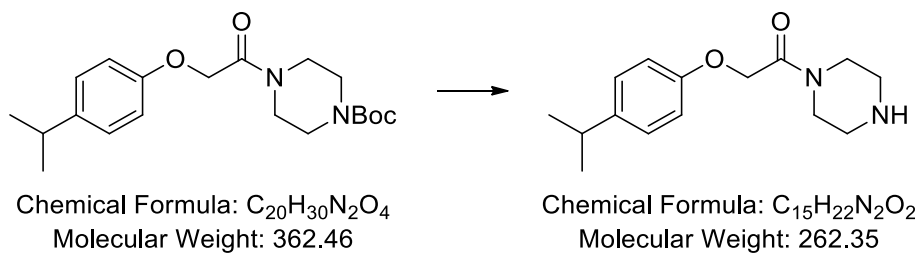


4-*t*-Butoxycarbonyl-1-(4-*i*-propylphenoxyacetyl)piperazine

A solution of 4-*N*-Boc-piperazine (0.95 g, 5.13 mmol) in DCM (10 mL) was added to a solution of 4-*i*-Propylphenoxyacetyl chloride (1.09 g, 5.13 mmol) and TEA (0.86 mL, 6.16 mmol) in DCM (10 mL) at 0°C. The reaction mixture was stirred at RT for 3 h, diluted with DCM (20 mL), washed twice with 10% aqueous $NaHCO_3$ (2 × 10 mL) and once with brine (10 mL), dried over Na_2SO_4 , filtered and concentrated under vacuum to give 1.86 g of 4-*t*-Butoxycarbonyl-1-(4-*i*-propylphenoxyacetyl)piperazine as a yellow oil.

Yield = Quantitative

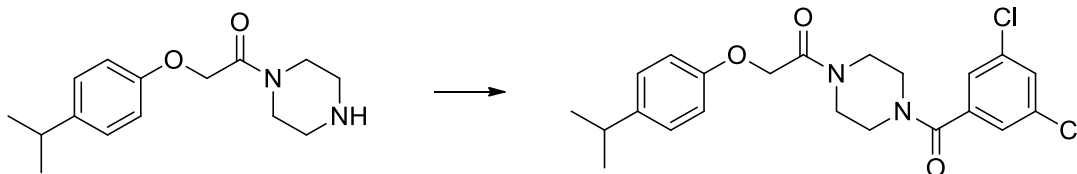
1H NMR ($CDCl_3$): δ 7.14 (d, $J = 7.1$ Hz, 2H), 6.86 (d, $J = 7.1$ Hz, 2H), 4.66 (s, 2H), 3.57 (m, 4H), 3.43 (m, 4H), 2.85 (set, $J = 6.8$ Hz, 1H), 1.45 (s, 9H), 1.21 (d, $J = 6.8$ Hz, 6H).

1-(4-*i*-propylphenoxyacetyl)piperazine

TFA (5.80 mL, 51.50 mmol) was added to a solution of *t*-Butoxycarbonyl-1-(4-*i*-propylphenoxyacetyl)piperazine (1.86 g, 5.15 mmol) in DCM (20 mL) at 0°C. The reaction mixture was stirred at RT for 18 h, diluted with DCM, washed once with 10% aqueous NaOH (15 mL), once with brine (15 mL), dried over Na_2SO_4 , filtered, and concentrated under vacuum to give 1.35 g of 1-(4-*i*-propylphenoxyacetyl)piperazine as a yellowish oil.

Yield = Quantitative

1H NMR ($CDCl_3$): δ 7.14 (d, $J = 8.7$ Hz, 2H), 6.87 (d, $J = 8.7$ Hz, 2H), 4.65 (s, 2H), 3.59 (m, 4H), 2.85 (m, 4H), 2.82 (set, $J = 7.0$ Hz, 1H) 1.22 (d, $J = 7.0$ Hz, 6H).

(XXXVII) 4-(3,5-Dichlorobenzoyl)-1-(4-*i*-propylphenoxyacetyl)piperazine

Chemical Formula: C₁₅H₂₂N₂O₂
Molecular Weight: 262.35

Chemical Formula: C₂₂H₂₄Cl₂N₂O₃
Molecular Weight: 435.34

A solution of 1-(4-*i*-propylphenoxyacetyl)piperazine (1.36 g, 5.19 mmol) in DCM (10 mL) was added to a solution of 3,5-Dichlorobenzoyl chloride (1.09 g, 5.19 mmol) and TEA (0.87 mL, 6.23 mmol) in DCM (10 mL) at 0°C. The reaction mixture was stirred at RT for 3 h, diluted with DCM (20 mL), washed twice with 10% aqueous NaHCO₃ (2 × 10 mL) and once with brine (10 mL), dried over Na₂SO₄, filtered and concentrated under vacuum. Crystallization with 7/3 Cyclohexane/Ethyl acetate (5 vol) gave 0.95 g of 4-(3,5-Dichlorobenzoyl)-1-(4-*i*-propylphenoxyacetyl)piperazine as a white solid.

Yield = 42.0%

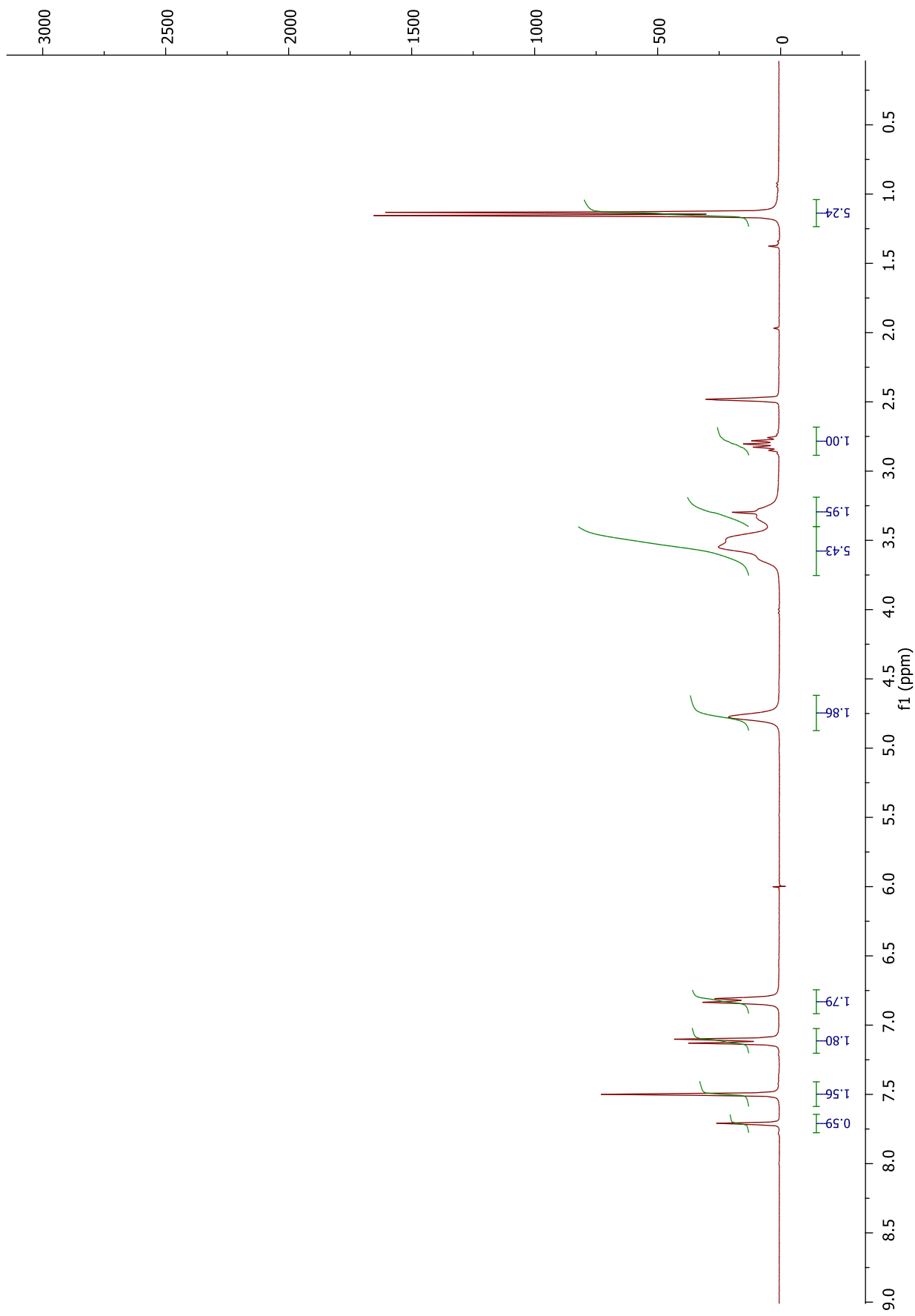
M.p. = 104.1°C

Tr (HPLC, Isocratic, H₂O with 0.10% TFA / Acetonitrile with 0.10% TFA 50/50. 30 min run time. Flow rate: 1.5 mL/min) = 6.67 min, Purity = 98.0%

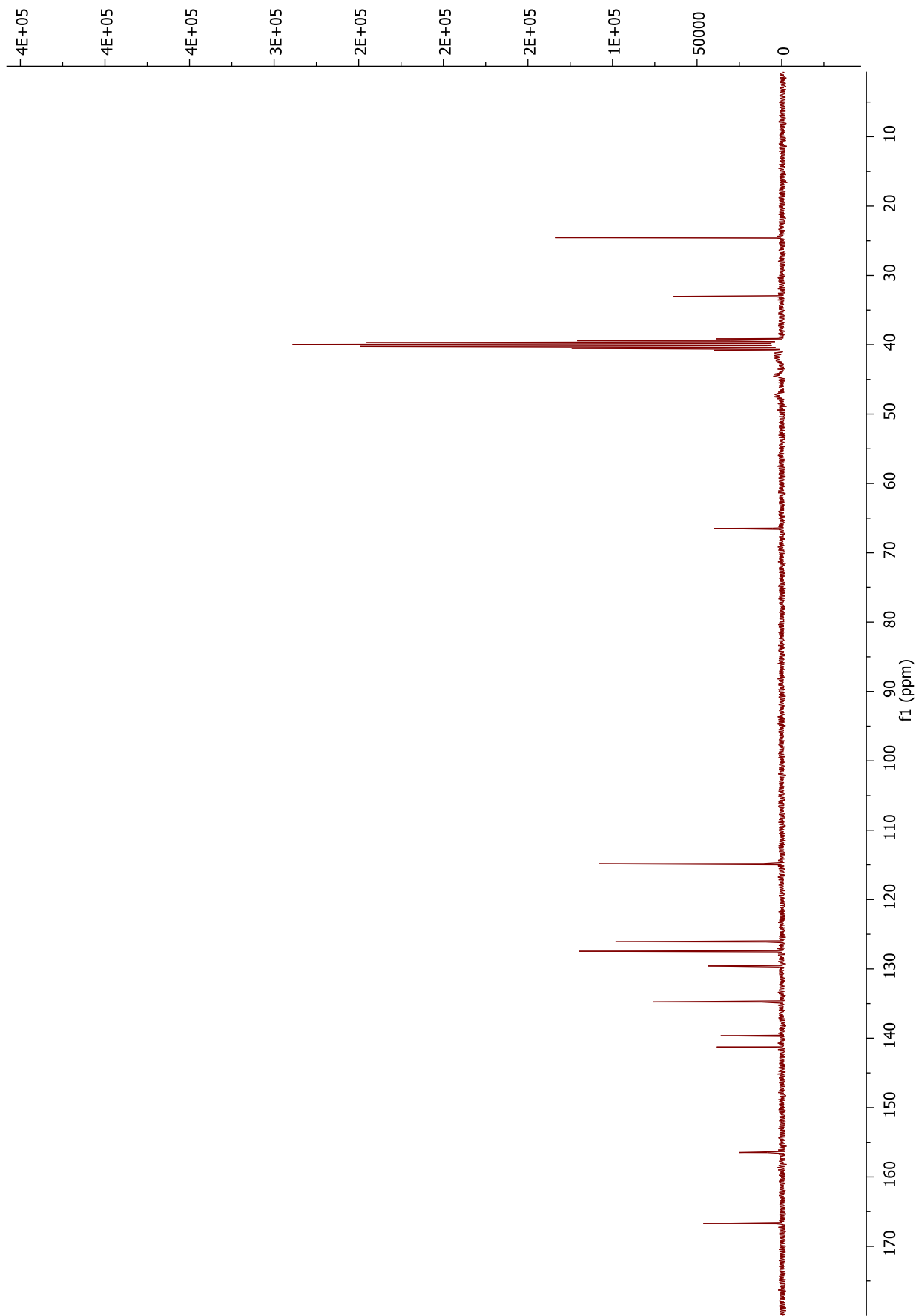
¹H NMR (d₆-DMSO): δ 7.72 (m, J = 1.7 Hz, 1H), 7.50 (m, 2H), 7.12 (d, J = 8.1 Hz, 2H), 6.82 (d, J = 8.1 Hz, 2H), 4.78 (s, 2H), 3.44 (m, 8H), 2.80 (set, J = 6.9 Hz, 1H), 1.14 (d, J = 6.9 Hz, 6H).

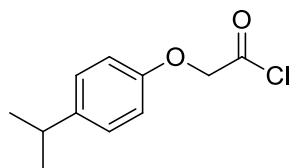
¹³C NMR (d₆-DMSO): δ 166.70, 166.62, 156.48, 141.27, 139.65, 134.76, 129.58, 127.47, 126.09, 114.85, 66.49, 33.02, 24.55 ppm.

Experimental

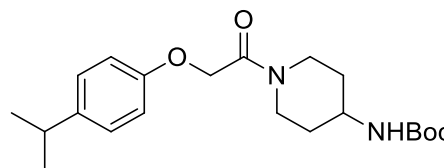


Experimental



4-*t*-Butoxycarbonylamino-1-(4-*i*-propylphenoxyacetyl)piperidine

Chemical Formula: C₁₁H₁₃ClO₂
Molecular Weight: 212.67



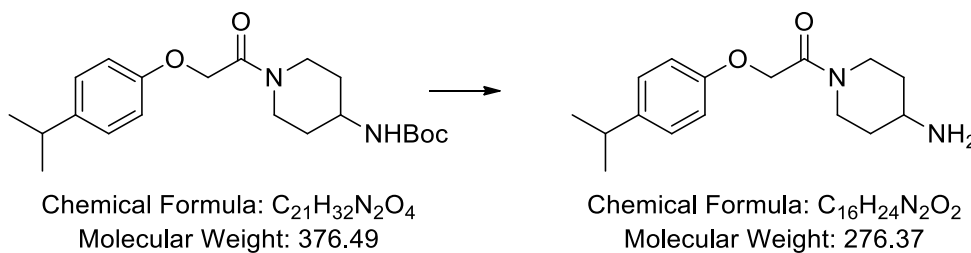
Chemical Formula: C₂₁H₃₂N₂O₄
Molecular Weight: 376.49

A solution of 4-*N*-Boc-aminopiperidine (2.48 g, 12.39 mmol) in DCM (10 mL) was added to a solution of 4-*i*-Propylphenoxyacetyl chloride (2.63 g, 12.39 mmol) and TEA (2.07 mL, 14.87 mmol) in DCM (10 mL) at 0°C. The reaction mixture was stirred at RT for 3 h, diluted with DCM (20 mL), washed twice with 10% aqueous NaHCO₃ (2 × 10 mL) and once with brine (10 mL), dried over Na₂SO₄, filtered and concentrated under vacuum. Crystallization with MeOH (7.5 vol) gave 2.80 g of 4-*t*-Butoxycarbonylamino-1-(4-*i*-propylphenoxyacetyl)piperidine as a white solid.

Yield = 60.0%

M.p. = 160.5°C

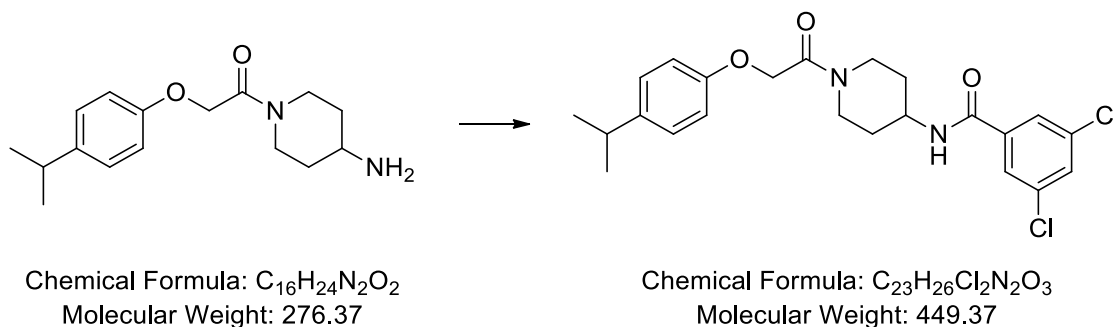
¹H NMR (CDCl₃): δ 7.13 (d, *J* = 8.5 Hz, 2H), 6.85 (d, *J* = 8.5 Hz, 2H), 4.63 (s, 1H), 4.44 (m, 2H), 3.95 (d, *J* = 13.1 Hz, 1H), 3.66 (bs, 1H), 3.13 (t, *J* = 12.2 Hz, 1H), 2.83 (m, 1H), 2.82 (set, *J* = 6.9 Hz, 1H) 1.97 (t, *J* = 12.5 Hz, 2H), 1.43 (s, 9H), 1.20 ppm (d, *J* = 6.9 Hz, 6H).

4-amino-1-(4-*i*-propylphenoxyacetyl)piperidine

TFA (5.66 mL, 73.80 mmol) was added to a solution of 4-*t*-Butoxycarbonylamino-1-(4-*i*-propylphenoxyacetyl)piperidine (2.78 g, 7.38 mmol) in DCM (30 mL) at 0°C. The reaction mixture was stirred at RT for 18 h, diluted with DCM, washed once with 10% aqueous NaOH (15 mL), once with brine (15 mL), dried over Na_2SO_4 , filtered, and concentrated under vacuum to give 2.04 g of 4-Amino-1-(4-*i*-propylphenoxyacetyl)piperidine as a yellowish oil.

Yield = Quantitative

1H NMR ($CDCl_3$): δ 7.13 (d, $J = 8.6$ Hz, 2H), 6.86 (d, $J = 8.6$ Hz, 2H), 4.64 (s, 2H), 4.44 (d, $J = 13.6$ Hz, 1H), 3.96 (d, $J = 13.6$ Hz, 1H), 3.10 (t, $J = 12.4$ Hz, 1H), 2.85 (m, 2H), 2.82 (set, $J = 6.9$ Hz, 1H), 1.84 (m, 2H), 1.30 (m, 2H), 1.21 ppm (d, $J = 6.9$ Hz, 6H).

(XXXVIII) 4-(3,5-Dichlorobenzoylamino)-1-(4-*i*-propylphenoxyacetyl)piperidine

A solution of 4-Amino-1-(4-*i*-propylphenoxyacetyl)piperidine (1.16 g, 4.19 mmol) in DCM (10 mL) was added to a solution of 3,5-Dichlorobenzoyl chloride (0.88 g, 4.19 mmol) and TEA (0.70 mL, 5.03 mmol) in DCM (10 mL) at 0°C. The reaction mixture was stirred at RT for 3 h, diluted with DCM (20 mL), washed twice with 10% aqueous $NaHCO_3$ (2 × 10 mL) and once with brine (10 mL), dried over Na_2SO_4 , filtered and concentrated under vacuum. Crystallization with MeOH (5 vol) gave 0.81 g of 4-(3,5-Dichlorobenzoylamino)-1-(4-*i*-propylphenoxyacetyl)piperidine as a white solid.

Yield = 43.0%

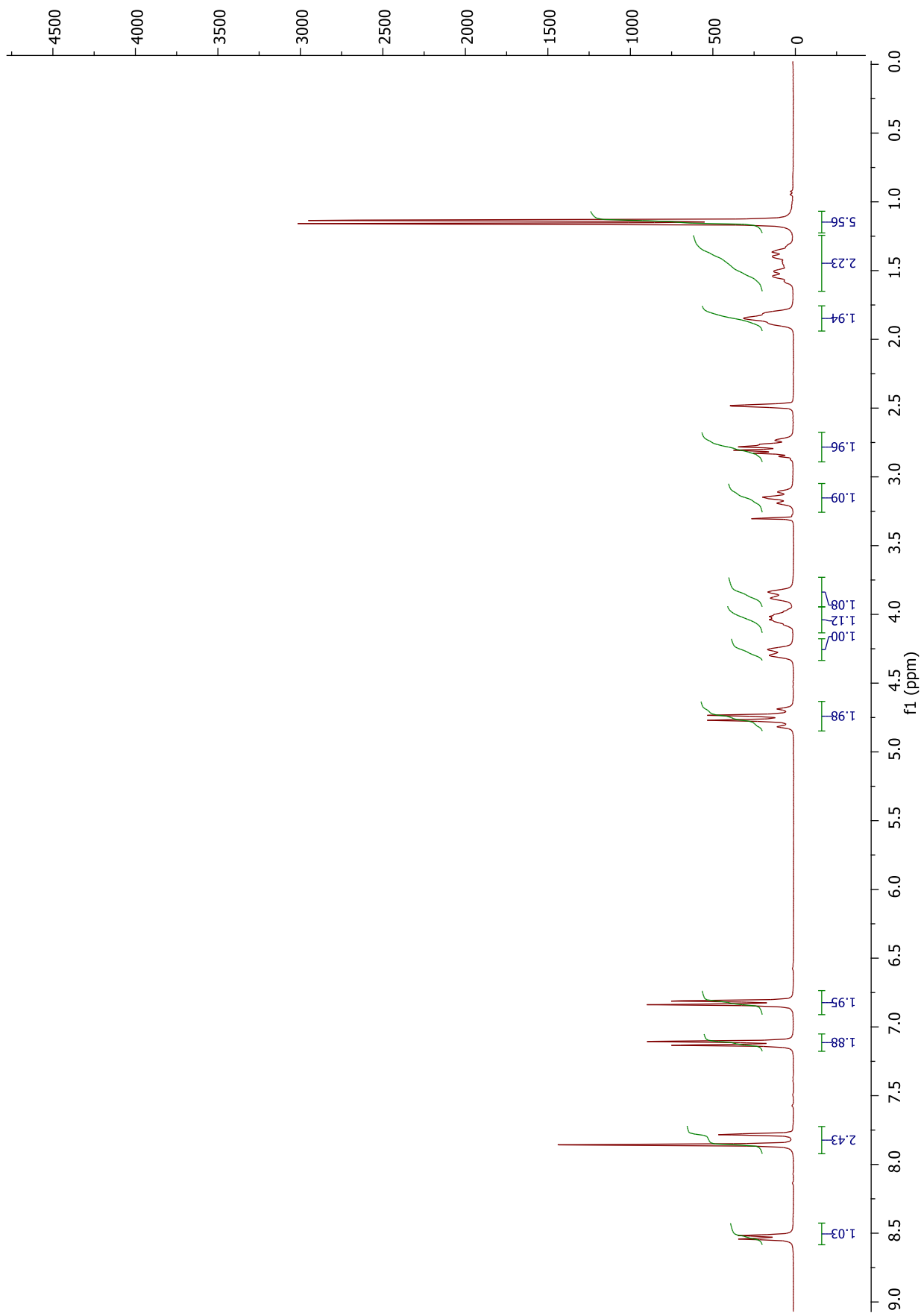
M.p. = 135.9°C

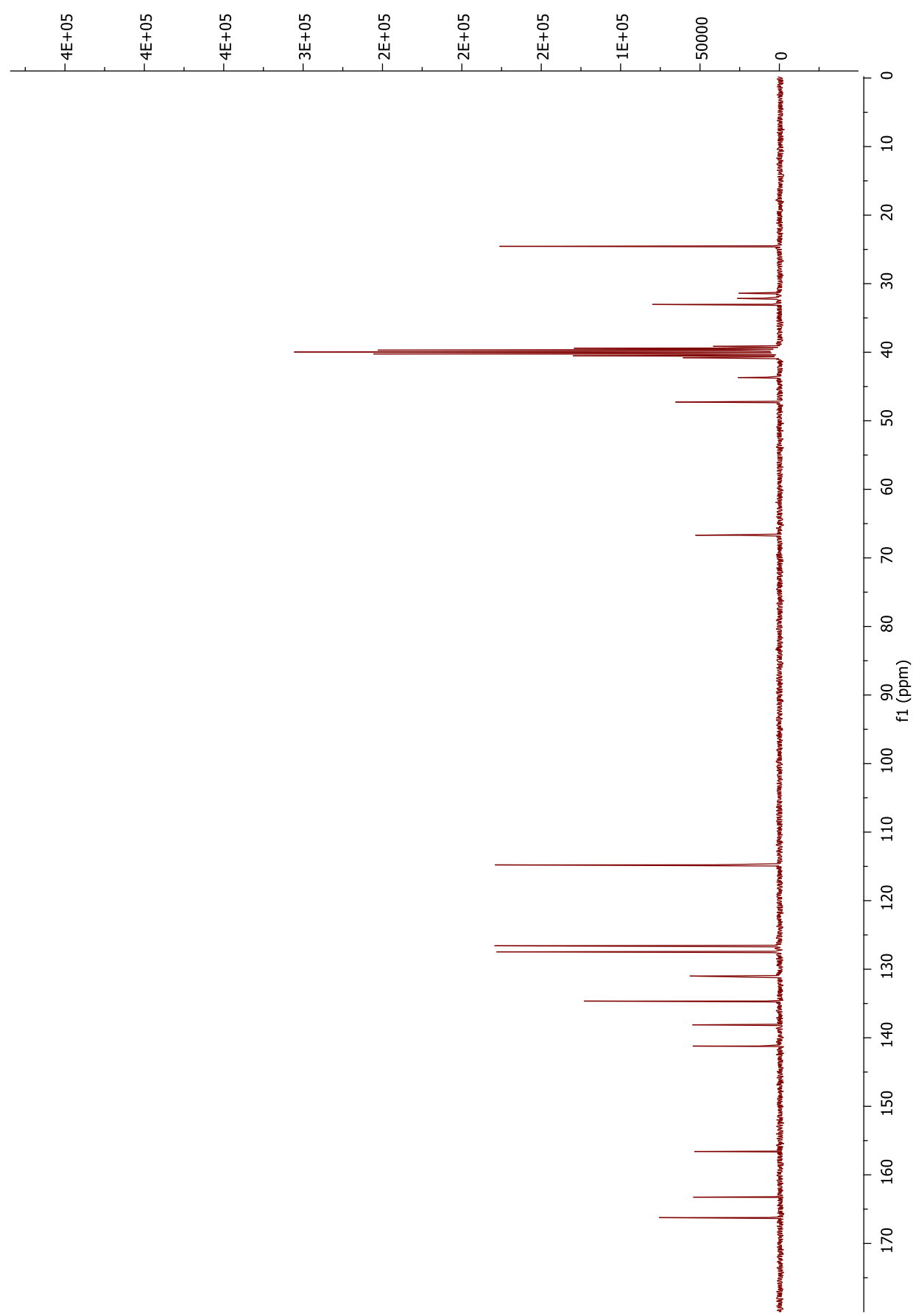
Tr (HPLC, Isocratic, H_2O with 0.10% TFA / Acetonitrile with 0.10% TFA 55/45. 30 min run time. Flow rate: 1.5 mL/min) = 14.83 min, Purity = 98.4%

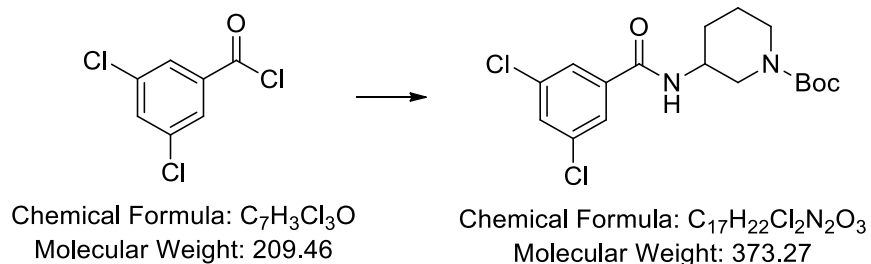
1H NMR (d_6 -DMSO): δ 8.53 (d, J = 7.5 Hz, 1H), 7.86 (m, 2H), 7.78 (m, 1H), 7.12 (d, J = 8.2 Hz, 2H), 6.83 (d, J = 8.2 Hz, 2H), 4.79 (d, J = 14.0 Hz, 1H), 4.71 (d, J = 14.0 Hz, 1H), 4.28 (d, J = 13.1 Hz, 1H), 4.02 (m, 1H), 3.86 (d, J = 13.1 Hz, 1H), 3.15 (t, J = 12.1 Hz, 1H), 2.82 (set, J = 6,8 Hz, 1H), 2.80 (m, 1H), 1.85 (m, 2H), 1.53 (m, 1H), 1.37 (m, 1H), 1.15 ppm (d, J = 6.8 Hz, 6H)

^{13}C NMR (d_6 -DMSO): δ 166.23, 163.25, 156.59, 141.21, 138.11, 134.66, 131.00, 127.47, 126.59, 114.79, 66.69, 47.27, 43.69, 33.03, 32.16, 31.40, 24.55 ppm.

Experimental





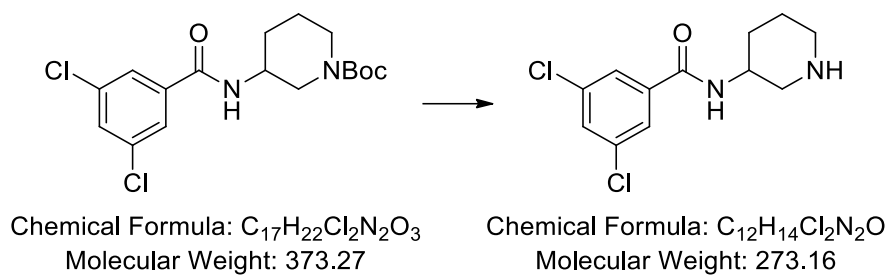
N-Boc-(3-(3,5-dichlorobenzamido)piperidine)

A solution of 1-*N*-Boc-3-amino-piperidine (2.10 g, 10.47 mmol) in DCM (20 mL) was added to a solution of 3,5-dichlorobenzoic acid (2.19 g, 10.47 mmol) and TEA (2.92 mL, 20.94 mmol) in DCM (20 mL) at 0°C. The reaction mixture was stirred at RT for 3 h, diluted with DCM (20 mL), washed twice with 10% aqueous $NaHCO_3$ (2 × 10 mL) and once with brine (10 mL), dried over Na_2SO_4 , filtered and concentrated under vacuum to give 3.68 g of *N*-Boc-(3-(3,5-dichlorobenzamido)piperidine) as a yellow oil.

Yield = 94.1%

1H NMR ($CDCl_3$): δ 7.60 (s, 2H), 7.45 (s, 1H), 6.60 (bs, 1H), 4.11 (dq, $J = 9.3, 4.5$ Hz, 1H), 3.53 (m, 3H), 3.24 (m, 1H), 1.77 (m, 2H), 1.60 (m, 2H), 1.44 (s, 9H).

3-(3,5-dichlorobenzamido)piperidine

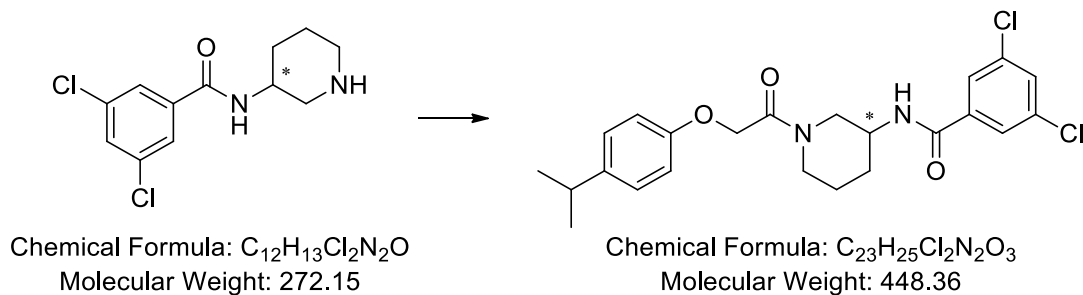


TFA (7.55 mL, 98.6 mmol) was added to a solution of *N*-Boc-3-(3,5-dichlorobenzamido)piperidine (3.68 g, 9.86 mmol) in DCM (30 mL) at 0°C. The reaction mixture was stirred at RT for 18 h, diluted with DCM, washed once with 10% aqueous NaOH (15 mL), once with brine (15 mL), dried over Na_2SO_4 , filtered, and concentrated under vacuum to give 2.10 g of 3-(3,5-dichlorobenzamido)piperidine as a white solid.

Yield = 77.0%

M.p. = 186.50°C

1H NMR ($CDCl_3$): δ 7.64 (s, 2H), 7.47 (m, 1H), 6.86 (bs, 1H), 4.17 (m, 1H), 3.05 (d, J = 11.8 Hz, 1H), 2.83 (m, 3H), 2.25 (bs, 1H), 1.76 (m, 3H), 1.57 (m, 1H).

(XXXIX) 3,5-dichloro-*N*-(1-(2-(4-isopropylphenoxy)acetyl)piperidin-3-yl)benzamide

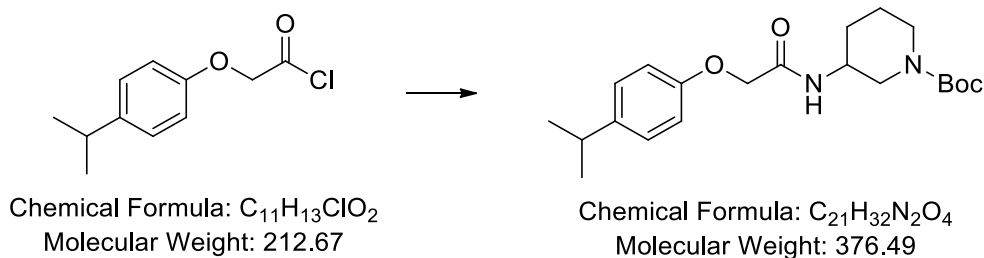
A solution of 3-(3,5-dichlorobenzamido)piperidine (2.10 g, 7.69 mmol) in DCM (20 mL) was added to a solution of 4-*i*-Propylphenoxyacetyl chloride (1.63 g, 7.69 mmol) and TEA (2.14 mL, 15.37 mmol) in DCM (15 mL) at 0°C. The reaction mixture was stirred at RT for 3 h, diluted with DCM (20 mL), washed twice with 10% aqueous $NaHCO_3$ (2 × 10 mL) and once with brine (10 mL), dried over Na_2SO_4 , filtered and concentrated under vacuum. Elution with 6/4 Cyclohexane/Ethyl acetate and subsequent crystallization with MeOH (7 vol.) gave 1.36 g of 3,5-dichloro-*N*-(1-(2-(4-isopropylphenoxy)acetyl)piperidin-3-yl)benzamide as a white solid.

Yield = 39.5%

M.p. = 137.74°C

Tr (HPLC, Isocratic, H_2O with 0.10% TFA / Acetonitrile with 0.10% TFA 50/50. 30 min run time. Flow rate: 1.5 mL/min) = 9.05 min, Purity = 99.2%

The NMR characterization was difficult due to co-presence of several conformers in solution.

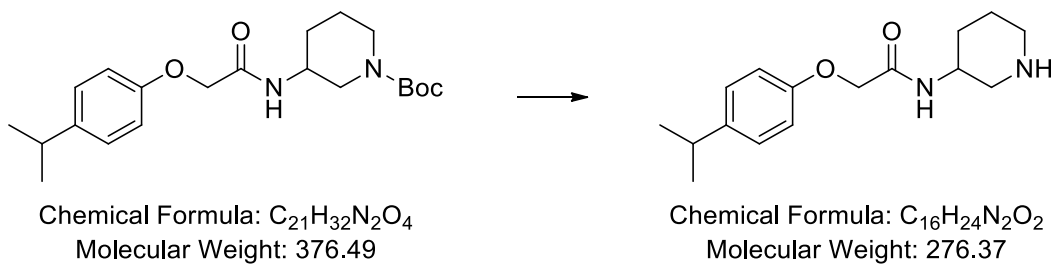
***N*-Boc-(3-(4-isopropylphenoxy)acetamido)piperidine**

A solution of 1-*N*-Boc-3-amino-piperidine (1.55 g, 7.75 mmol) in DCM (10 mL) was added to a solution of 4-*i*-Propylphenoxyacetyl chloride (1.65 g, 7.75 mmol) and TEA (2.16 mL, 15.5 mmol) in DCM (30 mL) at 0°C. The reaction mixture was stirred at RT for 3 h, diluted with DCM (20 mL), washed twice with 10% aqueous $NaHCO_3$ (2 × 10 mL) and once with brine (10 mL), dried over Na_2SO_4 , filtered and concentrated under vacuum to give 3.20 g of *N*-Boc-(3-(4-isopropylphenoxy)acetamido)piperidine as a yellow oil.

Yield = Quantitative

1H NMR ($CDCl_3$): δ 7.15 (d, $J = 8.6$ Hz, 2H), 6.83 (d, $J = 8.6$ Hz, 2H), 6.68 (bs, 1H), 4.45 (s, 2H), 4.02 (m, 1H), 3.60 (d, $J = 13.0$ Hz, 1H), 3.34 (m, 3H), 2.86 (m, 1H), 1.84 (d, $J = 4.0$ Hz, 1H), 1.57 (m, 3H), 1.43 (s, 9H), 1.22 (d, $J = 7.0$ Hz, 6H).

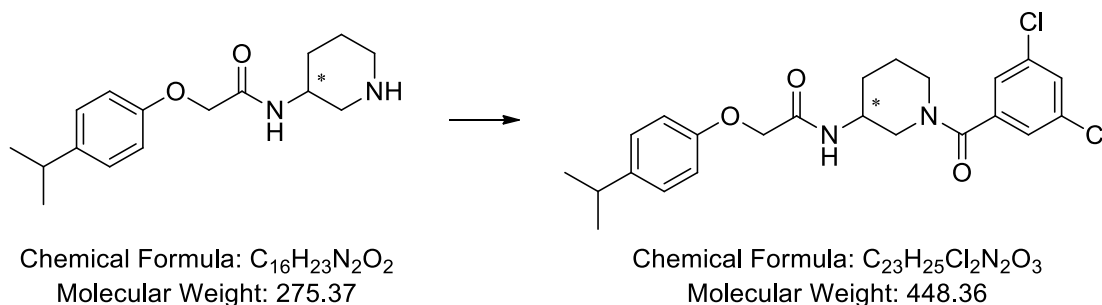
3-(4-isopropylphenoxy)acetamido)piperidine



TFA (6.50 mL, 85.00 mmol) was added to a solution of *N*-Boc-3-(4-isopropylphenoxy)acetamido)piperidine (3.20 g, 8.50 mmol) in DCM (30 mL) at 0°C. The reaction mixture was stirred at RT for 18 h, diluted with DCM, washed once with 10% aqueous NaOH (15 mL), once with brine (15 mL), dried over Na_2SO_4 , filtered, and concentrated under vacuum to give 1.94 g of 3-(4-isopropylphenoxy)acetamido)piperidine as a yellowish oil.

Yield = 82.5%

1H NMR ($CDCl_3$): δ 7.16 (d, $J = 8.6$ Hz, 2H), 6.94 (bs, 1H), 6.87 (d, $J = 8.6$ Hz, 2H), 4.46 (s, 2H), 4.03 (s, 1H), 3.08 (dd, $J = 12.0, 3.1$ Hz, 1H), 2.86 (m, 2H), 2.75 (m, 1H), 2.65 (dd, $J = 11.9, 7.1$ Hz, 1H), 2.43 (m, 1H), 1.81 (m, 1H), 1.56 (m, 3H), 1.22 (d, $J = 6.9$ Hz, 6H).

(XL) *N*-(1-(3,5-dichlorobenzoyl)piperidin-3-yl)-2-(4-isopropylphenoxy)acetamide

A solution of 3-(4-isopropylphenoxy)acetamidopiperidine (1.94 g, 7.02 mmol) in DCM (20 mL) was added to a solution of 3,5-Dichlorobenzoyl chloride (1.47 g, 7.02 mmol) and TEA (1.96 mL, 14.04 mmol) in DCM (15 mL) at 0°C. The reaction mixture was stirred at RT for 3 h, diluted with DCM (20 mL), washed twice with 10% aqueous $NaHCO_3$ (2 × 10 mL) and once with brine (10 mL), dried over Na_2SO_4 , filtered and concentrated under vacuum. Elution with 7/3 Cyclohexane/Ethyl acetate and subsequent crystallization with MeOH (7 vol.) gave 1.50 g of *N*-(1-(3,5-dichlorobenzoyl)piperidin-3-yl)-2-(4-isopropylphenoxy)acetamide as a white solid.

Yield = 47.6%

M.p. = 145.26°C

Tr (HPLC, Isocratic, H_2O with 0.10% TFA / Acetonitrile with 0.10% TFA 50/50. 30 min run time. Flow rate: 1.5 mL/min) = 8.29 min, Purity = 99.6%

The NMR characterization was difficult due to co-presence of several conformers in solution

CHAPTER 10 – REFERENCES

Adedeji W.A. (2021) 'The treasure called antibiotics', *Ann Ib Postgrad Med*, 14(2), pp. 56–57.

Aminov, R.I. (2010) 'A brief history of the antibiotic era: lessons learned and challenges for the future', *Frontiers in microbiology*, 1, p. 134. Available at: <https://doi.org/10.3389/fmicb.2010.00134>.

Andreu, J.M. *et al.* (2010) 'The antibacterial cell division inhibitor PC190723 is an FtsZ polymer-stabilizing agent that induces filament assembly and condensation', *Journal of Biological Chemistry*, 285(19), pp. 14239–14246. Available at: <https://doi.org/10.1074/jbc.M109.094722>.

Banks, J.L. *et al.* (2005) 'Integrated Modeling Program, Applied Chemical Theory (IMPACT)', *Journal of Computational Chemistry*, pp. 1752–1780. Available at: <https://doi.org/10.1002/jcc.20292>.

Bhambhani, A. *et al.* (2021) 'Bacteriophage SP01 gene product 56 inhibits bacillus subtilis cell division by interacting with FtsL and disrupting Pbp2B and FtsW recruitment', *Journal of Bacteriology*, 203(2). Available at: <https://doi.org/10.1128/JB.00463-20>.

Bi, F. *et al.* (2018) 'Design, synthesis and structure-based optimization of novel isoxazole-containing benzamide derivatives as FtsZ modulators', *European Journal of Medicinal Chemistry*, 159, pp. 90–103. Available at: <https://doi.org/10.1016/j.ejmech.2018.09.053>.

Bi, F. *et al.* (2019) 'Discovery of 1,3,4-oxadiazol-2-one-containing benzamide derivatives targeting FtsZ as highly potent agents of killing a variety of MDR bacteria strains', *Bioorganic and Medicinal Chemistry*, 27(14), pp. 3179–3193. Available at: <https://doi.org/10.1016/j.bmc.2019.06.010>.

Bolchi, C. *et al.* (2004) 'Structure-affinity studies for a novel series of homochiral naphtho and tetrahydronaphtho analogues of α 1 antagonist WB-4101', *Bioorganic and Medicinal Chemistry*, 12(18), pp. 4937–4951. Available at: <https://doi.org/10.1016/j.bmc.2004.06.040>.

Bolchi, C. *et al.* (2020) '1,4-Benzodioxane, an evergreen, versatile scaffold in medicinal chemistry: A review of its recent applications in drug design', *European Journal of Medicinal Chemistry*. Available at: <https://doi.org/10.1016/j.ejmech.2020.112419>.

Bosch, F. and Rosich, L. (2008) 'The contributions of paul ehrlich to pharmacology: A tribute on the occasion of the centenary of his nobel prize', *Pharmacology*, pp. 171–179. Available at: <https://doi.org/10.1159/000149583>.

Casiraghi, A. *et al.* (2020) 'Targeting bacterial cell division: A binding site-centered approach to the most promising inhibitors of the essential protein FtsZ', *Antibiotics*. MDPI AG. Available at: <https://doi.org/10.3390/antibiotics9020069>.

- Centre for Disease Control and Prevention (2019) *Antibiotic resistance threats in the United States, 2019*. Atlanta, Georgia. Available at: <https://doi.org/10.15620/cdc:82532>.
- Chiodini, G. *et al.* (2015) 'Benzodioxane-benzamides as new bacterial cell division inhibitors', *European Journal of Medicinal Chemistry*, 89, pp. 252–265. Available at: <https://doi.org/10.1016/j.ejmech.2014.09.100>.
- Colquhoun, J.M. *et al.* (2019) 'Identification of small molecule inhibitors of Staphylococcus aureus RnpA', *Antibiotics*, 8(2). Available at: <https://doi.org/10.3390/antibiotics8020048>.
- Czaplewski, L.G. *et al.* (2009) 'Antibacterial alkoxybenzamide inhibitors of the essential bacterial cell division protein FtsZ', *Bioorganic and Medicinal Chemistry Letters*, 19(2), pp. 524–527. Available at: <https://doi.org/10.1016/j.bmcl.2008.11.021>.
- Dai, K. and Lutkenhaus, J. (1991) 'ftsZ is an essential cell division gene in Escherichia coli', *Journal of bacteriology*, 173(11), pp. 3500–3506. Available at: <https://doi.org/10.1128/jb.173.11.3500-3506.1991>.
- Du, S. and Lutkenhaus, J. (2019) 'At the Heart of Bacterial Cytokinesis: The Z Ring', *Trends in microbiology*, 27(9), pp. 781–791. Available at: <https://doi.org/10.1016/j.tim.2019.04.011>.
- Duman, R. *et al.* (2013) 'Structural and genetic analyses reveal the protein SepF as a new membrane anchor for the Z ring', *Proceedings of the National Academy of Sciences of the United States of America*, 110(48). Available at: <https://doi.org/10.1073/pnas.1313978110>.
- Eidem, T.M. *et al.* (2015) 'Small-molecule inhibitors of Staphylococcus aureus RnpA-mediated RNA turnover and tRNA processing', *Antimicrobial Agents and Chemotherapy*, 59(4), pp. 2016–2028. Available at: <https://doi.org/10.1128/AAC.04352-14>.
- Elsen, N.L. *et al.* (2012) 'Mechanism of action of the cell-division inhibitor PC190723: modulation of FtsZ assembly cooperativity', *Journal of the American Chemical Society*, 134(30), pp. 12342–12345. Available at: <https://doi.org/10.1021/ja303564a>.
- Erickson, H.P. (1997) 'FtsZ, a tubulin homologue in prokaryote cell division', *Trends in Cell Biology*, 7(9), pp. 362–367. Available at: [https://doi.org/10.1016/S0962-8924\(97\)01108-2](https://doi.org/10.1016/S0962-8924(97)01108-2).
- Erickson, H.P. (2007) 'Evolution of the cytoskeleton', *BioEssays*, pp. 668–677. Available at: <https://doi.org/10.1002/bies.20601>.
- Fang, Z., Li, Y., *et al.* (2019) 'Antibacterial activity and mechanism of action of a thiophenyl substituted pyrimidine derivative', *RSC Advances*, 9(19), pp. 10739–10744. Available at: <https://doi.org/10.1039/c9ra01001g>.
- Fang, Z., Zheng, S., *et al.* (2019) 'Design, synthesis and antibacterial evaluation of 2,4-disubstituted-6-thiophenyl-pyrimidines', *European Journal of Medicinal Chemistry*, 161, pp. 141–153. Available at: <https://doi.org/10.1016/j.ejmech.2018.10.039>.
- Foye, W.O. (2005) *Principles of Medicinal Chemistry*.

- Friesner, R.A. *et al.* (2006) 'Extra precision glide: Docking and scoring incorporating a model of hydrophobic enclosure for protein-ligand complexes', *Journal of Medicinal Chemistry*, 49(21), pp. 6177–6196. Available at: <https://doi.org/10.1021/jm051256o>.
- FtsZ Wikipedia page* (2022). Available at: <https://en.wikipedia.org/wiki/FtsZ> (Accessed: 25 November 2022).
- Gueiros-Filho, F.J. and Losick, R. (2002) 'A widely conserved bacterial cell division protein that promotes assembly of the tubulin-like protein FtsZ', *Genes and Development*, 16(19), pp. 2544–2556. Available at: <https://doi.org/10.1101/gad.1014102>.
- Ha, L. *et al.* (2018) 'Crystal structure of the ribonuclease-P-protein subunit from *Staphylococcus aureus*', *Acta Crystallographica Section F: Structural Biology Communications*, 74(10), pp. 632–637. Available at: <https://doi.org/10.1107/S2053230X18011512>.
- Haeusser, D.P. and Margolin, W. (2016) 'Splitsville: Structural and functional insights into the dynamic bacterial Z ring', *Nature Reviews Microbiology*. Nature Publishing Group, pp. 305–319. Available at: <https://doi.org/10.1038/nrmicro.2016.26>.
- Haydon, D.J. *et al.* (2008) 'An Inhibitor of FtsZ with Potent and Selective Anti-Staphylococcal Activity', *Science*, 321(5896), pp. 1670–1673. Available at: <https://doi.org/10.1126/science.1160446>.
- Haydon, D.J. *et al.* (2010) 'Creating an antibacterial with in vivo efficacy: Synthesis and characterization of potent inhibitors of the bacterial cell division protein FTSZ with improved pharmaceutical properties', *Journal of Medicinal Chemistry*, 53(10), pp. 3927–3936. Available at: <https://doi.org/10.1021/jm9016366>.
- Jorgensen, W.L., Maxwell, D.S. and Tirado-Rives, J. (1996) 'Development and Testing of the OPLS All-Atom Force Field on Conformational Energetics and Properties of Organic Liquids', *Journal of the American Chemical Society*, 118(45), pp. 11225–11236. Available at: <https://doi.org/10.1021/ja9621760>.
- Kaul, M. *et al.* (2013) 'Pharmacokinetics and in vivo antistaphylococcal efficacy of TXY541, a 1-methylpiperidine-4-carboxamide prodrug of PC190723', *Biochemical Pharmacology*, 86(12), pp. 1699–1707. Available at: <https://doi.org/10.1016/j.bcp.2013.10.010>.
- Lee Ventola, C. (2015) 'The Antibiotic Resistance Crisis Part 1: Causes and Threats', *Pharmacy & Therapeutics*, 40(4).
- Levin, P.A. and Janakiraman, A. (2021) 'Localization, Assembly, and Activation of the *Escherichia coli* Cell Division Machinery', *EcoSal Plus*, 9(2). Available at: <https://doi.org/10.1128/ecosalplus.ESP-0022-2021> (Accessed: 25 November 2022).
- Liang, X. *et al.* (2006) 'Inactivation of a two-component signal transduction system, SaeRS, eliminates adherence and attenuates virulence of *Staphylococcus aureus*', *Infection and Immunity*, 74(8), pp. 4655–4665. Available at: <https://doi.org/10.1128/IAI.00322-06>.

- Lock, R.L. and Harry, E.J. (2008) 'Cell-division inhibitors: new insights for future antibiotics.', *Nature reviews. Drug discovery*, pp. 324–338. Available at: <https://doi.org/10.1038/nrd2510>.
- Lounsbury, N. *et al.* (2018) 'Novel inhibitors of *Staphylococcus aureus* RnpA that synergize with mupirocin', *Bioorganic and Medicinal Chemistry Letters*, 28(6), pp. 1127–1131. Available at: <https://doi.org/10.1016/j.bmcl.2018.01.022>.
- Löwe, J. (1998) 'Crystal Structure Determination of FtsZ from *Methanococcus jannaschii*', *Journal of Structural Biology*, 124, pp. 235–243.
- Lu, Y. *et al.* (2012) 'An overview of tubulin inhibitors that interact with the colchicine binding site', *Pharmaceutical Research*, pp. 2943–2971. Available at: <https://doi.org/10.1007/s11095-012-0828-z>.
- Lui, H.K. *et al.* (2019) 'Boosting the efficacy of anti-MRSA β -lactam antibiotics via an easily accessible, non-cytotoxic and orally bioavailable FtsZ inhibitor', *European Journal of Medicinal Chemistry*, 163, pp. 95–115. Available at: <https://doi.org/10.1016/j.ejmech.2018.11.052>.
- Lutkenhaus, J.F., Wolf-Watz, H. and Donachie, W.D. (1980) 'Organization of Genes in the *ftsA-envA* Region of the *Escherichia coli* Genetic Map and Identification of a New *fts* Locus (*ftsZ*)', *Journal of Bacteriology*, 142(2), pp. 615–620.
- Margolin, W. (2005) 'FtsZ and the division of prokaryotic cells and organelles', *Nature reviews. Molecular cell biology*, 6(11), pp. 862–871. Available at: <https://doi.org/10.1038/nrm1745>.
- Marincola, G. *et al.* (2012) 'RNase Y of *Staphylococcus aureus* and its role in the activation of virulence genes', *Molecular Microbiology*, 85(5), pp. 817–832. Available at: <https://doi.org/10.1111/j.1365-2958.2012.08144.x>.
- Monahan, L.G. *et al.* (2014) 'Division site positioning in bacteria: One size does not fit all', *Frontiers in Microbiology*. Frontiers Research Foundation. Available at: <https://doi.org/10.3389/fmicb.2014.00019>.
- Morris, G.M. *et al.* (2009) 'Software news and updates AutoDock4 and AutoDockTools4: Automated docking with selective receptor flexibility', *Journal of Computational Chemistry*, 30(16), pp. 2785–2791. Available at: <https://doi.org/10.1002/jcc.21256>.
- Newman, J.A. *et al.* (2012) 'Dissection of the network of interactions that links RNA processing with glycolysis in the *Bacillus subtilis* degradosome', *Journal of Molecular Biology*, 416(1), pp. 121–136. Available at: <https://doi.org/10.1016/j.jmb.2011.12.024>.
- Nicolaou, K.C. and Rigol, S. (2018) 'A brief history of antibiotics and select advances in their synthesis', *The Journal of antibiotics*, 71(2), pp. 153–184. Available at: <https://doi.org/10.1038/ja.2017.62>.
- Nogales, E., Wolf, S.G. and Downing, K.H. (1998) 'Structure of the tubulin dimer by electron crystallography', *Nature*, 391, pp. 199–203.

- Ohashi, Y. *et al.* (1999) 'The Lethal Effect of a Benzamide Derivative, 3-Methoxybenzamide, Can Be Suppressed by Mutations within a Cell Division Gene, *ftsZ*, in *Bacillus subtilis*', *Journal of Bacteriology*, 181(4), pp. 1348–1351.
- Olson, Patrick D *et al.* (2011) 'Small molecule inhibitors of *Staphylococcus aureus* RnpA alter cellular mRNA turnover, exhibit antimicrobial activity, and attenuate pathogenesis', *PLoS pathogens*, 7(2), p. e1001287. Available at: <https://doi.org/10.1371/journal.ppat.1001287>.
- Olson, Patrick D. *et al.* (2011) 'Small molecule inhibitors of *staphylococcus aureus* RnpA alter cellular mRNA turnover, exhibit antimicrobial activity, and attenuate pathogenesis', *PLoS Pathogens*, 7(2). Available at: <https://doi.org/10.1371/journal.ppat.1001287>.
- Paul Erlich (no date). Available at: https://en.wikipedia.org/wiki/Paul_Ehrlich (Accessed: 25 November 2022).
- Pradhan, P., Margolin, W. and Beuria, T.K. (2021) 'Targeting the Achilles Heel of FtsZ: The Interdomain Cleft', *Frontiers in Microbiology*. Frontiers Media S.A. Available at: <https://doi.org/10.3389/fmicb.2021.732796>.
- Read, A.F. and Woods, R.J. (2014) 'Antibiotic resistance management', *Evolution, Medicine and Public Health*, 2014(1), p. 147. Available at: <https://doi.org/10.1093/emph/eou024>.
- Reija, B. *et al.* (2011) 'Development of a homogeneous fluorescence anisotropy assay to monitor and measure FtsZ assembly in solution', *Analytical Biochemistry*, 418(1), pp. 89–96. Available at: <https://doi.org/10.1016/j.ab.2011.07.001>.
- Rice, L.B. (2008) 'Federal funding for the study of antimicrobial resistance in nosocomial pathogens: No ESKAPE', *Journal of Infectious Diseases*, pp. 1079–1081. Available at: <https://doi.org/10.1086/533452>.
- Rico, A.I., Krupka, M. and Vicente, M. (2013) 'In the beginning, *escherichia coli* assembled the proto-ring: An initial phase of division', *Journal of Biological Chemistry*, pp. 20830–20836. Available at: <https://doi.org/10.1074/jbc.R113.479519>.
- Rivas, G. *et al.* (2000) 'Magnesium-induced Linear Self-association of the FtsZ Bacterial Cell Division Protein Monomer', *The Journal of Biological Chemistry*, 275(16), pp. 11740–11749. Available at: <http://www.jbc.org/>.
- Rollo, J.M. and Williamson, J. (1952) 'Acquired resistance to Penicillin and to Neoarsphenamine in *Spirochaeta Recurrentis*', *British Journal of Pharmacology*, 7(33). Available at: <https://doi.org/10.1111/j.1476-5381.1952.tb00686.x> (Accessed: 25 November 2022).
- le Scornet, A. and Redder, P. (2019) 'Post-transcriptional control of virulence gene expression in *Staphylococcus aureus*', *Biochimica et Biophysica Acta - Gene Regulatory Mechanisms*. Elsevier B.V., pp. 734–741. Available at: <https://doi.org/10.1016/j.bbagr.2018.04.004>.

- Sengupta, S., Chattopadhyay, M.K. and Grossart, H.P. (2013) 'The multifaceted roles of antibiotics and antibiotic resistance in nature', *Frontiers in Microbiology*. Frontiers Research Foundation. Available at: <https://doi.org/10.3389/fmicb.2013.00047>.
- Stokes, N.R. *et al.* (2013) 'An improved small-molecule inhibitor of FtsZ with superior in vitro potency, drug-like properties, and in vivo efficacy', *Antimicrobial Agents and Chemotherapy*, 57(1), pp. 317–325. Available at: <https://doi.org/10.1128/AAC.01580-12>.
- Straniero, V. *et al.* (2016) '3-(Benzodioxan-2-ylmethoxy)-2,6-difluorobenzamides bearing hydrophobic substituents at the 7-position of the benzodioxane nucleus potentially inhibit methicillin-resistant Sa and Mtb cell division', *European Journal of Medicinal Chemistry*, 120, pp. 227–243. Available at: <https://doi.org/10.1016/j.ejmech.2016.03.068>.
- Straniero, V. *et al.* (2017) '2,6-Difluorobenzamide Inhibitors of Bacterial Cell Division Protein FtsZ: Design, Synthesis, and Structure–Activity Relationships', *ChemMedChem*, 12(16), pp. 1303–1318. Available at: <https://doi.org/10.1002/cmdc.201700201>.
- Straniero, V., Suigo, L., *et al.* (2020) 'Benzamide derivatives targeting the cell division protein ftsz: Modifications of the linker and the benzodioxane scaffold and their effects on antimicrobial activity', *Antibiotics*, 9(4). Available at: <https://doi.org/10.3390/antibiotics9040160>.
- Straniero, V., Sebastián-Pérez, V., *et al.* (2020) 'Benzodioxane-Benzamides as Antibacterial Agents: Computational and SAR Studies to Evaluate the Influence of the 7-Substitution in FtsZ Interaction', *ChemMedChem*, 15(2), pp. 195–209. Available at: <https://doi.org/10.1002/cmdc.201900537>.
- Straniero, V. *et al.* (2021) 'Computational design and development of benzodioxane-benzamides as potent inhibitors of FtsZ by exploring the hydrophobic subpocket', *Antibiotics*, 10(4). Available at: <https://doi.org/10.3390/antibiotics10040442>.
- Sun, N. *et al.* (2014) 'Rational design of berberine-based FtsZ inhibitors with broad-spectrum antibacterial activity', *PLoS ONE*, 9(5). Available at: <https://doi.org/10.1371/journal.pone.0097514>.
- Sun, N. *et al.* (2017) 'A thiazole orange derivative targeting the bacterial protein FtsZ shows potent antibacterial activity', *Frontiers in Microbiology*, 8(MAY). Available at: <https://doi.org/10.3389/fmicb.2017.00855>.
- Tan, C.M. *et al.* (2012) 'Restoring Methicillin-Resistant Staphylococcus aureus Susceptibility to β -Lactam Antibiotics', *Science Translational Medicine*, 4(126). Available at: <https://www.science.org>.
- TAXIS pharmaceuticals, inc. (2022).
- University of Oxford (2022) *An estimated 1.2 million people died in 2019 from antibiotic-resistant bacterial infections*. Available at: [https://www.ox.ac.uk/news/2022-01-20-estimated-12-million-people-died-2019-antibiotic-resistant-bacterial-infections#:~:text=More%20than%201.2%20million%20people,of%20antimicrobial%20resistance%20\(AMR\)](https://www.ox.ac.uk/news/2022-01-20-estimated-12-million-people-died-2019-antibiotic-resistant-bacterial-infections#:~:text=More%20than%201.2%20million%20people,of%20antimicrobial%20resistance%20(AMR).). (Accessed: 25 November 2022).

World Health Organization (2015) *Global Action Plan on Antimicrobial Resistance*.

World Health Organization (2021) 'Antibacterials in clinical and preclinical development'.

Zorrilla, S. *et al.* (2021) 'FtsZ Interactions and Biomolecular Condensates as Potential Targets for New Antibiotics', *Antibiotics (Basel, Switzerland)*, 10(3). Available at: <https://doi.org/10.3390/antibiotics10030254>.